

Conformal Mapping and Elliptic Functions

Harald Dalichau

Munich 1993

© Copyright, Prof. Dr.-Ing. Dalichau, Munich 1993, 2005
All rights reserved.

Preface

This book is for engineers, who want to solve a technical problem with the method of conformal mapping. The basic principles of conformal mapping are given in almost all textbooks of electromagnetic theory, field theory and static electric fields. The new approach in this book is the appendix with more than 500 BASIC-programs, with which all given mappings can immediately be calculated.

The following procedure has to be met:

1. Find out the number of your conformal mapping resp. the electrode-configuration of your problem in Chapter 15, the table of all conformal mappings.
2. Load the program with the mapping number (You need to have HTBasic-software on your PC or server. There is a free demo version that you can download from www.htbasic.com) and modify the input parameters to match your specific geometry.
3. Run the program and watch the output on the screen.
4. Store the field-map on your computer.
5. Add the computed field to a presentation or a document.

There is actually no necessity to read the text or to learn the method of conformal mapping.

Today, where automatic design software with two- and threedimensional field computations belongs to the standard tools of many R&D engineers, the method of conformal mapping has to a large extent lost its relevance. It is only used in the education of engineers and physicists, for the presentation of field-maps and to derive analytical formulas.

During my professional career I have used conformal mappings rather often (a major reason for that was probably because I know the method quite well). Therefore I started at the completion of my doctoral thesis to collect conformal transformations and to derive systematically new transformations. For a couple of years I made this my private hobby. As time passed by, this accumulated to a large number of transformations and consequently there was the idea to publish all this: the library of conformal mappings, the collection of BASIC-programs and the methods used, to derive all this.

If you start to work extensively with the method of conformal mappings, you are inevitably confronted with elliptic integrals and elliptic functions. It is rather heavy for an engineer to become acquainted with this very specialized field, mainly because the correspondent literature does not use a consistent nomenclature. In order to remedy this drawback, I have introduced new notations in chapters 12 and 13, with which it is possible to differentiate between the various types of functions. The different notations of Jacobi's Zeta Function for instance, which are all denoted as $Z(\underline{w}, k)$ in the literature, are divided into the algebraic form $Z_a(\underline{w}, k)$, the trigonometric form $Z_t(\underline{w}, k)$ and the elliptic form $Z_e(\underline{w}, k)$.

Munich, October 1993

Harald Dalichau

Contents

1. Conformal Mapping and Complex Variables

- 1.1 Introduction
- 1.2 Computation of an Electric Field without Conformal Mapping
- 1.3 Analytic Functions
- 1.4 Conformal Mapping
- 1.5 Theory of Images

2. Simple Conformal Mappings

- 2.1 The Transformation $\underline{z} = \underline{w}^{\varphi/\pi}$
- 2.2 The Transformation $\underline{z} = \exp(\underline{w}\pi)$
- 2.3 The Transformation $\underline{z} = \ell n \underline{w}$
- 2.4 The Transformation $\underline{z} = \arcsin \underline{w}$
- 2.5 The Transformation $\underline{z} = \sin \underline{w}$
- 2.6 The Transformation $\underline{z} = \tanh \underline{w}$
- 2.7 The Transformation $\underline{z} = 1/\underline{w}$

3. Superposition of Complex Potentials

4. Mapping of Polygonal Boundaries

5. Pre-Transformations

6. Successive Transformations

- 6.1 The Function $\underline{z} = \underline{w}_1^{\varphi/\pi}$
- 6.2 Arcsine
- 6.3 Sine
- 6.4 Logarithm
- 6.5 Exponential Function
- 6.6 Inversion $\underline{z} = 1/\underline{w}_1$
- 6.7 Transformation of Regions
- 6.8 Table of Transformations of Regions

7. Superposition of Fields

8. Electrodes in a Uniform Field

- 8.1 Vertically Oriented Uniform Field
- 8.2 Oblique Incidence of the Uniform Field
- 8.3 Airfoils

9. Rounded Corners

- 9.1 Neighboring Field Line
- 9.2 Rounding of Corners by Superposition of Partly Differing Boundaries
- 9.3 Rounding of Outside Corners with the Schwarz-Christoffel-Transformation
- 9.4 Rounding of Inside Corners

10. Electrodes with Constant Fieldstrength

11. Elliptic Functions

- 11.1 Introduction
- 11.2 The Function $\text{sn}(\underline{w}, k)$
- 11.3 The Functions $\text{cn}(\underline{w}, k)$ and $\text{dn}(\underline{w}, k)$
- 11.4 Some Calculation Formulas

12. Elliptic Integrals

- 12.1 Elliptic Integrals of the First Kind
- 12.2 Elliptic Integrals of the Second Kind
- 12.3 Jacobi's Zeta Function; the Functions $B(\underline{w}, k)$ und $D(\underline{w}, k)$
- 12.4 Elliptic Integrals of the Third Kind

13. Theta Functions

14. Applications

15. Table of Conformal Mappings

Elementary und Special Functions

Elementary und Special Curves

- Group A: One Conducting Boundary with Infinite Extension
- Group B: One Conducting Boundary with Finite Extension
- Group C: Two Conducting Boundaries with Infinite Extension,
Symmetrically Arranged, Same Charge, Opposite
Polarity
- Group D: Two Conducting Boundaries with Infinite Extension,
Same Charge, Opposite Polarity
- Group E: Two Conducting Boundaries with Finite Extension,
Symmetrically Arranged, Same Charge, Opposite
Polarity
- Group F: Two Conducting Boundaries with Finite Extension,
Same Charge, Opposite Polarity
- Group G: Fields with Radial Symmetry
- Group H: Fields with Periodicity in One Dimension
- Group I: Fields with Periodicity in Two Dimensions
- Group J: Surfaces with Periodicity in One Dimension
- Group K: One Conducting Boundary with Finite Extension and
One with Infinite Extension, Same Charge, Opposite
Polarity
- Group L: More Fields with Line Charges
- Group M: Boundaries with Rounded Corners
- Group N: Conducting Boundaries with Constant Field Strength
- Group P: Three and More Conducting Boundaries
- Group Q: Fields with Dipoles
- Group R: Conducting Boundaries in a Uniform Field
- Group S: Conducting Boundaries, Symmetrically Arranged,
Same Charge, Same Polarity
- Group T: Mappings with Nonconducting Boundaries
- Group U: More Mappings, Special Functions

16. Basic-Subroutines

16.1 Elliptic Functions

- 16.1.1 Elliptic Function $\text{sn}(z, k)$
- 16.1.2 Elliptic Function $\text{cn}(z, k)$
- 16.1.3 Elliptic Function $\text{dn}(z, k)$
- 16.1.4 Zeta Function $Z_a(z, k)$
- 16.1.5 Zeta Function $Z_t(\phi, k)$
- 16.1.6 Zeta Function $Z_e(z, k)$

- 16.1.7 Elliptic Functions sn , cn , dn , $Z_e(x,k)$
as well as $K(k)$ and $E(k)$
- 16.1.8 Elliptic Functions sn , cn , dn and
 $Z_e(z,k)$

16.2 Elliptic Integrals

- 16.2.1 Complete Elliptic Integrals $K(k)$ and $E(k)$
- 16.2.2 Complete Elliptic Integrals K , E , Π ,
 $-\infty < k_c, p, a, b < +\infty$
- 16.2.3 Elliptic Integral of the First Kind $F_a(x,k)$,
Real Argument
- 16.2.4 Elliptic Integral of the First Kind $F_t(\phi,k)$,
Real Argument
- 16.2.5 Elliptic Integral of the First Kind $F_a(z,k)$
- 16.2.6 Elliptic Integral of the First Kind $F_t(\phi,k)$
- 16.2.7 Elliptic Integral of the Second Kind $E_a(z,k)$
- 16.2.8 Elliptic Integral of the Second Kind $E_t(\phi,k)$
- 16.2.9 Elliptic Integral of the Second Kind $E_e(z,k)$
- 16.2.10 Elliptic Integral of the Second Kind $E_a(z,k_c,a,b)$,
 $B_a(z,k,a=1,b=0)$, $D_a(z,k,a=0,b=1)$
- 16.2.11 Elliptic Integral of the Third Kind $\Pi_a(z,k,n)$
- 16.2.12 Elliptic Integral of the Third Kind $\Pi_t(\phi,k,n)$
- 16.2.13 Elliptic Integral of the Third Kind $\Pi_e(z,k,a)$
- 16.2.14 Elliptic Integral of the Third Kind $\Pi_j(z,k,a)$

16.3 Theta Functions

- 16.3.1 Theta Function $\vartheta_1(z,k)$
- 16.3.2 Theta Function $\vartheta_2(z,k)$
- 16.3.3 Theta Function $\vartheta_3(z,k)$
- 16.3.4 Theta Function $\vartheta_4(z,k)$

References

Appendix

Basic Programs

1. Conformal Mapping and Complex Variables

1.1 Introduction

Conformal mapping is a very powerful method for the analytical solution of two-dimensional potential fields. Potential fields are solutions of Laplace's equation,

$$\Delta u = 0, \quad (1)$$

which in e.g. Cartesian coordinates x and y reads

$$\frac{d^2 u(x,y)}{dx^2} + \frac{d^2 u(x,y)}{dy^2} = 0. \quad (2)$$

The potential distribution $u(x,y)$ satisfies the differential equation. If the given boundary conditions are unique the solution $u(x,y)$ is unique as well. In case a function $u_1(x,y)$ satisfies the boundary conditions and is at the same time a solution of the differential equation, then this function $u_1(x,y)$ is the wanted solution of the accompanying physical problem and no other solution exists, which is different from $u(x,y)$.

The two-dimensional potential fields that can be solved with the method of conformal mapping or conformal transformation respectively are for instance:

- static electric fields,
- static magnetic fields,
- stationary electric flow fields,
- fields of TEM-waves,
- stationary thermal flow fields,
- stationary hydrodynamic flow fields,
- stationary aerodynamic flow fields.

Further applications for the method of conformal mapping are amongst others the theory of elasticity (e.g. torsion of a cylindrical rod, deformation of a rubber membrane and plane stress) and in the projection of curved planes (e.g. Mercator projection in the field of cartography). In the following text only terms and examples from the field of static electric fields, from the field of transmission line theory and from the field of stationary electric flow will be used.

1.2 Computation of an Electric Field without Conformal Mapping

Example 1: Two concentric circular cylinders

As an example for a two dimensional electrostatic field two very long, concentric circular cylinders are analyzed (Figure 1.1a). The outer cylinder has the potential 0 and the inner one has the potential u_1 . The planes of constant potential, $u = \text{const}$ (Figure 1.1c) are to be calculated. As the field map is identical in all cross-sections $z = \text{const}$, the distribution of the traces of the potential lines $u = \text{const}$ have to be determined in the x - y -plane only (Figure 1.1b). Furthermore the traces of the field lines (Figure 1.1d), which are everywhere perpendicular to the potential lines: The tangent of a field line gives in every point (x,y) of the plane the direction of the local vector of the electric field strength $\vec{E}(x,y)$.

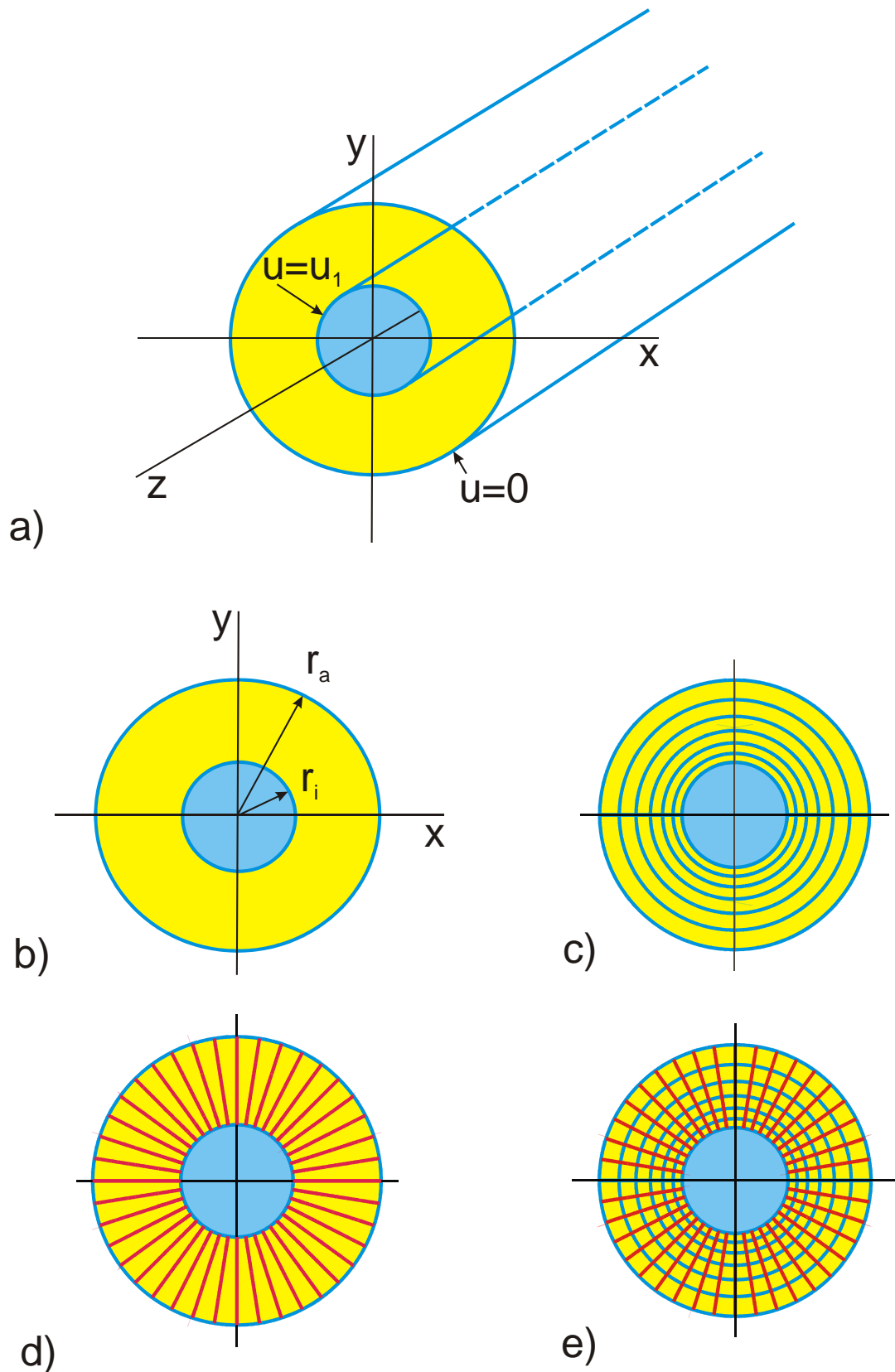


Figure 1.1: Example 1, a) 2 concentric circular cylinders with electrostatic field, b) two-dimensional problem, c) equipotential lines (blue), d) electric field lines (red), e) complete field map

The calculation of the potential distribution $u(x,y)$ (Figure 1.1e) between the two metal cylinders can for instance be accomplished in that way, that the real configuration is substituted by the field of a fictive line charge ρ_L in the center of the metal cylinder (Figure 1.2). The potential $u(x,y)$ in this equivalent configuration is known.

$$u(r) = \frac{\rho_L}{2\pi\epsilon} \ln \frac{r}{r_0}. \quad (3)$$

The reference radius r_0 is the radius, at which the potential has the value $u = 0$. In the case of the potential distribution of Figure 1.2 r_0 can be arbitrarily chosen.

According to Eq. (1.2) all potential lines in the equivalent configuration are concentric circles. With the theorem about the uniqueness of the solution of Laplace's equation follows, that the field map between two concentric, metallic circular cylinders is enclosed in the field map of a line charge. In order to match both fields also quantitatively, the reference radius r_0 and the value of ρ_L are chosen in such a way, that the two boundary conditions

$$u(r = r_a) = 0 \quad (4)$$

$$u(r = r_i) = u_1 \quad (5)$$

are satisfied.

With $r_0 = r_a$ and $\rho_L = \frac{2\pi\epsilon u_1}{\ln \frac{r_i}{r_a}}$ the potential distribution is

$$u(r) = \frac{u_1}{\ln \frac{r_i}{r_a}} \ln \frac{r}{r_a} \quad (6)$$

or

$$u(r) = \frac{u_1}{\ln \frac{r_i}{r_a}} \ln r_a + \frac{u_1}{\ln \frac{r_i}{r_a}} \ln r \quad (7)$$

or

$$u(x, y) = -\frac{u_1}{\ln \frac{r_i}{r_a}} \ln r_a + \frac{u_1}{\ln \frac{r_i}{r_a}} \ln \sqrt{x^2 + y^2} \quad (8)$$

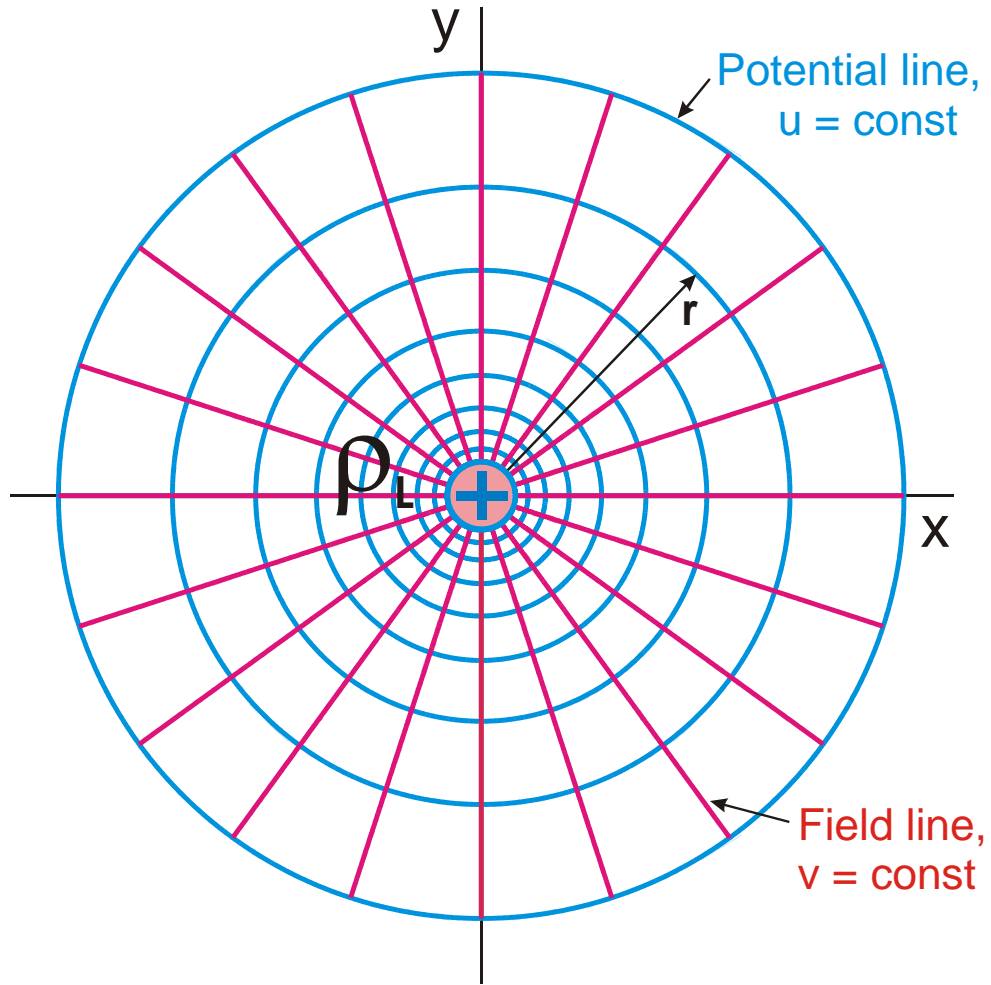


Figure 1.2: Potential lines (blue) and field lines (red) of a line charge ρ_L in the origin of the x-y-coordinate system

Example 2: Sector of an annulus

As an example from the field of stationary electric flow a thin sheet of conducting material is analyzed. Figure 1.3 shows the sheet with thickness d and electric conductivity σ . The sheet has the shape of the sector of an annulus with the angle φ_1 .

The two blue electrodes have the potential 0 and u_0 respectively. Due to the conductivity of the material a current flows through the sheet. Because the sheet ends at the red boundaries, where the non-conducting outer region begins, the red circular arcs at $r = r_i$ and $r = r_a$ are fixed boundary conditions and as that electric flow lines or flux lines respectively. In the region inside the blue-red boundaries the potential distribution $u(x, y)$ has to be determined.

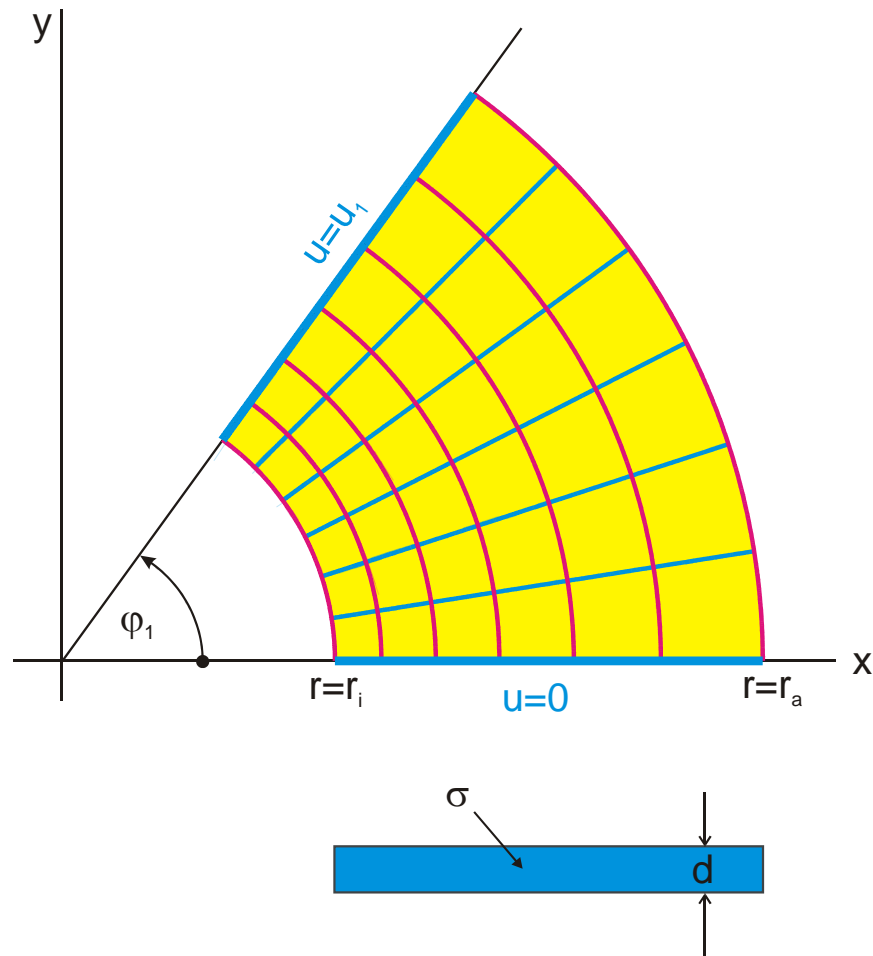


Figure 1.3: Stationary electric flow field in a conductive sheet with thickness d

Because flux lines and potential lines are perpendicular to each other and because in the differential equation (1.3) the x - and the y -dependencies are equal, it can be assumed, that also the field map of this configuration is given by the field map of a line charge in the origin of the coordinate system according to Figure 1.2. Only the field lines (electric

flow lines) and the potential lines have changed places in this case. The electric flow lines are parts of concentric circles and the potential lines are parts of straight lines through the origin.

$$u(\varphi) = u_1 \frac{\varphi}{\varphi_1} \quad (9)$$

$$u(x, y) = u_1 \frac{\varphi}{\varphi_1} \arctan\left(\frac{y}{x}\right). \quad (10)$$

Every potential field like that in Figure 1.2 thus solves two problems. The second one, the dual problem, is found by exchanging potential lines and field lines: If the blue lines were interpreted as potential lines in the first problem, they are taken as field lines in the second problem.

If a closed region like that in Figure 1.3 is examined, whose boundaries completely comply with a sector of an infinite or bigger field map, like e.g. that in Figure 1.2, which is defined for the complete x-y-plane, then there is also a complete agreement between the field map inside the closed region and that inside the sector.

1.3 Analytic Functions

A function \underline{w} of a complex variable $\underline{z} = x + jy$

$$\underline{w} = f(\underline{z}) \quad (11)$$

is termed analytic, if the derivative of the function

$$\frac{d\underline{w}}{d\underline{z}} = \lim_{\Delta \underline{z} \rightarrow 0} \frac{\underline{w}(\underline{z} + \Delta \underline{z}) - \underline{w}(\underline{z})}{\Delta \underline{z}} \quad (12)$$

exists and if it is independent of the direction $\Delta \underline{z} = \Delta x + j\Delta y$. To prove this, the function can be differentiated in Cartesian coordinates once in the x direction and once in the y direction. If the real part of \underline{w} is u and the imaginary part is v , $\underline{w} = u + jv$, this leads to:

$$\text{In } x \text{ direction: } \frac{d\underline{w}}{d\underline{z}} = \lim_{\Delta x \rightarrow 0} \frac{u(x + \Delta x, y) - u(x, y) + j[v(x + \Delta x, y) - v(x, y)]}{\Delta x} \quad (13)$$

$$\text{In } y \text{ direction: } \frac{d\underline{w}}{d\underline{z}} = \lim_{\Delta y \rightarrow 0} \frac{u(x, y + \Delta y) - u(x, y) + j[v(x, y + \Delta y) - v(x, y)]}{j\Delta y} \quad (14)$$

The function $f(\underline{z})$ is analytic, if the real parts and the imaginary parts of both equations are equal.

$$\text{Real parts: } \lim_{\Delta x \rightarrow 0} \frac{u(x + \Delta x, y) - u(x, y)}{\Delta x} = \lim_{\Delta y \rightarrow 0} \frac{v(x, y + \Delta y) - v(x, y)}{\Delta y} \quad (15)$$

$$\text{Imaginary parts: } \lim_{\Delta x \rightarrow 0} \frac{v(x + \Delta x, y) - v(x, y)}{\Delta x} = \lim_{\Delta y \rightarrow 0} \left(-\frac{u(x, y + \Delta y) - u(x, y)}{\Delta y} \right) \quad (16)$$

Equation (15) and (16) written as differential equations read:

$$\frac{\partial u}{\partial x} = \frac{\partial v}{\partial y} \quad (17)$$

$$\frac{\partial v}{\partial x} = -\frac{\partial u}{\partial y} \quad (18)$$

These are the Cauchy-Riemann equations.

In cylinder coordinates they read:

$$\frac{\partial u}{\partial r} = \frac{1}{r} \frac{\partial v}{\partial \phi}; \quad \frac{\partial v}{\partial r} = -\frac{1}{r} \frac{\partial u}{\partial \phi} \quad (19)$$

These differential equations are, as mentioned above, usually used, to prove, that a function $\underline{w} = f(\underline{z})$

$$\underline{w}(\underline{z}) = u(x, y) + j v(x, y) \quad (20)$$

is analytic. These conditions are necessary and sufficient.

If they are differentiated again and inserted, it is evident that the real part u and the imaginary part v satisfy Laplace's equation.

$$\Delta u(x, y) = \frac{\partial^2 u(x, y)}{\partial x^2} + \frac{\partial^2 u(x, y)}{\partial y^2} = 0 \quad (21)$$

$$\Delta v(x, y) = \frac{\partial^2 v(x, y)}{\partial x^2} + \frac{\partial^2 v(x, y)}{\partial y^2} = 0. \quad (22)$$

A function is in a region analytic (different terms: regular, holomorph), if the derivatives (Eq. (17, 18)) exist and are unique in all points of this region. Single singular points, where the derivative is undetermined or infinite are allowed. An analytic function, whose singularities are only poles, is a meromorphic function. As for instance all elementary algebraic and transcendental functions satisfy this condition, there are very many analytic functions. Furthermore holds that analytic functions of analytic functions are also analytic.

Analytic functions can be divided into three classes:

- nonperiodic,
- single-periodic and
- double-periodic

analytic functions. Single-periodic functions are for instance the trigonometric functions and the exponential function. Double-periodic analytic functions are called elliptic functions.

Real part and imaginary part of an analytic function are harmonic functions. If for instance the real part is known, the imaginary part can be calculated in such a way, that both together form an analytic function. $v(x,y)$ is the conjugate harmonic function of $u(x,y)$ and $-u(x,y)$ is the conjugate harmonic function of $v(x,y)$.

This coincidence that when working on physical problems Laplace's equation is to be solved in a region with the local coordinates x and y and that for analytic functions $\underline{w} = f(x + jy)$, the real part of \underline{w} as well as the imaginary part of \underline{w} satisfy Laplace's equation, opens up the possibility, to solve these physical problems with the methods of the theory of complex variables:

- The local coordinates x and y (Figure 1.1 and 1.3) are renamed as real axis x and imaginary axis y of the complex \underline{z} -plane.
- The solution that is to be found is no longer a potential function $u(x,y)$ or a field function $v(x,y)$, but the complex function $\underline{w} = u(x,y) + jv(x,y)$ with the real part $u(x,y)$ and the imaginary part $v(x,y)$.

The function $\underline{w}(x,y)$ is called complex potential. The real part and the imaginary part can be either interpreted as potential function or as field function of the associated physical problem. In the case of example 1 and 2 respectively this means:

$$\underline{w}(x,y) = \ell n \underline{z} \quad (23)$$

with

$$\ell n \underline{z} = \ell n(x + jy) = \ell n \left[\sqrt{x^2 + y^2} \cdot \exp(j \arctan(y/x)) \right] \quad (24)$$

$$\ell n \underline{z} = \ell n \sqrt{x^2 + y^2} + j \arctan(y/x) \quad (25)$$

this leads to

$$\text{Re } \underline{w} = \ell n \sqrt{x^2 + y^2} \quad (26)$$

$$\text{Im } \underline{w} = \arctan(y / x) . \quad (27)$$

A comparison with Eq. (1.13) and (1.18) yields that $\text{Re } \underline{w}$ is the potential function in example 1 and $\text{Im } \underline{w}$ is the potential function in example 2. All constant factors and additive constants, which are missing in these cases, are irrelevant for the solution of the potential problem. The field between two concentric circular cylinders always looks like Figure 1.3, independent of the fact, which specific numerical values are chosen for the potential of the inner and the outer cylinder.

The first, in some cases rather difficult step on the way to find a solution for a potential problem is to determine the potential function $u(x,y)$. The second, trivial step is then the choice of the constants a and b , that belong to the specific physical problem.

$$u_{\text{special}}(x,y) = a + b u(x,y) \quad (28)$$

1.4 Conformal Mapping

The potential function $u(x,y)$ or the complex potential $\underline{w}(x,y)$ can be used to calculate for a given problem in every point (x,y) the local potential $u(x,y)$. However in many cases the field map of the configuration is needed, this means the traces of the potential lines $u = \text{const}$ and the traces of the field lines $v = \text{const}$ in the x - y -plane (Figure 1.2). This results from the inverse function $\underline{z}(u,v)$. The function $\underline{z}(u,v)$ yields for every value $u = \text{const}$ the trace of the corresponding potential line. In the case of example 1 and 2 respectively:

$$\text{Complex potential:} \quad \underline{w} = \ell n \underline{z} \Rightarrow \underline{z} = \exp(\underline{w}) \quad (29)$$

$$\text{Field map:} \quad \underline{z} = \exp(u + j v) \quad (30)$$

$$\text{Potential line } u = u_0, v \text{ variable: } \underline{z}_0 = \exp(u_0) \cdot \exp(jv). \quad (31)$$

The potential line, that we are looking for, thus is a circle around the origin of the \underline{z} -plane with the radius $\exp(u_0)$.

$$\text{Field line } v = v_0, u \text{ variable: } \underline{z}_0 = \exp(u) \cdot \exp(jv_0). \quad (32)$$

The field line or flux line, that we are looking for, thus is a straight line through the origin of the \underline{z} -plane with the angle v_0 measured from the positive x-axis (Figure 1.2, 1.3).

The equation $\underline{z} = f(\underline{w})$, which can be used to draw the field map, may be depicted as a mapping or a transformation: In the \underline{w} -plane the lines $u = \text{const}$ (red) and $v = \text{const}$ (blue) are because of $\underline{w} = u + jv$ straight lines that build a Cartesian coordinate system or a uniform field respectively (Figure 1.4). The straight lines $u = \text{const}$ are mapped onto concentric circular arcs in the \underline{z} -plane and the parallel straight lines $v = \text{const}$ are mapped onto radial rays through the origin of the \underline{z} -plane. The inside of the rectangle ABCD is mapped onto the inside of a sector of an annulus ABCD. Just as well as it is possible to calculate with the equation for each value of \underline{w}_1 the corresponding value of \underline{z}_1 , the graphic representation of the \underline{z} -plane and the \underline{w} -plane gives for every point in the \underline{w} -plane the corresponding point in the \underline{z} -plane.

The graphic representation according to Figure 1.4 that maps the \underline{w} -plane onto the \underline{z} -plane with an analytic function $\underline{z} = f(\underline{w})$ is termed conformal mapping. To every analytic function $\underline{z} = f(\underline{w})$ belongs a conformal mapping.

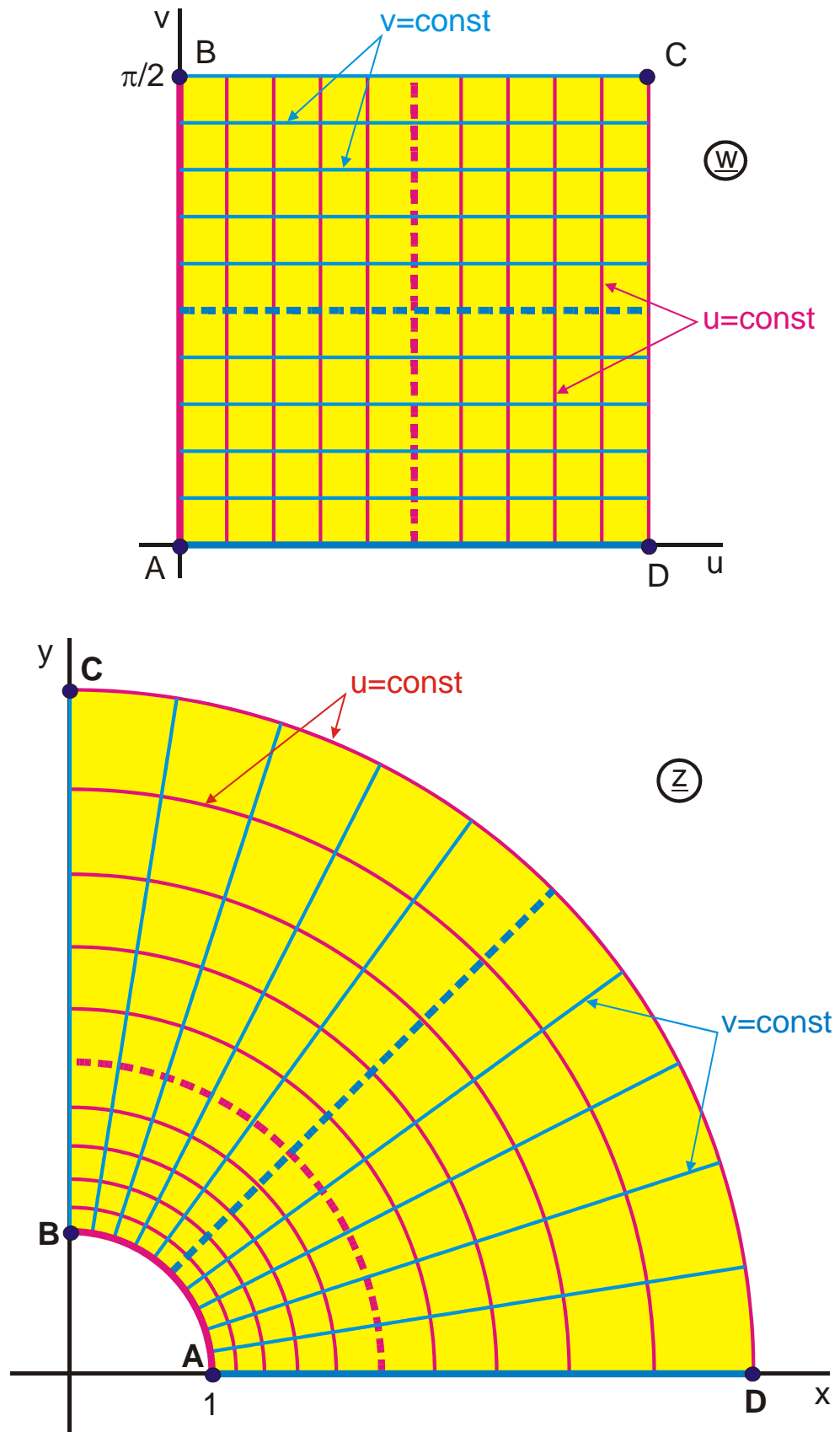


Figure 1.4: The transformation $z = \exp(w)$, mapping B 1

Properties of the conformal mapping:

- Orthogonal sets of curves are transformed into orthogonal sets of curves.
- Every point in the \underline{z} -plane corresponds exactly to one point in the \underline{w} -plane, nevertheless are periodically recurring allocations, like for instance with the function $\underline{z} = \sin \underline{w}$, allowed.
- When considering infinitesimally small regions, every structure in the \underline{w} -plane is transformed into a similar structure in the \underline{z} -plane. This means, an infinitesimally small circle remains a circle and an infinitesimally small triangle remains a triangle.

Through the mapping process they are only rotated and reduced or magnified, respectively. For every point of the \underline{z} -plane a complex number can be determined. The magnitude of this number is the scale factor, with which all lengths in the corresponding point of the \underline{w} -plane have to be multiplied and the phase angle of this number determines, by which angle all lines have to be rotated.

As rotation and magnification vary continuously from each point of the \underline{z} -plane to its neighboring point, the similarity is not achieved for larger areas.

- The conformal mapping is isogonic (it conserves the angles).
- As a result of this a given sense of circulation around any arbitrarily defined closed region is conserved. (In Figure 1.4 the vertices of the rectangle ABCD are lettered clockwise in both planes.)
- The conformal mapping is a similarity transformation (therefore the adjective "conformal").

As analytic functions are allowed to have certain isolated singularities, where they cannot be differentiated, all properties listed above are not satisfied at the location of the singularity.

1.5 Theory of Images

Image behind a plane:

In the field map of two line charges of same size and opposite polarity (Mapping E 1, Figure 1.5a) and in the field map of a symmetrical two wire line in odd mode respectively, the potential line at $y = 0$ is a straight line of infinite length. This line is a symmetry axis of the field (Figure 1.5b). In the three-dimensional field of the two line charges the plane $y = 0$ is the symmetry plane. The boundary conditions of the field on this plane are:

1. The blue line $y = 0$ is a magnetic field line.
2. The potential U of this symmetry plane is constant.
3. The electric field lines are perpendicular to this plane.

Or

4. $U(y)$ is an odd function.
5. $E(y)$ is an even function.

Every potential line in an electrostatic field may be replaced by a conducting surface, without any change in the field above the conducting plane. Therefore it is possible in Figure 5.1a, b to replace the symmetry plane by a conducting half space with infinite extension (Figure 1.5c). The field above the half space is identical to the field in the upper half plane of Figure 1.5a.

From the statements above follows, that the field of a line charge above a conducting half plane can be calculated, by removing the conducting half plane and replacing it with a line charge, which is of same size and has opposite polarity and which is placed at the same distance h below the plane $y = 0$.

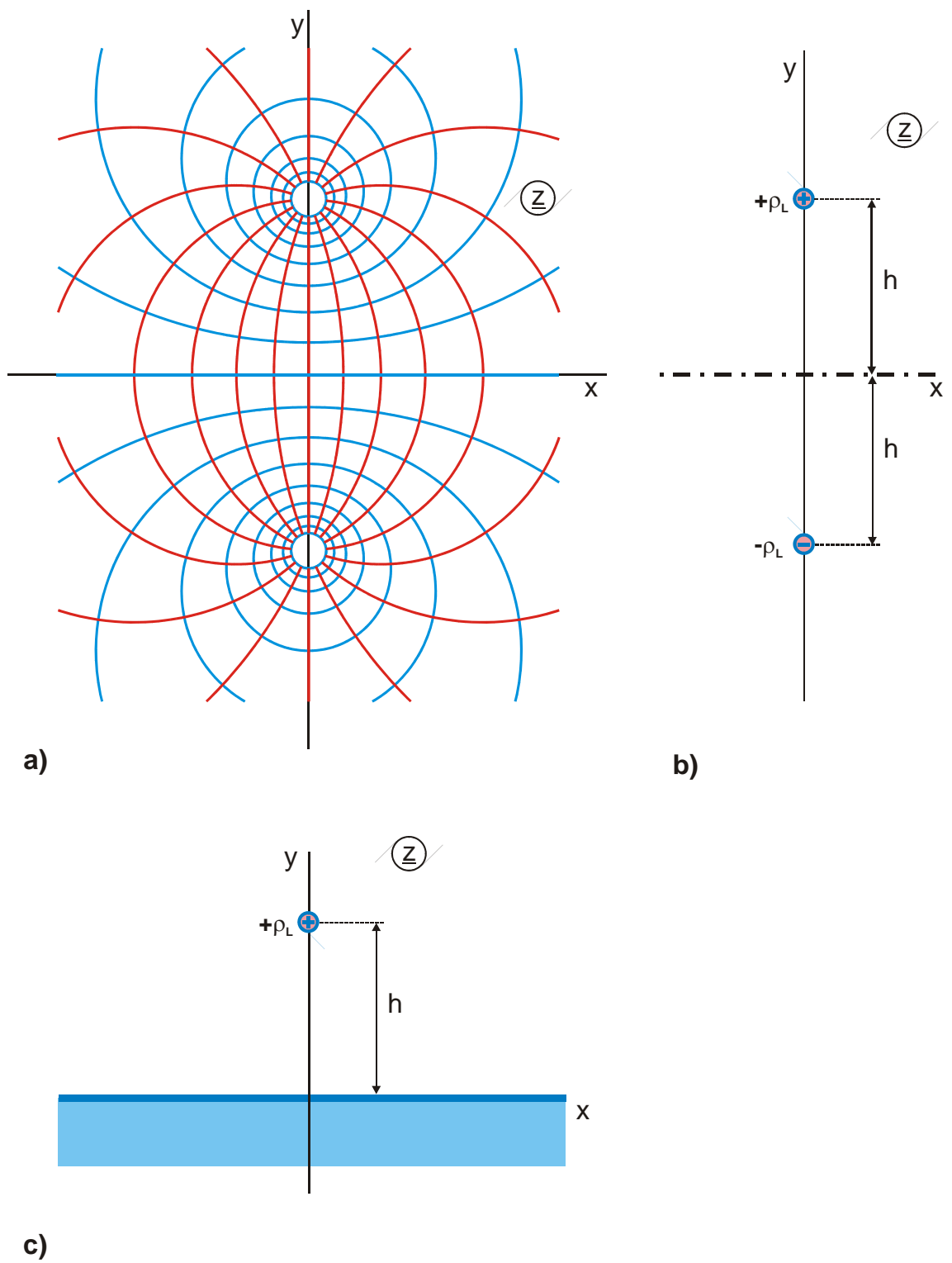


Figure 1.5: Field map of a symmetric two wire line in odd mode with a symmetry plane at $y = 0$

This method of images is also useful and valid respectively for other types of reflecting surfaces (Figure 1.6). It is not only possible to image line charges but also dipoles or in general arbitrary charge distributions and electrode shapes (Figure 1.6d). The theory of images is not restricted to electrostatics but it is valid in analog manner also for electromagnetic wave fields, consequently also for that range of frequencies that covers the visible light. Thus it is possible to visualize the phenomena described above with optical mirrors instead of conducting planes and optical images instead of line charges.

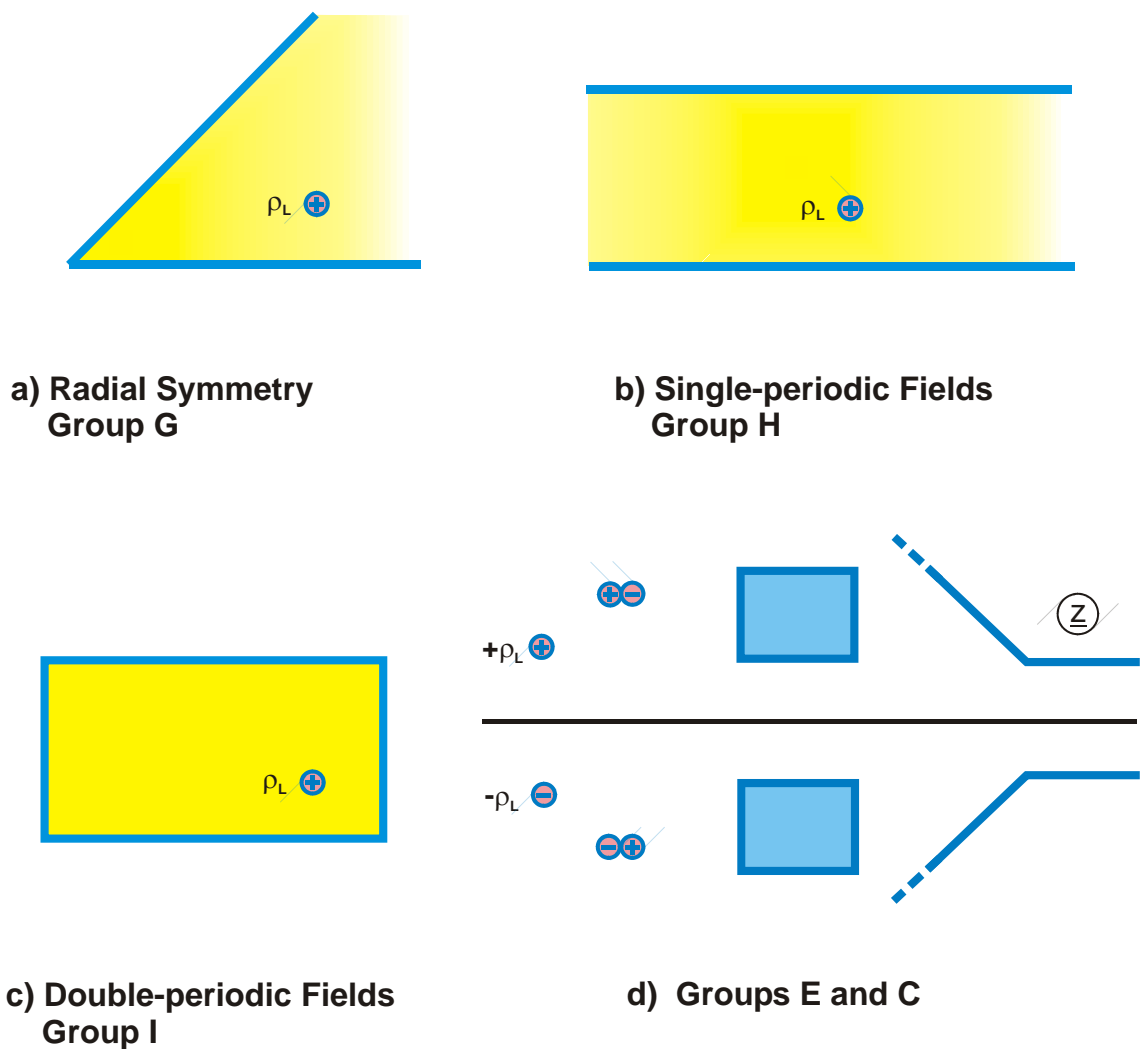


Figure 1.6: Imaging at different planes; various charge configurations

The theory of images has lead to an additional analytical method to calculate specific static fields: As the fields of line charges, point charges and dipoles are analytically known and as they can be superposed arbitrarily (Chapter 3), it is possible to determine the field of Figure 1.6b, by imaging the line charge in the first step once at the upper plane and once at the lower plane. In the second step these image charges of first degree are imaged once again at both planes, thus producing the image charges of second degree, etc. The superposition of the fields of all these charges leads to a fast converging series, with which the total field of the configuration can be calculated with good approximation.

When looking at Figure 1.5a it is evident, that there is still another symmetry plane existing: The y-axis of the coordinate system is a straight field line (red line) with infinite extension, except for the two poles at the location of the line charges. The potential lines (blue lines) are perpendicular to this line and the field in the 1. quadrant is the mirror image of the field in the 2. quadrant.

Figure 1.7 visualizes once again this type of symmetry at the example of the field of two line charges with same size and same polarity (Mapping S 1). This is the field of a symmetric two wire line in even mode. The plane $y = 0$ is the symmetry plane of the field. In analogy to the electrically conducting wall in Figure 1.5, where the electric field lines are perpendicular to, this plane is termed magnetically conducting wall. In this case the magnetic field lines (blue lines) are perpendicular to the wall. The boundary conditions of the field on this plane are:

1. The red line $y = 0$ is an electric field line.
2. The magnetic field lines run perpendicular to this plane.

Or

3. $U(y)$ is an even function.
4. $H(y)$ is an even function.

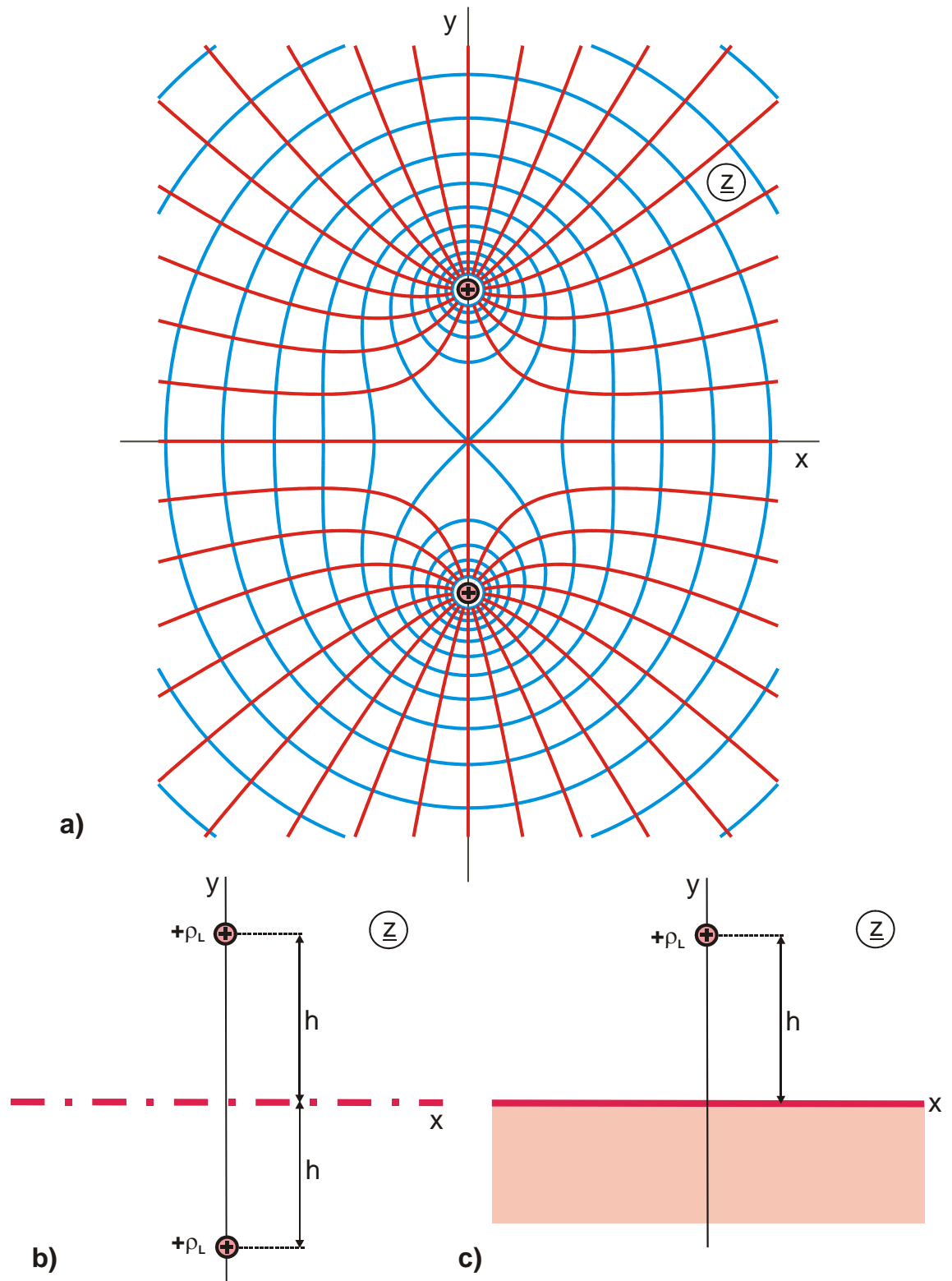


Figure 1.7: Imaging at a magnetically conducting wall illustrated by the field of two line charges with same size and same polarity (Mapping S 1)

Images inside/outside a circle (cylinder):

Field maps, calculated with the method of conformal mapping, consist of sets of orthogonal curves. Therefore it is possible to interpret every field line and every potential line as curvilinear mirror. The correspondence between a point in front of the mirror and its image behind the mirror is defined by the individual mapping function. This interpretation however does not yield new insights. Only for a few special types of mirrors, like for instance straight lines, circles and ellipses, it is possible to put up imaging laws of universal validity.

For the unit circle there is the law of the reciprocal radii (Figure 1.8a): A positive line charge with the distance r_1 from the origin of the coordinate system generates, with the unit circle being a potential line (mirror), as an image a line charge with the same size but opposite polarity in a distance $r_2 = 1/r_1$.

From this follows for instance, that in the field map of a coplanar wave guide (Mapping E 3, Figure 1.8b), which contains a circular potential line (pale green), the end point of the inner conductor at $x_1 = \sqrt{k}$ is mapped onto the end point of the outer conductor at $x_2 = 1/\sqrt{k}$. All points in between are mapped as well, following the same relationship. The midpoint of the inner conductor at $x = 0$ is finally mapped onto $x = \infty$.

With the same mapping function the field maps of a circular inner conductor between two planar outer conductors (Figure 1.5c) and that of a conducting strip inside a circular outer conductor (Figure 1.5d) can be determined. Further examples for images inside/outside a circle are found in the table of mappings (E 5, G 7.3, L 1.2 etc.).

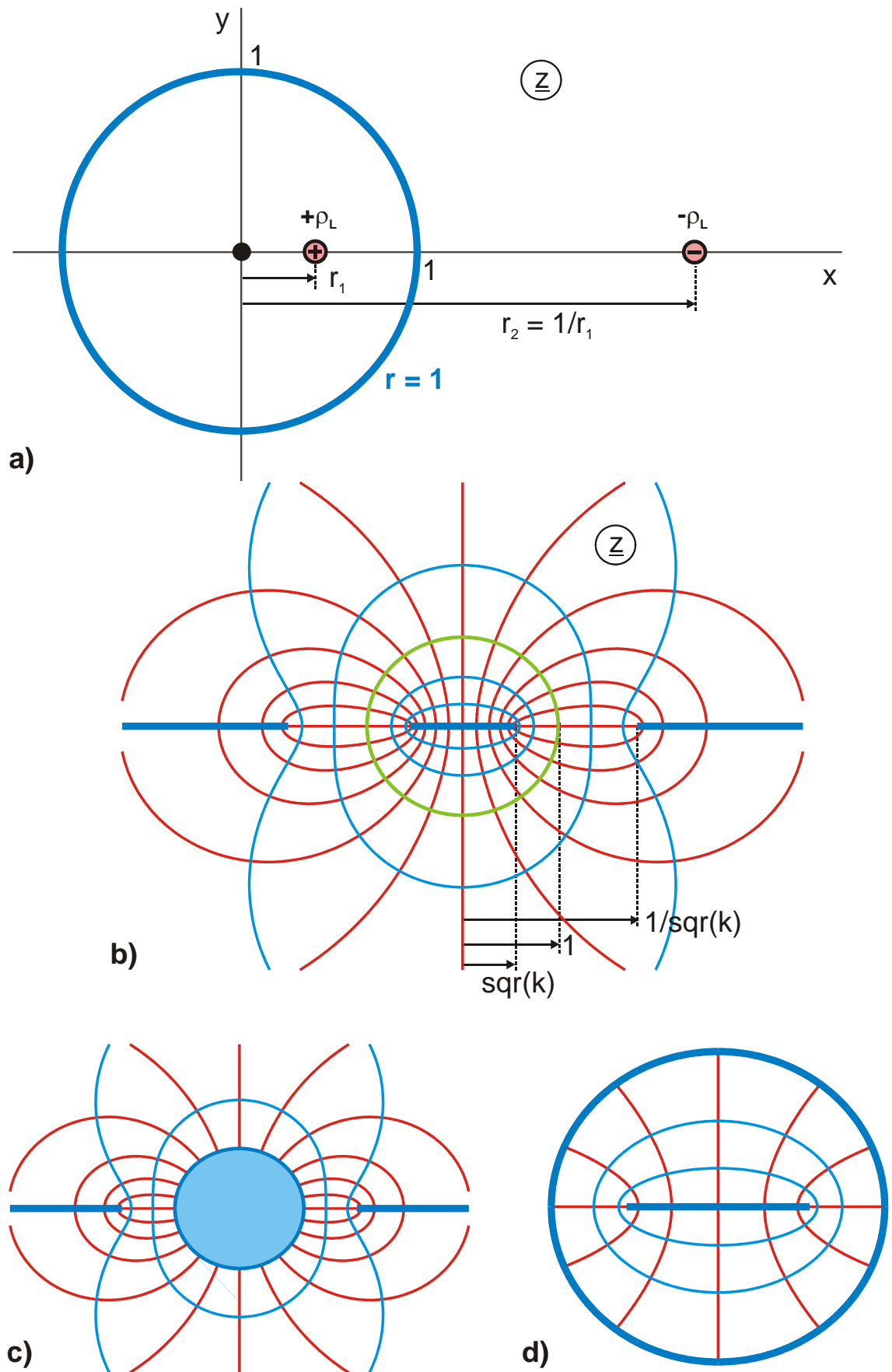


Figure 1.8: Images inside and outside of a circle

Images of an electrode with constant field strength:

Electrodes with constant field strength have also the property, that the image of a straight line is again a straight line. Figure 1.9a shows the field map of a channel of width b that is bent by 90° . Along the pale green colored potential line in the middle the electric field strength is constant. In the transformation from the uniform channel in the \underline{w} -plane to the bent channel in the \underline{z} -plane this line is the "neutral fiber". Its length ℓ is not changed. In the imaging process at this electrode, the lower boundary with the right inside angle at A is transformed into the upper boundary with a right outside angle at B. The electric field strength is "inverse symmetric" with regard to the mirror electrode at $v = b/2$:

$$E(u, v = b/2 + \Delta v) = \frac{1}{E(u, v = b/2 - \Delta v)} \quad (33)$$

The normalized electric field strength in the \underline{w} -plane $E(v)$ equals 1 on the mirror electrode. Below it is smaller and above it is bigger. In the extreme cases it is 0 in point A and ∞ in point B.

Chapter 10 covers transformations containing electrodes with constant field strength. They compose the group of mappings N.

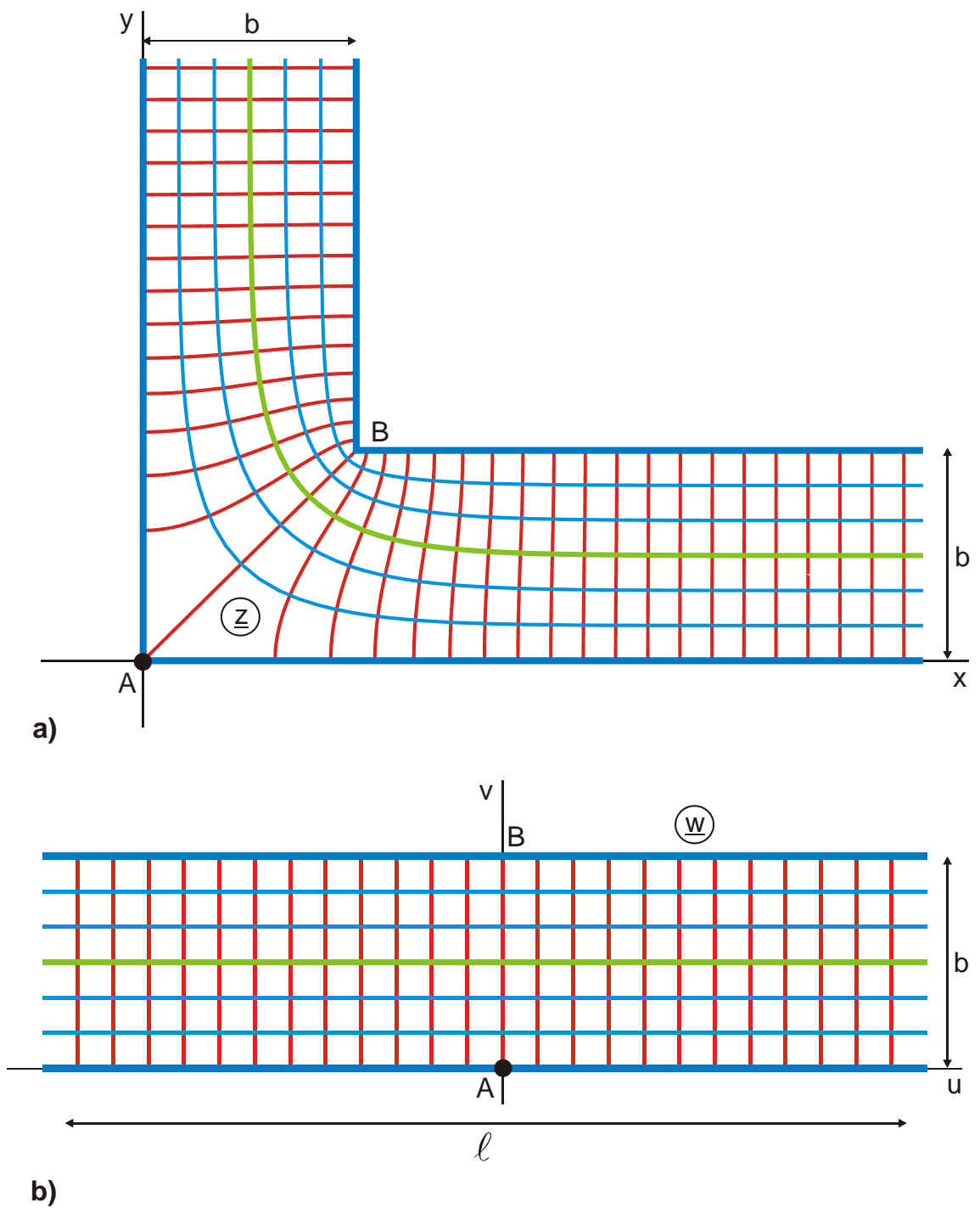


Figure 1.9: Imaging at an electrode with constant field strength (green line)
(Mappings D 4 and N 1)

2. Simple Conformal Mappings

This chapter examines simple conformal mappings with elementary functions. A Cartesian coordinate system in the w -plane is mapped onto the z -plane in each case. There is a uniform field in the w -plane with blue horizontal potential lines ($v = \text{const}$) and red vertical field lines ($u = \text{const}$). After the transformation of the individual points with the mapping function the wanted non-uniform field (the field map) in the z -plane results, also with blue potential lines and red field lines.

w-plane:	Cartesian coordinates $\underline{w} = u + jv$ uniform field
z-plane:	image plane non-uniform field field map

To find out, onto which point \underline{z}_1 the point \underline{w}_1 is mapped, \underline{w}_1 is inserted into the mapping function $\underline{z} = f(\underline{w})$ and the result is

$$\underline{z}_1 = f(\underline{w}_1). \quad (1)$$

Normally it is sufficient to look at the mapping of the boundaries, in order to study the properties of the individual conformal mapping.

2.1 The Mapping $\underline{z} = \underline{w}^{\varphi/\pi}$

In the process of the mapping the real axis is bent in the origin (Figure 2.1). All points $\underline{w} = u$ on the positive real axis are transformed into points $\underline{z} = u^{\varphi/\pi}$, which are also on the positive real axis. The negative real axis $\underline{w} = u \cdot \exp(j\pi)$ is transformed into $\underline{z} = u \cdot \exp(j\varphi)$, a straight line through the origin with the angle φ . Point B stays in the origin of each coordinate system. Point $\underline{w} = 1$ is transformed unchanged into point $\underline{z} = 1$; all points on the circle $w = 1$ are transformed into points on the circle $z = 1$.

In the special case $\varphi = 2\pi$ the function $\underline{z} = \underline{w}^2$ maps the upper w -half plane onto the complete z -plane (Figure A1.2). The point $\underline{z} = 0$ is the singular point of this mapping function.

To understand the process of conformal mapping the following can be envisaged:

- a) The field map in the \underline{z} -plane is produced by looking at the uniform field in the \underline{w} -plane through a curved or deformed mirror.
- b) The field map in the \underline{z} -plane is produced by looking at the uniform field in the \underline{w} -plane through an optical lens with an appropriate continuously deformed surface.
- c) Field lines and potential lines have the flexibility of thin steel wires and at the same time the elasticity of rubber straps. They form an easily deformable planar lattice, where field lines and potential lines are always perpendicular to each other. In the case of the mapping in Figure 2.1, there is a hinge in point B of the \underline{w} -plane (at the position of the singularity). When the left boundary electrode AB is turned around this rotational axis, the lattice of formerly parallel lines is deformed and the field map in the \underline{z} -plane is produced.

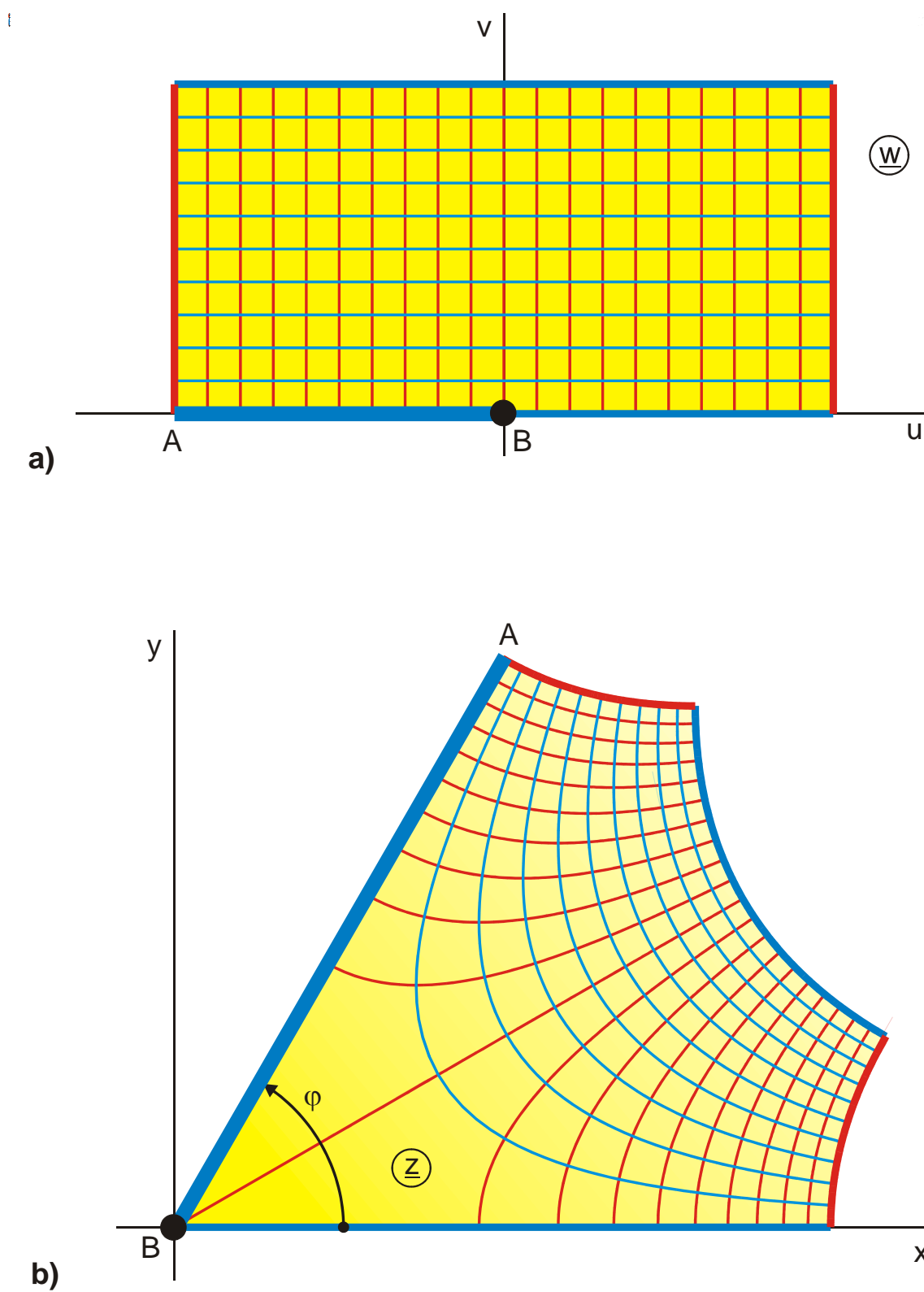


Figure 2.1: The transformation equation $\underline{z} = \underline{w}^{\varphi/\pi}$ with $\varphi = 60^\circ$

2.2 The Mapping $\underline{z} = \exp(\underline{w}\pi)$

This mapping was already mentioned in Chapter 1 (Figure 1.4). A Cartesian coordinate system is transformed into a polar coordinate system by the exponential function. Figure 2.2 shows that a parallel strip in the w -plane is mapped onto the 1. quadrant of the z -plane. The points on the straight line \overline{ADC}

$$\underline{w} = u + j/2 \quad (2)$$

are because of

$$\begin{aligned} \underline{z} &= \exp(u\pi + j\pi/2) = \exp(u\pi) \cdot \exp(j\pi/2) \\ \underline{z} &= j \exp(u\pi) \end{aligned} \quad (3)$$

mapped onto \overline{ADC} on the positive imaginary axis. The straight line is bent upward by 90° and the point $-\infty$ is transformed into the origin. All vertical lines turn into circular arcs. The straight line \overline{BD} is transformed into a quarter circle with the radius 1. As there are infinitely many blue lines up to the point A, a line charge is generated in the origin of the z -plane.

The complete z -plane results as the image of the parallel strip between $v=-1$ und $v=+1$. The other strips in parallel to this one produce periodically the same mapping.

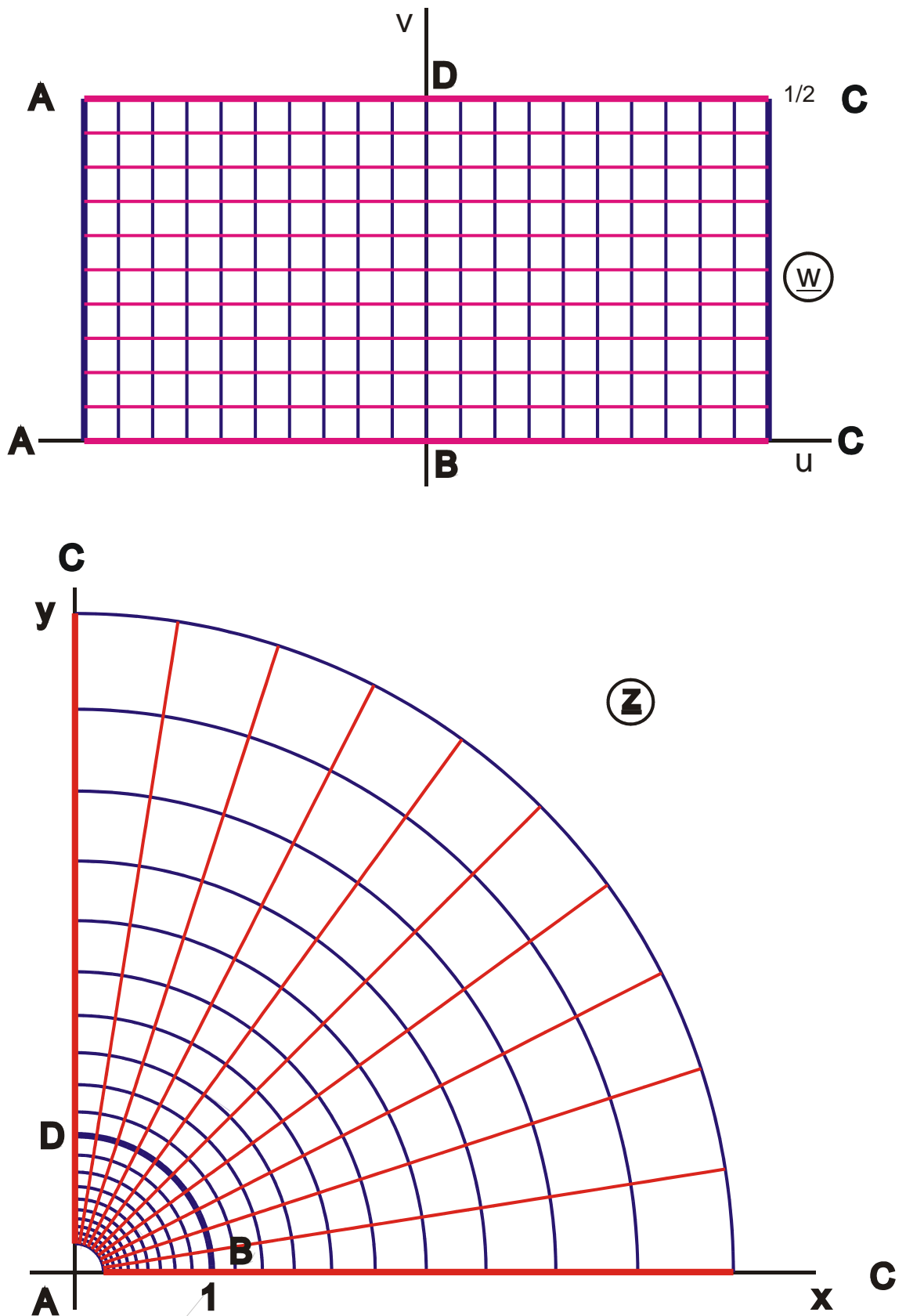


Figure 2.2: The transformation equation $z = \exp(w\pi)$, Mapping B 1

2.3 The Mapping $\underline{z} = \ell n \underline{w}$

The logarithm is the inverse of the exponential function. The wanted mapping therefore results out of Figure 2.2, when a Cartesian lattice in the \underline{z} -plane is transformed onto the parallel strip in the \underline{w} -plane.

Figure 2.3 shows that the I. quadrant of the w -plane is mapped onto the parallel strip between $v = 0$ and $v = \pi/2$.

$$\text{Point B:} \quad \underline{z}_B = \ell n 1 = 0 \quad (4)$$

$$\text{Point D:} \quad \underline{z}_D = \ell n(j) = \ell n \exp(j\pi/2) = j\pi/2 \quad (5)$$

The complete w -plane is mapped onto a parallel strip from $v = -\pi$ to $+\pi$. The mapping is termed single-periodic, this means the periodicity is only in one dimension, in the y direction.

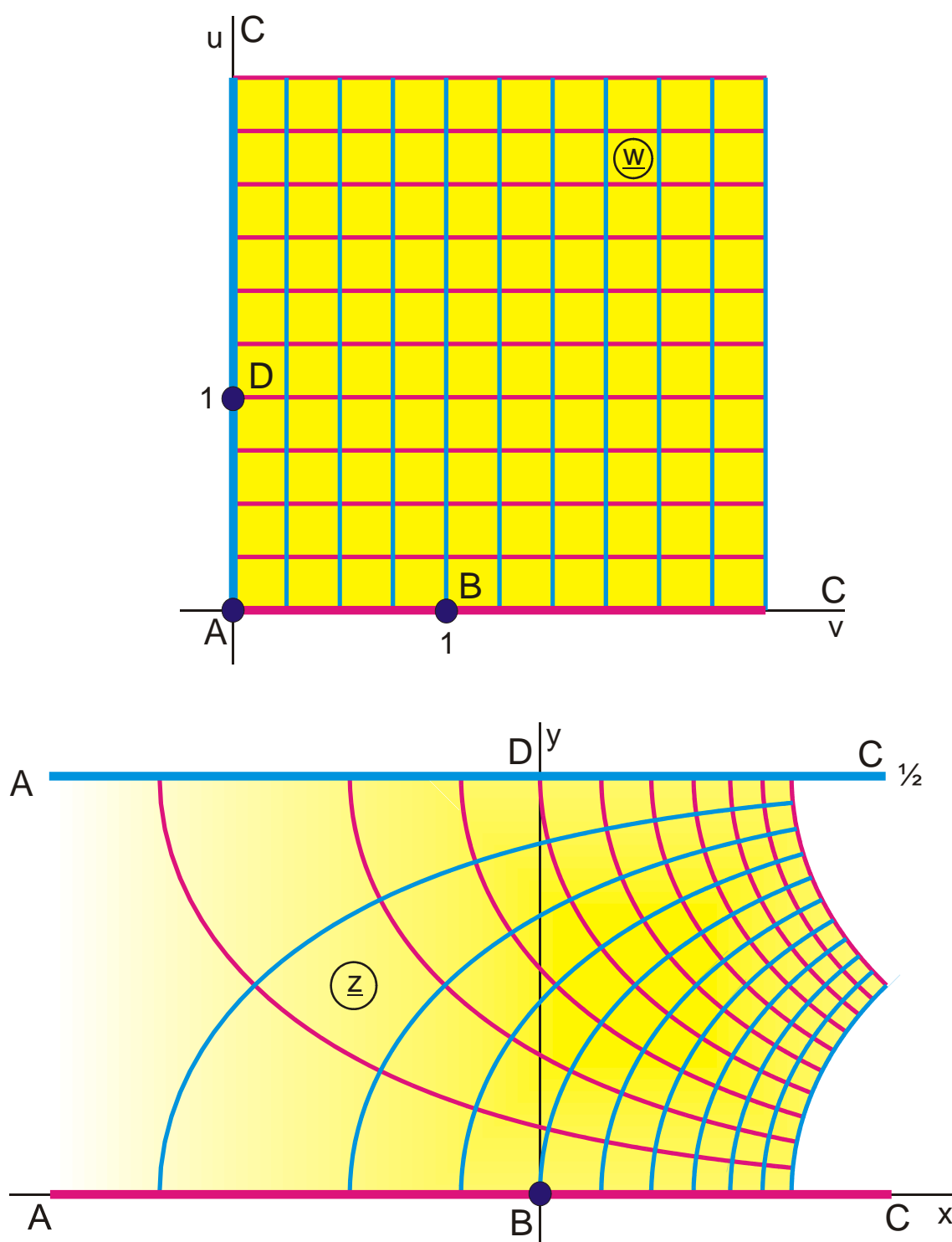


Figure 2.3: The transformation equation $\underline{z} = \ln \underline{w}$, Mapping H 1

2.4 The Mapping $\underline{z} = \arcsin \underline{w}$

As Figure 2.4 shows, the mapping with the arcsine bents the real axis in the points -1 and +1 by 90° . The upper w -half plane is mapped onto the half strip from $u = -\pi/2$ bis $u = +\pi/2$ and the complete w -plane is mapped onto the complete parallel strip respectively. As with the logarithm the mapping with the arcsine is single-periodic. The similarity of the mapping of the boundaries in both cases yields from

$$\arcsin \underline{w} = -j \ln (j\underline{w} + \sqrt{1 - \underline{w}^2}). \quad (6)$$

According to Chapter 5 this is the transformation with the logarithm together with a pre-transformation with the equation in brackets.

The points on the real axis between A and C are:

$$x = \arcsin u. \quad (7)$$

The points between C and D result with Eq. 6 to

$$\underline{z} = \frac{\pi}{2} + j \operatorname{arcosh} u. \quad (8)$$

All points on the imaginary axis of the w -plane are mapped onto the imaginary axis likewise in the image plane.

$$y = \operatorname{arsinh} v. \quad (9)$$

An ellipse with the half axes $a = \cosh y_1$ and $b = \sinh y_1$ is mapped onto the straight line $\underline{z} = \pm y_1$.

The functions $\underline{z} = \arccos \underline{w}$, $\underline{z} = \operatorname{arcosh} \underline{w}$ and $\underline{z} = \operatorname{arsinh} \underline{w}$ produce topologically similar mappings (Figure 2.5). Here again the half plane is folded up into a half strip. All three functions can in analogy to Eq. (6) be expressed by the logarithm and by the arcsine respectively.

$$\arccos \underline{w} = \frac{\pi}{2} - \arcsin \underline{w} \quad (10)$$

$$\operatorname{arsinh} \underline{w} = -j \arcsin(j\underline{w}) \quad (11)$$

$$\operatorname{arcosh} \underline{w} = -j \arcsin \underline{w} + j\pi / 2 \quad (12)$$

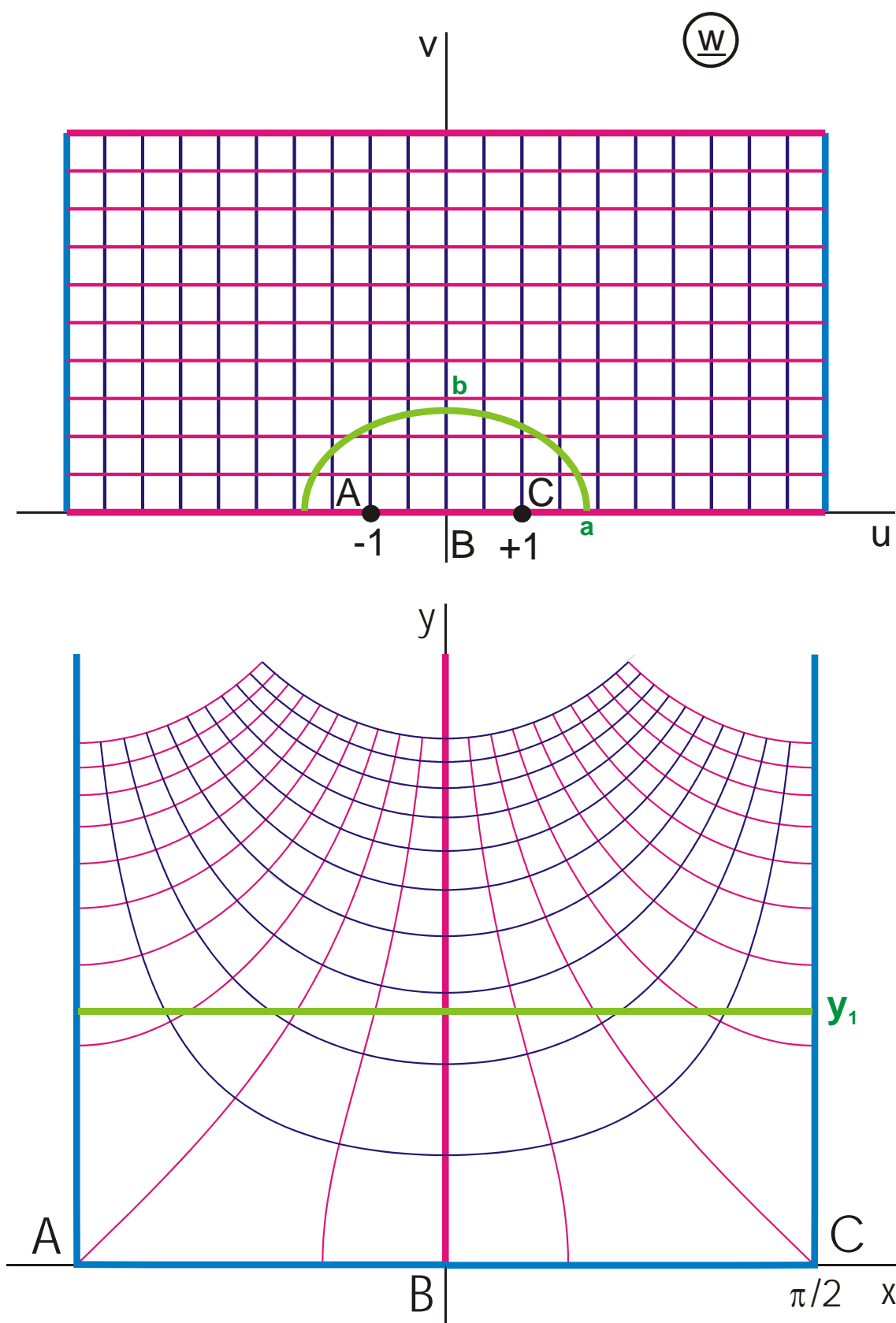


Figure 2.4: The transformation equation $z = \arcsin w$, Mapping H 1.5

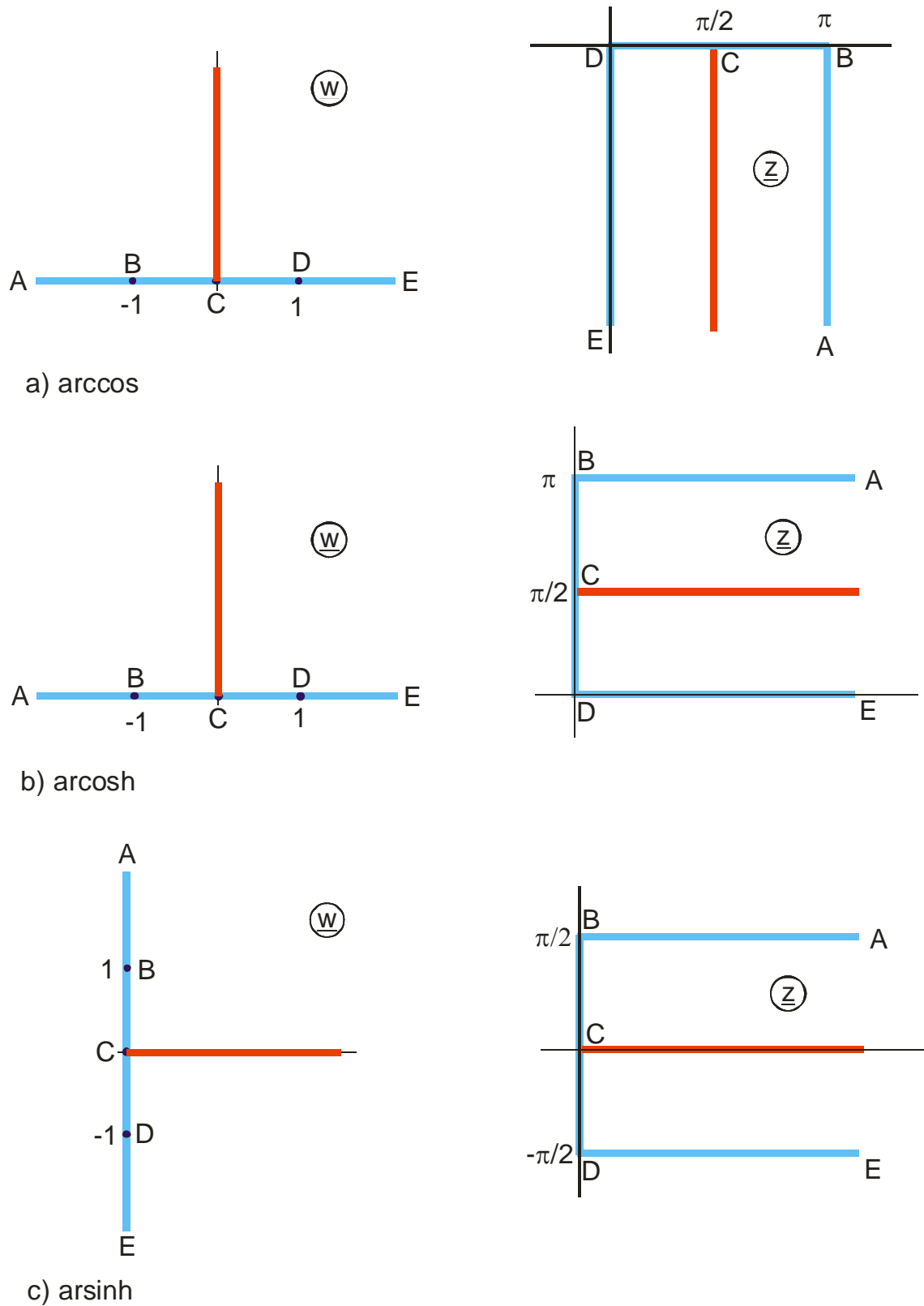


Figure 2.5: The transformation equations $\underline{z} = \arccos \underline{w}$, $\underline{z} = \operatorname{arcosh} \underline{w}$ and $\underline{z} = \operatorname{arsinh} \underline{w}$

2.5 The Mapping $\underline{z} = \sin \underline{w}$

The properties of the mapping with the function $\sin \underline{w}$ are following directly from Figure 2.4, because the arcsine is the inverse function. Thus Figure 2.4 and Figure 2.6 are equal, except for the interchange of w and z . As the sine is a periodic function, the half strip from $u = -\pi/2$ through $u = +\pi/2$ is mapped onto the complete z -plane. Every horizontal straight line at $v = v_1$ is transformed into a half ellipse with the half axes $a = \cosh v_1$ and $b = \sinh v_1$. The ellipses are confocal with the foci at $x = -1$ and $x = +1$. All vertical lines in the w -plane are mapped onto confocal hyperbolas. The foci are also at $x = \pm 1$ and the cusps are at $x = \pm \sin u_1$.

The functions $\underline{z} = \cos \underline{w}$, $\underline{z} = \sinh \underline{w}$ and $\underline{z} = \cosh \underline{w}$ yield topologically similar mappings. They can be represented by the sine function:

$$\cos \underline{w} = \sin(\underline{w} + \pi/2) \quad (13)$$

$$\sinh \underline{w} = -j \sin(j\underline{w}) \quad (14)$$

$$\cosh \underline{w} = \sin(j\underline{w} + \pi/2). \quad (15)$$

The mappings are found in Figure 2.5, by interchanging the labels w -plane and z -plane.

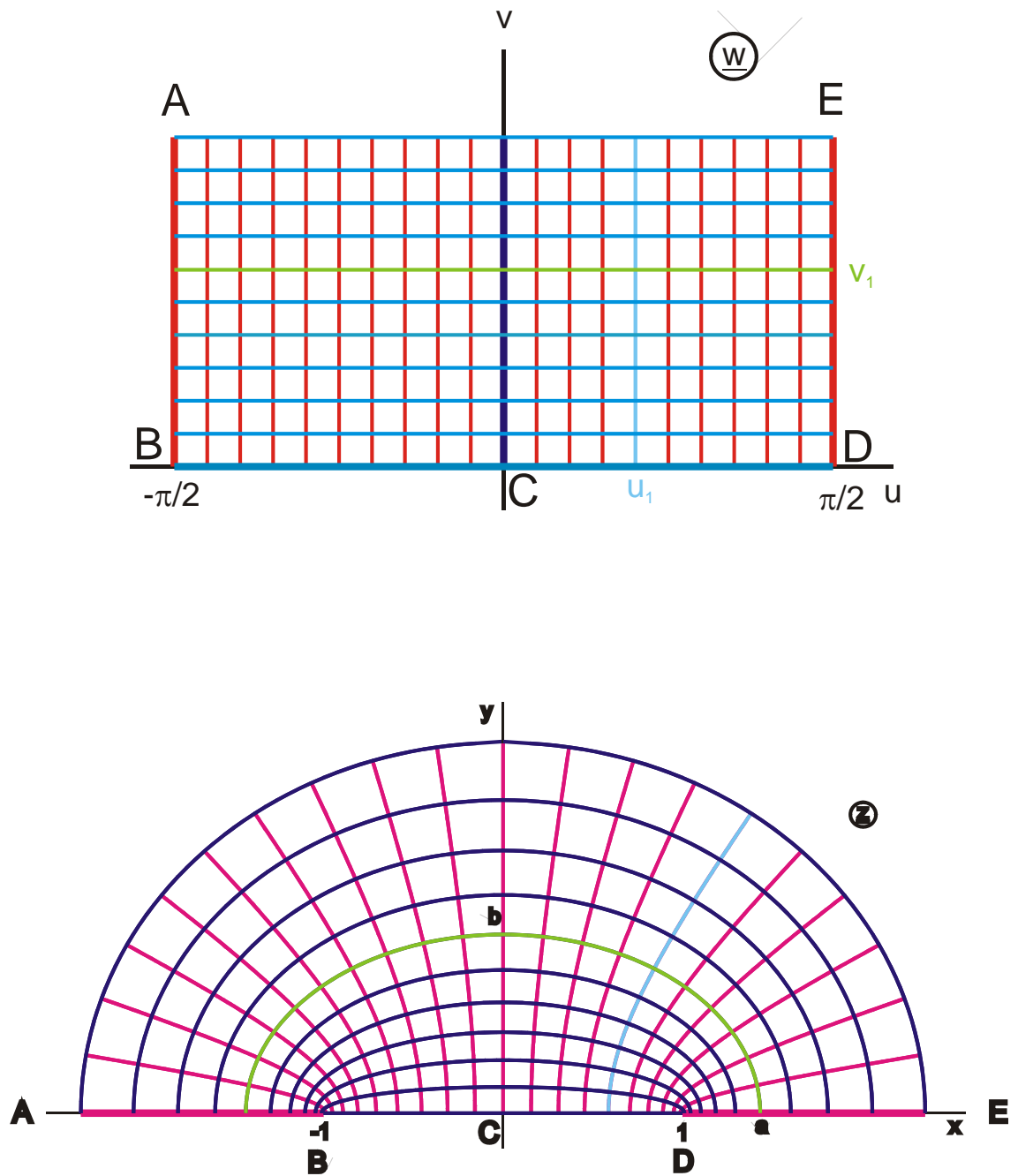


Figure 2.6: The transformation equation $\underline{z} = \sin \underline{w}$.

2.6 The Mapping $\underline{z} = \tanh \underline{w}$

The parallel strip between $v = -\pi/2$ and $v = +\pi/2$ is mapped onto the z -plane. Point $u = +\infty$ is transformed onto $x = +1$ and $u = -\infty$ onto $x = -1$. The generation of the uniform field in the parallel strip can be envisaged as the field between a positive line charge $+\rho_L$ at $u = +\infty$ and a negative line charge $-\rho_L$ at $u = -\infty$ (line dipole or doublet at $\underline{w} = \infty$). By the mapping with the function $\tanh \underline{w}$ both line charges move closer together and end up in the points $x = +1$ and $x = -1$. Thus the field map in the z -plane is the field of two line charges with equal size and opposite polarity.

The blue potential lines $u = u_1 = \text{const}$ are in the image plane circles with the radius

$$r_1 = (x_I - x_H) / 2 \quad (16)$$

and the center point at

$$x_M = r + x_H \quad (\text{Figure 2.7}). \quad (17)$$

They are termed Apollonian circles.

Inserting in the transformation equation yields:

$$\text{Point I: } x_I = \tanh \underline{w}_I = \tanh(u_1 + j\pi/2) = 1 / \tanh u_1 \quad (18)$$

$$\text{Point H: } x_H = \tanh \underline{w}_H = \tanh u_1. \quad (19)$$

This gives

$$r_1 = (1 / \tanh u_1 - \tanh u_1) / 2 = 1 / \sinh(2 u_1) \quad (20)$$

$$r_M = (1 / \tanh u_1 + \tanh u_1) / 2 = 1 / \tanh(2 u_1). \quad (21)$$

The red field lines $v = v_1 = \text{const}$ are mapped onto circles as well. Their radii

$$r_1 = (y_F - y_G) / 2 \quad (22)$$

and their center points

$$y_M = y_F - r_1 \quad (23)$$

are equated analogously by inserting the coordinates of the points F and G into the transformation equation:

$$\text{Point F: } j y_F = \tanh(j v_1) = j \tan v_1 \quad (24)$$

$$\text{Point G: } j y_G = \tanh(j v_1 - j\pi/2) = -j / \tan v_1 \quad (25)$$

this gives:

$$r_1 = (\tan v_1 + 1 / \tan v_1) / 2 = 1 / \sin(2 v_1) \quad (26)$$

$$y_M = (\tan v_1 - 1 / \tan v_1) / 2 = -1 / \tan(2 v_1). \quad (27)$$

The straight lines $v_1 = \pm\pi/4$ are transformed into the unit circle. The field map has also the name "bipolar coordinate system".

The functions $\underline{z} = \tan \underline{w}$, $\underline{z} = \cot \underline{w}$ and $\underline{z} = \coth \underline{w}$ yield topologically similar mappings (Figure 2.8). They can be represented by the hyperbolic tangent:

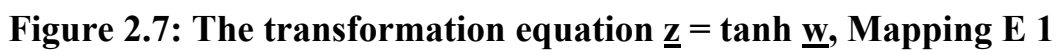
$$\tan \underline{w} = -j \tanh(j \underline{w})$$

$$\cot \underline{w} = 1 / \tan \underline{w}$$

$$\coth \underline{w} = 1/\tanh \underline{w}$$

The field map is not changed by the inversion in the equations for \cot and \coth : The line charges remain at ± 1 and $\pm j$ respectively; the points 0 and ∞ change places.

A representation of the w -plane and the z -plane like in Figure 2.7 is sufficient, to describe the function $\tanh \underline{w}$ completely. The z -plane gives for every point magnitude and phase of the function $\tanh \underline{w}$. $\tanh \underline{w}$ has a zero at $\underline{w} = 0$ (point A). At $\underline{w} = \pm\pi/2$ the function $\tanh \underline{w}$ is infinite. The function has a pole at these points (points E, B). This way to represent a function of a complex variable is more descriptive and clearer than the relief representation, where in a three dimensional picture the magnitude of the function is represented by the height above the w -plane. In most cases the phase of the function is included in this relief as an additional lattice.



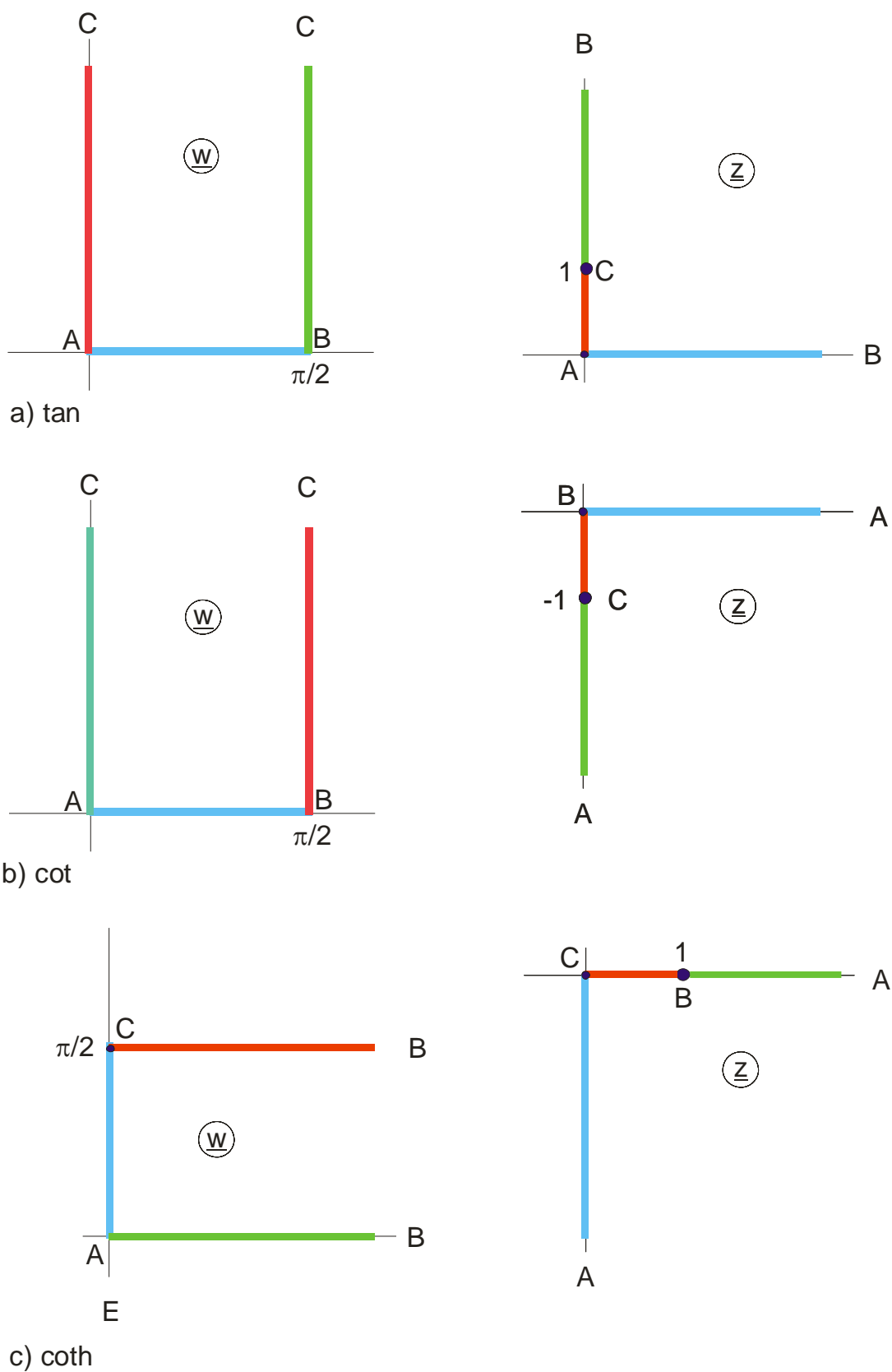


Figure 2.8: The transformation equations $\underline{z} = \tan \underline{w}$, $\underline{z} = \cot \underline{w}$ and $\underline{z} = \coth \underline{w}$

2.7 The Mapping $\underline{z} = 1 / \underline{w}$

Whereas with the transformation function $\tanh \underline{w}$ the two line charges at $+\infty$ and at $-\infty$, which generate the uniform field \underline{w} , are mapped onto the points $+1$ and -1 , these line charges are mapped into the origin by the inversion $1/\underline{w}$. The field of a positive and a negative line charge of equal magnitude located in the same point is termed “line dipole field” and in the following text abbreviated “dipole field”. As this book covers only two dimensional fields, there is no danger of confusion with the field of a point dipole (whose field map is different from that of a line dipole).

Figure 2.9d shows the sign for the dipole field that will be used in the following text, two small circles, arranged as an eight, in this case in the origin of the z -plane. The dipole field, labeled by this sign, is generated by the field of two line charges, same size but opposite polarity, which are symmetrically placed on the imaginary axis, when their distance d is infinitesimally small (Figure 2.9c).

In the technical application the dipole field is for instance the far field of two line charges like in Figure 2.9c or the far field of a two wire line respectively, that means an approximation of the function $\underline{z} = j \tanh \underline{w}$ in those regions of the z -plane, where $|\underline{z}| \gg d$ is valid, this is far away from the two line charges.

The field map (Figure 2.9b) consists of two sets of mutually orthogonal circles, which all go through the origin of the z -plane. The point $\underline{w} = 1$ is mapped onto the point $\underline{z} = 1$. A red straight line $u_1 = \text{const}$ is mapped onto a red circle that crosses the real axis at

$1/u_1$. Its center point is also on the real axis at $1/(2u_1)$. In the same manner all blue straight lines $v_1 = \text{const}$ are mapped onto blue circles. Because of

$$\underline{z} = 1/\underline{w} = \frac{1}{w \cdot \exp(j\varphi)} = \frac{1}{w} \exp(-j\varphi) \quad (28)$$

the I. quadrant of the w -plane is mapped onto the IV. quadrant of the z -plane and vice versa. The unit circle in the w -plane is mapped onto the unit circle in the z -plane. Only the sense of circulation is reversed. The field map in the z -plane is equivalent to the backside of the complex Riemann sphere, that means it is the top view on the point ∞ .

The bilinear transformation (Möbius transformation) and the transformation with a fractional linear function respectively

$$\underline{z} = \frac{a\underline{w} + b}{c\underline{w} + d} \quad \text{with } ad - bc \neq 0 \quad (29)$$

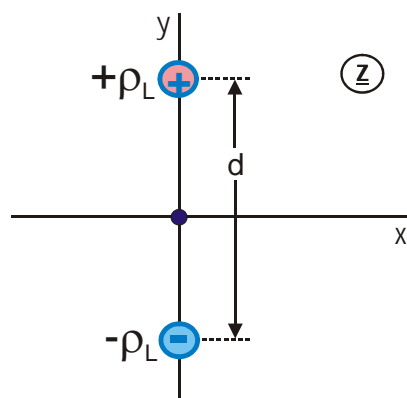
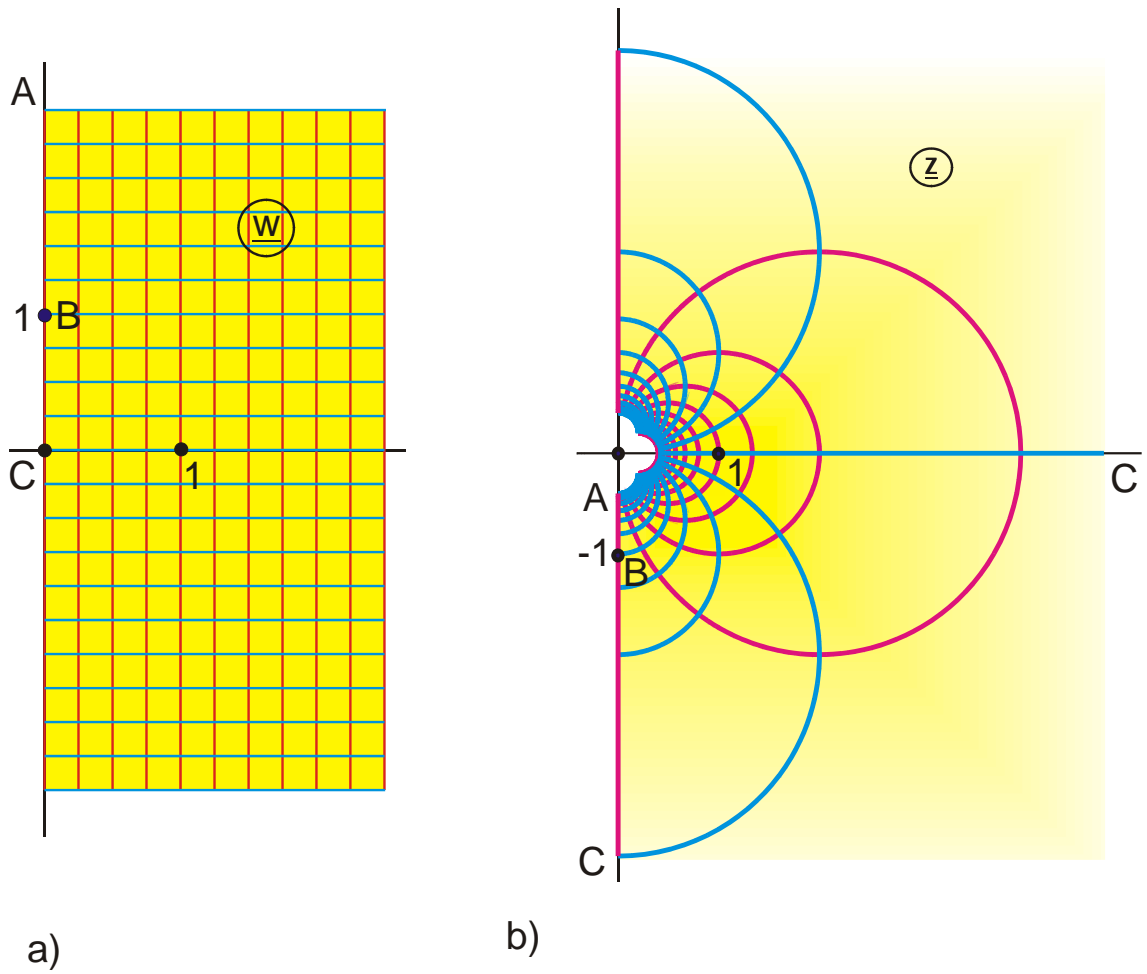
with arbitrary complex constants a , b , c and d , which often also has the simpler form

$$\underline{z} = \frac{\underline{w} + 1}{\underline{w} - 1} \quad (30)$$

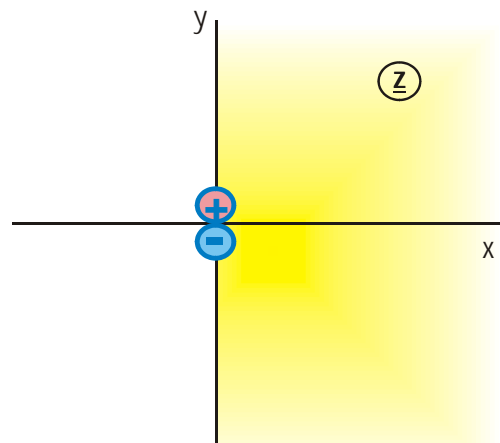
or

$$\underline{z} = \frac{\underline{w} + j}{\underline{w} - j}, \quad (31)$$

yields topologically the same field map as the inversion $\underline{z} = 1/\underline{w}$. The constants only cause a magnification, a rotation and a displacement of the coordinate system (translation). Examples: Mapping of regions No.: 7, 8, 24, 25, 26, 31, 32 in 6.8 and Example 6.8.



c) Dipole field with line charges

d) Sign for the dipole field in c)
with $d \rightarrow 0$ **Figure 2.9: The transformation equation $\underline{z} = 1/\underline{w}$, Mapping Q 1**

3. Superposition of Complex Potentials

The \underline{w} -plane is the plane of the complex potential \underline{w} . The real potential distribution (voltage distribution) of a given technical problem, whose geometry exists in the \underline{z} -plane, is found as real part $u(\underline{z})$ or as imaginary part $v(\underline{z})$. The superposition principle for real potential fields is likewise valid for complex potential fields: The total potential \underline{w} is the sum of the single potentials of all sources, which are present in the \underline{z} -plane. Simple sources, which are qualified for superposition, are:

Table 3.1: Complex notation of elementary potential sources

Source	Potential
Uniform field	$\underline{w} = a_o \underline{z} \quad (1)$
Uniform field, rotated by the angle φ_o (Oblique flow)	$\underline{w} = a_o \cdot \underline{z} \cdot \exp(-j \varphi_o) \quad (2)$
Line charge at \underline{z}_o	$\underline{w} = a_o \cdot \ln(\underline{z} - \underline{z}_o) \quad (3)$
Line dipole at \underline{z}_o	$\underline{w} = \frac{a_o}{\underline{z} - \underline{z}_o} \quad (4)$
Line dipole at \underline{z}_o , rotated by the angle φ_o	$\underline{w} = \frac{a_o}{\underline{z} - \underline{z}_o} \cdot \exp(j \varphi_o) \quad (5)$

Provided there are n sources with the amplitude a_i at the points \underline{z}_i given in the \underline{z} -plane, then the total potential \underline{w} of the configuration is the sum of the potentials \underline{w}_i of all sources.

$$\underline{w} = \sum_{i=1}^n \underline{w}_i(\underline{z}) \quad (6)$$

The superposition of potential fields \underline{w}_i is permitted if and only if all fields \underline{w}_i satisfy the same boundary conditions throughout the whole \underline{z} -plane (singular points excluded). Because line charges and line dipoles originate from singular points, it is possible to superpose their fields. On the contrary to these, **potential fields**, which are **created by spacious electrodes**, being located at different points \underline{z}_i , **cannot be superposed**. Example: The potential field of a conducting strip at point \underline{z}_1 and the potential field of a cylinder at point \underline{z}_2 are not superposable, because the field of the conducting strip does not have an equipotential plane at the location of the cylinder surface and because the field of the cylinder does not have an equipotential plane at the location of the conducting strip as well. Hence only the elementary sources of Eq. (1) through (5) are feasible for the method of superposition of complex potentials.

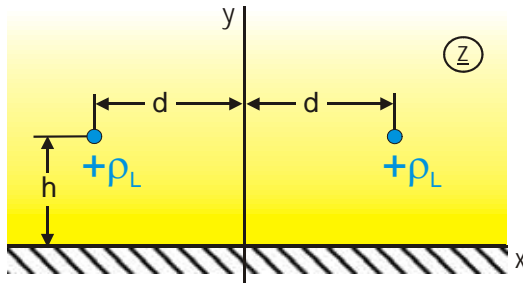
With Eq. (6) it is possible to calculate the potential of all configurations that consist of a uniform field and of line charges and/or line dipoles. The associated field map $\underline{z} = f(\underline{w})$ is found by inverting the potential function $\underline{w} = f(\underline{z})$ {Eq. (6)}. In those cases, where it is not possible to write down this equation for the field map explicitly, numerical line tracing methods can be used, to plot the field.

The procedure of employing the method of superposition of complex potentials will be demonstrated with some simple examples:

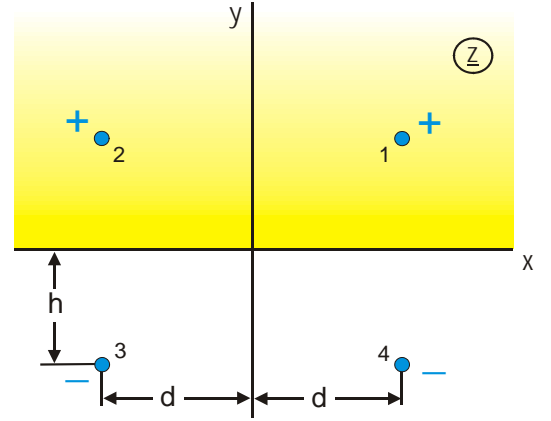
Example 1: Two equal line charges above a conducting plane.

Figure 3.1a shows the geometry of the configuration. According to the theory of images the conducting plane is replaced by the mirror images of the two line charges in the upper half plane (Figure 3.1b). In every point (x, y) of the \underline{z} -plane the complex potential \underline{w} is given as the sum of the potentials of the 4 line charges:

$$\underline{w} = a_1 \cdot \ln(\underline{z} - \underline{z}_1) + a_2 \cdot \ln(\underline{z} - \underline{z}_2) + a_3 \cdot \ln(\underline{z} - \underline{z}_3) + a_4 \cdot \ln(\underline{z} - \underline{z}_4) \quad (7)$$



a) Initial problem: 2 equal line charges above a conducting plane



b) Replacement of the conducting plane by two image charges

Figure 3.1: Example 1

As all four line charges have the same size, the magnitudes of a_1 through a_4 are equal. They are chosen to be 1. The line charges 1 and 2 are positive, therefore $a_1 = a_2 = 1$. The remaining two are negative, therefore $a_3 = a_4 = -1$. The points \underline{z}_1 through \underline{z}_4 are found directly from Figure 1b.

$$\underline{w} = \ln[\underline{z} - (d + jh)] + \ln[\underline{z} - (-d + jh)] - \ln[\underline{z} - (-d - jh)] - \ln[\underline{z} - (d - jh)] \quad (8)$$

$$\underline{w} = \ln \frac{[\underline{z} - (d + jh)][\underline{z} - (-d + jh)]}{[\underline{z} + (d + jh)][\underline{z} + (-d + jh)]} \quad (9)$$

With Eq. (9) it is possible to determine the potential in every point of the \underline{z} -plane.

The field map of the configuration is found by inversion (Mapping L 2):

$$\underline{z} = -jh \frac{1 + \exp(\underline{w})}{1 - \exp(\underline{w})} \pm \sqrt{d^2 + h^2 \left[1 - \left(\frac{1 + \exp(\underline{w})}{1 - \exp(\underline{w})} \right)^2 \right]} \quad (10)$$

Example 2: Two line charges, opposite sign, different size.

For a negative line charge at $x = +1$ and another one in the origin with opposite sign, whose magnitude differs by the factor σ (Figure 3.2), the complex potential is:

$$\underline{w} = \sigma \ln \underline{z} - \ln(\underline{z} - 1) \quad (11)$$

$$\underline{w} = \ln \frac{\underline{z}^\sigma}{\underline{z} - 1} \quad (12)$$

In the case $\sigma = 2$ the equation can be solved for \underline{z} . The field map of this configuration is then (Mapping L 3):

$$\underline{z} = \frac{\exp(\underline{w})}{2} \pm \sqrt{\left(\frac{\exp(\underline{w})}{2} \right)^2 - \exp(\underline{w})} \quad (13)$$

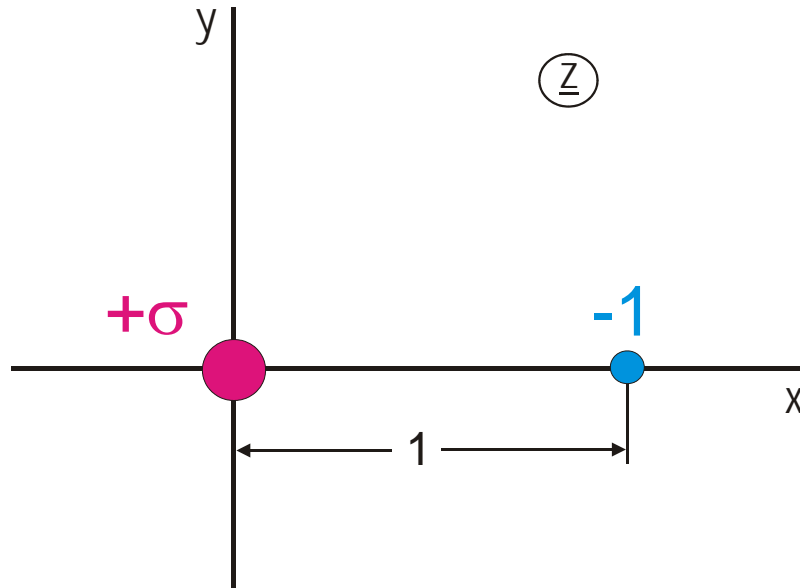


Figure 3.2: Example 2

Example 3: Two equal line dipoles.

Two dipoles with the same orientation are located at $x = +a$ and $x = -a$ (Figure 3.3). The potential \underline{w} is found by superposition:

$$\underline{w} = \frac{1}{\underline{z} + a} + \frac{1}{\underline{z} - a} \quad (14)$$

$$\underline{w} = \frac{2\underline{z}}{\underline{z}^2 - a^2} \quad (15)$$

The corresponding field map is then (Mapping Q 2.1):

$$\underline{z} = \frac{1}{\underline{w}} \pm \sqrt{\frac{1}{\underline{w}^2} + a^2} \quad (16)$$

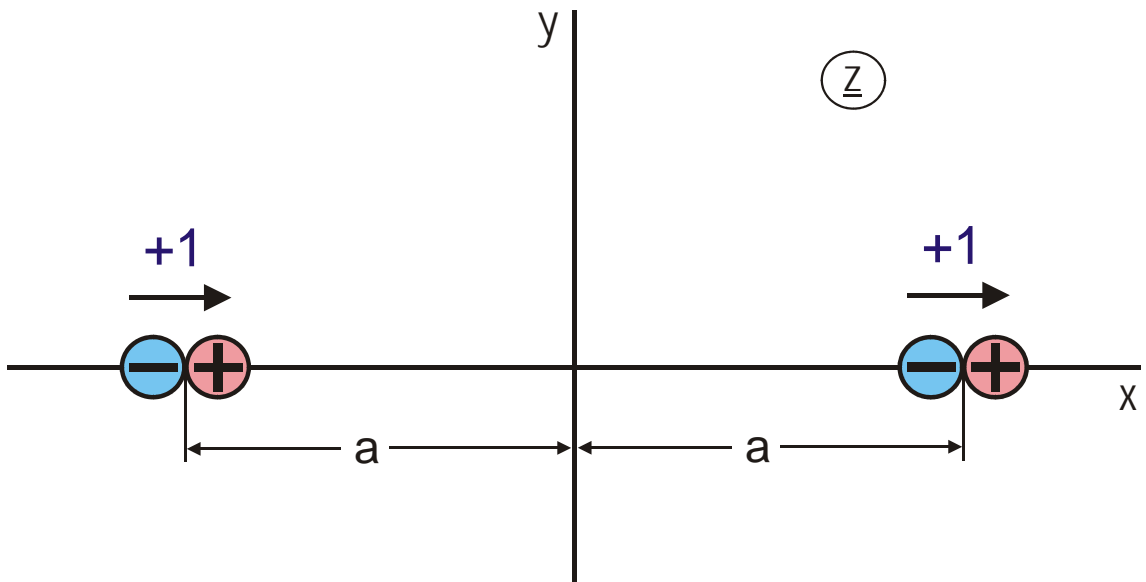


Figure 3.3: Example 3

Example 4: Conducting cylinder in a uniform field.

The field map of a conducting cylinder in a uniform electrostatic field is derived by superposition of a dipole field and a uniform field (Figure 3.4).

The corresponding complex potential is:

$$\underline{w} = \underline{z} + 1/\underline{z} \quad (17)$$

Solving for \underline{z} results in the field map:

$$\underline{z} = \frac{\underline{w}}{2} + \sqrt{\left(\frac{\underline{w}}{2}\right)^2 - 1}. \quad (18)$$

As the coordinate system in the \underline{w} -plane may be scaled arbitrarily, the mapping remains unchanged, if $\underline{w}/2$ is replaced by \underline{w} . Hence the solution is (Mapping A 3)

$$\underline{z} = \underline{w} + \sqrt{\underline{w}^2 - 1}. \quad (19)$$

In the resulting field map the unit circle is an equipotential line. Outside, in great distance, the uniform field is found; inside, in the center, there is the dipole field.

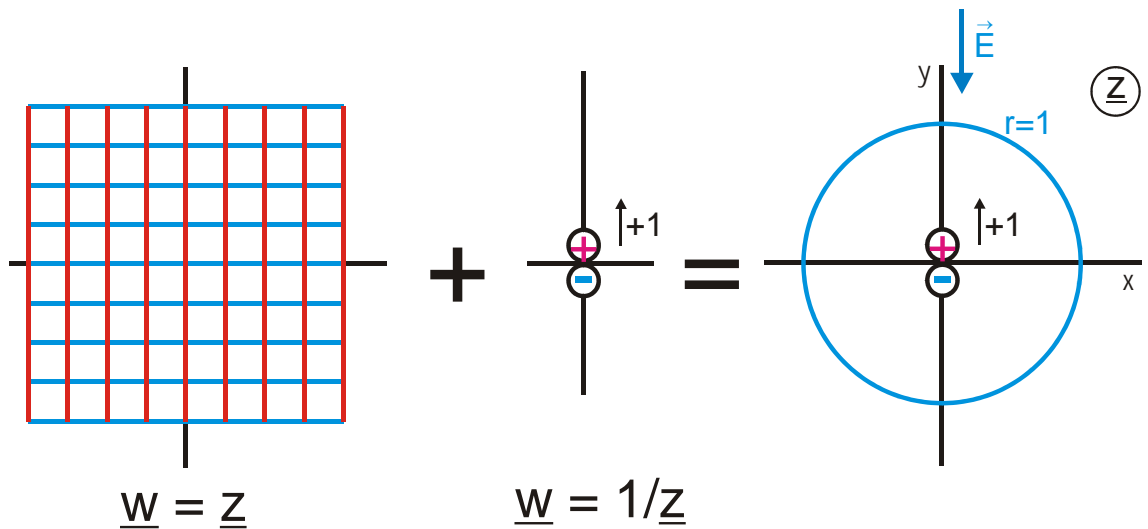
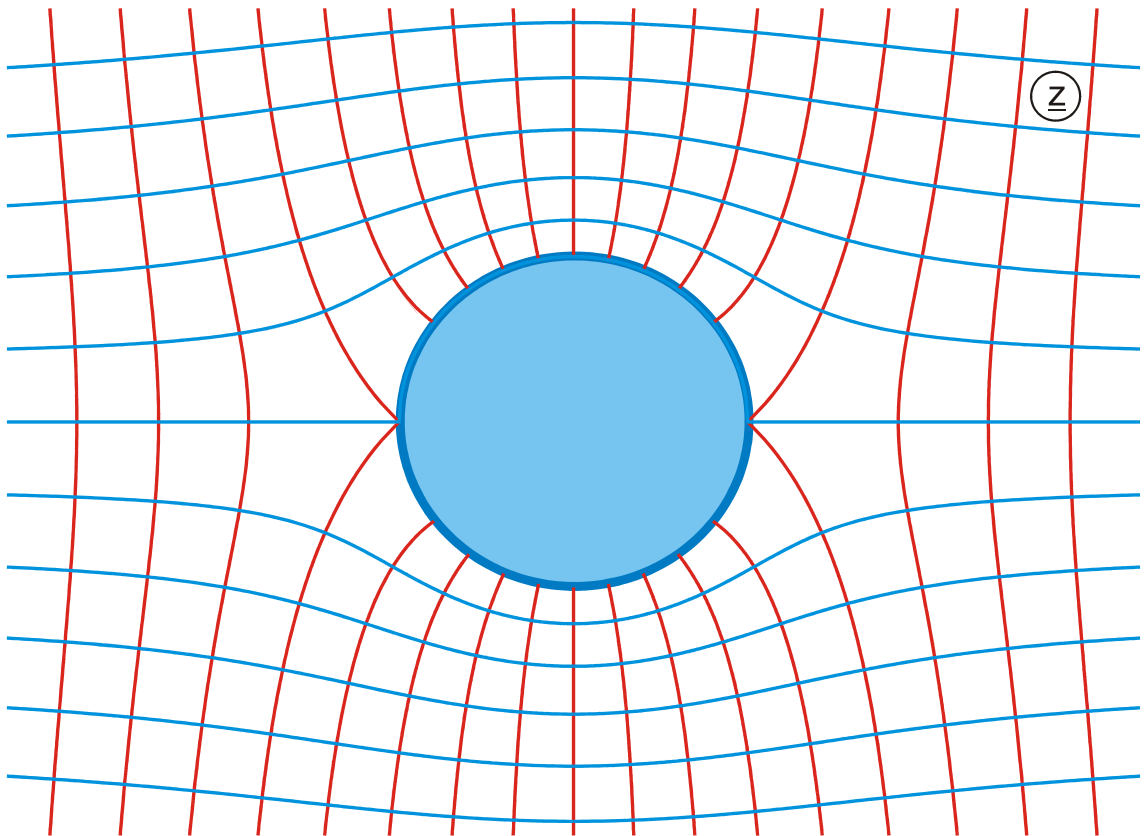
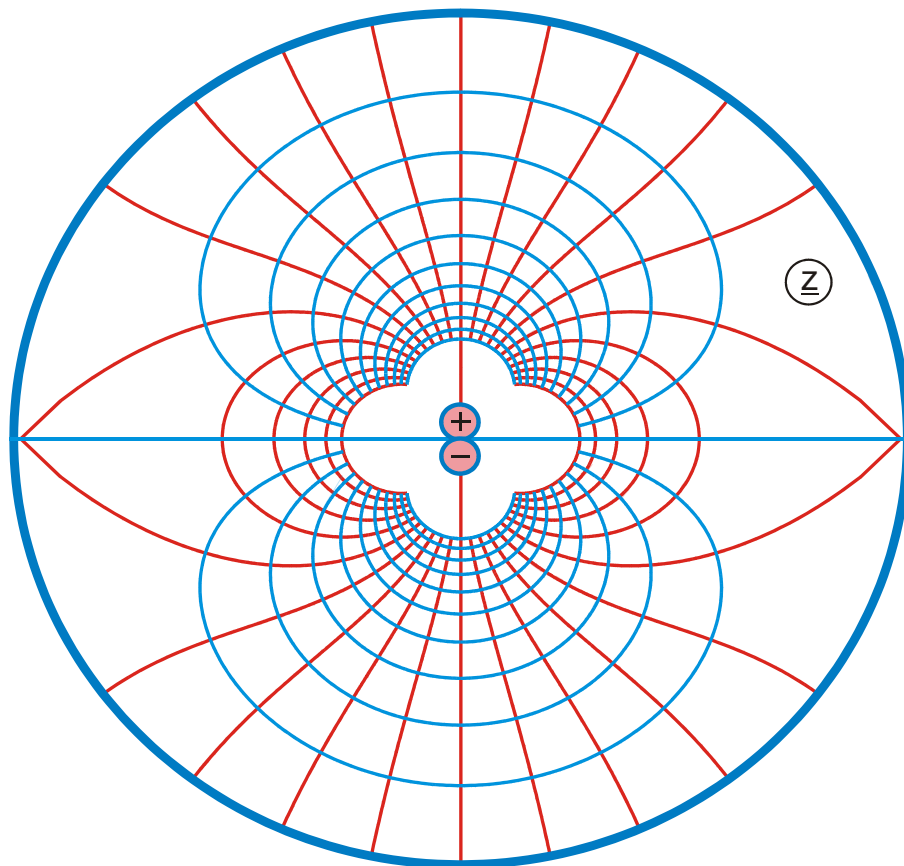


Figure 3.4: Example 4



a)



b)

Figure 3.5: Exterior field a) and interior field b) of the conducting cylinder from

Example 4

4. Mapping of Polygonal Boundaries

The field map in the interior of a closed polygon is to be determined (Figure 4.1b). It is permitted that one or several vertices of the polygon are at infinity (Figure 4.1c, d). In the context of conformal mapping this is expressed as follows: The analytical function $\underline{z} = f(\underline{w})$ is sought, which maps the uniform field in the upper w -plane onto the interior of the polygon. In this mapping the real axis of the w -plane corresponds with the boundary of the polygon.

For open polygons like e.g. in Figure 4.1c the ambiguity exists, whether the calculated field map is above or below the polygonal line. The answer follows from the theorem that conformal mapping preserves the sense of circulation (Chapter1): Going from A to B, the uniform field is to the left of the straight line \overline{AB} . Consequentially the calculated field map in the image plane is also left of the straight line \overline{AB} , when going from A to B in that plane.

According to the chosen coordinate system, the potential lines are the lines $v = \text{const.}$ The potential distribution in the z -plane is $v(x, y)$. Then the electric field strength in the z -plane is

$$\vec{E} = -\text{grad } v(x, y) = -\frac{\partial v}{\partial x} \vec{e}_x - \frac{\partial v}{\partial y} \vec{e}_y. \quad (1)$$

The magnitude of the field strength is:

$$E = \sqrt{\left(\frac{\partial v}{\partial x}\right)^2 + \left(\frac{\partial v}{\partial y}\right)^2} = \left| \frac{d\mathbf{w}}{d\mathbf{z}} \right|. \quad (2)$$

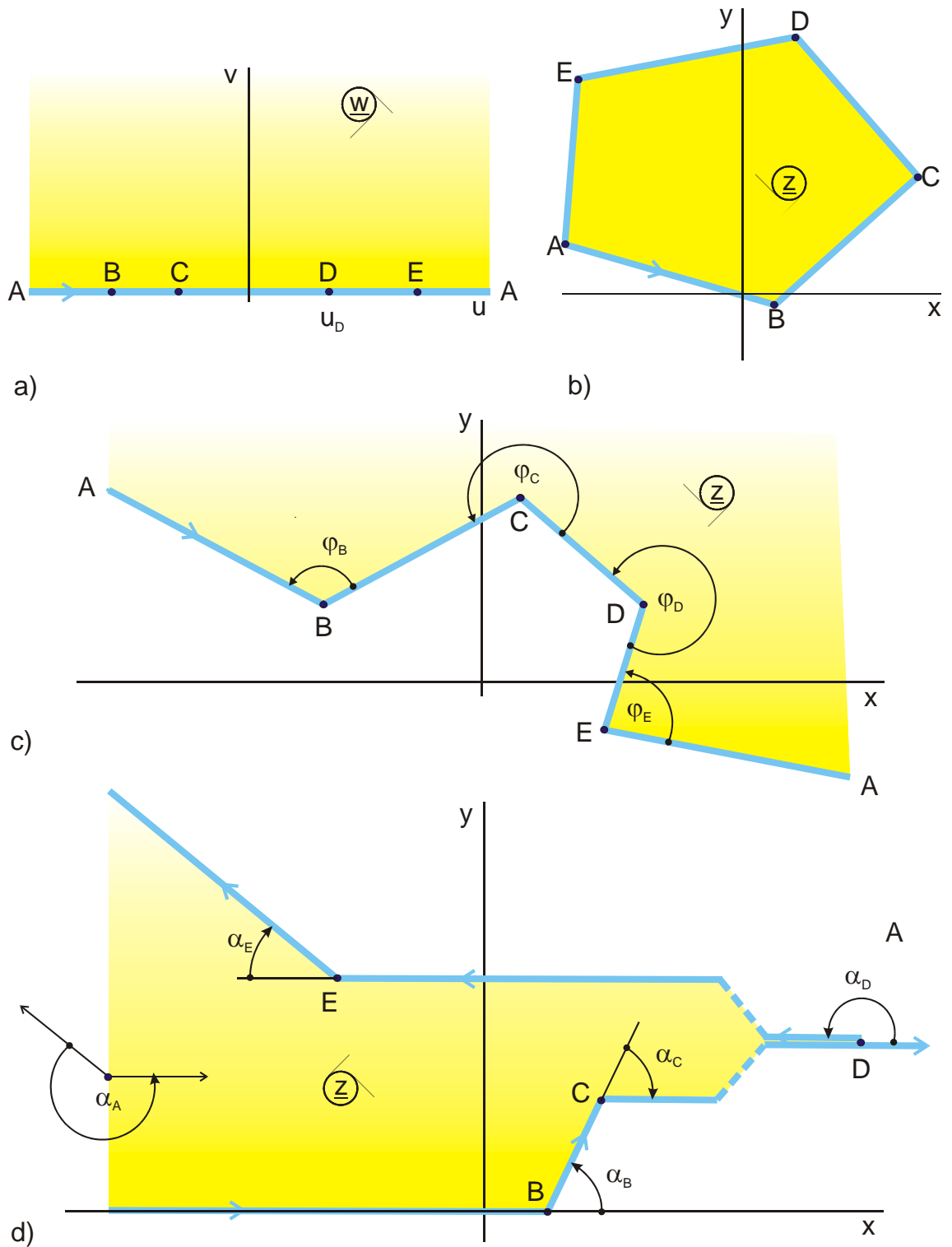


Figure 4.1: Mapping the upper half plane onto the interior of a polygon

As the electric field strength E on a conducting surface is infinite at an exterior angle ($\varphi > \pi$) and vanishes in an interior angle ($\varphi < \pi$), for the contour in Figure 4.1c follows:

$$\text{Point C:} \quad \varphi > \pi \Rightarrow E_C = \infty$$

$$\text{Point D:} \quad \varphi > \pi \Rightarrow E_D = \infty$$

$$\text{Point B:} \quad \varphi < \pi \Rightarrow E_B = 0$$

$$\text{Point E:} \quad \varphi < \pi \Rightarrow E_E = 0 .$$

Hence the function $d\underline{w}/d\underline{z}$ can be written in the form

$$\frac{d\underline{w}}{d\underline{z}} = f_1 \left(\frac{(\underline{w} - u_B)(\underline{w} - u_E)}{(\underline{w} - u_C)(\underline{w} - u_D)} \right) \quad (3)$$

with zeros at $\underline{w} = u_B$ and $\underline{w} = u_E$ and poles at $\underline{w} = u_C$ and $\underline{w} = u_D$. The inverse of this function is:

$$\frac{d\underline{z}}{d\underline{w}} = f_2 \left(\frac{(\underline{w} - u_C)(\underline{w} - u_D)}{(\underline{w} - u_B)(\underline{w} - u_E)} \right). \quad (4)$$

It was shown in Chapter 2 that the function $\underline{z} = \underline{w}^{\varphi/\pi}$ creates a corner of the boundary (a vertex) at the origin with the interior angle φ . As field maps may be rotated and displaced arbitrarily, this is valid in general for a corner in the boundary at an arbitrary point B (Figure 4.2). From

$$\underline{z} = (\underline{w} - u_B)^{\varphi_B/\pi} \quad (5)$$

follows

$$\frac{d\underline{z}}{d\underline{w}} = \frac{\varphi_B}{\pi} (\underline{w} - u_B)^{\varphi_B/\pi - 1}. \quad (6)$$

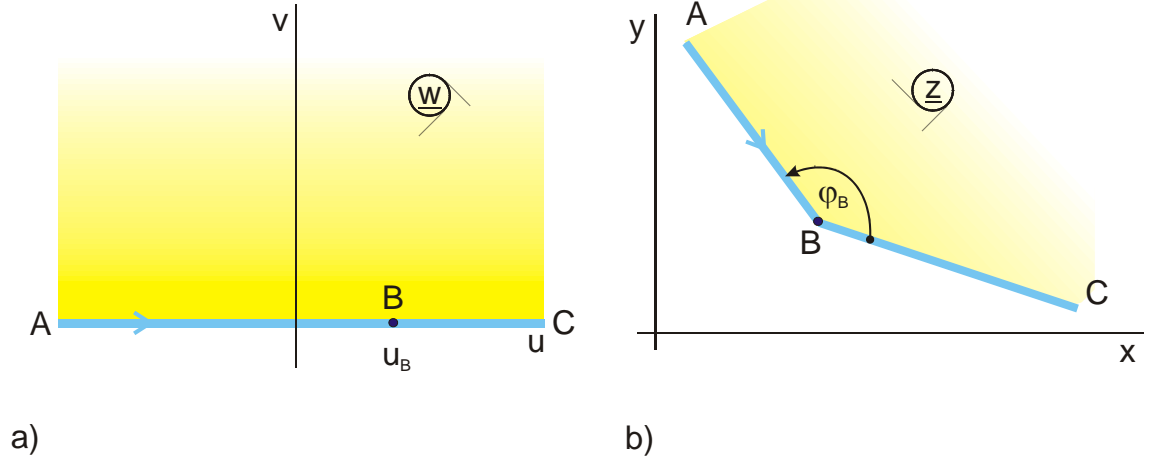


Figure 4.2: The transformation $\underline{z} = (\underline{w} - u_B)^{\phi_B / \pi}$

The function $d\underline{z} / d\underline{w}$ that is sought-after, is therefore evidently for the example in Figure 4.1c

$$\frac{d\underline{z}}{d\underline{w}} = \underline{A} \frac{(\underline{w} - u_C)^{\phi_C / \pi - 1} (\underline{w} - u_D)^{\phi_D / \pi - 1}}{(\underline{w} - u_B)^{1 - \phi_C / \pi} (\underline{w} - u_E)^{1 - \phi_E / \pi}} \quad (7)$$

All points, where the field strength reaches infinity ($\phi > \pi$, outside corner), are in the numerator and all points, where the field strength vanishes ($\phi < \pi$, inside corner: $\phi / \pi - 1 < 0$) are in the denominator. Integration of Eq. (7) yields the transformation equation $\underline{z} = f(\underline{w})$.

The above illustrated relations can also be derived and proven with more mathematical stringency (e.g. [6, 15]).

For the mapping of the upper w -half plane onto the interior of a region with polygonal boundaries and with n vertices in the z -plane is valid:

$$\frac{d\underline{z}}{d\underline{w}} = \prod_{i=1}^n (\underline{w} - u_i)^{\phi_i / \pi - 1} . \quad (8)$$

The corresponding transformation equation is:

$$\underline{z} = \underline{B} \int_0^{\underline{w}} \prod_{i=1}^n (\underline{w} - u_i)^{\varphi_i/\pi-1} d\underline{w} + \underline{C}. \quad (9)$$

As the constants \underline{B} and \underline{C} do not influence the field map, they may be chosen arbitrarily for practical problems. Hence the equation is:

$$\underline{z} = \int_0^{\underline{w}} \prod_{i=1}^n (\underline{w} - u_i)^{\varphi_i/\pi-1} d\underline{w} . \quad (10)$$

Because this book is intended for engineers and not for mathematicians, for the sake of clarity the same letter \underline{w} is used for the variable and the upper integration limit.

If a point lies at infinity ($u_i = \infty$), like e.g. point A in Figure 4.1a, the corresponding term is omitted. The angles φ_i are the interior angles of the polygon. They are in the interior of the field maps. Points with $u_i \neq \infty$, which are at ∞ in the image plane (e.g. point D in Figure 4.1d), must of course be included. For two parallel straight lines, like in point D, Figure 4.1d, φ_D equals 0.

Because the sum of the interior angles of a closed polygon is $\pi(n-2)$, the equation can be checked with:

$$\sum_{i=1}^n \varphi_i = \pi(n-2) \quad (11)$$

Instead of using the interior angles φ_i , it is easier, to work with the rotation angles α_i .

$$\varphi_i/\pi - 1 = -\alpha_i/\pi \quad (12)$$

As the complete change of direction is 360° when circumscribing a closed region, for the sum of the rotation angles α_i holds:

$$\sum_{i=1}^n \alpha_i = 2\pi . \quad (13)$$

If the boundary line in the z -plane is run through in such a sense of circulation that the field map is to the left, then α_i is the angle of the change of direction in point i (Figure 4.1d). Angles like α_E , which rotate in a mathematically negative sense, are inserted into Eq. (14) with negative sign. Hence all outside corners with $E_i = \infty$ are in the numerator of the integral. Equation 8 thus gets the form

$$\frac{d\underline{z}}{d\underline{w}} = \prod_{i=1}^n \frac{1}{(\underline{w} - u_i)^{\alpha_i/\pi}} . \quad (14)$$

and Eq.10 is

$$\underline{z} = \int_0^{\underline{w}} \frac{d\underline{w}}{\prod_{i=1}^n (\underline{w} - u_i)^{\alpha_i/\pi}} . \quad (15)$$

Due to the two mathematicians, who first published Eq. (9) independently from each other, this method to find the transformation equation is termed "Schwarz-Christoffel transformation".

The equation for the mapping of the upper w -half plane onto the [exterior](#) of a polygon (Figure 4.3) is:

$$\underline{z} = \int_0^{\underline{w}} \prod_{i=1}^n (\underline{w} - u_i)^{\varphi_i/\pi-1} \frac{d\underline{w}}{(\underline{w} - \underline{w}_\infty)^2 (\underline{w} - \underline{w}_\infty^*)^2} \quad (16)$$

and

$$\underline{z} = \int_0^{\underline{w}} \frac{d\underline{w}}{\prod_{i=1}^n (\underline{w} - u_i)^{\alpha_i/\pi} \cdot (\underline{w} - \underline{w}_\infty)^2 (\underline{w} - \underline{w}_\infty^*)^2} . \quad (17)$$

The point $\underline{w} = \underline{w}_\infty$ is mapped onto the point $\underline{z} = \infty$ by this transformation. Hence the transformation equation has a pole at $\underline{w} = \underline{w}_\infty$ and at the conjugate complex value

$\underline{w} = \underline{w}_\infty^*$. Like for the preceding mapping onto the interior of a polygon in this case the following is also valid:

- The term with $u_i = \infty$ is omitted.
- The angles φ_i are inside the field map. They are the exterior angles of the polygon.
- For the sum of the angles holds:

$$\sum_{i=1}^n (\varphi_i / \pi - 1) = 2 \quad (18)$$

$$\sum_{i=1}^n \alpha_i = -2\pi \quad (19)$$

If $\underline{w} = \infty$ is mapped onto $\underline{z} = \infty$, then Eq. (10) is valid without modification, because this case can also be interpreted as mapping onto the interior of a polygon.

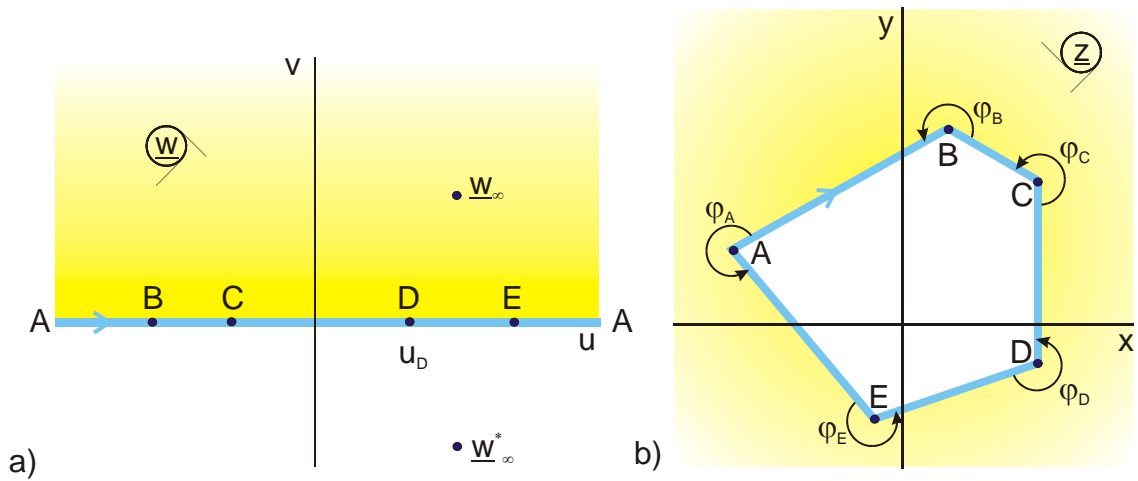


Figure 4.3: Mapping of the upper half plane onto the exterior of a polygon

When the transformation equation for a polygon mapping is calculated, three of the unknowns u_i , u_∞ and v_∞ can be arbitrarily chosen. With these three the location of the polygon in the z -plane is well-defined. In case the polygon is symmetrical, up to five unknowns can be arbitrarily chosen, by similar symmetrical arrangement of the points in the w -plane.

The evaluation of the Schwarz-Christoffel integral in Eq. (9) yields only in special cases analytical solutions. These cases can be roughly categorized as follows:

- For up to two vertices with angles of $\pi/2$ or $3\pi/2$ and additional vertices with angles of 0 or π , solutions are found with elementary functions.
- For up to three or four vertices with angles of $\pi/2$ or $3\pi/2$ and additional vertices with angles of 0 or π , solutions are found with elliptic functions.
- For symmetrical field maps the above given number of vertices can be duplicated.

In all other cases, i.e. for more vertices with angles of $\pi/2$ or $3\pi/2$ and for polygons with angles, which are not multiples of $\pi/2$, the solution of the integral is only possible in a few special cases. But also in those cases, where the field map cannot be determined, under certain circumstances the distribution of the field strength can be determined with Eq. (7).

For the evaluation of the Schwarz-Christoffel integral partial fraction expansion and substitution are commonly used. Quite often used substitutions are e.g. of the form:

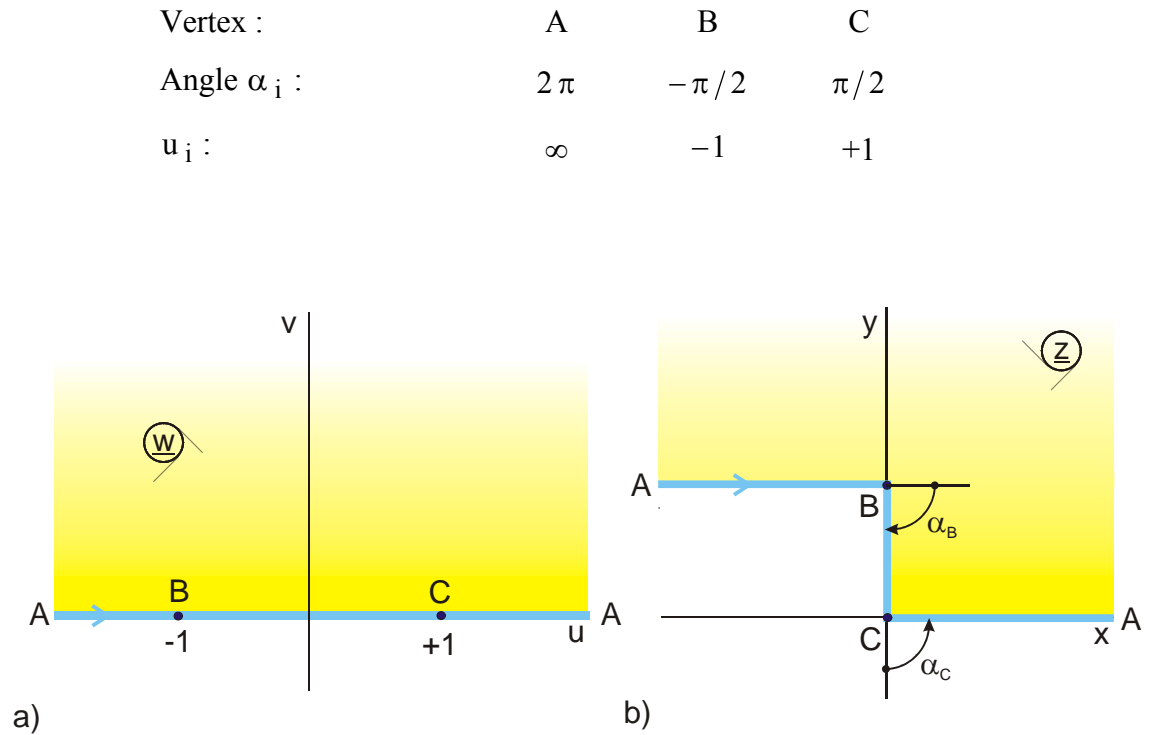
$$\underline{w} = \cos \underline{w}_1 \quad \Rightarrow \quad \underline{w}_1 = \arccos \underline{w}_1 \quad \text{and} \quad d\underline{w} = -\sqrt{1 - \underline{w}^2} d\underline{w}_1 \quad (20)$$

$$\underline{w} = \frac{1}{\cos^2 \underline{w}_1} \quad \Rightarrow \quad \underline{w}_1 = \arccos \left(\frac{1}{\sqrt{\underline{w}}} \right) \quad \text{and} \quad d\underline{w} = 2 \underline{w} \sqrt{\underline{w} - 1} d\underline{w}_1 \quad (21)$$

$$\underline{w} = \sinh^2 \underline{w}_1 \quad \Rightarrow \quad \underline{w}_1 = \operatorname{arcsinh} \sqrt{\underline{w}} \quad \text{and} \quad d\underline{w} = 2\sqrt{\underline{w}} \sqrt{\underline{w} + 1} d\underline{w}_1 \quad (22)$$

Example 1: Field map of a right-angled step (Mapping A 6)

According to Figure 4.4 the uniform field of the upper w-half plane shall be mapped on- to a step in the z-plane. In order to have a simple integral, the three freely selectable vertices u_i are placed at ∞ and at ± 1 .

**Figure 4.4: Example 1**

Condition (13) is satisfied. The term for point A is omitted because $u_A = \infty$. From Eq. (14) follows:

$$\frac{d\underline{z}}{d\underline{w}} = \frac{1}{(\underline{w}+1)^{-1/2} (\underline{w}-1)^{1/2}} \quad (23)$$

$$\underline{z} = \int_0^{\underline{w}} \sqrt{\frac{\underline{w}+1}{\underline{w}-1}} d\underline{w} \quad (24)$$

From a table of integrals the following solution for the integral is found:

$$\underline{z} = \sqrt{\underline{w}^2 - 1} + \operatorname{ar} \cosh \underline{w} + \ell n 2 . \quad (25)$$

The constant $\ell n 2$ is omitted, because it has no influence on the field map. The solution of the problem is:

$$\underline{z} = \sqrt{\underline{w}^2 - 1} + \operatorname{ar} \cosh \underline{w} . \quad (26)$$

The location of the points B and C in the z-plane are found by inserting into the equation.

$$\text{Point C:} \quad \underline{w}_C = 1 \quad \Rightarrow \quad \underline{z}_C = 0$$

$$\text{Point B:} \quad \underline{w}_B = -1 \quad \Rightarrow \quad \underline{z}_B = j\pi .$$

Example 2: Two parallel half planes above a conducting infinite plane (Mapping P 3.6)

According to Figure 4.5 the upper w-half plane shall be mapped onto two parallel half planes above a conducting infinite plane. The three freely selectable points u_i are determined so that A lies at ∞ , C at -1 and D at 0 .

Vertex :	A	B	C	D	E
Rotation angle α_i :	2π	$-\pi$	π	$-\pi$	π
u_i :	∞	$-a$	-1	0	b

With Eq. (14) can be written:

$$\underline{z} = \int_0^{\underline{w}} \frac{(\underline{w} + a) \underline{w}}{(\underline{w} + 1)(\underline{w} - b)} d\underline{w} \quad (27)$$

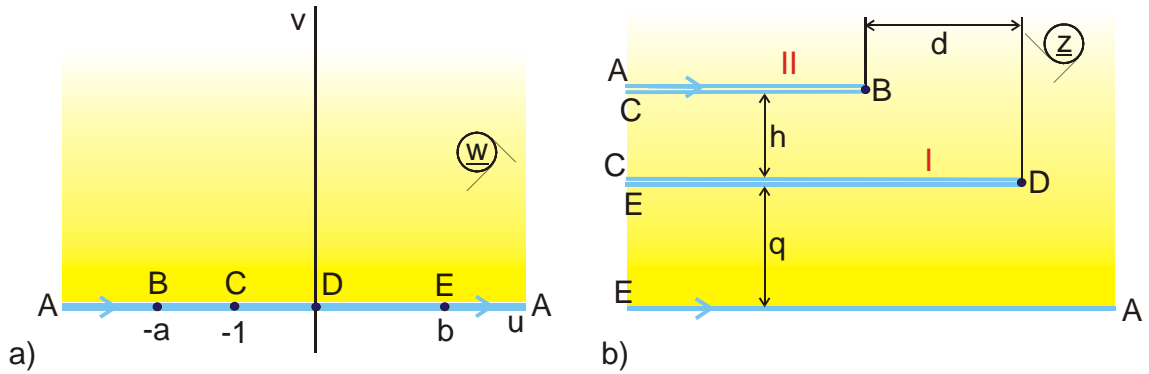


Figure 4.5: Example 2

The integrand has to be converted first, so that it is possible to find the corresponding integrals in a table of integrals:

$$\underline{z} = \int_0^{\underline{w}} \left(\frac{\underline{w}^2}{(\underline{w}+1)(\underline{w}-b)} + a \frac{\underline{w}}{\underline{w}^2 + \underline{w}(1-b) - b} \right) d\underline{w} . \quad (28)$$

The solution is:

$$\underline{z} = \underline{w} + \frac{a+b-1}{2} \ln((\underline{w}+1)(\underline{w}-b)) + \frac{1+b^2-a(1-b)}{2(1+b)} \ln \frac{\underline{w}-b}{\underline{w}+1} . \quad (29)$$

By inserting the points B and D into this equation, the conditional equations $h(a,b)$, $q(a,b)$ and $d(a,b)$ are found, with which it is possible to calculate the location of the half planes as functions of the parameters a and b . In Mapping P 3.6 the same transformation equation (29) is used. In addition the line \overline{CDE} in the w -plane is set to a different potential with the help of a pre-transformation. This finally produces the field map of a conducting half plane I with the potential u_1 between a conducting infinite plane and a parallel conducting half plane II, both with the potential 0.

Example 3: Rectangular conductor in a uniform field (Mapping A 10.1)

If a rectangular conductor is placed into a uniform electric field (Figure 4.6a), then the horizontal center lines on the right and left side of the conductor are a potential line. The field map is found by mapping the upper w -half plane onto the boundary in Figure 4.6c. By taking advantage of the symmetry the vertices C and D are chosen at ± 1 and the vertices B and E at $\pm 1/k$ (with $k < 1$).

Vertex :	A	B	C	D	E
Angle α_i :	2π	$\pi/2$	$-\pi/2$	$-\pi/2$	$\pi/2$
u_i :	∞	$-1/k$	-1	1	$1/k$

With Eq. (14) this leads to:

$$\frac{d\underline{z}}{d\underline{w}} = \frac{1}{(\underline{w} + 1/k)^{1/2} (\underline{w} + 1)^{-1/2} (\underline{w} - 1/k)^{1/2} (\underline{w} - 1)^{-1/2}} \quad (30)$$

$$\underline{z} = \int_0^{\underline{w}} \frac{\sqrt{\underline{w}^2 - 1}}{\sqrt{\underline{w}^2 - 1/k^2}} d\underline{w} = k \int_0^{\underline{w}} \frac{\sqrt{1 - \underline{w}^2}}{\sqrt{1 - k^2 \underline{w}^2}} d\underline{w} . \quad (31)$$

If the constant factor k is omitted, the solution can be written as:

$$\underline{z} = \int_0^{\underline{w}} \frac{\sqrt{1 - \underline{w}^2}}{\sqrt{1 - k^2 \underline{w}^2}} d\underline{w} = B_a(\underline{w}, k) , \quad (32)$$

the algebraic form of the function $B(\underline{w}, k)$, a specific elliptic integral (see Chapter 12.3).

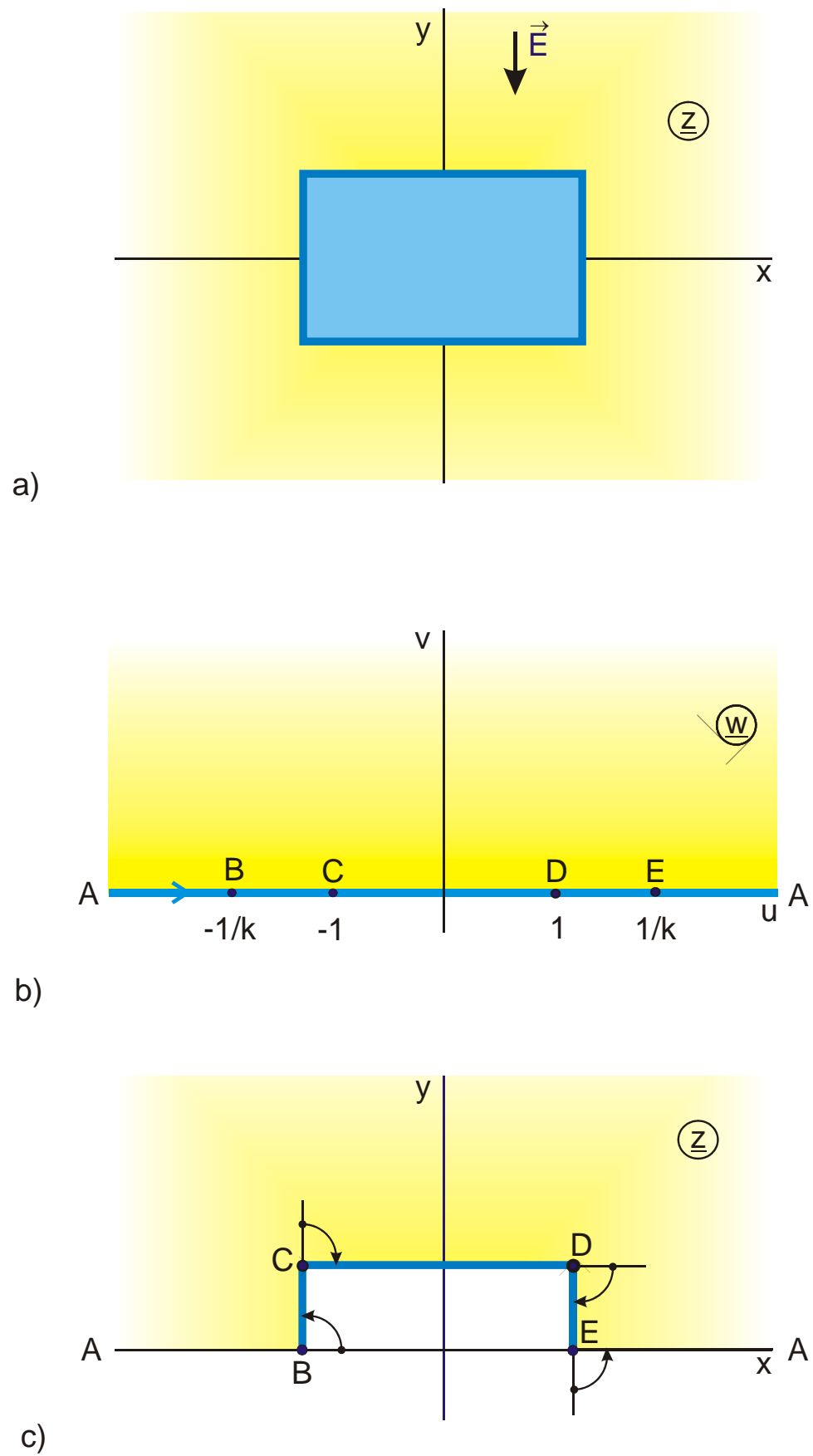


Figure 4.6: Example 3

Example 4: Mapping of the upper w-half plane onto the exterior of a thin strip

The three arbitrary selectable coordinates in the w-plane are determined as follows by taking advantage of the symmetry of the field map:

1. Coordinate: The two vertices on the sides of the strip, B and C, are placed at $u = \pm 1$.
2. Coordinate: The point A in the origin below the strip is placed at $u = \pm \infty$.
3. Coordinate: The point ∞ in the z-plane is placed at $v = 1$ and $w_\infty = j$ respectively.

Vertex :	A	B	C
Angle α_i :	0	$-\pi$	$-\pi$
u_i :	∞	-1	+1

Inserting in Eq. (17) gives:

$$\underline{z} = \int_0^{\underline{w}} \frac{d\underline{w}}{(\underline{w}+1)^{-1}(\underline{w}-1)^{-1}(\underline{w}-j)^2(\underline{w}+j)^2} \quad (33)$$

$$\underline{z} = \int_0^{\underline{w}} \frac{\underline{w}^2 - 1}{(\underline{w}^2 + 1)^2} d\underline{w} \quad (34)$$

$$\underline{z} = \int_0^{\underline{w}} \frac{\underline{w}^2}{(\underline{w}^2 + 1)^2} d\underline{w} - \int_0^{\underline{w}} \frac{d\underline{w}}{(\underline{w}^2 + 1)^2} \quad (35)$$

These integrals can be expressed by elementary functions. The solution is:

$$\underline{z} = \frac{\underline{w}}{\underline{w}^2 + 1} . \quad (36)$$

A factor 2 is added, so that the points B and C of the field map are located at ± 1 .

$$\underline{z} = \frac{2\underline{w}}{\underline{w}^2 + 1} . \quad (37)$$

The transformation equation in this form is not feasible for a technical application. The two line charges at $\pm\infty$, which create the uniform field in the w -plane, have been mapped into the origin below the strip. There is now the source of a dipole field (Figure 4.7).

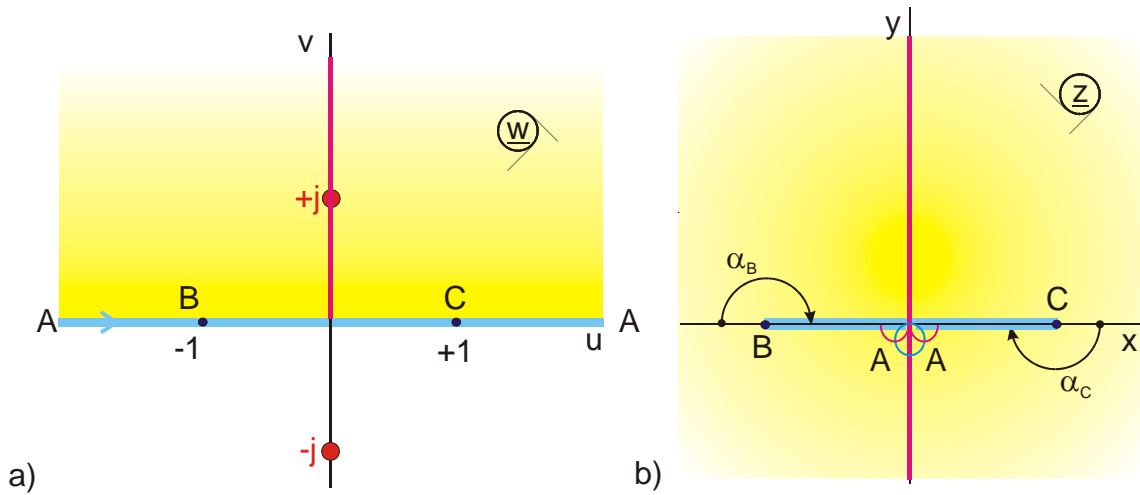


Figure 4.7: Example 4

In this mapping the real axis is bent downwards in the points B and C by 180° . The complete lower w -half plane is folded up and vanishes in the interior of the thin strip. The point $\underline{w} = j$ is mapped onto $\underline{z} = \infty$. Therefore a pre-transformation (see Chapter 5) is used in Mapping B 2 which places two line charges with the magnitude ± 1 at $\pm j$ in the w -plane, so that the real axis remains a potential line. These two line charges create

in the image plane the field map of a charged thin conducting strip, where all field lines emanate from the strip and end at the infinite point (Figure 4.8).

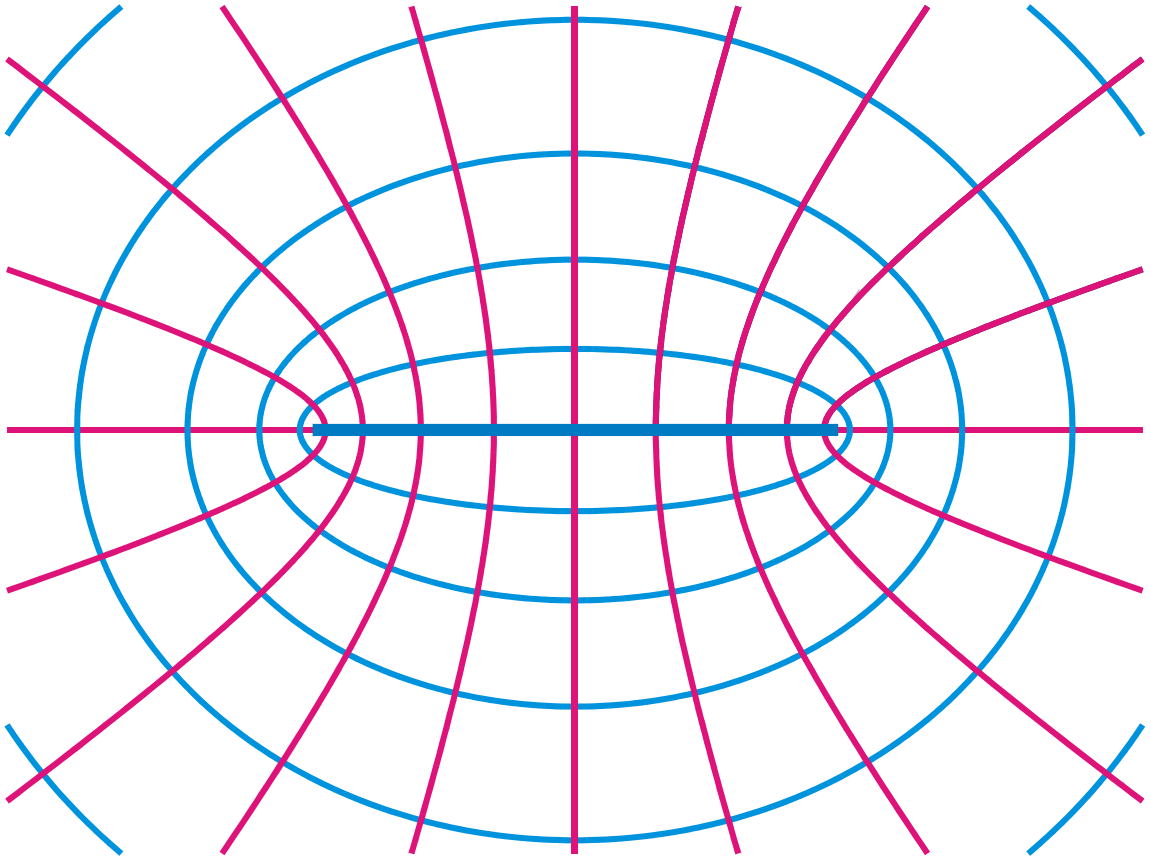


Figure 4.8: Mapping B 2, conducting strip against ∞

5. Pre-Transformations

In the preceding chapters always the uniform field in the w -plane was mapped onto the z -plane for the conformal mapping $\underline{z} = f(\underline{w})$. All these mappings can be varied or modified, if not the uniform field, but a non-uniform field in the w -plane is mapped onto the z -plane. This method is termed pre-transformation. Mathematically this means

$$\underline{z} = f_1(\underline{w}_1) \quad \text{and} \quad \underline{w}_1 = f(\underline{w}) \quad (1)$$

where $f_1(\underline{w}_1)$ is the original transformation equation and $\underline{w}_1 = f(\underline{w})$ the newly added, non-uniform field. Such pre-transformations can be employed multiple times successively, e.g.:

$$\begin{aligned} \underline{w}_1 &= f(\underline{w}) \\ \underline{w}_2 &= f_1(\underline{w}_1) \\ \underline{w}_3 &= f_2(\underline{w}_2) \\ \underline{z} &= f_3(\underline{w}_3). \end{aligned} \quad (2)$$

In the following some examples are given to illustrate the procedure.

Example 1: Line charge between two parallel planes

The field map of a line charge, located in the middle between two parallel planes, is to be determined (Figure 5.1). From Chapter 2.3 it is known that the function $\underline{z} = \ell \ln \underline{w}$ maps the upper half plane onto a parallel strip in the image plane. Hence the logarithm solves the first part of the mapping problem. This function produces two parallel conducting electrodes. Only the line charge in the middle is missing. In Figure 2.3 it can be seen that this point E is at $+j$. If a line charge is created there, the field map, which is

sought, is found. Furthermore the condition has to be satisfied that the real axis in the w -plane in Figure 5.2 must be a potential line. Therefore, according to the theory of images, two line charges of equal size and opposite sign must be placed in the w -plane (Figure 5.3). The transformation equation, which belongs to this charge distribution, is according to Chapter 2.7:

$$\underline{z} = j \tanh \underline{w}. \quad (3)$$

This field map is now transformed with the logarithm and thus solves the problem (Figure 5.4).

$$\text{Pre-transformation: } \underline{w}_1 = j \tanh \underline{w} \quad (4)$$

$$\text{Transformation: } \underline{z} = \ell n \underline{w}_1 \quad (5)$$

The complete transformation equation is

$$\underline{z} = \ell n (j \tanh \underline{w}). \quad (6)$$

This function maps the uniform field in the w -plane onto the field map of two parallel conducting planes with a line charge in the middle.

Finally this transformation equation can be rewritten in order to center the field map in the image plane. With Eq. (2.13)

$$\tanh \underline{w} = j \tan(-j w) \quad (7)$$

$$\text{and } \underline{z} = \ell n(-\tan(-j w)) = \ell n \tan(j \underline{w}). \quad (8)$$

The transition from $\tan(j \underline{w})$ to $\tan(\underline{w})$ does not change the transformation. Only the assignment between u , v and potential lines and field lines is exchanged. By the addition

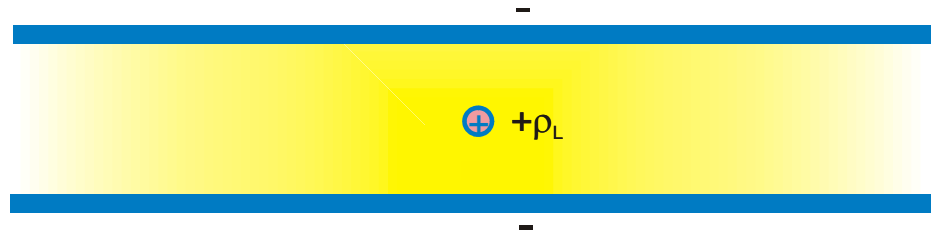
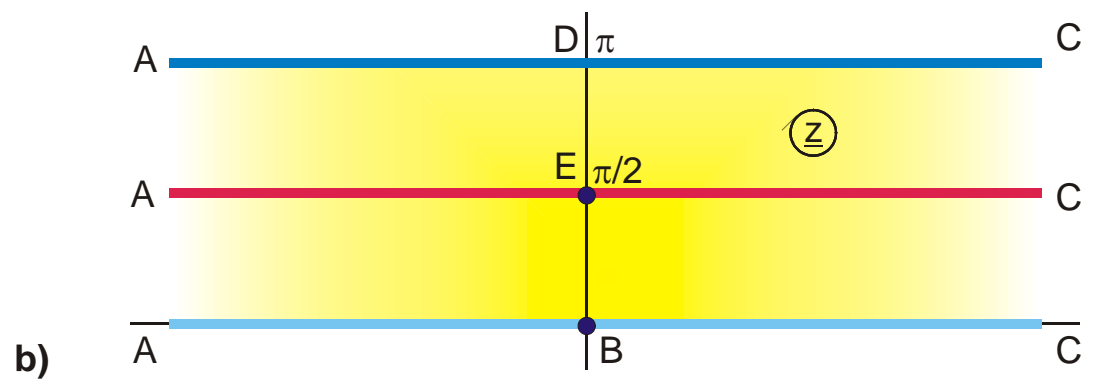
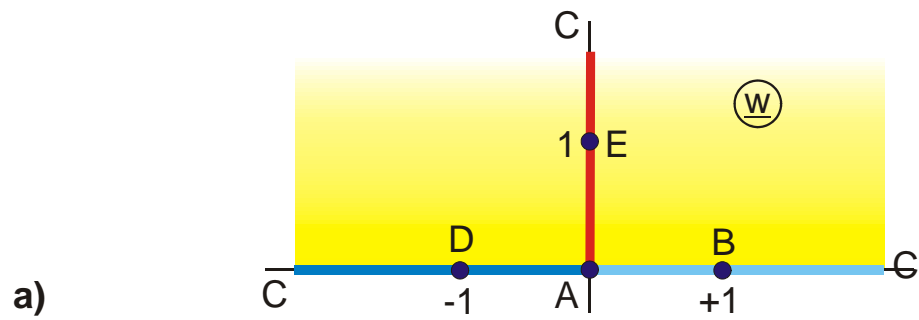
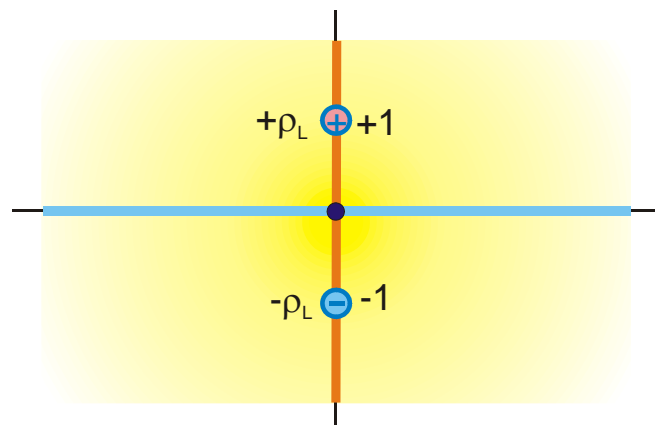


Figure 5.1: Example 1

Figure 5.2: $z = \ln w$, (Mapping H 1)Figure 5.3: $z = j \tanh w$

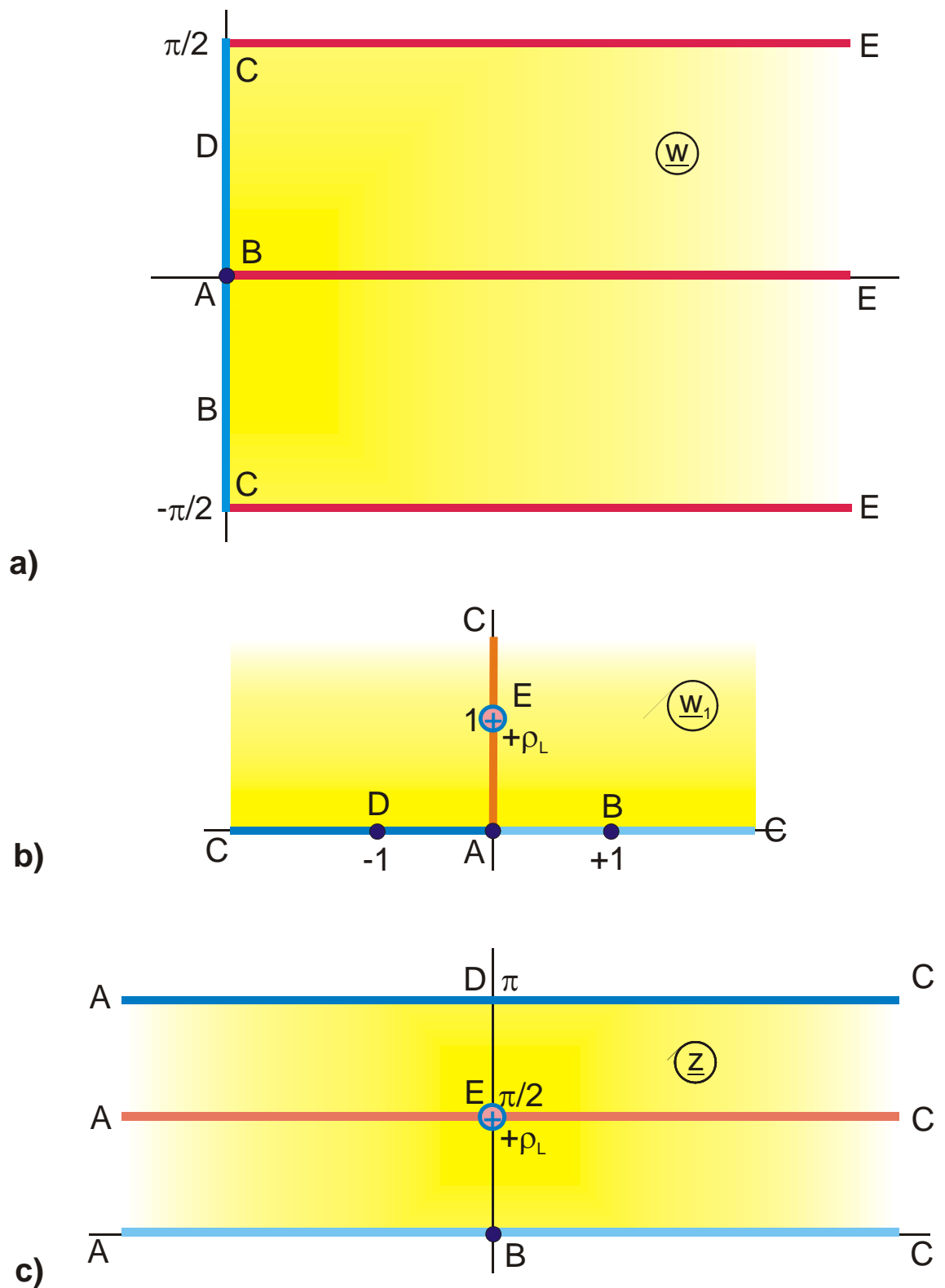


Figure 5.4: Pre-transformation for the mapping $z = \ln(j \tanh w)$

of the constant $-j\pi/2$ the line charge is moved into the origin of the image plane. So the final solution is (Figure 5.5, Mapping H 2):

$$\underline{z} = \ell \ln \tan \underline{w} - j\pi/2 . \quad (9)$$

In the same manner as in this example arbitrary configurations of line charges or line dipoles can be placed between the two parallel planes. Spacious electrodes can also be added to a mapping by a pre-transformation. In the following Example 2 a thin conducting strip is placed between the two parallel planes.

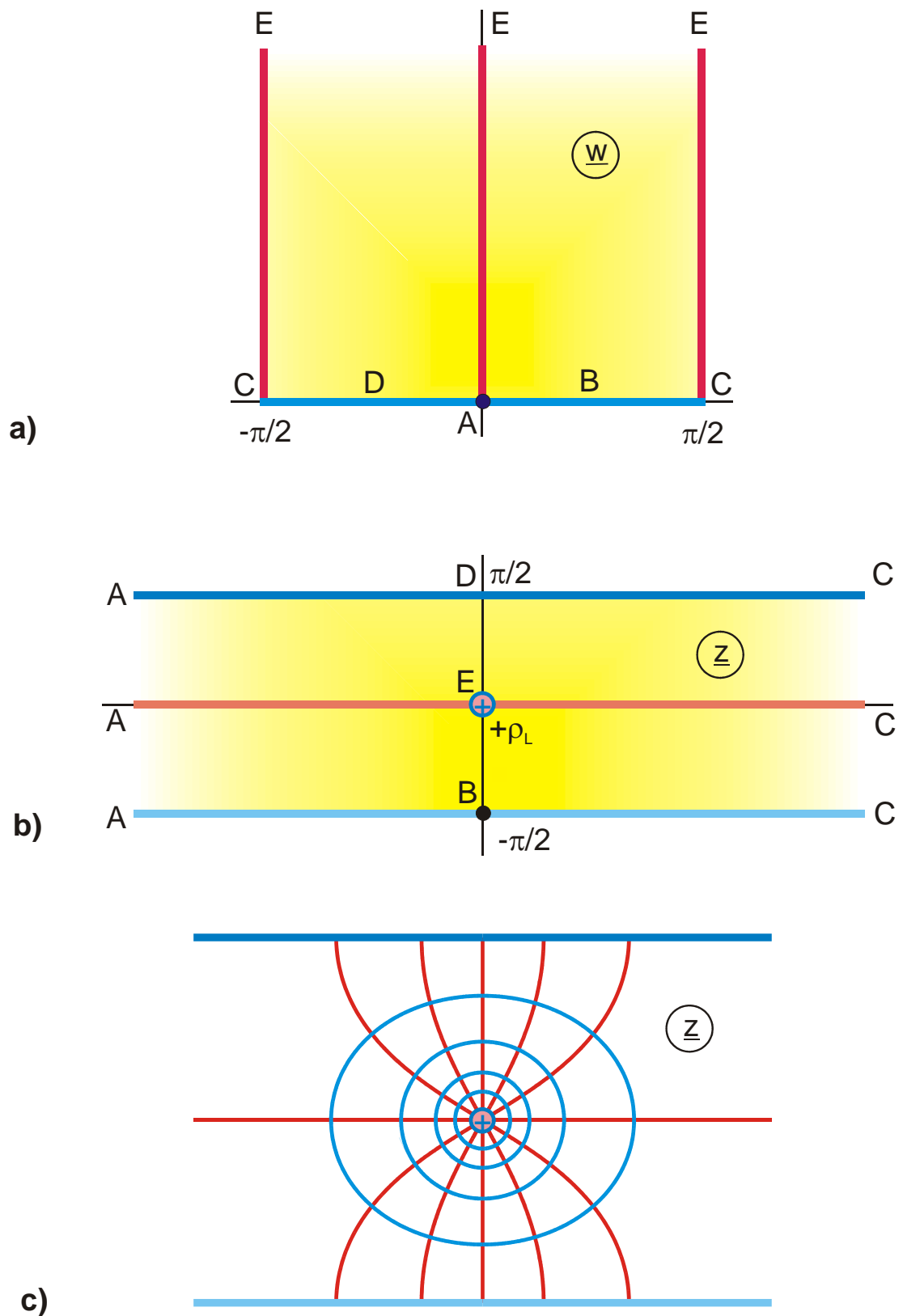


Figure 5.5: Final solution for Example 1: $z = \ln \tan w - j \pi/2$ (H 2)

Example 2: Field map of a strip transmission line

The field map of a conducting strip in the middle between two parallel, infinite conducting planes (Figure 5.6) is to be determined. To solve this problem, a pre-transformation is sought for the mapping $\underline{z} = \ell n \underline{w}$, which contains a conducting strip on the imaginary axis of the w -plane and where the real axis is a potential line. From the table of mappings the Mapping E 3, rotated by $+90^\circ$, is found.

$$\text{Transformation:} \quad \underline{z} = \ell n \underline{w}_1 \quad (10)$$

$$\text{Pre-transformation:} \quad \underline{w}_1 = j \cdot \text{sn}(\underline{w}, k) . \quad (11)$$

Figure 5.7 illustrates the two mappings. The conducting strip starts in the image plane at point E, there, where in Example 1 the line charge was located, and extends up to the point D and F respectively. Hence the width d of the strip is:

$$d = \text{Re } \ell n(j/k) = \ell n k . \quad (12)$$

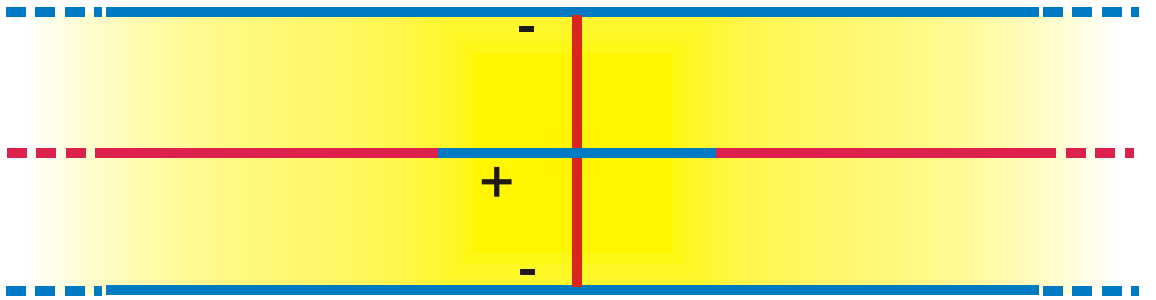


Figure 5.6: Symmetrical strip line (Example 2)

In order to center the field map, the center of the conducting strip is moved into the origin of the z -plane (Mapping H 7):

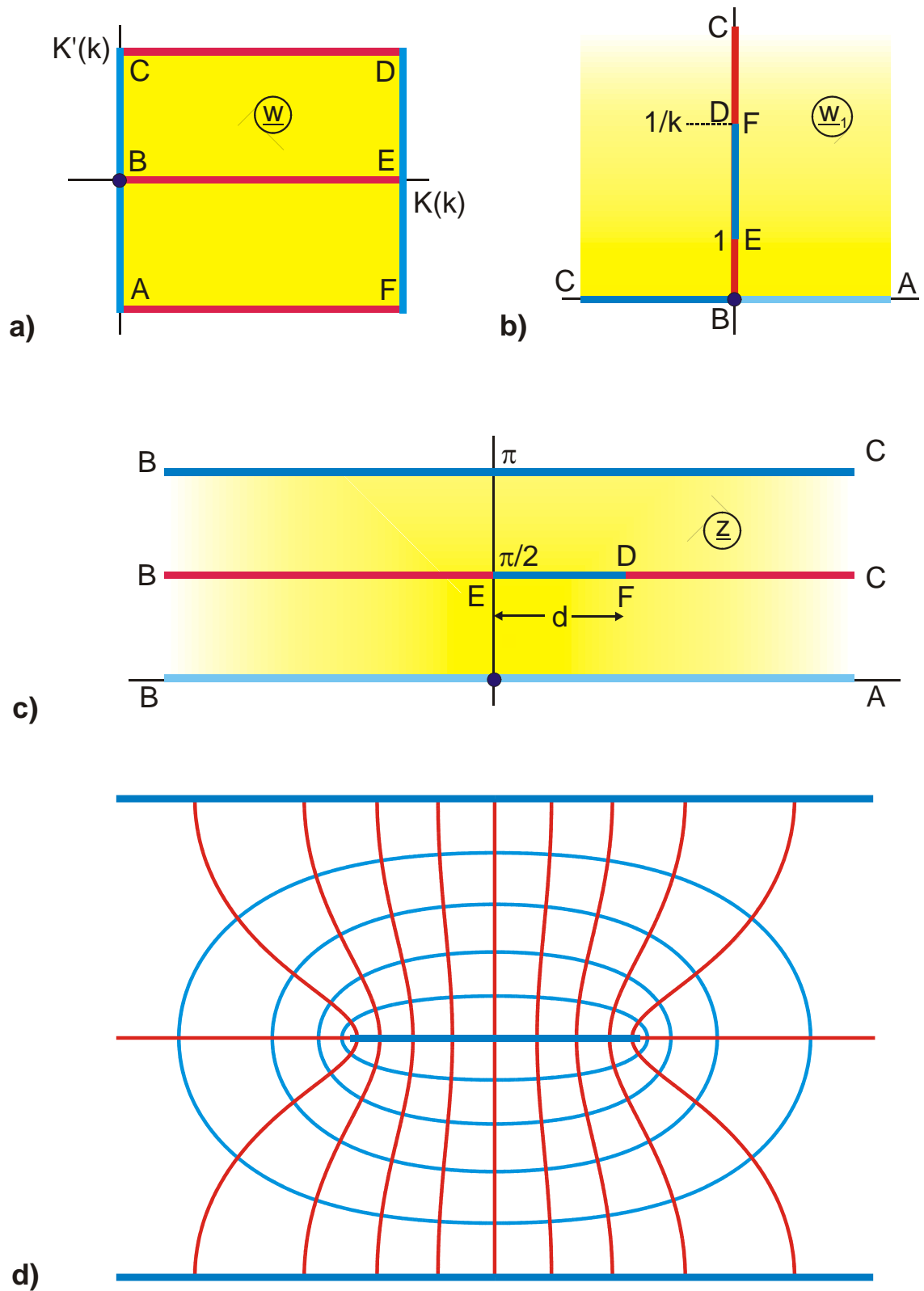
$$\underline{z} = \ell n(j \operatorname{sn}(\underline{w}, k)) - j\frac{\pi}{2} - d/2 \quad (13)$$

$$\underline{z} = \ell n \operatorname{sn}(\underline{w}, k) - d/2 \quad (14)$$

The conducting strip, which is imported into the w_1 -plane by the pre-transformation, remains to be a strip, despite the transformation with the logarithm, only because he lies on a straight line in the w_1 -plane, which is again mapped onto a straight line. As shown in Figure 5.2 the vertical, red straight line \overline{AC} is mapped onto the horizontal, red straight line \overline{AC} by $\underline{z} = \ell n \underline{w}$. Strips or line segments, which are placed on this straight line, maintain their shape throughout the process of the pre-transformation.

Whereas point-shaped sources (line charges, line dipoles) can be placed into existing mappings at arbitrary locations with an appropriate pre-transformation, this method is restricted for spacious electrodes to special cases, as long as exact solutions are wanted. Usually only thin strips like in Example 2, which may also extend up to infinity, can be created in this way. Furthermore they must lie in symmetry planes of the field map, in order to maintain their shape.

In case that only an approximate solution is sought, there are a lot more possibilities given by the method of pre-transformations, to determine unknown potential fields with the help of known mappings.

Figure 5.7: Example 2, $z = \ln \{j \operatorname{sn}(w, k)\}$ (H 7)

Example 3: Conducting strip

In Example 4.4 the upper half plane was mapped onto the exterior of a conducting strip. This resulted in a line dipole in point A (Figure 4.7). However the field map of a charged thin strip against the point ∞ is sought. In order to get this, a line charge has to be placed into the point ∞ of the z -plane. This point lies at $\pm j$ in the w -plane. As already employed in Example 1, the necessary pre-transformation is:

$$\text{Pre-transformation: } \underline{w}_1 = j \tanh \underline{w} \pi .$$

(15)

The transformation used in Example 4.4 was:

$$\text{Transformation: } \underline{z} = \frac{2 \underline{w}_1}{\underline{w}_1^2 + 1} \quad (16)$$

Both functions combined and converted yields:

$$\underline{z} = j \sinh (2\underline{w}\pi).$$

According to Chapter 2.5 this mapping is topologically the same as

$$\underline{z} = \cosh (\underline{w} \pi).$$

This is Mapping B 2 in the table of mappings.

Example 4: Thick conducting plate

The field map in the vicinity of the edge of a thick right-angled plate according to Figure 5.8a is should be determined. From the symmetry of the configuration follows that the center line is a field line. This leads to the new boundary in Figure 5.8b. This boundary has been solved already in Example 4.1, however as a continuous potential line (Figure 4.4). Figure 5.9 shows this mapping once again, but the straight line \overline{CA} is now plotted in red as a field line and the former w -plane is named w_1 -plane. The corresponding mapping is Eq. (4.13):

$$\underline{z} = \operatorname{arccosh} \underline{w}_1 + \sqrt{\underline{w}_1^2 - 1} . \quad (17)$$

In order to convert \overline{CA} into a field line, a pre-transformation is needed, which creates the field in the w_1 -plane. From the table of mappings the Mapping A 1.2 is found, however multiplied by -1 and displaced by $+1$:

$$\underline{w}_1 = 1 - \underline{w}^2 . \quad (18)$$

Thus the problem is solved.

The solution given in the table of mappings for Mapping A 5 is in this case a completely different equation. There are many ways, to find a transformation equation for a given problem. Depending on the method used, the derived functions are very often completely different. Even a different choice of the origin changes the transformation equation. The corresponding field maps are nevertheless all topologically identical.

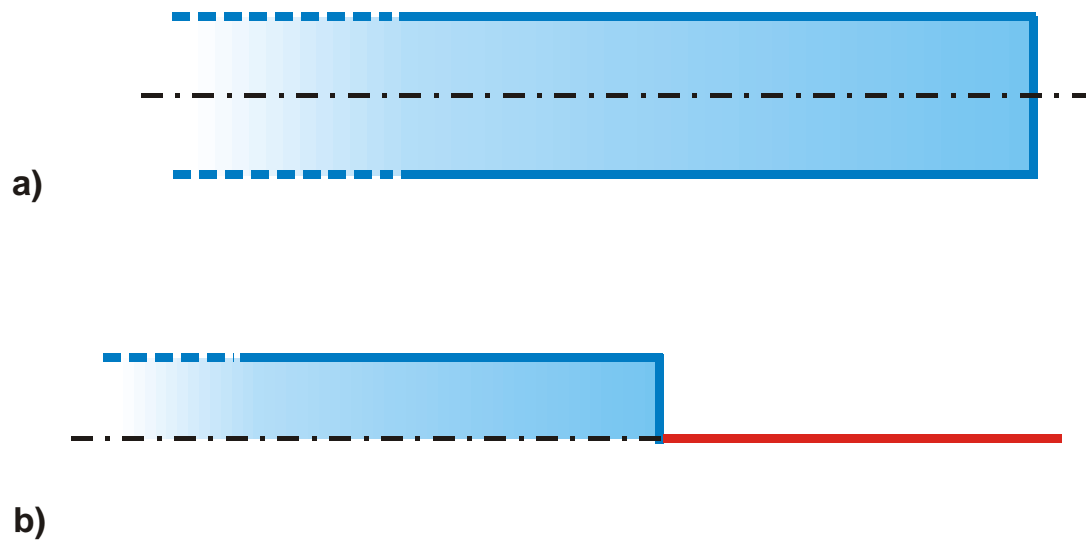
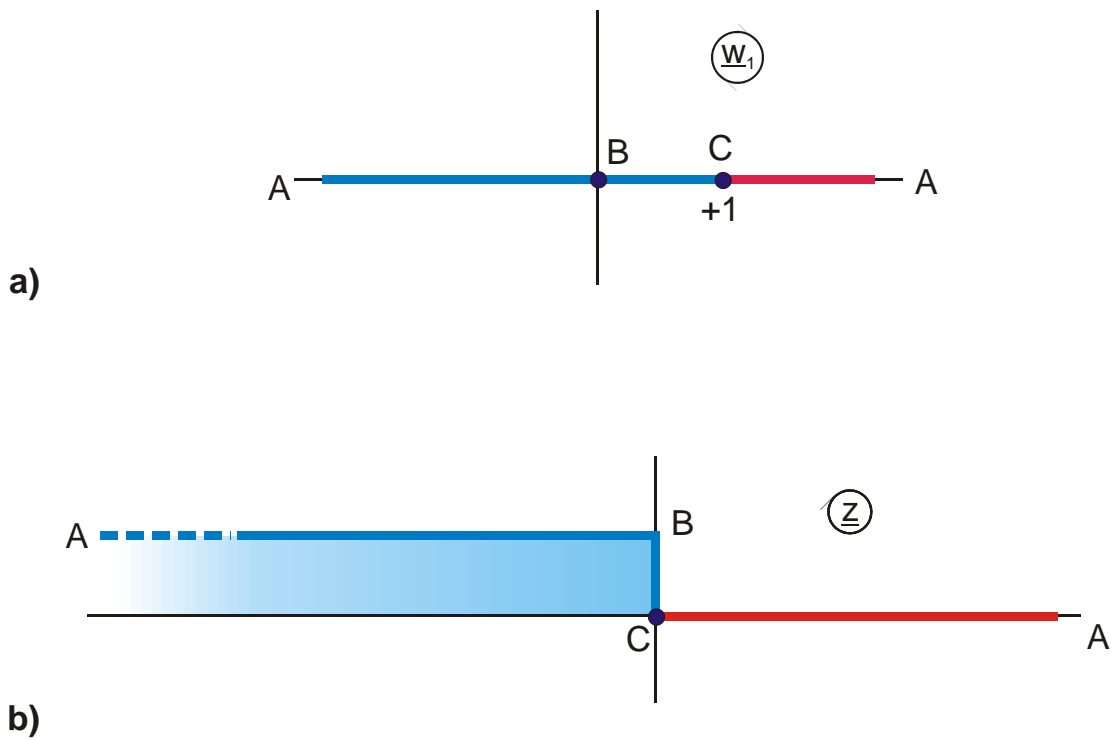


Figure 5.8: Thick conducting plate, Example 4

Figure 5.9: w_1 - and z -plane, Example 4

Example 5: Two coplanar conducting sheets centered between two parallel planes

The field map of the configuration illustrated in Figure 5.10a is to be determined. According to symmetry the vertical symmetry axis is a potential line and the horizontal axis a field line. Thus the mapping problem is reduced to the contour in Figure 5.10b. From Chapter 1.4 it is known that the function arcsine maps the upper half plane onto a half strip (Figure 5.11). The colors used in this figure already indicate that the line \overline{DE} should be a field line. To reach this, the field of a conducting strip like in Example 3 is used as pre-transformation. However this conducting strip is displaced by $1 + a/2$ from the origin of the w_1 -plane in Figure 5.11a. With this the pre-transformation is:

$$\underline{w}_1 = \frac{a}{2} \cdot \cosh(\underline{w} \pi) + 1 + \frac{a}{2}. \quad (19)$$

In Figure 5.11a the straight line \overline{DE} , which was interpreted as conducting strip in Example 3, is plotted in red, according to the problem in Figure 5.10b. Field maps are generally orthogonal sets of curves and the denotation as field line or potential line is arbitrary, as well as the assignment of the colors red and blue.

In order to place the field map in the I. quadrant as in Figure 5.10b, the configuration in Figure 5.11b is displaced by $\pi/2$ and rotated by 90° . Then the transformation equation is (Mapping H 6.4)

$$\underline{z} = j \left(\frac{\pi}{2} - \arcsin \underline{w}_1 \right) \quad (20)$$

$$\underline{w}_1 = 1 + \frac{a}{2} (1 + \cosh(\underline{w} \pi)). \quad (21)$$

The parameter a is determined from the mapping of point E with Eq. (20) and (2.12):

$$s = \operatorname{ar} \cosh(1 + a) \quad (22)$$

$$a = \cosh(s) - 1. \quad (23)$$

Determination of point B:

In Eq. (19) $\underline{w}_1 = -1$ is inserted.

$$-1 = 1 + a/2(1 + \cosh(u_D \pi + j\pi))$$

$$u_B = \frac{1}{\pi} \operatorname{arccosh}(1 + 4/a). \quad (24)$$

It is evident from inspection of Figure 5.11 that it is possible to create a whole family of mappings only by displacing and/or magnifying the red straight line \overline{DE} in the w_1 -plane (e.g.. H 1.4, H 6.1, H 6.2, H 6.3, H 6.4, J 1).

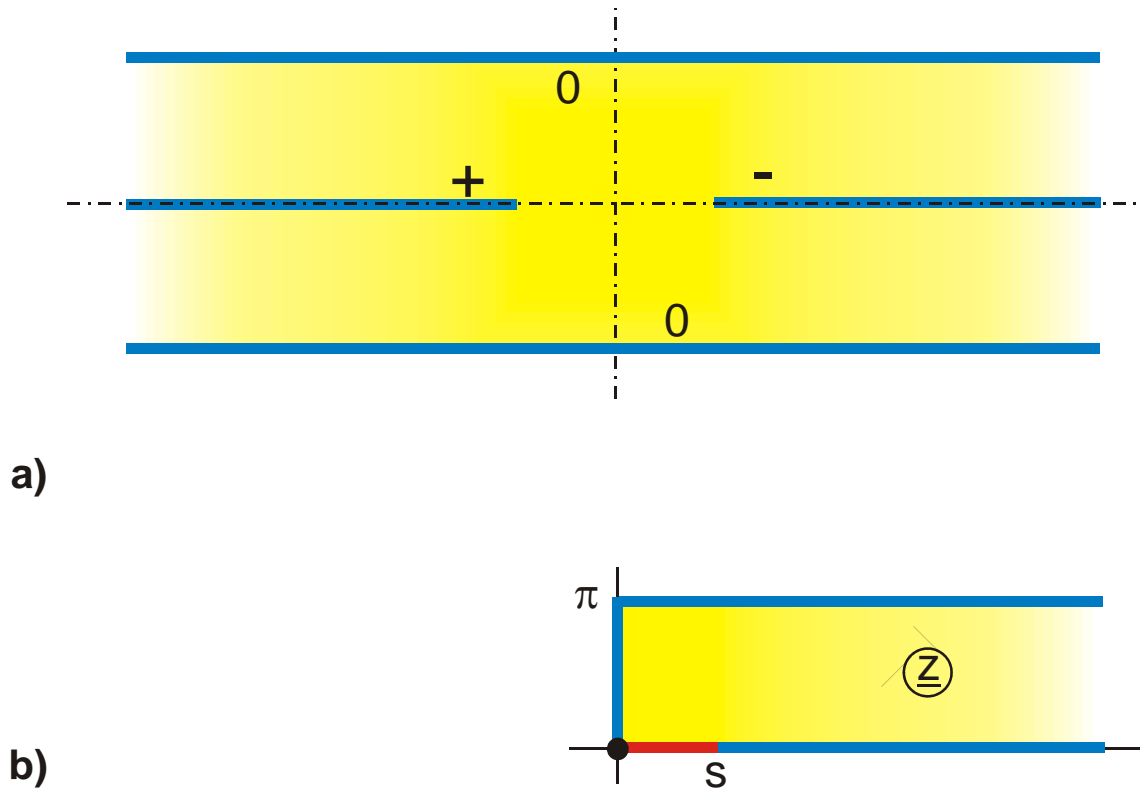


Figure 5.10: Example 5

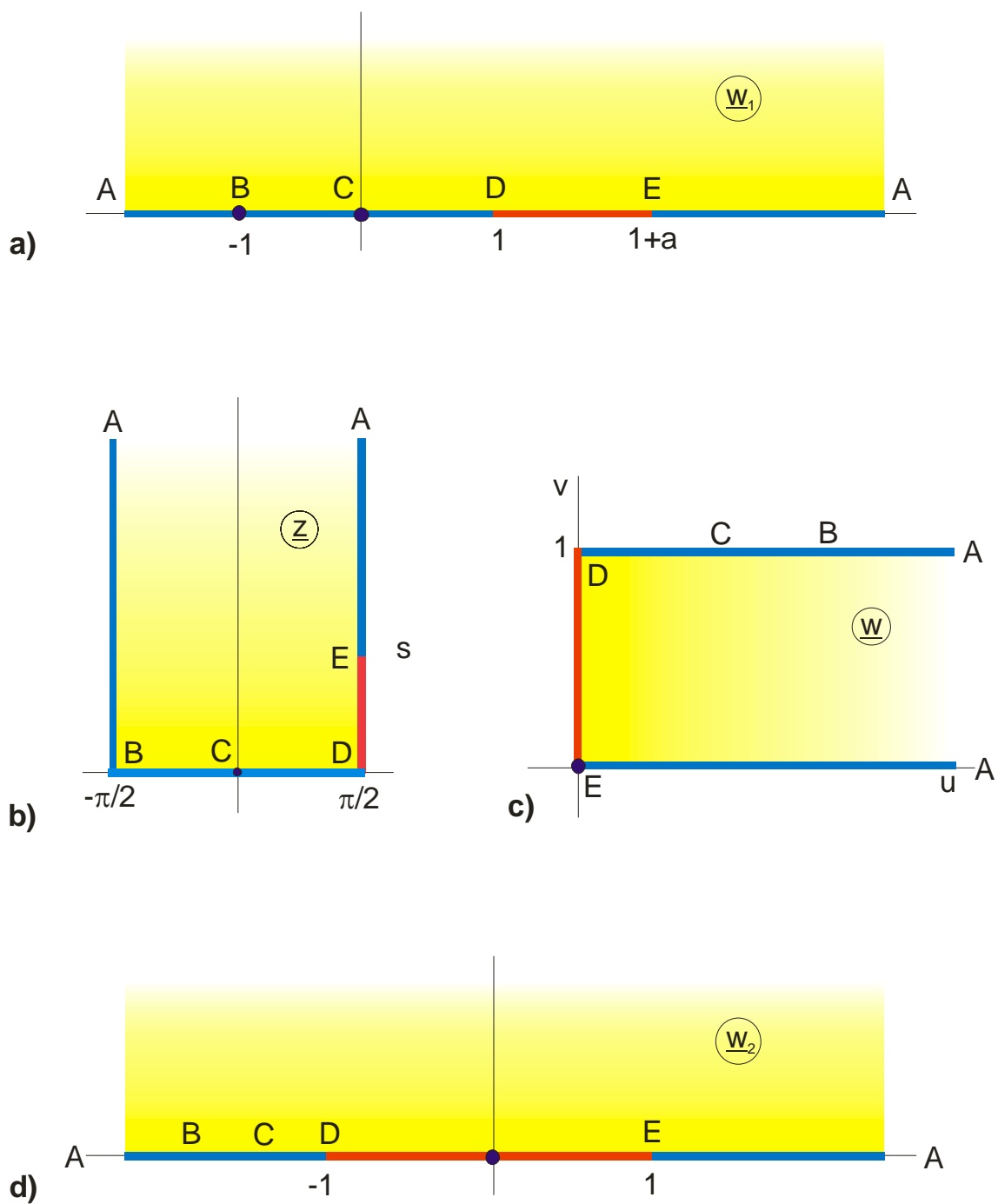


Figure 5.11: $z = \arcsin w_1$ (Figure a, b)
 $w_2 = \cosh (w\pi)$ (Figure c, d)

Example 6: Two coplanar conducting sheets excentric between two parallel planes

Figure 5.12a shows the boundary of the field map sought-after. Due to the symmetry the symmetry plane is a potential line (Figure 5.12b). With the method of mapping of polygonal boundaries, the function

$$\underline{z} = 2 \operatorname{ar} \coth \left(\frac{\underline{w}_1}{a} \right) + 2b \operatorname{ar} \coth (a \underline{w}_1) \quad (25)$$

is derived, which maps the upper half of the w_1 -plane onto the interior of the region and the real axis according to Figure 5.13a onto the boundary.

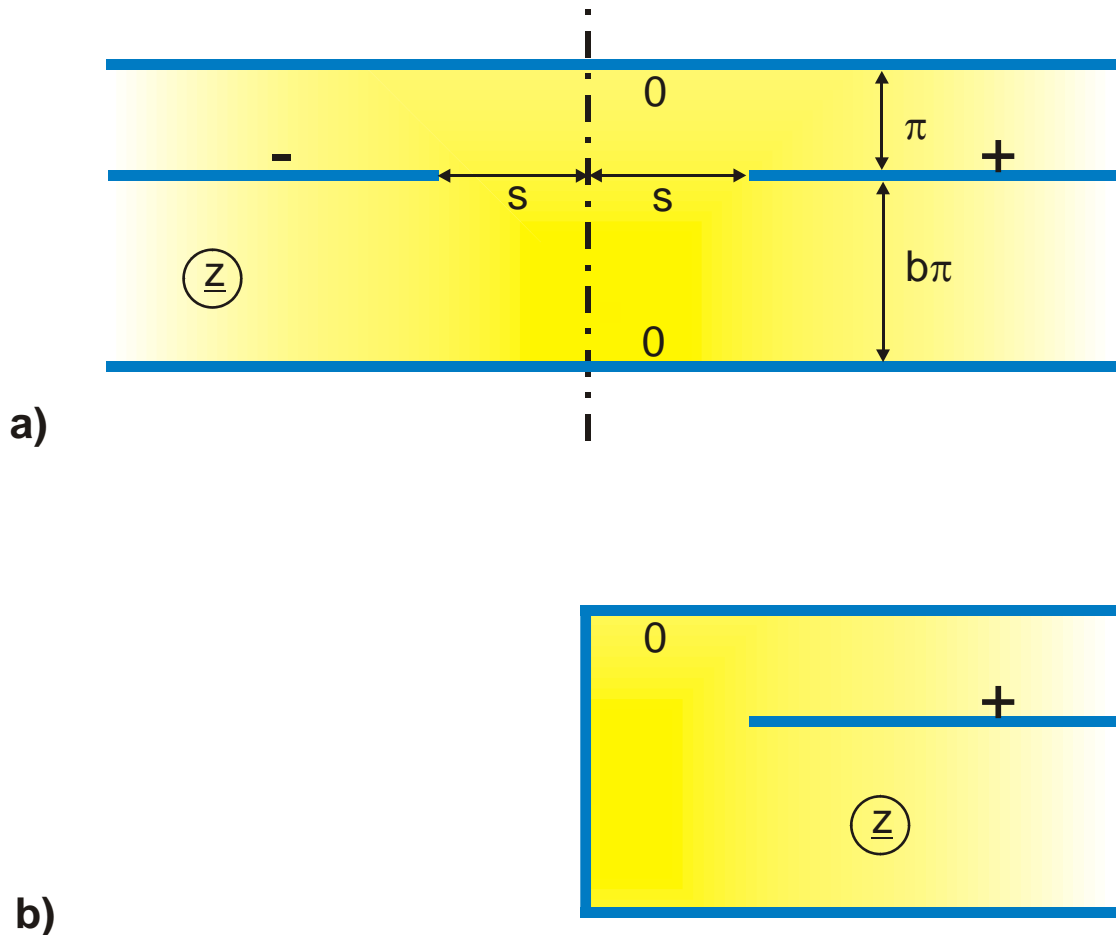


Figure 5.12: Example 6

In the next step a pre-transformation is needed, with which the boundary FGH in Figure 5.13b gets a constant potential u_1 and the boundary FEAH a differing constant potential u_2 . In the w_1 -plane both boundaries touch each other in the points F and H. There the field strength is infinite. The appropriate pre-transformation therefore must have a line charge in point F and another one in point H. As also the line AE must be a potential line, a distribution of the charges like in Figure 5.13d is necessary, to create the final potential distribution. The corresponding transformation equation is found in the table of mappings (Mapping L 4 with $p = a^2$, multiplied by $1/a$ and rotated by -90°):

$$\underline{w}_1 = -\frac{j}{a} \sqrt{\frac{\exp(\underline{w}\pi) - a^4}{1 - \exp(\underline{w}\pi)}}. \quad (26)$$

In Figure 5.13e it is indicated that both line charges are at $+\infty$ in the image plane. Far away from the origin they create the uniform field in the parallel channels above and below, which later on in the vicinity of the points E, G and A turns into a non-uniform field. When circulating the boundary in Figure 5.13b there is a change of direction in the points C and G. Mathematically this is:

$$\left. \frac{d\underline{z}}{d\underline{w}_1} \right|_{\underline{w}_1 = a} = 0. \quad (27)$$

With this equation the parameter a is determined and inserted in Eq. (25) the dimension s . All other values are found in the same way as in the preceding examples by insertion of the corresponding points. The results are assembled at Mapping D 5.

Hence the problem is solved. By the choice of other, appropriate pre-transformations in combination with Eq. (25) the Mappings H 6.7, H 6.8, H 6.9 and H 6.10 are produced.

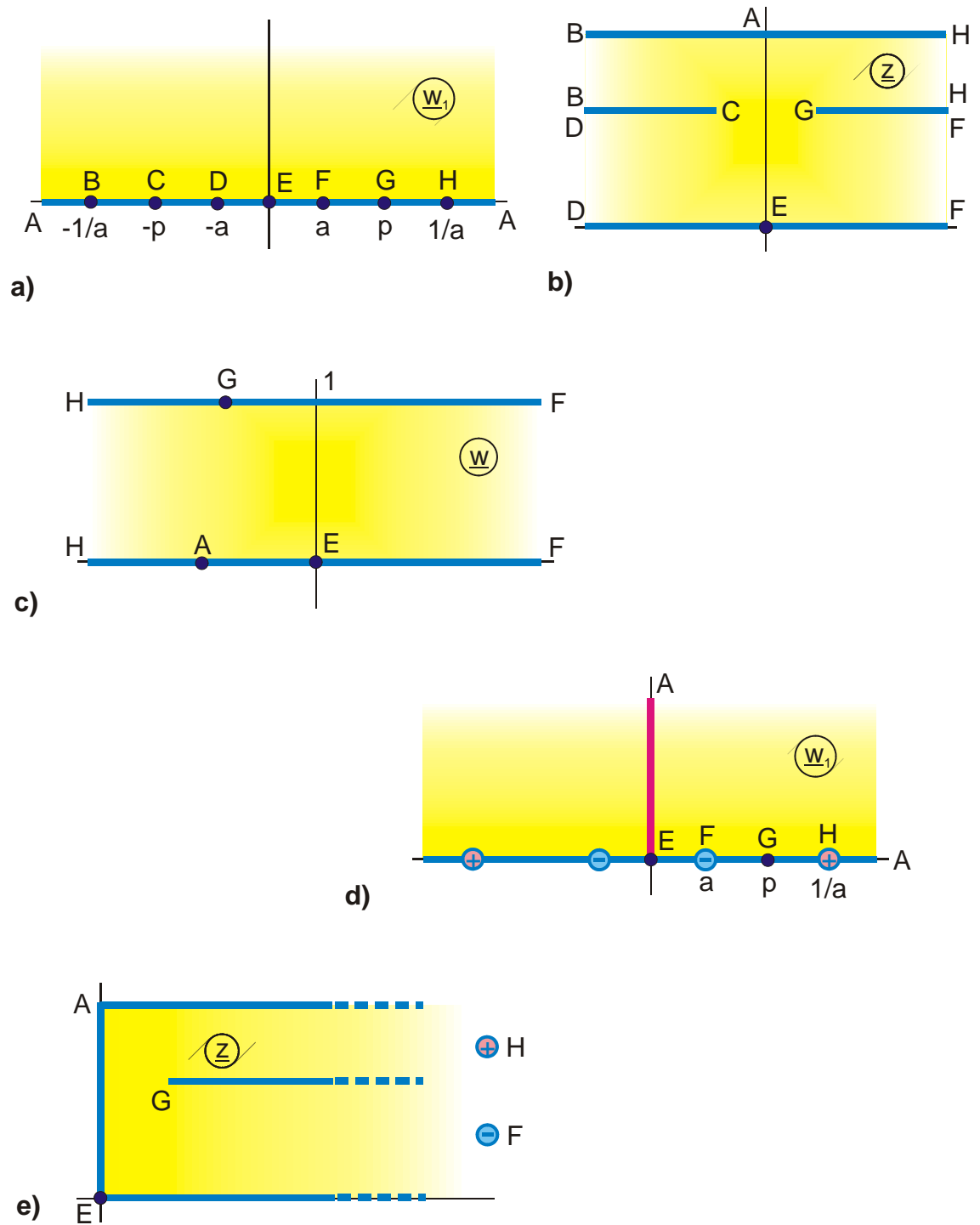
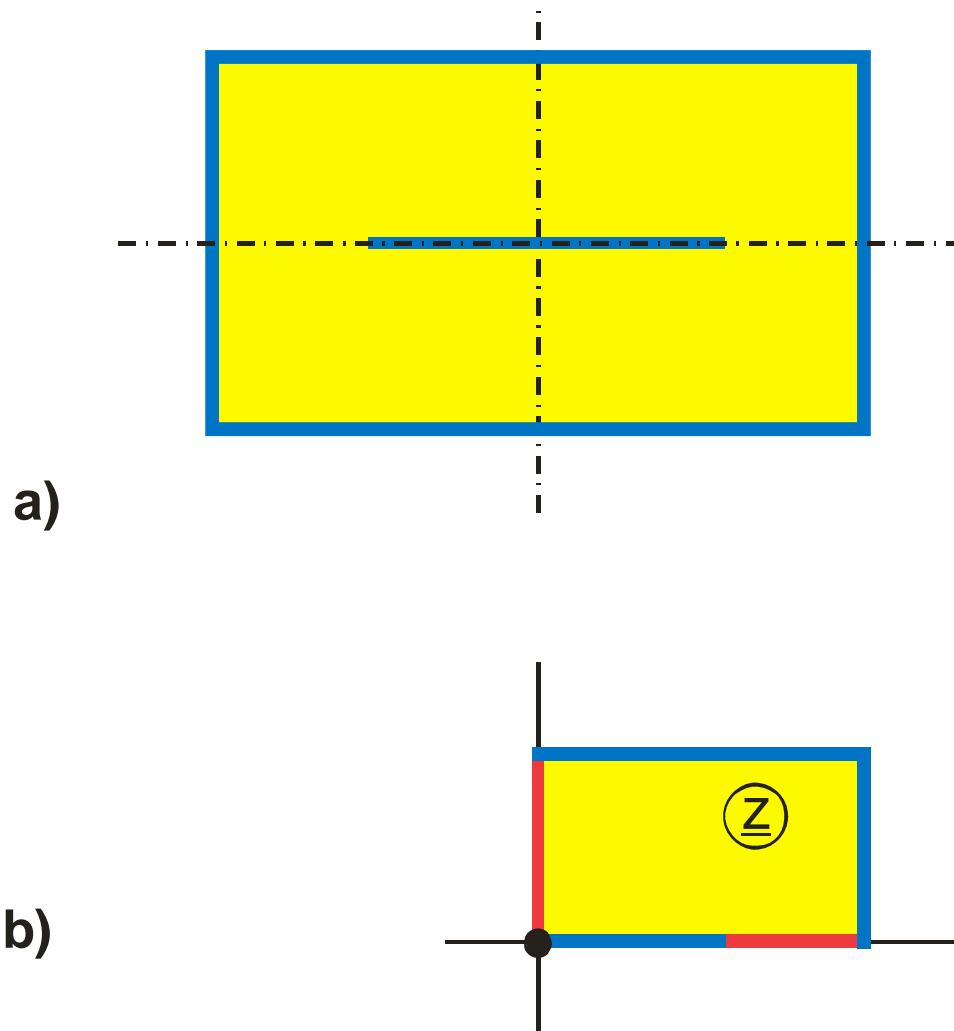


Figure 5.13: Solution for Example 6

**Example 7: Rectangular Outer Conductor, Symmetric Strip as
Inner Conductor**

Figure 5.14a illustrates the electrode configuration whose field map is to be determined. Because of the symmetry it is sufficient to consider the rectangular region shown in Figure 5.14b. The elliptic integral of the first kind (Chapter 12, Figure 4) is used to map the I. quadrant onto the interior of the rectangle.

$$\underline{z} = F_a(\underline{w}_1, k_1) . \quad (28)$$



**Figure 5.14: Example 7, a) Physical problem,
b) Transformation problem**

With an appropriate pre-transformation the straight lines \overline{AB} and \overline{CDE} must be transformed into potential lines and the straight lines \overline{AE} and \overline{BC} must be transformed into field lines in the \underline{w}_1 -plane (Figure 5.15c). The denotation potential line and field line may of course be exchanged. The corresponding transformation equation is found either with Chapter 11, Figure 2, or from the table of mappings with Mapping E 3:

$$\underline{w}_2 = \text{sn}(\underline{w}, k) . \quad (29)$$

In order to place point C at $z = 1$, the function is multiplied with k .

$$\underline{w}_1 = k \cdot \underline{w}_2 = k \cdot \text{sn}(\underline{w}, k) . \quad (30)$$

Hence the solution of the initial problem is:

$$\underline{z} = F_a(k \cdot \text{sn}(\underline{w}, k), k_1) . \quad (31)$$

This function maps a rectangle (Figure 5.15a) onto another rectangle (Figure 5.15d). It is evident that by magnifying and/or moving the red straight line \overline{BC} in the transition from \underline{w}_2 to \underline{w}_1 , more, different mappings are produced (e.g.. Mapping I 2.2, I 2.3 and I 2.6). Corresponding to Example 1 it is also possible to place a line charge into the rectangle (Group of mappings I, e.g. I 1) or a dipole (Group Q, e.g. Q 4).

To normalize the mapping, so that the rectangle has the side length 1 and the aspect ratio τ , the transformation equation is divided by $K(k_1)$ (Mapping I 2):

$$\underline{z} = F_a(k \cdot \text{sn}(\underline{w}, k), k_1) / K(k_1) . \quad (32)$$

Inserting point B gives

$$d = F_a(k, k_1) / K(k_1) . \quad (33)$$

This equation can be solved for k:

$$k = \operatorname{sn}(d \cdot K(k_1), k_1) . \quad (34)$$

If the aspect ratio τ is given, k_1 can be determined (Eq. 13.13):

$$k_1 = \left(\vartheta_2(\tau, 0) / \vartheta_3(\tau, 0) \right)^2 . \quad (35)$$

Point D is found in the w-plane by insertion:

$$\frac{1}{k_1} = k \operatorname{sn}[u_D + j K'(k), k] \Rightarrow u_D = \operatorname{Re} F_a\left(\frac{1}{k k_1}, k\right) . \quad (36)$$

Now all parameters and coordinates of this mapping are known.

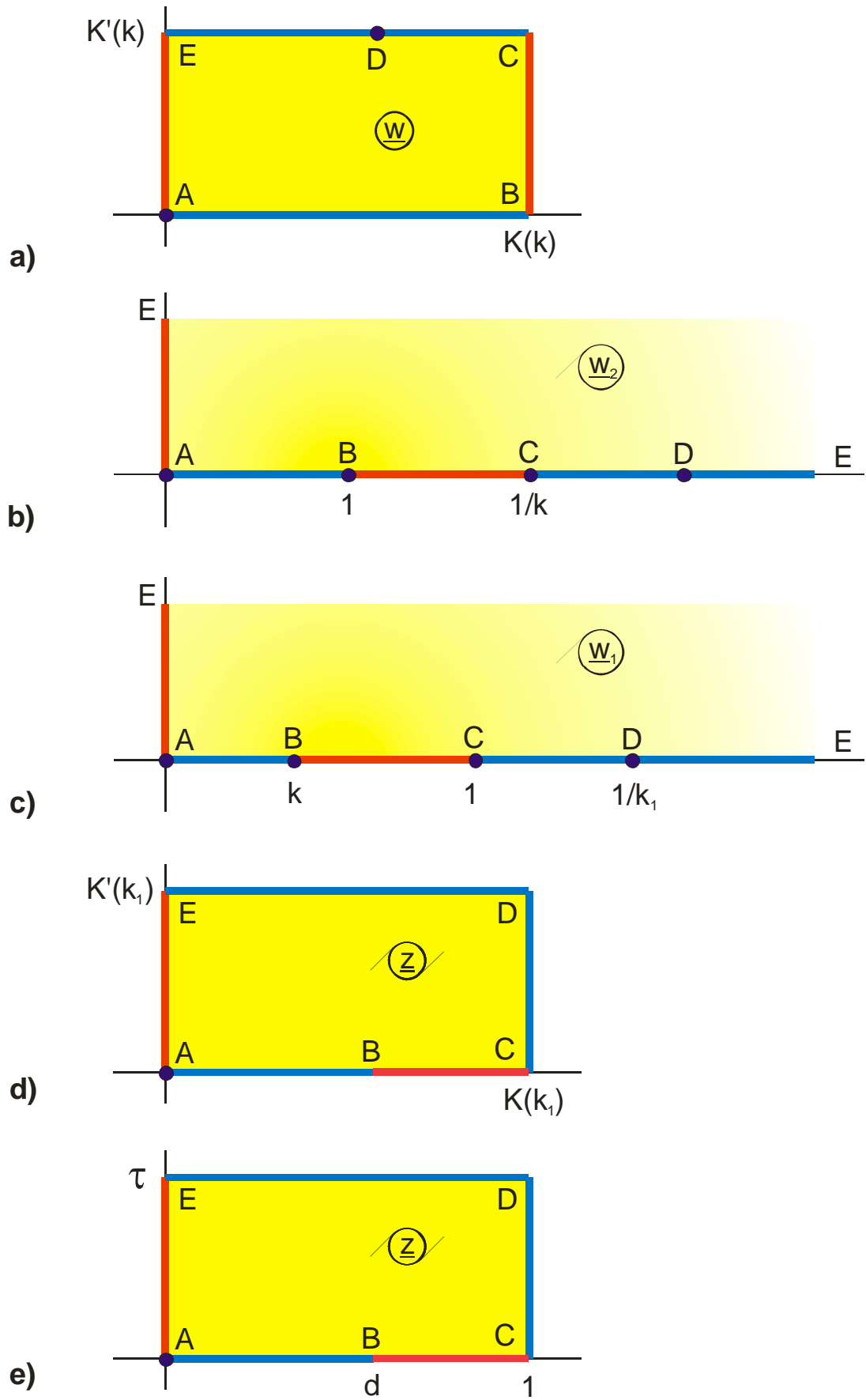


Figure 5.15: Sequence of the pre-transformations for Example 7

Example 8: Symmetrical transmission line with three conducting strips

Figure 5.16a shows a conducting strip symmetrically arranged between two more strips. Figure 5.16b is the reduction on the I. quadrant. Utilizing the method of pre-transformations to determine the field map, a mapping must be found, whose outside contour corresponds with Figure 5.16b, whereas the potential distribution along this contour may be arbitrary. From Chapter 12, Figure 11, or from Mapping E 2 the Zeta function is found to be appropriate:

$$\underline{z} = Z_e(\underline{w}_1, k'_1) + ja . \quad (37)$$

This maps the I. quadrant of the field map sought-after onto the interior of a rectangle (Figure 5.17c, d). The pre-transformation, necessary to create the appropriate potential distribution on the boundary of this rectangle (Figure 5.17c), is already known from Example 7. The transformation

$$\underline{w}_2 = F_a(k \cdot \text{sn}(\underline{w}, k), k_1) \quad (38)$$

(Figure 5.17a, b) has to be rotated by 90° and to be displaced by $K'(k_1)$

$$\underline{w}_1 = K'(k_1) + j \underline{w}_2 . \quad (39)$$

When rotating a rectangle by 90° it has to be taken into account that

$$K(k'_1) = K'(k_1) \quad (40)$$

and

$$K'(k'_1) = K(k_1) \quad (41)$$

holds; i.e. the modulus changes from k'_1 to k_1 or in general from k to k' .

Hence this mapping problem is solved. The individual parameters are given at Mapping P 5.4. They are determined as in the preceding examples by insertion of the individual points into the transformation equation. When inspecting Figure 5.17 it is evident that it

is easily achieved with another, similar pre-transformation, to rotate the center conductor of the transmission line by 90° , so that all three strips are parallel to each other (Mapping P 5.3).

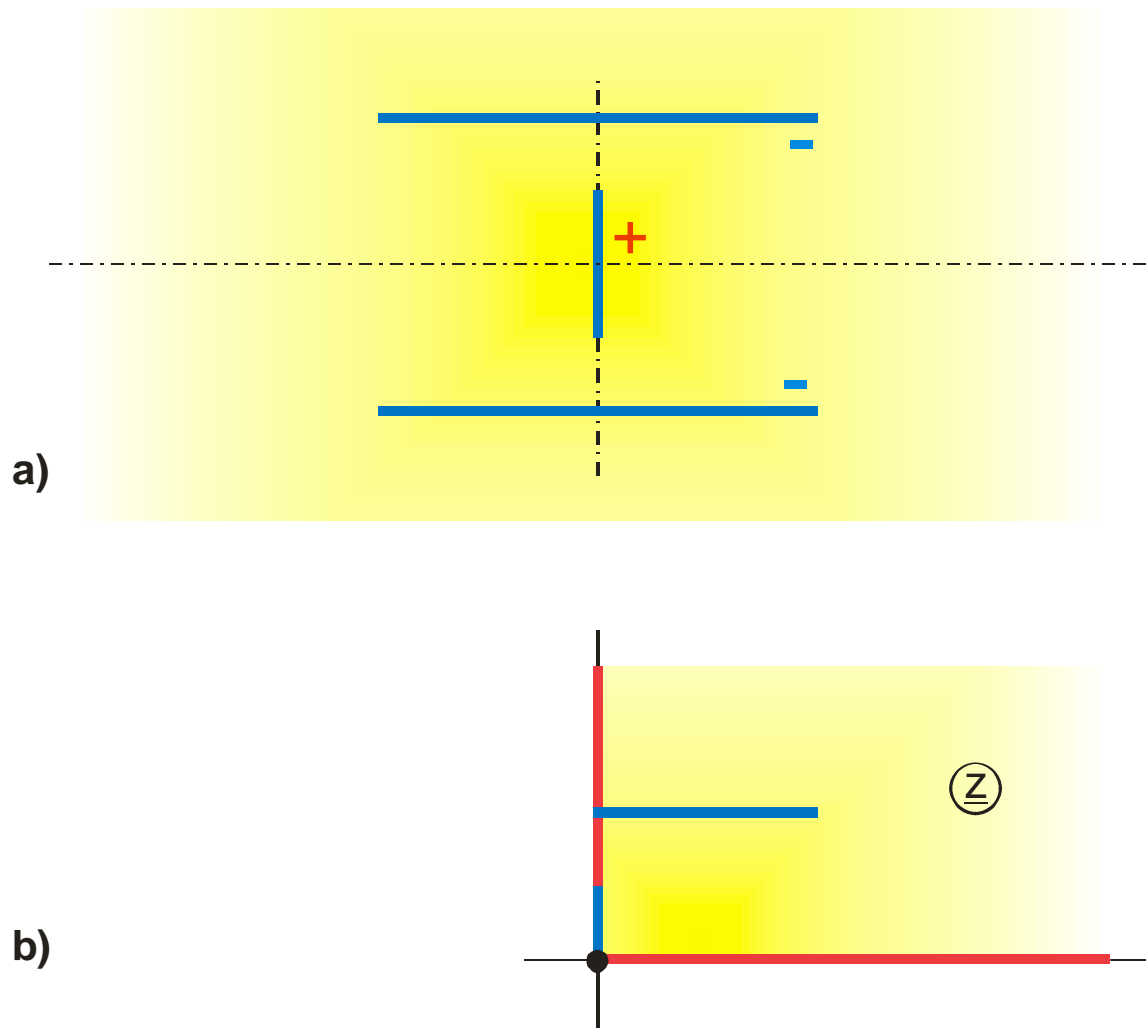


Figure 5.16: Example 8 a) Physical problem,
b) Mapping problem

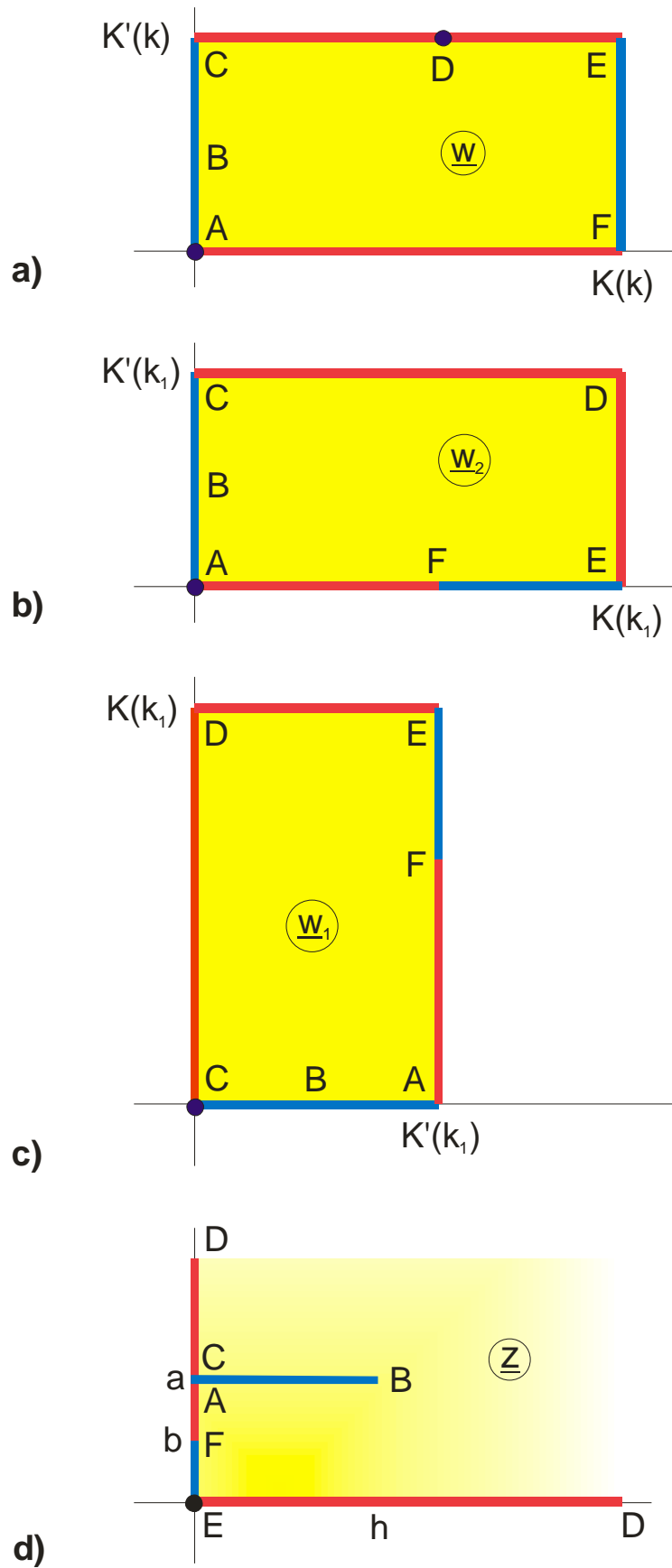


Figure 5.17: Sequence of the pre-transformations for Example 8

6. Successive Transformations

A given mapping $f_1(\underline{w})$ can be transformed once again by a second mapping $f_2(\underline{w})$. In this way it is possible, to modify a given mapping $f_1(\underline{w})$ systematically. The procedure is the following:

$$\text{Given mapping:} \quad \underline{w}_1 = f_1(\underline{w}) \quad (1)$$

$$\text{Successive transformation:} \quad \underline{z} = f_2(\underline{w}_1) \quad (2)$$

$$\text{Result:} \quad \underline{z} = f_2[f_1(\underline{w})]. \quad (3)$$

Three successive transformations consecutively:

$$\underline{z} = f_4(f_3(f_2(f_1(\underline{w})))) \quad (4)$$

The procedure is similar to the pre-transformation. Only the sequence of the transformations is reversed. The main difference is that [the boundaries of the given mapping are altered by the successive transformation](#). A first successive transformation may be succeeded by second one and so on.

This method, which looks quite complicated in this notation, is extremely simple in the practical application, because each single successive transformation can be analyzed and carried through by itself.

$$\begin{aligned} \text{Given:} \quad \underline{w}_1 &= f_1(\underline{w}) \\ 1. \text{ Step:} \quad \underline{w}_2 &= f_2(\underline{w}_1) \\ 2. \text{ Step:} \quad \underline{w}_3 &= f_3(\underline{w}_2) \\ 3. \text{ Step:} \quad \underline{z} &= f_4(\underline{w}_3) \end{aligned} \quad (5)$$

The procedure is similar to the solution of an integral by several substitutions in a row. However with the difference that it is possible, to find the result, as demonstrated in the following, target-oriented and easily interpretable. For instance for mapping R 7.2 in the table of mappings there were five mappings carried through consecutively. In fact there were even more successive transformations, because e.g. the first transformation equation, as shown in the following Example 1, can be separated into three successive transformations.

Besides being illustratively and simple because of the separation in simple single steps the method of successive transformations has a further advantage: In most cases it is very easy to find the inverse of the transformation equation (e.g. Mapping R 7.2).

Inverse function of Eq. (4):

$$\begin{aligned}
 \underline{w}_3 &= f_4^{-1}(\underline{z}) \\
 \underline{w}_2 &= f_3^{-1}(\underline{w}_3) \\
 \underline{w}_1 &= f_2^{-1}(\underline{w}_2) \\
 \underline{z} &= f_1^{-1}(\underline{w}_1).
 \end{aligned} \tag{6}$$

The pre-transformations of the preceding chapter are strictly spoken not an independent method, but may as well be referred to as successive transformations.

6.1 The Function $\underline{z} = \underline{w}_1^{\varphi/\pi}$

Some basic possibilities, to modify a given mapping $\underline{w}_1(\underline{w})$ by a successive transformation with the function $\underline{z} = \underline{w}_1^{\varphi/\pi}$, are comprised in Figure 6.1.

In Figure 6.1a the field of a thin conducting strip against ∞ (Mapping B 2) is changed into the field of two thin conducting strips, symmetrically arranged, with equal charge

(Mapping S 2.2), after moving the strip away from the origin and using a successive transformation with $\underline{z} = \underline{w}_1^{1/2}$. Due to the exponent 1/2 the negative real axis is bent upwards by 90° and creates the symmetry plane of the new mapping.

In Figure 6.1b the field of two symmetrically arranged thin conducting strips with equal but opposite charge (Mapping E 3) is transformed with $\underline{z} = \underline{w}_1^2$ into the field of a thin conducting strip against a thin half plane (Mapping K 3). In this case the positive imaginary axis is bent by 90° to the left and creates the half plane of the new mapping. The same Mapping E 3 yields after a displacement by +1 with $\underline{z} = \underline{w}_1^{1/2}$ a symmetrical three strip transmission line (Figure 6.1c). This is a special case of Mapping P 5. However a different successive transformation was used for Mapping P 5, because the widths of the conducting strips cannot be varied independently from one another in the mapping of this example. Alternatively it is yet possible to reach this more general result with $\underline{z} = \underline{w}_1^{1/2}$, if as initial mapping the field of two conducting strips with different widths (Mapping F 5.1) is used.

With the successive transformation $\underline{z} = \underline{w}_1^{\varphi/\pi}$ all elements along the positive real axis remain there. It is possible to duplicate them in this way or to expand them to symmetrical multi-conductor configurations.

Furthermore this successive transformation yields a large part of the mappings with radial symmetry of Group G. The procedure is demonstrated in Figure 6.1d. Starting with Mapping F 3, the field map of a coaxial line with a slotted, thin outer conductor, the successive transformation $\underline{z} = \underline{w}_1^{1/n}$ yields a field map in an angular range from 0 through π/n , which can be symmetrically complemented to the field map of a coaxial line with a uniformly, n-fold divided outer conductor (Mapping G 4). All elements that are placed on circles concentric to the origin, maintain their shape by the successive transformation $\underline{z} = \underline{w}_1^{\varphi/n}$.

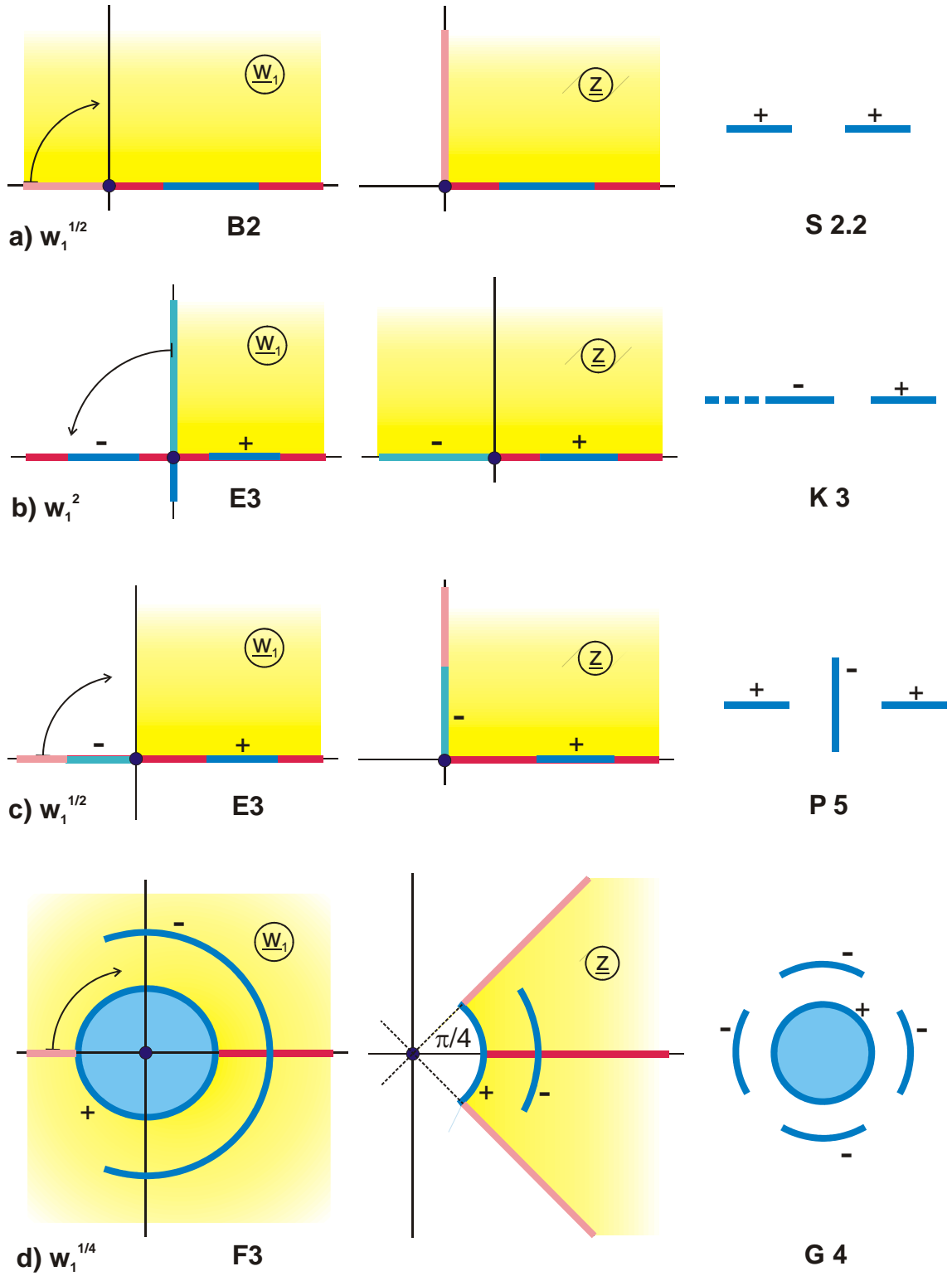


Figure 6.1: The successive transformation $\underline{z} = \underline{w}_1^{\phi/\pi}$

Example 1: Conducting plane with salient edge

Mapping 2.1 is an example where the successive transformation $\underline{z} = \underline{w}_1^{\varphi/\pi}$ is applied twice. According to the sequence of the pictures in Figure 6.2 the uniform field \underline{w} is transformed with $\underline{w}_1 = \underline{w}^2$ into the field map of a thin plate. This is displaced by -1 with $\underline{w}_2 = \underline{w}_1 - 1$ and then folded up to the final result with $\underline{z} = \sqrt{\underline{w}_2}$. If the equations are combined, the result is $\underline{z} = \sqrt{\underline{w}^2 - 1}$, the Mapping A 2.1.

Summary: With the successive transformation $\underline{z} = \underline{w}_1^{\varphi/\pi}$ it is possible amongst others to complement a mapping symmetrically or to generate configurations with radial symmetry. All elements, being located on rays through the origin and on concentric circles around the origin maintain their shape.

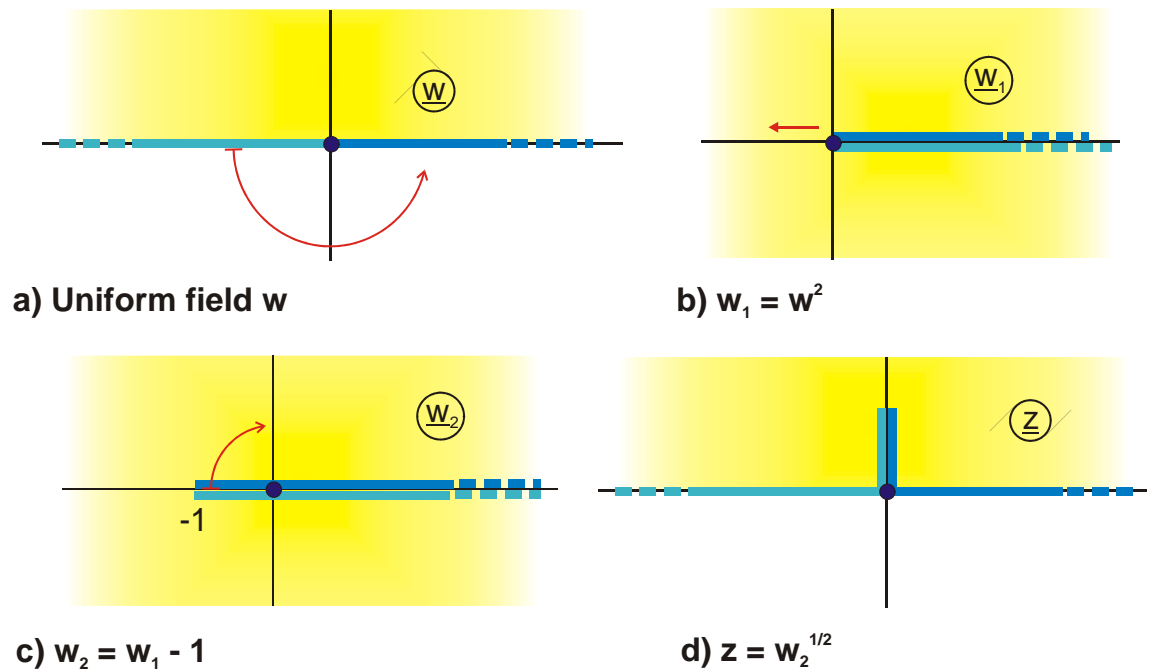


Figure 6.2: Example 1, $\underline{z} = \sqrt{\underline{w}^2 - 1}$, Mapping A 2.1

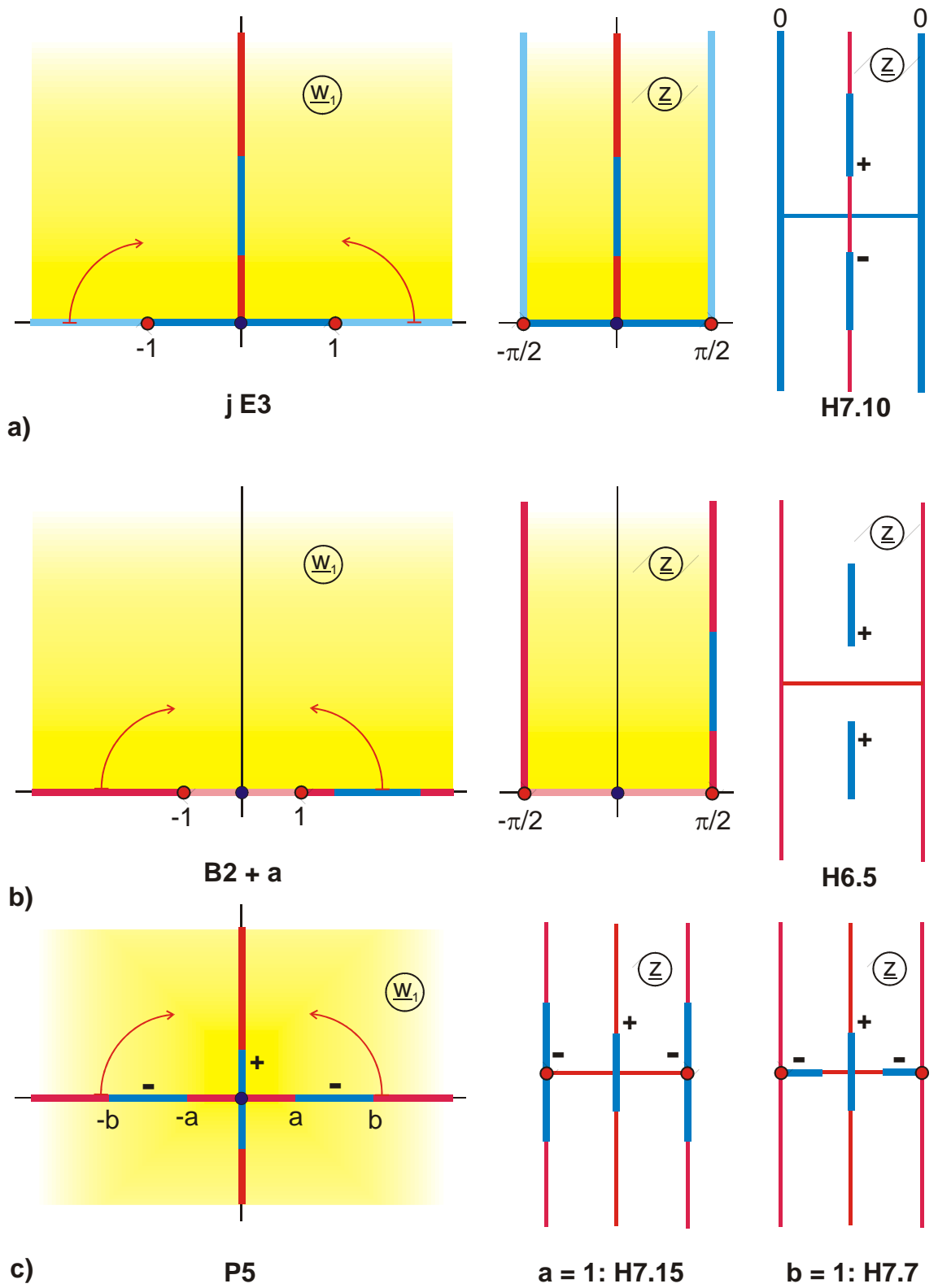
6.2 Arcsine

Figure 6.3 gives an overview, which modifications of a given mapping \underline{w}_1 are obtainable by a successive transformation with the function arcsine. In all three examples the real axis is bent downwards and upwards at ± 1 by 90° , so that a parallel strip of the width π is created. All mappings produced in this manner are single periodic (Group of mappings H) along the real axis. All elements on the real axis and on the imaginary axis of the original mapping \underline{w}_1 maintain their shape (Exception: see Mapping H 6.3). Elements that are on the real axis between -1 and $+1$, are mapped onto the real axis of the z -plane between $-\pi/2$ and $+\pi/2$; all elements outside are mapped onto the straight line $\pm\pi/2 \pm jy$.

Two different results are found in Figure 6.3c, depending upon if $a = 1$ or $b = 1$ in the \underline{w}_1 -plane. [In the first case the function \underline{w}_1 is divided by a , in the second case divided by b].

The successive transformation with the arcsine leads to useful results, if the real axis in the \underline{w}_1 -plane is for $|u_1| \geq 1$ continuously composed of field line segments and/or potential line segments. Then the result is a single periodic function, which can be perpetuated via mirror imaging at $x = \pm \pi/2$.

Successive transformations with the functions $\arccos \underline{w}_1$, $\operatorname{arsinh} \underline{w}_1$ and $\operatorname{arcosh} \underline{w}_1$ yield similar mappings (see Figure 2.5 and Eq. (2.10) through (2.12)).

Figure 6.3: Successive transformations with $\underline{z} = \arcsin \underline{w}_1$

Now the successive transformation with the sine function yields the solution of the problem (Figure 6.5c):

$$\underline{z} = \sin \underline{w}_2. \quad (9)$$

The distances b and c are determined to:

$$jb = \sin[j(a-d)] \Rightarrow b = \sinh(a-d) \quad (10)$$

$$jc = \sin(ja) \Rightarrow c = \sinh a. \quad (11)$$

In the same way Mapping P 2.3 is produced from Mapping H 3, Mapping P 2.2 from Mapping H 2.1 and Mapping P 3.7 from Mapping H 1.6.

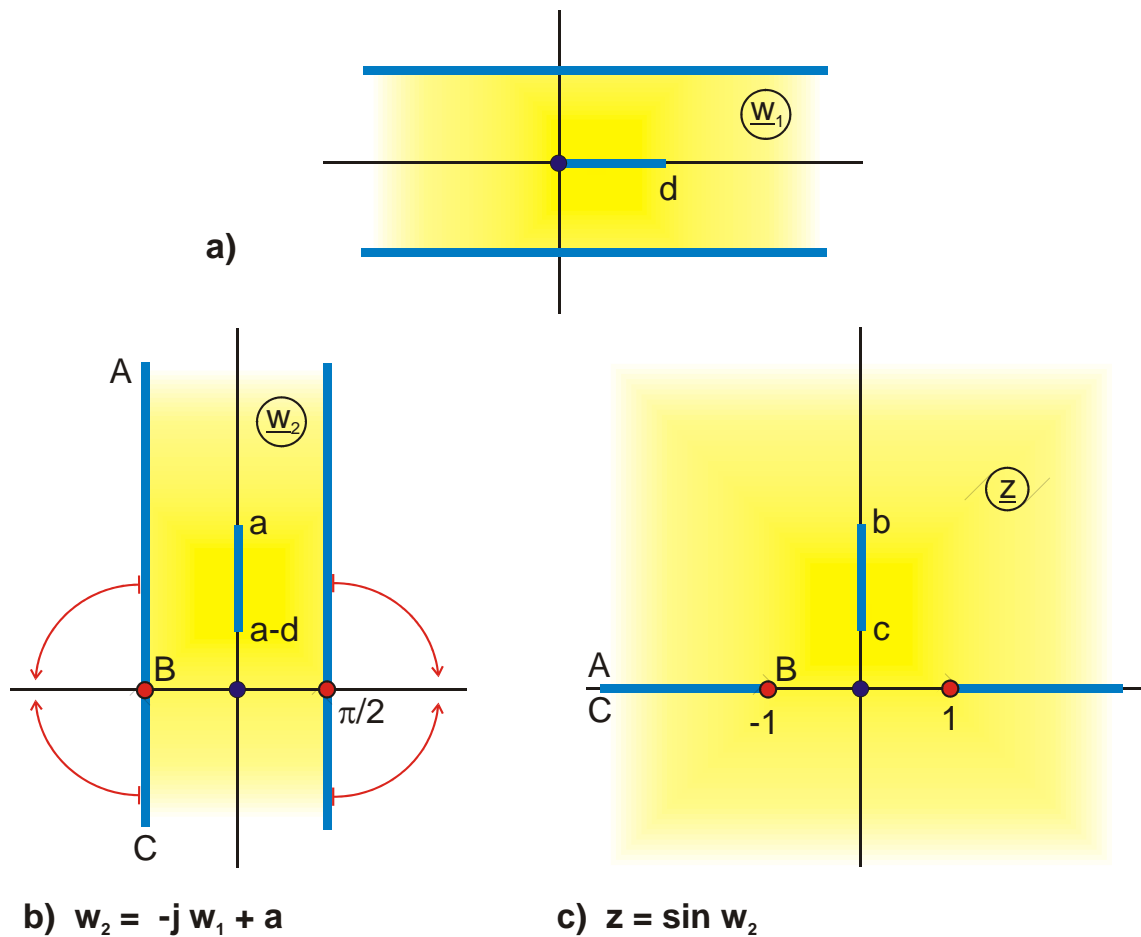


Figure 6.5: Example 2, Mapping P 4.1

Example 3: Conducting strip in elliptical outer conductor

In order to determine the field map of a conducting strip, which is centered inside an elliptic outer conductor, it is possible according to Chapter 5, Example 3, to use the transformation equation $\underline{z} = \cosh(\pi \underline{w})$ (Mapping B 2). All potential lines in this field map of a conducting strip against ∞ are ellipses. Yet this mapping has unfortunately only one freely selectable parameter v_1 . For $a = 1$ holds (Figure 5.4):

$$b = \tanh v_1 \quad (12)$$

$$\text{and} \quad d = 2 / \cosh v_1. \quad (13)$$

The dimension b as well as d is defined by v_1 .

However a field map, where the aspect ratio b/a of the ellipse and the width of the conducting strip d could be preset independently from each other, would be much more useful. To reach this, in Mapping I 2.2 (Figure 6.6a)

$$\underline{w}_1 = F_a \left(\frac{k}{k_1} \operatorname{sn}(\underline{w}, k), k_1 \right), \quad (14)$$

which is generated corresponding to Example 5.7, the width of the rectangle is normalized to $\pi/2$

$$\underline{w}_2 = \frac{\underline{w}_1}{K(k_1)} \cdot \frac{\pi}{2}. \quad (15)$$

Afterwards the rectangle is mapped by the successive transformation with the sine function onto an ellipse. According to Figure 6.4 a straight line parallel to the real axis is mapped onto an elliptical arc in this successive transformation.

$$\underline{z} = \frac{\sin \underline{w}_2}{\cosh(\tau \cdot \pi/2)} \quad (16)$$

In order to normalize the semi-major of the ellipse to the length 1, the mapping is divided by $\cosh(\tau \cdot \pi/2)$. The semi-minor b is then

$$b = \frac{\sinh(\tau \cdot \pi/2)}{\cosh(\tau \cdot \pi/2)} = \tanh(\tau \cdot \pi/2). \quad (17)$$

Provided that the aspect ratio of the ellipse is given, i.e. if $a = 1$ the magnitude of b , then also τ is known

$$\tau = \frac{2}{\pi} \operatorname{ar} \tanh b. \quad (18)$$

τ is the aspect ratio of the resulting rectangle in Mapping I 2.2. With τ the (complementary) modulus k_1 of the elliptic integral of the first kind is defined (see Chapter 13 and 14):

$$k_1 = \left[\vartheta_2(0, \tau) / \vartheta_3(0, \tau) \right]^2. \quad (19)$$

The distance \overline{AE} in the original rectangle in the w_1 - plane has the length f . According to Mapping I 2.2 the length f is defined by the modulus k of the sn function:

$$k = k_1 \cdot \operatorname{sn}(f, k_1). \quad (20)$$

If $\underline{w}_1 = f$ is inserted into Eq. (14), the width of the conducting strip d can be determined with Eq. (16). With the inverse of all three successive transformations, f and hence k can be written as functions of d :

$$k = k_1 \cdot \operatorname{sn} \left\{ \frac{2}{\pi} K(k_1) \cdot \arcsin(a \cdot d), k_1 \right\}. \quad \text{for } k \leq k_1 \quad (21)$$

For the case of a very wide conducting strip as illustrated in Figure 6.6b, the corresponding calculation yields:

$$k = k_1 \cdot \operatorname{Re} \operatorname{sn} \left\{ K(k_1) + j \frac{\pi}{2} K(k_1) \operatorname{arcosh}(a \cdot d), k_1 \right\}. \quad \text{for } k > k_1 \quad (22)$$

Hence all parameters of this mapping are known.

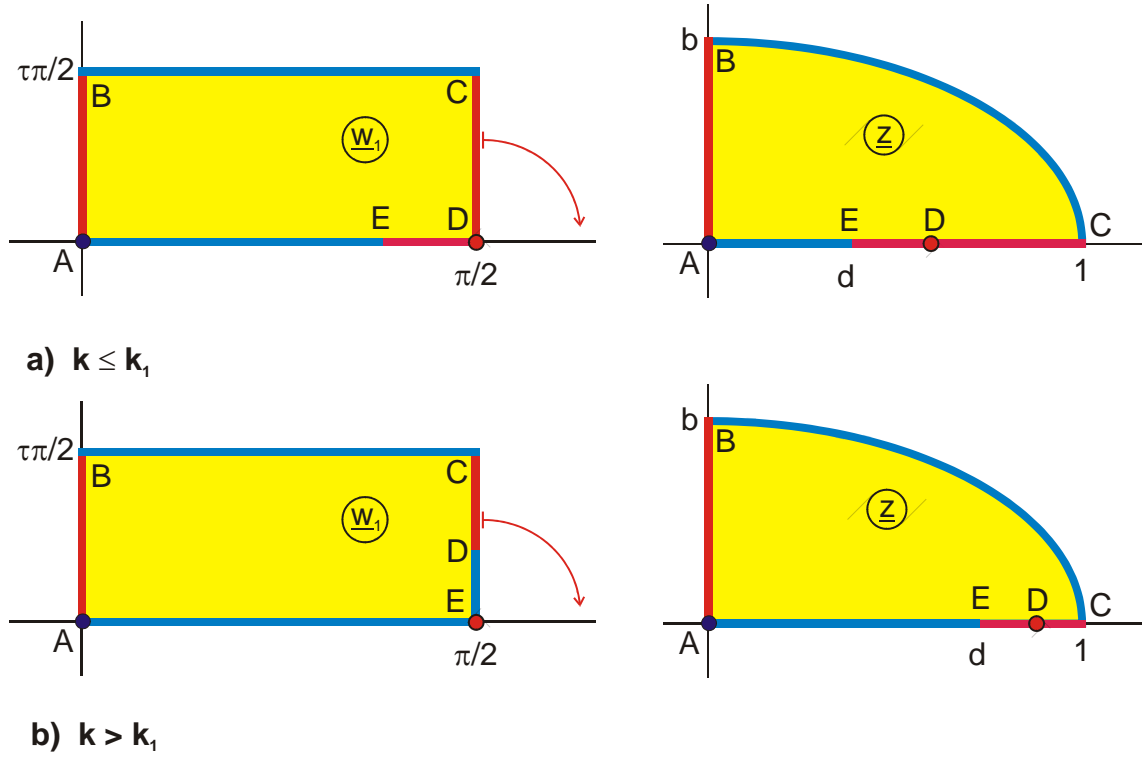


Figure 6.6: Example 3, Mapping F 4.1

Example 4: Conducting strip in a slotted, elliptical outer conductor

Starting point is Mapping H 7.9, rotated by 90° (Figure 6.7):

$$\underline{w}_1 = -j \ln \frac{\vartheta_4 \left\{ \frac{\pi}{2K(k)} (\underline{w} + ja), \tau \right\}}{\vartheta_4 \left\{ \frac{\pi}{2K(k)} (\underline{w} - ja), \tau \right\}} + jb \quad (23)$$

The parallel strip has in this case the width π . By the successive transformation with the sine function

$$\underline{z} = \sin \underline{w}_1 \quad (24)$$

the right half of the lower boundary is bent downwards by 180° in point D. The horizontal strip AGF is transformed into an elliptical arc. The semi axes of the ellipse are:

$$a_1 = \cosh b \quad (25)$$

$$b_1 = \sinh b. \quad (26)$$

If the width of the parallel strip is not normalized to π but to $\pi/2$, the resulting field map is that of a conducting strip in an elliptical outer conductor with two slots.

In an analogous manner like in these 4 examples a multitude of further mappings can be produced from single periodic mappings (Group H and J) and from double periodic mappings (Group I), which are not listed in the table of mappings. Elements along the outer boundary of the half strip and on the imaginary axis maintain their shape. Horizontal straight lines are transformed into elliptical arcs and vertical straight lines into hyperbolic arcs.

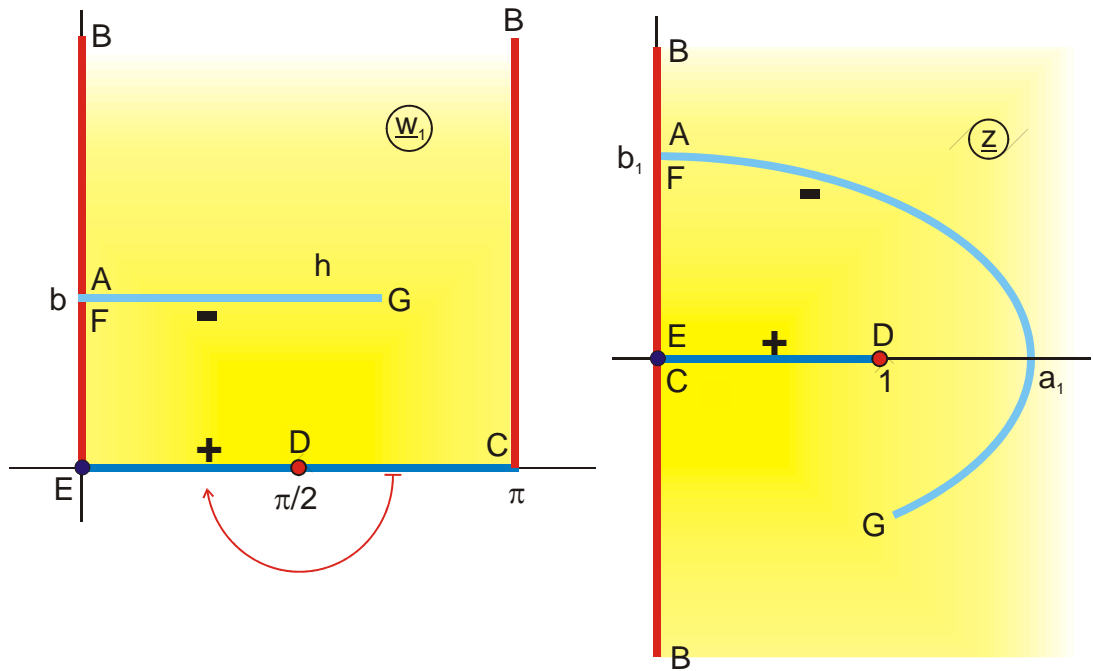


Figure 6.7: Example 4, Mapping F 4.4

6.4 Logarithm

The successive transformation $\underline{z} = \ell n \underline{w}_1$ maps the upper half plane onto a parallel strip of the width π (Figure 6.8). The lower half plane (in Figure 6.8 not shown) is accordingly mapped onto the parallel strip between $y = 0$ and $y = -\pi$. The negative real axis is bent upwards by 180° in the origin, until both axes are parallel to each other. During this rotation the origin moves to the left into the point $-\infty$. All concentric circles around the origin become vertical straight lines; all rays through the origin become horizontal straight lines.

The unit circle is mapped onto the imaginary axis between $y = +\pi$ and $y = -\pi$. The interior of the unit circle goes over into the left half of the parallel strip, the exterior into the right half. The result of this successive transformation is a single periodic mapping.

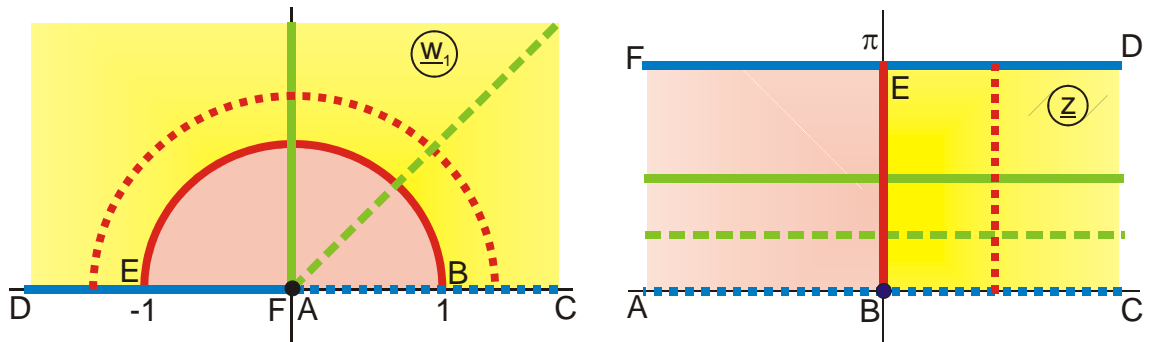


Figure 6.8: The Mapping $\underline{z} = \ln \underline{w}_1$

Figure 6.9 illustrates some examples. In Figure 6.9a the positive imaginary axis \overline{BC} is mapped onto the upper boundary of the parallel strip at $y = \pi/2$ and the negative imaginary axis onto the lower boundary. The origin moves to $-\infty$. In Figure 6.9b the mapping of the boundary is carried out likewise and the two circular arcs are transformed into vertical straight lines.

Figure 6.9c is an example for the mapping of the unit circle onto the imaginary axis between $+\pi$ and $-\pi$.

Figure 6.9d contains the same mapping of the unit circle. The conducting strip on the real axis remains on the real axis.

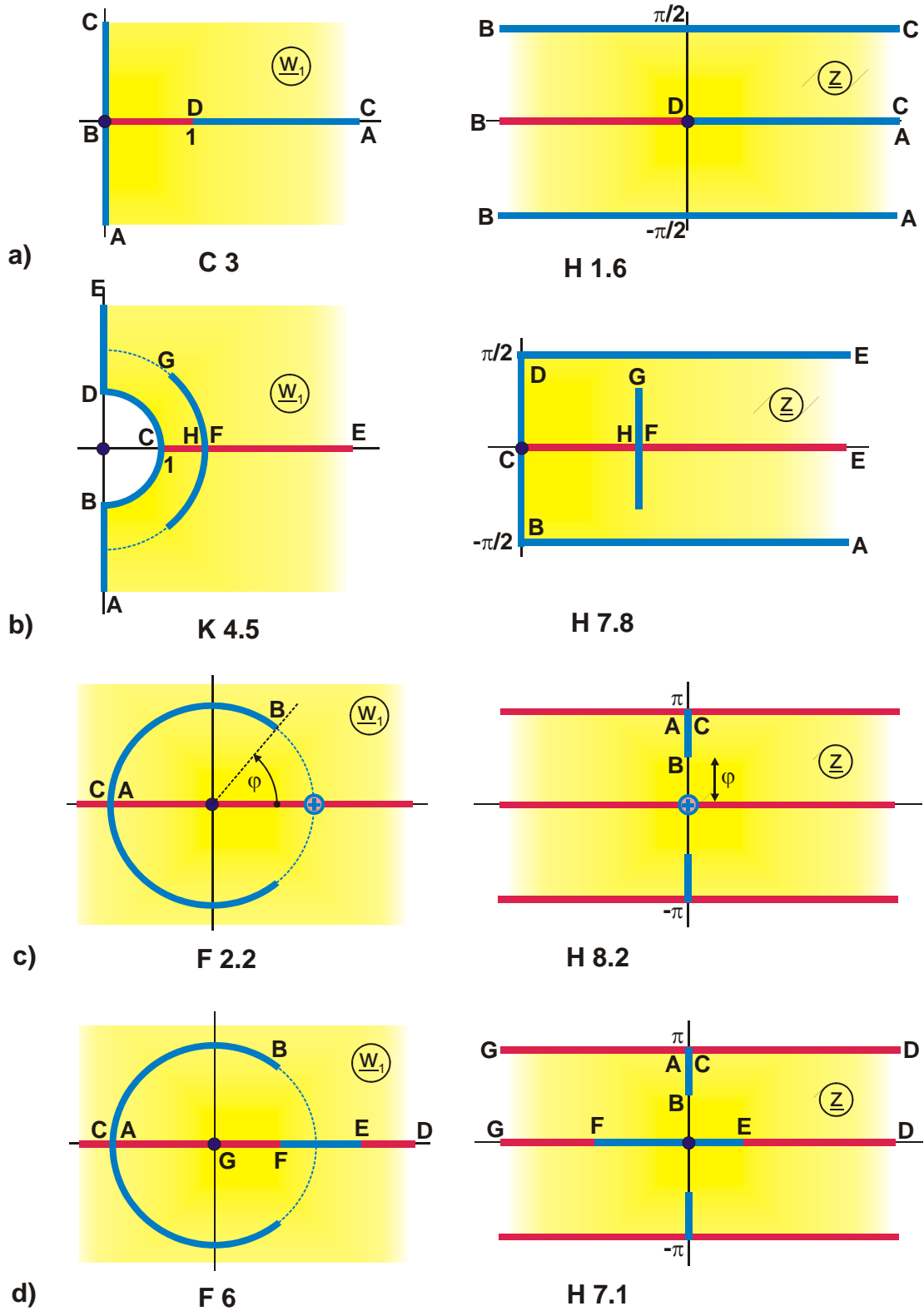


Figure 6.9: Successive transformations with $\underline{z} = \ln \underline{w}_1$

Example 5: Line charges, periodically arranged, displaced against each other

The number of mappings which can be created by successive transformation with the logarithm may be increased, if not only those field maps are transformed, which are symmetrical to the imaginary axis, but also those, which are not symmetrical. It is possible for instance, with the already known field of two equal and opposite line charges (Figure 6.10a), to move the negative line charge into any predefined point. The positive line charge remains at $+1$, in order to be in the origin of the z -plane after the successive transformation. To reach all this, the positive line charge is first moved into the origin $\rightarrow (\underline{w}_1 - 1)$ and the distance is normalized to $1 \rightarrow (\underline{w}_1 - 1) / 2$. Then the predefined distance $(1 + a)$ is created by multiplication with $(1 + a)$ and finally the positive line charge is moved to $+1$ by addition of 1. All steps together yield:

$$\underline{w}_2 = \frac{\underline{w}_1 - 1}{2} (1 + a) + 1. \quad (27)$$

With the successive transformation

$$\underline{z} = \ell n \underline{w}_2 \quad (28)$$

the mapping problem is completed. The displacement d of the negative line charge is:

$$d = \ell n a. \quad (29)$$

For the case illustrated in Figure 6.10b and c the coordinates a and d are negative.

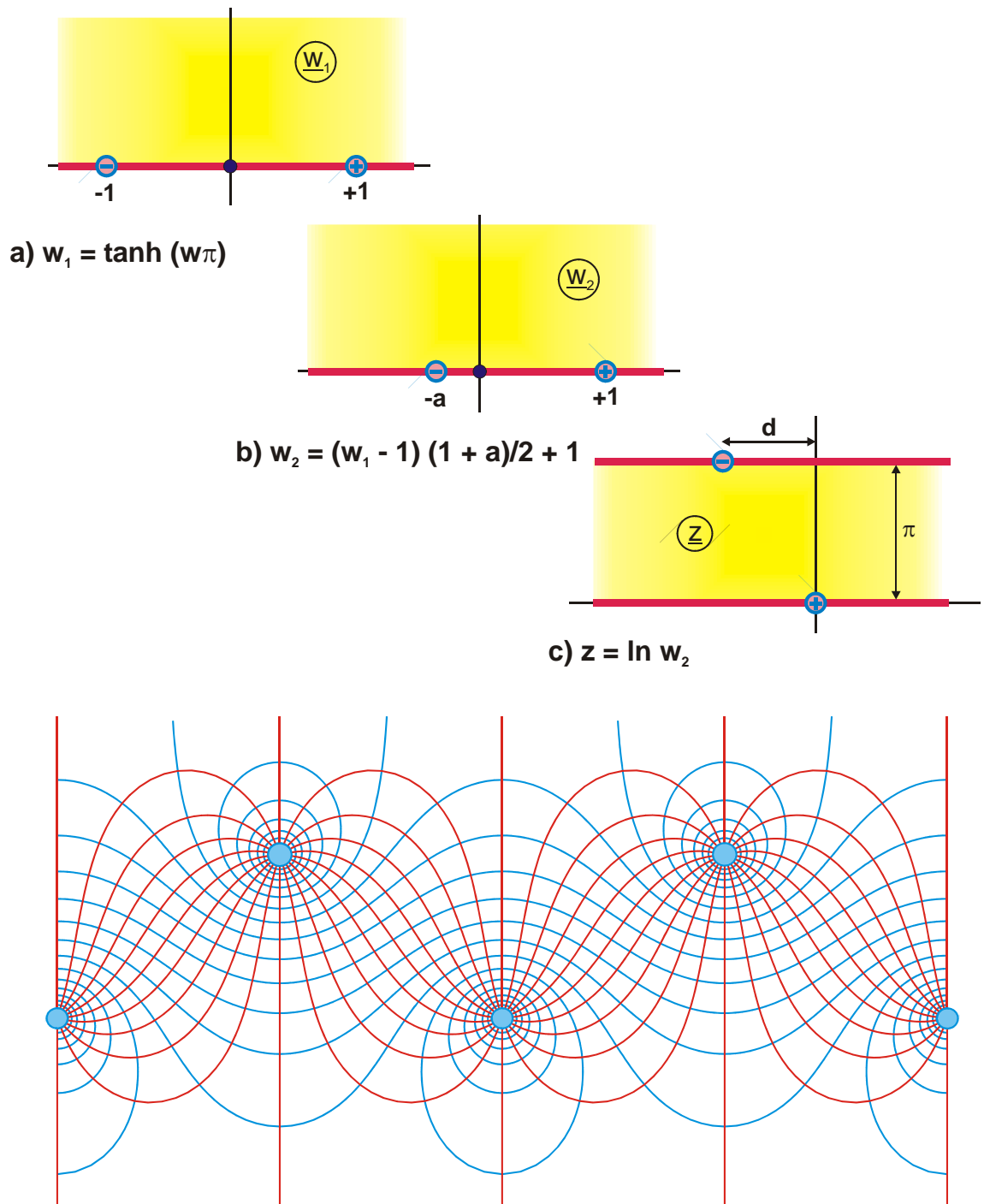


Figure 6.10: Example 5, Mapping H 5

Example 6: Asymmetrical stripline

Mapping E 5 is the field map of a conducting strip in front of a conducting plane, which is rotated by the angle α from the horizontal, (Figure 6.11). With the successive transformation

$$\underline{z} = \ell \ln \underline{w}_1 \quad (30)$$

the surface of the conducting plane in the IV. quadrant (straight line \overline{AB})

$$\underline{w}_1 = r \cdot e^{-j\alpha} \quad (31)$$

is mapped onto a horizontal straight line, displaced by $-j\alpha$.

$$\underline{z} = \ell \ln r - j\alpha \quad (32)$$

and the surface of the conducting plane in the II. quadrant (straight line \overline{AC})

$$\underline{w}_1 = r \cdot e^{j(\pi-\alpha)} \quad (33)$$

is mapped onto a horizontal straight line, displaced by $j(\pi - \alpha)$

$$\underline{z} = \ell \ln r + j(\pi - \alpha). \quad (34)$$

The width s of the conducting strip is

$$s = \ell \ln h = -\ell \ln(1/h). \quad (35)$$

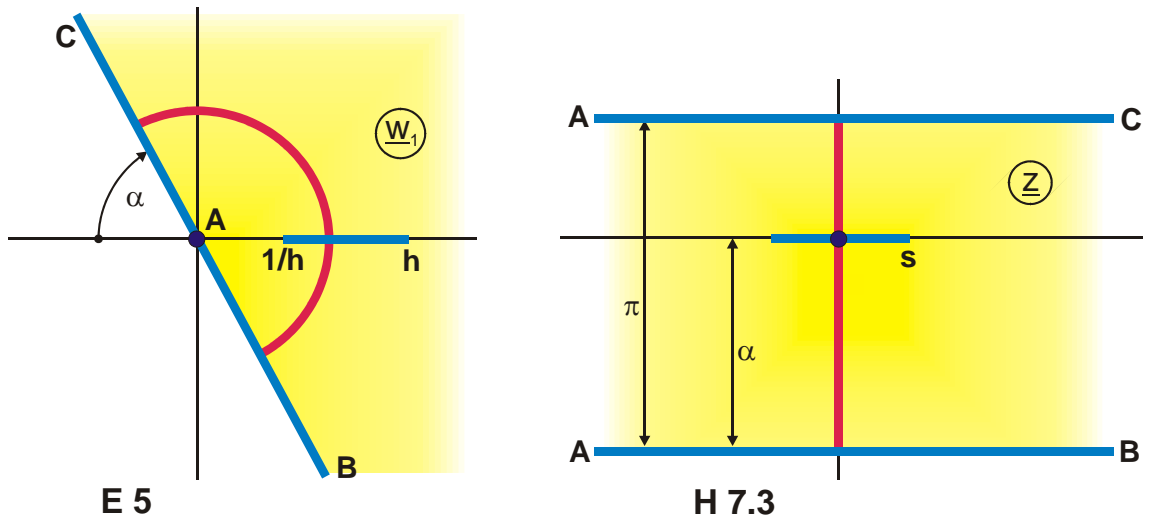


Figure 6.11: Example 6, Mapping H 7.3

6.5 Exponential function

The mapping properties of the exponential function can be directly extracted from the preceding chapter, because it is the inverse of the logarithm. Only the sequence of the mappings has to be exchanged in the Figures 6.8 and 6.9. The exponential function maps the right side onto the left side.

Further examples are compiled in Figure 6.12. Figure 6.12a and b illustrate how horizontal straight lines are transformed into rays through the origin. By the successive transformation with the exponential function, the upper boundary is rotated to the left by 180° , comparable to the course of motions, when the cover of a thick book is opened, and at the same time the point $-\infty$ moves into the origin of the z -plane. The Figures 6.10c, d and e contain examples, how vertical straight lines are transformed into circular arcs. Straight line segments on the imaginary axis are transformed into sectors of the unit circle.

All illustrated examples can be modified, if the parallel strip of the initial mapping is not normalized to the width π but to the width α . Thus the angle α is created in the z -plane. This means that (if the positive real axis remains fixed) the negative real axis together with all other boundaries along this axis, can be rotated around the origin, upwards as well as downwards, depending upon the magnitude of α , i.e. if α is chosen $\alpha > \pi$ or $\alpha < \pi$.

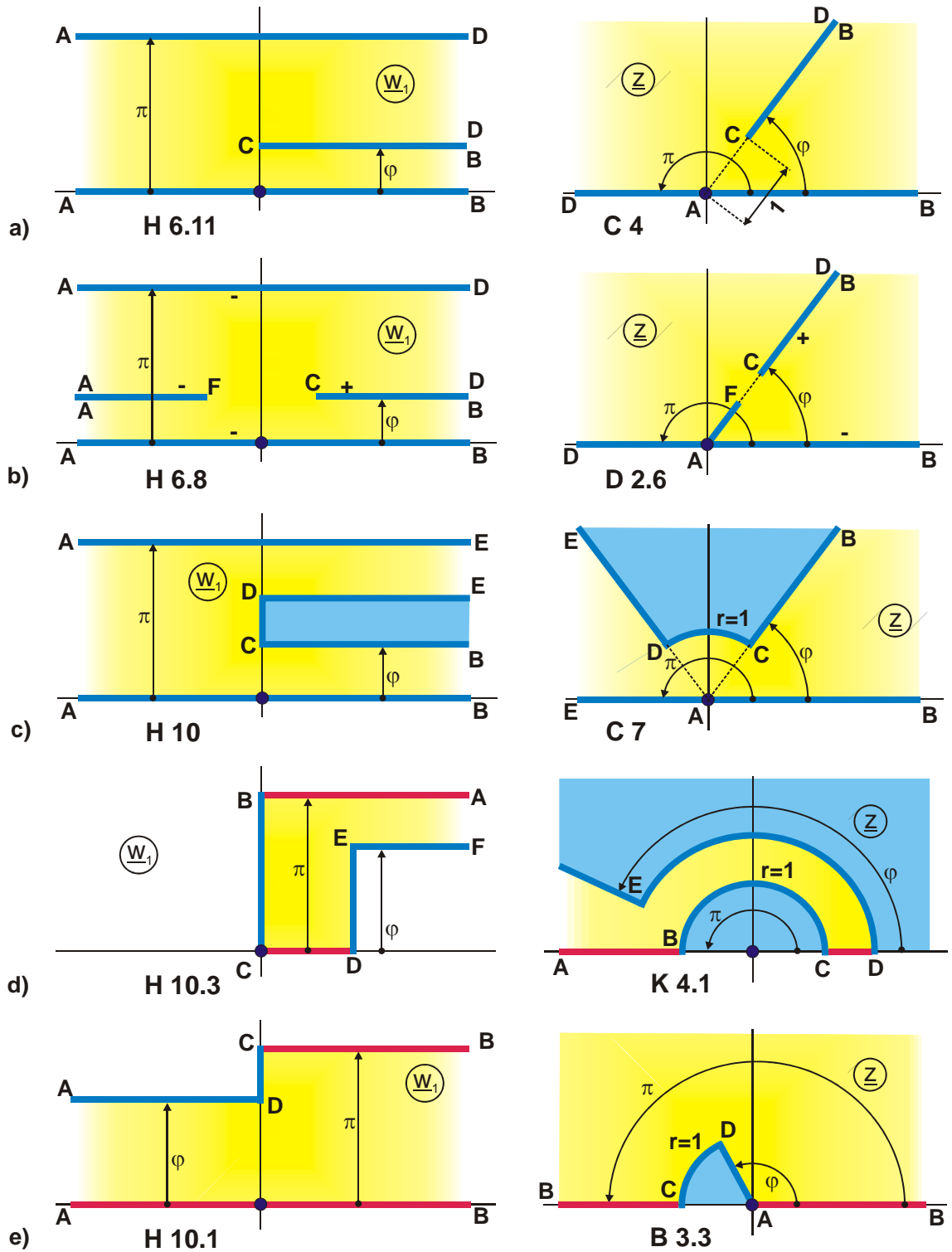


Figure 6.12: Successive transformations with the exponential function,

$$\underline{z} = \exp \underline{w}_1$$

Example 7: Line charge between two concentric metal cylinders

A successive transformation with the exponential function is not only possible for single periodic functions, but also for double periodic functions. As an example for this, the field map of a line charge inside a rectangle is the starting point (Figure 6.13). The initial mapping I 1.1

$$\underline{w}_1 = F_a(a + jb \cdot \tanh(\underline{w} \pi), k) \quad (36)$$

is converted such that the rectangle is located in the II. quadrant and that its height is φ

$$\underline{w}_2 = \varphi \cdot \left(\frac{\underline{w}_1}{K'(k)} - \frac{K(k)}{K'(k)} \right) = \varphi \left(\frac{\underline{w}_1}{K'(k)} - \frac{1}{\tau} \right). \quad (37)$$

Thus it is obtained that the straight line \overline{DC} is on the unit circle after the successive transformation

$$\underline{z} = \exp(\underline{w}_2) \quad (38)$$

and that the circular arc has the aperture angle φ . This follows immediately from Eq. (38) by insertion of $\underline{w}_2 = j\varphi$. The complete rectangle is mapped onto a segment of an annulus. The radius of the inner circle r is found by insertion of point A:

$$r = \exp\left(-\frac{\varphi}{2\tau}\right). \quad (39)$$

The line charge, in the w_2 -plane at $\underline{r}_0 = \alpha + j\beta$, is mapped onto

$$\underline{r}_1 = \exp(\underline{r}_0) = e^\alpha \cdot e^{j\beta}. \quad (40)$$

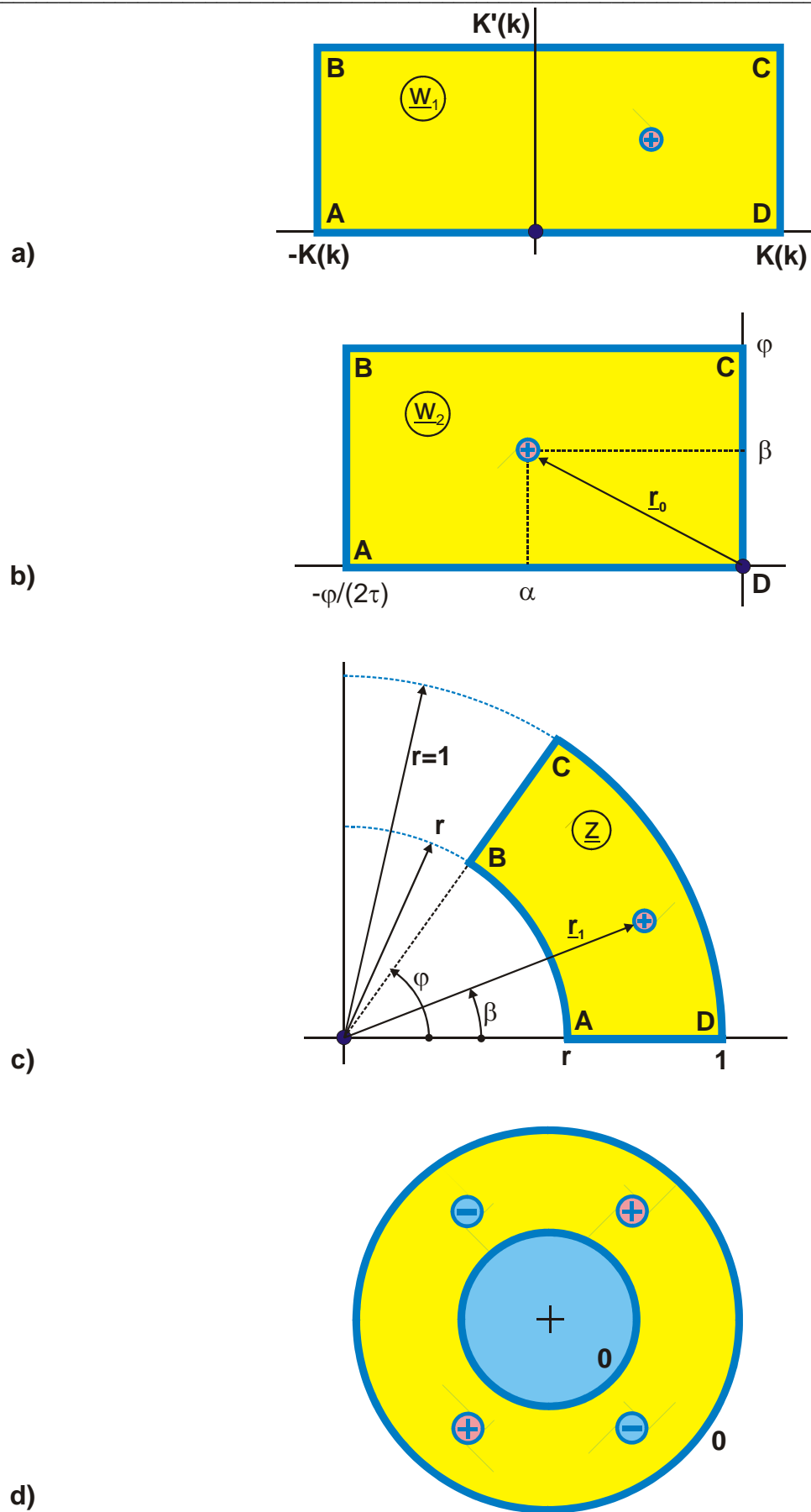


Figure 6.13: Example 7, Mapping G 7

By modification of a and b the line charge can be positioned anywhere within the segment of the annulus. The corresponding equations are assembled in Mapping G 7. If φ is set to $\pi/2$, then the result is, complemented to a configuration with radial symmetry, the field map of 4 line charges of equal size and opposite sign between two grounded, concentric circular cylinders (Figure 6.13d). Further examples for this type of successive transformation are the Mappings G 7.1 through G 7.3.

6.6 The function $\underline{z} = 1/\underline{w}_1$

If a given mapping is inverted with $\underline{z} = 1/\underline{w}_1$, due to

$$\frac{1}{r \cdot e^{j\varphi}} = \frac{1}{r} \cdot e^{-j\varphi} \quad (41)$$

all points outside the unit circle are transformed into points inside the unit circle. The upper half plane is mapped onto the lower and vice versa. Only the points $+1$ and -1 stay unchanged. As Figure 6.14 illustrates, rays through the origin are again mapped onto rays through the origin. Horizontal and vertical straight lines go over into sets of mutually perpendicular circles through the origin. In general circular arcs in arbitrary positions in the w_1 -plane are transformed into circular arcs in the z -plane. The point ∞ is mapped into the origin.

Figure 6.15 illustrates the effect of the inversion on various mappings. In Figure 6.15a the two conducting strips on the real axis remain there, and the negative charge at infinity is mapped into the origin. Figure 6.15b illustrates the reverse effect. A ray from ∞ to B is mapped into the origin. Figure 6.15c illustrates the reverse effect. A ray from ∞ to B is transformed into a ray from B to the origin. Basically it is valid for all examples that the mapping sequence can also be reversed. Because the reciprocal function of the inversion is again the inversion, all mappings on the left side are created by inverting the mapping on the right side. Figure 6.15c illustrates, that a straight line \overline{BA} , parallel

to one axis turns into a semi circle and Figure 6.15d is an example for the mirror image of a mapping in the unit circle. Figure 6.15e illustrates, that two straight lines starting in the same point, are transformed into a biangle. Their intersecting angle φ is preserved. Because the two straight lines intersect at the point ∞ with the same angle φ , the resultant biangle is symmetric.

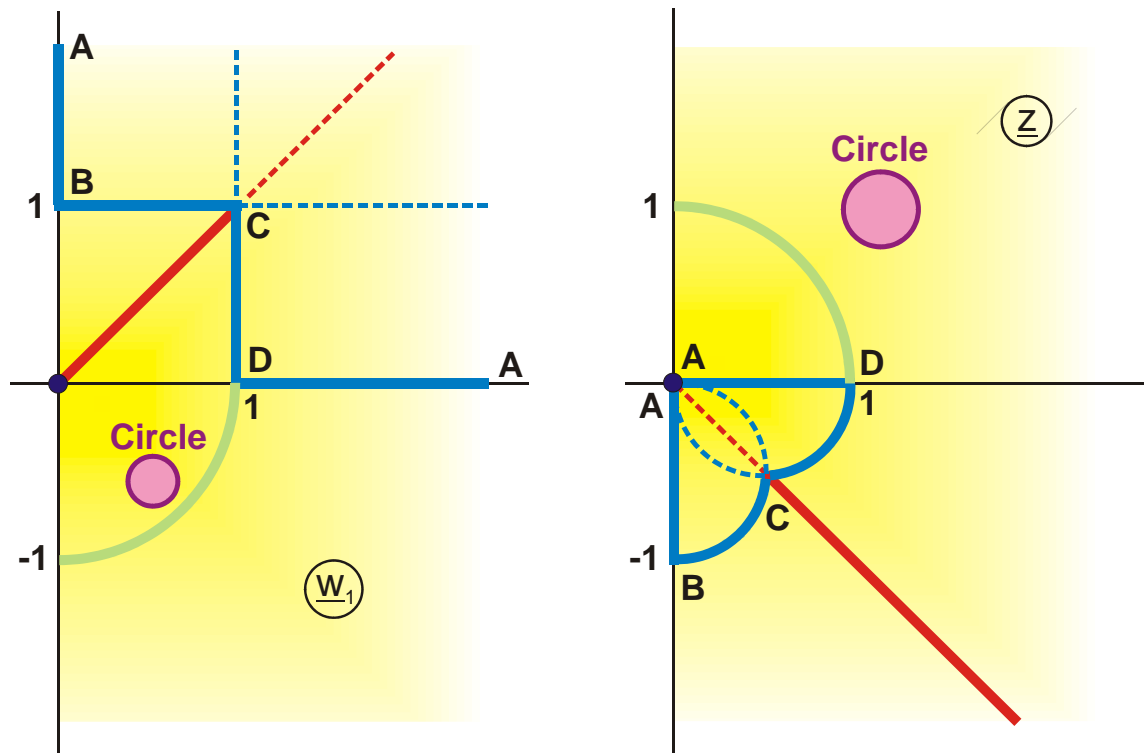


Figure 6.14: The Mapping $\underline{z} = 1/\underline{w}_1$

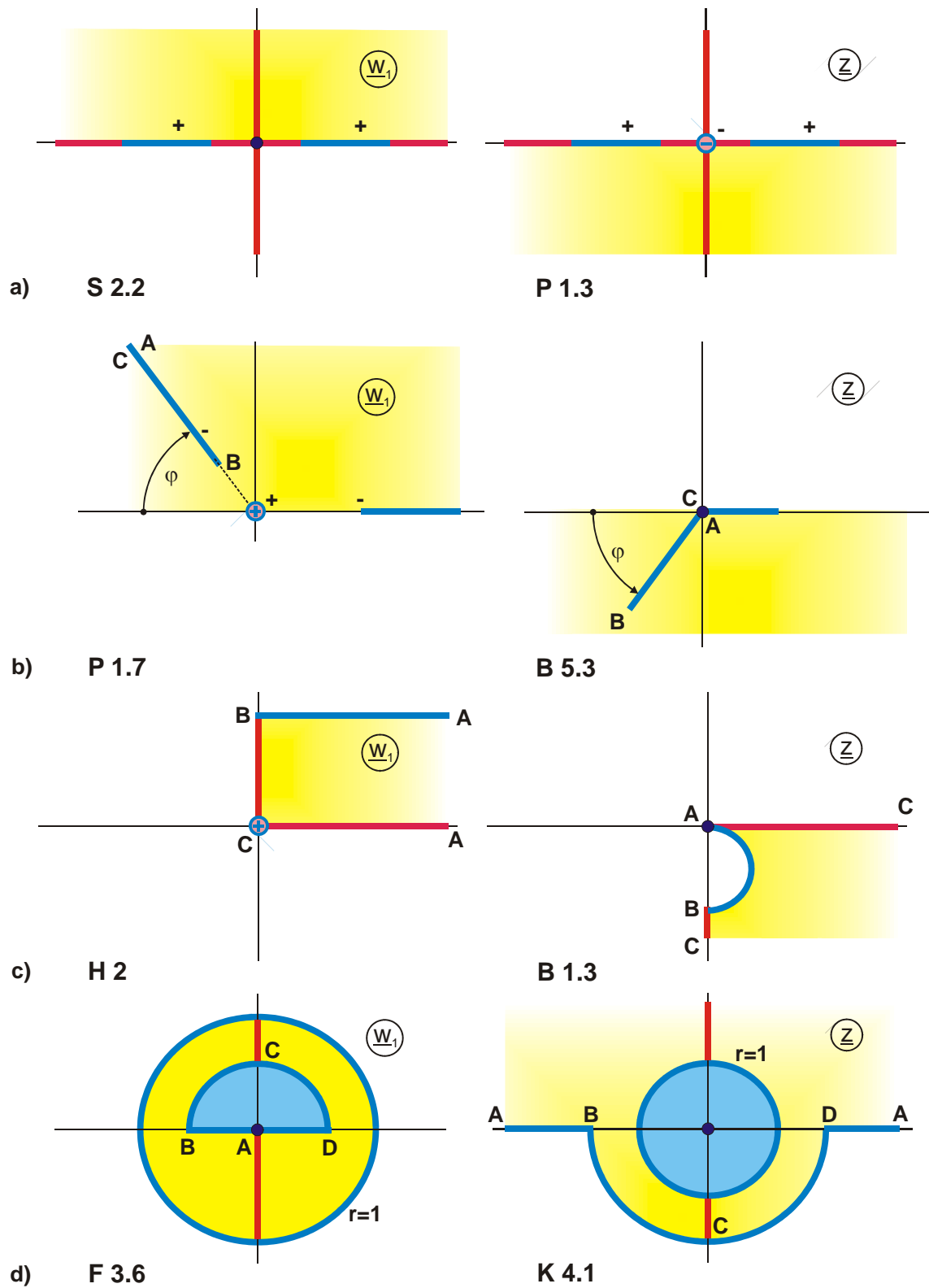


Figure 6.15: Successive transformations with $\underline{z} = 1/\underline{w}_1$

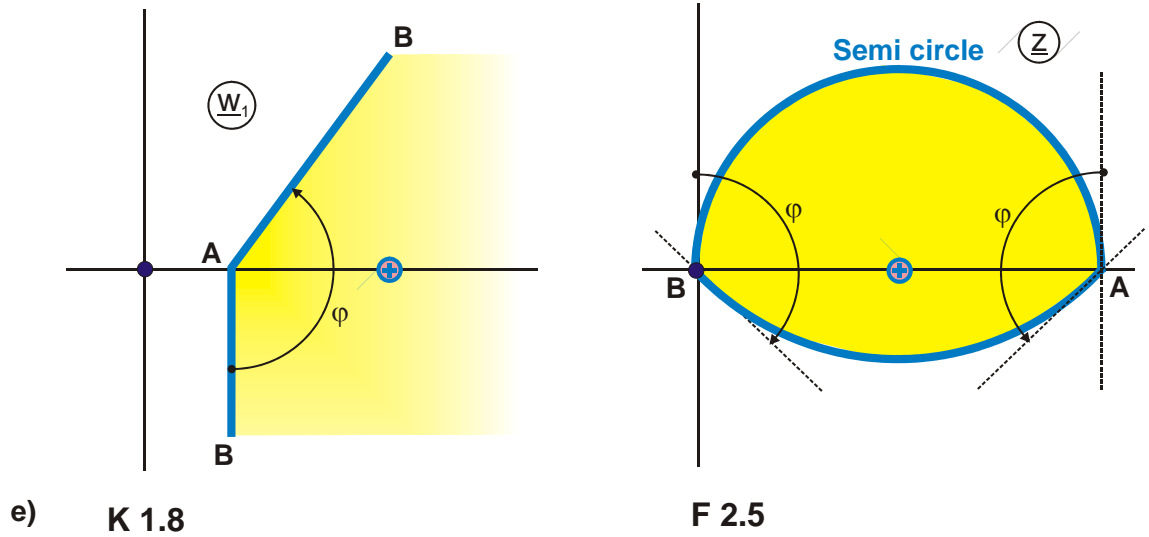


Figure 6.15: Successive transformations with $\underline{z} = 1/\underline{w}_1$

Example 8: Field map I of a conducting strip against a circular cylinder

As a vertical straight line, which does not coincide with a coordinate axis, is according to Figure 6.14 mapped onto a circle, the field map of a strip against a conducting plane (Mapping E 3) is used as initial mapping.

$$\underline{w}_1 = \operatorname{sn}(\underline{w}, k). \quad (42)$$

This mapping is multiplied by a , in order to get a further parameter, and the conducting plane is displaced from the origin by 1

$$\underline{w}_2 = 1 + a \cdot \underline{w}_1. \quad (43)$$

After the successive transformation

$$\underline{w}_3 = 1/\underline{w}_2 \quad (44)$$

the conducting plane goes over into a circle through the points 1 and 0; the strip maintains its shape. Only the length is altered.

Hence the objective is achieved. Because of normalization reasons of the field maps in the table of mappings, the center point of the circle is moved into the origin and the radius is set to 1

$$\underline{z} = \left(\underline{w}_3 - \frac{1}{2} \right) \cdot 2. \quad (45)$$

The end points of the strips are thus found as (Figure 6.16d):

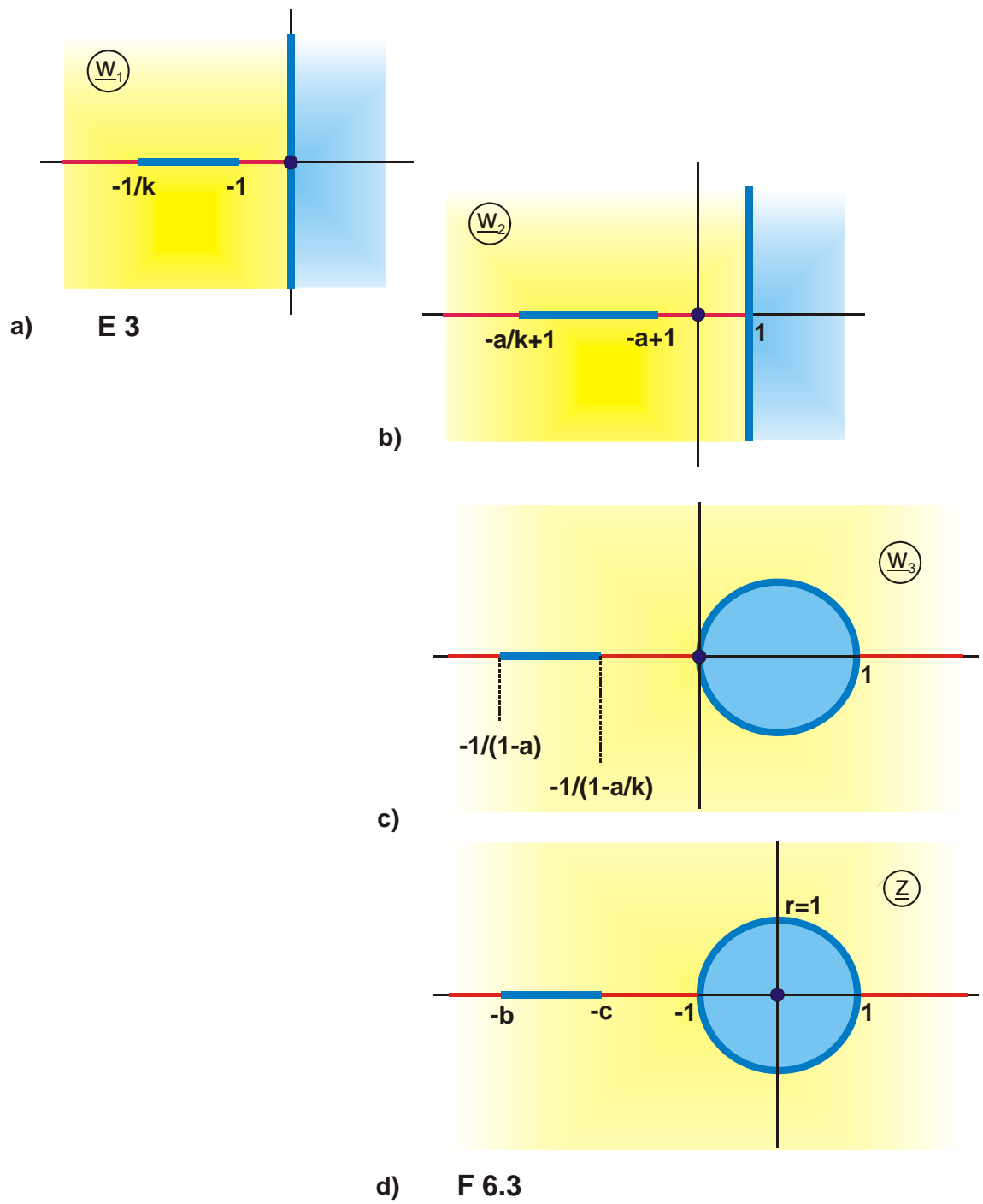
$$-b = \left(\frac{1}{1-a} - \frac{1}{2} \right) 2 = \frac{1+a}{1-a} \quad (46)$$

$$-c = \left(\frac{1}{1-a/k} - \frac{1}{2} \right) 2 = \frac{1+a/k}{1-a/k}. \quad (47)$$

The equations (43) through (45) can be combined to

$$\left(\frac{1}{1+a\underline{w}_1} - \frac{1}{2} \right) 2 = \frac{1-a\underline{w}_1}{1+a\underline{w}_1}. \quad (48)$$

Instead of the 3 single steps in Figure 6.16 it is as well possible to utilize directly a successive transformation with this special case of the bilinear transformation. Equation (48) maps the imaginary axis onto the unit circle. The left half plane is transformed into the exterior and the right half plane into the interior of the unit circle.

Figure 6.16: Example 8, Mapping $F_{6.3}$

Example 9: Field map II of a conducting strip against a circular cylinder

In the case that the conducting strip is rotated by 90° (Figure 17d), a more suitable starting point is Mapping F 3.1.

$$\underline{w}_1 = r \cdot \frac{\wp_4 \left\{ \frac{\pi}{2K(k)} (\underline{w} + j a), \tau \right\}}{\wp_4 \left\{ \frac{\pi}{2K(k)} (\underline{w} - j a), \tau \right\}}. \quad (49)$$

The field map is moved out of the origin by r

$$\underline{w}_2 = r + \underline{w}_1, \quad (50)$$

in order to achieve that the inner circular arc lies on a circle through the origin. With the successive transformation

$$\underline{w}_3 = 1/\underline{w}_2, \quad (51)$$

this arc is mapped onto a vertical straight line, the conducting strip sought-after. The outer circular cylinder remains a circular cylinder (Circles are mapped onto circles). In order to standardize the mappings, the radius of the circle is normalized to 1 and the center is moved back into the origin.

$$\underline{z} = r + \underline{w}_3 / \rho. \quad (52)$$

With the successive transformation $\underline{z} = 1/\underline{w}_1$ circles are indeed mapped onto circles, but concentric circles do not remain concentric. The common center $\underline{w}_2 = r$ of the two circular cylinders in Figure 17b is not preserved. The new center M of the outer circle has to be determined from the geometry of Figure 17c:

$$\rho = \left(\frac{1}{1+r} + \frac{1}{1-r} \right) / 2 = \frac{1}{1-r^2} \quad (53)$$

$$M = \frac{1}{r-1} + \rho = -\frac{r}{1-r^2} = -\rho \cdot r. \quad (54)$$

The height b of the strip is found from

$$\underline{r}_1 = \frac{1}{r + r \cdot \exp(-j\varphi)} \quad (55)$$

$$b = \frac{1}{\rho} \operatorname{Im} \underline{r}_1. \quad (56)$$

The distance from the center s follows with Eq. (52):

$$s = r + \frac{1}{2r\rho}. \quad (57)$$

Mapping F 6.6 is a modification of this mapping. As it is evident when examining Figure 6.17, a multiplication of the initial mapping in Figure 6.17a with $\exp(j\beta)$ creates a displacement of the conducting strip in Figure 6.17d in vertical direction. For a positive angle β the circular arc electrode is rotated in mathematically positive sense. The conducting strip moves downwards while the distance s and the location of the circular cylinder remain unchanged. The geometry of the electrodes is therefore no longer symmetrical with respect to the real axis.

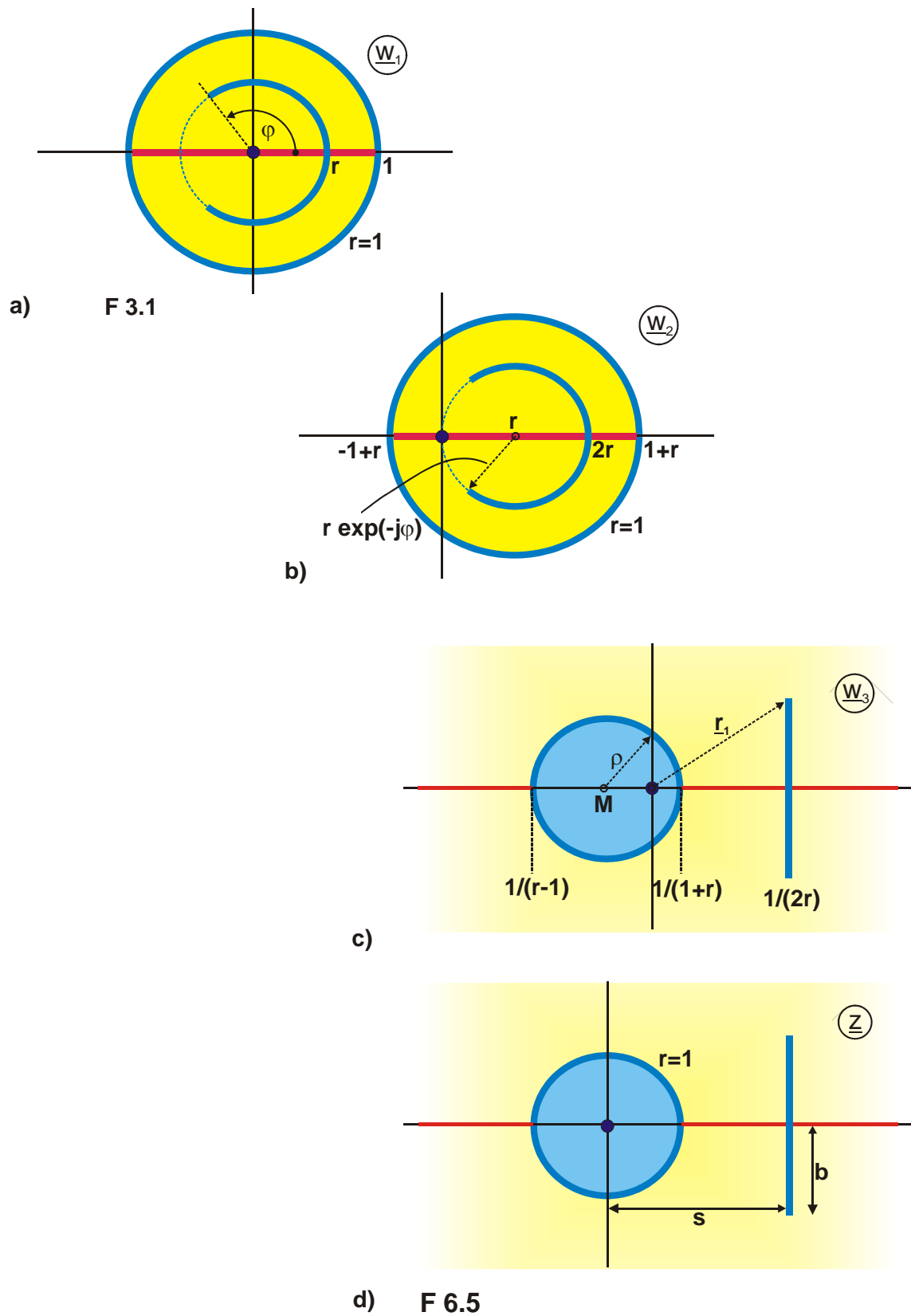


Figure 6.17: Example 9, Mapping F 6.5

6.7 Transformation of Regions

The preceding chapters have illustrated how a given mapping can be deliberately transformed into another mapping by a successive transformation with an elementary function. Of course it is also possible to employ more complicated functions to solve a given mapping problem and also to execute several successive transformations consecutively. Another target oriented procedure in this context is, to transform a complete region in a given mapping into a differently shaped region. For this purpose Chapter 6.8 contains an assembly of frequently used transformations of regions. The procedure is illustrated with some examples.

Example 10: Vertical strip against horizontal strip

In order to create the field map of a vertical strip against a horizontal strip (Figure 6.10c), where all dimensions are arbitrarily selectable, Mapping E 3 is chosen as initial mapping

$$\underline{w}_1 = \operatorname{sn}(\underline{w}, k) . \quad (58)$$

With the conversion

$$\underline{w}_2 = j \cdot a \cdot \underline{w}_1 \quad (59)$$

the field map of a vertical strip against a conducting plane is found. Now the upper half plane is mapped onto the exterior of a conducting strip with mapping of regions X 6 as successive transformation

$$\underline{z} = -2 \frac{\underline{w}_2}{1 + \underline{w}_2^2} . \quad (60)$$

Due to the fact that in this mapping the imaginary axis is again mapped onto the imaginary axis, the vertical strip is maintained. The conducting plane (the real axis) is folded up into a horizontal strip.

The coordinates of the vertical strip are found by insertion of the points E and D in Eq. (60). Point E is moved from $\underline{w}_2 = j a$ onto $j h = -2 j a / (1 - a^2)$:

$$h = \frac{2 a}{a^2 - 1}. \quad (61)$$

Point D is moved from $\underline{w}_2 = j a / k$ onto $\underline{z} = j d$ with

$$d = \frac{2 a k}{a^2 - k^2}. \quad (62)$$

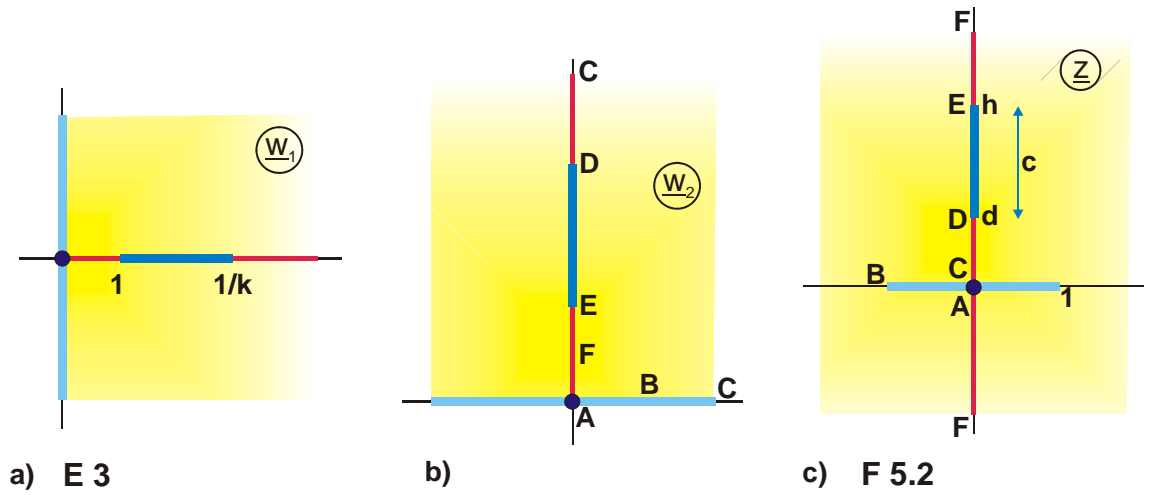


Figure 6.18: Example 10, Mapping F 5.2

Example 11: Strip against rectangular cylinder

With the mapping of regions X 12 a strip on the real axis between -1 and $+1$ can be transformed into a rectangle. Hence the field map is found with the result of the preceding Example 10

$$\underline{w}_1 = -2 \frac{j a \operatorname{sn}(\underline{w}, k)}{1 - a^2 \operatorname{sn}^2(\underline{w}, k)} \quad (63)$$

and the successive transformation

$$\underline{z} = B_a \left(\frac{\underline{w}_1}{k_1}, k_1 \right) + j b_1 . \quad (64)$$

The sides a_1 and b_1 are functions of the modulus k_1

$$a_1 = \frac{E(k_1) - k_1'^2 K(k_1)}{k_1'^2} \quad (65)$$

$$b_1 = \frac{E'(k_1)}{k_1'^2} - K'(k_1) . \quad (66)$$

The vertical strip on the imaginary axis is maintained. The new coordinates of the strip are determined by insertion of the corresponding two points

$$h_1 = \operatorname{Im} B_a \left(j \frac{h}{k_1}, k_1 \right) + b_1 \quad (67)$$

$$d_1 = \operatorname{Im} B_a \left(j \frac{d}{k_1}, k_1 \right) + b_1 . \quad (68)$$

Like in the Examples 10 and 11 the mapping of regions as successive transformation opens the possibility to transform a specific region in a given field map into another region with different shape. In this way it is without any difficulty possible, to transform e.g. a strip into a circle or into an ellipse and the other way round to transform circles or ellipses into a strip. Nevertheless it has to be kept in mind that the remaining field map

is transformed as well. In case the electrodes outside the mapped region are not located on symmetry planes, it is possible only in a few special cases to describe the shape of the transformed electrode configuration with simple analytical functions. One of those special cases is given in the following example.

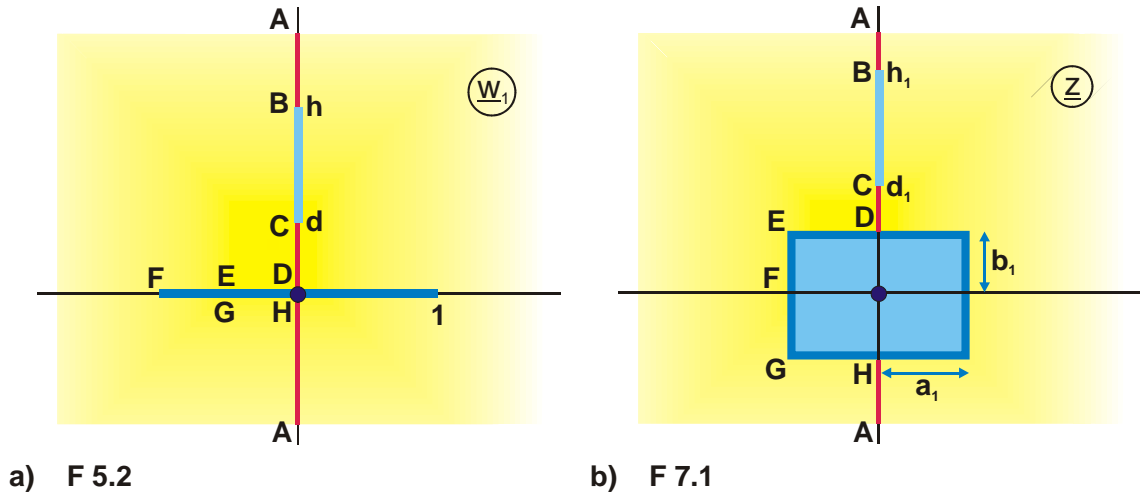


Figure 6.19: Example 11, Mapping F 7.1

Example 12: Strip and circular arc

The mapping of regions X 6 used in Example 10

$$\underline{z} = -2 \frac{\underline{w}_1}{1 + \underline{w}_1^2} \quad (69)$$

does not only fold up the real axis into a strip, but at the same time maps the upper half of the unit circle onto the real axis for $|x| \geq 1$.

If the initial field map is chosen according to Figure 6.20a, where the oblique strip is mirror imaged at the unit circle, then after the mapping of regions with Eq. (69) this strip is transformed into a circular arc and the unit circle becomes part of the real axis.

1. The transformation equations f_I and f_{II} , which have the regions I and II as resulting field map, are gathered from the table of mappings.
2. Transformation equation f_I is inverted into f_I^{-1} .
3. Function f_I^{-1} is used as pre-transformation for the function f_{II} .

Example 13: 2 Circles onto 2 strips

As an example for this procedure the region exterior to two circles of the same size shall be mapped onto the region exterior to two coplanar strips. Function f_I is found with Mapping E 1.1

$$f_I: \quad \underline{w}_1 = \frac{1}{r_1} \tanh(\underline{w}_2 \pi) \quad (70)$$

with

$$r_1 = \frac{1}{\sinh(2\pi u_c)} \quad (71)$$

and

$$u_c = \frac{1}{2\pi} \cdot \operatorname{ar sinh} \sqrt{d^2 - 1} . \quad (72)$$

This function maps according to Figure 6.21 the interior of a rectangle onto the region between two circles of the same size.

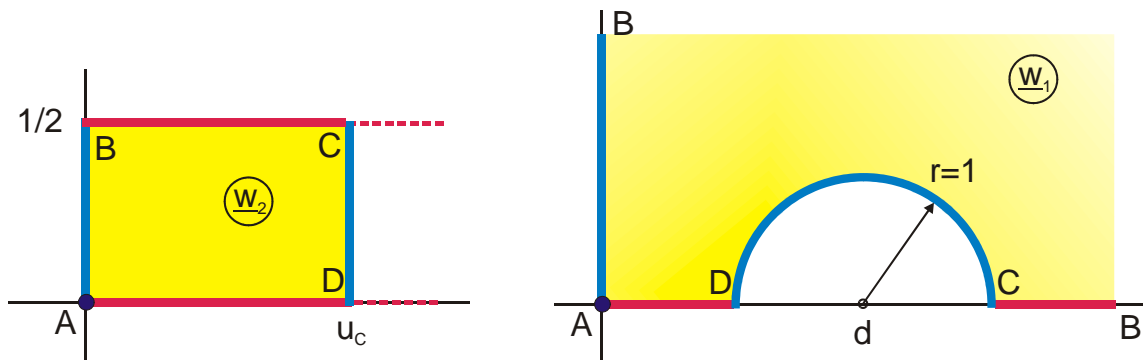


Figure 6.21: Function f_I from Example 13, only the I. quadrant of the mapping is shown

The function f_{II} is found with Mapping E 3

$$f_{II} : \quad \underline{z} = \operatorname{sn}(\underline{w}_3, k) \quad (73)$$

and maps the interior of a rectangle onto the region exterior to two coplanar strips (Figure 6.22).

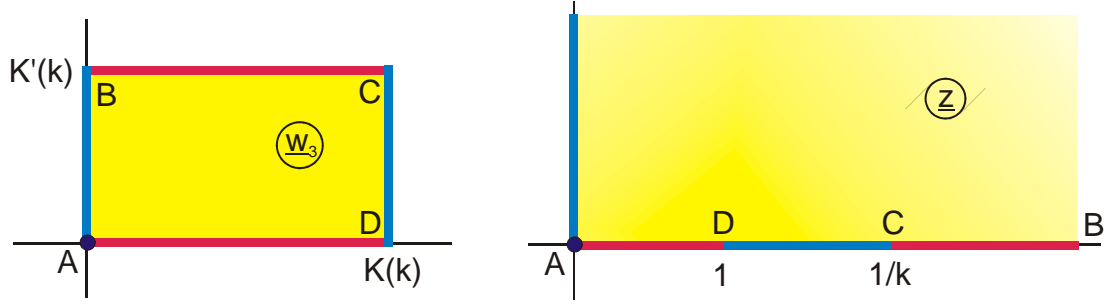


Figure 6.22: Function f_{II} from Example 13

In Figure 6.23 the final result due to three successive mappings is illustrated. The inverse of f_I

$$f_I^{-1} : \quad \underline{w}_2 = \frac{1}{\pi} \operatorname{ar tanh}(r_1 \cdot \underline{w}_1) \quad (74)$$

maps the region exterior to two circles onto the interior of a rectangle. With the in-between mapping

$$\underline{w}_3 = \frac{\underline{w}_2}{u_c} \cdot K(k) \quad (75)$$

with

$$\tau = \frac{K'(k)}{K(k)} = \frac{1}{2u_c} \quad (76)$$

and

$$k = \left[\vartheta_2(0, \tau) / \vartheta_3(0, \tau) \right]^2 \quad (77)$$

this rectangle is converted such that it is of the same shape as that, which belongs to the function f_{II} . The complete mapping, from plane w_1 onto plane z is found by inserting the equations (73) through (75) into one another:

$$\underline{z} = \operatorname{sn} \left[\frac{K(k)}{u_c \cdot \pi} \cdot \operatorname{ar} \tanh (r_1 \cdot \underline{w}_1), k \right]. \quad (78)$$

This function maps two circles of the same size onto two strips of the same size. The inverse function, which can be written down immediately, accordingly maps two strips onto two circles.

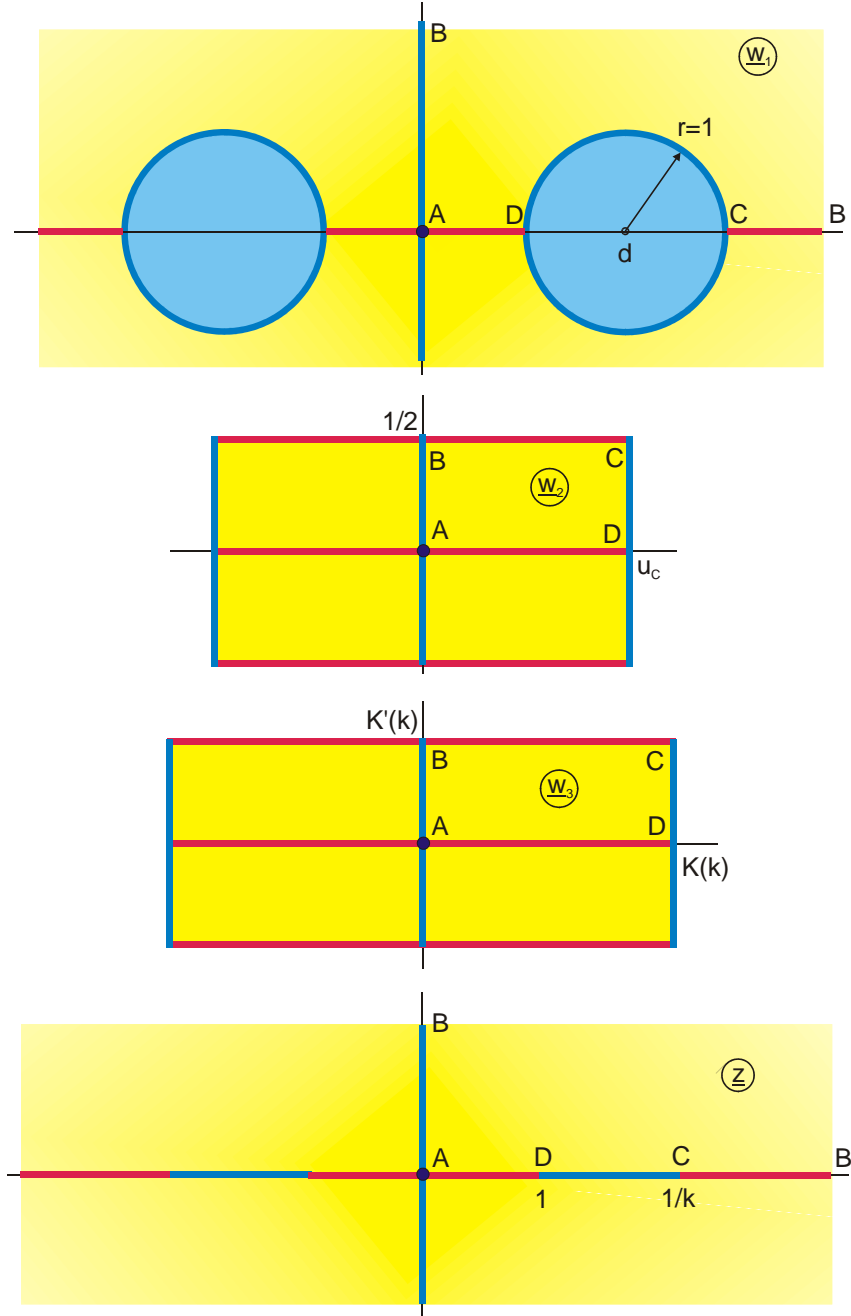
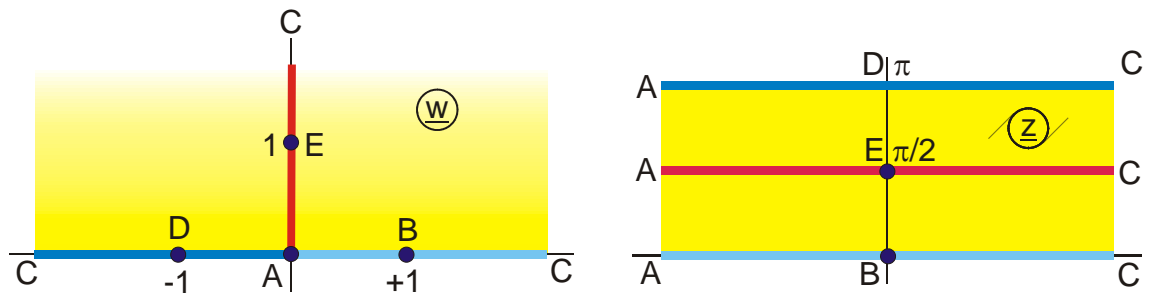


Figure 6.23: Complete sequence of mappings for Example 13

6.8 Table of Transformations of Regions

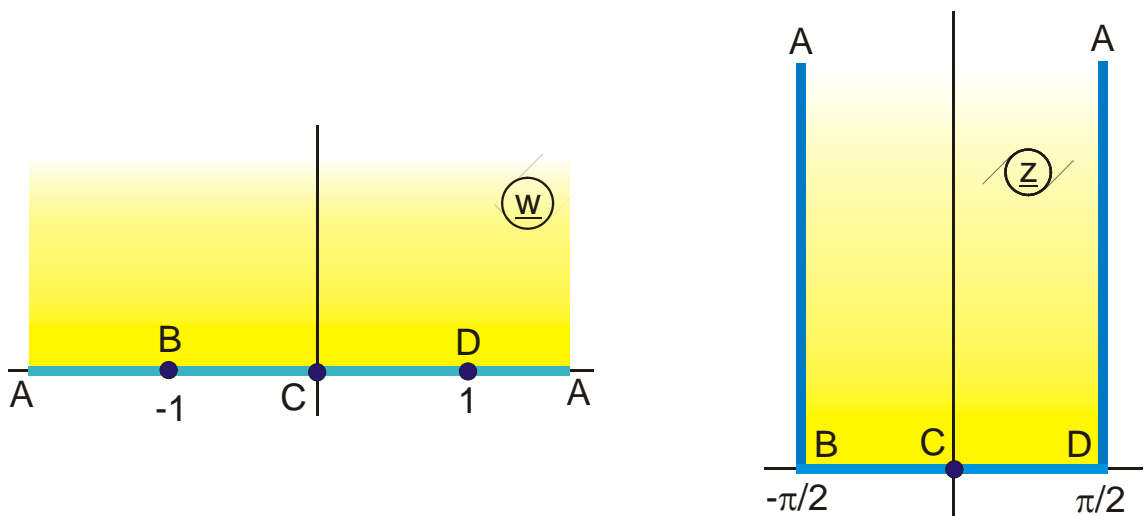
1. Upper half plane onto parallel strip

$$z = \ln w_1$$



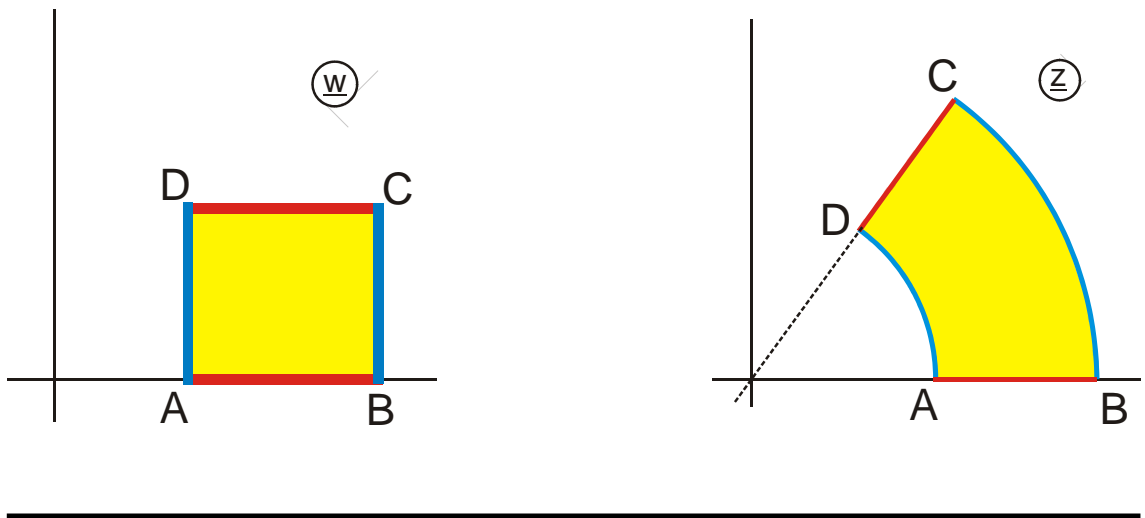
2. Upper half plane onto half strip

$$z = \arcsin w_1$$



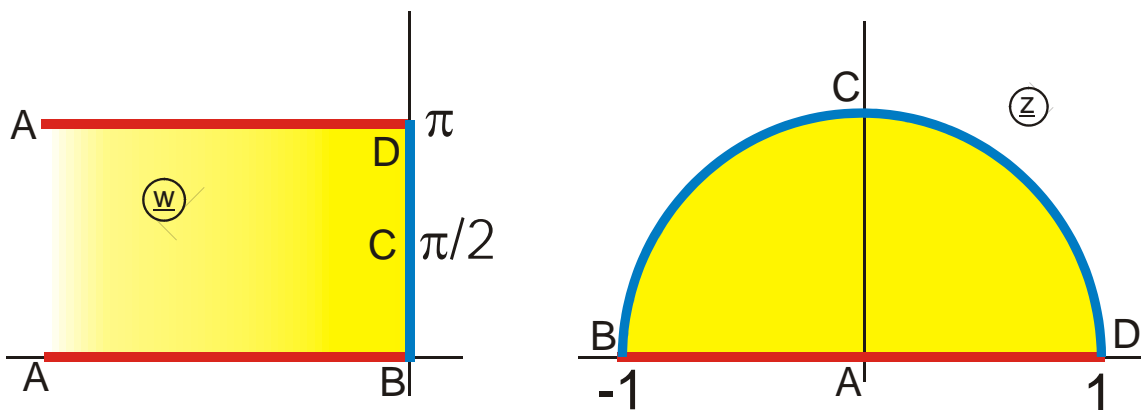
3. Interior of rectangle onto the interior of a sector of an annulus

$$z = \exp w$$



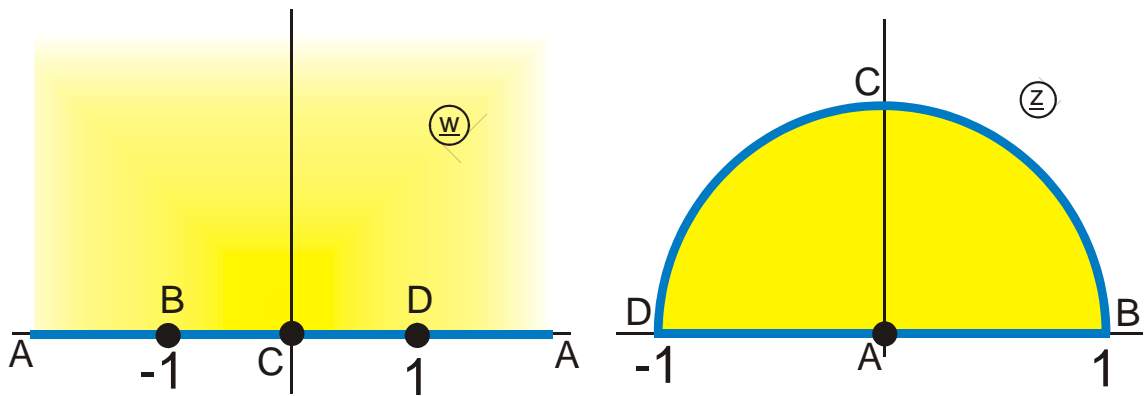
4. Half strip onto interior of semi circle

$$z = \exp w$$



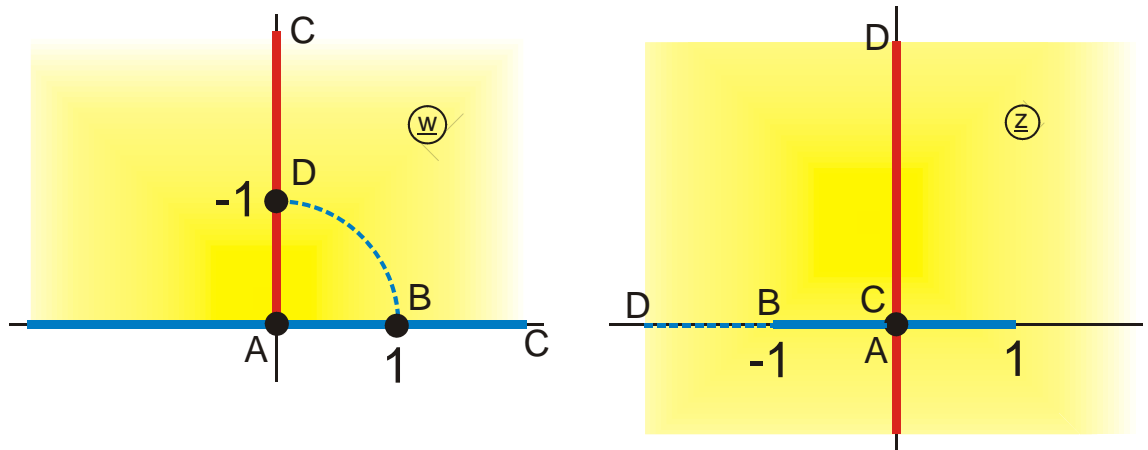
5. Upper half plane onto interior of semi circle

$$z = \sqrt{w^2 - 1} - w$$



6. Upper half plane onto strip

$$z = -2 \frac{w}{1 + w^2}$$

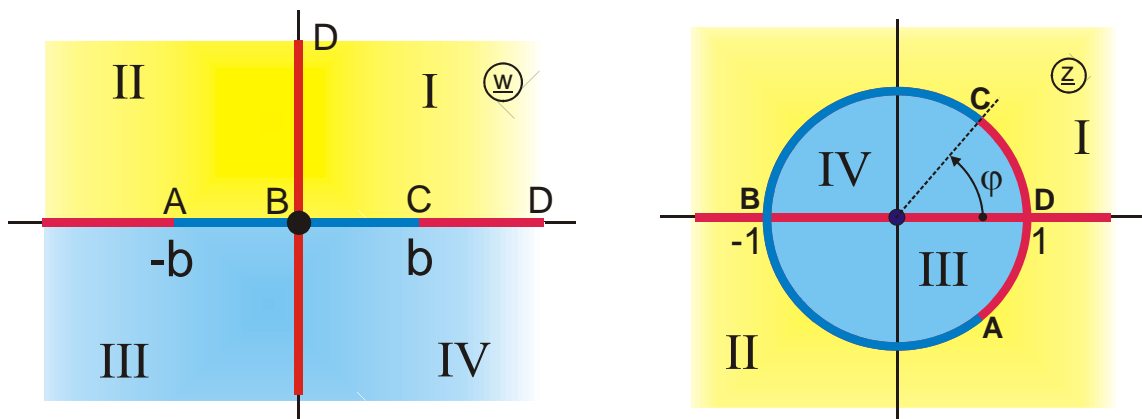
Dipole at C in the z -plane

7. Upper half plane onto exterior of circle

Lower half plane onto interior of circle

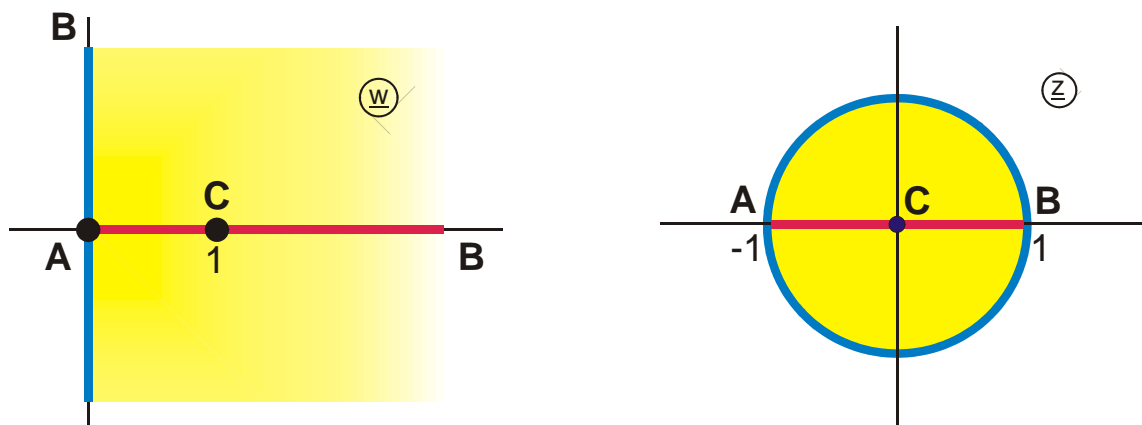
$$z = \frac{w + j}{w - j}$$

$$b = \frac{1}{\tan(\varphi/2)}$$



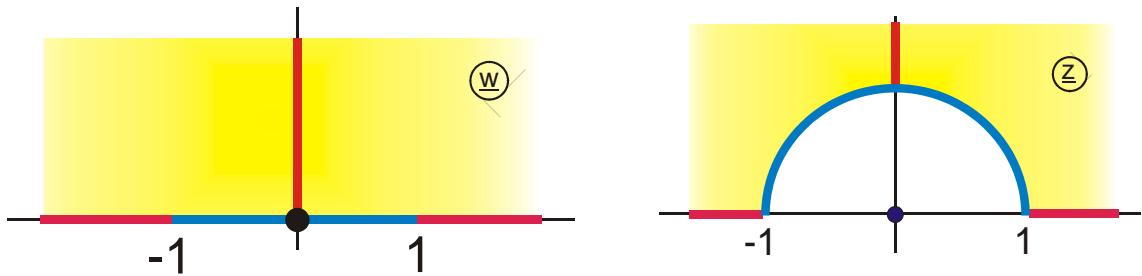
8. Right half plane onto interior of circle (Smith-Diagram)

$$z = \frac{w - 1}{w + 1}$$



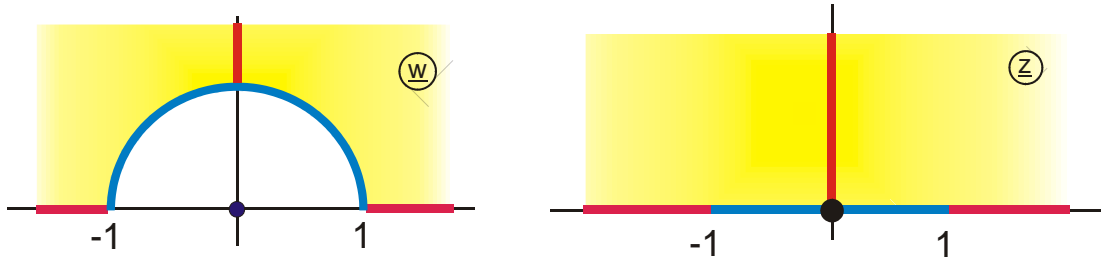
9. Strip onto circle

$$z = w + \sqrt{w^2 + 1}$$



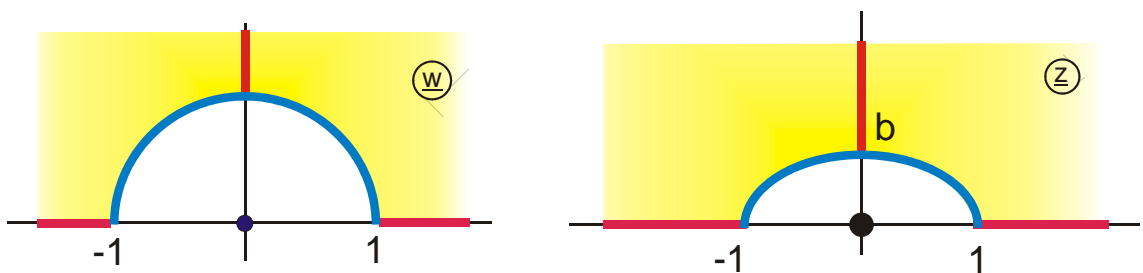
10. Circle onto strip

$$z = \frac{1}{2}(w + 1/w)$$



11. Circle onto ellipse

$$z = \frac{1}{2} \left\{ w(1+b) + \frac{1-b}{w} \right\}$$

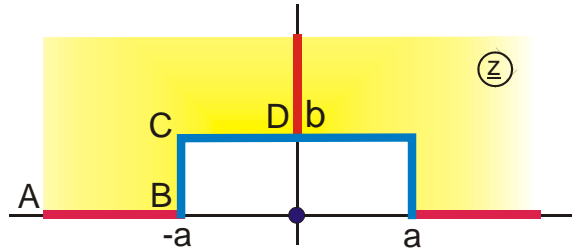
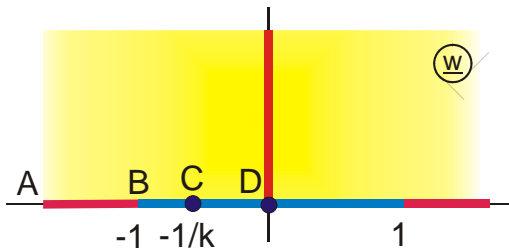


12. Strip onto rectangle

$$z = B_a \left(\frac{w}{k}, k \right) + jb$$

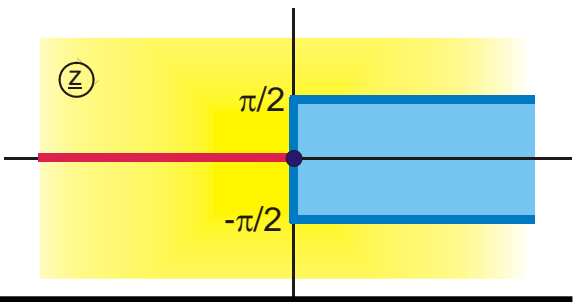
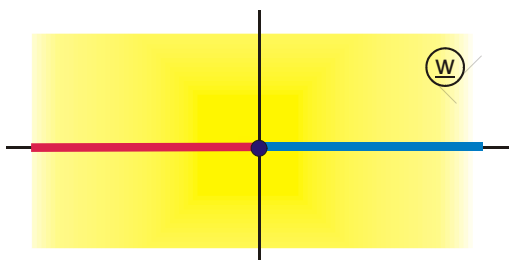
$$a = \frac{E(k) - k'^2 K(k)}{k^2}$$

$$b = \frac{E'(k)}{k^2} - K'(k)$$



13. Half straight line onto half strip

$$z = \sqrt{w(w-1)} + j \arcsin \sqrt{w}$$



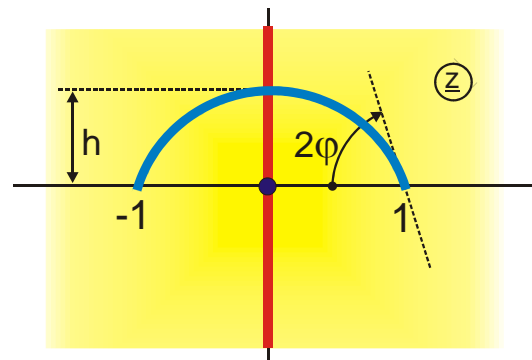
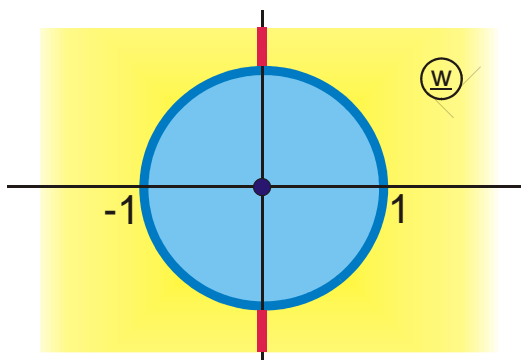
14. Circle onto circular arc

$$z = \frac{1}{2} (w_1 + 1/w_1)$$

$$w_1 = \frac{w + j \sin \varphi}{\cos \varphi}$$

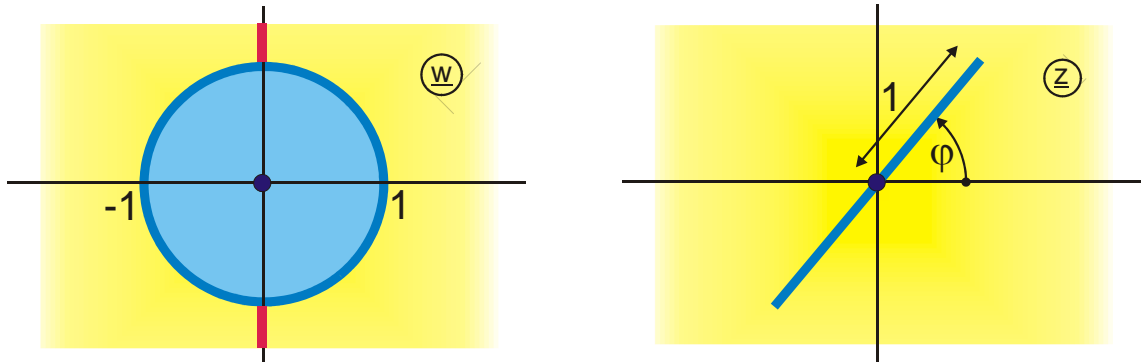
$$h = \tan \varphi$$

$$r = 1/\sin(2\varphi)$$



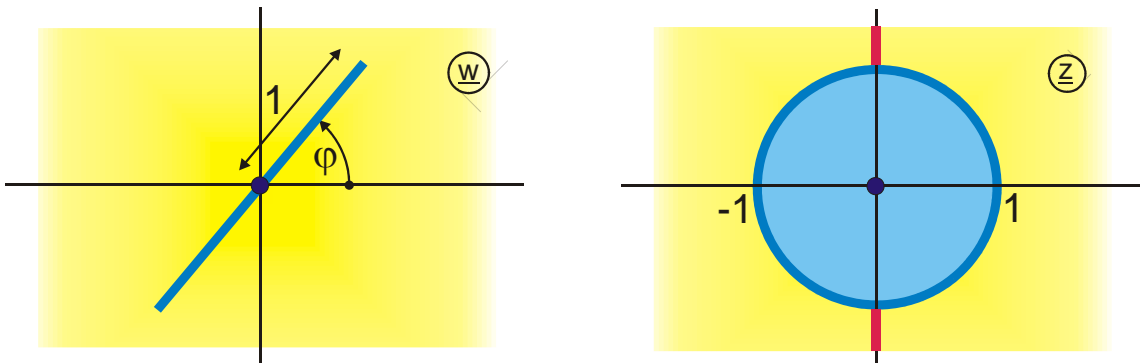
15. Circle onto rotated strip

$$z = \frac{1}{2} \left(w + \frac{\exp(j2\varphi)}{w} \right)$$



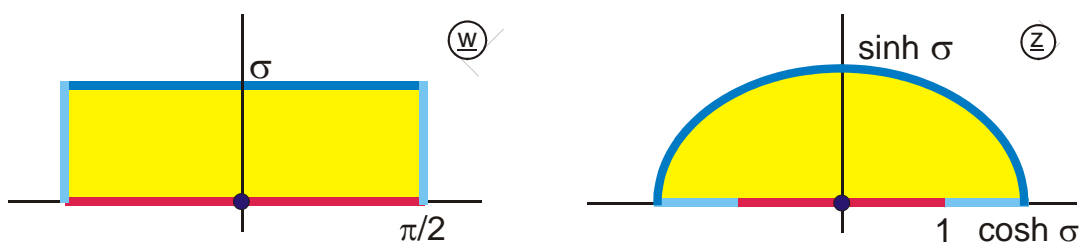
16. Rotated strip onto circle

$$z = w + \sqrt{w^2 - \exp(j2\varphi)}$$

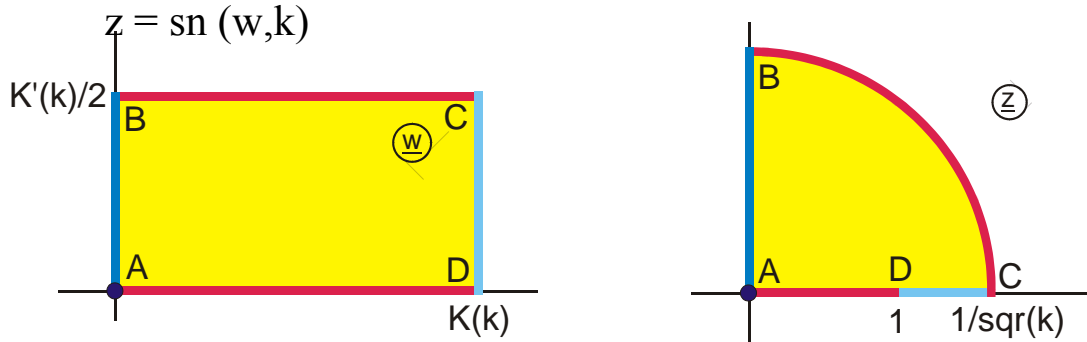


17. Interior of rectangle onto interior of ellipse

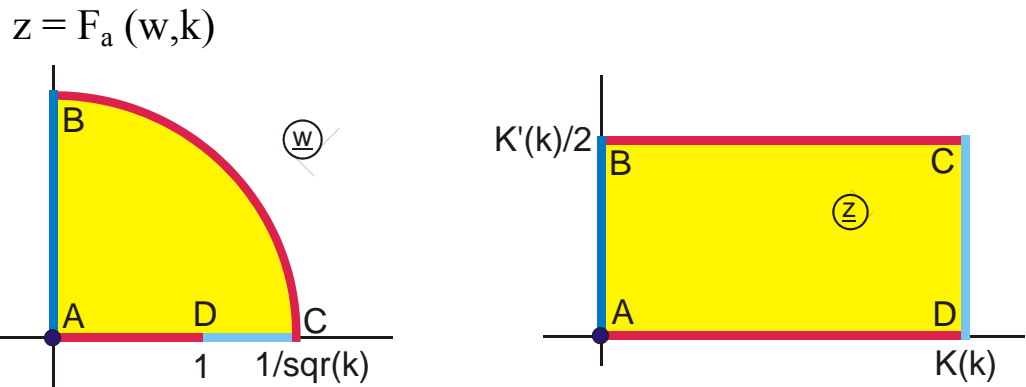
$$z = \sin w$$



18. Interior of rectangle onto interior of circle



19. Interior of circle onto interior of rectangle

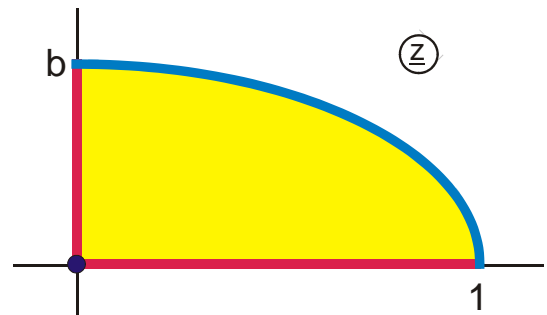
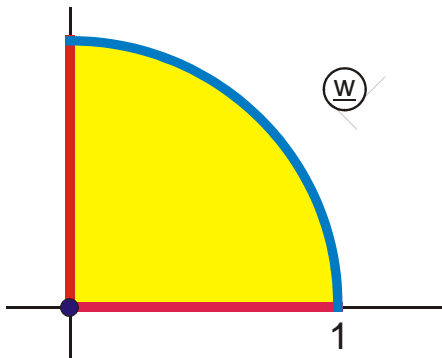


20. Interior of circle onto interior of ellipse

$$z = \sqrt{1-b^2} \sin \left\{ \frac{\pi}{2K(k)} F_a \left(\frac{w}{\sqrt{k}}, k \right) \right\}$$

$$\tau = \frac{4}{\pi} ar \tanh b$$

$$k = [\mathcal{G}_2(0, \tau) / \mathcal{G}_3(0, \tau)]^2$$

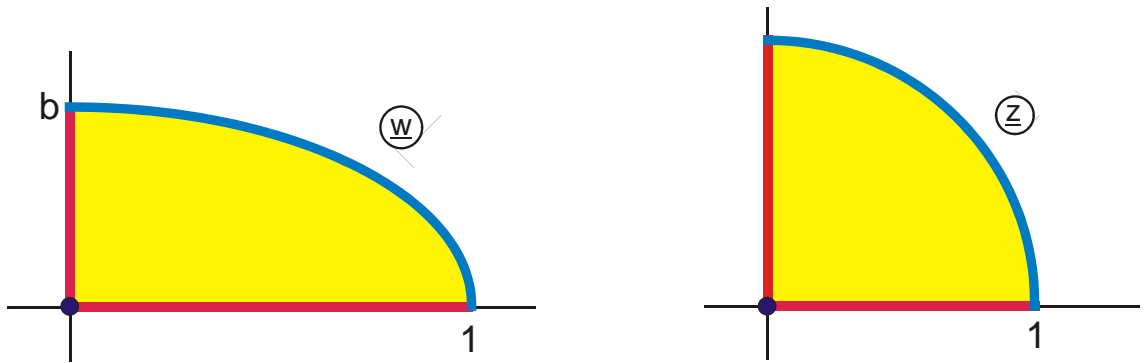


21. Interior of ellipse onto interior of circle

$$z = \sqrt{k} \operatorname{sn} \left\{ \frac{2K(k)}{\pi} \arcsin \frac{w}{\sqrt{1-b^2}}, k \right\}$$

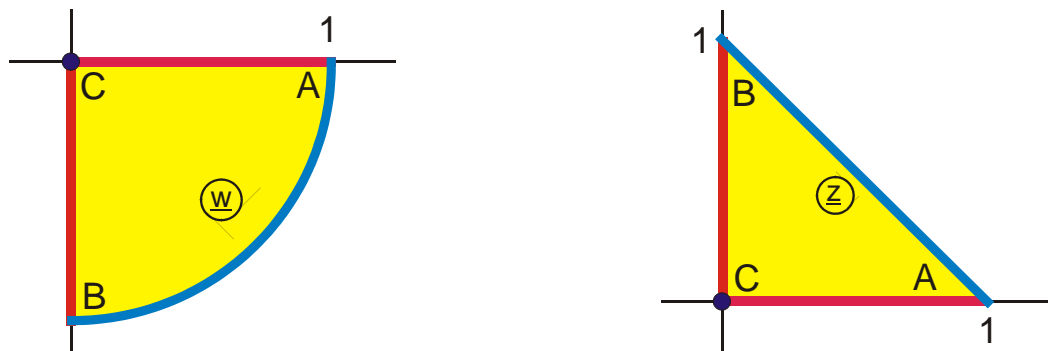
$$\tau = \frac{4}{\pi} \operatorname{ar} \tanh b$$

$$k = [\mathcal{G}_2(0, \tau) / \mathcal{G}_3(0, \tau)]^2$$



22. Interior of quarter circle onto interior of triangle

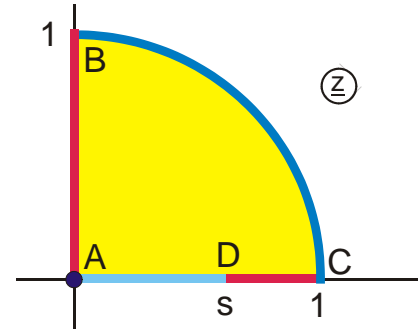
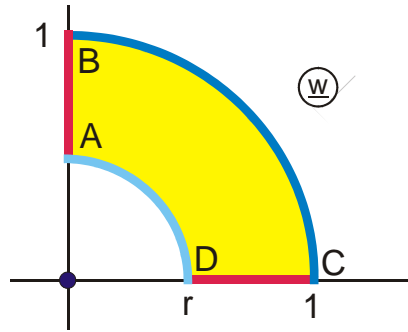
$$z = \frac{1}{K(k)} F_a \left(\sqrt{\frac{2w^2}{1+w^2}}, k \right) \quad \text{mit} \quad k = \frac{1}{\sqrt{2}}$$



23. Interior of annulus onto interior of circle with strip

$$z = \sqrt{k} sn \left[K(k) + K'(k) \frac{\ln w}{\pi}, k \right] \quad \text{mit} \quad \tau = -\frac{\pi}{\ln r}$$

$$k = [\vartheta_2(0, \tau) / \vartheta_3(0, \tau)]^2 \quad s = \sqrt{k}$$



24. Annulus onto the region exterior to two circles

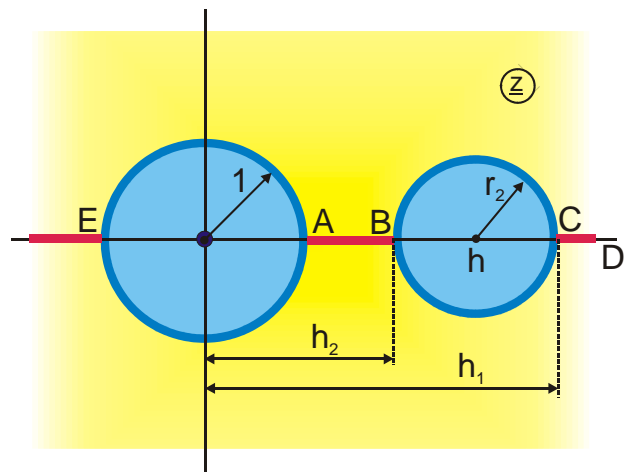
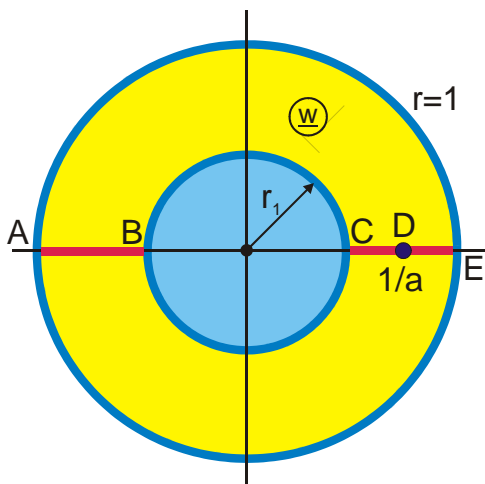
$$z = \frac{w-a}{aw-1}$$

$$a = \frac{h_1 h_2 + 1 + \sqrt{(h_1^2 - 1)(h_2^2 - 1)}}{h_1 + h_2}$$

$$r_1 = \frac{h_1 h_2 - 1 - \sqrt{(h_1^2 - 1)(h_2^2 - 1)}}{h_1 - h_2}$$

$$r_2 = r_1 \frac{1-a^2}{a^2 r_1^2 - 1}$$

$$h = a \frac{r_1^2 - 1}{a^2 r_1^2 - 1}$$



25. Region exterior to two circles onto annulus

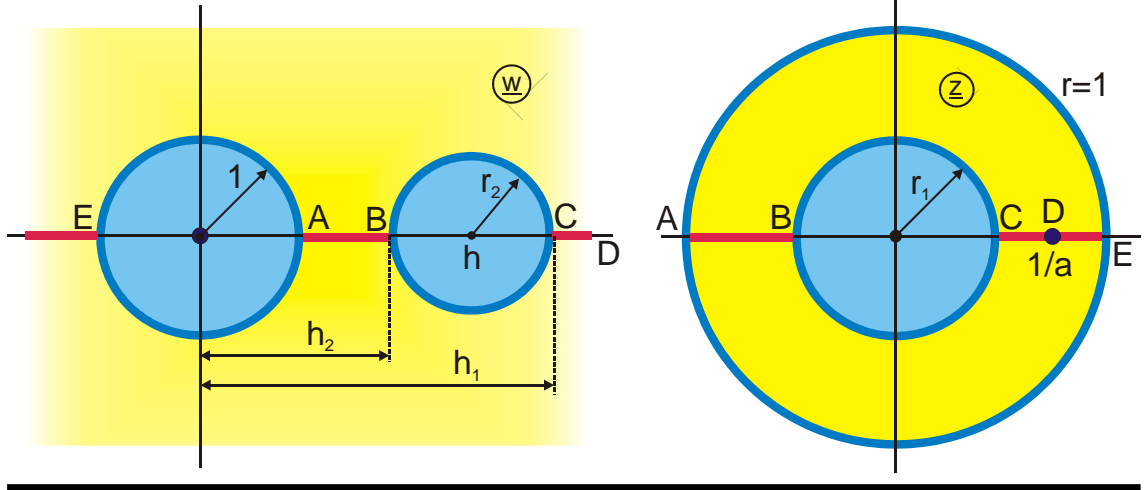
$$z = \frac{w - a}{aw - 1}$$

$$a = \frac{h_1 h_2 + 1 + \sqrt{(h_1^2 - 1)(h_2^2 - 1)}}{h_1 + h_2}$$

$$r_1 = \frac{h_1 h_2 - 1 - \sqrt{(h_1^2 - 1)(h_2^2 - 1)}}{h_1 - h_2}$$

$$r_2 = r_1 \frac{1 - a^2}{a^2 r_1^2 - 1}$$

$$h = a \frac{r_1^2 - 1}{a^2 r_1^2 - 1}$$

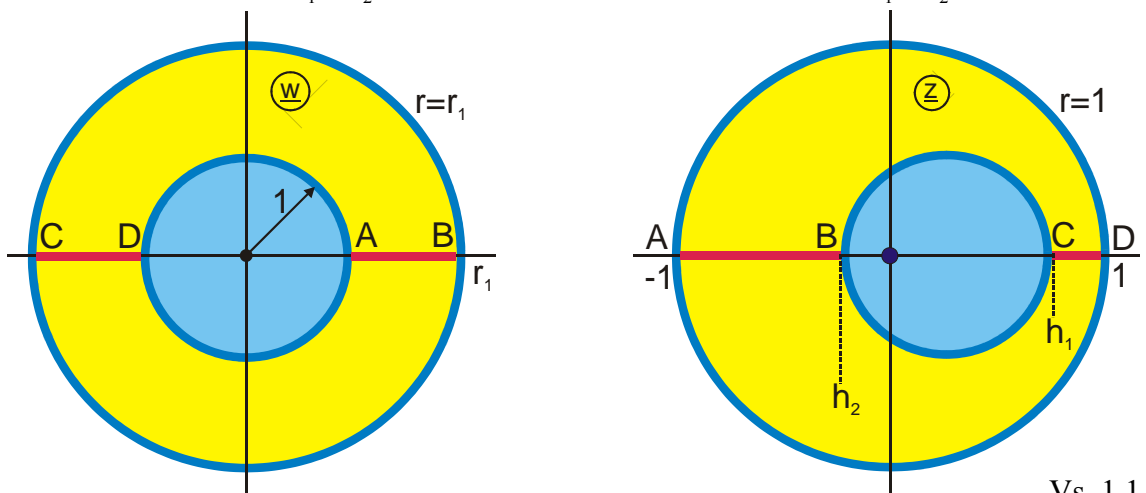


26. Annulus onto excentric annulus

$$z = \frac{w - a}{aw - 1}$$

$$a = \frac{h_1 h_2 + 1 + \sqrt{(1 - h_1^2)(1 - h_2^2)}}{h_1 + h_2}$$

$$r_1 = \frac{-h_1 h_2 + 1 + \sqrt{(1 - h_1^2)(1 - h_2^2)}}{h_1 - h_2}$$



27. Two circles onto two strips

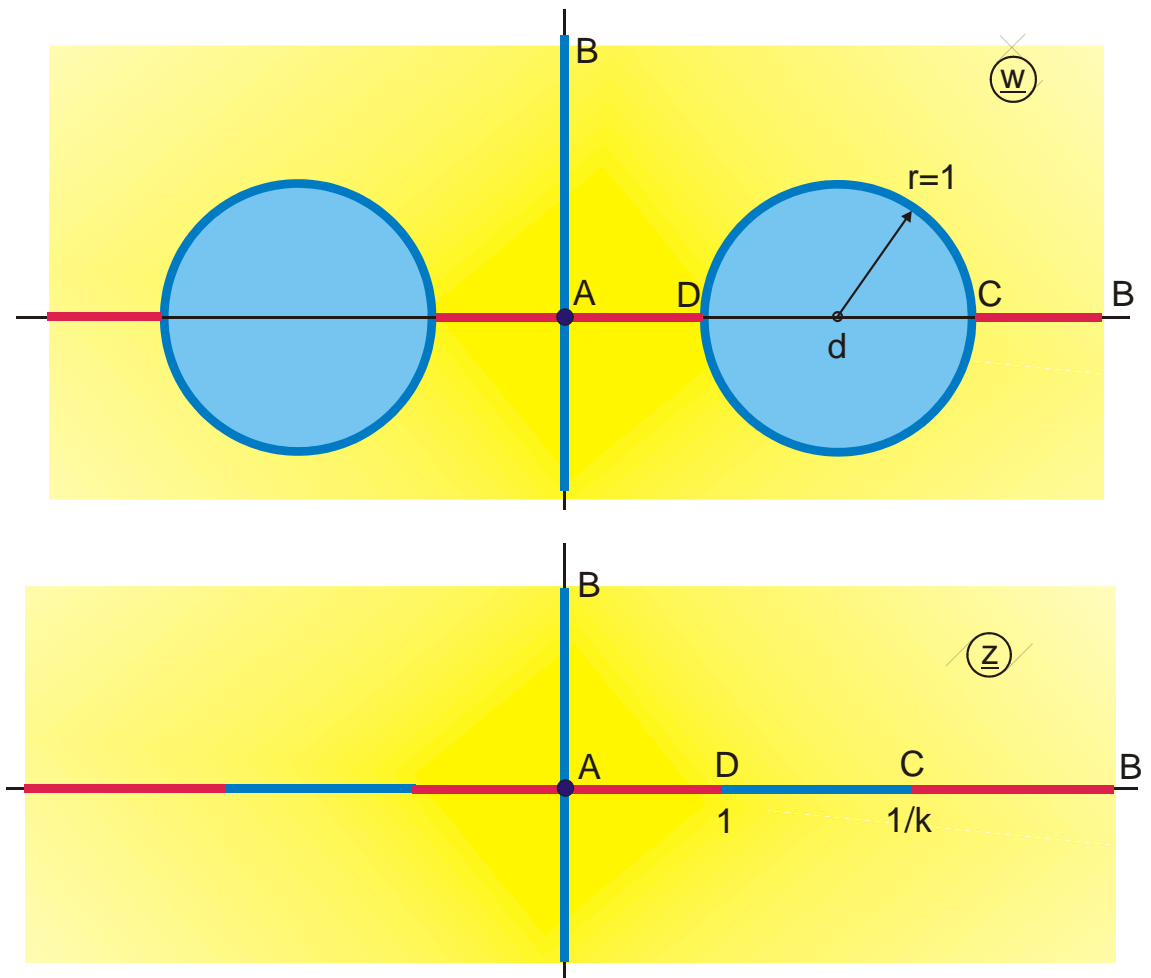
$$\underline{z} = sn \left[\frac{K(k)}{u_c \cdot \pi} \cdot ar \tanh(r_1 \cdot \underline{w}), k \right].$$

$$k = [\mathcal{G}_2(0, \tau) / \mathcal{G}_3(0, \tau)]^2$$

$$\tau = \frac{K'(k)}{K(k)} = \frac{1}{2u_c}$$

$$r_1 = \frac{1}{\sinh(2\pi u_c)}$$

$$u_c = \frac{1}{2\pi} \cdot ar \sinh \sqrt{d^2 - 1}$$

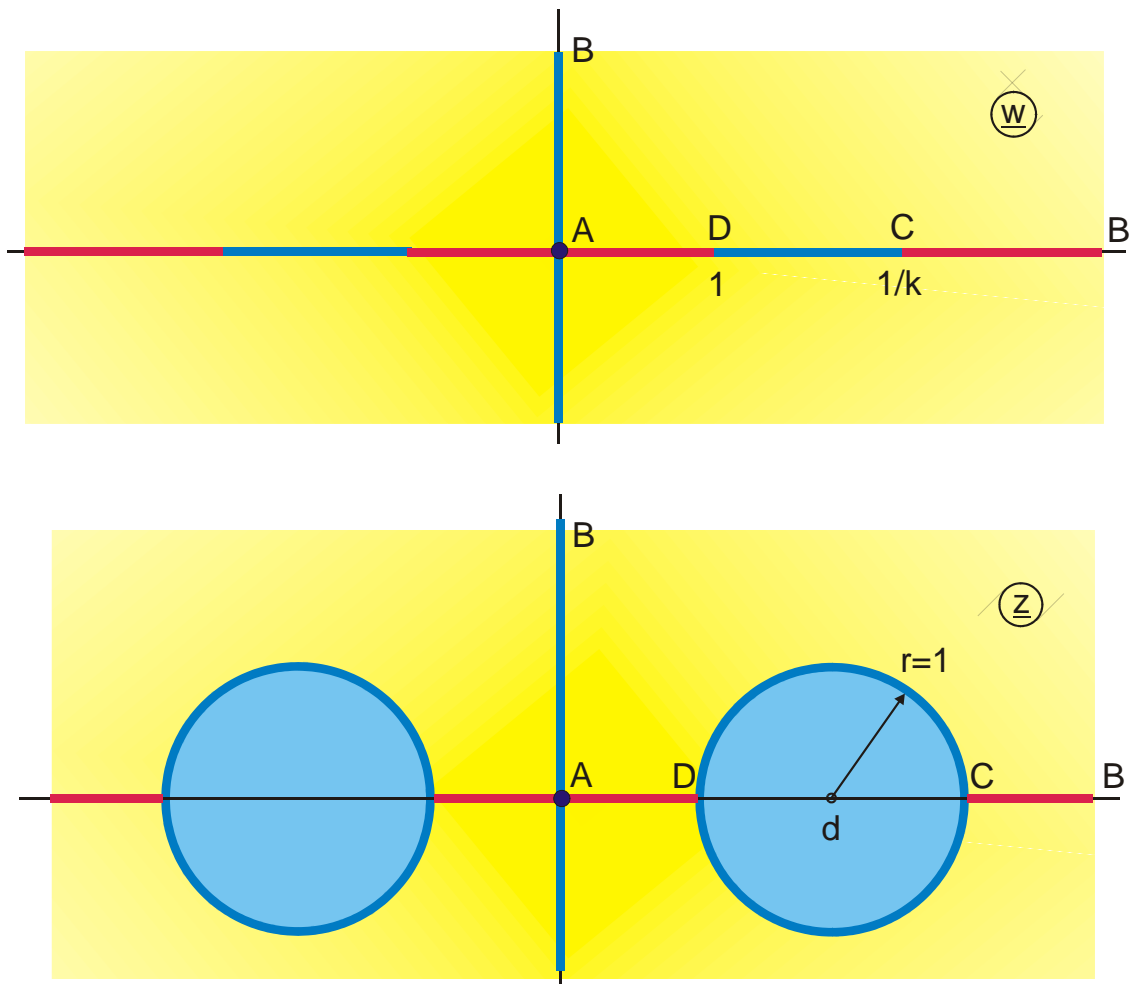


28. Two strips onto two circles

$$\underline{z} = \frac{1}{r_1} \tanh \left[\frac{u_c \pi}{K(k)} F_a(\underline{w}, k) \right]$$

$$r_1 = \frac{1}{\sinh(2\pi u_c)}$$

$$u_c = \frac{1}{2\pi} \cdot \operatorname{arsinh} \sqrt{d^2 - 1}$$



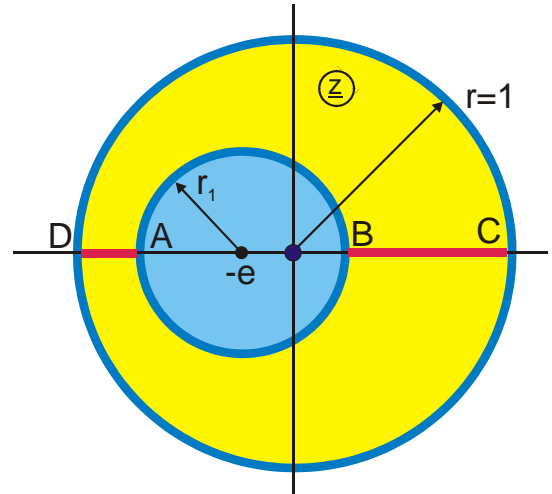
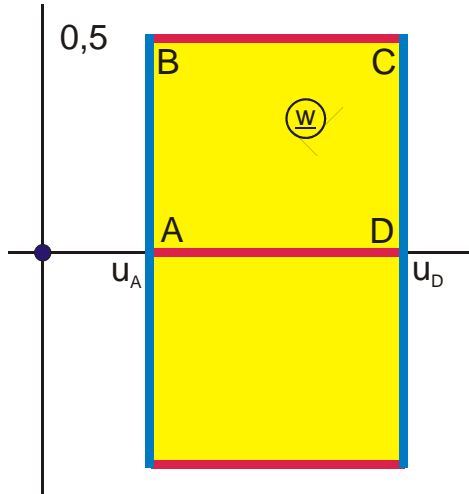
29. Interior of rectangle onto excentric annulus (F 1.1)

$$z = a \tanh(w\pi) - \sqrt{a^2 + 1}$$

$$a = \sqrt{(r_1^2 + 1 - e^2)^2 / 4 - r_1^2} / e$$

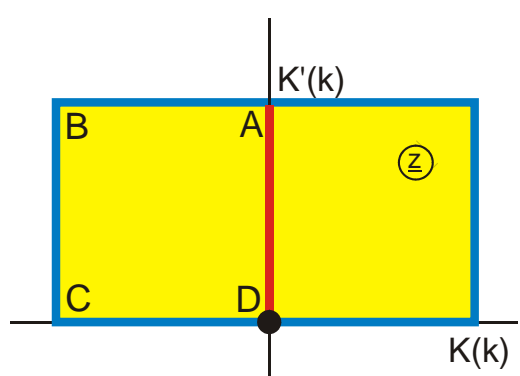
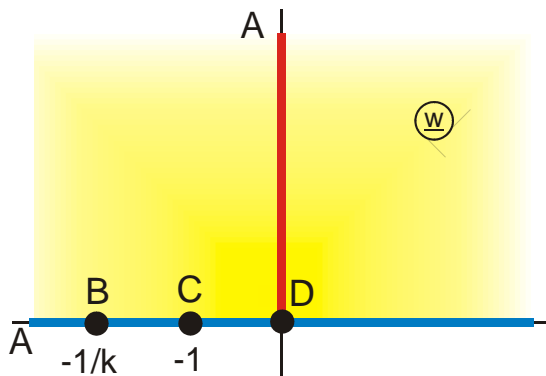
$$u_a = \frac{1}{2\pi} \operatorname{arsinh} a$$

$$u_D = \frac{1}{2\pi} \operatorname{arsinh}(a / r_1)$$



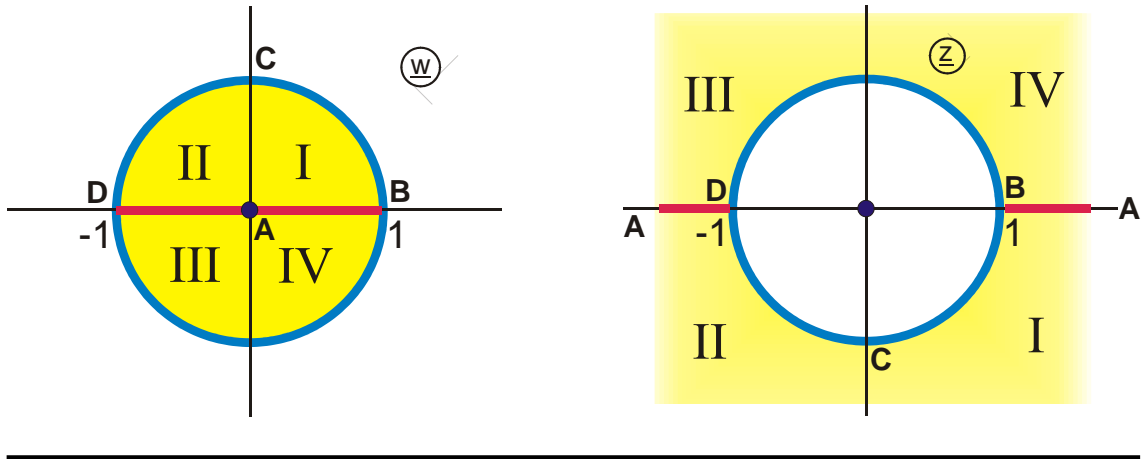
30. Upper half plane onto interior of rectangle

$$z = F_a(w, k)$$



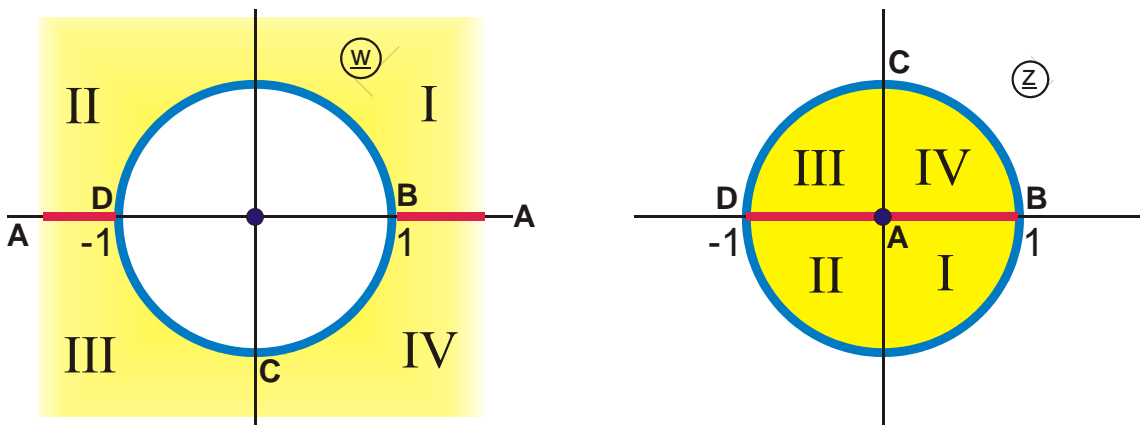
31. Interior of circle onto exterior of circle (Q 1)

$$z = 1/w$$



32. Exterior of circle onto interior of circle (Q 1)

$$z = 1/w$$



7. Superposition of Fields

When the superposition of two fields in the \underline{z} -plane takes place

$$\underline{z} = \underline{f}_1(\underline{w}) + \underline{f}_2(\underline{w}) \quad (1)$$

two complex numbers \underline{f}_1 and \underline{f}_2 or two vectors \vec{f}_1 and \vec{f}_2 respectively are added in every point $P(x,y)$. As a field is well-defined by its electrodes or more general by its boundary conditions, it is sufficient, to constrain the analysis to these boundaries. The superposition of fields in the \underline{z} -plane is a method, where several known field maps are combined in such a way that the result is a field with the new boundary that was sought after.

Example 1: Creating a Circle or an Ellipse

If a uniform field $\underline{f}_2(\underline{w}) = \underline{w}$ (Figure 7.1) is added to the field of a half plane with a salient edge (Mapping A 2.1)

$$\underline{f}_1(\underline{w}) = \sqrt{\underline{w}^2 + 1}, \quad (2)$$

then along the boundary with increasing u , starting at $-\infty$, there is at first an interval between point A and B, where both functions run into the same direction along the real axis (Figure 7.1, right side, \underline{z} -plane). Therefore their sum also remains on the negative real axis. In the interval between point B and C the function $\underline{f}_1(\underline{w})$ runs vertically upwards and $\underline{f}_2(\underline{w})$ continues horizontally: Hence the sum of both functions is a circular arc pointing upwards. Between point C and D this circular arc goes downwards again. From point D until point E at $+\infty$ the sum is once again the same straight line along the positive real axis.

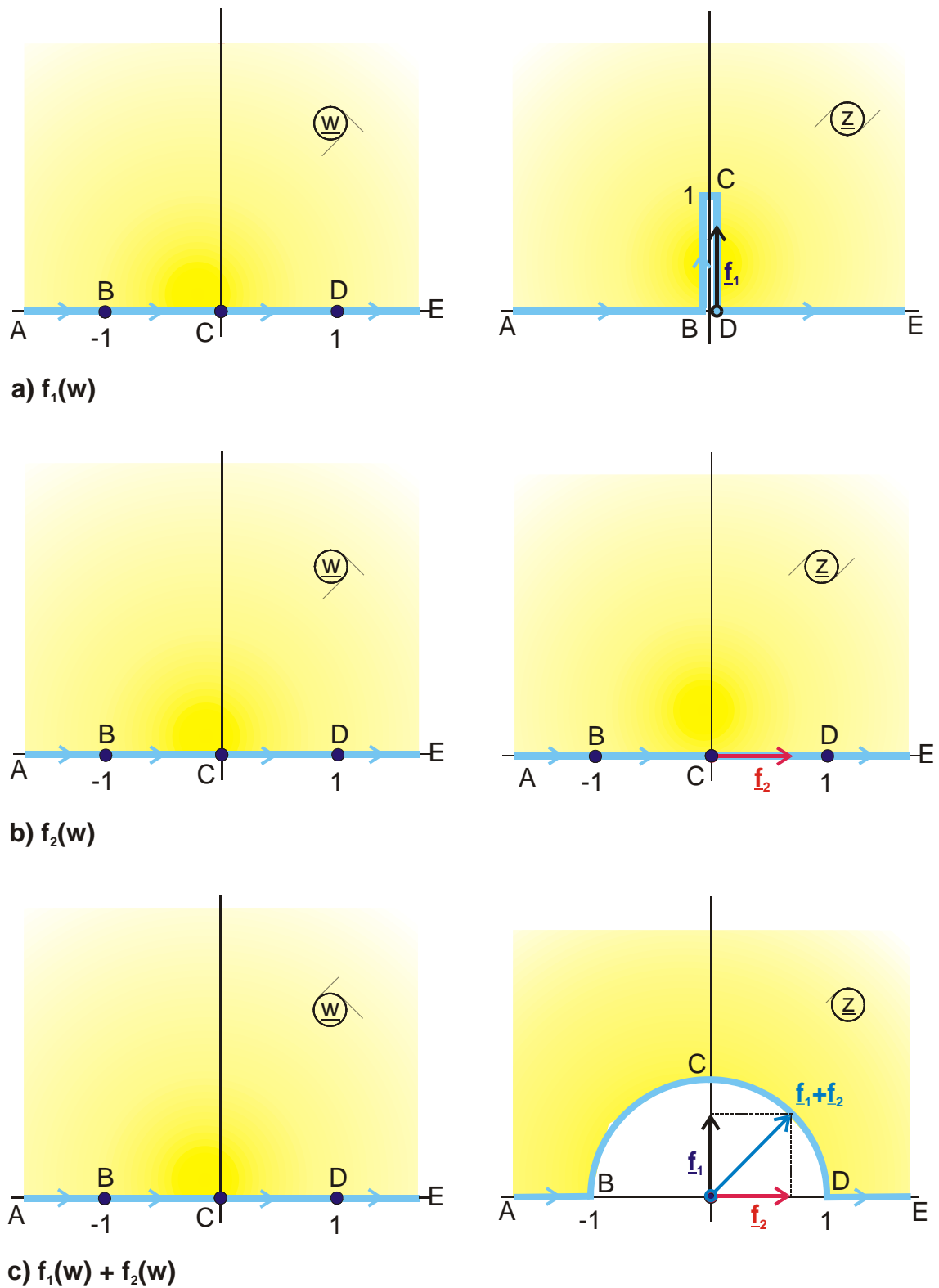


Figure 7.1: Example 1 – Creating a semi circle

For a point between C and D, the two radius vectors of the complex numbers are plotted in Figure 7.1, $\underline{f}_1(\underline{w})$ in black and $\underline{f}_2(\underline{w})$ in red. Their sum is a point $\underline{f}_1(\underline{w}) + \underline{f}_2(\underline{w})$, which lies on the circular arc.

The complete transformation equation is (Mapping A 3):

$$\underline{z} = w + \sqrt{w^2 - 1} \quad (3)$$

The proof that this curve is an exact circle, can be provided e.g. as follows:

$$\text{Curve } \overline{CD}: \quad \underline{w} = u \text{ with } u < 1 \quad \Rightarrow \quad x + jy = u + \sqrt{u^2 - 1} \quad (4)$$

$$x = u \quad y = \sqrt{1 - u^2} \quad (5)$$

$$\sqrt{x^2 + y^2} = 1 \quad (\text{equation of a circle}). \quad (6)$$

If $\underline{f}_1(\underline{w})$ is multiplied with b , in order to achieve that the edge has no longer the height 1, but the height b , then the field map after the superposition contains an ellipse (Mapping A 3.2) instead of the circle, with the vertical semi-minor b and the horizontal semi-major 1:

$$\underline{z} = w + b\sqrt{w^2 - 1} \quad (7)$$

Example 2: Conversion Edge into Half Strip

If from the field of Mapping A 8

$$\underline{f}_1(\underline{w}) = \underline{w}\sqrt{w^2 - 1} \quad (8)$$

the interior of a half strip (Mapping A 7) is subtracted

$$\underline{f}_2(\underline{w}) = \text{arcosh}(\underline{w}) - j\pi/2, \quad (9)$$

then this yields Mapping A 5. (Figure 7.2):

$$\underline{z} = f_1(\underline{w}) - f_2(\underline{w}) = \underline{w}\sqrt{\underline{w}^2 - 1} - \operatorname{ar} \cosh \underline{w} + j\frac{\pi}{2}. \quad (10)$$

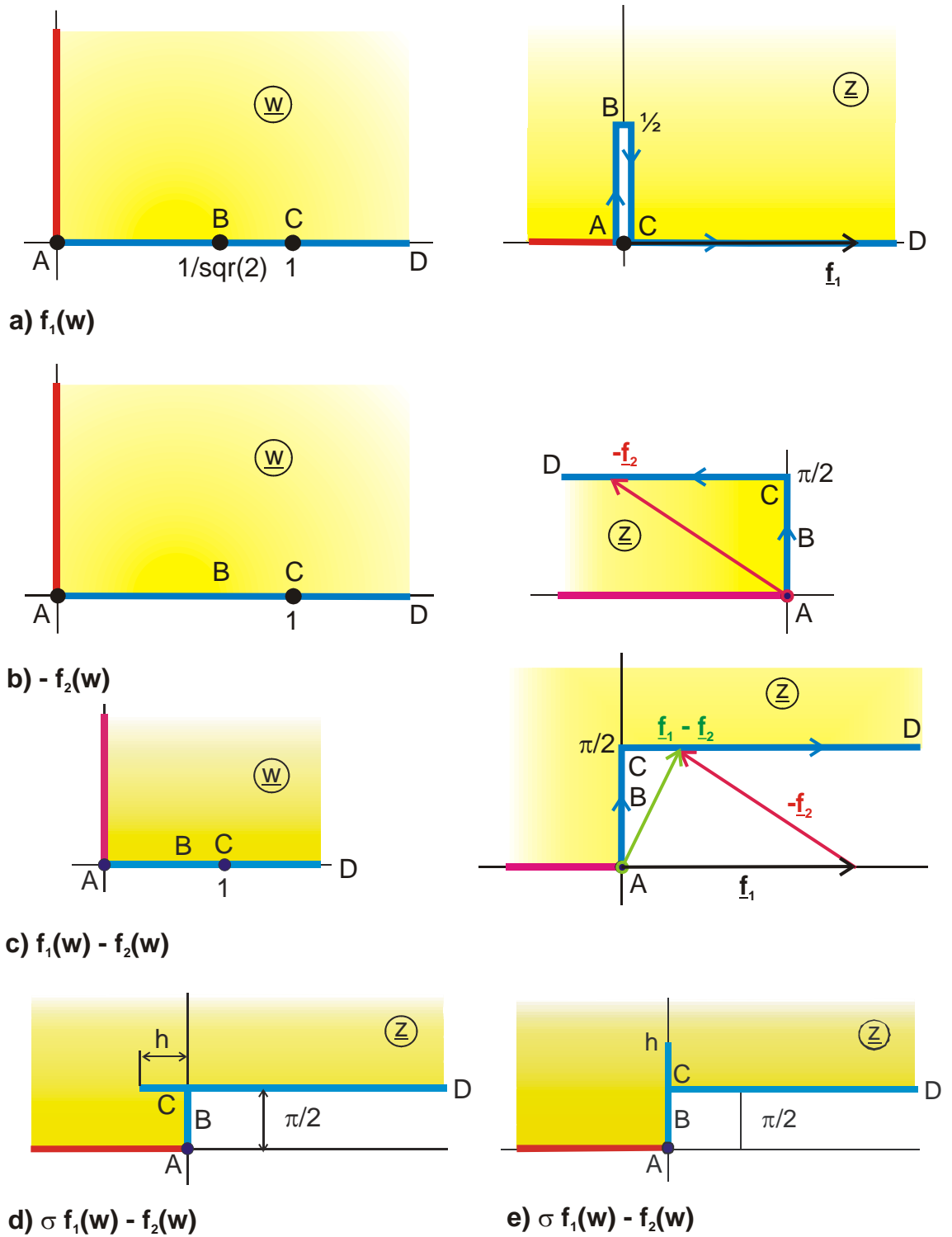


Figure 7.2: Example 2

In order to illustrate the procedure, $f_1(\underline{w})$ is shown in Figure 7.2a and $-f_2(\underline{w})$ in Figure 7.2b. Figure 7.2c shows the sum $f_1(\underline{w}) + \{-f_2(\underline{w})\}$. From point A to point C both curves run vertical on the imaginary axis, hence also the sum yields values lying on the imaginary axis. In the interval between point C and D both curves run horizontally, displaced against each other by $j\pi/2$. Because the real part of $f_1(\underline{w})$ is always bigger than the magnitude of the real part of $f_2(\underline{w})$, the sum lies always on the straight line $x + j\pi/2$ in the I. quadrant.

If this relationship of the magnitudes is changed by a factor $\sigma < 1$ for $f_2(\underline{w})$, then the sum lies in a certain interval in the II. quadrant and this leads to Mapping A 5.3 (Figure 7.2d).

$$z = \sigma f_1 - f_2 = \sigma w \sqrt{w^2 - 1} - \operatorname{ar} \cosh w + j \frac{\pi}{2} \quad (11)$$

For $\sigma > 1$ the vertical boundary in the interval A-C swings higher up than $\pi/2$ and afterwards down again to $\pi/2$ (Mapping A 5.4 , Figure 7.2e).

Example 3: Bent Channel with Right Angle

The function

$$f_1(\underline{w}) = 2a \operatorname{ar} \tanh \underline{w}_1 \quad \text{with} \quad \underline{w}_1 = \sqrt{\frac{\exp(\pi \underline{w}) - 1}{\exp(\pi \underline{w}) + a^2}} \quad (12)$$

yields the field map of a line charge at point A in a half strip, which points to the right (Mapping H 2.3). The function

$$f_2(\underline{w}) = -2 \operatorname{arctan}(a \underline{w}_1) \quad (13)$$

yields the field map of a line charge at point C in a half strip, which points upwards. The sum of both transformation equations $z = f_1(\underline{w}) + f_2(\underline{w})$ yields the field map of a bent channel with a right angle (Mapping D 4).

As can be seen in Figure 7.3 $f_1(\underline{w})$ and $f_2(\underline{w})$ run from point A to point B vertically on the imaginary axis. The sum $f_1(\underline{w}) + f_2(\underline{w})$ is therefore the right vertical boundary of the channel. Point A of $f_2(\underline{w})$ remains unchanged at $+j\infty$. From B to C both functions run on the real axis. The sum yields the upper horizontal boundary of the channel.

Likewise the lines from D to E produce the left vertical boundary of the channel and the lines from E to F the lower horizontal boundary of the channel. The line charges in the points $A = D$ and $C = F$ are mapped to ∞ . They are the reason, why the streamlines in the channel flow from one end to the other. Both branches of the channel have the same width for $a = 1$.

With the same method the Mappings H 10, C 5, C 5.1 and C 5.2 were found.

Example 4: Superposition of the same Function, Displaced by Δ

The function

$$f(\underline{w}) = Z_e(\underline{w}, k) + ja \quad (14)$$

maps a rectangle onto a conducting strip, parallel to an infinite conducting plane (Mapping E 2, Figure 7.4). With the transformation

$$f(\underline{w}) = f(\underline{w} + \Delta) + f(\underline{w} - \Delta) \quad (15)$$

and $\Delta = j\sigma$ this turns into

$$\underline{z} = Z_e(\underline{w} + j\sigma, k) + Z_e(\underline{w} - j\sigma, k). \quad (16)$$

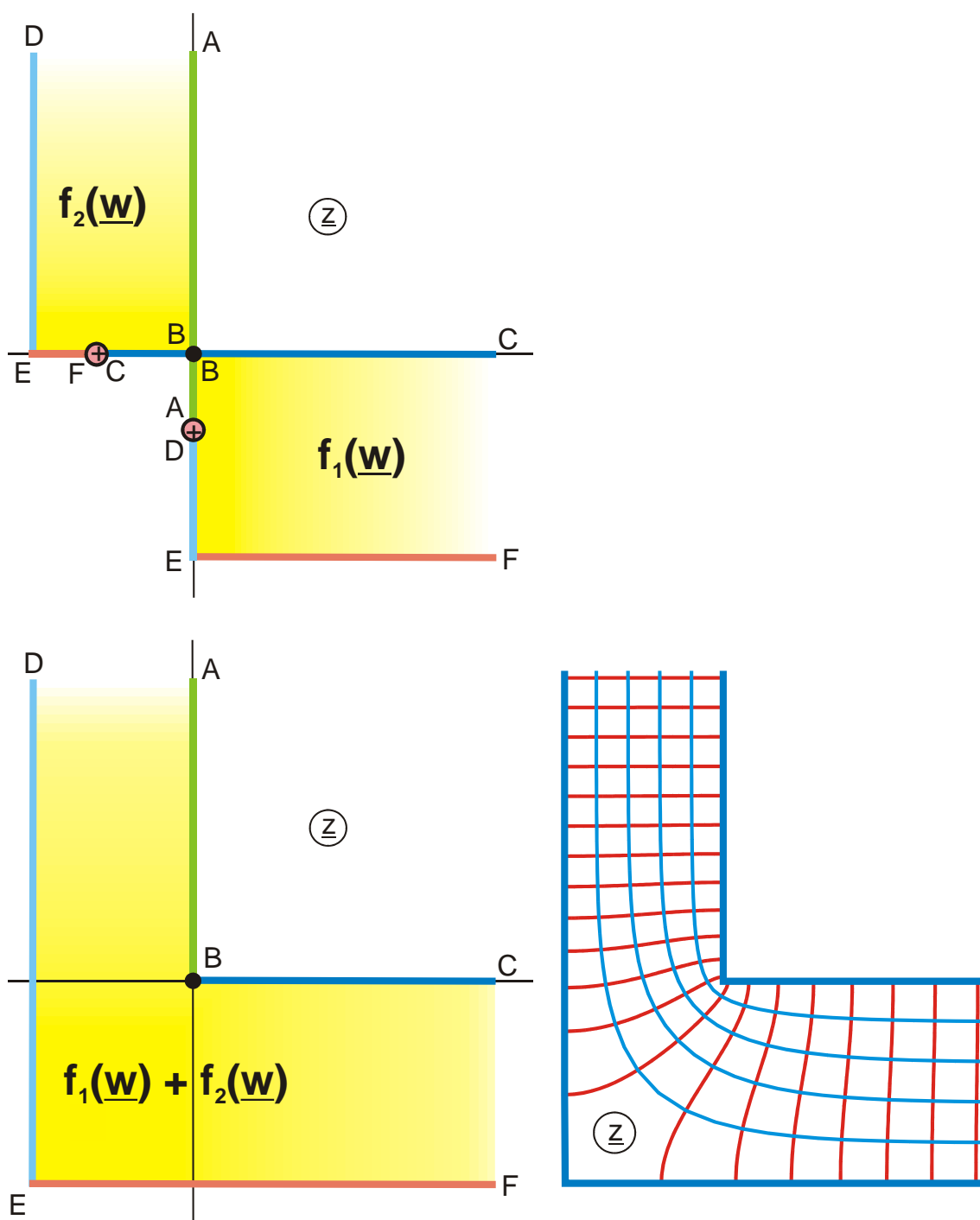


Figure 7.3: Example 3, Mapping D 4

Due to the displacement by $j\sigma$ in the uniform field of the w -plane, the bottom line, the **infinite** potential line DE in the z -plane in Figure 7.4 is omitted. Because of the $\pm\Delta$ -transformation the curvilinear **finite** potential line, which is displaced by $j\sigma$, is mapped onto a straight line parallel to the real axis ($+j\sigma - j\sigma = 0$, the imaginary parts of the two functions cancel each other). The result is the field map of two parallel conducting strips with different width (Mapping F 5, Figure 7.5) and the distance $2a$. With the same method, amongst others, the Mappings P 4.2 and P 4.3 were produced.

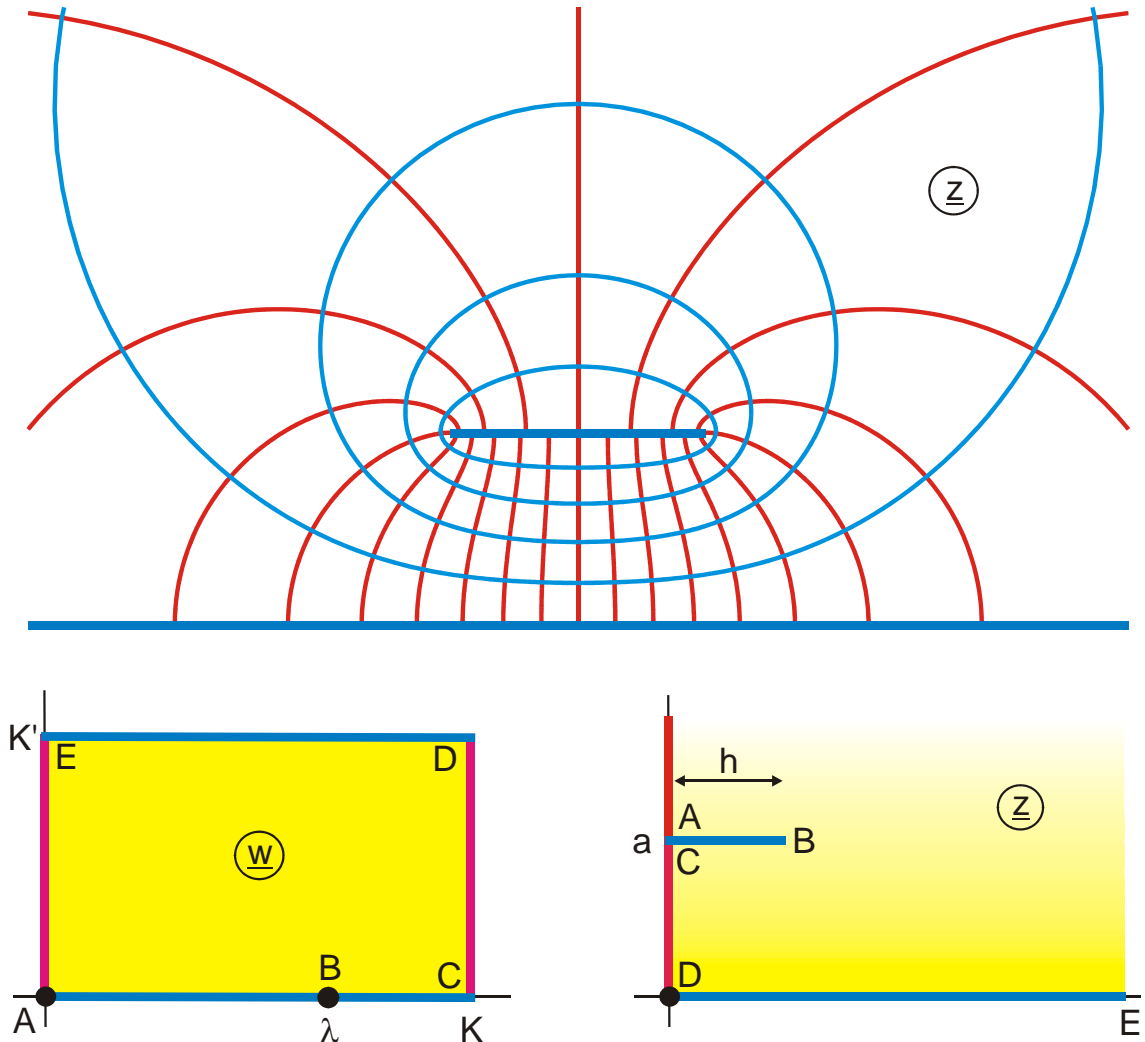


Figure 7.4: Mapping E 2

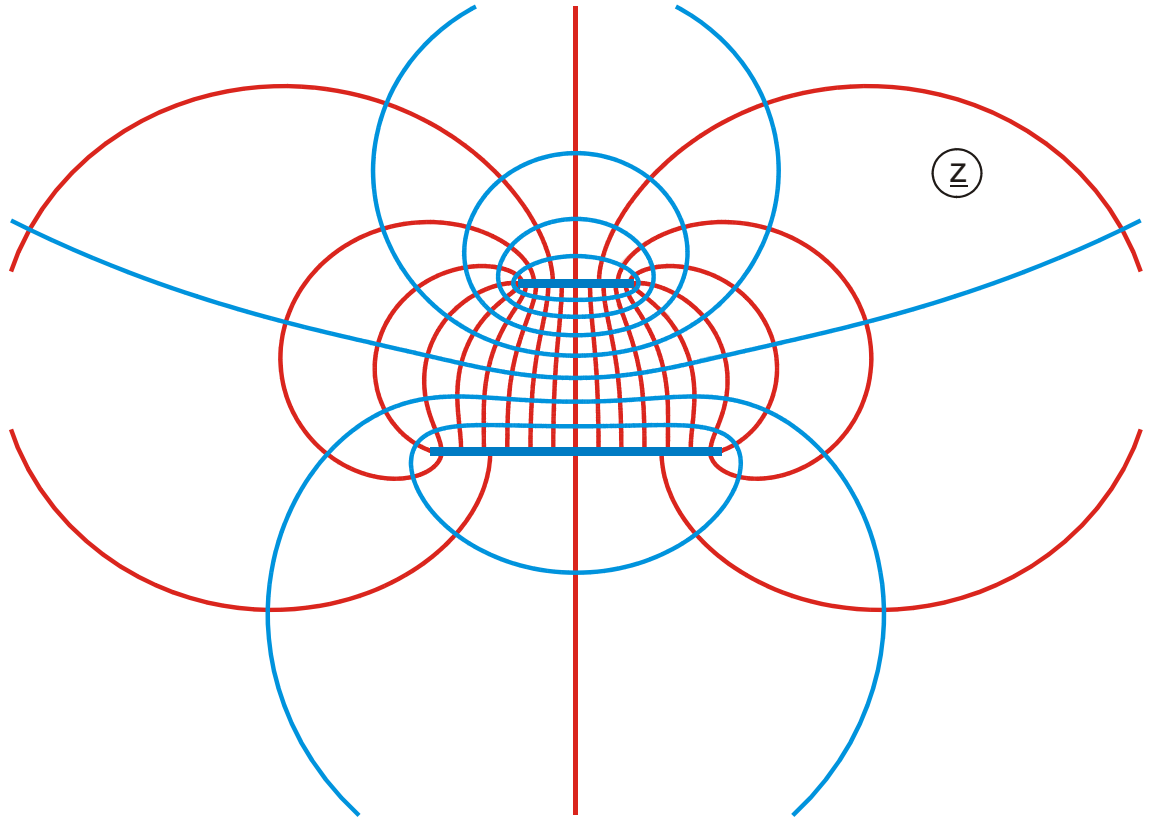


Figure 7.5: Example 4, Mapping F 5

Example 5: Inserting a Gap into a Boundary

The Mapping P 7.3:

$$z = B_a(w_1, k) + jB_a(w_2, k) - h - jh = f_1(\underline{w}) + f_2(\underline{w}) \quad (17)$$

$$w_1 = \sqrt{1 + w_0} \quad (18)$$

$$w_2 = \sqrt{1 + 1/w_0} \quad w_0 = \cosh(w\pi) \quad (19)$$

$$k = 1/\text{sqr}(2) \quad h = 2E(k) - K(k) \quad (20)$$

is produced by addition of the two functions $f_1(\underline{w})$ and $f_2(\underline{w})$. As illustrated in Figure 7.6, both functions $f(\underline{w})$ have similarity with a sector of 1/8 of the outside field of a

quadratic electrode (Special case of Mapping B 4, but with a different pre-transformation). The field map has a circumferential closed boundary from point A to point E with a single pole. Both boundaries are equal and have the same dimensions. Only the sense of circulation and their position in the \underline{z} -plane are different. In Figure 7.6 are shown:

$$f_1(w) = B_a(w_1, k) - h/2 - jh/2 \quad (21)$$

and

$$f_2(w) = jB_a(w_2, k) - h/2 - jh/2 \quad (22)$$

When the superposition $f_1(\underline{w}) + f_2(\underline{w})$ takes place, the radius vectors ending on the dark blue colored boundary from C to A are added, and the curve of the sum $f(\underline{w})$ begins, because of $C_1 = h/2 (1+j)$ and $C_2 = \infty$, inclined by 45° , in the infinite point at C. Thereafter it runs along the 45° -straight line in the direction of the origin. Because f_1 is always increasing and f_2 is constantly decreasing, the sum never reaches the origin. In point B the movement comes to a standstill and afterwards the sum reverses the direction. Point B is located at $d (1+j)$ with $d > h$. Because of $A_2 = h/2 (1+j)$ and $A_1 = \infty$ the curve ends in Point A again inclined by 45° in the infinite point. Thus the boundary, which is closed in both individual functions, is opened between B and D in the case of the sum function.

Point D_1 is at $h/2 (1-j)$ and point D_2 is at $h/2 (-1+j)$. Therefore the sum lies in the origin. The sum of all radius vectors, whose end points are located on the pale blue horizontal straight line, lies on the real axis in the \underline{z} -plane. The vertical offset by $\pm jh/2$ is mutually canceled.

In the same way the points on the two red straight lines DC add to sum points on the imaginary axis of the \underline{z} -plane. The offset by $\pm h/2$ is mutually canceled. The direction of movement along the straight lines DE and DC is the same for both functions; hence there is no change of direction in this case. The positive real axis and the positive imaginary axis are occupied continuously.

The transformation of the same boundaries, as used above, can also be done without elliptic functions (Mapping D 2.5 with $\alpha = 90^\circ$, $\beta = 45^\circ$ and modified pre-transformation).

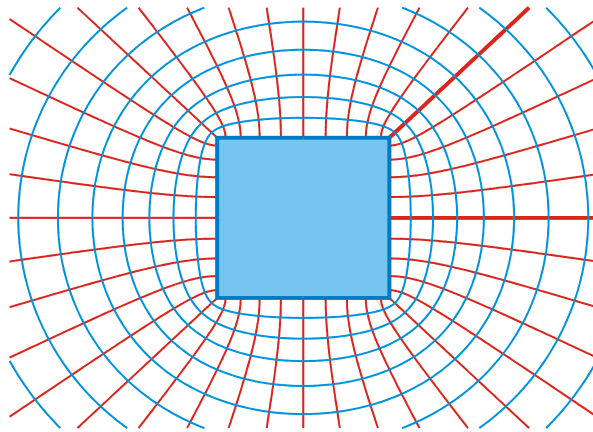


Abb. B 4

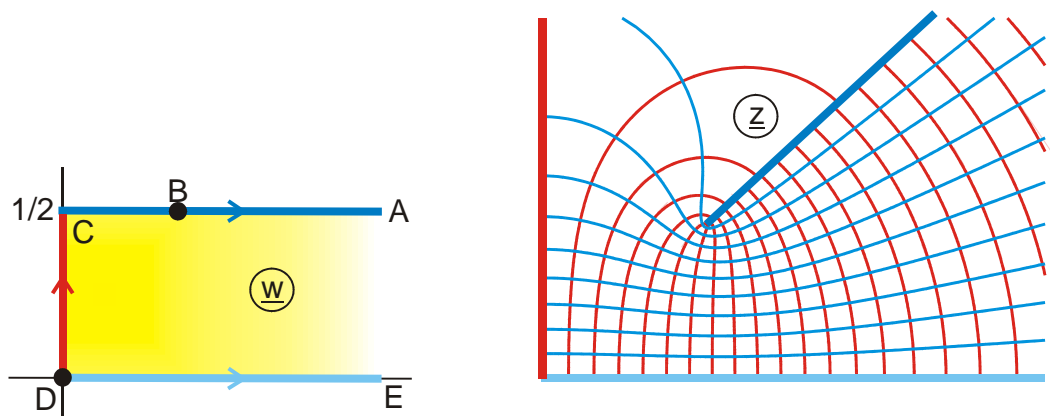
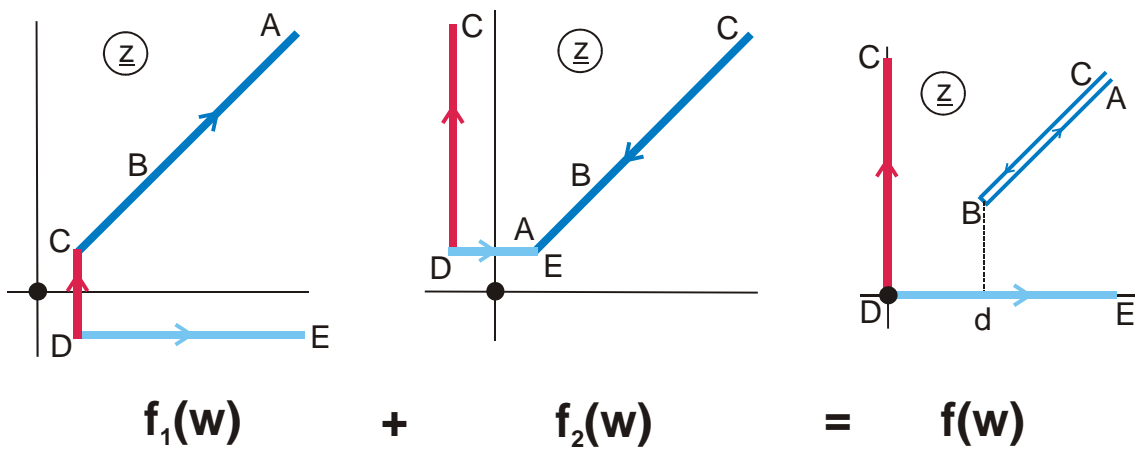
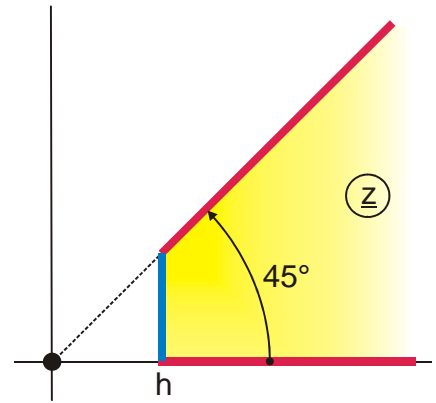


Abb. P 7.3

Figure 7.6: Example 5

8. Electrodes in a Uniform Field

8.1 Vertical Incidence of the Uniform Field

Figure 8.1 illustrates with the example of a circular cylinder the difference between the field of an electrode against the infinite point (Figure 8.1a) and the field of an electrode in a uniform field or in a uniform flow (Figure 8.1b). In the first case there is a line charge at the point $z = \infty$. In the second case there is a line dipole at ∞ . This line dipole can be visualized as two separate line charges: The uniform field is created from a positive line charge at $y = +\infty$ and a negative line charge at $y = -\infty$.

The existence of a uniform field in the z -plane will be indicated with the vector of the electric field strength \vec{E} . The arrowhead points in the direction of the field lines (flux lines, stream lines). The vector of \vec{E} is perpendicular to the potential lines. The field maps of electrodes in a uniform field are comprised in the group of mappings R. In addition many other mappings of other groups (e.g. A, D, C ...) belong to this family. Most of these are supplemented in Chapter 15 R. As illustrated in Figure 8.2, e.g. Mapping A 10.2 yields, when complemented symmetrically, the field map of a rectangular cylinder in a uniform field. In Figure 8.2b the real axis is (outside of the rectangle) a potential line due to the symmetry of the configuration. In Figure 8.2a this line is interpreted as a conducting surface.

Fields with two infinite electrodes of opposite charge can be converted into those with a uniform field, by placing a line dipole in the point ∞ with an appropriate pre-transformation.

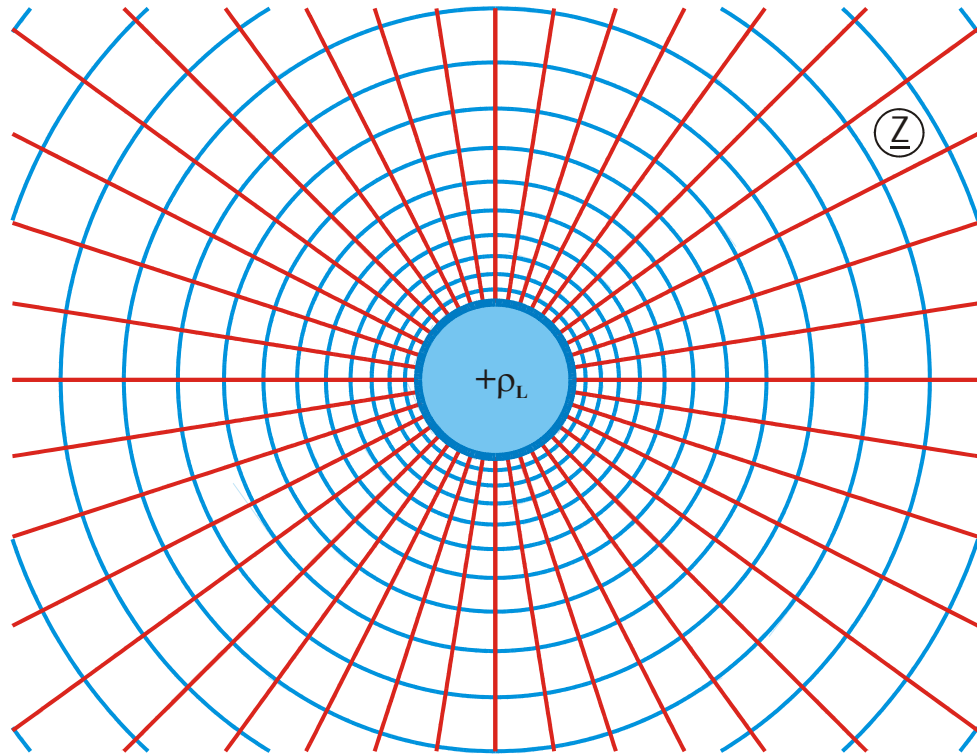


Figure 8.1a: Circular cylinder charged against ∞ (B 1)

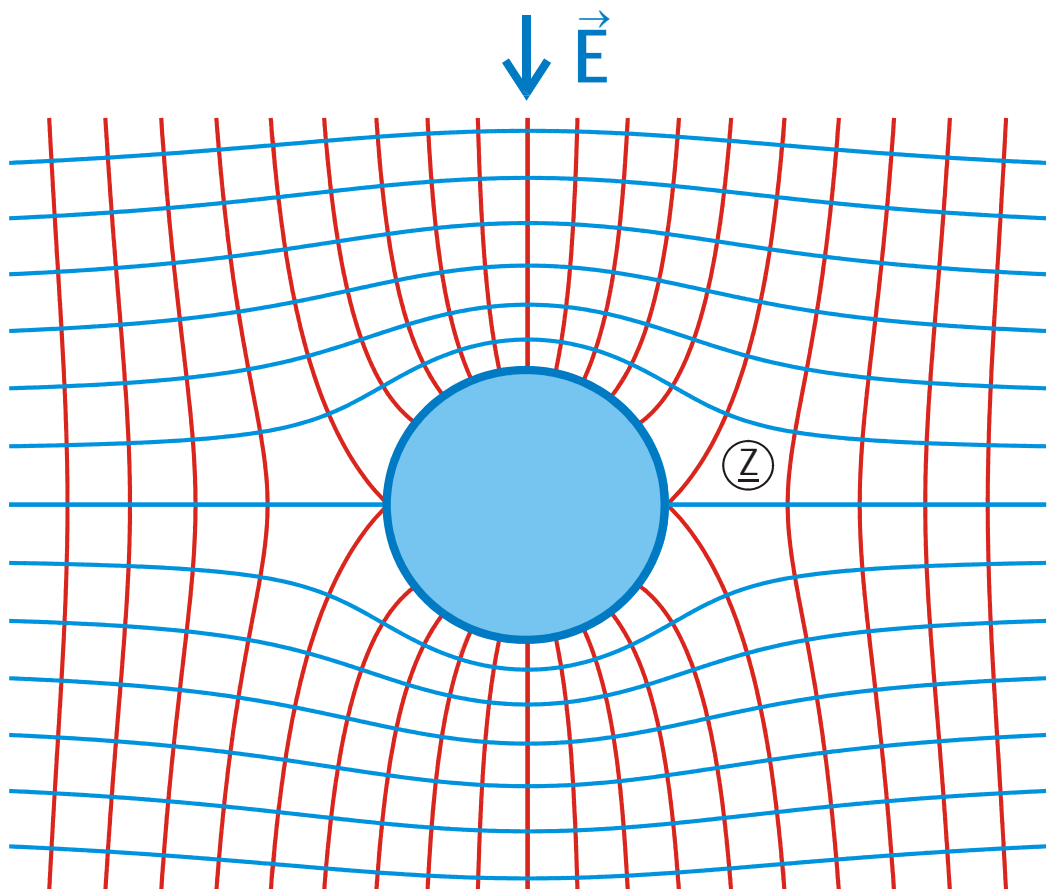


Figure 8.1b: Conducting circular cylinder in a uniform field (A 3)

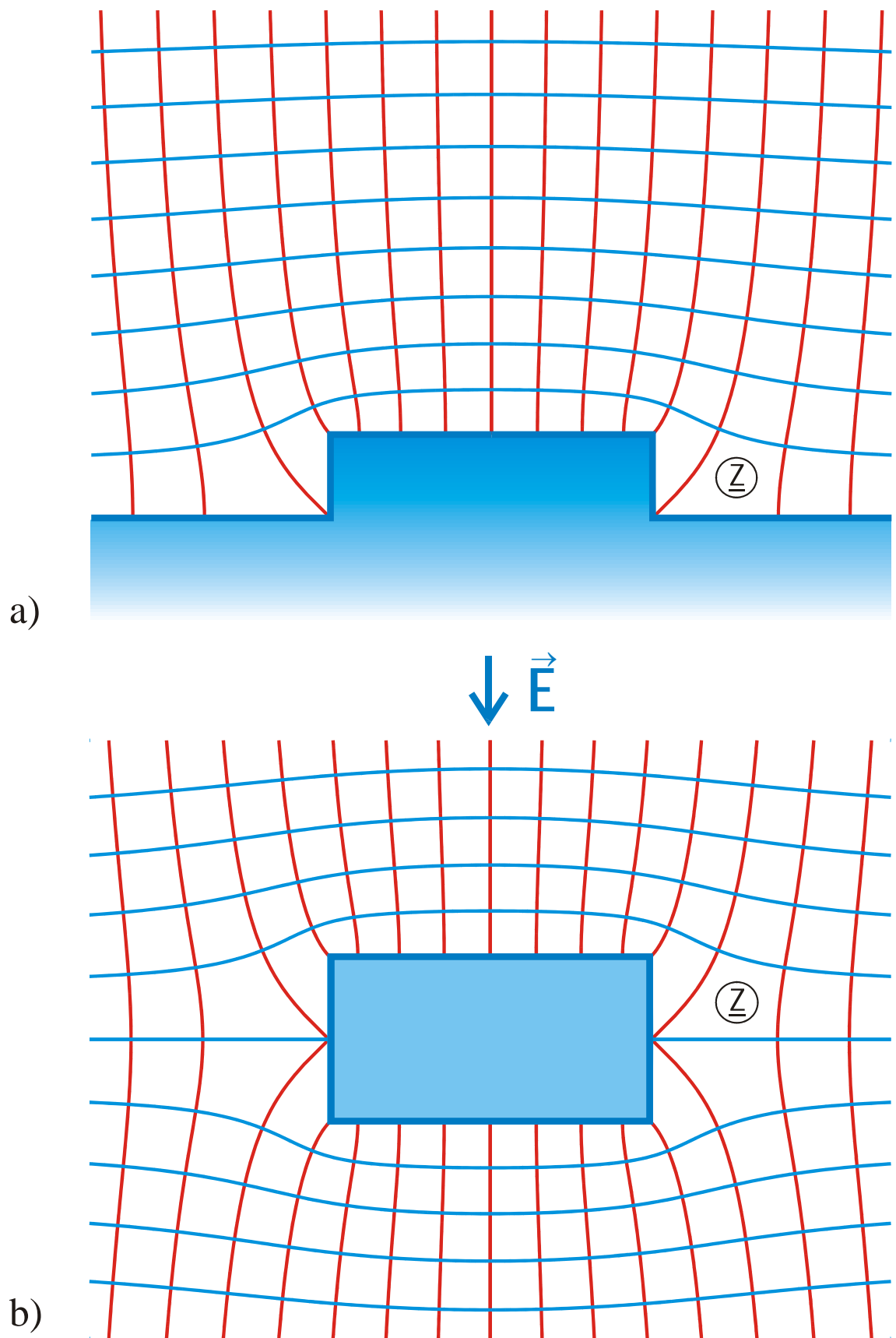


Figure 8.2: An infinite electrode a) and a conducting rectangular cylinder in a uniform field b) have the same transformation equation (A 10.2)

Example 1: Two coplanar plates in uniform field (Conducting plane with slot)

The field map of two coplanar plates on the real axis with equal and opposite charge is given by mapping C 3. According to Figure 8.3a the uniform field between the plates \overline{FED} and \overline{ABC} in the w -plane is transformed by the function

$$\underline{z} = \cosh(\underline{w}\pi) \quad (1)$$

onto the region between the two coplanar plates. In order to create a uniform field on top of these two plates, as depicted in the z -plane in Figure 8.3b, a positive line charge in point D and a negative line charge in point C must be created by an appropriate pre-transformation. This implies for the w_1 -plane that a line dipole must be at $u_1 = +\infty$, at the right end of the parallel strip. Furthermore both boundaries of the parallel strip must be potential lines and must have the same potential. These conditions are satisfied by Mapping H 1 (Figure 8.3c):

$$\underline{w}_1 = \ln(\underline{w}\pi) \quad (2)$$

Both mappings combined together with

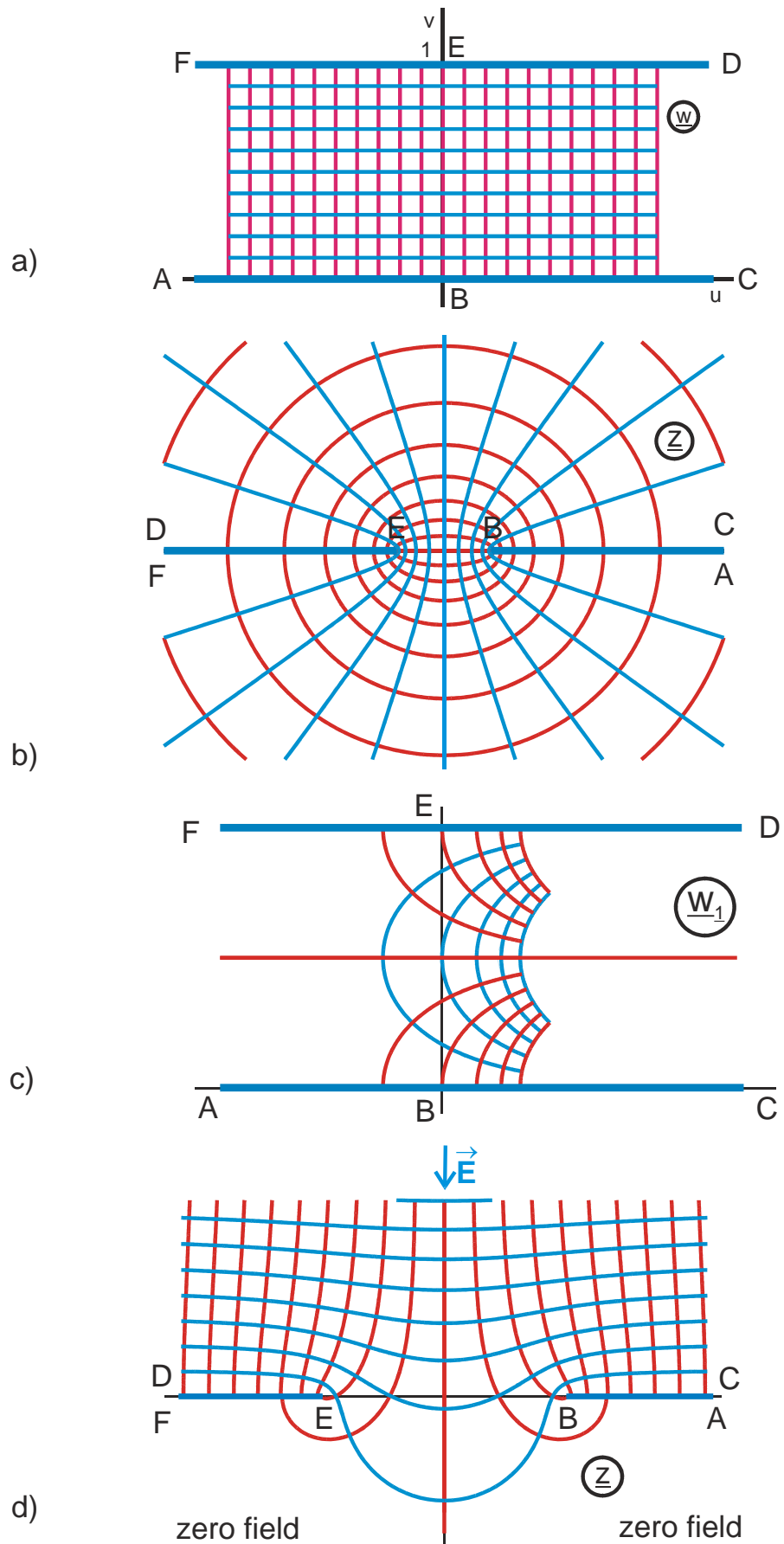
$$\cosh(\underline{w}\pi) = \frac{1}{2} [\exp(\underline{w}\pi) + \exp(-\underline{w}\pi)] \quad (3)$$

leads to
$$\underline{z} = \frac{1}{2}(\underline{w} + 1/\underline{w}) \quad (4)$$

the field map of a uniform field, which is confined by a conducting plane with slot (Mapping R 4). If the sign of the pre-transformation in Eq. (2) is changed

$$\underline{w}_1 = -\ln(\underline{w}\pi), \quad (5)$$

the line dipole moves to the left end of the parallel strip, into the points F and A. Now the uniform field is below the two plates. Because the two electrodes in this example are symmetrical on the real axis, the same field map is produced. In those cases, where no symmetry exists, it is possible in this way to exchange the region with the uniform field and the region with zero field (e.g. Mapping R 4.2).



The method introduced in the example above can be applied to all mappings of the groups C and D. These mappings were not included in the table of mappings. Group R contains only some typical examples.

8.2 Oblique Incidence of the Uniform Field

In Example 4.3 the field map of a conducting circular cylinder in a uniform field was derived from the superposition of a uniform field and the field of a line dipole. The superposition was done in the plane of the complex potential:

$$\underline{w} = \underline{z} + 1/\underline{z}. \quad (6)$$

From this the transformation equation was found:

$$\underline{z} = \underline{w} + \sqrt{\underline{w}^2 - 1}. \quad (7)$$

If in the same manner the potential of a uniform field, which is rotated by the angle φ (Table 3.1),

$$\underline{w}_1 = \underline{z} \cdot \exp(-j\varphi) \quad (8)$$

and the potential of a line dipole, which is rotated by the angle φ

$$\underline{w}_2 = \frac{1}{\underline{z}} \cdot \exp(j\varphi) \quad (9)$$

$$\text{are added } \underline{w} = \underline{w}_1 + \underline{w}_2 = \underline{z} \cdot \exp(-j\varphi) + \frac{1}{\underline{z}} \cdot \exp(j\varphi), \quad (10)$$

then this yields the transformation equation

$$\underline{z} = e^{j\varphi} \left(\underline{w} + \sqrt{\underline{w}^2 - 1} \right), \quad (11)$$

the field map of a circular cylinder in a uniform field, which is rotated by the angle φ in the direction of the imaginary axis (Figure 8.4a). The solution seems to be trivial at first sight, because from experience as well as from the derived function follows that the field map of a circular cylinder in a uniform field always remains the same, irrespective of the fact, that the direction of the incident field is changed, or that, at constant angle of incidence, the circular cylinder is rotated.

Nevertheless the derived equation is very useful, if it is considered that according to Chapter 7 it is easily accomplished, to map a circular cylinder onto a strip, onto a rectangle, onto an ellipse or onto an arbitrary biangle (region with circular arc sides and two corners). All these mapping problems are solved with this equation (Group of mappings R 3). The following example explains the procedure.

Example 2: Strip in uniform field with oblique incidence.

The field map of a circular cylinder in a uniform field with oblique incidence is (Eq. (11)):

$$\underline{w}_1 = e^{j\varphi} \left(\underline{w} + \sqrt{\underline{w}^2 - 1} \right). \quad (12)$$

A circle is mapped onto a strip with the successive transformation X 10

$$\underline{z} = \frac{1}{2} \left(\underline{w}_1 + 1/\underline{w}_1 \right). \quad (13)$$

Furthermore the circle must have the radius 1 and must be concentric to the origin. Both conditions are already satisfied by Eq. (12). Thus the successive transformation can be employed directly, without any other transformation in-between. Hence the field map sought-after in the z-plane is found (Figure 8.4b).

If Equation (12) is inserted into Equation (13), the solution can be written, with the relation

$$\frac{1}{\underline{w} + \sqrt{\underline{w}^2 - 1}} = \underline{w} - \sqrt{\underline{w}^2 - 1} \quad (14)$$

as

$$\underline{z} = \underline{w} \cdot \cos \varphi + j \sqrt{\underline{w}^2 - 1} \cdot \sin \varphi. \quad (15)$$

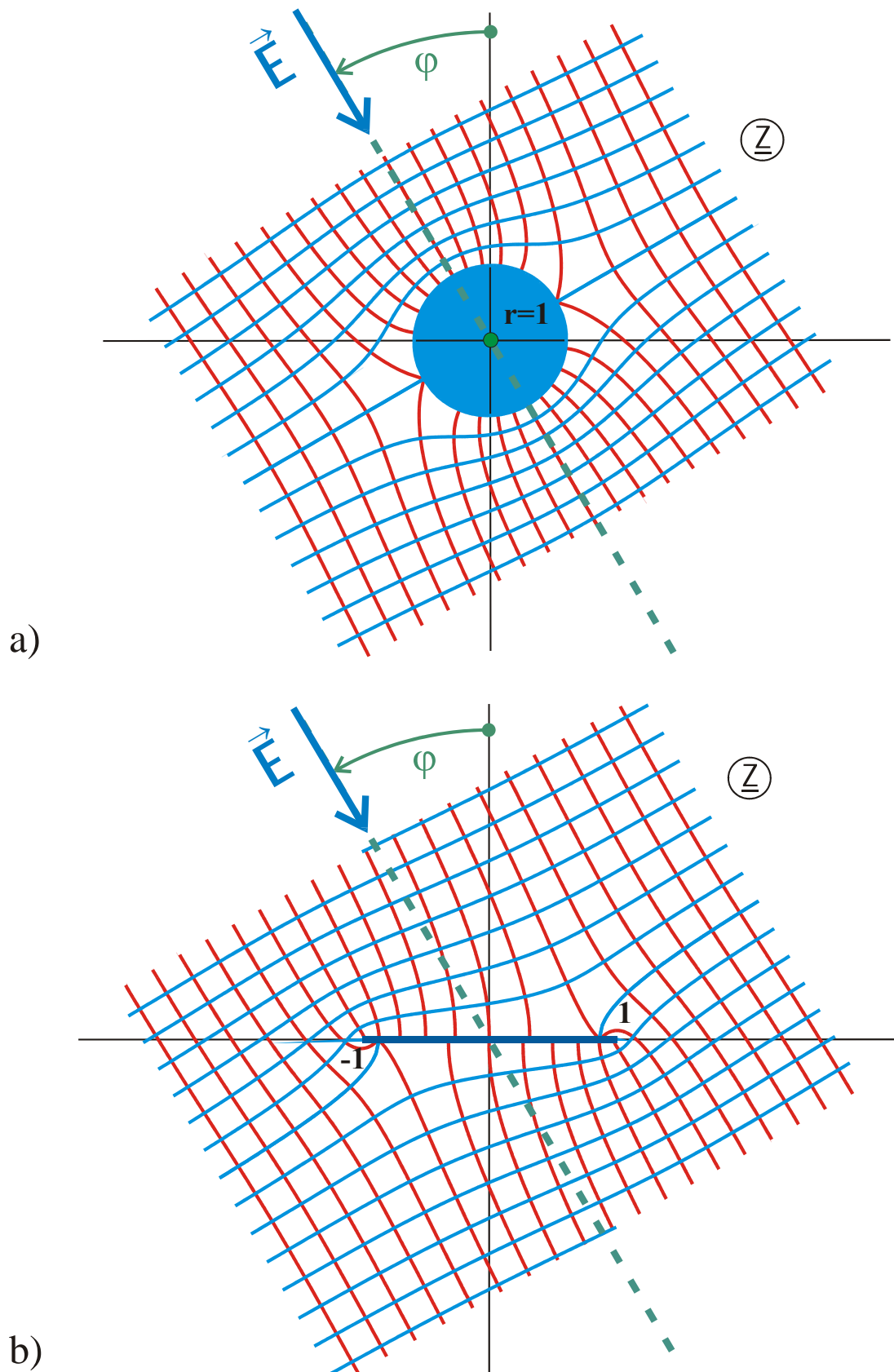


Figure 8.4: Example 2, conducting strip in a uniform field with oblique incidence
(A 3 and R 3)

8.3 Airfoil Profiles

In the fields of aerodynamics and hydrodynamics it is possible to determine physical parameters like e.g. velocity, pressure and uplift for a certain cross section, which is in a laminar flow, with the help of conformal mapping [29, 30]. The medium, in which the body to be analyzed is submerged, is assumed to be approximately inviscid and incompressible. As an example for cross sections, which are analytically solvable in such potential flows, the transformation equations for Joukowski profiles [3] and for Kármán-Trefftz profiles [3] are derived in the following.

Example 3: Joukowski profiles

The mapping is based on a circular arc in a uniform flow with oblique incidence. As illustrated in Figure 8.5, the starting point is a circle in a uniform flow with oblique incidence

$$\underline{w}_1 = e^{j\alpha} \left(\underline{w} + \sqrt{\underline{w}^2 - 1} \right) \quad (16)$$

and this circle is mapped onto a circular arc with equation X 14 of the transformation of domains.

$$1. \text{ Step: } \underline{w}_2 = \frac{\underline{w}_1 + j \sin \varphi}{\cos \varphi} \quad (17)$$

$$2. \text{ Step: } \underline{z} = \frac{1}{2} \left(\underline{w}_2 + 1/\underline{w}_2 \right). \quad (18)$$

In the general case that not the unit circle, like in Figure 8.6a, but a slightly bigger circle is transformed, a region with a curvilinear boundary is created in the z -plane, which covers the former circular arc completely. In the special case, where the slightly bigger circle in the w_2 -plane touches the unit circle in a single point and where the center point is not on the real axis, the created region in the z -plane is termed Joukowski profile.

Mathematically the slightly bigger circle is created by an additional mapping:

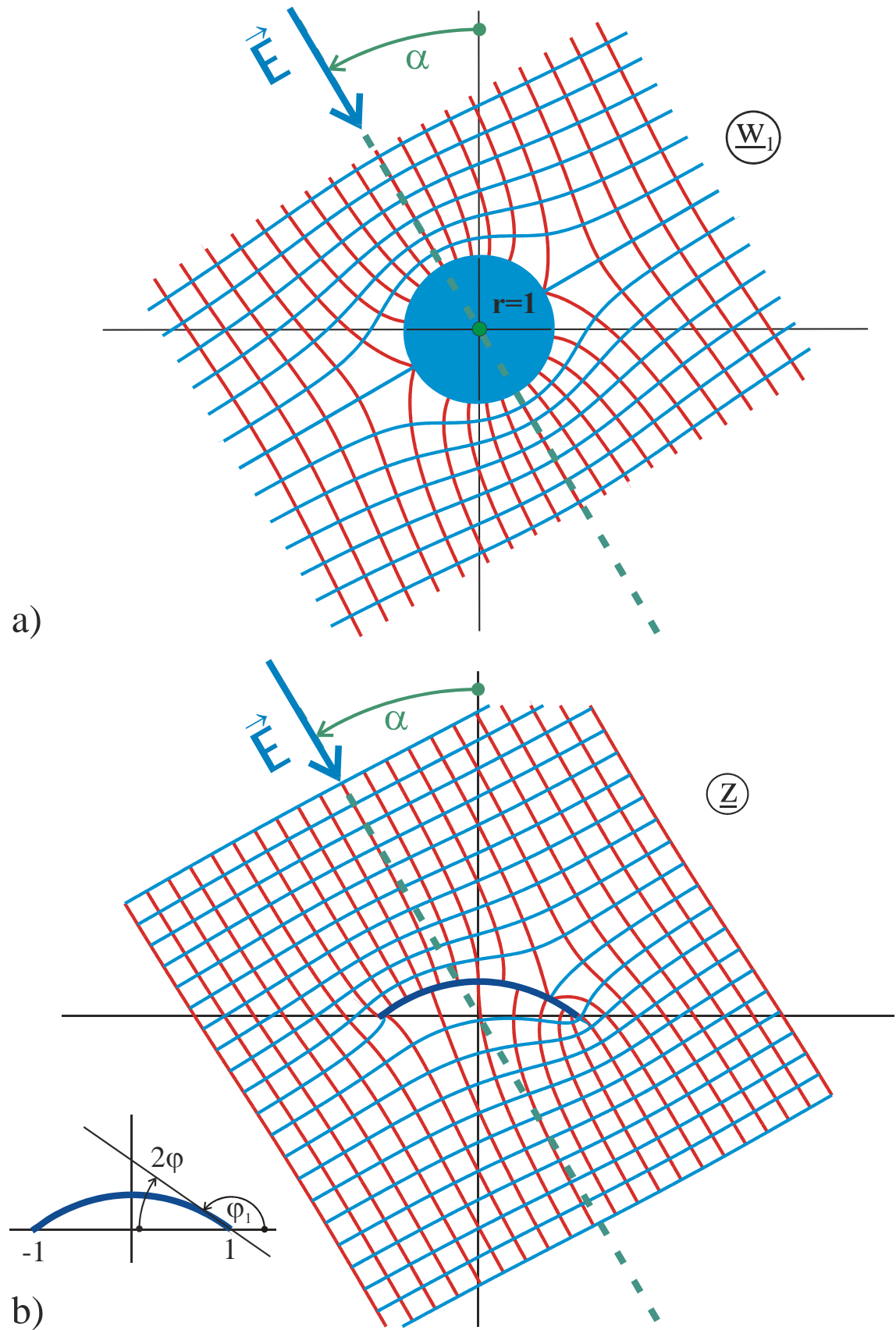


Figure 8.5: Circular arc in uniform flow with oblique incidence (R 3.1)

The starting point is again the unit circle in a uniform flow with oblique incidence

$$\underline{w}_1 = e^{j\alpha} \left(\underline{w} + \sqrt{\underline{w}^2 - 1} \right). \quad (19)$$

This circle is magnified by the factor $r > 1$ i.e. $(r \cdot \underline{w}_1)$, then this bigger circle is moved back to the unit circle $(r \cdot \underline{w}_1 - (r-1))$, moved away from the unit circle by the distance b $(r \cdot \underline{w}_1 - (r-1) + b)$ and finally rotated by the angle $-\beta$ (Figure 8.6b).

$$\underline{w}_2 = e^{-j\beta} [r \underline{w}_1 - (r-1) + b]. \quad (20)$$

After this the unit circle (in Figure 8.6b and c plotted in black) is mapped onto a circular arc and this procedure at the same time transforms the bigger circle (red) into a universal airfoil profile.

$$1. \text{ Step: } \underline{w}_3 = \frac{\underline{w}_2 + j \sin \varphi}{\cos \varphi} \quad (21)$$

$$2. \text{ Step: } \underline{z} = \frac{1}{2} (\underline{w}_3 + 1/\underline{w}_3). \quad (22)$$

In the special case $b = 0$, a Joukowski profile is created. It has a sharp edge at the right end. Figure 8.8a shows an example for the complete stationary flow field. The tangent to this edge has the same angle φ_1 as the tangent to the circular arc (Figure 8.5b). For $b = r-1$ the profiles are symmetrical to the imaginary axis; for $\beta = 0$ the profiles are symmetrical to the real axis. The shape of the profile can be systematically modified by adjustment of the parameters r , b and β . Further classes of profiles are generated, by modifying the transformation, e.g. in such a way that the rotation by the angle β is not like in Eq. (20) around the origin of the w_2 - plane, but instead around an arbitrary chosen different point.

If α is given a value between 0 and 2π the angle of incidence γ can be arbitrarily chosen.

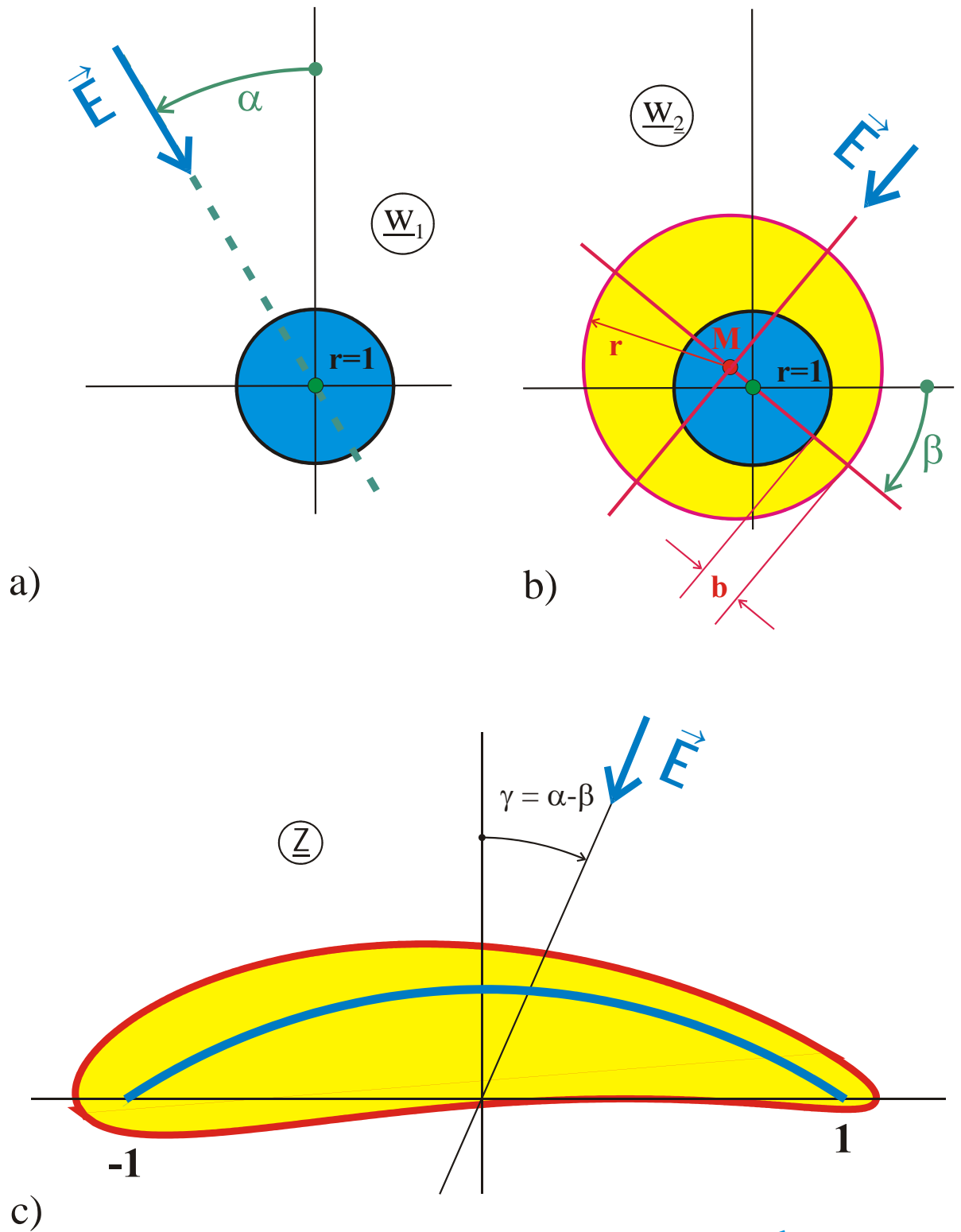


Figure 8.6: Airfoil profile, Example 3 (R 7.1)

Example 4: Kármán-Trefftz profiles

Another class of airfoil profiles is found, if the domain transformation used is not from circle onto circular arc, but from circle onto circular arc biangle. For $b = 0$ the cross sections created in the z -plane are termed Kármán-Trefftz profiles. The transformation equation for this case is (Figure 8.7):

$$\underline{w}_1 = e^{j\alpha} \left(\underline{w} + \sqrt{\underline{w}^2 - 1} \right) \quad (23)$$

$$\underline{w}_2 = e^{-j\beta} \left[r \underline{w}_1 - (r-1) + b \right] \quad (24)$$

$$\underline{w}_3 = a - jb \frac{1 + \underline{w}_2}{1 - \underline{w}_2} \quad (26)$$

$$\underline{w}_4 = e^{j\delta_2} \cdot \underline{w}_3^{(2-\delta_2/\pi+\delta_1/\pi)} \quad (26)$$

$$\underline{z} = \frac{1 + \underline{w}_4}{1 - \underline{w}_4} \quad (27)$$

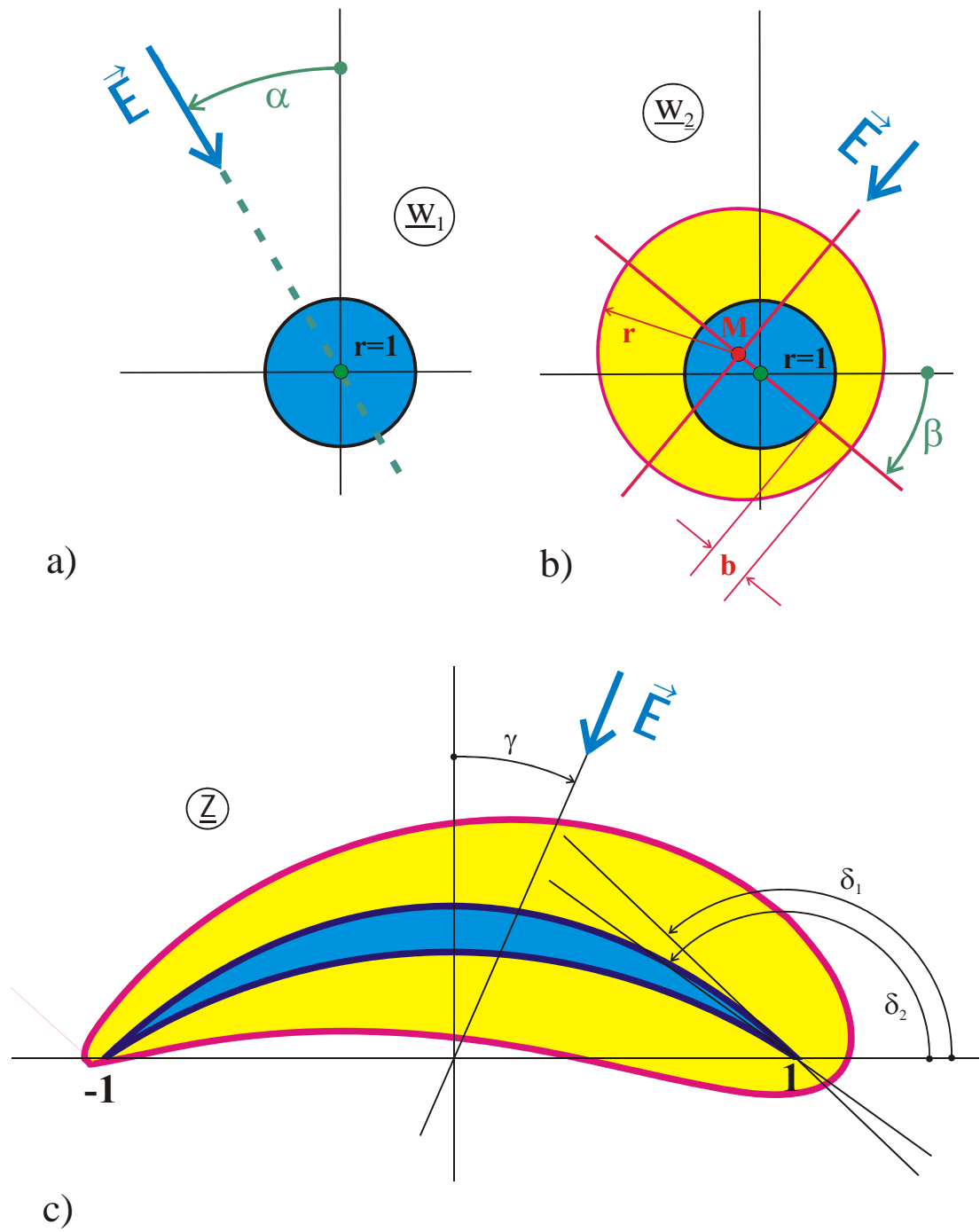
$$\text{with } a = \cos \varphi \quad (28)$$

$$b = \sin \varphi \quad (29)$$

$$\text{and } \varphi = \frac{2\pi - \delta_2}{2 - \frac{\delta_2}{\pi} + \frac{\delta_1}{\pi}} \quad (30)$$

Figure 8.8b illustrates a flow map of this type of profile with $b = 0,15$.

The profiles of Example 3 are special cases of this profile: For $\vartheta_1 = \vartheta_2$ the circular arc biangle fades into a circular arc.



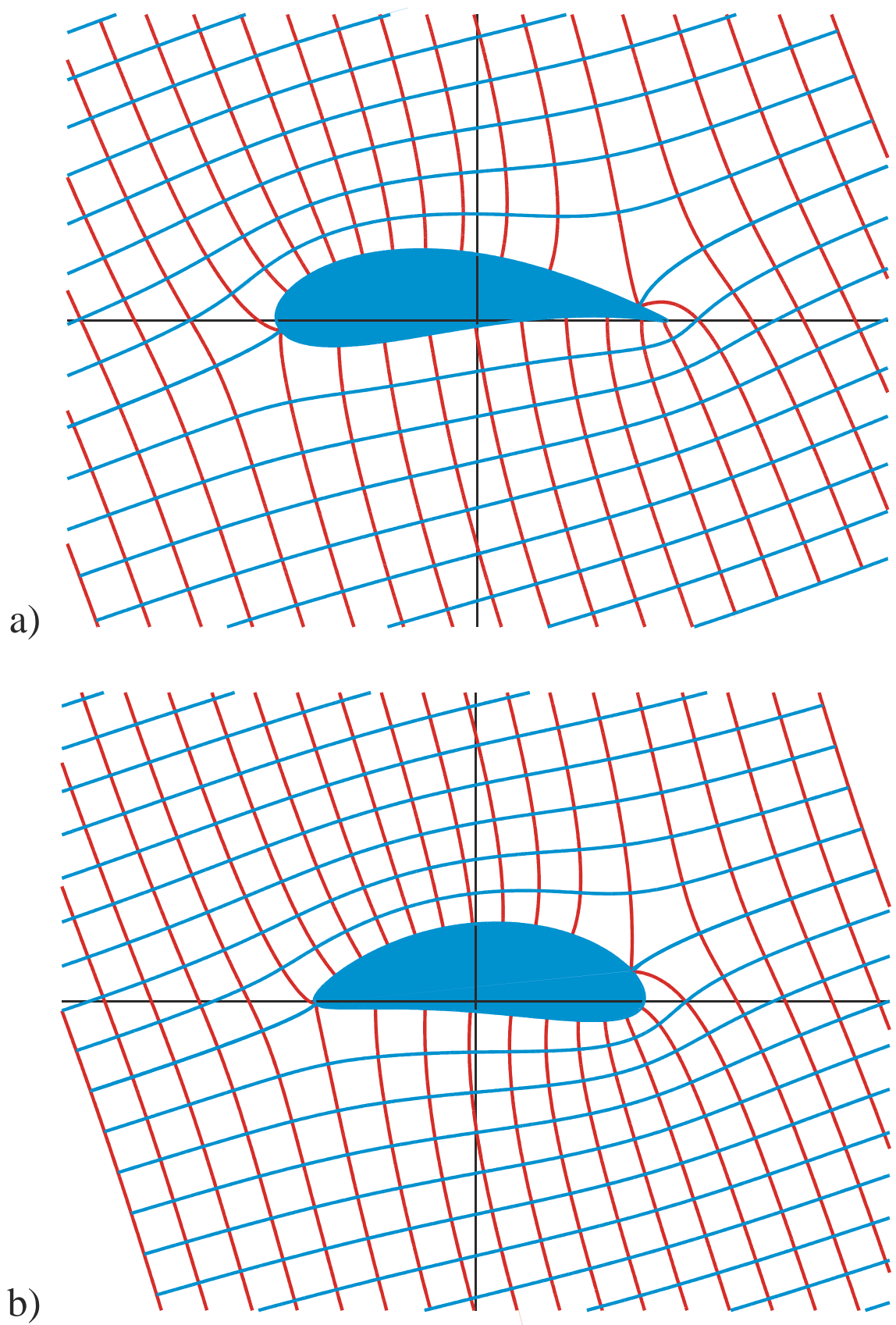


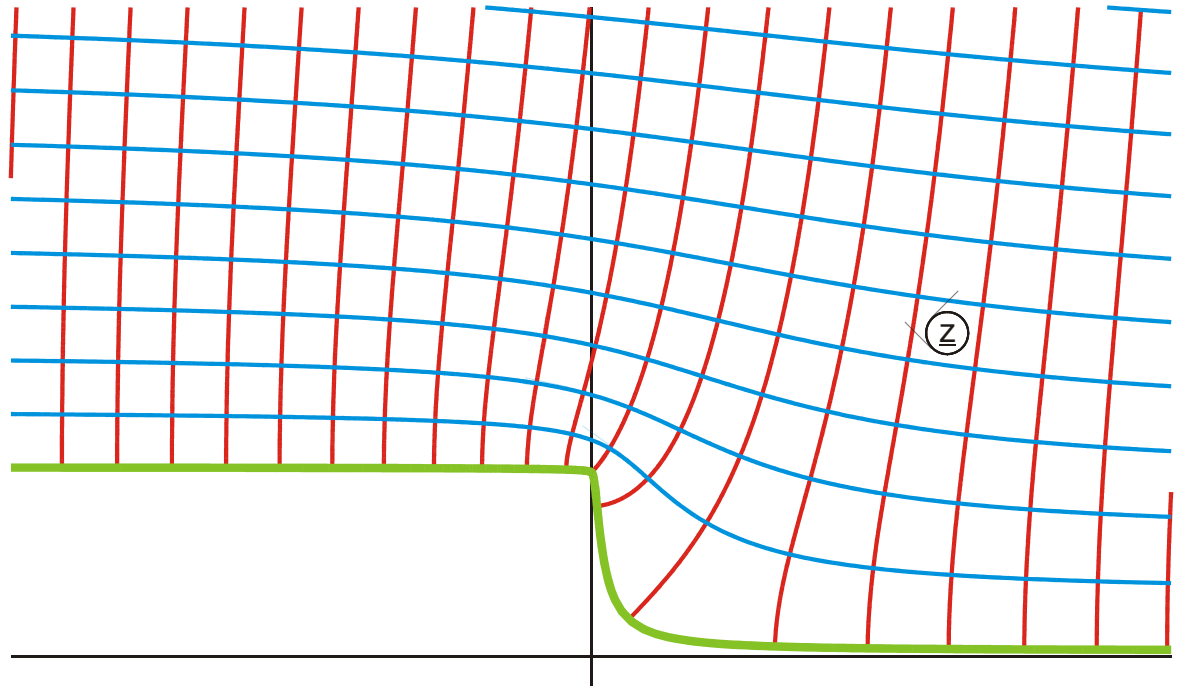
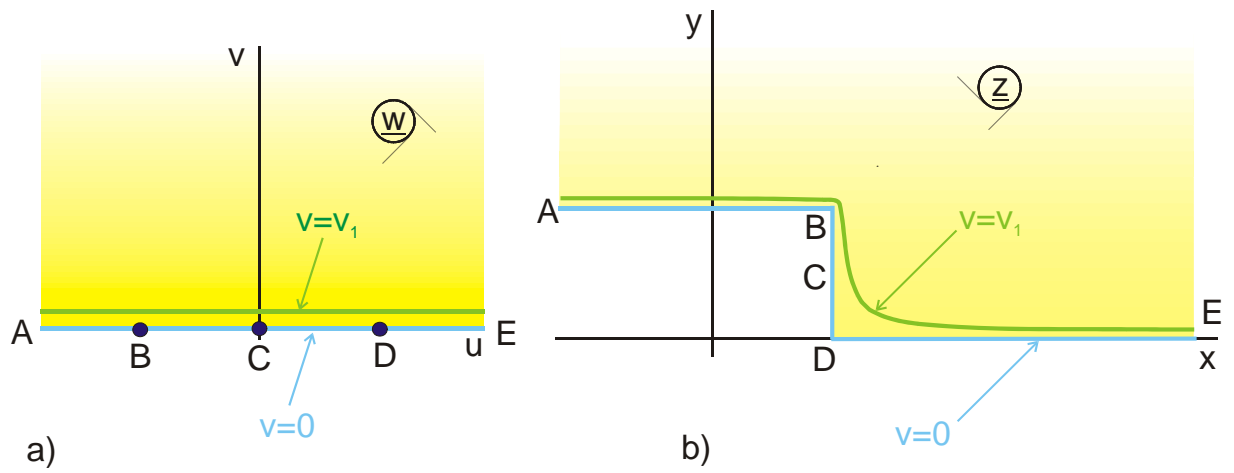
Figure 8.8: a) Flow map with Joukowski profile (R 7)

b) Flow map of the profile in Example 4 with $b = 0,15$ (R 7.2)

9. Rounded Corners

9.1 Neighboring Field Line

A simple procedure for rounding a corner of a given mapping with angled boundaries is illustrated in Figure 1. Instead of the boundary line $v=0$ another equipotential line $v=v_1$ is used as new boundary, which lies a little bit more inside, within the region of the field. This procedure has been used already in Example 8.3, when the airfoil was mapped. There the unit circle was mapped onto an area between two circular arcs with two sharp corners, and a bigger, adjacent circle that nevertheless did nowhere touch the unit circle, was mapped onto the airfoil, without any corners. As shown in Figure 9.1, the complete boundary changes its position when this method is used, to round a corner. Furthermore the effect is much more pronounced with inside corners (point D) than with outside corners or salient angles respectively (point B). Technically interesting is in general the rounding of outside corners, because there e.g. in the case of the electrostatic field, the electric field strength reaches infinite values, at least in the mathematical model.



c) $v_1 = 0,1$

Figure 9.1: Rounding of a corner by omitting the border line $v = 0$ and using an adjacent potential line $v = v_1$ as new boundary (A 6)

9.2 Rounding of Corners by Superposition of Partly Differing Boundaries

If to a field $f_1(\underline{w})$, whose boundary line runs with increasing \underline{w} , e.g. vertically, a second field $f_2(\underline{w})$, whose boundary line runs perpendicular to the other one, also with increasing \underline{w} , hence in this case horizontally, is added, then this yields in the field map of the function

$$f(\underline{w}) = f_1(\underline{w}) + f_2(\underline{w}) \quad (1)$$

in general a curved boundary as new border line (The addition of two complex numbers in the complex plane equals the addition of two vectors in the two-dimensional plane).

Example 1: Conducting plane with semi circle convexity

(Conducting circular cylinder in uniform field).

According to Figure 9.2a the boundary line of the function runs

$$f_1(\underline{w}) = \sqrt{\underline{w}^2 - 1} \quad (2)$$

from A to B in vertical direction, when u runs from 0 to 1 in the w -plane. The boundary line ($v = 0$) of the function

$$f_2(\underline{w}) = \underline{w} \quad (3)$$

runs according to Figure 9.2b with increasing u in horizontal direction. If both are added

$$f(\underline{w}) = f_1(\underline{w}) + f_2(\underline{w}) = \underline{w} + \sqrt{\underline{w}^2 - 1}, \quad (4)$$

then every point of the new boundary curve, as illustrated in Figure 9.2c, is found as the sum of the two complex numbers $f_1(\underline{w})$ and $f_2(\underline{w})$. The starting point A lies at $j + 0 = j$, the end point B lies at $0 + 1 = 1$ and all points in between create a curve, which is bent to the right. It is easily proven that in this case the curvilinear line is an exact semi circle with $x^2 + y^2 = 1$. In the interval between point B and point C both boundary lines have the same direction, they run vertically, with increasing u to the right. Thus the superposition yields the same curve there.

By the superposition of two field maps, whose boundaries are orthogonal to each other in a certain interval (between A and B) and whose boundaries are parallel aligned outside of this interval (between B and C), it is achieved in this example that a sharp blade, which extends into the upper half plane ($f_1(\underline{w})$, A 2.1) is converted into a semi circle (A 3). This procedure can be used systematically, to convert given field maps with sharp corners into field maps with rounded boundaries.

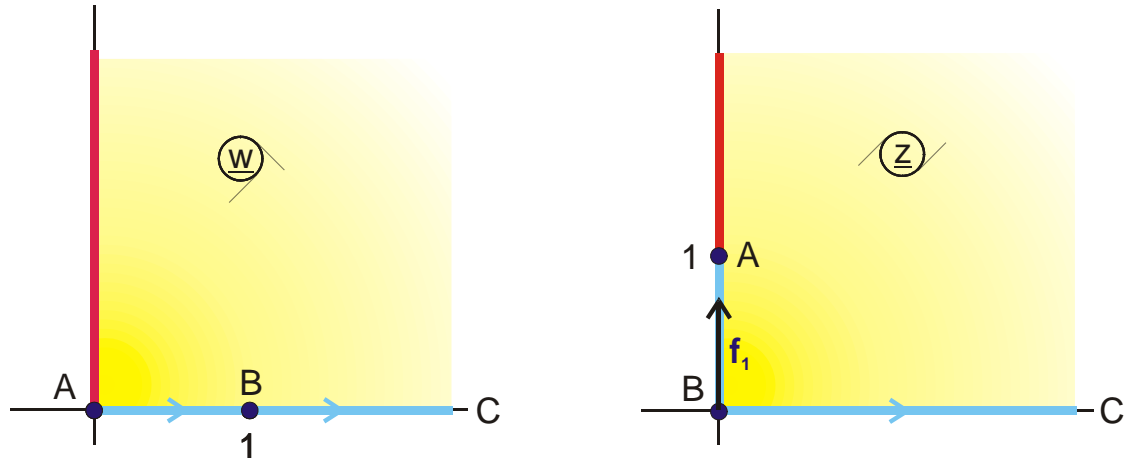
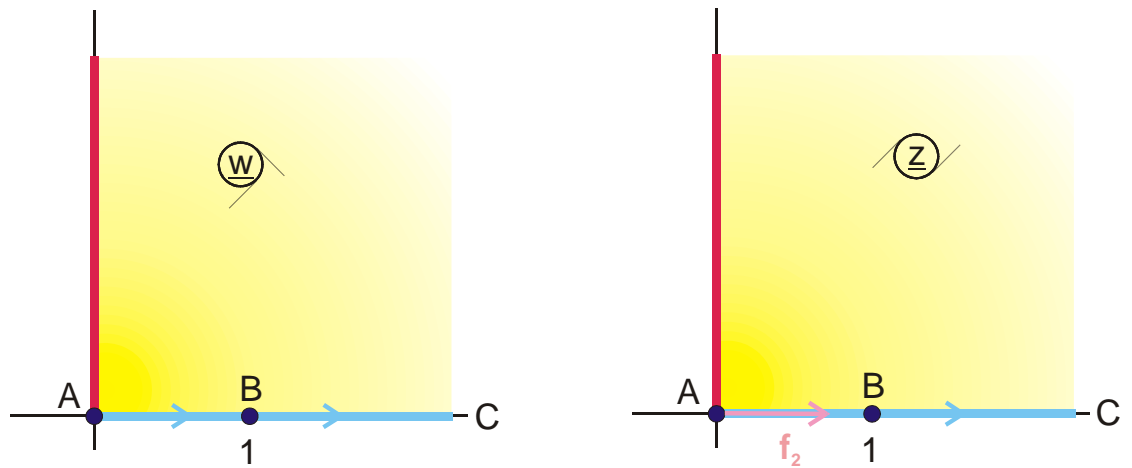
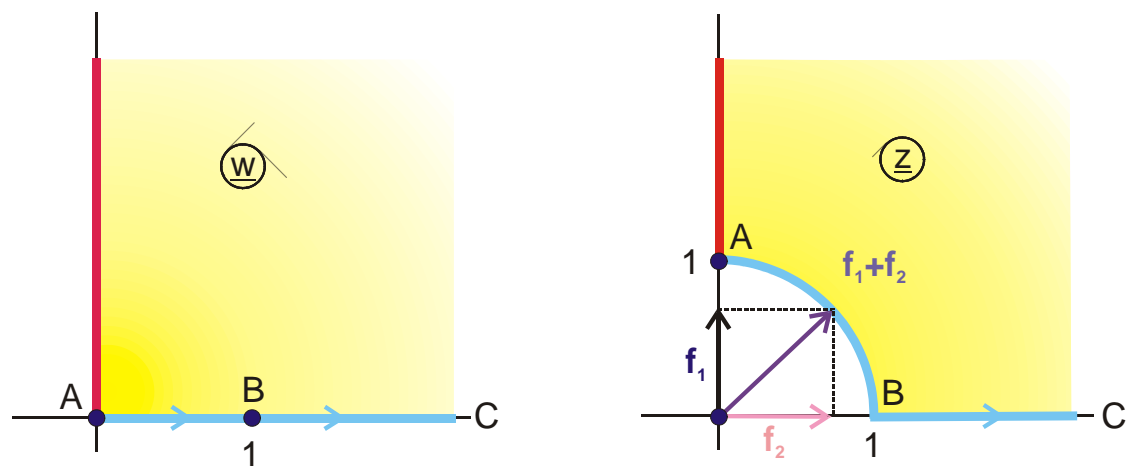
a) $f_1(w)$ b) $f_2(w)$ c) $f_1(w) + f_2(w)$

Figure 9.2: Example 1, details of the method used in Mapping A 3

Example 2: Rounded rectangle

In Figure 9.3a the contour of the boundary is a rectangle. If another boundary is added to this, which runs vertical in the complete interval from A through B to C, then the sum of the two curves is between A and B a curvilinear boundary and between B and C a vertical straight line.

$$\text{Rectangle:} \quad f_1(\underline{w}) = B_a \left(\frac{\sin(\underline{w}\pi)}{k}, k \right) + jb \quad (5)$$

$$\text{Vertical strip:} \quad f_2(\underline{w}) = j\sigma \cdot \cos(\underline{w}\pi) \quad (6)$$

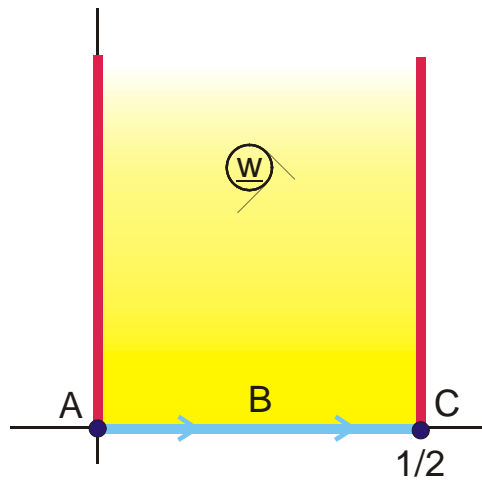
$$\text{Sum:} \quad \underline{z} = B_a \left(\frac{\sin(\underline{w}\pi)}{k}, k \right) + jb + j\sigma \cdot \cos(\underline{w}\pi). \quad (7)$$

In point A there is a horizontal tangent. In point B the contour of the boundary is discontinuous. Point B is at $u_B = \frac{1}{\pi} \arcsin k$. There $f_1(\underline{w})$ has the value $a + jb$ and $f_2(\underline{w})$ has the value $j\sigma\sqrt{1-k^2} = j\sigma k'$. Hence point B of the sum function is at $j(b + \sigma k')$. The contour of the boundary is approximately circular for

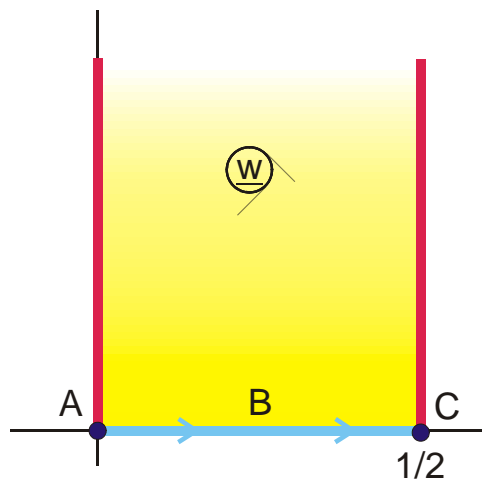
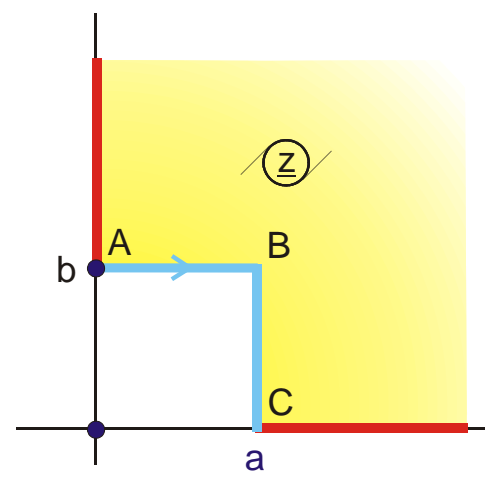
$$\sigma(1-k') = a, \quad (8)$$

which is evident, when looking at Figure 9.3c. Further examples for rounding one side of a rectangle or of a half strip with the same procedure are the Mappings M 1, M 1.1 and M 3.

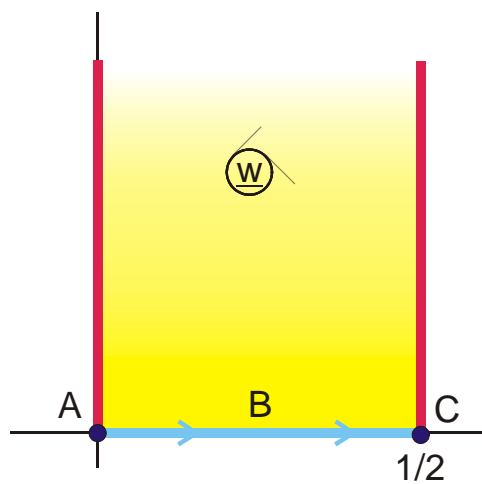
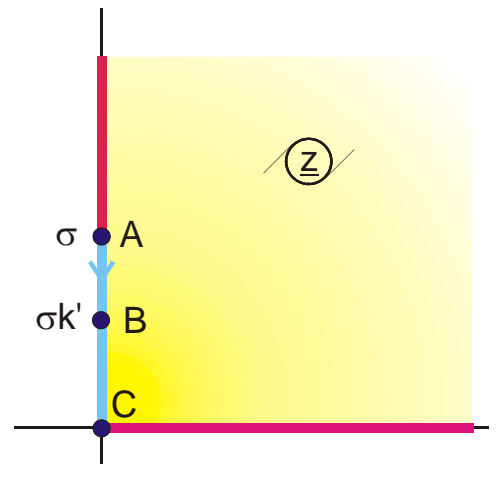
Instead of superposing two different field maps, like in the example above, it is also possible to superpose two similar field maps. Mapping 1 differs from mapping 2 in such a way that the outside corner, which is to be rounded, is displaced for a certain amount in the w -plane.



a) Rectangle



b) Vertical Strip



c) Sum: Mapping M1.2

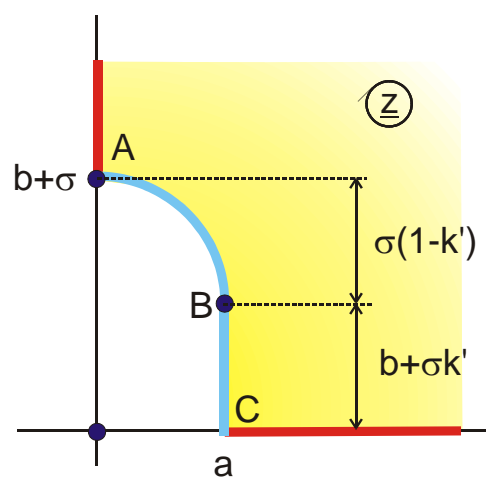


Figure 9.3: Example 2

Example 3: Rounded outside corner

The easiest case for the application of this procedure is the single corner

$$\underline{z} = \underline{w}^{\varphi/\pi}. \quad (9)$$

The vertex lies in the w -plane at $\underline{w} = 0$. If this point is moved for $f_1(\underline{w})$ to $\underline{w} = +a$ and for $f_2(\underline{w})$ to $\underline{w} = -a$

$$f_1(\underline{w}) = (\underline{w} - a)^{\varphi/\pi} \quad (10)$$

$$f_2(\underline{w}) = (\underline{w} + a)^{\varphi/\pi}, \quad (11)$$

then the sum of both functions contains in the interval between point B and point C in Figure 9.4c the superposition of a vertical boundary, function $f_1(\underline{w})$, and a horizontal boundary, function $f_2(\underline{w})$. The result is a rounded corner.

$$f(\underline{w}) = f_1(\underline{w}) + f_2(\underline{w}) \quad (12)$$

By insertion the location of point C is found:

$$b = (2a)^{\varphi/\pi}. \quad (13)$$

Further examples for the application of this procedure are the Mappings M 2 and M 2.1. In Figure 9.5 the basic principle of this procedure is illustrated. Both transformations $f_1(\underline{w})$ and $f_2(\underline{w})$ create the same boundary with a corner. The outside corner, which is to be rounded, in Figure 9.5 at point D, is in $f_1(\underline{w})$ slightly displaced compared to $f_2(\underline{w})$. All other vertices are in the w -plane at the same locations. The superposition of both fields then yields a rounded corner in point D. The shape and the extension of the rounded contour can be controlled by the choice of the distance Δu between the two points. Furthermore it is possible to influence the shape by repeated employment of this procedure, i.e. by multiple, weighted superpositions.

$$f(\underline{w}) = f_1(\underline{w}) + g_2 \cdot f_2(\underline{w}) + g_3 \cdot f_3(\underline{w}) + \dots \quad (14)$$

With the superposition of field maps it is also possible to create rounded inside corners.

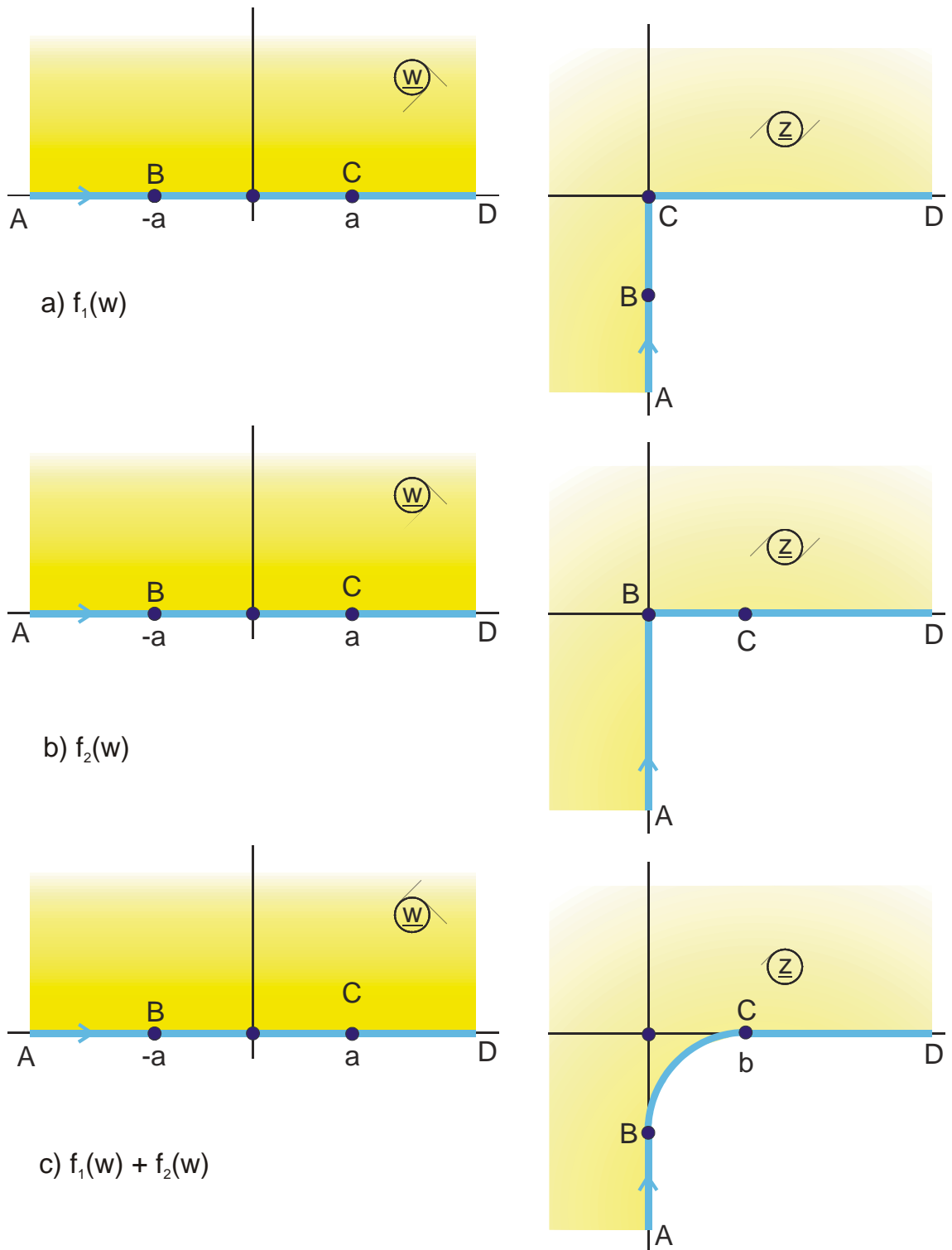


Figure 9.4: Example 3

Example 4: Rounded inside corner

Analogously to Example 3 the function

$$f_1(\underline{w}) = (\underline{w} + a)^{1+\varphi/\pi} \quad (15)$$

and the function

$$f_2(\underline{w}) = -(\underline{w} - a)^{1+\varphi/\pi} \quad (16)$$

are added to yield the function

$$f(\underline{w}) = f_1(\underline{w}) + f_2(\underline{w}) = (\underline{w} + a)^{1+\varphi/\pi} - (\underline{w} - a)^{1+\varphi/\pi} \quad (17)$$

Along the straight lines \overline{AB} and \overline{CD} the two different boundaries run into opposite directions (Figure 9.5). The function with the biggest magnitude dominates. The result is again a straight line. Between the points B and C the two functions run into different directions and the result is a curvilinear boundary, the rounded inside corner.

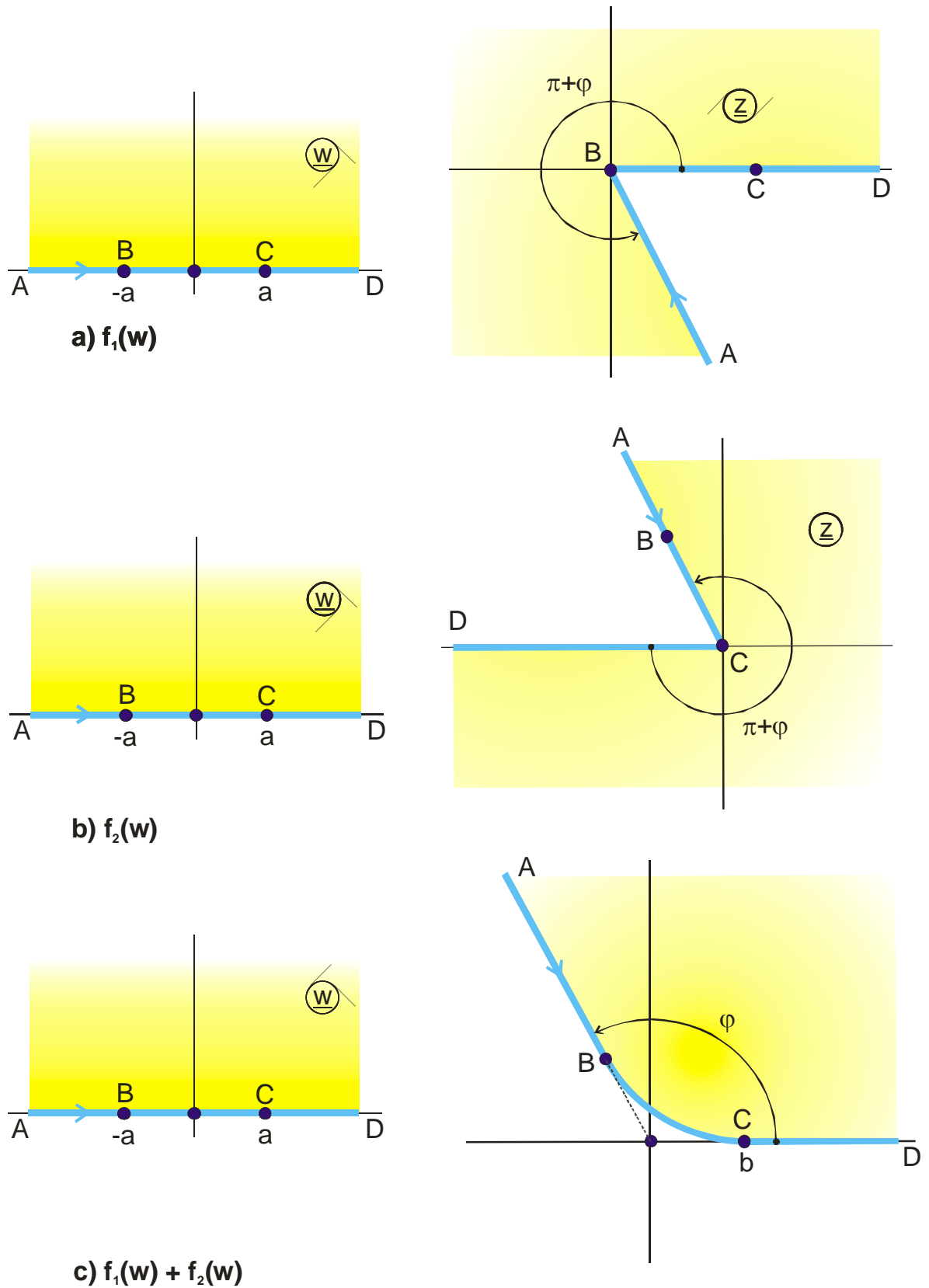


Figure 9.5: Example 4, rounded inside corner, (Mapping M 2.3)

9.3 Rounding of Outside Corners with the Schwarz-Christoffel Transformation

In the preceding chapter a method to create rounded outside corners has been introduced, where two transformation equations are added. The corner, which is to be modified, lies for each of these transformation equations at a different point of the real axis in the w -plane (Figure 9.5). Each transformation equation alone yields an outside corner at point D . The sum of both functions yields a rounded outside corner, where the curved boundary, whose shape is not mathematically defined, starts at D_1 and ends at D_2 .

In the Schwarz-Christoffel formula, Eq. (4.15), an outside corner is described by the term

$$\frac{1}{(\underline{w} - u_i)^{\alpha_i / \pi}} \quad (18)$$

with $\alpha_i < 0$. For $i = D$, according to Figure 9.5, it can be written

$$\frac{1}{(\underline{w} - u_D)^{\alpha_D / \pi}} \quad (19)$$

The two functions for the superposition result from the Schwarz-Christoffel formula with the term

$$\frac{1}{(\underline{w} - u_{D1})^{\alpha_D / \pi}} \quad \text{for } f_1(\underline{w}) \quad (20)$$

$$\text{and} \quad \frac{1}{(\underline{w} - u_{D2})^{\alpha_D / \pi}} \quad \text{for } f_2(\underline{w}) \quad (21)$$

The arc length of the curved line is controlled by the distance Δu from u_{D1} to u_{D2} . The shape of the curve is furthermore influenced by the weighting factor g_2 in the addition.

$$f(\underline{w}) = f_1(\underline{w}) + g_2 \cdot f_2(\underline{w}) \quad (22)$$

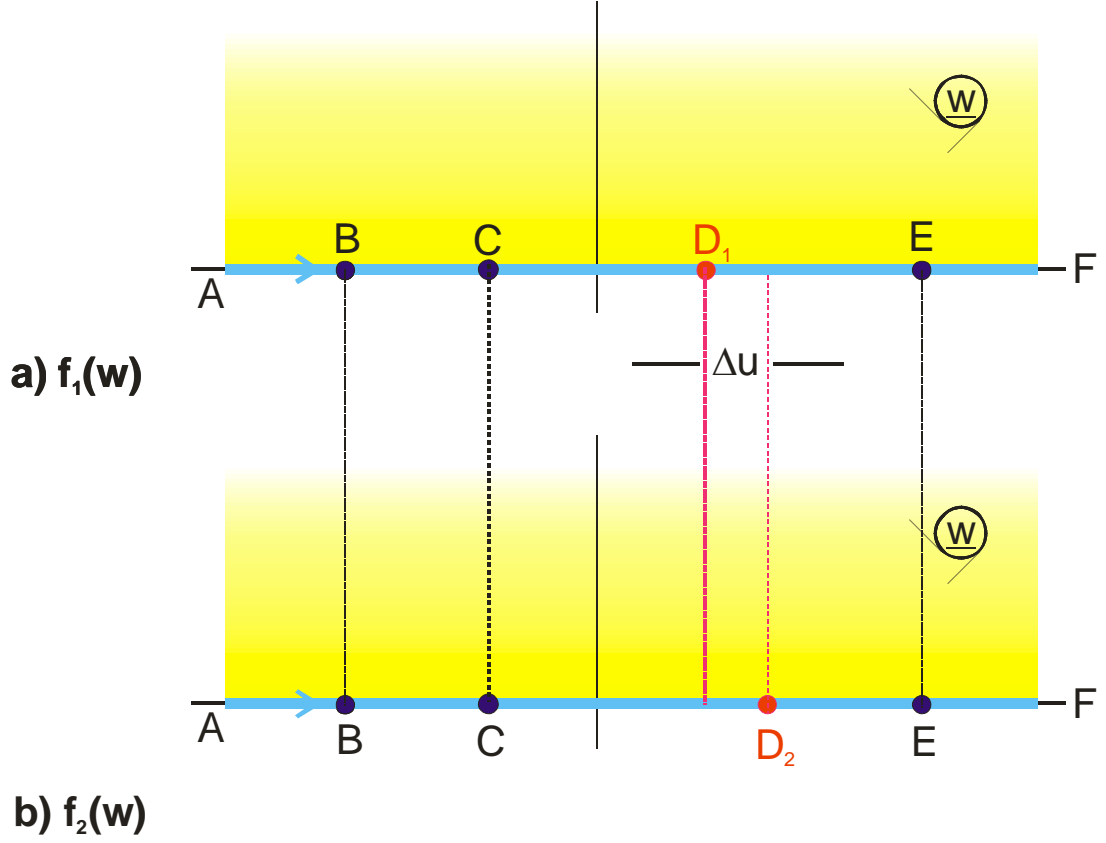


Figure 9.6: Allocation of the vertices of $f_1(w)$ and $f_2(w)$ in the w -plane

Example 5: Mapping M 4, rounding of the corner in Mapping C 1 [10]

With the method for the mapping of regions with polygonal boundaries, the following integral is found for the polygon in Figure 9.7

$$\underline{z} = \int_0^{\underline{w}_1} \frac{\sqrt{\underline{w}_1 - b_1}}{\underline{w}_1} d\underline{w}_1 \quad (23)$$

with the solution

$$\underline{z} = 2\sqrt{\underline{w}_1 - b_1} - 2\sqrt{b_1} \cdot \arctan \sqrt{\frac{\underline{w} - b_1}{b_1}}. \quad (24)$$

In order to have different potential on both electrodes AC the pre-transformation

$$\underline{w}_1 = \exp(\pi \underline{w}) \quad (25)$$

has to be used.

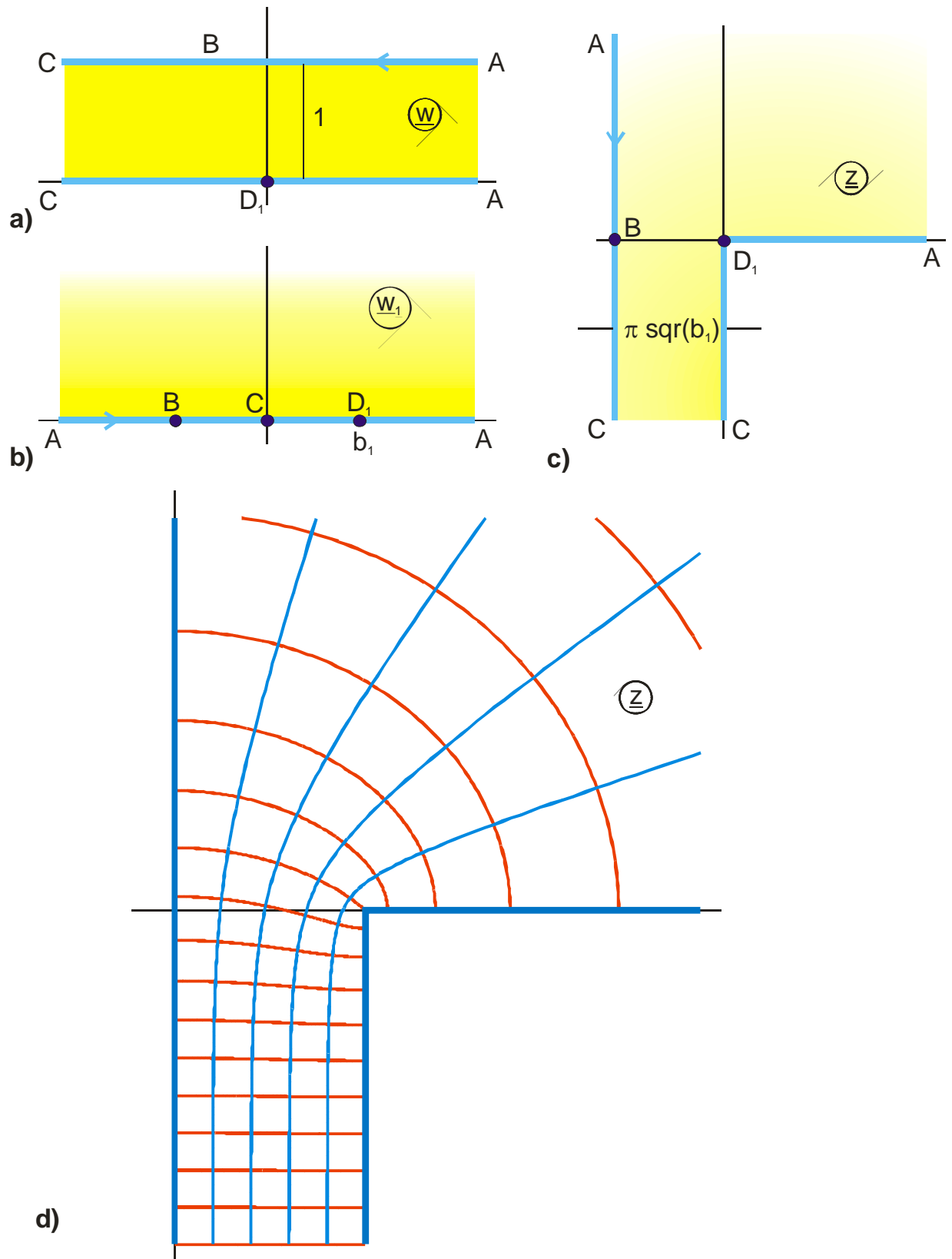


Figure 9.7: Mapping C 1 for Example 5

In order to get a rounded corner in point D_1 , to this function

$$f_1(\underline{w}_1) = 2\sqrt{\underline{w}_1 - b_1} - 2\sqrt{b_1} \cdot \arctan \sqrt{\frac{\underline{w}_1 - b_1}{b_1}} \quad (26)$$

another function

$$f_2(\underline{w}_1) = 2\sqrt{\underline{w}_1 - b_2} - 2\sqrt{b_2} \cdot \arctan \sqrt{\frac{\underline{w}_1 - b_2}{b_2}}, \quad (27)$$

multiplied with the weighting factor λ , is added.

$$f(\underline{w}_1) = f_1(\underline{w}_1) + \lambda \cdot f_2(\underline{w}_1). \quad (28)$$

The function $f_1(\underline{w}_1)$ has an outside corner at D_1 ; $f_2(\underline{w}_1)$ has an outside corner at D_2 .

For $\Delta u_1 \neq 0$, with

$$\Delta u_1 = |b_1 - b_2|, \quad (29)$$

the weighted addition of both functions yields a rounded corner. The smaller Δu_1 , the smaller the radius of curvature. For $b_1 = b_2$ the original, sharp angled corner is restored. For $b_1 = 1 - \Delta u_1/2$ and $b_2 = 1 + \Delta u_1/2$ point D_1 is moved downwards in the z -plane for $\lambda > 1$. For $\lambda < 1$ point D_2 is moved to the right.

To normalize the mapping to the width 1 and to move point B into the origin of the z -plane (Figure 9.8) Eq. (28) is modified to

$$f(\underline{w}_1) = \frac{1}{\pi(\sqrt{b_1} + \lambda\sqrt{b_2})} \{f_1(\underline{w}_1) + \lambda \cdot f_2(\underline{w}_1)\} + 1. \quad (30)$$

Mapping M 4.1 is a further example for this method of creating a rounded outside corner.

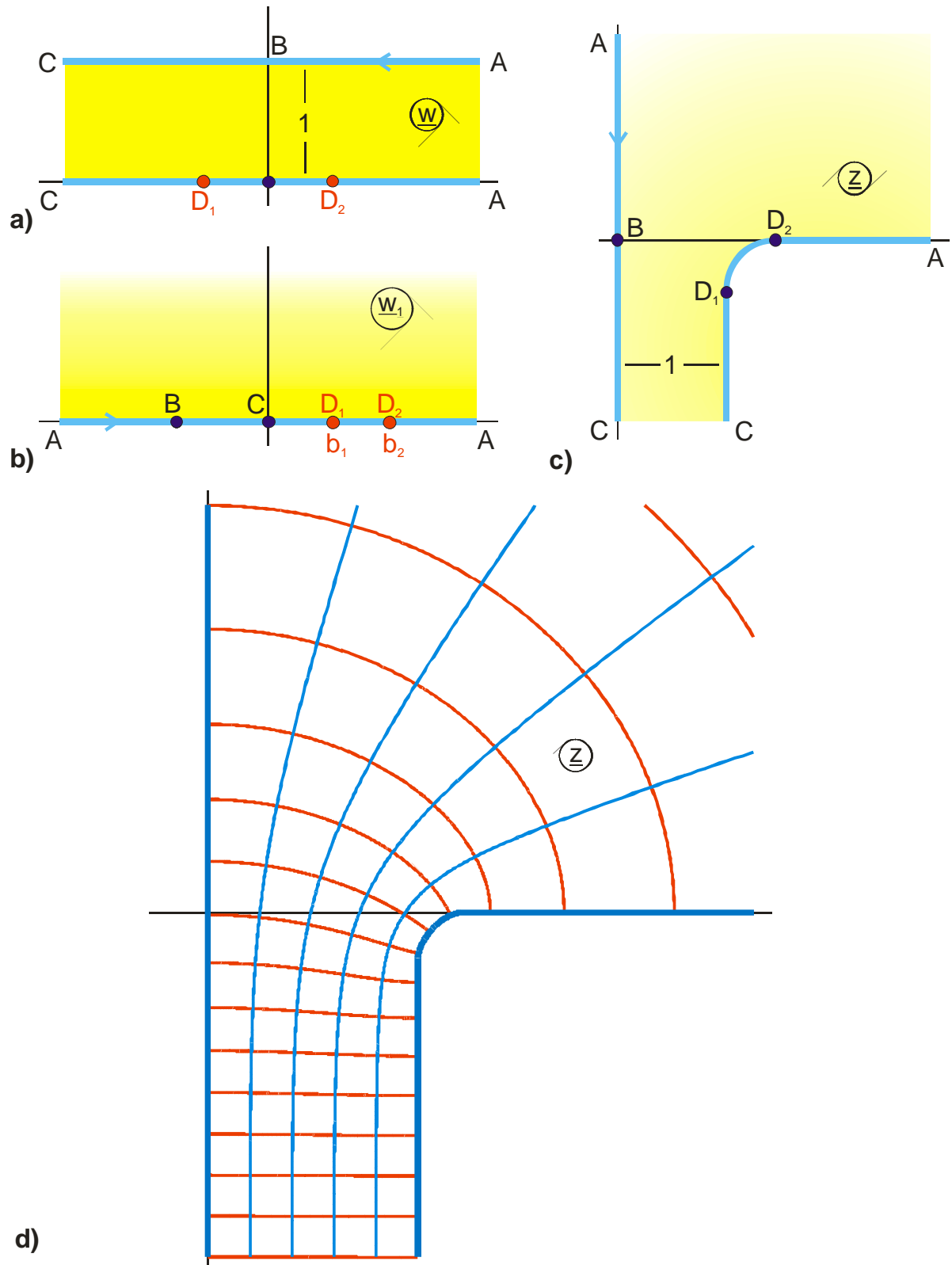


Figure 9.8: Example 5, Mapping M 4

9.4 Rounding of Inside Corners

In Chapter 9.1. it was said that a simple rounding of a corner is possible, if instead of the bent boundary line another potential line, lying slightly more inside, is used as new boundary line. This procedure may be improved, if the boundary is only left for a detour through the region inside the field, in the immediate vicinity of the corner, which is to be modified. As illustrated in Figure 9.9b, in this manner the corner, which lies at point D on the real axis, is by-passed. In the z -plane, exclusively between D_1 and D_2 , a curvilinear boundary is created. The remaining boundary stays unchanged. Corner D is cut out with the help of a pre-transformation.

Example 6: M 5, rounding of the inside corner in Mapping A 6

A suitable pre-transformation is e.g. Mapping A 3.11 [15]:

$$\underline{w}_1 = \underline{w} - \frac{h}{a^2} \left\{ \left[(\underline{w} - b_1)(\underline{w} - b_2) \right]^{3/2} - (\underline{w} - b_1)(\underline{w} - b_2)(\underline{w} - b) \right\} \quad (31)$$

$$\text{with } a = (b_2 - b_1) / 2. \quad (32)$$

The parameters b_1 and b_2 determine the length of the curved area. With the parameter h the degree of the curvature is influenced. The height c of the cut out area in the w_1 - plane, is proportional to h ($c = h a$). At D_1 and D_2 in the w_1 -plane the boundary has a horizontal tangent.

Now the task is to round the inside corner in Mapping A 6. As seen in Figure 9.9, b equals 1 and the field map in the z -plane is given by

$$\underline{z} = \sqrt{\underline{w}_1^2 - 1} + \ell n \left(\underline{w}_1 + \sqrt{\underline{w}_1^2 - 1} \right). \quad (33)$$

As the pre-transformation Eq. (31) does only affect the interval between D_1 and D_2 , it is possible to employ it several times successively. In this manner each inside corner that has to be rounded, can be treated individually, independent from all others.

The procedure is **in principle** also applicable for outside corners. However, in this case, as the dashed line at point B in Figure 9.9c shows, a swelling of the outside corner is created.

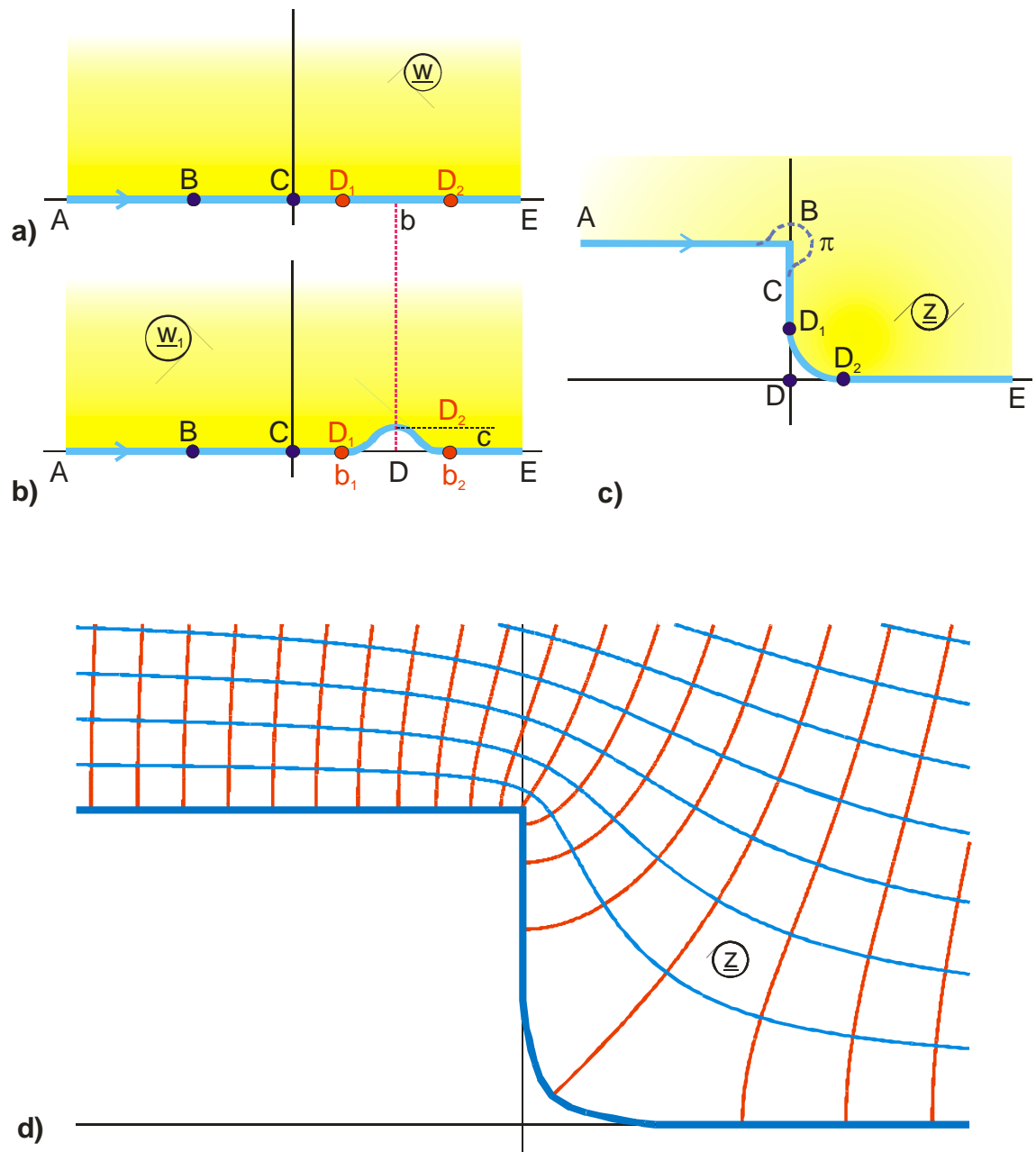


Figure 9.9: M 5, rounding of an inside corner according to Example 6

A further example for the application of this method is Mapping M 5.1.

10. Electrodes with Constant Field Strength

In the conformal mappings discussed so far, the surfaces of the conducting electrodes were planes of constant potential. Through the process of conformal mapping from an original plane onto an image plane this property of a boundary, to be a potential line, was preserved. The electric field strength on this potential line, i.e. the distribution of the density of the field lines, which ended there, was always altered by the mapping. The task, which was to be solved by the application of the method of conformal mapping, is in most cases: How can the straight boundary of a uniform field (with constant field strength everywhere) be mapped onto the non-uniform field of a given problem with curvilinear boundaries, in order to be able to determine the local distribution of the electric field strength of this non-uniform field. By conformal mapping into another plane the electric field strength on a potential line will be altered in principle.

However there are some technical applications, where systematically electrode configurations are searched, on which the electric field strength is constant (e.g. in the field of high voltage engineering) or the task is to determine the trace of those boundaries with constant velocity, which were found experimentally (e.g. in the field of fluid dynamics). In the case of electrostatics an electrode with constant field strength in a field map $\underline{z} = f(\underline{w})$ is defined by

$$1. \quad u = \text{const} \quad \text{or} \quad v = \text{const} \quad (\text{potential line}) \quad (1)$$

$$\text{and} \quad 2. \quad |\vec{E}| = \left| \frac{d\underline{w}}{d\underline{z}} \right| = \frac{1}{\left| \frac{d\underline{z}}{d\underline{w}} \right|} = \text{const} \quad (\text{const. field strength}). \quad (2)$$

In the case of fluid dynamics such boundary resembles either a solid boundary (potential line), where the velocity of flow v is constant

$$|\vec{v}| = \text{const}, \quad (3)$$

or the boundary of a free jet, e.g. as border line between streaming water and air or between streaming water and stagnant water, where the magnitude of the velocity of flow \bar{v} is constant as well.

In the two trivial cases, the uniform field

$$\underline{z} = \underline{w} \quad (4)$$

and the field of a line charge

$$\underline{z} = \exp(\underline{w}\pi) \quad (5)$$

all potential lines are as well lines of constant field strength. In the case of all other potential fields

$$\underline{z} = f(\underline{w}) \quad (6)$$

there exists at most one potential line, where the magnitude of the electric field strength is constant. Figure 10.1 shows an example for such an electrode opposite to an inside right angle corner. The field lines are equidistant along the line CD. The electric field strength E is in the w -plane (uniform field) as well as in the z -plane constant. For the normalized case $E = 1$ follows

$$\left| \frac{d\underline{z}}{d\underline{w}} \right|_{\underline{w}=\underline{w}_h} = 1. \quad (7)$$

The line CD in the z -plane has even sector-wise the same length as in the w -plane. For every point on this curve holds that the relative elongation is constant and equal to 1 respectively

$$\left| \frac{d\underline{z}}{d\underline{w}} \right| = 1 \quad \text{and} \quad \frac{\Delta z_h}{\Delta w_h} = 1. \quad (8)$$

The arc length in the z -plane is therefore

$$\int_{z_1}^{z_2} \underline{z}_h d\underline{z} = u_2 - u_1, \quad (9)$$

if the boundary with the uniform field strength (Index h for homogeneous) is mapped like in Figure 10.1a onto a line $v = \text{const}$. Elsewise the arc length is $v_2 - v_1$.

From this follows directly that a field with **two** neighboring lines, which satisfy this condition, is either a uniform field or the field of a line charge. **Every non-uniform field can possess just one of these lines.** In the case of symmetric fields or single or double

periodic fields this sentence is valid only for the non-uniform field within a non-symmetric sector or within a periodic strip or within a periodic rectangle.

With the help of fluid mechanics it can be derived that in the case of boundaries with infinite extension the channel width h_1 at one end must be the same as the channel width h_2 at the other end (Figure 10.1b). The flow must be uniform in each point at infinite distance. Because the flow rate is constant in the case of two continuous solid boundaries, the channel widths must be the same in the uniform part of the field, as long as also the velocity is constant at the boundary. The proof of this property is even easier if the z -plane is looked upon as a complex Riemann sphere. Point C merges into point D and point B merges into point E in the infinite point. The channel ends are connected with each other in this point and there is a smooth transition of the boundaries.

For the potential line with constant field strength follows from $1 / \left| \frac{dw}{dz} \right| = 1$

$$\left(\frac{\partial x_h}{\partial u} \right)^2 + \left(\frac{\partial y_h}{\partial u} \right)^2 = 1 \quad (10)$$

$$\left(\frac{\partial x_h}{\partial v} \right)^2 + \left(\frac{\partial y_h}{\partial v} \right)^2 = 1 \quad (11)$$

Example 1: Line with constant field strength in front of an inside corner

The field map of Figure 10.1b is found with the conformal transformation

$$\underline{w}_1 = \tanh(\underline{w}\pi) \quad (12)$$

$$\underline{w}_2 = \sqrt{\underline{w}_1} \quad (13)$$

$$\underline{z} = 2j[\arctanh \underline{w}_2 - \arctan \underline{w}_2] + \pi + j\pi. \quad (14)$$

On the potential line CD the electric field strength E is constant. There is (for $\underline{z} = \underline{z}_h$)

$$|\vec{E}| = \left| \frac{dw}{dz} \right| = |\underline{w}'| = \text{const.} \quad (15)$$

The w' -plane or the $(-w')$ -plane respectively is termed hodograph-plane in hydrodynamics. The hodograph is the image of the line CD in this plane. Because the magnitude of \underline{w}' is constant along this line, it is the arc of a circle, which is concentric to the origin.

If instead of this the conformal mapping

$$\underline{z}' = \frac{d\underline{z}}{d\underline{w}}. \quad (16)$$

is analyzed in the z' -plane, it is found from Eq. (12 through 14)

$$\frac{d\underline{z}}{d\underline{w}} = \frac{d\underline{z}}{d\underline{w}_2} \cdot \frac{d\underline{w}_2}{d\underline{w}_1} \cdot \frac{d\underline{w}_1}{d\underline{w}} \quad (17)$$

$$\frac{d\underline{z}}{d\underline{w}} = j2\pi \sqrt{\tanh(\underline{w}\pi)}. \quad (18)$$

Also in this plane it is obtained that

$$\left| \frac{d\underline{z}}{d\underline{w}} \right|_{\underline{w}=\underline{w}_h} = \text{const} \quad (19)$$

with $\underline{w}_h = u + j/4$.

In this plane the line DC is a circular arc, concentric to the origin, with the radius 2π (Figure 10.1c).

If the field map in the z -plane is symmetrically complemented by mirror imaging at the axes, in such a way that all 4 quadrants are filled with field, then it is found that the image of the total of 4 lines with constant field strength are mapped onto a full circle around the origin in the z' -plane. Outside this circle the field map in the z' -plane is completely defined.

The images in electrodes with constant field strength are also examined in Chapter 1.5.

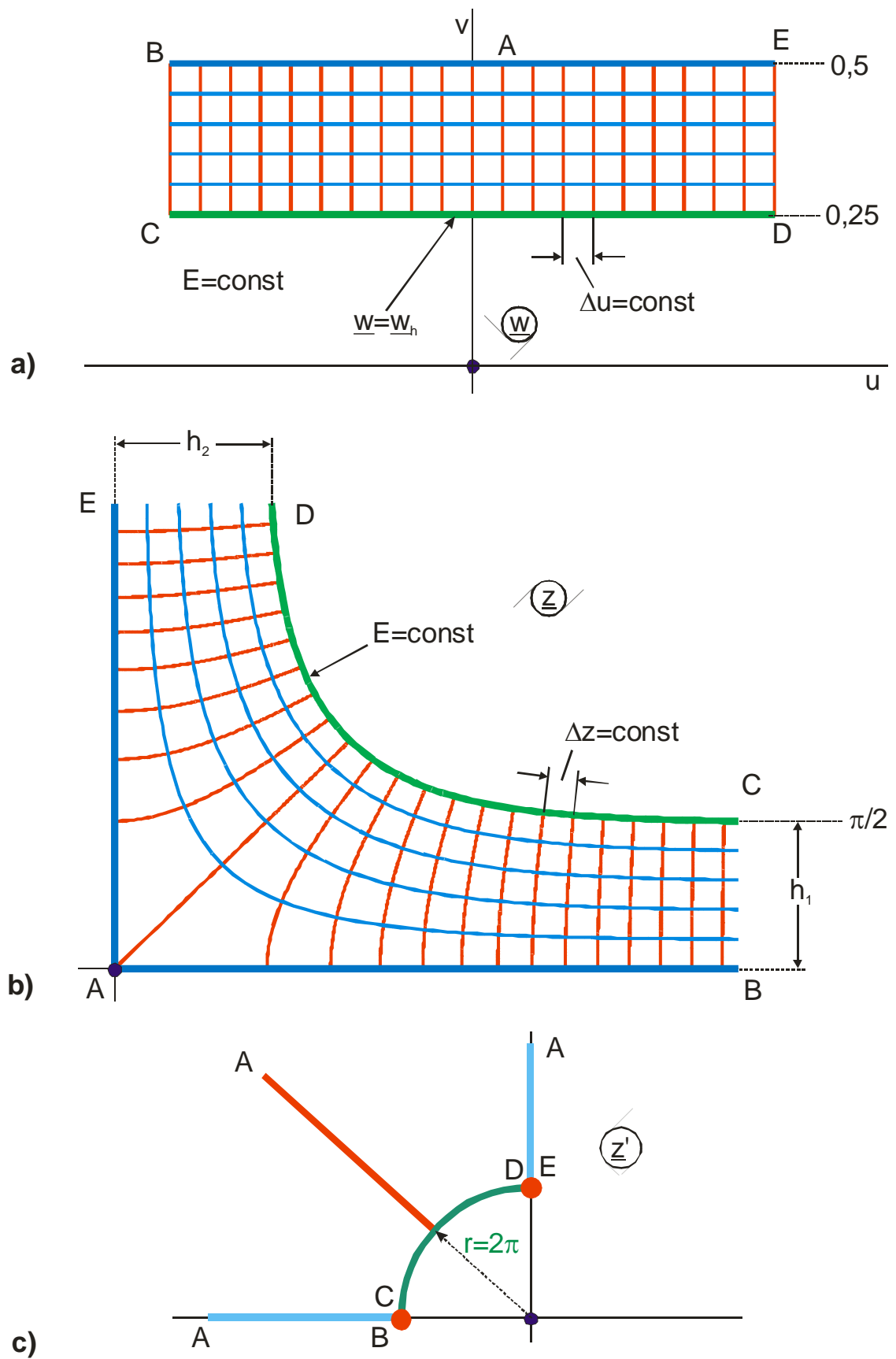


Figure 10.1: Field map of an infinite electrode with constant field strength (N 1)

According to the theory of images (Chapter 1.5) the field map inside the circle is also defined and known. The potential line BAE outside the circle has as mirror image the potential line HGF inside the circle. This line is shown dotted in Figure 2c. This boundary is also enclosed in the z -plane and in the w -plane. The interrelationship is straightforward and simple in the w -plane. The imaging at the line CD is there the imaging at a straight line. The correspondence between the points in the lower half strip and those in the upper half strip are well defined. From the examination of the point $\underline{w} \rightarrow \pm \infty$ results in the z -plane that the channel widths must be the same there. The correspondence between all other points is easily determined as well. It can be calculated as the image in the circle of the z' -plane and by the transformation from the z' -plane in the z -plane.

Having added the imaged boundary HGF in Figure 10.2b, it is evident that the Mapping N 1 in Figure 10.1 is nothing else but one half of the Mapping D 4 from the table of Mappings. The transformation equation Eq. (12-14), which was given in Example 1 without explanation, in order to illustrate the shown relationships, was known already in advance, due to the theory of images.

The potential line CD in Figure 10.1b, upon which the electric field strength is constant, has in parametric form the notation

$$x_h = \pi - \frac{\pi}{2} \left[1 - \frac{1}{\pi} \ell n \frac{1 + \cos \varphi}{1 - \cos \varphi} \right] \quad (20)$$

$$y_h = \pi - \frac{\pi}{2} \left[1 - \frac{1}{\pi} \ell n \frac{1 - \sin \varphi}{1 + \sin \varphi} \right] \quad (21)$$

with $0 \leq \varphi \leq \pi/2$.

The relationships shown in this example are valid for all fields with lines of constant field strength:

- Potential lines with constant field strength in the z -plane are circular arcs concentric to the origin in the z' -plane.

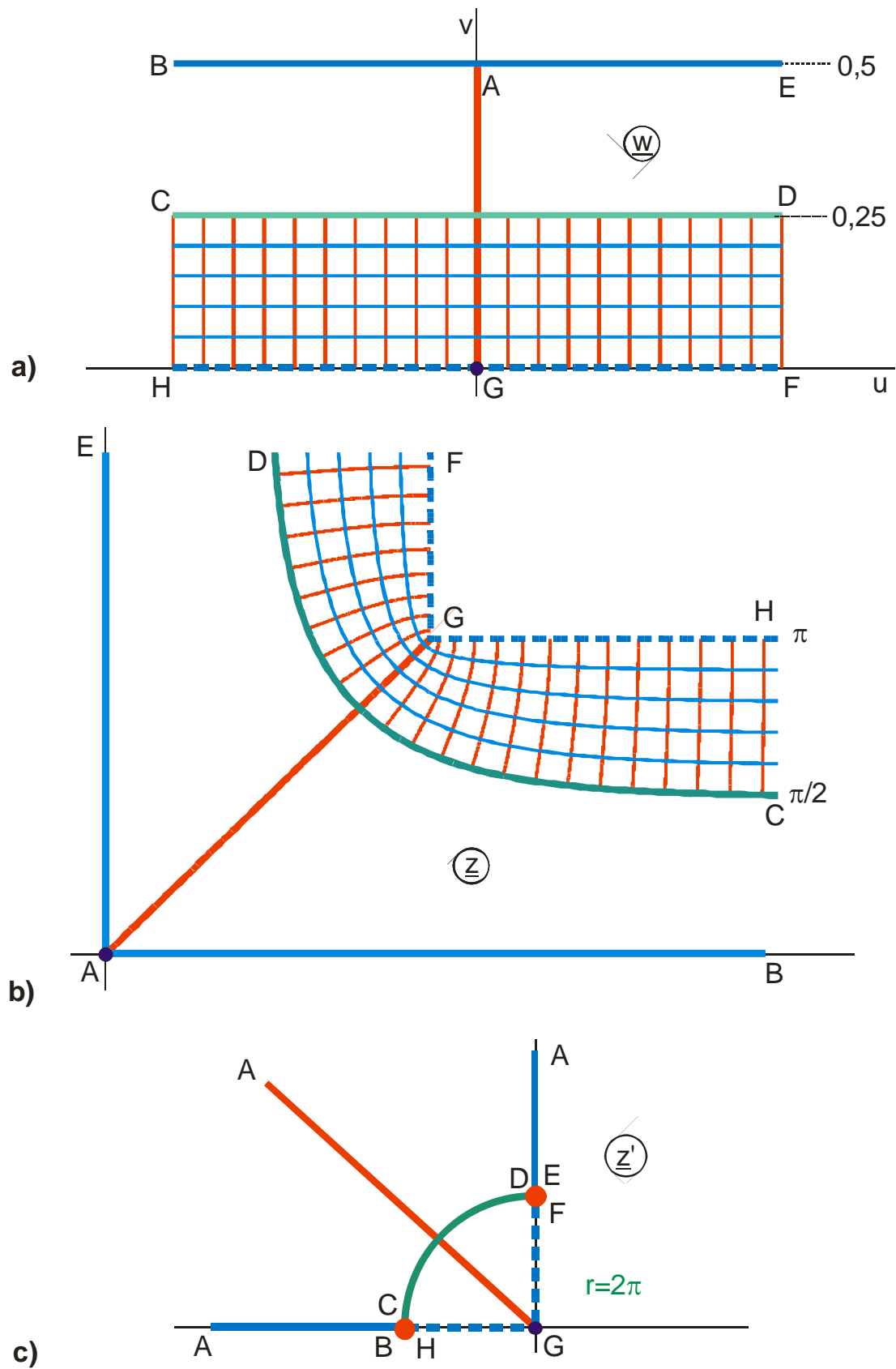


Figure 10.2: Example 1 with mirror image of potential line BAE

- A potential line with constant field strength has analogously to straight and circular potential lines the property of a mirror. If the field map is known on one side, the field map on the other side is known too.
- If a transformation equation, whose field map contains a potential line, which is a circular arc, concentric to the origin, is integrated, then this line is transformed into a potential line with constant field strength.
- The line of constant field strength is always the center line (symmetry line) in the w-plane.

With the help of these imaging laws it is possible to find more field maps with conducting boundaries with constant field strength (Group of Mappings N). Figure 10.3 illustrates some examples. The imaged boundary is shown dashed.

In Mapping N 1 (Figure 10.1) the line of constant field strength is:

$$y_h = \ln \coth(x_h / 2). \quad (22)$$

In Mapping N 1.3 (Figure 10.3b) the line of constant field strength is:

$$x_h = -\frac{1}{2} \ln \cos(2y_h). \quad (23)$$

In Mapping N 1.1 (Figure 10.3c) the line of constant field strength is:

$$x_h = \ln \left\{ \frac{1+k}{k} \frac{[1 - k \operatorname{sn}^2(v, k)]^2}{\operatorname{dn}^2(v, k) + k^2 \operatorname{sn}^2(v, k) \operatorname{cn}^2(v, k)} \right\} \quad (24)$$

$$y_h = 2 \arctan \left\{ k \frac{\operatorname{sn}(v, k) \operatorname{cn}(v, k)}{\operatorname{dn}(v, k)} \right\}. \quad (25)$$

In Mapping N 1.2 (Figure 10.3f) the line of constant field strength is:

$$x_h = \ln(1 + \sqrt{2}) - \ln \left\{ \frac{\sqrt{2} + \operatorname{sn}^2(v, k)}{\sqrt{2} - \operatorname{sn}^2(v, k)} \right\} \quad (26)$$

$$y_h = 2 \arctan \frac{\operatorname{sn}(v, k) \operatorname{dn}(v, k)}{\operatorname{cn}(v, k)} = 2 \arctan \sqrt{\frac{1 - \operatorname{cn}(2v, k)}{1 + \operatorname{cn}(2v, k)}}. \quad (27)$$

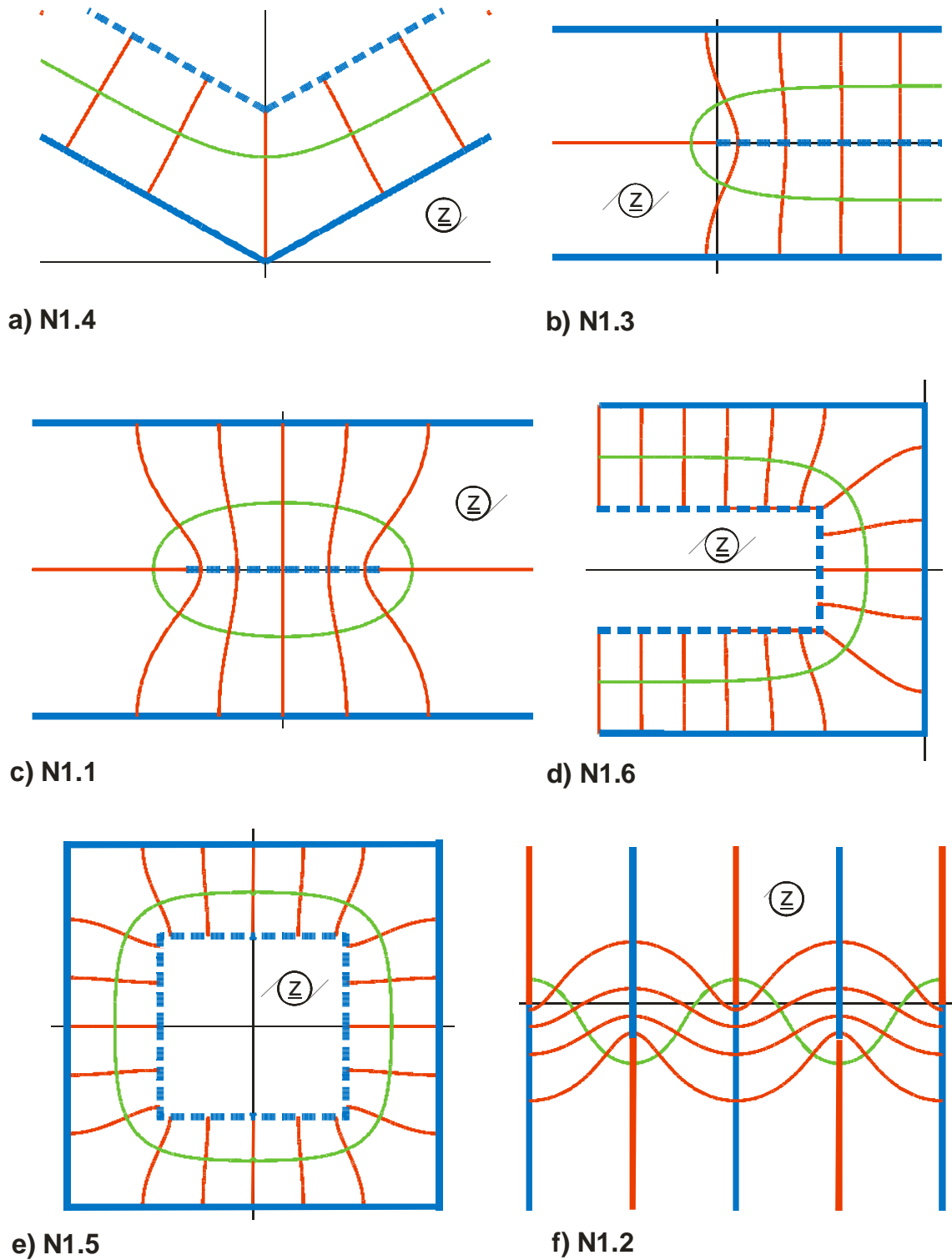


Figure 10.3: Field maps, which contain potential lines with constant field strength (pale green). The imaged boundary is shown dashed.

Example 2: Borda's mouthpiece

In the field of high voltage engineering [1] and in the field of hydrodynamics [28, 30] an electrode configuration according to Figure 10.4 is known. It is termed π -Borda profile [1] or Borda's mouthpiece [3]. In a large fluid tank there is a long channel with parallel side walls AB and A'B' (dark green). Through this empty channel the fluid flows out of the tank. Though the direction of flow is downwards in Figure 10.4 the influence of the gravitational force is not accounted for. Provided that this yields a potential flow, the curves BC and B'C' are the boundary lines of the free jet. In the pale green regions there is no fluid or stagnant fluid respectively.

In the field of fluid dynamics several methods exist, with which it is possible to determine the boundary lines of free jets analytically [30, 28, 32, 1, 3]. In parametric form line BC is found as

$$x = \sin \varphi - \varphi \quad (28)$$

$$y = 1 - \cos \varphi + 2 \ln \cos(\varphi / 2) \quad (29)$$

with $0 \leq \varphi \leq \pi$.

To calculate the field map we return to the notations of electrostatic fields and consider only one half of the symmetrical arrangement (Figure 10.5a). According to the laws of mirror imaging, which are valid for the dashed line BC with constant field strength E , at first point E is mapped into point D and the distances DC and CE are the same (imaging at a straight line). Point B apparently remains unchanged at the same location. The complete large area to the right from line ABC is imaged onto the dashed small area to the left from DBC. The field in the large area emanates from a positive line charge $+1$ at $-\infty$ and ends in a negative line charge -1 at $+\infty$. The field in the mirror imaged area also ends in a line charge -1 at $+\infty$. Consequently there must be a positive line charge with the magnitude $+1$ on the line DB that creates this field. This location G is the mirror image of the points A and F respectively.

Because line charges can be arbitrarily added by pre-transformations, the first task is: Which transformation equation creates the field map between a half straight line ABD and an infinite straight line FE? From the table of Mappings the Mapping C2 is found. The function

$$\underline{z} = -\underline{w}_1 - \ln \underline{w}_1 \quad (30)$$

maps the lower w_1 – half plane (Figure 10.5b) onto the upper z -half plane (Figure 10.5a). The complete line charge of magnitude -2 in point C = point D = point E at $+\infty$ is mapped onto the origin of the w_1 -plane. Point B goes to -1 . The line charge of magnitude $+1$ is located somewhere between B and D. The line charge of magnitude $+1$ at point A = point F lies at $\underline{w}_1 = \infty$.

In the next step the pre-mapping is searched, which creates this line charge distribution on the real axis. From Example 3.2 or from the Mapping L 3 in the table of Mappings the following transformation equation is found

$$\underline{w}_1 = -a \left\{ \frac{\exp(\underline{w}\pi)}{2} \left[1 + \sqrt{1 - 4 \cdot \exp(\underline{w}\pi)} \right] \right\}. \quad (31)$$

The factor a , that fixes the location of the point G in the w_1 – plane, still has to be determined. As exactly that transformation equation is searched, for which

$$\left| \frac{d\underline{z}}{d\underline{w}} \right| = \text{const} \quad (32)$$

is valid on line BC, this condition is used to determine $a = 1/2$. After this the transformation equation and the field map of the π -Borda profile are completely known.

The π -Borda profile is used for example in the field of high voltage engineering, to avoid extreme field strength spikes or to create uniform fields. This results in considerably smaller fringing regions as compared to the Rogowski profile (Center line $v = 0,5$ in Mapping C 2), which is used in the majority of cases.

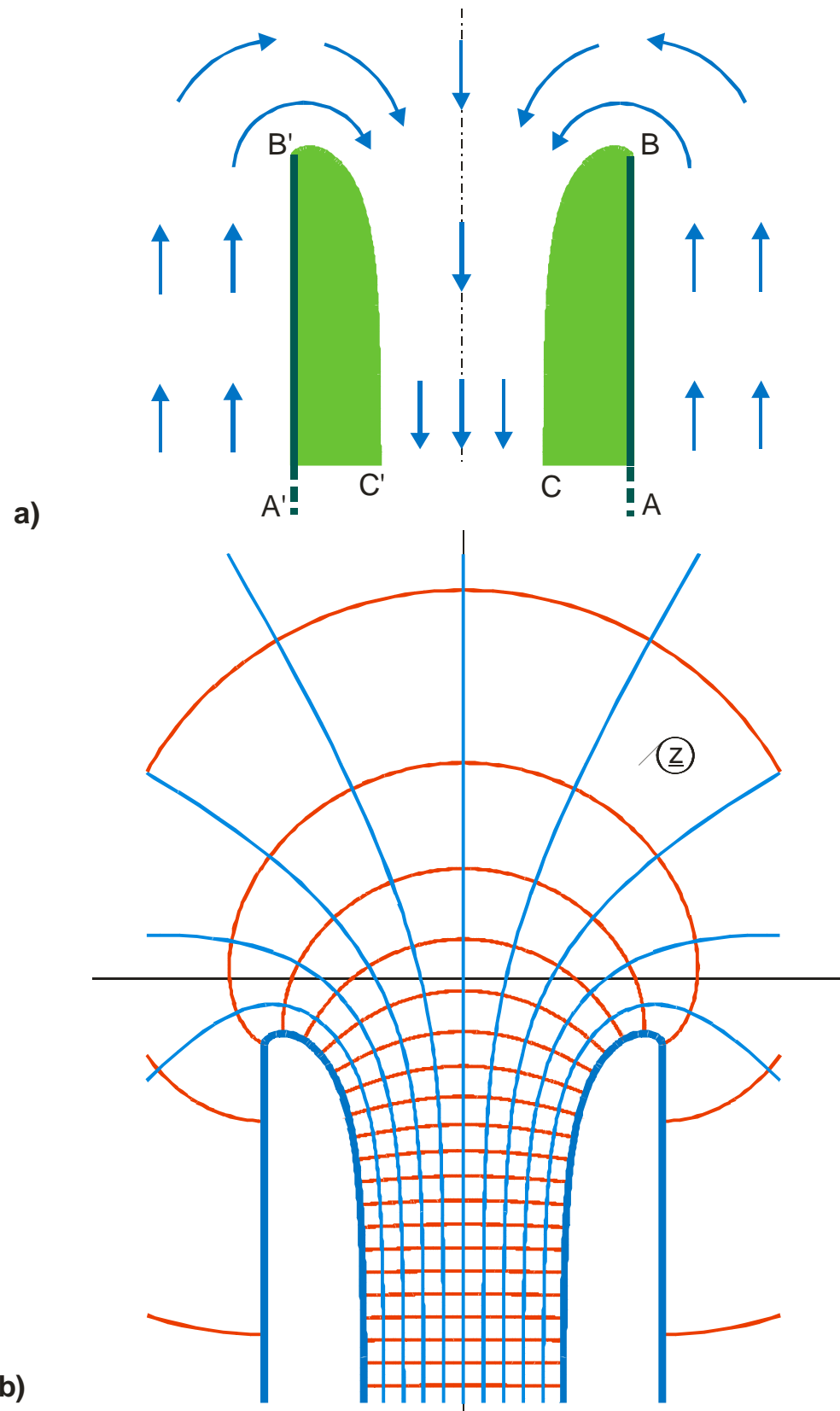
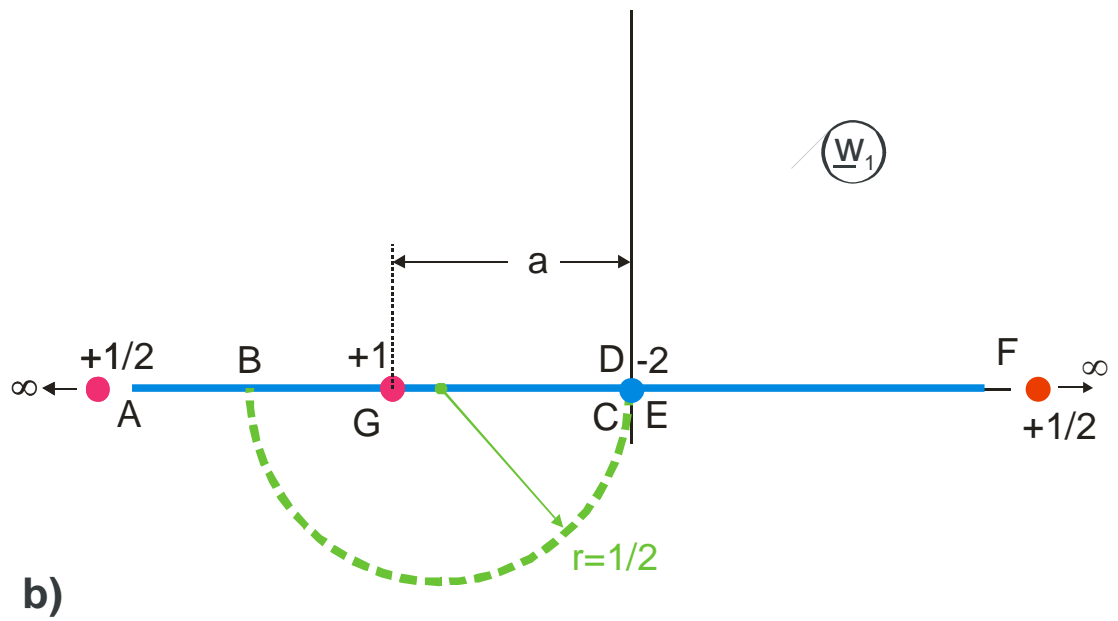
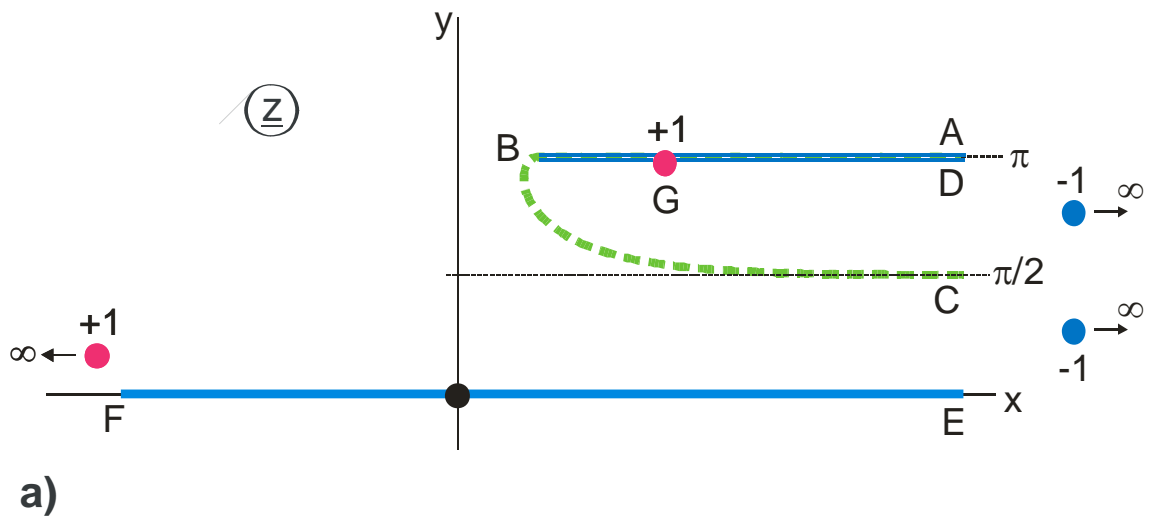


Figure 10.4: Plane fluid flow in an open channel (Borda's mouthpiece, N 2.2)

Figure 10.5: Example 2, π -Borda profile

Example 3: Fluid flow against a perpendicular plate

The field map of a wide-stretching flow is to be determined, which strikes a thin plate of width $2a$ perpendicularly. The velocity of flow vanishes in point B. On the line BC the flow is exclusively horizontal. Due to this, the flow leaves the plate in point C. On the line CD the border line of a free jet is created (green line, Figure 10.6).

The problem is solved with the method of superposition of fields. Only one half of the symmetrical configuration is considered. The field of a step, already known from Example 4.1

$$\underline{z}_1 = \sqrt{\underline{w}} \cdot \sqrt{1 - \underline{w}} + \arcsin \sqrt{\underline{w}} \quad (33)$$

is superposed with a field, which has the same boundaries from A to C in the w -plane as well as in the z -plane and which creates a horizontal flow component along the boundary CD (Figure 10.7), because now the boundary continues horizontally to the infinite point, instead of vertically, as the step does:

$$\underline{z}_2 = b \sqrt{\underline{w}}. \quad (34)$$

The solution is

$$\underline{z} = \underline{z}_1 + \underline{z}_2. \quad (35)$$

The still unknown factor b is determined by the condition

$$\left| \frac{d\underline{z}}{d\underline{w}} \right|_{u \geq 1} = \text{const}. \quad (36)$$

It follows $b = 2$. The complete solution is

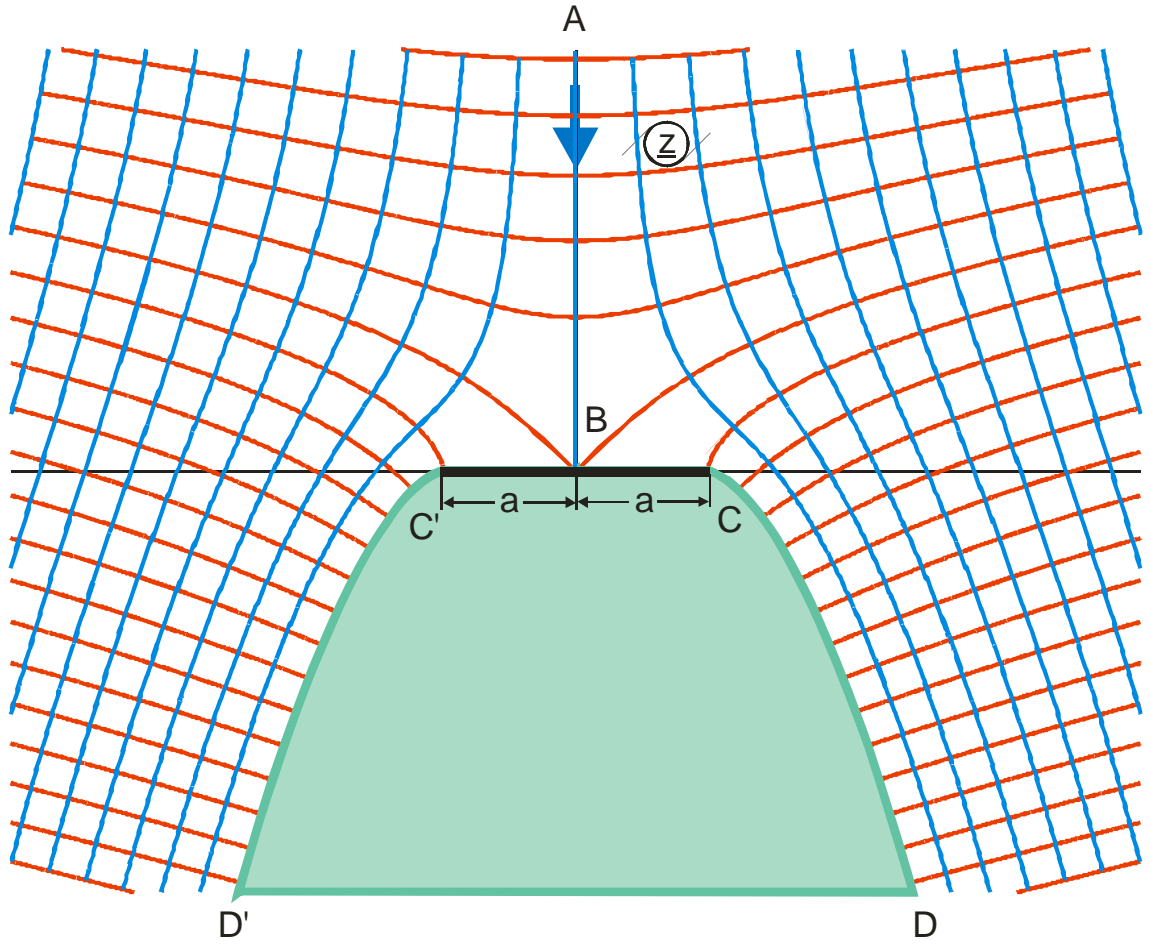
$$\underline{z} = 2\sqrt{\underline{w}} + \sqrt{\underline{w}} \sqrt{\underline{w} - 1} + \arcsin \sqrt{\underline{w}} \quad (37)$$

with $a = 2 + \pi / 2$ (Mapping N 2.1).

In order to keep this example as simple as possible, the transformation equation for z_1 that was given as solution in Example 4.1 {Eq. (4.32)}, where the points B and C are at $w = \pm 1$, was not used in this case. If Eq. (4.32) is taken, the field which is to be superposed would be

$$\underline{z}_2 = 2\sqrt{\underline{w}-1} \quad (38)$$

Nevertheless this variant of the solution yields as a matter of course the same field map.



**Figure 10.6: Example 3, uniform fluid flow against a perpendicular plate,
Mapping N 2.1**

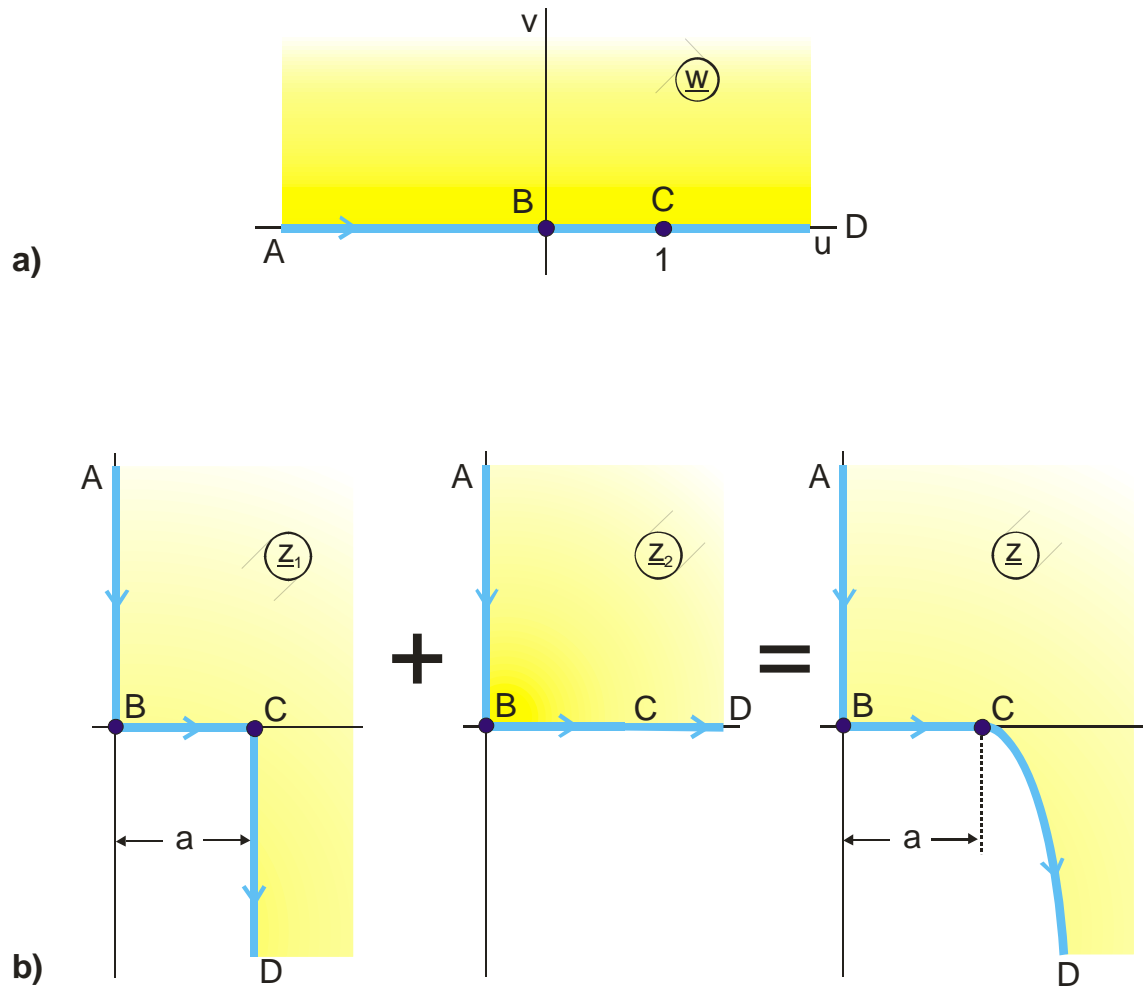


Figure 10.7: Solution method for Example 3

Example 4: Laminar flow out of a slot

In a large fluid tank, as illustrated in Figure 10.8, there is a slot of width $2a$. Once again the outpouring fluid gets a horizontal velocity component because of the boundary CD. The result is the borderline of a free jet DA ($\pi/2$ -Borda profile) with the parametric form

$$x = \sin \varphi - \ell n \tan \left(\frac{\varphi}{2} + \frac{\pi}{4} \right) \quad (33)$$

$$y = 1 - \cos \varphi \quad (34)$$

with $0 \leq \varphi \leq \pi/2$.

The transformation equation is found analogously to Example 3 by the superposition of two fields $\underline{z}_1(\underline{w})$ and $\underline{z}_2(\underline{w})$ (Figure 10.9).

$$\underline{z}_1 = \arctan \sqrt{\underline{w}_1^2 - 1} - \sqrt{\underline{w}_1^2 - 1} - \frac{\pi}{2} \quad (35)$$

$$\underline{z}_2 = b \cdot \underline{w}_1 \quad (36)$$

$$\text{with } \underline{w}_1 = \exp(\underline{w}\pi). \quad (37)$$

From the condition

$$\left| \frac{d(\underline{z}_1 + \underline{z}_2)}{d\underline{w}} \right|_{\overline{DA}} = \text{const} \quad (38)$$

the constant b is determined as $b = 1$. Thus the solution is:

$$\underline{z} = \underline{w}_1 + \arctan \sqrt{\underline{w}_1^2 - 1} - \sqrt{\underline{w}_1^2 - 1} - \frac{\pi}{2} \quad (39)$$

$$\text{with } \underline{w}_1 = \exp(\underline{w}\pi) \quad (40)$$

$$\text{and } a = 1 + \pi/2, \quad b = \pi/2. \quad (41)$$

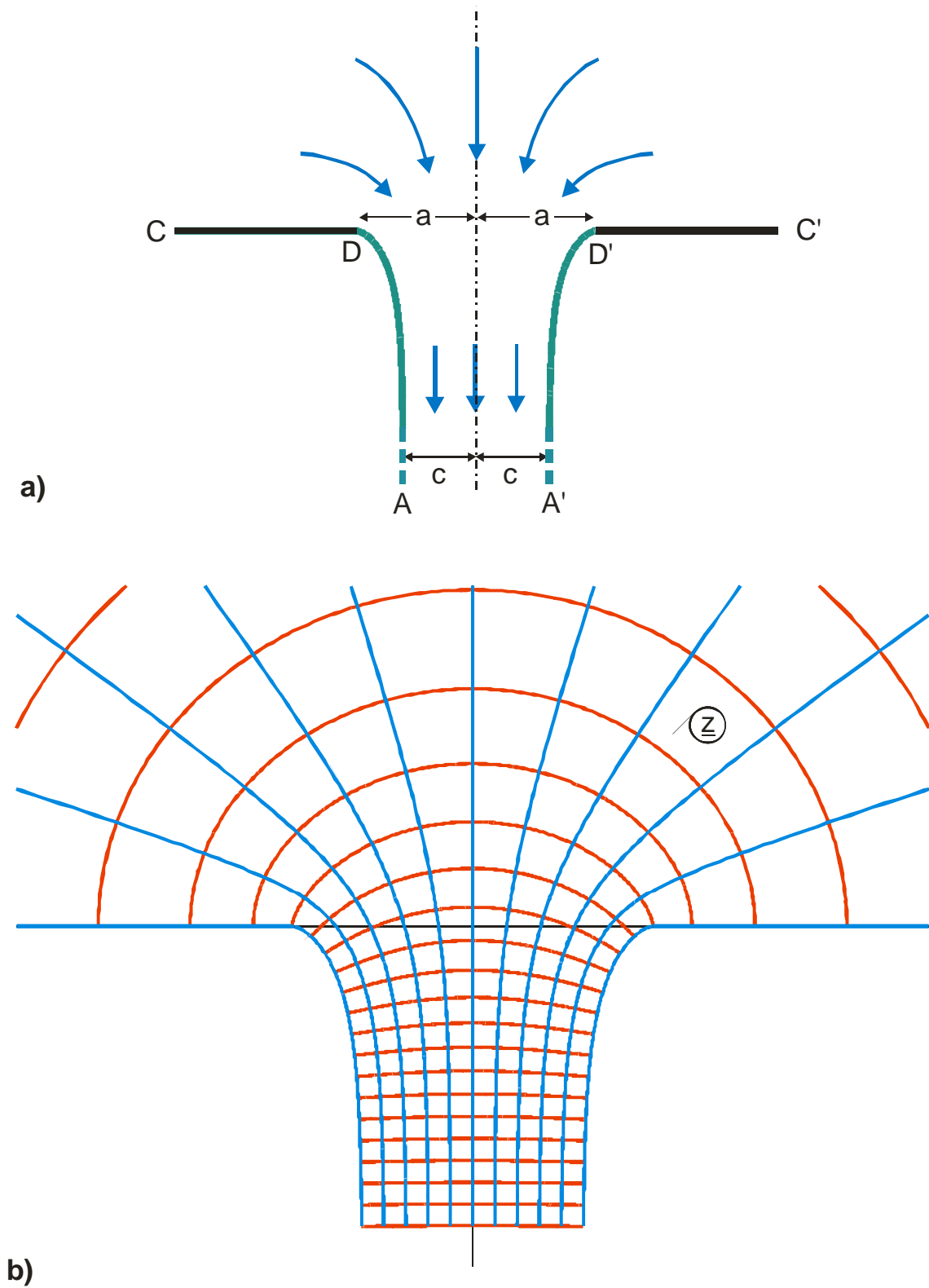


Figure 10.8: Mapping N 2, fluid flowing out of a slot, $\pi/2$ -Borda profile

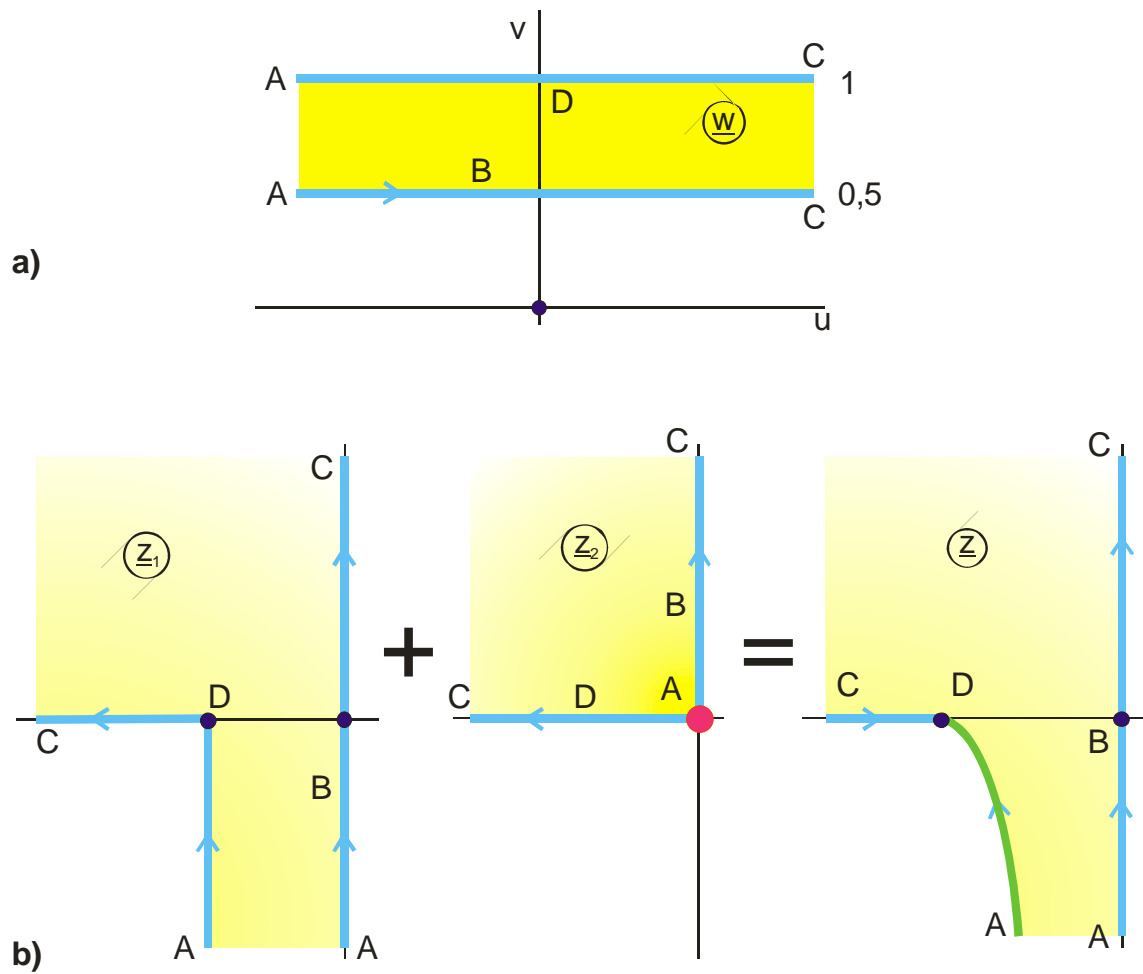


Figure 10.9: Solution method for Example 4, Mapping N 2

11. Elliptic functions

11.1 Introduction

In order to illustrate the difference between elliptic functions and trigonometric functions, at first the function $\underline{z} = \tanh \underline{w}$ is examined as an example for a conformal mapping with a trigonometric function. As shown in Figure 11.1, the transformation with $\tanh \underline{w}$ yields the field map of a line charge in front of a conducting plane. If the potential of the plane is set to 0, the potential increases when the line charge is approached. In the location of the line charge the value of the potential reaches infinity.

As a result, the number of the field lines (in Figure 11.1a the field lines $n = 0$ through 5 are plotted as continuous blue lines) is infinite and thus the field in the I. quadrant of the z -plane is mapped onto a half strip in the w -plane of infinite length.

All 4 quadrants of the field map are transformed into an infinitely long parallel strip of width π in the w -plane (Figure 11.1c).

The function $\tanh \underline{w}$ has in the direction of the imaginary axis the period π . In the direction of the real axis there is no periodicity. The function is termed "single-periodic".

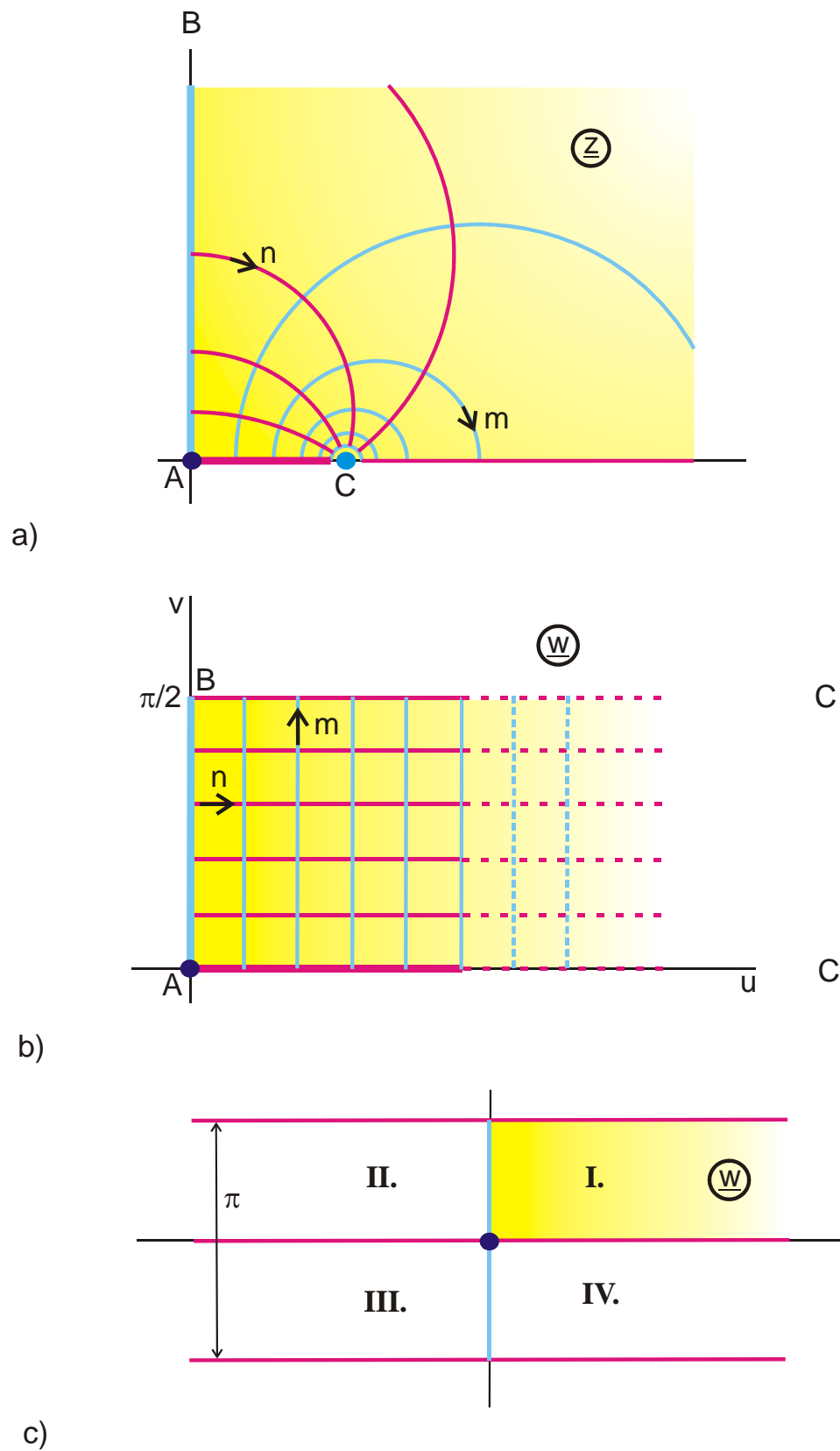


Figure 11.1: Transformation with a trigonometric function, $z = \tanh(\underline{w})$

$$\tanh(u + jv) = \frac{\sinh(2u) + j\sin(2v)}{\cosh(2u) + \cos(2v)} \quad (1)$$

$$\tanh(\underline{w} \pm jn\pi) = \tanh(\underline{w}) \quad n = 0, 1, 2, \dots \quad (2)$$

Symptomatic for a conformal transformation with a trigonometric function is therefore that the field of the electrode configuration in the z -plane is produced by the mapping of a parallel strip in the w -plane of infinite extension. The orientation of this parallel strip in the w -plane is basically irrelevant. Every transformation function $f(\underline{w})$ can be rotated arbitrarily by multiplication with the constant $\exp(j\varphi)$. Trigonometric functions are single-periodic functions.

In case the parallel strip has the width 2π and is parallel to the real axis this means:

$$f(\underline{w} \pm n \cdot 2\pi) = f(\underline{w}) \quad \text{with } n = 0, 1, 2, \dots \quad (3)$$

The transformation equations are infinitely ambiguous, that means all parallel strips that are displaced by $\pm n2\pi$ yield the same field map in the z -plane. Transformations with trigonometric functions are for example the mappings B 1, B 2.2, B 3.3, C 1, D 4, F 2, G 1, H 2, K 1 etc.

In comparison to this, the field of a metal strip in front of a grounded, conducting plane is analyzed (Figure 11.2a). If the metal strip is given the potential $U_s = 10\text{ V}$ and if the

potential lines are plotted with a potential difference of $\Delta U = 1V$, than this results in 11 potential lines, including the boundaries ($n = 0$ through 10). Because also the number of field lines is finite (e.g. $m = 0$ through 5 as in Figure 11.2a), this field map in the z -plane corresponds to a uniform field in a rectangle in the w -plane. All 4 quadrants of the z -plane are mapped onto a rectangle in the w -plane with the edge length $2K$ in the u direction and $2K'$ in the v direction.

The function, which yields this transformation, is the elliptic function $\underline{z} = \text{sn}(\underline{w}, k)$ (pronounced "ess-enn of w and k "). k is the modulus of the function. The magnitudes of K and K' and the aspect ratio K'/K of the rectangle respectively is determined by the modulus. For $\text{sn}(\underline{w}, k)$ both, the real part

$$f(\underline{w} \pm n4K) = f(\underline{w}) \quad n = 0, 1, 2, \dots \quad (4)$$

and the imaginary part are periodic.

$$f(\underline{w} \pm jm2K') = f(\underline{w}) \quad m = 0, 1, 2, \dots \quad (5)$$

$\text{sn} = (\underline{w}, k)$ is a "double-periodic" function.

The function is infinitely ambiguous, i.e. all rectangles displaced by $\pm n2K$ or $\pm m2K'$ yield the same field map in the z -plane. Analogous to the trigonometric example in Figure 11.1 the function is continued perpendicular to the red boundaries as an even function and perpendicular to the blue boundaries as an odd function.

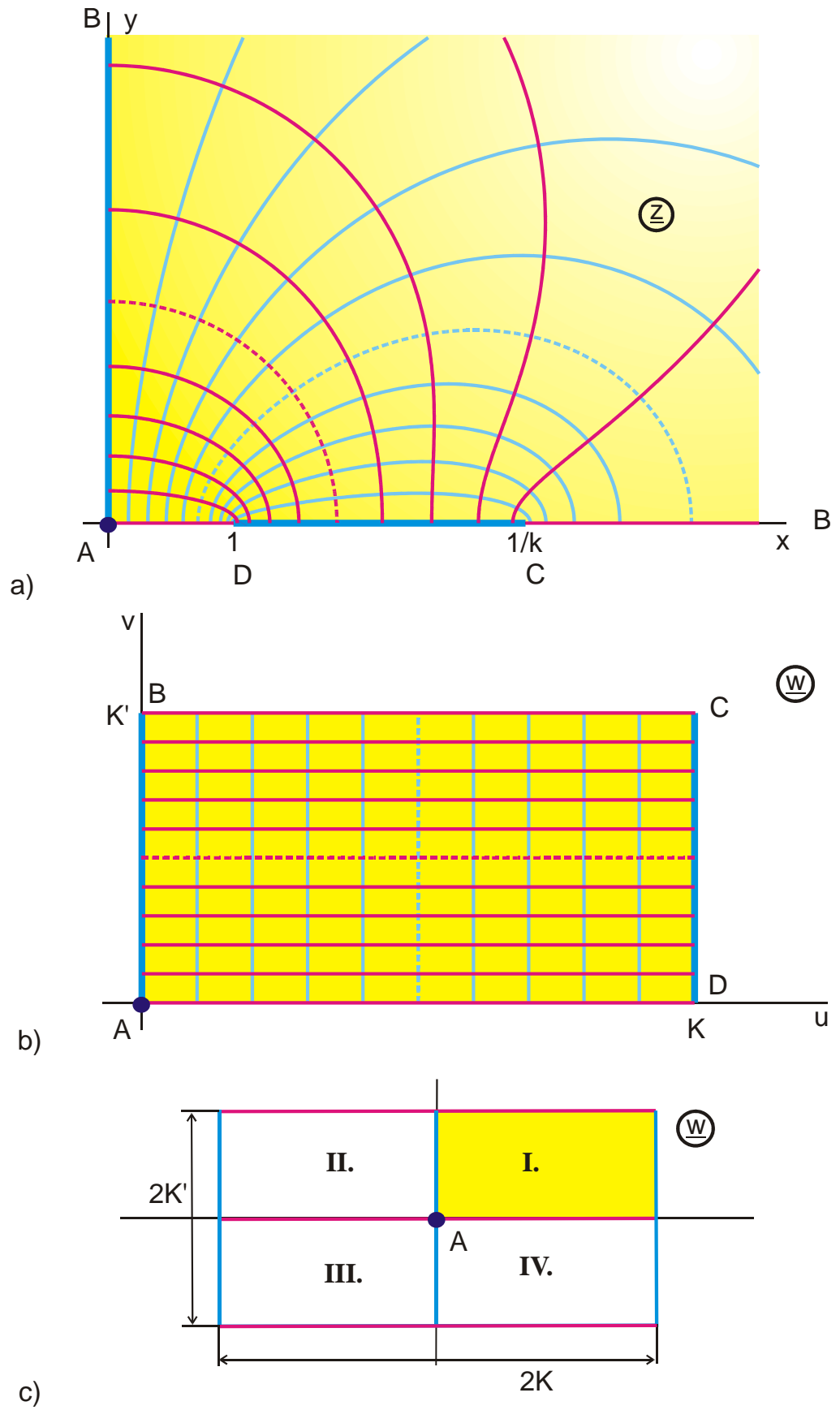


Figure 11.2: Transformation with an elliptic function, $z = \text{sn}(\underline{w}, k)$ with $k=0,3$

The general property of a mapping with an elliptic function is thus that the complete z -plane is mapped onto a rectangle in the w -plane. Elliptic functions are double-periodic, meromorphic functions of a complex variable. The three elliptic functions that will be used in this book are the Jacobian elliptic functions $\text{sn}(\underline{w}, k)$, $\text{cn}(\underline{w}, k)$ and $\text{dn}(\underline{w}, k)$ [13-16].

The mapping of a sector of a field map in the z -plane onto a rectangle in the w -plane is also possible with trigonometric functions (e.g. Mapping E 1). Only if the complete z -plane or the complete area of a fundamental period of a field map which is periodic in the z -plane is to be mapped, then the use of elliptic functions is mandatory.

Irrespective of the fact that the **potential** in the field map in Figure 11.2a has only finite values, the **field strengths** in points D and C and likewise in point C in Figure 11.1a reaches an infinite magnitude.

11.2 The Function $\text{sn}(\underline{w}, k)$

The function $\text{sn}(\underline{w}, k)$ is periodic.

$$\text{sn}(\underline{w} \pm n4K, k) = \text{sn}(\underline{w}, k) \quad (6)$$

$$\operatorname{sn}(\underline{w} \pm jn2K', k) = \operatorname{sn}(\underline{w}, k) \quad n = 0, 1, 2, \dots \quad (7)$$

$$\operatorname{sn}(\underline{w} \pm n(4K + j4K'), k) = \operatorname{sn}(\underline{w}, k) \quad (8)$$

Analogous to the function $\sin x$ with the period 2π , which is well-defined by the values of the function between $x = 0$ and $x = \pi/2$, also for the function $\operatorname{sn}(\underline{w}, k)$ all other values of the function in the complete w -plane are found from those inside the fundamental rectangle with the edge lengths K and K' by the mirror images beyond the boundaries and by periodic recurrence of this rectangle respectively.

The value of the function $\operatorname{sn}(\underline{w}, k)$ is, just as well as the value of the trigonometric functions, calculated by evaluating a series expansion. One example amongst the various possible series expansions is given in the BASIC program $\operatorname{Csn}(\operatorname{Re} \underline{w}, \operatorname{Im} \underline{w}, k, \operatorname{Re} \underline{z}, \operatorname{Im} \underline{z})$ in the appendix.

With the modulus k of the function $\operatorname{sn}(\underline{w}, k)$ it is possible to calculate the side lengths K and K' of the fundamental rectangle (see Chapter 12). The aspect ratio K'/K is defined by k . K , K' , k and K/K' may be determined with excellent accuracy using elementary functions (see Eq. (13.37) – (13.45)).

The value $v = K'/2$ yields a circle in the z -plane. The center point is $z = 0$ and the radius $r = 1/\sqrt{k}$. By using this circle as a mirror, point D is imaged into point C .

There is no circle for $u = K/2$, for no value of $k \neq 0$ (Figure 11.3).

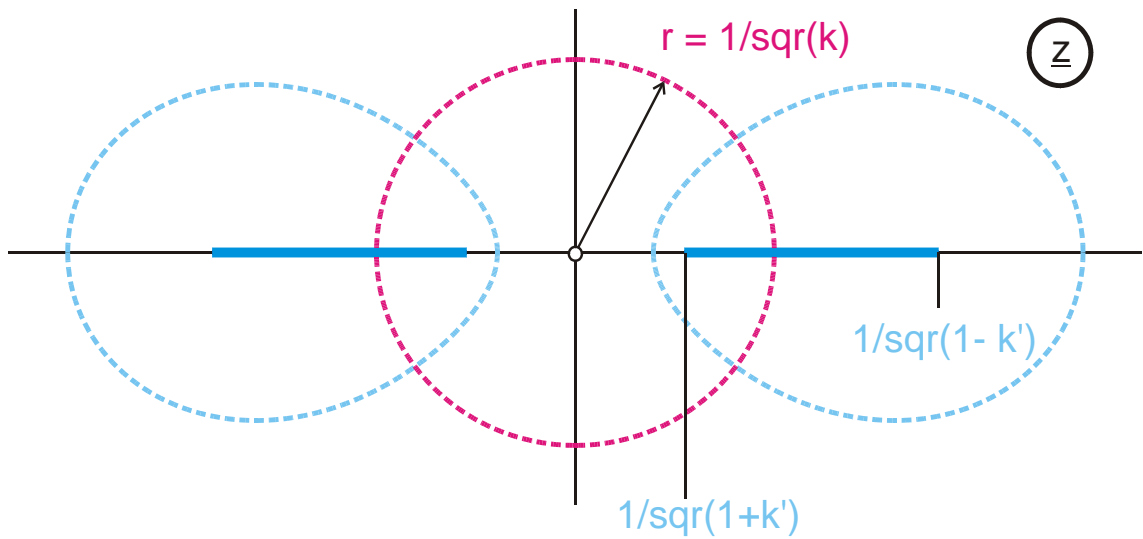


Figure 11.3: Mapping of $u=K/2$ (blue) and $v=K'/2$ (red) for $\underline{z} = \text{sn}(\underline{w}, k)$ with $k=0,3$

Special cases:

With increasing modulus k the side K of the rectangle increases and K' decreases. The strip in the z -plane becomes more and more narrow. For $k = 1$ the width of the strip is 0. The conducting strip fades to a line charge. The rectangle in the w -plane becomes a half strip, which extends to infinity.

$$\text{sn}(\underline{w}, k=1) = \tanh \underline{w} \quad (9)$$

$$K(k=1) = \infty \quad (10)$$

$$K'(k=1) = \pi/2 \quad (11)$$

For $k = 0$ the conducting strip begins at $x = 1$ and extends to infinity. The rectangle in the w -plane is infinitely high.

$$\operatorname{sn}(\underline{w}, k = 0) = \sin \underline{w} \quad (12)$$

$$K(k = 0) = \pi/2 \quad (13)$$

$$K'(k = 0) = \infty \quad (14)$$

Hence it is evident that the elliptic functions are a generalization and an extension of the trigonometric and of the hyperbolic functions respectively.

11.3 The Functions $\operatorname{cn}(\underline{w}, k)$ and $\operatorname{dn}(\underline{w}, k)$

The elliptic functions $\operatorname{cn}(\underline{w}, k)$ and $\operatorname{dn}(\underline{w}, k)$ (likewise pronounced as single letters: see-enn and dee-enn), are derived from the function $\operatorname{sn}(\underline{w}, k)$. According to Chapter 6 they are successive transformations.

Therefore they do not yield fundamentally novel mappings. They can be used to shorten the notation of the transformation equations.

From the function $\operatorname{sn}(\underline{w}, k)$ it is derived analogously to $\sin \underline{w}$ and $\cos \underline{w}$ with

$$\cos \underline{w} = \sqrt{1 - \sin^2 \underline{w}}$$

from

$$\operatorname{sn}^2(\underline{w}, k) + \operatorname{cn}^2(\underline{w}, k) = 1 \quad (15)$$

$$\operatorname{cn}(\underline{w}, k) = \sqrt{1 - \operatorname{sn}^2(\underline{w}, k)} \quad (16)$$

and from

$$k^2 \operatorname{sn}^2(\underline{w}, k) + \operatorname{dn}^2(\underline{w}, k) = 1 \quad (17)$$

$$\operatorname{dn}(\underline{w}, k) = \sqrt{1 - k^2 \operatorname{sn}^2(\underline{w}, k)} . \quad (18)$$

$\operatorname{cn}(\underline{w}, k)$ is periodic with $4K, j4K', 2K + j2K'$

$\operatorname{dn}(\underline{w}, k)$ is periodic with $2K, j4K', 4K + j4K'$.

Figure 11.4 shows the mapping with $\operatorname{cn}(\underline{w}, k)$.

In contrast to $\operatorname{sn}(\underline{w}, k)$ the rectangles in the w -plane are not arranged in the same pattern as the quadrants in the z -plane, onto which they are mapped. The point $z = 0$ lies at $\underline{w} = K$ (Point D). Therefore the four quadrants of the z -plane are mapped onto those rectangles in the w -plane, which have point D in common. According to the laws of the conformal mapping with the same sense of rotation (Figure 11.5c).

The transformation by $\operatorname{dn}(\underline{w}, k)$ (Figure 11.5) yields the same electrode configuration like the function $\operatorname{sn}(\underline{w}, k)$ (see Eq. (35)). Likewise there is also a circle in this case for $u = K/2$. The mirror image of point D in this circle is point A.

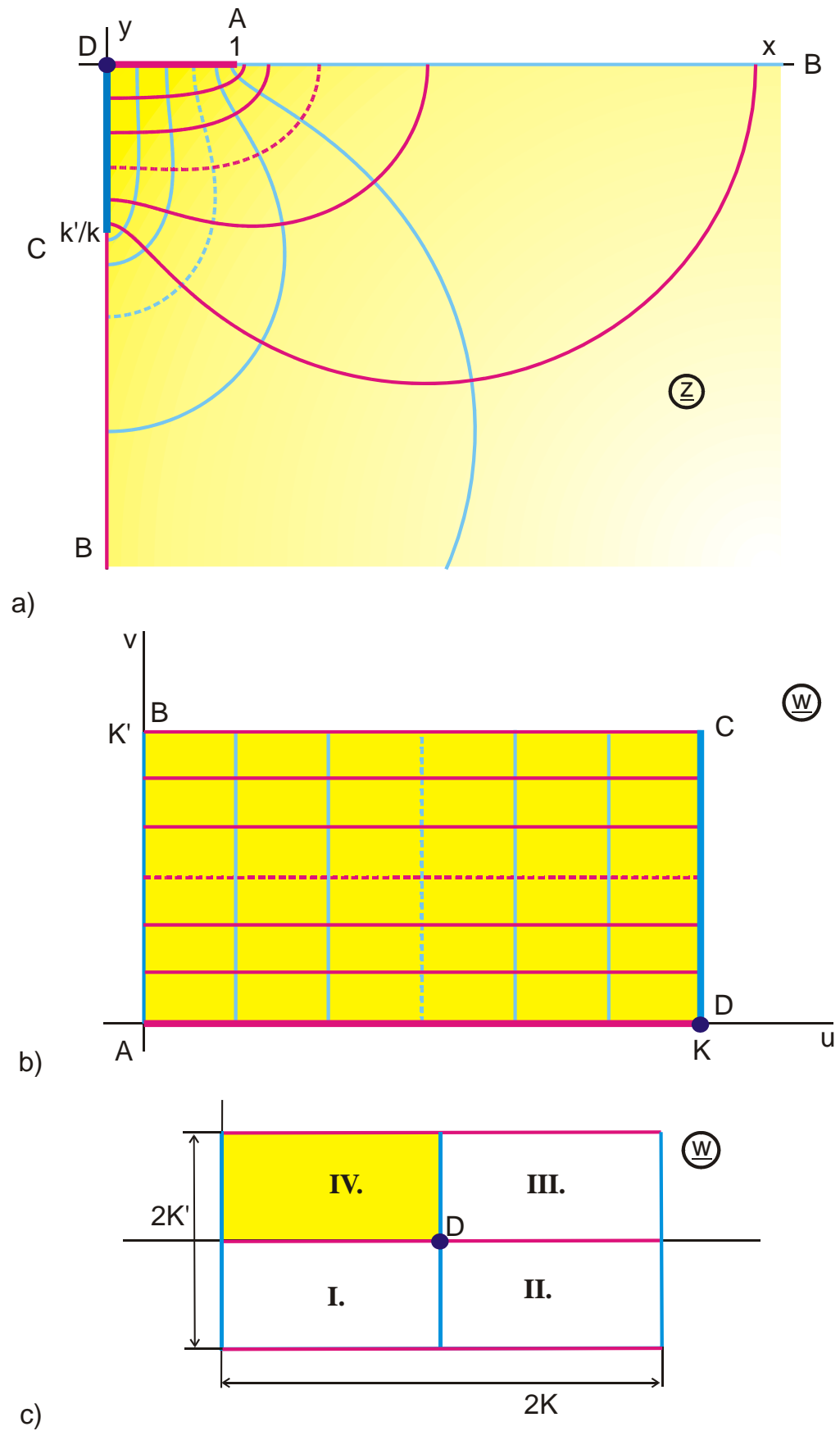


Figure 11.4: Transformation with the elliptic function $\underline{z} = \text{cn}(\underline{w}, k)$ with $k=0,6$

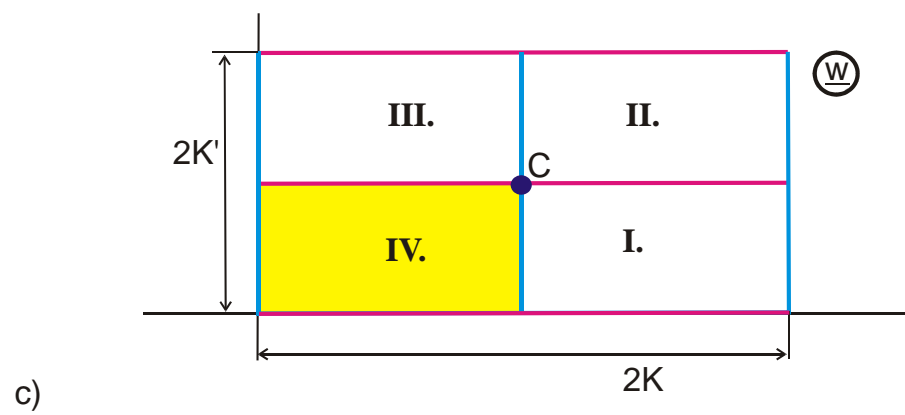
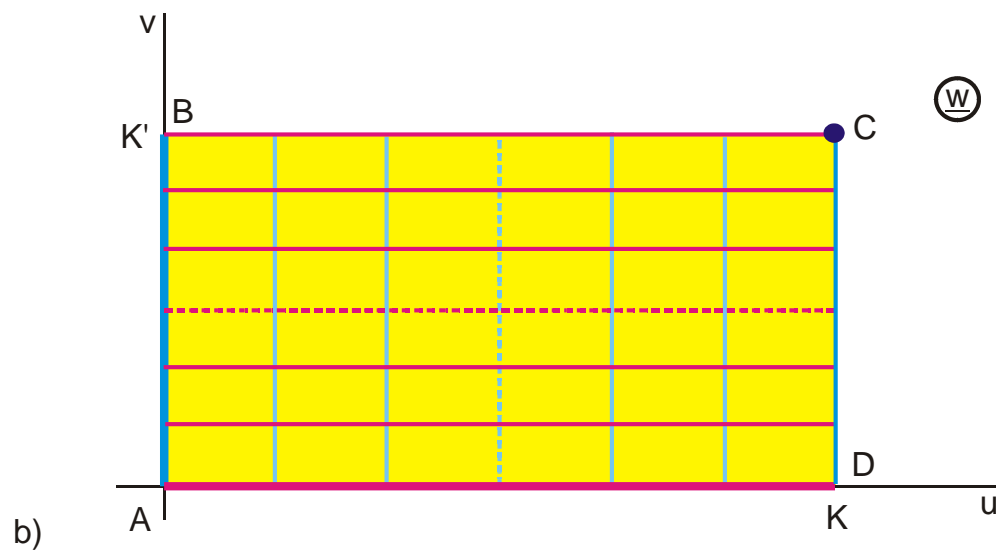
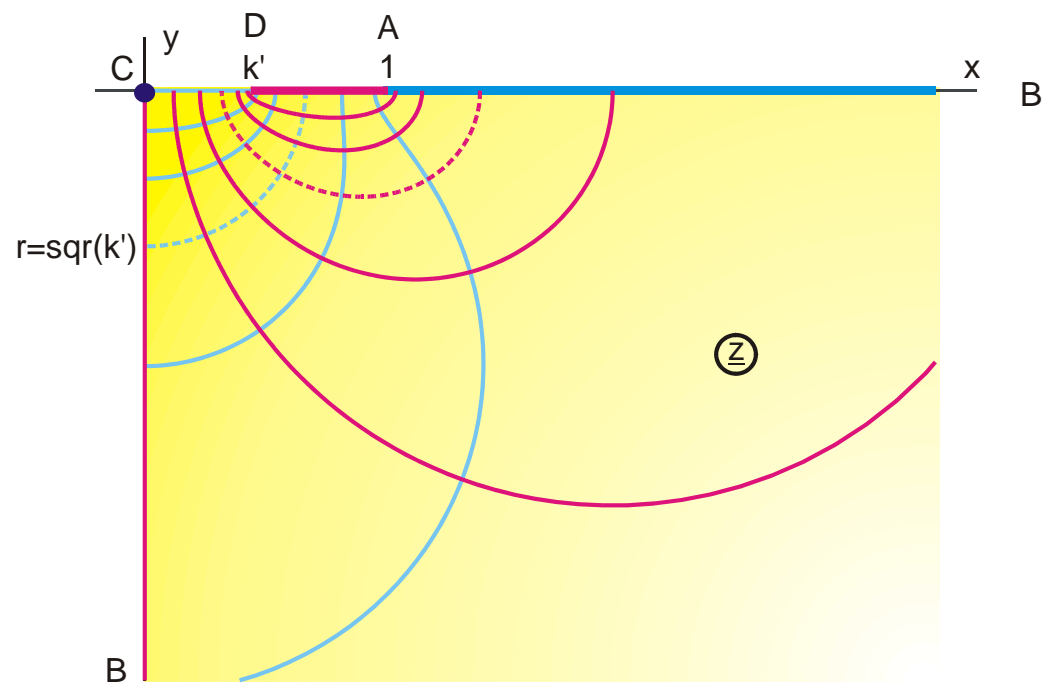


Figure 11.5: Transformation with the elliptic function $z = \text{dn}(\underline{w}, k)$ with $k=0,9$

Limiting values:

$$\text{cn}(\underline{w}, k = 0) = \cos \underline{w} \quad (19)$$

$$\text{cn}(\underline{w}, k = 1) = 1/\cosh \underline{w} \quad (20)$$

$$\text{dn}(\underline{w}, k = 0) = 1 \quad (21)$$

$$\text{dn}(\underline{w}, k = 1) = 1/\cosh \underline{w} \quad (22)$$

Once again the origin of the z -plane is not mapped onto the origin of the w -plane. Point C is mapped onto $K + jK'$. The four quadrants of the z -plane are arranged around this point counter clockwise (Figure 11.6c).

11.4 Some Calculation Formulas

$$\text{sn}(-\underline{w}, k) = -\text{sn}(\underline{w}, k) \quad (23)$$

$$\text{cn}(-\underline{w}, k) = \text{cn}(\underline{w}, k) \quad (24)$$

$$\text{dn}(-\underline{w}, k) = \text{dn}(\underline{w}, k) \quad (25)$$

$$\frac{\partial}{\partial \underline{w}} (\text{sn}(\underline{w}, k)) = \text{cn}(\underline{w}, k) \cdot \text{dn}(\underline{w}, k) \quad (26)$$

$$\frac{\partial}{\partial \underline{w}} (\text{cn}(\underline{w}, k)) = -\text{sn}(\underline{w}, k) \cdot \text{dn}(\underline{w}, k) \quad (27)$$

$$\frac{\partial}{\partial \underline{w}} (\text{dn}(\underline{w}, k)) = -k^2 \cdot \text{sn}(\underline{w}, k) \cdot \text{cn}(\underline{w}, k) \quad (28)$$

$$\int \text{sn}(\underline{w}, k) d\underline{w} = \frac{1}{k} \ell n \left(\text{dn}(\underline{w}, k) - \frac{1}{k} \text{cn}(\underline{w}, k) \right) \quad (29)$$

$$\int \text{cn}(\underline{w}, k) d\underline{w} = \frac{1}{k} \arccos \text{dn}(\underline{w}, k) \quad (30)$$

$$\int \text{dn}(\underline{w}, k) d\underline{w} = \arcsin \text{sn}(\underline{w}, k) \quad (31)$$

$$\frac{\text{sn}(\underline{w}, k) \cdot \text{dn}(\underline{w}, k)}{\text{cn}(\underline{w}, k)} = \sqrt{\frac{1 - \text{cn}(2\underline{w}, k)}{1 + \text{cn}(2\underline{w}, k)}} = -\frac{\partial}{\partial \underline{w}} (\ell n \text{cn}(\underline{w}, k)) \quad (32)$$

$$\frac{\text{sn}(\underline{w}, k) \cdot \text{cn}(\underline{w}, k)}{\text{dn}(\underline{w}, k)} = \frac{1}{k} \sqrt{\frac{1 - \text{dn}(2\underline{w}, k)}{1 + \text{dn}(2\underline{w}, k)}} = -\frac{1}{k^2} \frac{\partial}{\partial \underline{w}} (\ell n \text{dn}(\underline{w}, k)) \quad (33)$$

$$\frac{\text{cn}(\underline{w}, k) \cdot \text{dn}(\underline{w}, k)}{\text{sn}(\underline{w}, k)} = \frac{\text{cn}(2\underline{w}, k) + \text{dn}(2\underline{w}, k)}{\text{sn}(2\underline{w}, k)} = \frac{\partial}{\partial \underline{w}} (\ell n \text{sn}(\underline{w}, k)) \quad (34)$$

$$\text{dn}(\underline{w}, k) = k' \text{sn}(j\underline{w} + K'(k) + jK(k), k') \quad (35)$$

$$\text{sn}[\underline{w} + jK'(k), k] = \frac{1}{k \text{sn}(\underline{w}, k)} \quad (36)$$

$$\text{sn}(jy, k) = j \frac{\text{sn}(y, k')}{\text{cn}(y, k')} \quad (37)$$

$$k = \frac{1}{\text{sn}[K(k) + jK'(k), k]} \quad (38)$$

$$k' = \operatorname{dn}[K(k), k] \quad (39)$$

More calculation formulas and properties of the elliptic functions are given in the two following chapters about elliptic integrals and about Theta functions. Comprehensive calculation formulas are compiled in [2].

12. Elliptic Integrals

To get acquainted with the elliptic integrals they are compared to the trigonometric functions.

The inverse function of the function $t = \sin \varphi$ is the function

$$\varphi = \arcsin t = \int_0^t \frac{dt}{\sqrt{1-t^2}} \quad (1)$$

The function $\arcsin t$ is defined by an integral. “Exact“ numerical values for $\sin \varphi$ as well as for $\arcsin t$ cannot be calculated in an elementary way, but only as the sum of an infinite series.

The inverse function of the function $t = \operatorname{sn}(u, k)$ is the function

$$u = F_a(t, k) = \int_0^t \frac{dt}{\sqrt{(1-t^2)(1-k^2t^2)}} \quad (2)$$

$F_a(t,k)$ is termed the elliptic integral of the first kind. The notation used in this case is the algebraic form, therefore the index a . Numerical values for $\text{sn}(u,k)$ and $F_a(t,k)$ can only be calculated as the sum of an infinite series.

Integrals of the form

$$\int R(x,y)dx \quad (3)$$

where $R(x,y)$ is a rational function of x and y and where y is the root of a polynomial of 3. or 4. order in x without multiple zeros, are called elliptic integrals. In those special cases where the integral can be expressed by elementary functions, it is called pseudo elliptic.

Every elliptic integral can be expressed by the three standard forms, the elliptic integral of the first kind, of the second kind and of the third kind as well as by additional integrals of rational functions. Comprehensive tables of integrals are contained in [18] and [21].

The adjective “elliptic” derives historically from the fact that the arc length of an ellipse is defined by the elliptic integral of the second kind. With the terms in Figure 12.1 follows, if the ellipse is defined by $x = a \sin \varphi$ and $y = b \cos \varphi$:

$$ds = \sqrt{dx^2 + dy^2} = \sqrt{a^2 \cos^2 \varphi + b^2 \sin^2 \varphi} d\varphi \quad (4)$$

Thus the arc length s is:

$$s = \int_0^{\varphi} \sqrt{a^2 \cos^2 \varphi + b^2 \sin^2 \varphi} \, d\varphi \quad (5)$$

With the abbreviation $k = \sqrt{1 - b^2 / a^2}$ results

$$s = a \int_0^{\varphi} \sqrt{1 - k^2 \sin^2 \varphi} \, d\varphi \quad (6)$$

$$s = a E_t(\varphi, k) \quad (7)$$

$E_t(\varphi, k)$ is the elliptic integral of the second kind in trigonometric form.

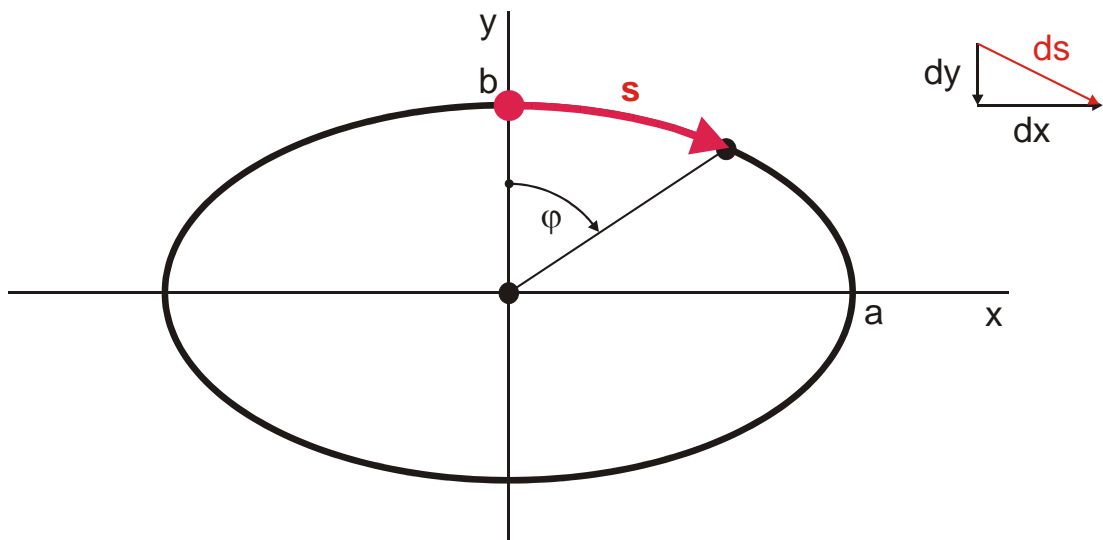


Figure 12.1: Calculation of the arc length of an ellipse

Again this example shows the relationship to the trigonometric functions. There the values of the functions can be defined geometrically with the help of a circle.

Elliptic integrals are very often used to calculate conformal mappings. According to chapter 4 there is in the mapping of polygonal boundaries for every right angle a term in the integrand of the transformation equation like

$$\underline{z} = \int_0^{\underline{w}} \dots (\underline{w} - \underline{w}_0)^{\pm 1/2} \dots d\underline{w} \quad (8)$$

Thus transformation equations for polygonal domains with more than two right angles always contain elliptic (or pseudo elliptic) integrals.

12.1 The Elliptic Integral of the First Kind

In mathematical text books and formularies [2, 11 - 15, 18] the elliptic integral of the first kind is denoted by the letter F. The different forms of the elliptic integrals of the first kind are discriminated in such a way that each form uses an individual letter for the variable. The algebraic form is defined by:

$$F(t, k) = \int_0^t \frac{dt}{\sqrt{(1-t^2)(1-k^2t^2)}} \quad (9)$$

With the substitution $t = \sin \varphi$ the trigonometric form is found

$$F(\varphi, k) = \int_0^{\varphi} \frac{d\varphi}{\sqrt{1 - k^2 \sin^2 \varphi}} \quad (10)$$

and for the integrals of the second kind and of the third kind a third notation is added with the substitution $t = \operatorname{sn}(u, k)$.

As it is not possible in the practical application of these functions to stick to a fixed notation of the variables with t , φ and u , the consequence was that elliptic integrals are thought of as exotic, and in addition that their usage was prohibited for the standard user from the engineering sciences due to time constraints.

In order to avoid this variety of notations (the manifold of notations used by various authors were not even yet mentioned), three indices are introduced in the following text, with whom the different forms of the elliptic integrals can be clearly distinguished. For the elliptic integral of the first kind follows:

The algebraic form:

$$F_a(\underline{w}, k) = \int_0^{\underline{w}} \frac{d\underline{w}}{\sqrt{(1 - \underline{w}^2)(1 - k^2 \underline{w}^2)}} \quad (11)$$

The trigonometric form:

$$F_t(\underline{w}, k) = \int_0^{\underline{w}} \frac{d\underline{w}}{\sqrt{1 - k^2 \sin^2 \underline{w}}} = F(\underline{w}, k) \quad (12)$$

with the conversion equations:

$$F_t(\underline{w}, k) = F_a(\sin \underline{w}, k) \quad (13)$$

$$F_a(\underline{w}, k) = F_t(\arcsin \underline{w}, k) \quad (14)$$

Furthermore holds:

$$F_a(\underline{w}, k) = \underline{z} \Rightarrow \underline{w} = \operatorname{sn}(\underline{z}, k) \quad (15)$$

$$F_t(\underline{w}, k) = \underline{z} \Rightarrow \underline{w} = \arcsin(\operatorname{sn}(\underline{z}, k)) \quad (16)$$

For the upper limits of integration $\underline{w} = 1$ and $\underline{w} = \pi/2$ respectively the complete elliptic integrals of the first kind are obtained.

$$K(k) = F_a(\underline{w} = 1, k) = \int_0^1 \frac{d\underline{w}}{\sqrt{(1 - \underline{w}^2)(1 - k^2 \underline{w}^2)}} \quad (17)$$

$$K(k) = F_t(\underline{w} = \pi/2, k) = \int_0^{\pi/2} \frac{d\underline{w}}{\sqrt{1 - k^2 \sin^2 \underline{w}}} \quad (18)$$

For the complementary modulus $k' = \sqrt{1 - k^2}$ follows:

$$K'(k) = K(k') = F_a(\underline{w} = 1, k') \quad (19)$$

$$K'(k) = K(k') = F_t(\underline{w} = \pi/2, k') \quad (20)$$

$K(k)$ and $K'(k)$, the complete elliptic integrals of the first kind, are the lengths of the sides of the rectangles in the mapping with the function $\underline{z} = \text{sn}(\underline{w}, k)$ in Figure 11.2.

$K(k)$, $K'(k)$, k and K/K' can be determined approximately with very high accuracy with elementary functions (see Eq. (13.37) – (13.45)). For $k = 1/\sqrt{2}$ the rectangle turns into

a square with $k = k'$ and $K(k) = K'(k) = \frac{2\pi}{(1 + 2^{-1/4})^2} = 1,854$.

Instead of the modulus k with

$$k^2 + k'^2 = 1 \quad (21)$$

as well the parameter m may be used.

$$m = k^2 \quad (22)$$

$$m + m' = 1 \quad (23)$$

Furthermore the modular angle (or argument) α is in use:

$$k = \sin \alpha \quad (24)$$

$$k' = \cos \alpha \quad (25)$$

Figure 12.2 shows the mapping that belongs to the elliptic integral of the first kind $F_t(\underline{w}, k)$. A parallel strip with the width π in the w -plane is mapped onto a rectangle with the width $2K$ and the height $2K'$. The straight line \overline{CD} is rotated in point C by 90° and the point ∞ (point D) is mapped into jK' . Because the parallel strip contains an infinite number of lines $v = \text{const}$, this results in a line charge in point D of the z -plane.

The mapping is in both planes symmetrical with respect to the axes. The origin A is again mapped onto the origin. The allocation of the quadrants remains the same, i.e. the half strip in the III. quadrant of the w -plane is mapped onto the rectangle in the III. quadrant of the z -plane, etc.

Because the variable \underline{w} in Eq. (12) appears only as the argument of the sine function, a periodicity with π results from $\sin^2 \underline{w}$.

Because the integration from 0 through $\pi/2$ yields the value K and every further part of the integration from \underline{w} through $\underline{w} + \pi/2$ also yields K , all parallel strips in the w -plane displaced by $\pm n \cdot \pi$ are mapped onto the corresponding rectangular regions displaced by $\pm n \cdot 2K$ (Figure 12.2c).

$$F_t(\underline{w} \pm n\pi, k) = \pm n2K + F_t(\underline{w}, k) \quad \text{with} \quad n = 0, 1, 2, \dots \quad (26)$$

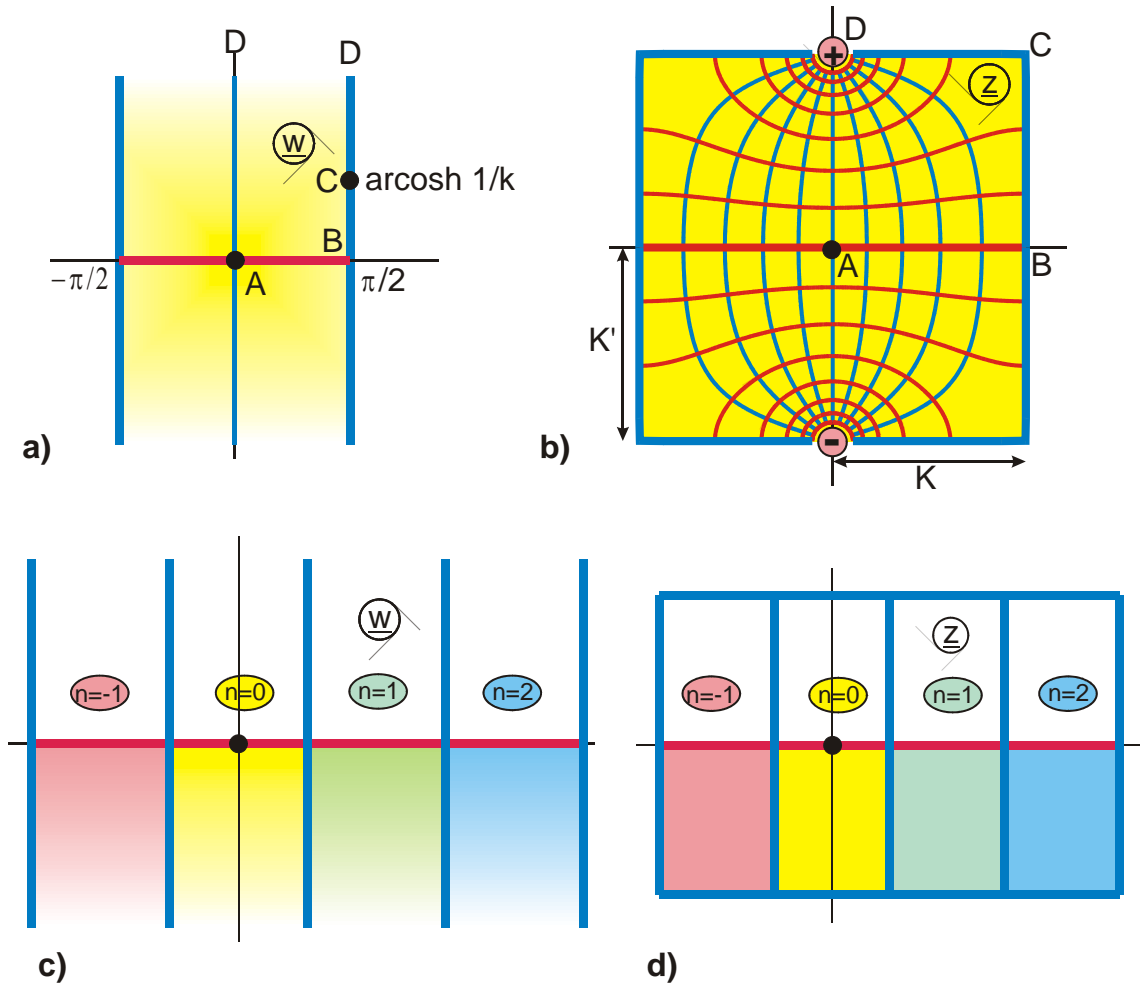


Figure 12.2: The transformation $z = F_t(w, k)$ for $0 \leq k \leq 1$, Mapping I 1.2

Limiting cases:

K' increases for $k \rightarrow 0$ and point D moves to ∞ . In the limit $k = 0$ the following is reached: $K = \pi/2$, $K' = \infty$ and the parallel strip of the w -plane is mapped onto an identical parallel strip in the z -plane (Figure 12.3a).

$$F_t(\underline{w}, k = 0) = \underline{w} \quad (27)$$

K increases for $k \rightarrow 1$ and point B moves to ∞ . In the limit $k=1$: $K = \infty$, $K' = \pi/2$ and the rectangle degenerates to a parallel strip.

$$F_t(\underline{w}, k=1) = \ln \tan(\underline{w} / 2 + \pi / 4) = \operatorname{ar} \tanh(\sin \underline{w}) \quad (28)$$

Because of $F_a(\underline{w}, k=1) = F_t(\arcsin \underline{w}, k)$ the algebraic form of the elliptic integral of the first kind is according to chapter 5 a pre-transformation with $\arcsin \underline{w}$. It follows that the geometry of the boundary in the z -plane, like it is seen in Figure 12.2, stays unchanged. Only the potential distribution along the boundary is modified. Figure 12.4 shows the mapping with $F_a(\underline{w}, k)$. The complete w -plane is mapped onto a rectangle with the sides $2K$ and $2K'$. The relationship with the inverse function $\underline{z} = \operatorname{sn}(\underline{w}, k)$ in Figure 6.2 is intuitively evident.

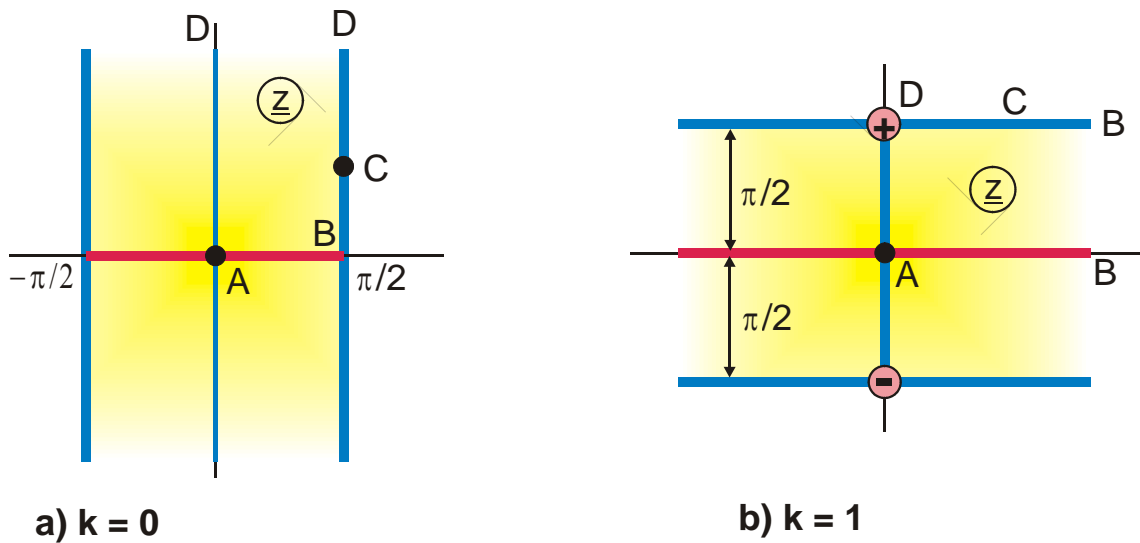


Figure 12.3: Limiting cases of the transformation $z = F_t(w, k)$

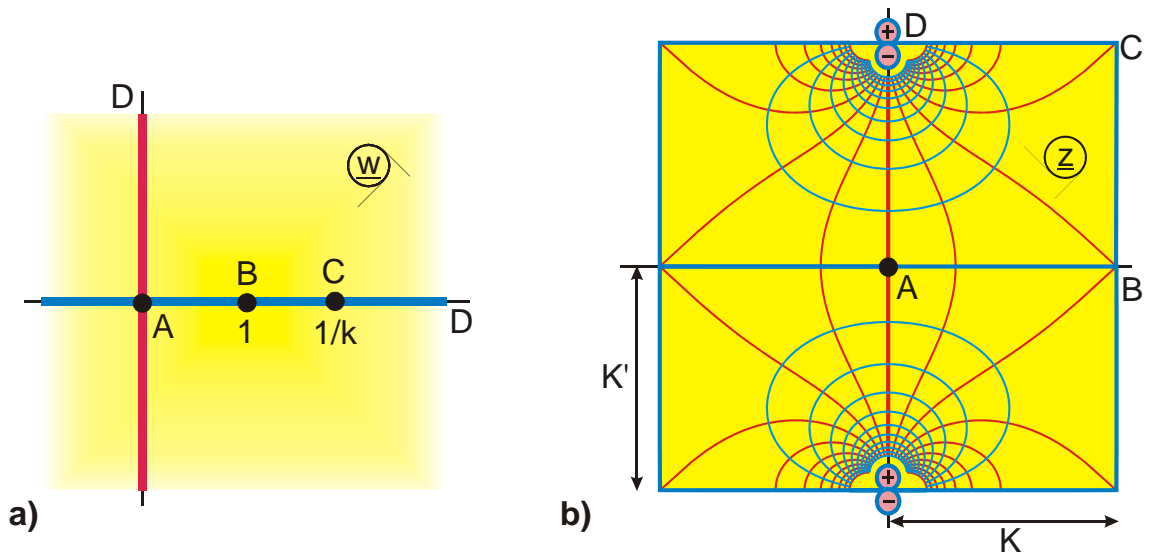


Figure 12.4: The transformation $z = F_a(w, k)$ for $0 \leq k \leq 1$, Mapping Q 4

Please pay attention to the difference: If according to Figure 12.4 a Cartesian lattice in the w -plane with an infinite number of potential lines and an infinite number of field lines is mapped onto a finite rectangle in the z -plane, than this results in a line dipole in point D of the z -plane.

If on the contrary according to Figure 11.2 the Cartesian lattice in a finite rectangle in the w -plane is mapped onto the complete z -plane, than this results in a field map with a finite number of potential lines and field lines.

More calculation formulas:

$$F_t(-\underline{w}, k) = -F_t(\underline{w}, k) \quad (29)$$

$$F_a(\operatorname{sn} \underline{w}, k) = \underline{w} \quad (30)$$

$$\frac{d}{d\underline{w}} F_a(\underline{w}, k) = \frac{1}{\sqrt{(1 - \underline{w}^2)(1 - k^2 \underline{w}^2)}} \quad (31)$$

$$\frac{d}{d\underline{w}} F_t(\underline{w}, k) = \frac{1}{\sqrt{1 - k^2 \underline{w}^2}} \quad (32)$$

In contrast to the Jakobian elliptic functions, where the modulus k is usually limited to a real number between 0 and 1, the modulus k of the elliptic integrals can be in principle an arbitrary complex number.

In the case of the elliptic integral of the first kind follows:

Modulus \underline{k} imaginary or $k' > 1$:

$$k' > 1, \text{ real} \Rightarrow \underline{k} = \sqrt{1 - k'^2} = j\sqrt{k'^2 - 1} = jk_0 \quad (33)$$

$$\underline{k}^2 = -k_0^2 \quad k' = \sqrt{1 + k_0^2} \quad (34)$$

$$F_t(\underline{w}, jk_0) = \int_0^{\underline{w}} \frac{d\underline{w}}{\sqrt{1 - k_0^2 \sin^2 \underline{w}}} \quad (35)$$

The values of the function for $k' > 1$ can be determined with the subroutine Cet ($u, v, k', 1, 1, \text{Re}, \text{Im}$), which is applicable for $0 \leq k' < \infty$. The subroutine Cfa ($u, v, k, 1, 1, \text{Re}, \text{Im}$), which is only valid for $0 \leq k' \leq 1$ can alternatively be used, with the help of the following conversion formulas:

$$F_t(\underline{w}, jk_0) = \frac{1}{k'} F_a \left(\frac{k' \sin \underline{w}}{\sqrt{1 + k_0^2 \sin^2 \underline{w}}}, \frac{k_0}{k'} \right) \quad (36)$$

Furthermore:

$$F_t(\underline{w}, jk_0) = \frac{1}{k'} \left[F_t \left(\underline{w} - \frac{\pi}{2}, k_0 / k' \right) + K(k_0 / k') \right] \quad (37)$$

Figure 12.5 shows the associated mapping. Starting from Figure 12.2 with $k' < 1$ the line charge moves in the z -plane for $k' \rightarrow 1$ along the imaginary axes to the point of infinity. For $k' > 1$ it moves backwards, parallel displaced on the straight line $\underline{z} = K$ with continuously decreasing imaginary part. Compared to the possibilities in the region $0 \leq k' \leq 1$ no topologically novel mappings are generated for $k' > 1$.

The dimensions of the rectangles are:

$$K(jk_0) = \frac{1}{k'} K \left(\frac{k_0}{k'} \right) \quad (38)$$

$$K'(jk_0) = \frac{1}{k'} K \left(\frac{1}{k'} \right) \quad (39)$$

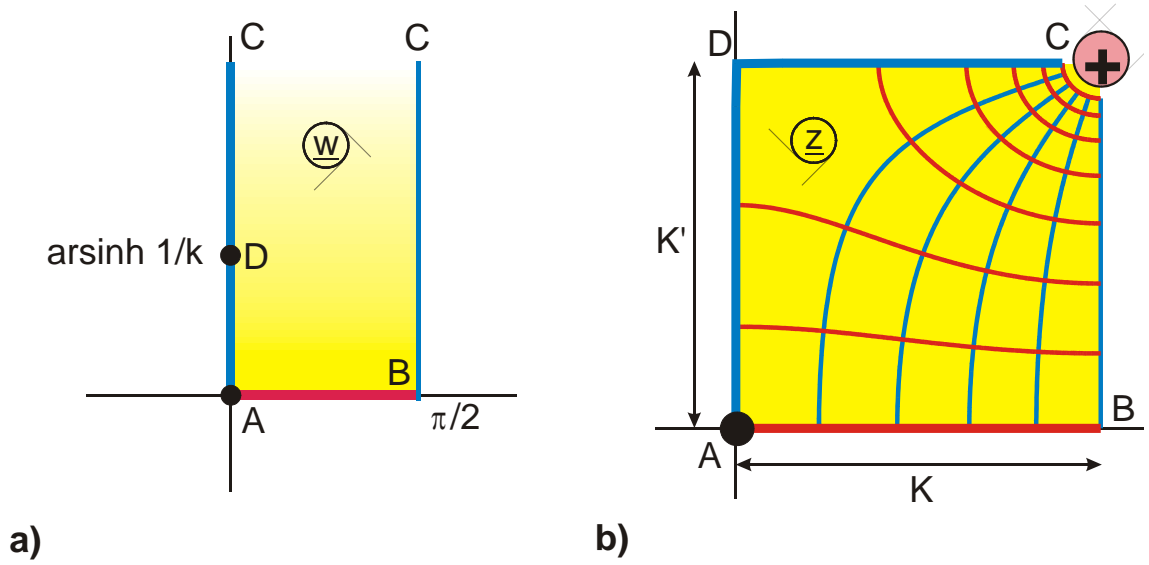


Figure 12.5: The transformation $z = F_t(w, jk_0)$

Modulus $k > 1$:

$$F_t(\underline{w}, k > 1) = \frac{1}{\sqrt{k}} F_a(k \sin \underline{w}, 1/k) \quad (40)$$

with

$$K(k > 1) = \frac{1}{\sqrt{k}} K(1/k) \quad (41)$$

$$K'(k > 1) = \frac{1}{\sqrt{k}} K'(1/k) \quad (42)$$

The transformation is shown in Figure 12.6. Compared to the case $k = 1$ in Figure 12.3b, it can be seen that the point of infinity, point B from Figure 12.3b moves to $K + jK'$ for $k > 1$. The line charge stays unchanged on the imaginary axis.

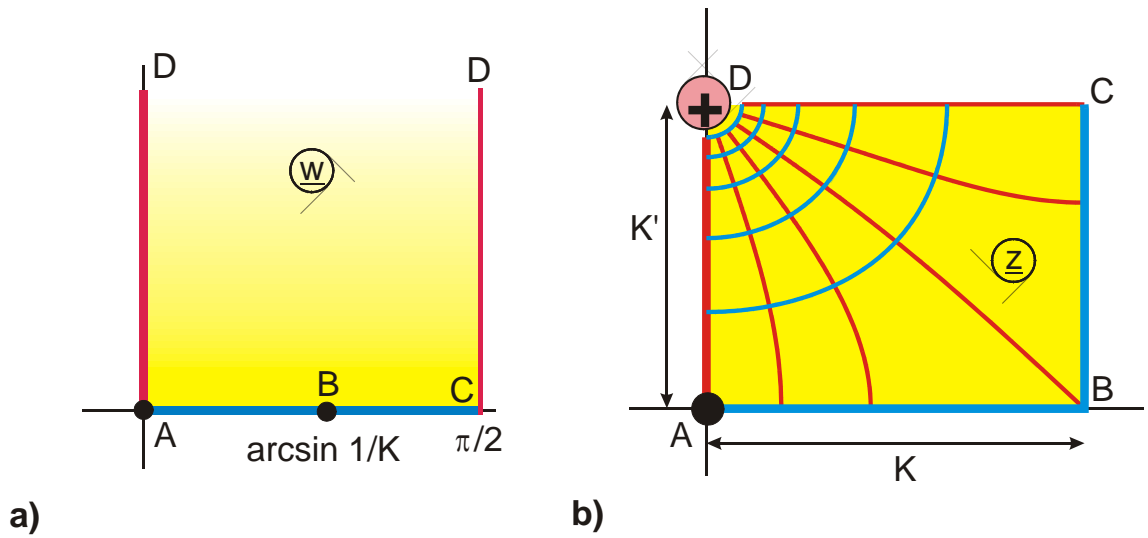


Figure 12.6: The transformation $z = F_t(w, k > 1)$

12.2 The Elliptic Integral of the Second Kind

The elliptic integral of the second kind is denoted by the letter E. The algebraic form is:

$$E_a(t, k) = \int_0^t \frac{\sqrt{1 - k^2 t^2}}{\sqrt{1 - t^2}} dt. \quad (43)$$

By substituting the variable in the integrand with $t = \sin \varphi$ the trigonometric form is found

$$E_t(\varphi, k) = \int_0^{\varphi} \sqrt{1 - k^2 \sin^2 \varphi} \, d\varphi. \quad (44)$$

If substituting in $E_a(t, k)$ with $t = \operatorname{sn} u$ the elliptic form results

$$E_e(u, k) = \int_0^u \operatorname{dn}^2(u, k) du \quad (45)$$

In common notation, with the complex variable \underline{w} , the algebraic form is

$$E_a(\underline{w}, k) = \int_0^{\underline{w}} \sqrt{\frac{1 - k^2 \underline{w}^2}{1 - \underline{w}^2}} \, d\underline{w}, \quad (46)$$

the trigonometric form is

$$E_t(\underline{w}, k) = \int_0^{\underline{w}} \sqrt{1 - k^2 \sin^2 \underline{w}} \, d\underline{w} = E(\underline{w}, k) \quad (47)$$

and the elliptic form is

$$E_e(\underline{w}, k) = \int_0^{\underline{w}} \operatorname{dn}^2(\underline{w}, k) \, d\underline{w}. \quad (48)$$

The three forms can be converted into each other with the following:

$$E_t(\underline{w}, k) = E_a(\sin \underline{w}, k) \quad (49)$$

$$E_a(\underline{w}, k) = E_t(\arcsin \underline{w}, k) \quad (50)$$

$$E_e(\underline{w}, k) = E_a[\operatorname{sn}(\underline{w}, k), k] \quad (51)$$

$$E_a(\underline{w}, k) = E_e[F_a(\underline{w}, k), k] \quad (52)$$

When discussing the elliptic integral of the first kind, the elliptic form $F_e(\underline{w}, k)$ was not mentioned, because for that one holds:

$$F_e(\underline{w}, k) = F_a[\operatorname{sn}(\underline{w}, k), k] = \underline{w}. \quad (53)$$

For the upper limits of integration $\underline{w} = 1$, $\underline{w} = \pi/2$ and $\underline{w} = K$ respectively the complete elliptic integral of the second kind is found:

$$E(k) = E_a(\underline{w} = 1, k) = E_t\left(\underline{w} = \frac{\pi}{2}, k\right) = E_e[\underline{w} = K(k), k] \quad (54)$$

For the complementary modulus $k' = \sqrt{1 - k^2}$ results

$$E'(k) = E(k'). \quad (55)$$

For the complete elliptic integrals of the first and second kinds holds:

$$EK' + E'K - KK' = \pi / 2 \quad (56)$$

For $k = 1 / \sqrt{2}$ it is found that $k = k'$ and accordingly $E = E'$. For $k = 0$ it is found that $E = \pi/2$ (see Eq. (57), circumference of a circle).

The complete elliptic integral of the second kind is geometrically defined by the circumference of an ellipse with the half axes a and b (see Figure 12.1):

$$\text{Circumference of an ellipse} = 4a E\left(k = \sqrt{1 - b^2/a^2}\right) \quad (57)$$

Normalized to $a = 1$ and $b = k$ this is:

$$\text{Circumference of an ellipse} = 4 E(k') \quad (58)$$

k is the numerical excentricity of the ellipse. The occurrence of this integral when calculating the arc length or the circumference of an ellipse has given the elliptic integrals and their inverse functions, the elliptic functions, their name.

Figure 12.7 shows the transformation, which belongs to $E_t(\underline{w}, k)$. A parallel strip in the w -plane is mapped onto the region that is depicted in the z -plane. The right boundary of the parallel strip is bent outside by 90° at the point D .

The left half plane, which is not shown, can be complemented as a mirror image.

$$E_t(-\underline{w}, k) = -E_t(\underline{w}, k) \quad (59)$$

$E_t(\underline{w}, k)$ is like $\sin^2 \underline{w}$ periodic with the period π . All other parallel strips, which are displaced by $\pm n\pi$ in the w -plane, yield the same mapping in the z -plane.

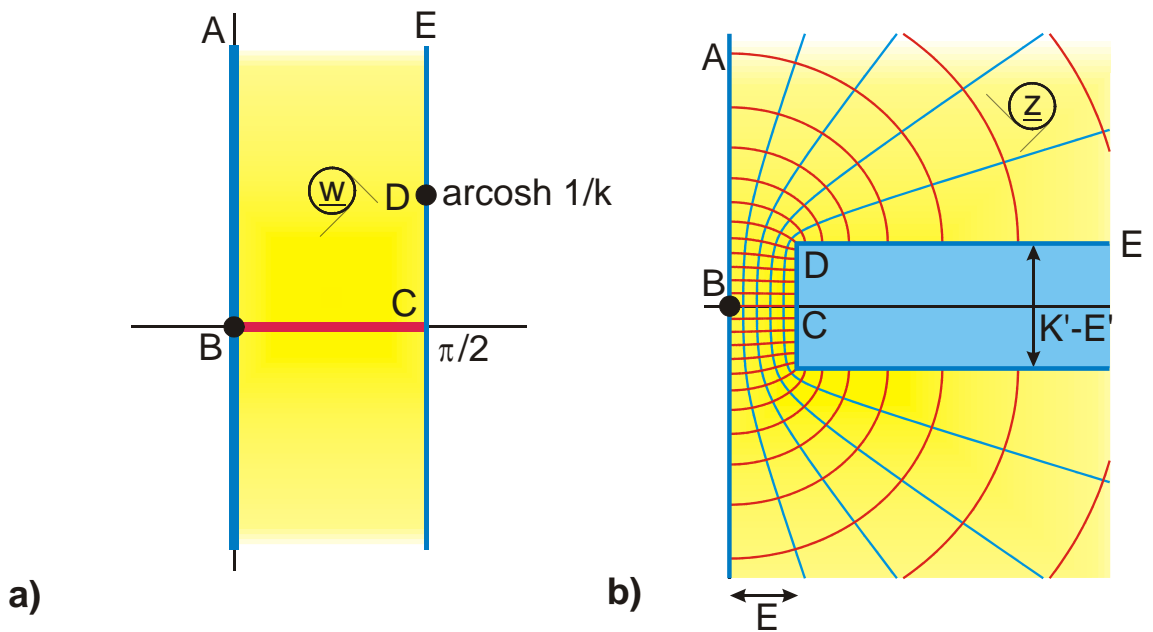


Figure 12.7: The transformation $z = E_t(w, k)$ for $0 \leq k \leq 1$, Mapping C 3.1

Limiting cases:

For $k \rightarrow 1$ the width of the half strip in the z -plane is decreasing. In the limit $k = 1$ it is

obtained that $K'(1) - E'(1) = \frac{\pi}{2} - \frac{\pi}{2} = 0$ and that the point D coincides with point C.

$$E_t(\underline{w}, k = 1) = \sin \underline{w} \quad (60)$$

When k decreases, the half strip becomes wider and wider. For $k = 0$ finally $K'(0) = \infty$ and $E'(0) = 1$. Point D moves in the z -plane to ∞ (Figure 12.8b).

$$E_t(\underline{w}, k = 0) = \underline{w} \quad (61)$$

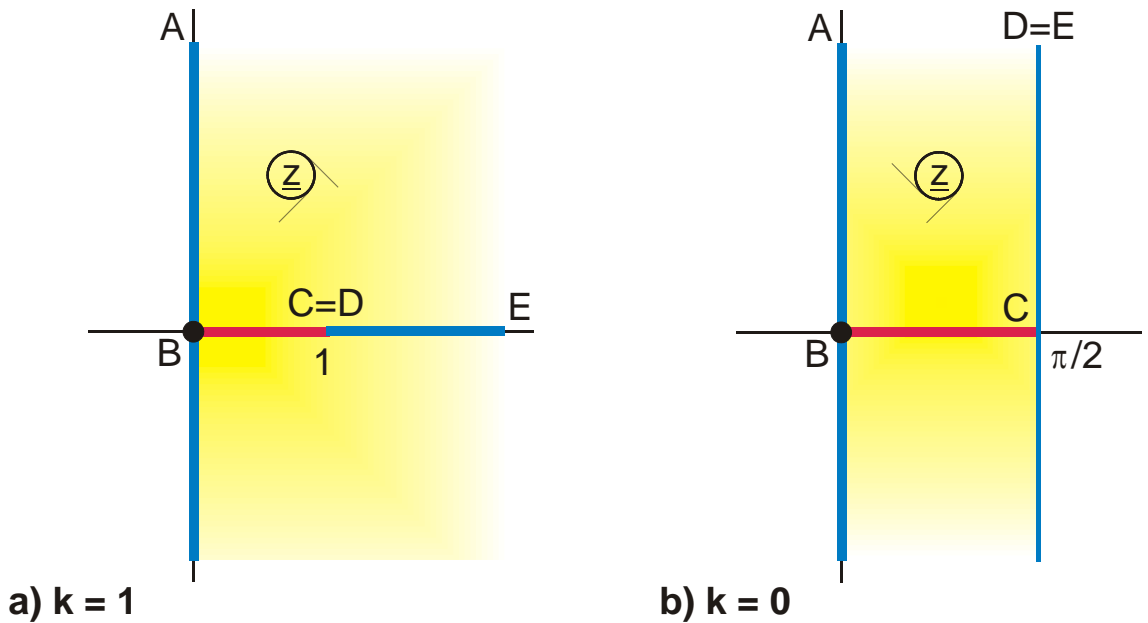


Figure 12.8: Limiting values of the transformation $z = E_t(w, k)$

As $E_t(z,k)$ differs from $E_a(z,k)$ only by the pre-transformation with the sine function, it follows that E_a and E_t have identical boundaries in the z -plane (Figure 12.9b). Only the potential distribution on the boundary is different.

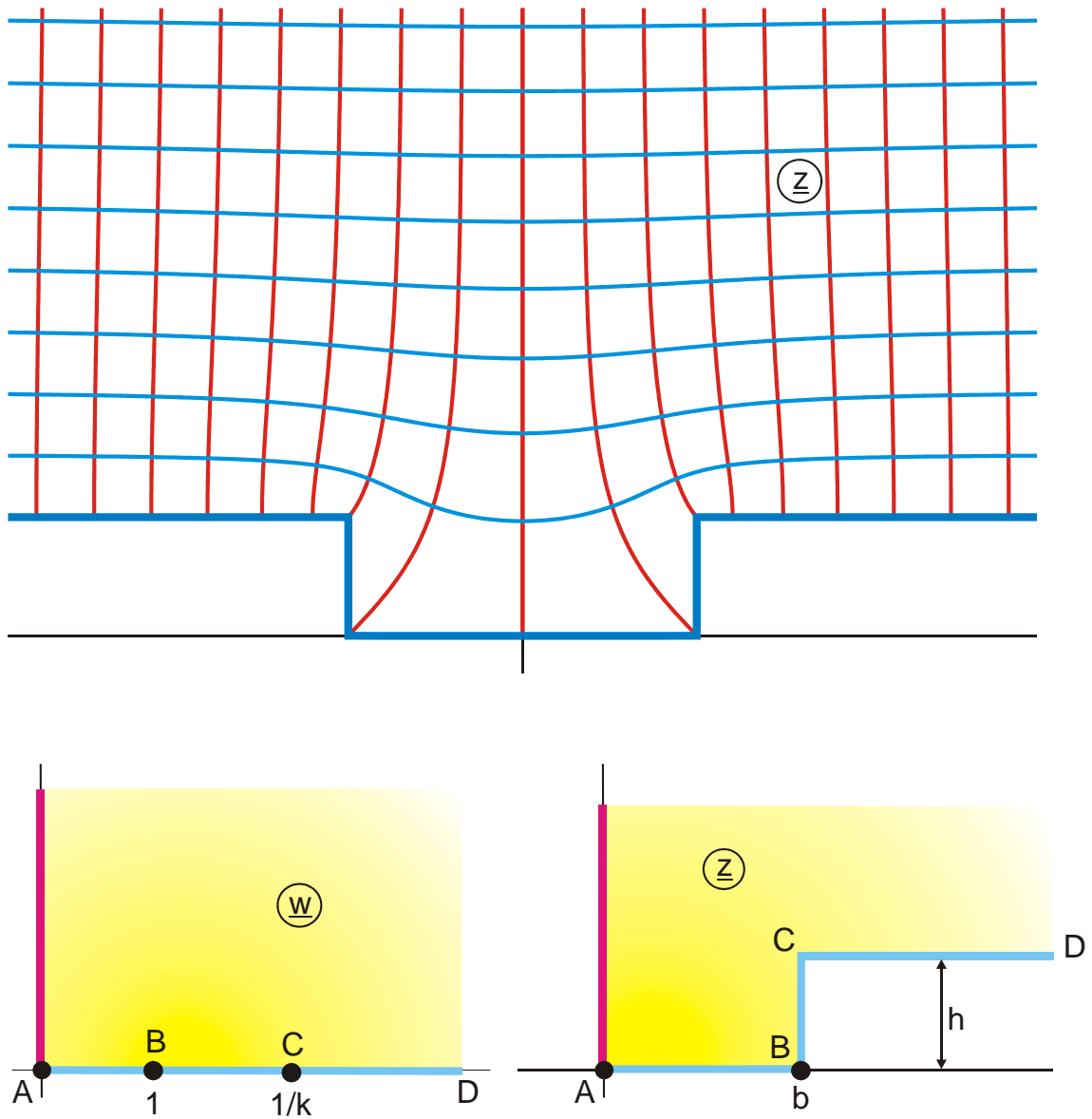


Figure 12.9: The transformation $z = E_a(w, k)$ for $0 \leq k \leq 1$, Mapping A 10

$$b = E(k), h = K'(k) - E'(k)$$

For the limiting cases $k = 1$ and $k = 0$ therefore the same is found:

$$E_a(\underline{w}, k = 1) = \underline{w} \quad (62)$$

$$E_a(\underline{w}, k = 0) = \arcsin \underline{w} \quad (63)$$

Figure 12.10 shows the transformation with $E_e(\underline{w}, k)$ for the I. quadrant of the w -plane. In the limiting cases $k = 1$ and $k = 0$ again Figure 12.8 is valid with appropriately changed distribution of the potential (the assignment of potential lines and field lines, which was chosen in Figure 12.8 and Figure 12.10 is arbitrary and can as well be the other way round).

$$E_e(\underline{w}, k = 1) = \tanh \underline{w} \quad (64)$$

$$E_e(\underline{w}, k = 0) = \underline{w} \quad (65)$$

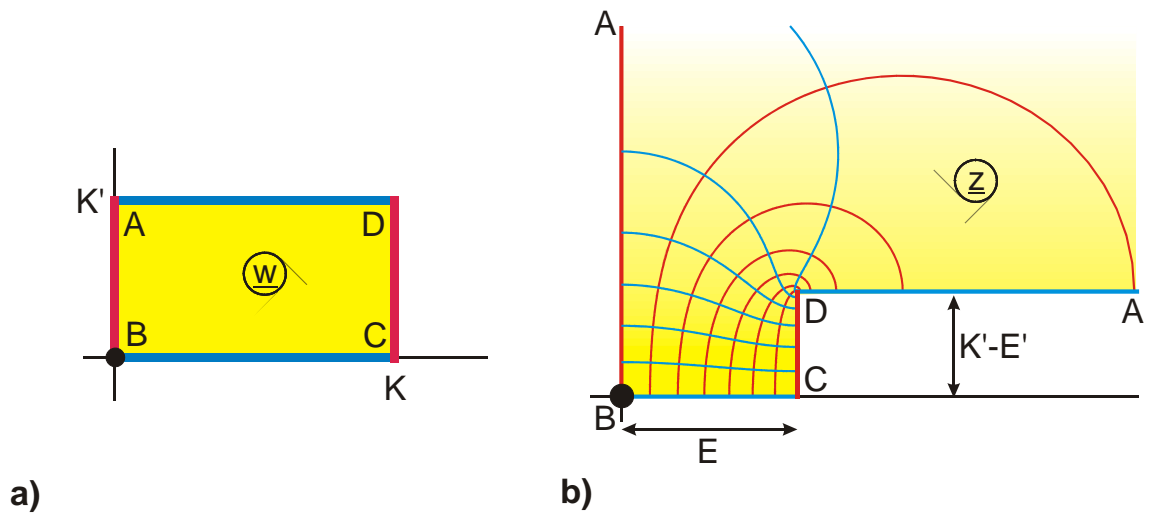


Figure 12.10: The transformation $z = E_e(w, k)$ for $0 \leq k \leq 1$, Mapping U 5

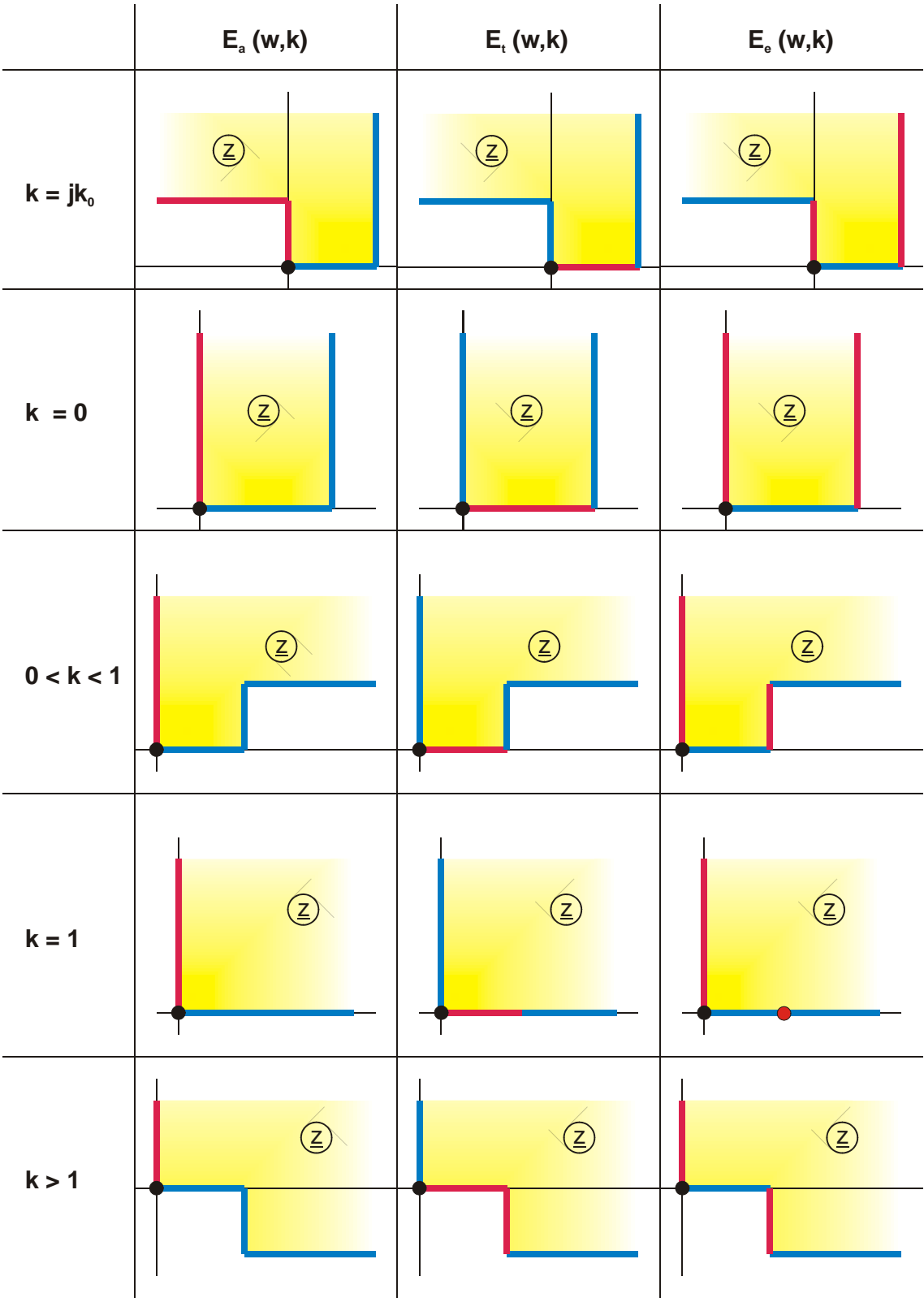


Table 12.1: General survey over the elliptic integral of the second kind

12.3 Jacobi's Zeta Function; the Functions $B(\underline{w}, k)$ and $D(\underline{w}, k)$

By linear combination of the elliptic integrals of the first and second kinds and of other rational functions it is possible to produce a variety of different other functions. In order to shorten the notation of equations, and also because they were used by various other authors, this book uses from these functions $Z(\underline{w}, k)$, $B(\underline{w}, k)$ and $D(\underline{w}, k)$.

Jacobi's Zeta function is defined by

$$Z(\underline{w}, k) = Z_e(\underline{w}, k) = E_e(\underline{w}, k) - \underline{w} \frac{E(k)}{K(k)} \quad (66)$$

in the elliptic form. In analogy to Eq. 16 - 18 the trigonometric form is found

$$Z_t(\underline{w}, k) = E_t(\underline{w}, k) - F_t(\underline{w}, k) \frac{E(k)}{K(k)} \quad (67)$$

and the algebraic form

$$Z_a(\underline{w}, k) = E_a(\underline{w}, k) - F_a(\underline{w}, k) \frac{E(k)}{K(k)} \quad (68)$$

The conversion is done by:

$$Z_t(\underline{w}, k) = Z_e[F_t(\underline{w}, k), k] \quad (69)$$

$$Z_a(\underline{w}, k) = Z_t(\arcsin \underline{w}, k) \quad (70)$$

$$Z_e(\underline{w}, k) = Z_t\{\arcsin[\operatorname{sn}(\underline{w}, k)], k\} \quad (71)$$

$$Z_a(\underline{w}, k) = Z_e[F_a(\underline{w}), k] \quad (72)$$

$$Z_e(\underline{w}, k) = Z_a[\operatorname{sn}(\underline{w}, k), k] \quad (73)$$

$$Z_t(\underline{w}, k) = Z_a(\sin \underline{w}, k). \quad (74)$$

Figure 12.11 shows the transformation with $Z_e(\underline{w}, k)$, Figure 12.12 that with $Z_t(\underline{w}, k)$ and Figure 12.13 that with $Z_a(\underline{w}, k)$.

Furthermore holds:

$$Z_e(\underline{w}, k) = \int_0^{\underline{w}} \left[\operatorname{dn}^2(\underline{w}, k) - \frac{E(k)}{K(k)} \right] d\underline{w} \quad (75)$$

$$Z_e(-\underline{w}, k) = -Z_e(\underline{w}, k) \quad (76)$$

$$Z_e(\underline{w}, k=0) = 0 \quad (77)$$

$$Z_e(\underline{w}, k=1) = \tanh \underline{w} \quad (78)$$

$$Z_e[\underline{w} + K(k), k] = Z_e(\underline{w}, k) - k^2 \cdot \operatorname{sn}(\underline{w}, k) \cdot \operatorname{cn}(\underline{w}, k) / \operatorname{dn}(\underline{w}, k) \quad (79)$$

$$Z_e[\underline{w} + jK'(k), k] = Z_e(\underline{w}, k) - j \frac{\pi}{2K(k)} + \operatorname{cn}(\underline{w}, k) \cdot \operatorname{dn}(\underline{w}, k) / \operatorname{sn}(\underline{w}, k) \quad (80)$$

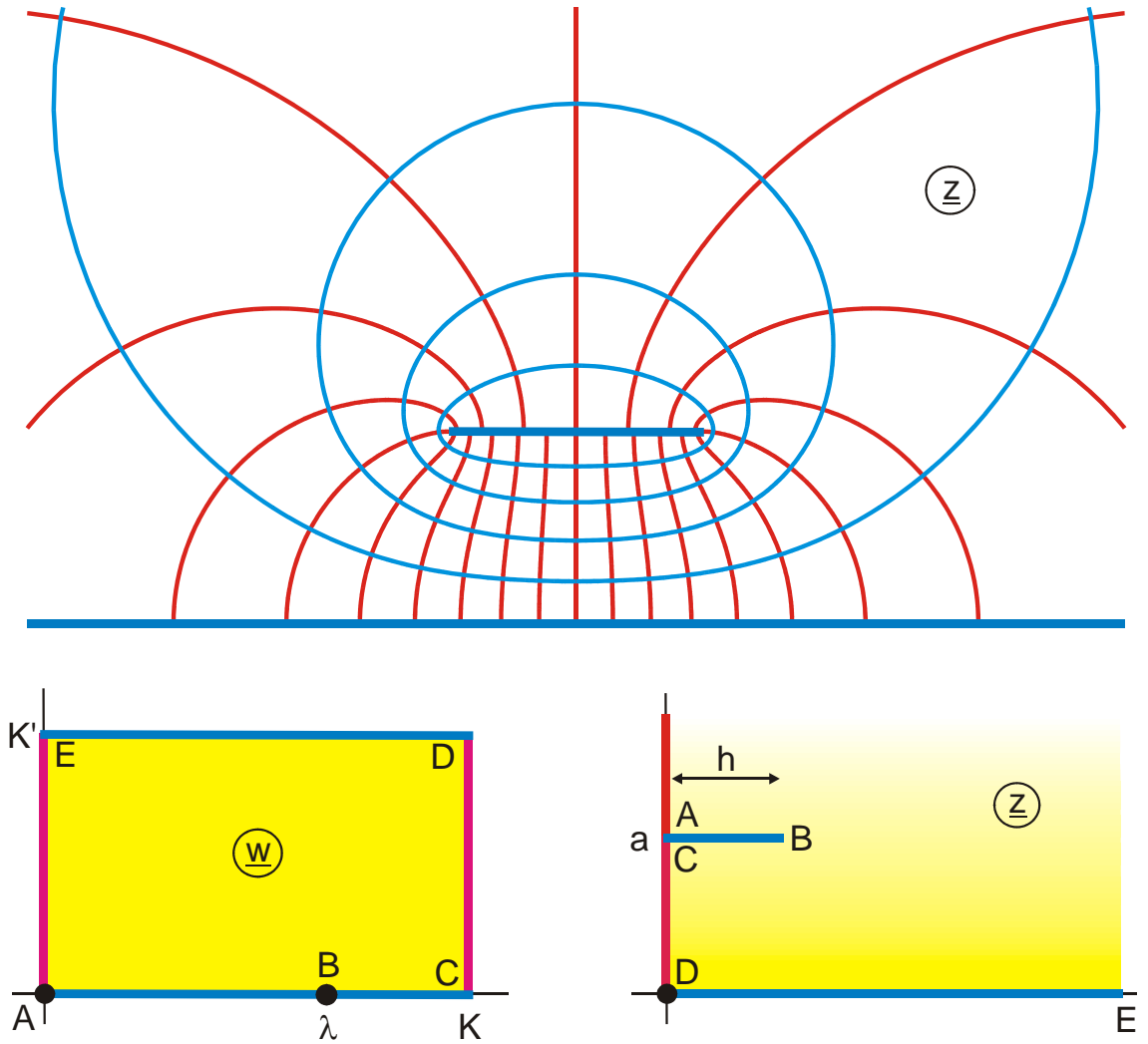


Figure 12.11: The transformation $z = Z_e(w, k)$, Mapping E 2,

with $h = Z_a\left(\frac{\sqrt{1-E/K}}{k}, k\right)$, $a = \frac{\pi}{2K}$ and $\lambda = F_a\left(\frac{1}{k}\sqrt{1-E/K}, k\right)$

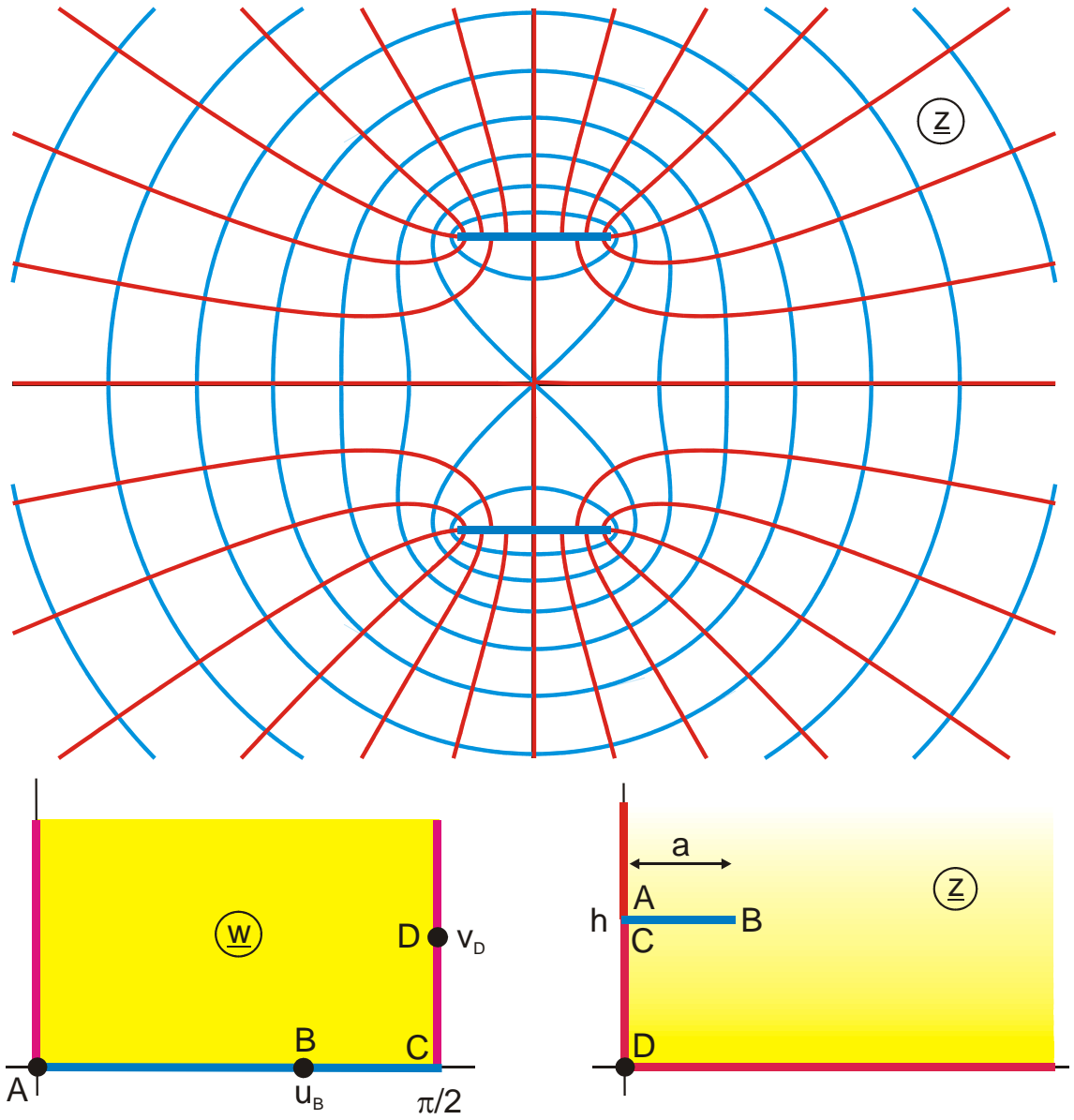


Figure 12.12: The transformation $z = Z_t(w, k)$, Mapping S 2, with

$$u_B = \sin \left(\frac{\sqrt{1 - E/K}}{k} \right)$$

$$a = \frac{\pi}{2K}$$

$$u_B = \arcsin b$$

$$h = Z_t(u_B, k) = Z_a(b, k)$$

$$b = \frac{1}{k} \sqrt{1 - \frac{E}{K}}$$

$$v_D = \operatorname{arcosh}(1/k)$$

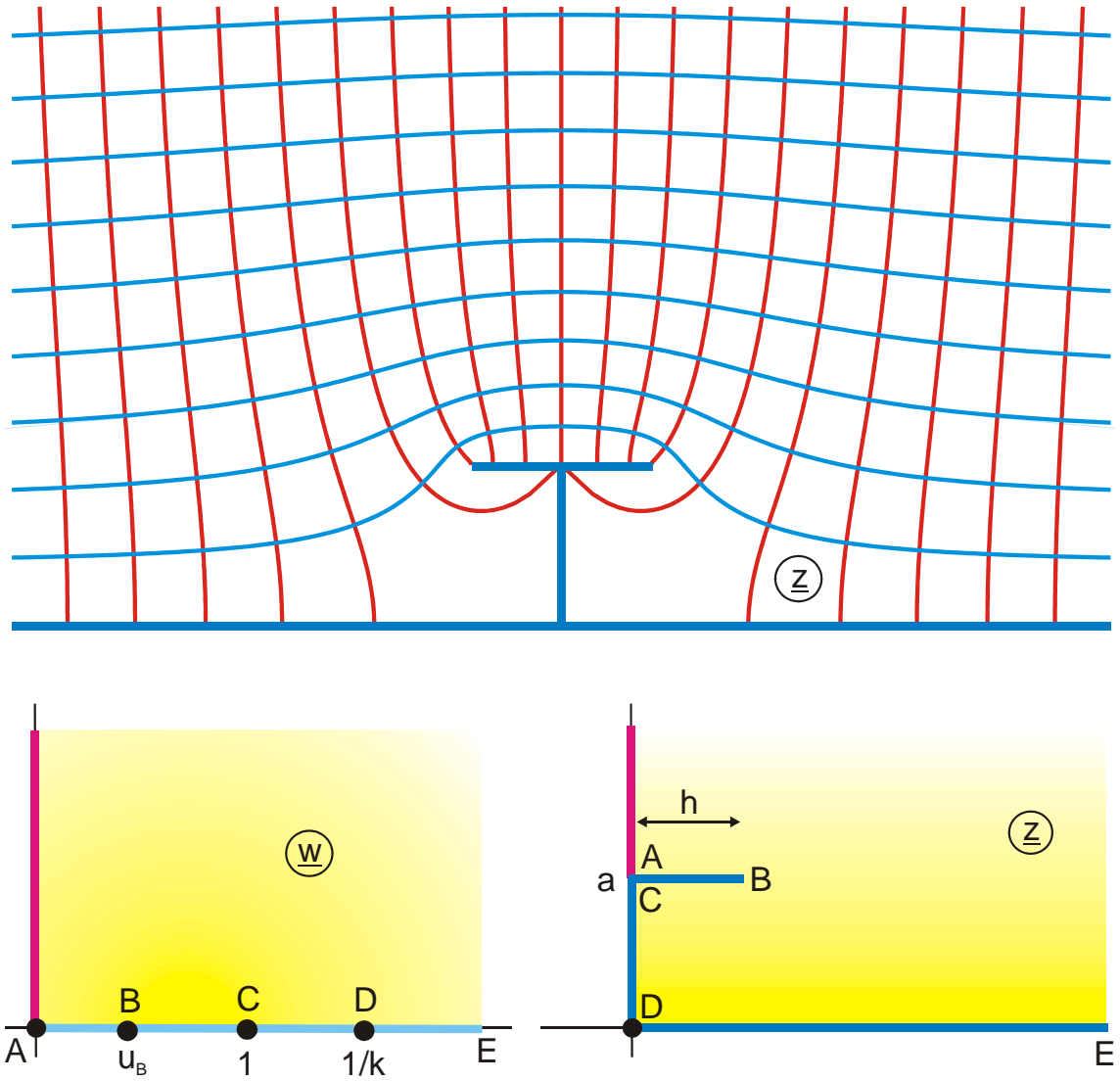


Figure 12.13: The transformation $z = Z_a(w, k)$, Mapping A 11.1,

with $h = Z_a\left(\frac{\sqrt{1-E/K}}{k}, k\right)$, $a = \frac{\pi}{2K}$ and $u_B = \frac{1}{k}\sqrt{1-E/K}$

The elliptic integral of the second kind can be separated in analogy to $\sin^2 \varphi + \cos^2 \varphi = 1$.

$$\int_0^\varphi \frac{\sin^2 \varphi}{\sqrt{1-k^2 \sin^2 \varphi}} d\varphi + \int_0^\varphi \frac{\cos^2 \varphi}{\sqrt{1-k^2 \sin^2 \varphi}} d\varphi = \int_0^\varphi \frac{1}{\sqrt{1-k^2 \sin^2 \varphi}} d\varphi$$

$$D_t(\varphi, k) + B_t(\varphi, k) = F_t(\varphi, k) \quad (81)$$

Trigonometric form (Figure 12.14):

$$D_t(\underline{w}, k) = \int_0^{\underline{w}} \frac{\sin^2 \underline{w}}{\sqrt{1-k^2 \sin^2 \underline{w}}} d\underline{w} \quad (82)$$

$$B_t(\underline{w}, k) = \int_0^{\underline{w}} \frac{\cos^2 \underline{w}}{\sqrt{1-k^2 \sin^2 \underline{w}}} d\underline{w} \quad (83)$$

Algebraic form (Figure 12.15):

$$D_a(\underline{w}, k) = \int_0^{\underline{w}} \frac{\underline{w}^2}{\sqrt{(1-\underline{w}^2)(1-k^2 \underline{w}^2)}} d\underline{w} \quad (84)$$

$$B_a(\underline{w}, k) = \int_0^{\underline{w}} \frac{\sqrt{1-\underline{w}^2}}{\sqrt{1-k^2 \underline{w}^2}} d\underline{w} \quad (85)$$

Elliptic form (Figure 12.16):

$$D_e(\underline{w}, k) = \int_0^{\underline{w}} \text{sn}^2(\underline{w}, k) d\underline{w} \quad (86)$$

$$B_e(\underline{w}, k) = \int_0^{\underline{w}} \text{cn}^2(\underline{w}, k) d\underline{w} \quad (87)$$

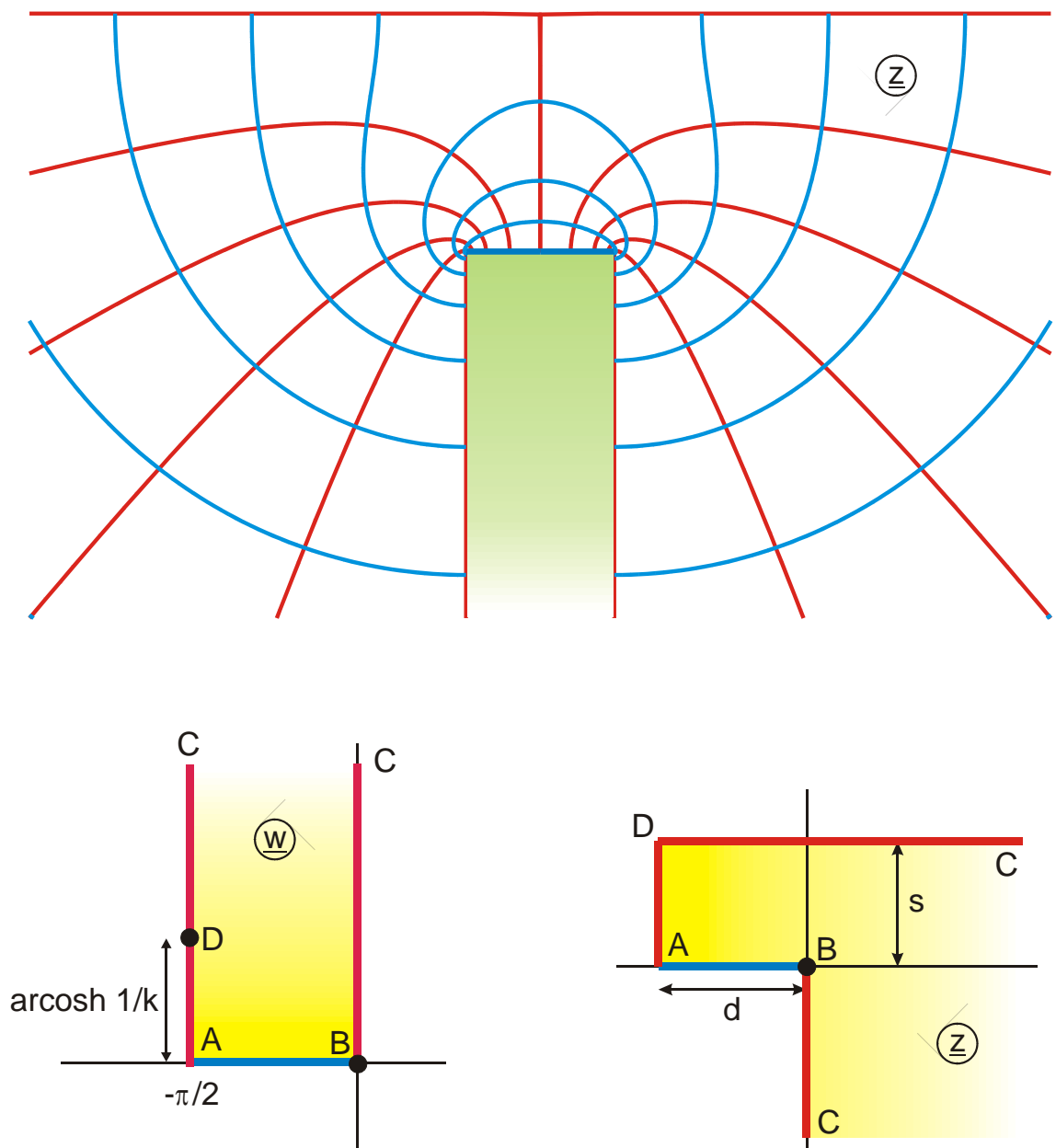


Figure 12.14 a: The transformation $z = D_t(w, k)$, Mapping U 2

$$d = \frac{K(k) - E(k)}{k^2}$$

$$s = \frac{E'(k)}{k^2}$$

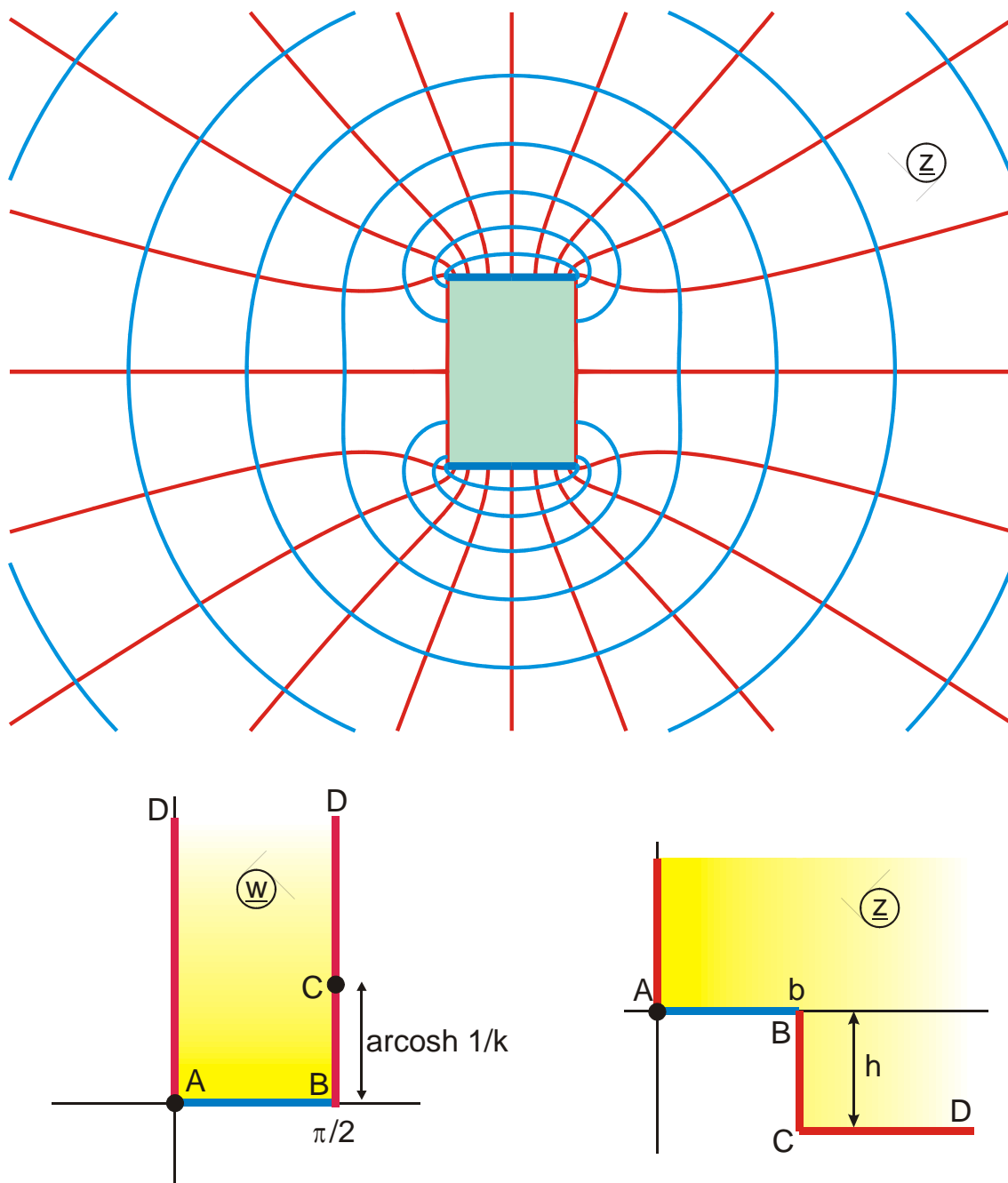


Figure 12.14 b: The transformation $z = B_t(w, k)$, Mapping U 1,

$$b = \frac{E(k) - k'^2 K(k)}{k^2}$$

$$h = \frac{E'(k)}{k^2} - K'(k)$$

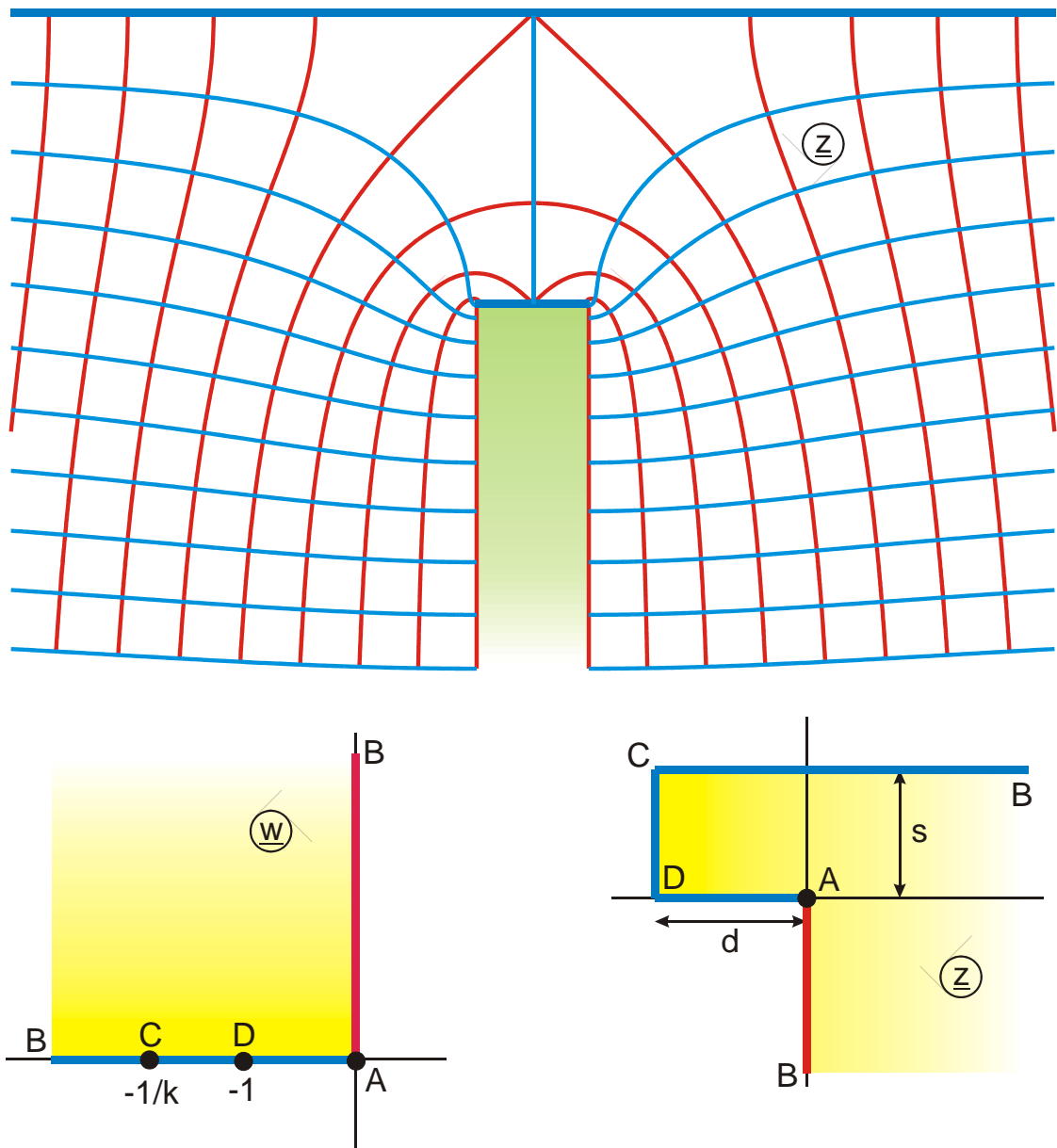


Figure 12.15 a: The transformation $z = D_a(w, k)$, Mapping U 2.1,

$$d = \frac{K(k) - E(k)}{k^2}$$

$$s = \frac{E'(k)}{k^2}$$

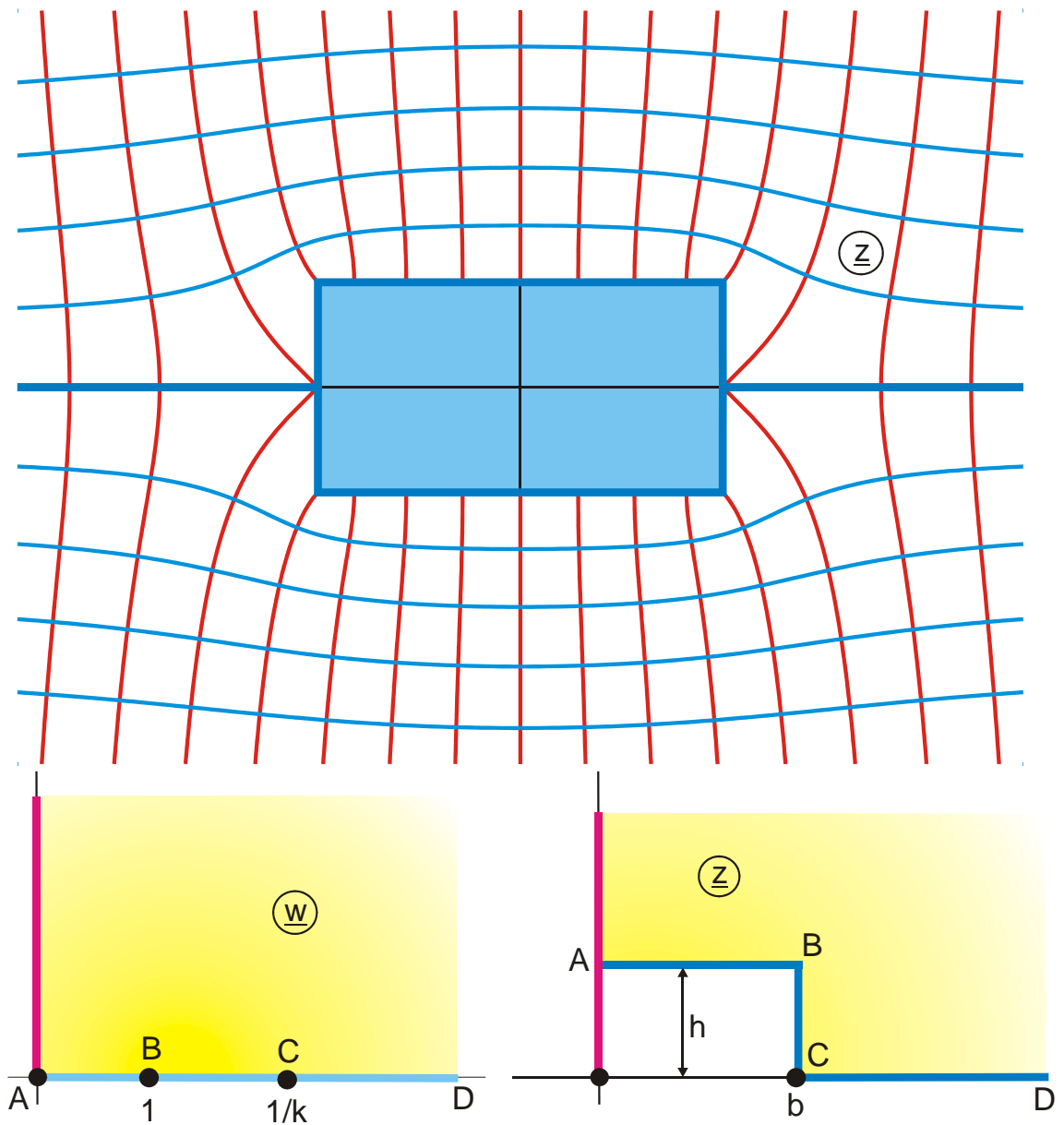


Figure 12.15 b: The transformation $z = B_a(w, k)$, Mapping A 10.2,

with $b = \frac{E - k'K}{k^2}$ and $h = \frac{E'}{k^2} - K'$

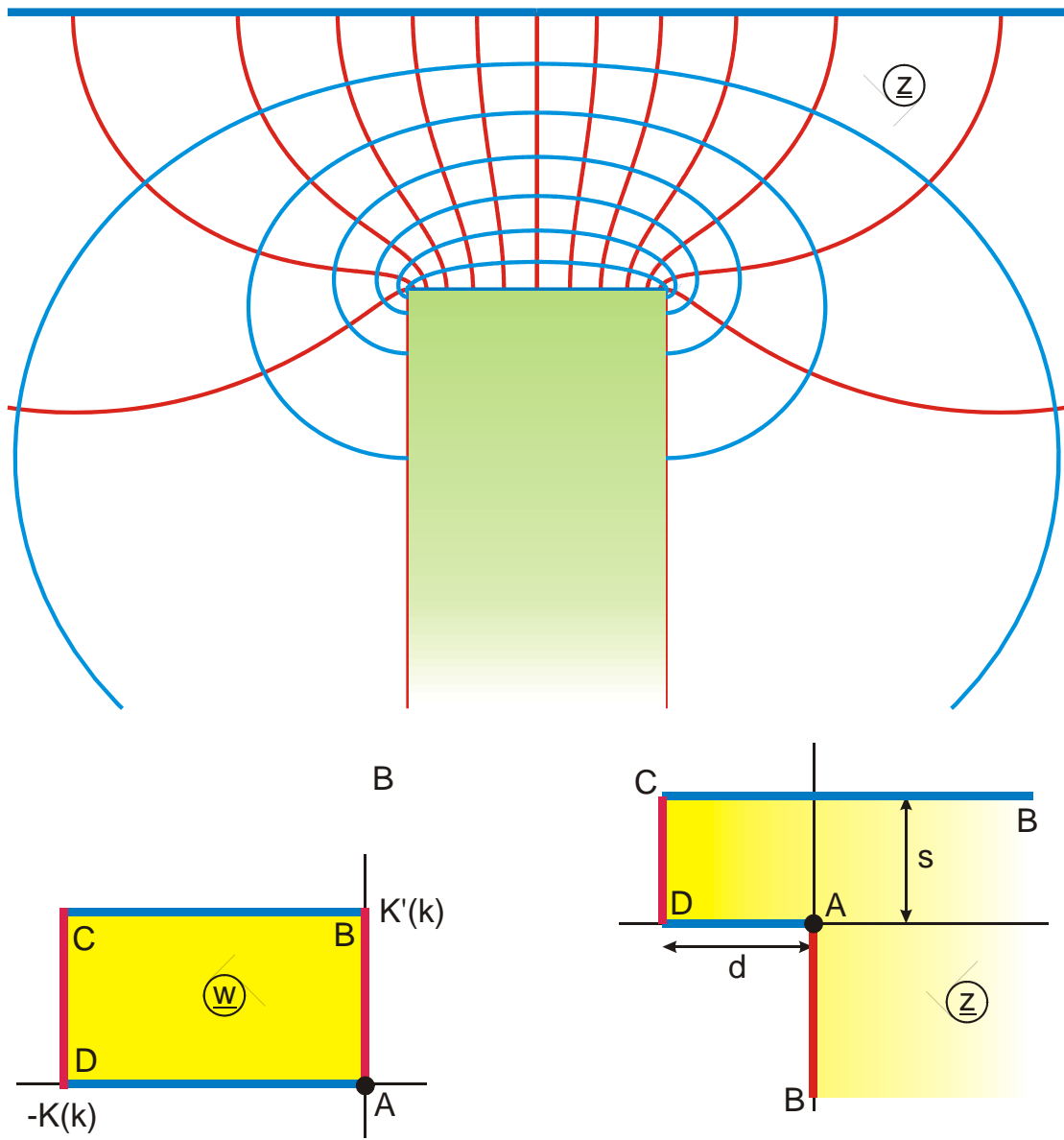


Figure 12.16 a: The transformation $z = D_e(w, k)$, Mapping U 2.2,

$$d = \frac{K(k) - E(k)}{k^2}$$

$$s = \frac{E'(k)}{k^2}$$

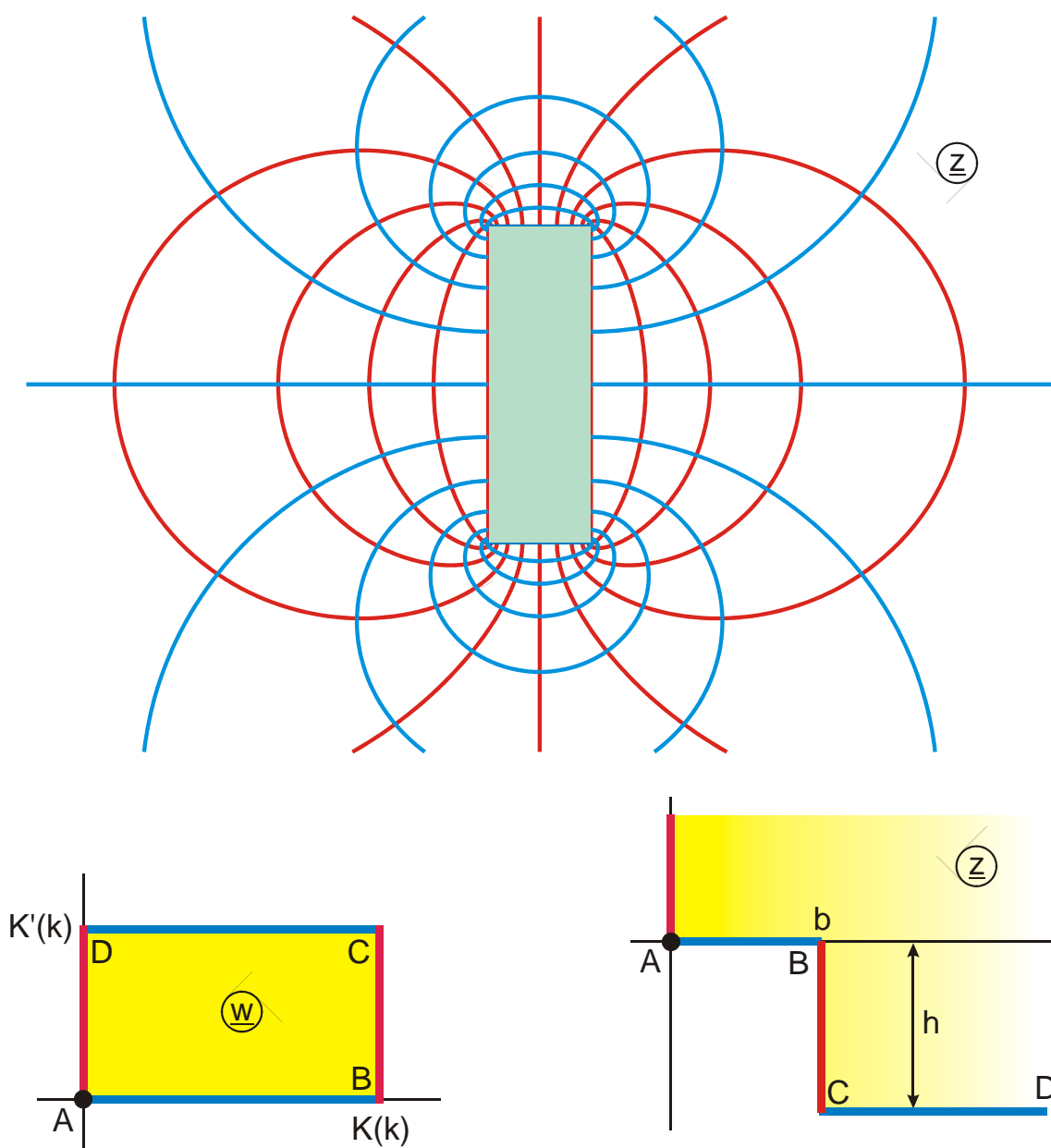


Figure 12.16 b: The transformation $z = B_e(w, k)$, Mapping U 1.1,

with $b = \frac{E - k'K}{k^2}$ and $h = \frac{E'}{k^2} - K'$

Complete integrals:

$$D(k) = \frac{K(k) - E(k)}{k^2} \quad (88)$$

$$B(k) = \frac{E(k) - k'^2 K(k)}{k^2} \quad (89)$$

Furthermore holds:

$$D(\underline{w}, k) = \frac{1}{k^2} [F(\underline{w}, k) - E(\underline{w}, k)] \quad (90)$$

$$B(\underline{w}, k) = \frac{1}{k^2} [E(\underline{w}, k) - k'^2 F(\underline{w}, k)] \quad (91)$$

The function $D(\underline{w}, k)$ does not yield any topologically novel conformal mappings. Transformations with $D(\underline{w}, k)$ can always be substituted by transformations with the elliptic integral of the second kind $E(\underline{w}, k)$. This is also immediately evident if Eq. (86) is compared with Eq. (45): The functions $\text{sn}(\underline{w}, k)$ and $\text{dn}(\underline{w}, k)$ in the integrand likewise yield similar mappings.

12.4 The Elliptic Integral of the Third Kind

The elliptic integral of the third kind is denoted by the capital letter Π . There are four forms in use:

The algebraic form:

$$\Pi_a(t, k, n) = \int_0^t \frac{dt}{(1 - nt^2)\sqrt{(1 - t^2)(1 - k^2 t^2)}} \quad (92)$$

By substituting $t = \sin \varphi$ the trigonometric form is found:

$$\Pi_t(\varphi, k, n) = \int_0^\varphi \frac{d\varphi}{(1 - n \sin^2 \varphi)\sqrt{1 - k^2 \sin^2 \varphi}} \quad (93)$$

By substituting $t = \operatorname{sn}(u, k)$ and $n = [k \cdot \operatorname{sn}(a, k)]^2$ the elliptic form is found:

$$\Pi_e(u, k, a) = \int_0^u \frac{du}{1 - k^2 \operatorname{sn}^2(a, k) \cdot \operatorname{sn}^2(u, k)} \quad (94)$$

The Jacobian form results from the elliptic form with the equation

$$\Pi_j(u, k, a) = \frac{\text{cn}(a, k) \text{dn}(a, k)}{\text{sn}(a, k)} [\Pi_e(u, k, a) - u] \quad (95)$$

$$\Pi_j(u, k, a) = k^2 \text{sn}(a, k) \text{cn}(a, k) \text{dn}(a, k) \int_0^u \frac{\text{sn}^2(u, k) du}{1 - k^2 \text{sn}^2(a, k) \cdot \text{sn}^2(u, k)} \quad (96)$$

The parameter (or characteristic) n is an arbitrary complex number. Yet for the conformal mappings treated in this book n and a are real numbers for the majority of mappings. The mappings usually have a totally different topology in the four regions:

- | | |
|-------|---------------|
| (I) | $n < 0$ |
| (II) | $0 < n < k^2$ |
| (III) | $k^2 < n < 1$ |
| (IV) | $n > 1$ |

Those cases, where \underline{a} is a complex number, are restricted to the special case $\underline{a} = \text{Re}\{\underline{a}\} + jK'(k)$ for the mappings D 6.2 and A 10.3.

When all four forms of the elliptic integral are used, it is sufficient for the purpose of conformal mapping, to restrict n to real numbers in the range $0 < n < k^2$ and a to real numbers in the range $0 < a < K(k)$.

In common notation, with the complex variable \underline{w} , follows

the algebraic form

$$\Pi_a(\underline{w}, k, n) = \int_0^{\underline{w}} \frac{d\underline{w}}{(1 - n\underline{w}^2) \sqrt{(1 - \underline{w}^2)(1 - k^2 \underline{w}^2)}} \quad (97)$$

the trigonometric form

$$\Pi_t(\underline{w}, k, n) = \int_0^{\underline{w}} \frac{d\underline{w}}{(1 - n \sin^2 \underline{w}) \sqrt{1 - k^2 \sin^2 \underline{w}}} \quad (98)$$

the elliptic form

$$\Pi_e(\underline{w}, k, a) = \int_0^{\underline{w}} \frac{d\underline{w}}{1 - k^2 \operatorname{sn}^2(a, k) \cdot \operatorname{sn}^2(\underline{w}, k)} \quad (99)$$

and the Jacobian form

$$\Pi_j(\underline{w}, k, a) = k^2 \operatorname{sn}(a, k) \operatorname{cn}(a, k) \operatorname{dn}(a, k) \int_0^{\underline{w}} \frac{\operatorname{sn}^2(\underline{w}, k) d\underline{w}}{1 - k^2 \operatorname{sn}^2(a, k) \cdot \operatorname{sn}^2(\underline{w}, k)} \quad (100)$$

For the conversion of the four forms into each other Table 12.2 can be used with respect for the variables together with

$$a = F_a(\sqrt{n} / k, k) \quad \text{and} \quad n = k^2 \operatorname{sn}^2(a, k). \quad (101)$$

The numerical values of the elliptic integrals of the third kind for \underline{w} complex and \underline{n} complex can be calculated with the subroutines Cpia, Cpit, Cpie and Cpij.

The complete elliptic integrals of the third kind are:

$$\Pi(k, n) = \Pi_a(\underline{w} = 1, k, n) = \Pi_t(\underline{w} = \frac{\pi}{2}, k, n) = \Pi_e[\underline{w} = K(k), k, a] \quad (102)$$

For $0 < n < k^2$:

$$\Pi(k, n) = K(k) \left[1 + \sqrt{\frac{n}{(1-n)(k^2-n)}} \cdot Z_a\left(\frac{\sqrt{n}}{k}, k\right) \right] \quad (103)$$

$$\Pi(k, a) = K(k) \left[1 + \frac{\text{sn}(a, k)}{\text{cn}(a, k) \text{dn}(a, k)} \cdot Z_e(a, k) \right] \quad (104)$$

The numerical values of the complete elliptic integrals of the third kind can be determined with the subroutine Kep in the appendix.

The Figures 12.17 through 12.20 illustrate the conformal mappings, which belong to the four forms of the elliptic integral of the third kind. In Figure 12.17 there is a line dipole in point E, in Figure 12.18 there is a line charge in point E.

	$E_a(\underline{w}, k)$	$E_t(\underline{w}, k)$	$E_e(\underline{w}, k)$
$E_a(\underline{w}, k) =$	$E_a(\underline{w}, k)$	$E_t(\arcsin \underline{w}, k)$	$E_e[F_a(\underline{w}, k), k]$
$E_t(\underline{w}, k) =$	$E_a(\sin \underline{w}, k)$	$E_t(\underline{w}, k)$	$E_e[F_t(\underline{w}, k), k]$
$E_e(\underline{w}, k) =$	$E_a[\text{sn}(\underline{w}, k), k]$	$E_t[\arcsin \{\text{sn}(\underline{w}, k)\}, k]$	$E_e(\underline{w}, k)$

Table 12.2: Conversion formulas for the elliptic integrals of the second kind

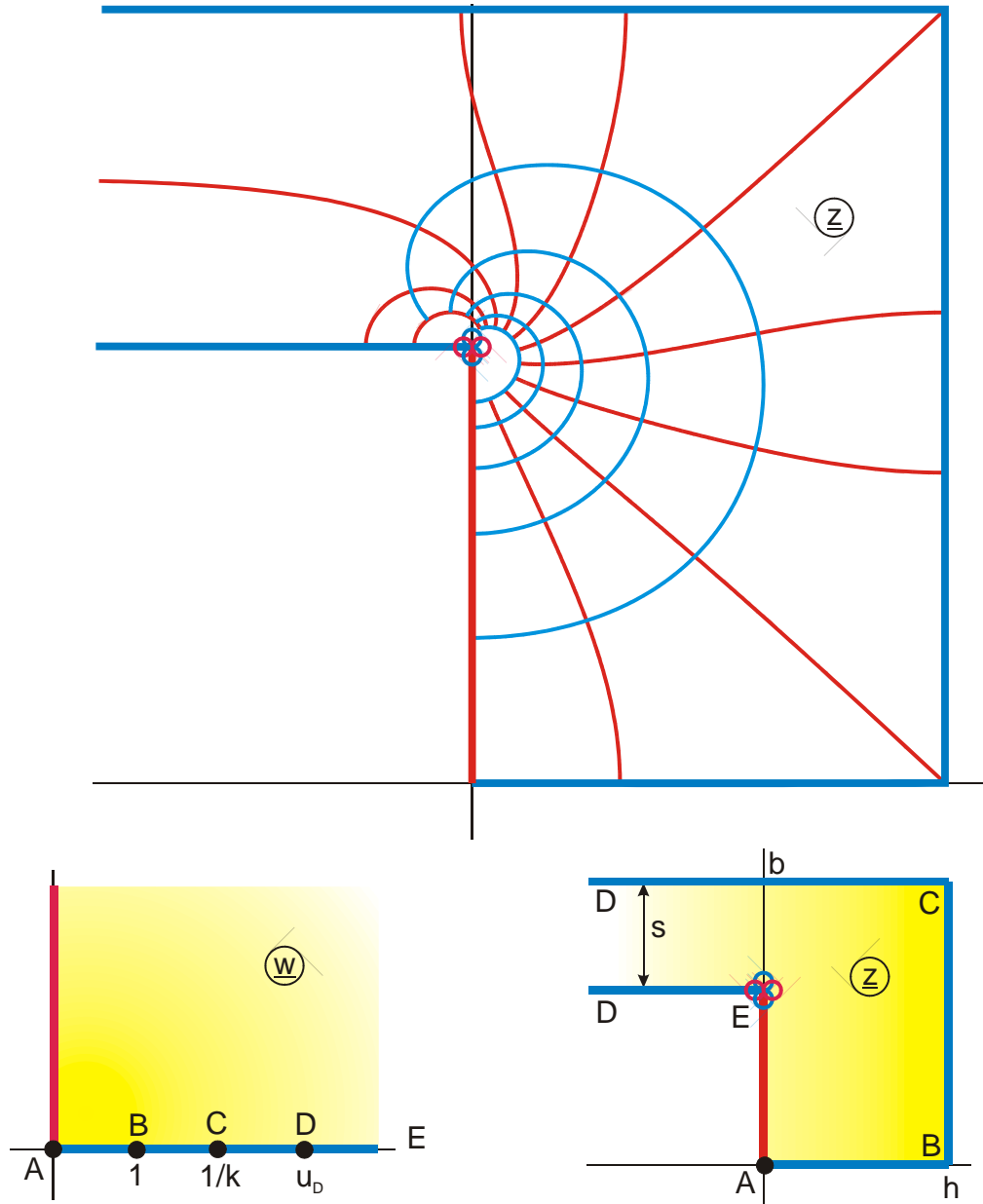


Figure 12.17: The transformation $z = \Pi_a(w, k, n)$ for $0 < n < k^2$, Mapping U 4.2

$$h = K(k) \left[1 + c Z_a \left(\frac{\sqrt{n}}{k}, k \right) \right] = \Pi(k, a) \quad u_D = \frac{1}{\sqrt{n}}$$

$$b = c \left[K'(k) Z_a \left(\frac{\sqrt{n}}{k}, k \right) \right] + K'(k) \quad s = c\pi/2$$

$$\text{with } a = F_a \left(\sqrt{n}/k, k \right) \quad \text{and}$$

$$c = \sqrt{\frac{n}{(1-n)(k^2-n)}}$$

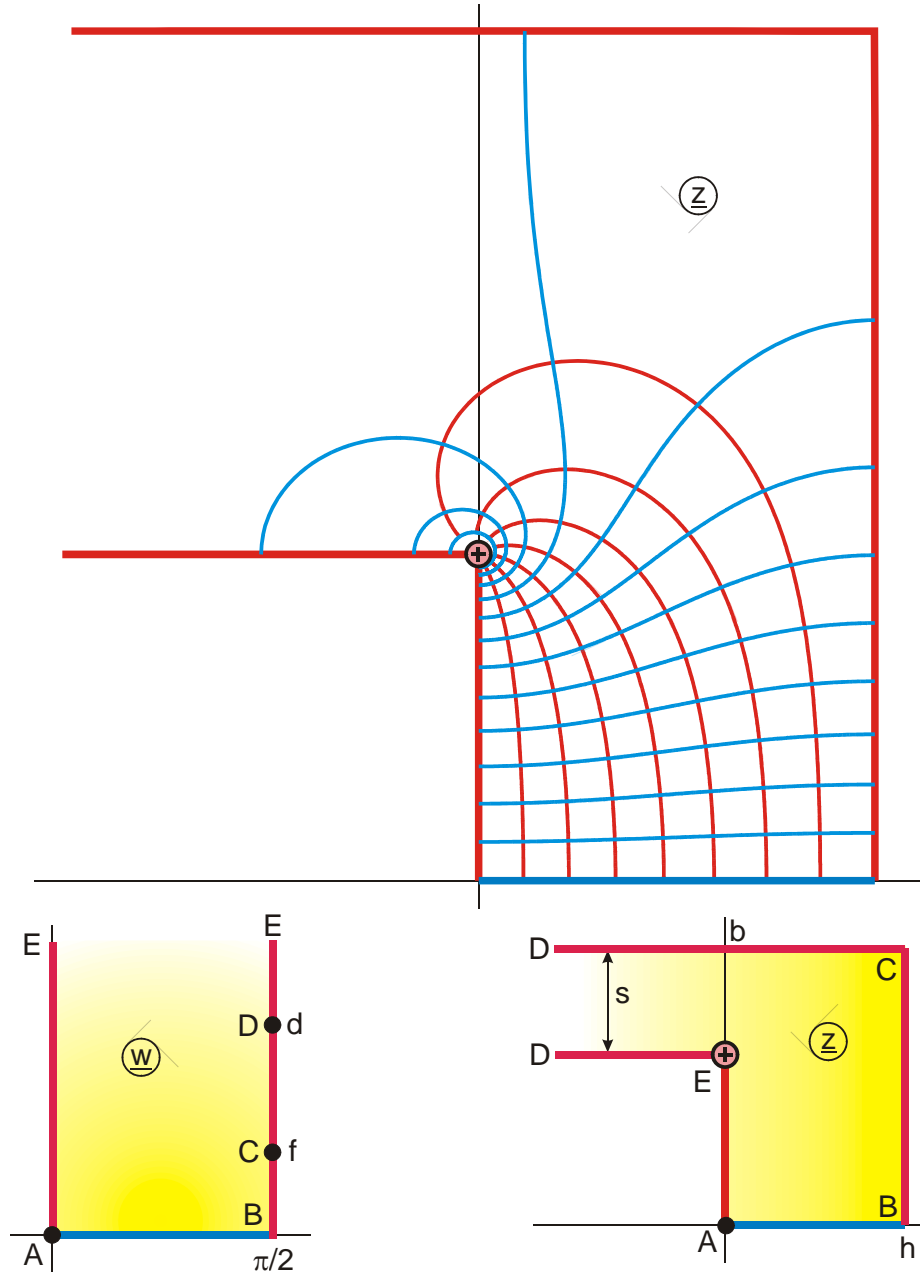


Figure 12.18: The transformation $z = \Pi_t(w, k, n)$ for $0 < n < k^2$, Mapping U 4.1

$$h = K(k) \left[1 + c Z_a \left(\frac{\sqrt{n}}{k}, k \right) \right] = \Pi(k, a)$$

$$b = c \left[K'(k) Z_a \left(\frac{\sqrt{n}}{k}, k \right) \right] + K'(k) \quad s = c\pi/2$$

$$d = \operatorname{arcosh}(1/\sqrt{n}) \quad c = \operatorname{arcosh}(1/k)$$

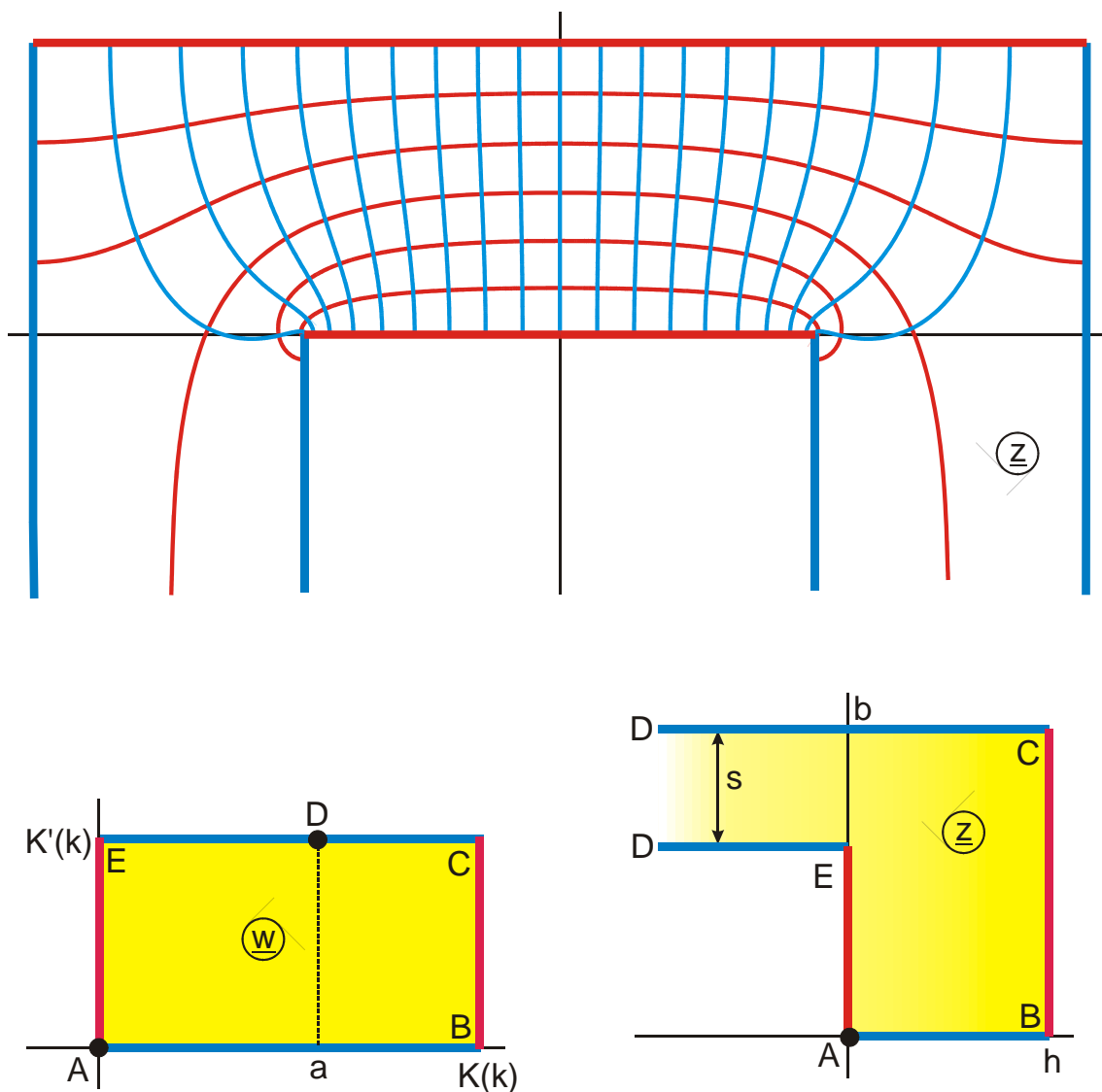


Figure 12.19: The transformation $z = \Pi_e(w, k, a)$ for $0 < a < K(k)$, Mapping U 4.3

$$h = c Z_e(a, k) K(k) + K(k) = \Pi(k, a)$$

$$b = c \left[K'(k) Z_e(a, k) + \frac{\pi a}{2K(k)} \right] + K'(k) \quad s = c\pi/2$$

$$c = \frac{sn(a, k)}{cn(a, k) dn(a, k)}$$

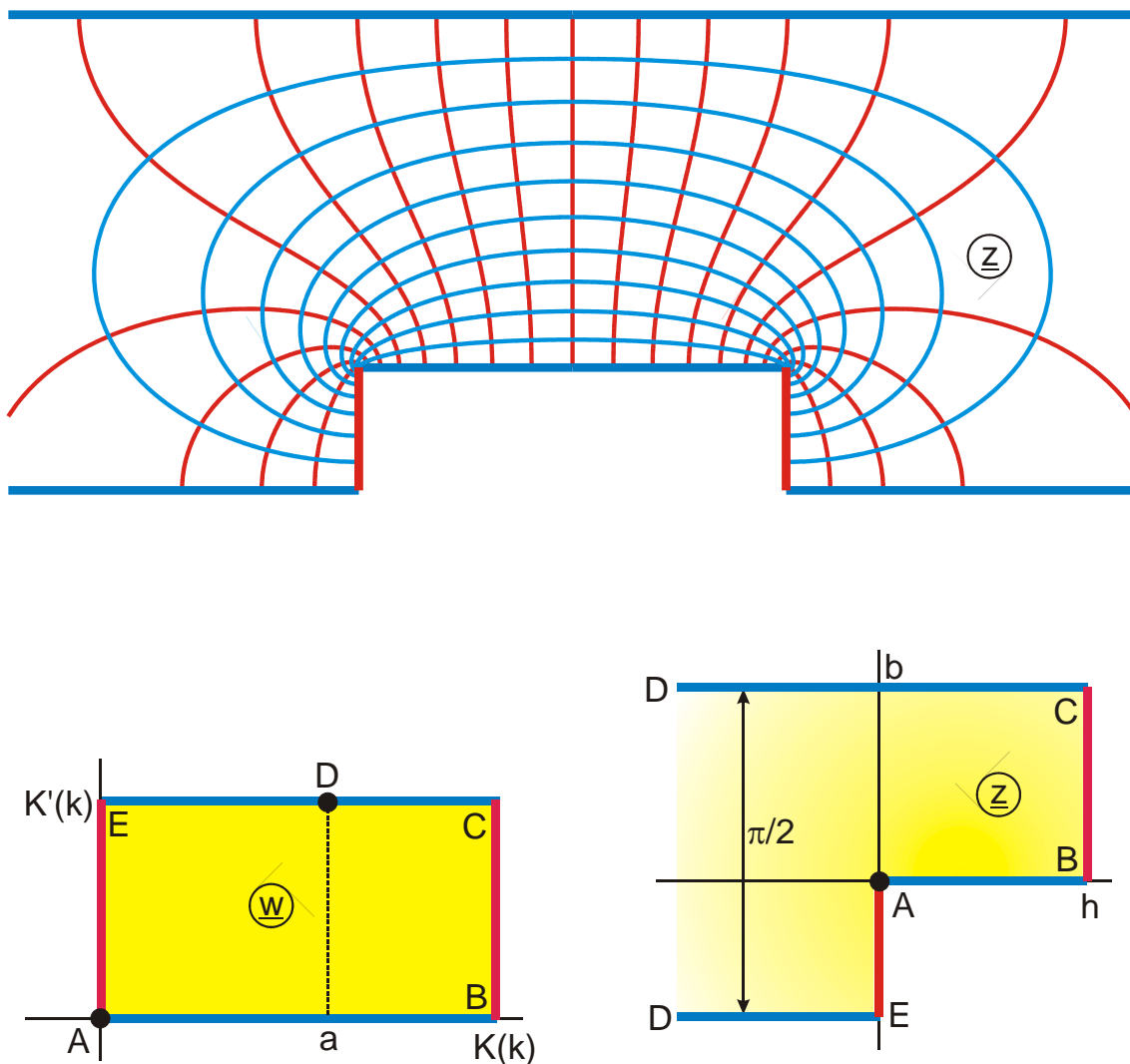


Figure 12.20: The transformation $z = \Pi_j(w, k, a)$ for $0 < a < K(k)$, Mapping U 3

$$h = Z_e(a, k) K(k)$$

$$b = K'(k) Z_e(a, k) + \frac{\pi a}{2K(k)}$$

Special values:

$$\Pi_t(\underline{w}, 0, 0) = \underline{w} \quad (105)$$

$$F_t(\underline{w}, 0) = \ln \left(\frac{1 + \sin \underline{w}}{\cos \underline{w}} \right) \quad (106)$$

$$\Pi_t(\underline{w}, 1, n) = \frac{1}{n-1} \left[\ln \left(\frac{1 + \sin \underline{w}}{\cos \underline{w}} \right) - \frac{\sqrt{n}}{2} \ln \left(\frac{1 + \sqrt{n} \sin \underline{w}}{1 - \sqrt{n} \sin \underline{w}} \right) \right] \quad (107)$$

$$\text{If } \underline{w} = \arcsin \frac{1}{\sqrt{1+k'}} \quad \text{then} \quad F_t(\underline{w}, k) = \frac{K(k)}{2} \quad (108)$$

$$\text{and} \quad E_t(\underline{w}, k) = \frac{E(k) + 1 - k'}{2} \quad (109)$$

$$\Pi_t(1, n) = \infty \quad (110)$$

$$\Pi_t(\underline{w}, k, 0) = F_t(\underline{w}, k) \quad (111)$$

$$\Pi_t(\underline{w}, k, 1) = F_t(\underline{w}, k) - \frac{E_t(\underline{w}, k)}{k'^2} + \left(\frac{\sqrt{1 - k^2 \sin^2 \underline{w}}}{k'^2} \right) \tan \underline{w} \quad (112)$$

$$\Pi_t(\underline{w}, k, k^2) = \frac{1}{k'^2} \left[E_t(\underline{w}, k) - \frac{k^2 \sin \underline{w} \cos \underline{w}}{\sqrt{1 - k^2 \sin^2 \underline{w}}} \right] \quad (113)$$

$$\text{If } k = \sqrt{2} - 1 \quad \text{then} \quad K'(k) = \sqrt{2}K(k) \quad (114)$$

$$\text{If } k = 3 - 2\sqrt{2} \quad \text{then} \quad K'(k) = 2K(k) \quad (115)$$

$$\text{If } k = \frac{\sqrt{3}-1}{2\sqrt{2}} \quad \text{then} \quad K'(k) = \sqrt{3}K(k) \quad (116)$$

$$\text{and} \quad E(k) = \frac{\pi}{4\sqrt{3}K(k)} + \frac{K(k)}{2} \left(1 + \frac{1}{\sqrt{3}} \right) \quad (117)$$

$$\text{and} \quad E'(k) = \frac{\pi\sqrt{3}}{4K'(k)} + \frac{K'(k)}{2} \left(1 - \frac{1}{\sqrt{3}} \right) \quad (118)$$

13. Theta Functions

Theta functions are solutions of the one-dimensional heat transfer equation in physics:

$$a \frac{\partial^2 \vartheta(z, t)}{\partial z^2} = \frac{\partial \vartheta(z, t)}{\partial t} \quad (1)$$

If in a very large isotropic, solid body with the specific thermal conductivity a that extends from $z = 0$ to $z = \pi$, at the time $t = 0$ in the center at $z = \pi/2$ a high temperature ϑ is abruptly generated (Dirac delta function δ)

$$\vartheta(z, t = 0) = \pi \delta(z - \pi/2), \quad (2)$$

then the heat transfer equation yields as the solution under the assumption that the boundaries at $z = 0$ and at $z = \pi$ have constant temperature $\vartheta = 0$, the series

$$\vartheta_1(z, q) = 2q^{1/4} \sum_{n=0}^{\infty} (-1)^n q^{n(n+1)} \sin[(2n+1)z] \quad (3)$$

with

$$q = e^{-4at}. \quad (4)$$

The series is found elementarily by first solving the differential equation via product solution

$$\vartheta(z, t) = \sum_{n=1}^{\infty} b_n \exp(-n^2 a t) \sin(nz) \quad (5)$$

and afterwards by calculating the Fourier coefficients b_n .

If the boundaries of the solid body are isolated, hence $\partial \vartheta / \partial z = 0$ at $z = 0$ and at $z = \pi$, then this yields the series

$$\vartheta_4(z, q) = 1 + 2 \sum_{n=1}^{\infty} (-1)^n q^{n^2} \cos(2nz) . \quad (6)$$

Figure 13.1a illustrates at equidistant times $m \cdot \Delta t$ the distribution of the temperature $\vartheta_1(z)$ in the infinite solid body. Figure 13.1b shows the temperature distribution $\vartheta_4(z)$. The above example from physics was chosen, in order to demonstrate that it is possible to visualize the course of the Theta functions with real argument. Furthermore it results from this that the name of the Theta functions originates from the temperature ϑ .

Two more Theta functions are defined by the series

$$\vartheta_2(z, q) = 2q^{1/4} \sum_{n=0}^{\infty} q^{n(n+1)} \cos[(2n+1)z] \quad (7)$$

and

$$\vartheta_3(z, q) = 1 + 2 \sum_{n=1}^{\infty} q^{n^2} \cos(2nz) \quad (8)$$

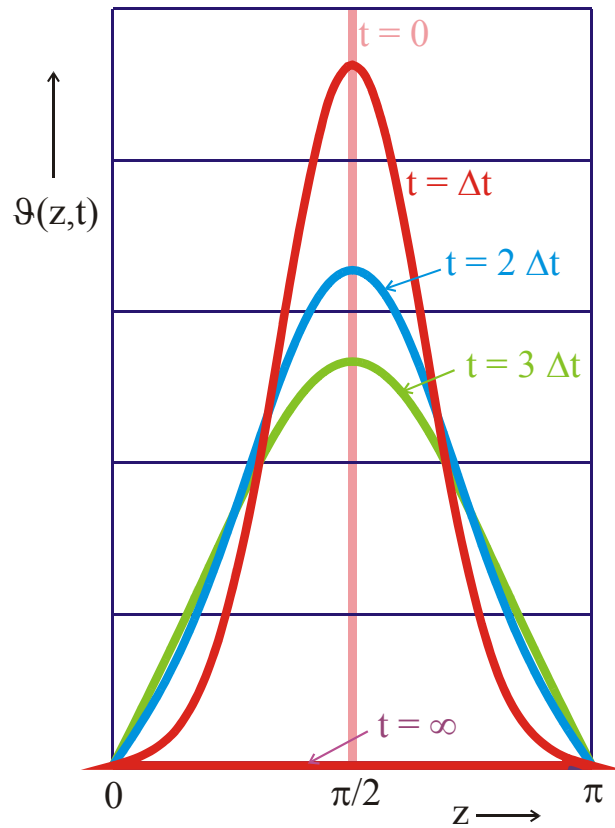
The Theta functions are defined for arbitrary complex numbers z and q with $|q| < 1$. With the restriction to real numbers q , with

$$q = e^{-\pi\tau} \quad (9)$$

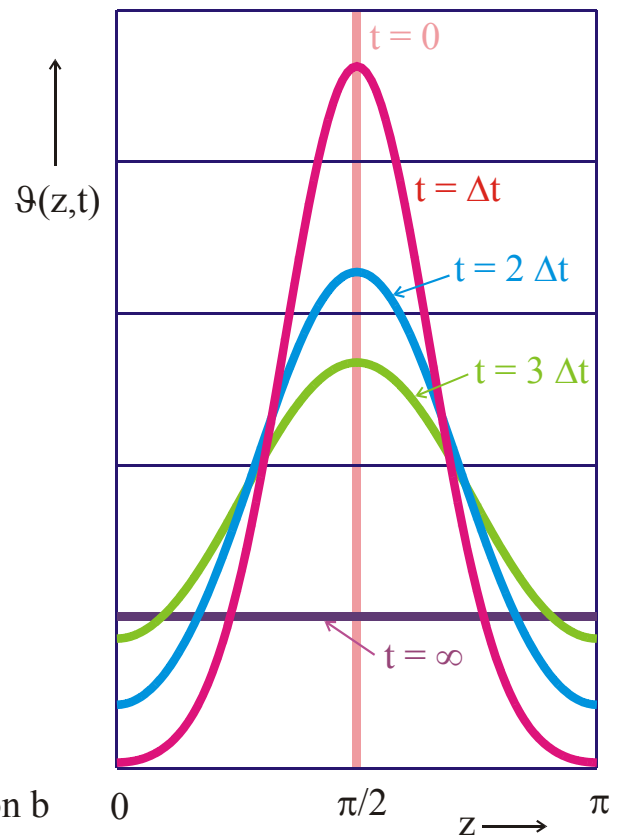
and

$$\tau = K'(k) / K(k) \quad (10)$$

the relationship with the elliptic functions and the elliptic integrals is found. The numerical values of these functions $\vartheta(z, \tau)$ are computed with the subroutines Theta 1 through Theta 4.



a) Temperature distribution a



b) Temperature distribution b

Figure 13.1: Calculation of the temperature distribution $\Theta(z,t)$ with Theta functions

Figures 13.2 through 13.5 show the conformal mappings that belong to the Theta functions. The trigonometric function in the element of the series causes that the function is, with respect to the variable z , periodic with periods $n\pi$ and $n \cdot 2\pi$ respectively.

$\vartheta_1(\underline{z})$ is an odd Function with the period 2π

$\vartheta_2(\underline{z})$ is an even Function with the period 2π

$\vartheta_3(\underline{z})$ is an even Function with the period π

$\vartheta_4(\underline{z})$ is an even Function with the period π

Because of the exponential function the trace of the boundary within a quarter period resembles a logarithmic spiral (Figure 13.6). The functions are quasi periodic with $\pi\tau$ and $\pi + \pi\tau$, with respect to the variable τ .

$$\vartheta_1(\underline{z} + \pi\tau) = \frac{1}{q} \exp((-j2\underline{z}) \vartheta_1(\underline{z})) \quad (11)$$

If the mapped domain is extended beyond the given region, it is seen that the transformation equation becomes infinitely ambiguous, the function has an infinite number of branches; the logarithmic spiral can be continued in the direction of increasing radii.

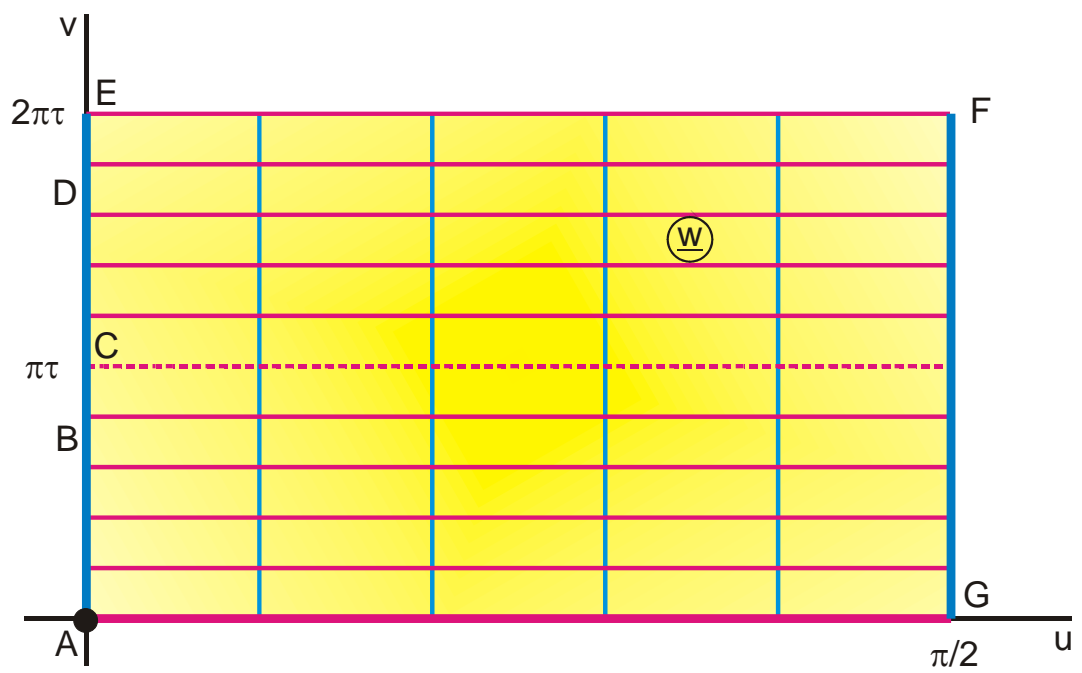
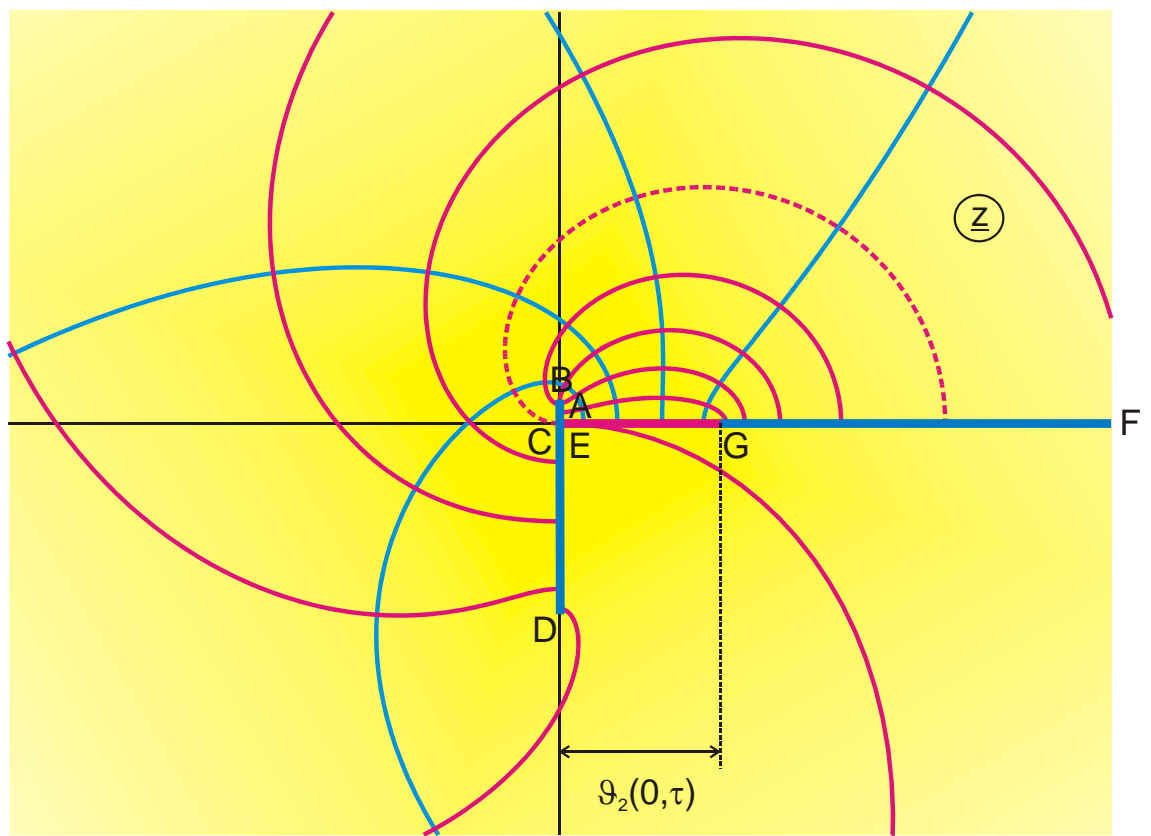
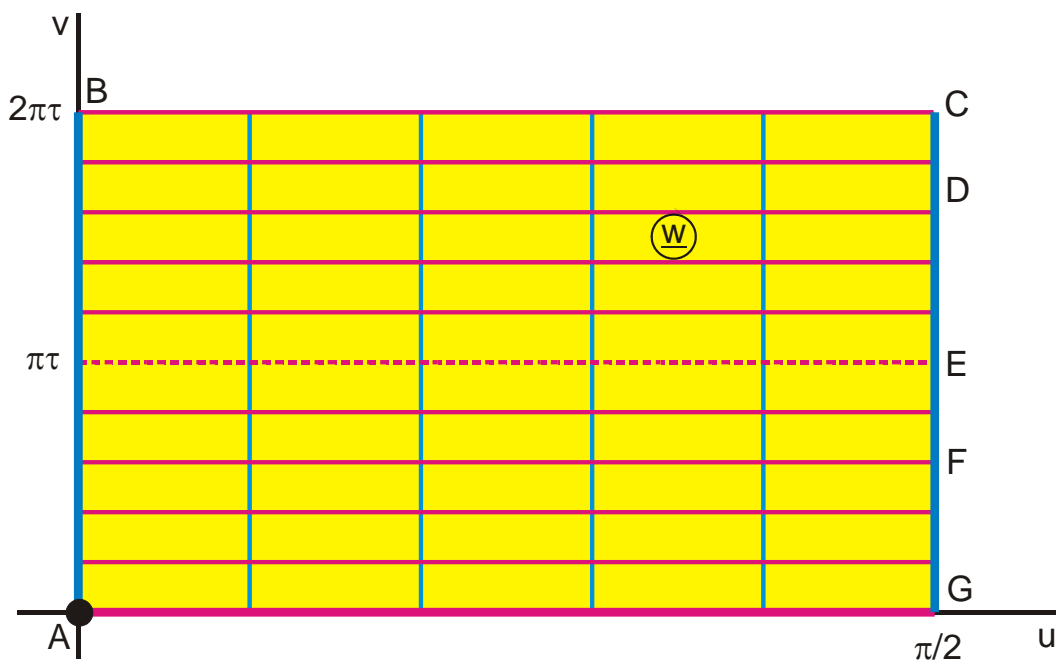


Figure 13.2: The transformation $\underline{z} = \vartheta_1(\underline{z}, \tau)$, with $\tau = 0,278$



Vs. 1.1

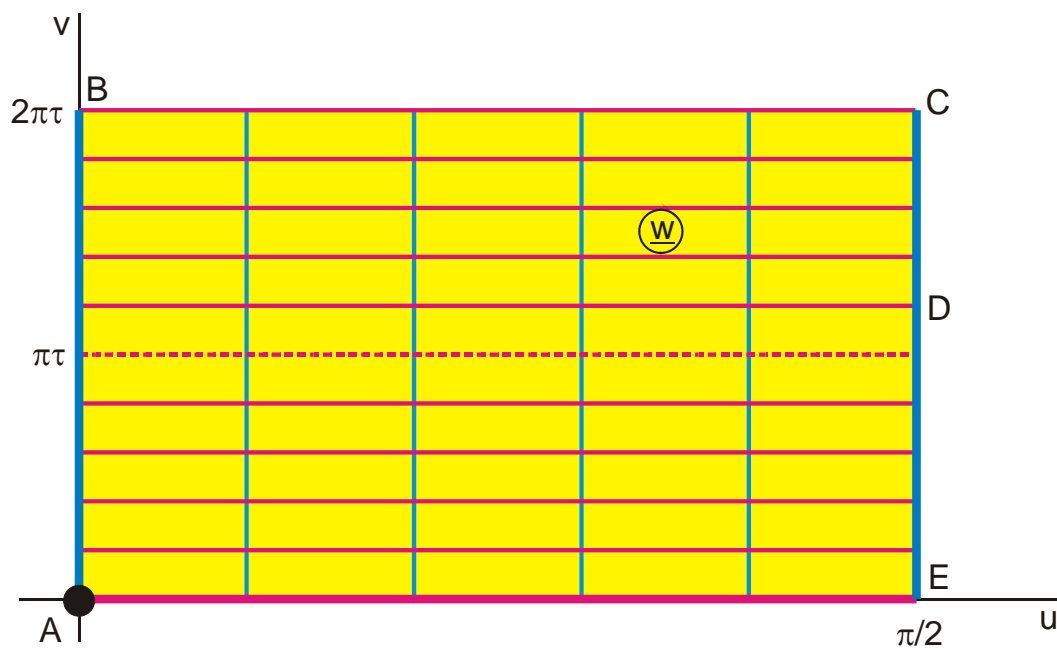
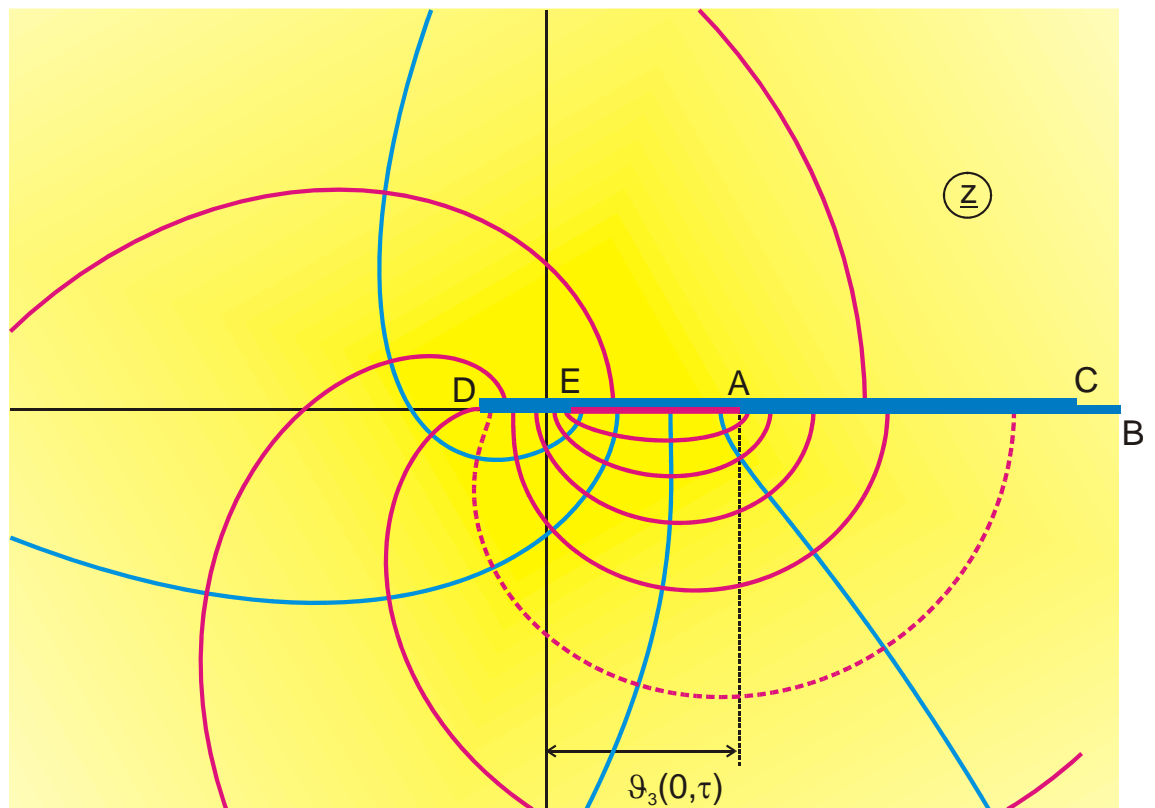


Figure 13.4: The transformation $\underline{z} = \vartheta_3(\underline{z}, \tau)$, with $\tau = 0,278$

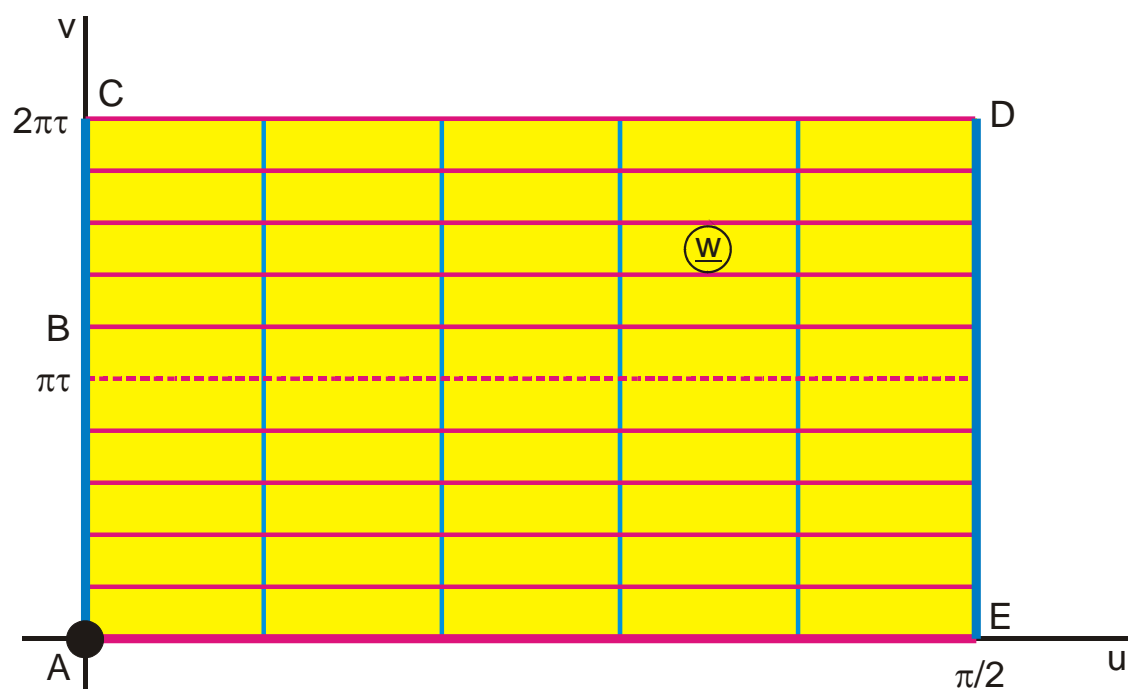
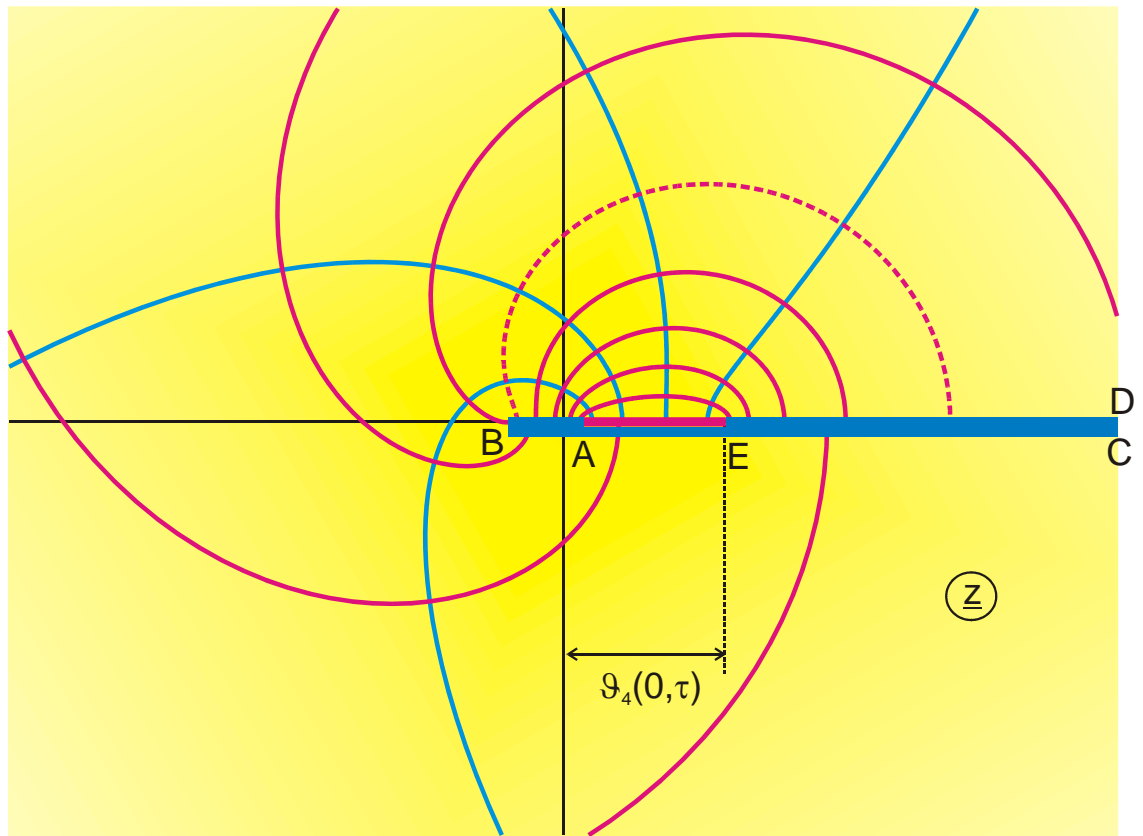


Figure 13.5: The transformation $\underline{z} = \vartheta_4(\underline{z}, \tau)$, with $\tau = 0,278$

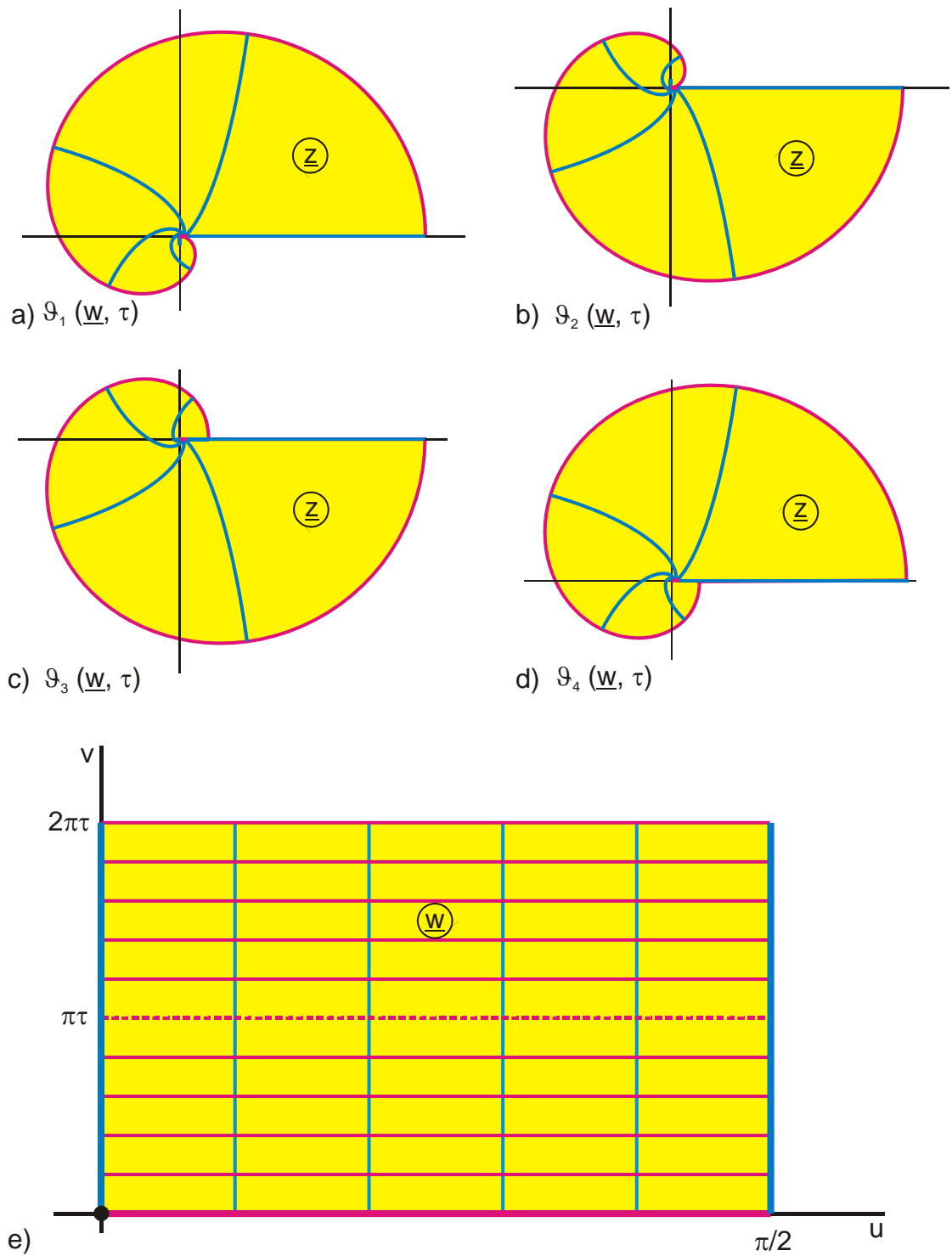


Figure 13.6: Complete mapping region of the four Theta functions

If the trigonometric functions are expressed by exponential functions and if $q = \exp\left(-\frac{\pi}{\tau}\right)$, it is found that:

$$\vartheta_1(\underline{z}, \tau) = -j \exp(-\pi \tau / 4) \sum_{n=-\infty}^{\infty} \exp(-\pi \tau n(n+1) + j(2n+1)\underline{z} + jn\pi) \quad (12)$$

$$\vartheta_2(\underline{z}, \tau) = \exp(-\pi \tau / 4) \sum_{n=-\infty}^{\infty} \exp(-\pi \tau n(n+1) + j(2n+1)\underline{z}) \quad (13)$$

$$\vartheta_3(\underline{z}, \tau) = \sum_{n=-\infty}^{\infty} \exp(-\pi \tau n^2 + j2n\underline{z}) \quad (14)$$

$$\vartheta_4(\underline{z}, \tau) = \sum_{n=-\infty}^{\infty} \exp(-\pi \tau n^2 + j2n\underline{z} + jn\pi) \quad (15)$$

The conversion from one Theta function to another is done by:

$$\vartheta_1(\underline{z}) = -\vartheta_2(\underline{z} + \pi / 2) \quad (16)$$

$$\vartheta_2(\underline{z}) = \vartheta_1(\underline{z} + \pi / 2) \quad (17)$$

$$\vartheta_3(\underline{z}) = \vartheta_4(\underline{z} + \pi / 2) \quad (18)$$

$$\vartheta_4(\underline{z}) = \vartheta_3(\underline{z} + \pi / 2) \quad (19)$$

The values of the functions for $z = 0$ are of particular importance for many applications:

$$\vartheta_1(z = 0, \tau) = \vartheta_1(\tau) = 0 \quad (20)$$

$$\vartheta_2(z=0, \tau) = \vartheta_2(\tau) = \sqrt{2kK(k) / \pi} \quad (21)$$

$$\vartheta_3(z=0, \tau) = \vartheta_3(\tau) = \sqrt{2K(k) / \pi} \quad (22)$$

$$\vartheta_4(z=0, \tau) = \vartheta_4(\tau) = \sqrt{2k'K(k) / \pi} \quad (23)$$

With the Theta zero-values it is possible to calculate the modulus k of an elliptic function for a given aspect ratio τ :

$$k = \left[\frac{\vartheta_2(0, \tau)}{\vartheta_3(0, \tau)} \right]^2 \quad (24)$$

$$K(k) = \frac{\pi}{2} \vartheta_3^2(0, \tau) \quad (25)$$

All elliptic functions can be expressed by Theta functions:

$$\text{sn}(\underline{z}, k) = \frac{\vartheta_3(\tau) \vartheta_1(\underline{z}, \tau)}{\vartheta_2(\tau) \vartheta_4(\underline{z}, \tau)} \quad (26)$$

$$\text{cn}(\underline{z}, k) = \frac{\vartheta_4(\tau) \vartheta_2(\underline{z}, \tau)}{\vartheta_2(\tau) \vartheta_4(\underline{z}, \tau)} \quad (27)$$

$$\text{dn}(\underline{z}, k) = \frac{\vartheta_4(\tau) \vartheta_3(\underline{z}, \tau)}{\vartheta_3(\tau) \vartheta_4(\underline{z}, \tau)} \quad (28)$$

$$\frac{\text{cn}(\underline{z}, k) \text{dn}(\underline{z}, k)}{\text{sn}(\underline{z}, k)} = k' \frac{\vartheta_2(\underline{z}, \tau) \vartheta_3(\underline{z}, \tau)}{\vartheta_1(\underline{z}, \tau) \vartheta_4(\underline{z}, \tau)} \quad (29)$$

$$\frac{\text{sn}(\underline{z}, k) \text{cn}(\underline{z}, k)}{\text{dn}(\underline{z}, k)} = \frac{1}{k} \frac{\vartheta_1(\underline{z}, \tau) \vartheta_2(\underline{z}, \tau)}{\vartheta_3(\underline{z}, \tau) \vartheta_4(\underline{z}, \tau)} \quad (30)$$

$$\frac{\operatorname{sn}(\underline{z}, k) \operatorname{dn}(\underline{z}, k)}{\operatorname{cn}(\underline{z}, k)} = \frac{\vartheta_1(\underline{z}, \tau) \vartheta_3(\underline{z}, \tau)}{\vartheta_2(\underline{z}, \tau) \vartheta_4(\underline{z}, \tau)} \quad (31)$$

Relation with the elliptic integrals:

$$\frac{d}{d\underline{z}} \ln \vartheta_1(\underline{z}, \tau) = Z_e(\underline{z}, k) + \frac{\operatorname{cn}(\underline{z}, k) \operatorname{dn}(\underline{z}, k)}{\operatorname{sn}(\underline{z}, k)} \quad (32)$$

$$\frac{d}{d\underline{z}} \ln \vartheta_2(\underline{z}, \tau) = Z_e(\underline{z}, k) - \frac{\operatorname{sn}(\underline{z}, k) \operatorname{dn}(\underline{z}, k)}{\operatorname{cn}(\underline{z}, k)} \quad (33)$$

$$\frac{d}{d\underline{z}} \ln \vartheta_3(\underline{z}, \tau) = Z_e(\underline{z}, k) - k^2 \frac{\operatorname{sn}(\underline{z}, k) \operatorname{cn}(\underline{z}, k)}{\operatorname{dn}(\underline{z}, k)} \quad (34)$$

$$\frac{d}{d\underline{z}} \ln \vartheta_4(\underline{z}, \tau) = Z_e(\underline{z}, k) \quad (35)$$

$$\Pi_j(\underline{z}, k, a) = \frac{1}{2} \ln \frac{\vartheta_4\left(\frac{\pi}{2K(k)}(\underline{z} - a), \tau\right)}{\vartheta_4\left(\frac{\pi}{2K(k)}(\underline{z} + a), \tau\right)} + \underline{z} Z_e(a, k) \quad (36)$$

Because of the term $\exp(\dots n^2)$ in the series representation of the Theta functions these series converge extremely well. This property can be utilized to derive approximation formulas with elementary functions which are of extraordinary accuracy [8]. If only the first element of the series in Eq. (8) is taken, then from Eq. (10) and (22) follows:

$$\frac{K(k)}{K'(k)} \approx \frac{1}{\pi} \ln \frac{2 + 2\sqrt{k}}{1 - \sqrt{k}} \quad \text{for} \quad k \geq \frac{1}{\sqrt{2}} \quad (37)$$

$$\frac{K(k)}{K'(k)} \approx \frac{\pi}{\ln \frac{2 + 2\sqrt{k'}}{1 - \sqrt{k'}}} \quad \text{for} \quad k \leq \frac{1}{\sqrt{2}} \quad (38)$$

with the inversion

$$k \approx \left(\frac{\exp\left(\frac{\pi K(k)}{K'(k)}\right) - 2}{\exp\left(\frac{\pi K(k)}{K'(k)}\right) + 2} \right)^2 \quad \text{for } K(k) \geq K'(k) \quad (39)$$

$$k' \approx \left(\frac{\exp\left(\frac{\pi K'(k)}{K(k)}\right) - 2}{\exp\left(\frac{\pi K'(k)}{K(k)}\right) + 2} \right)^2 \quad \text{for } K(k) \leq K'(k) \quad (40)$$

and

$$k \approx \frac{4 \sqrt{\exp\left(\frac{\pi K'(k)}{K(k)}\right) \left(\exp\left(\frac{2\pi K'(k)}{K(k)}\right) + 4 \right)}}{\left(\exp\left(\frac{\pi K'(k)}{K(k)}\right) + 2 \right)^2} \quad (41)$$

$$K(k) \approx \frac{2}{(1 + \sqrt{k})^2} \ln \frac{2 + 2\sqrt{k}}{1 - \sqrt{k}} \quad \text{for } k \geq \frac{1}{\sqrt{2}} \quad (42)$$

$$K'(k) \approx \frac{2\pi}{(1 + \sqrt{k})^2} \quad \text{for } k \geq \frac{1}{\sqrt{2}} \quad (43)$$

$$K(k) \approx \frac{2\pi}{(1 + \sqrt{k'})^2} \quad \text{for } k \leq \frac{1}{\sqrt{2}} \quad (44)$$

$$K'(k) \approx \frac{2}{(1 + \sqrt{k'})^2} \ln \frac{2 + 2\sqrt{k'}}{1 - \sqrt{k'}} \quad \text{for } k \leq \frac{1}{\sqrt{2}} \quad (45)$$

The relative error of the approximate values determined with these formulas is for $k > 10^{-5}$ less than 10^{-5} .

Theta functions can be expressed in terms of an infinite product:

$$\vartheta_1(\underline{z}, \tau) = 2 e^{-\pi\tau/4} \sin \underline{z} \prod_{n=1}^{\infty} \{1 - e^{-2n\pi\tau}\} \{1 - 2 e^{-2n\pi\tau} \cos(2\underline{z}) + e^{-4n\pi\tau}\} \quad (46)$$

$$\vartheta_2(\underline{z}, \tau) = 2 e^{-\pi\tau/4} \cos \underline{z} \prod_{n=1}^{\infty} \{1 - e^{-2n\pi\tau}\} \{1 + 2 e^{-2n\pi\tau} \cos(2\underline{z}) + e^{-4n\pi\tau}\} \quad (47)$$

$$\vartheta_3(\underline{z}, \tau) = \prod_{n=1}^{\infty} \{1 - e^{-2n\pi\tau}\} \{1 + 2 e^{-(2n-1)\pi\tau} \cos(2\underline{z}) + e^{-2(2n-1)\pi\tau}\} \quad (48)$$

$$\vartheta_4(\underline{z}, \tau) = \prod_{n=1}^{\infty} \{1 - e^{-2n\pi\tau}\} \{1 - 2 e^{-(2n-1)\pi\tau} \cos(2\underline{z}) + e^{-2(2n-1)\pi\tau}\} \quad (49)$$

This notation can be physically interpreted: The logarithm of the Theta functions is the complex potential of a double-periodic configuration of equal line charges according to Figure 13.7a through 13.7d. In each point \underline{z} the resulting complex potential \underline{w} is found as the sum of the potentials generated by each single line charge (see Table 3.1)

$$\underline{w} = C \sum_n \ell n \underline{z}_n . \quad (50)$$

This can be converted into an infinite product:

$$\underline{w} = C \ln \prod_n \underline{z}_n \quad (51)$$

With this example it is evident, why the elements of the series and the product respectively are converging so very well: The potential in a point \underline{z} is essentially due to the line charges in the immediate vicinity. Those fractions of the potential, which are caused by the remaining line charges, decrease rapidly with increasing distance of this charge. Likewise it is evident, why the function increases with increasing imaginary part. Because the plane $y = 0$ is a red field line, all field lines in the upper half plane run in the direction $+j\infty$ (Figure 13.8). With each step with the step size τ in the y direction the number of field lines increases by those emanating from the newly added line charge. Thus the density of the field lines is growing exponentially with increasing y .

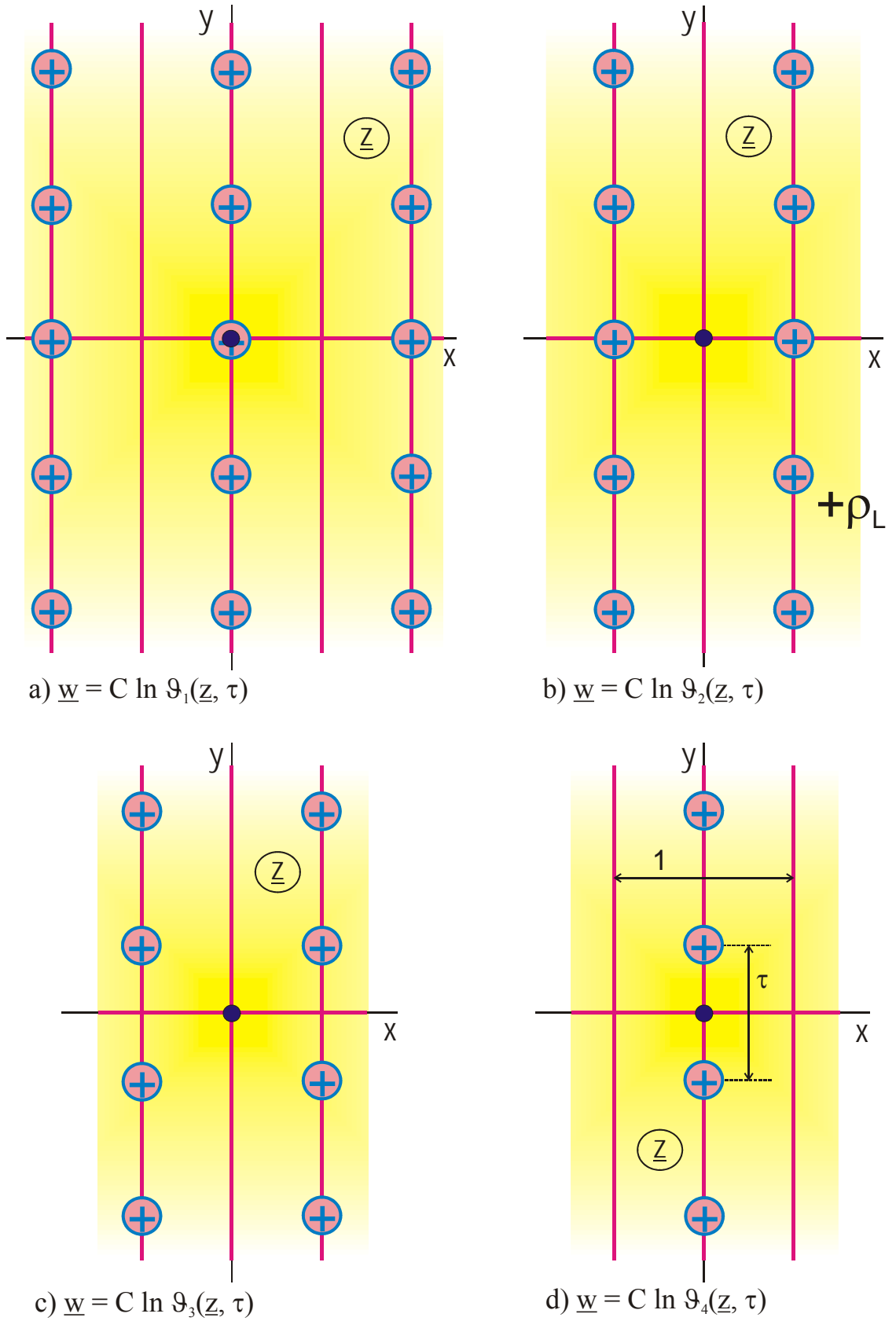


Figure 13.7: Allocation of the positive line charges in the z -plane for the transformation $w = C \ln \vartheta(z, \tau)$

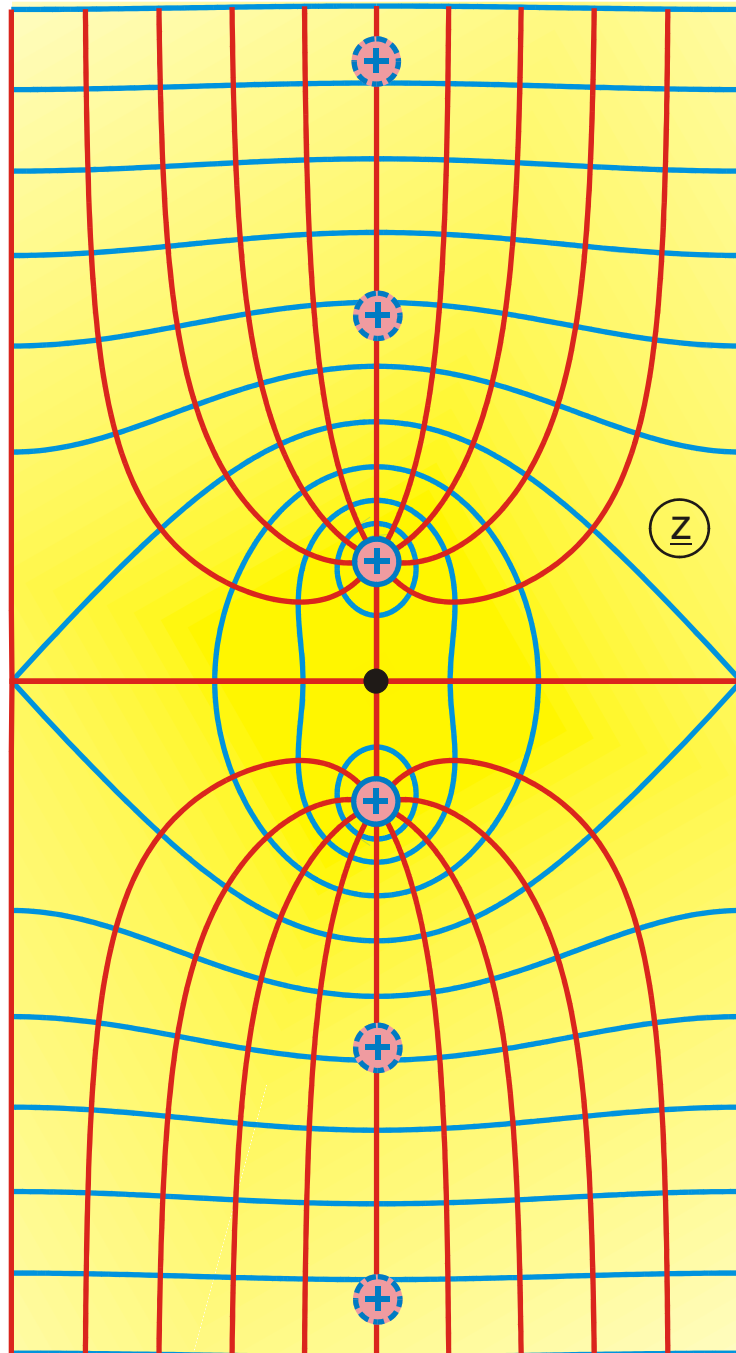


Figure 13.8: Field map of those two line charges, which are closest to the origin in Figure 13.7 d). The field of the remaining line charges (shown dotted) is omitted due to clarity. Because of the periodicity of the field in the x direction, all field lines stay within the vertical parallel strip of width 1.

14. Applications

Exercise 1: Electric Field Strength

The two dimensional electrostatic field of an inside corner with an opening angle of 60° is calculated with the mapping function $\underline{z} = \sqrt[3]{\underline{w}}$. The bent conducting sheet with the potential $V = \text{const}$ is transformed into the real axis of the \underline{w} -plane.

- Into which points of the z -plane are the points $u_1 = 0,5$, $v_1 = 0$ and $u_2 = 1$, $v_2 = 0$ mapped, when point $u = 1$, $v = 0$ is mapped into $x = 1$, $y = 0$?
- Sketch the field lines ($u=\text{const}$) and the lines of constant potential ($v=\text{const}$) given in the \underline{w} -plane in the \underline{z} -plane.
- Calculate the distribution of the electric field strength E as a function of x and y .

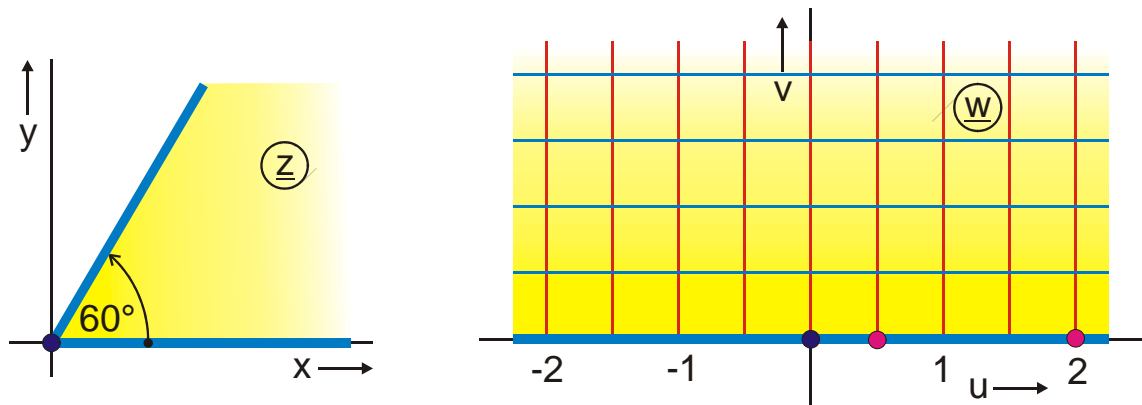


Figure 14.1: Exercise 1

Solution:

- Insertion of the coordinates into the mapping function $x + jy = \sqrt[3]{u + jv}$ results in:

$$\begin{aligned} x_1 &= 0,794, & y_1 &= 0 \\ x_2 &= 1,26, & y_2 &= 0 \end{aligned}$$

b)

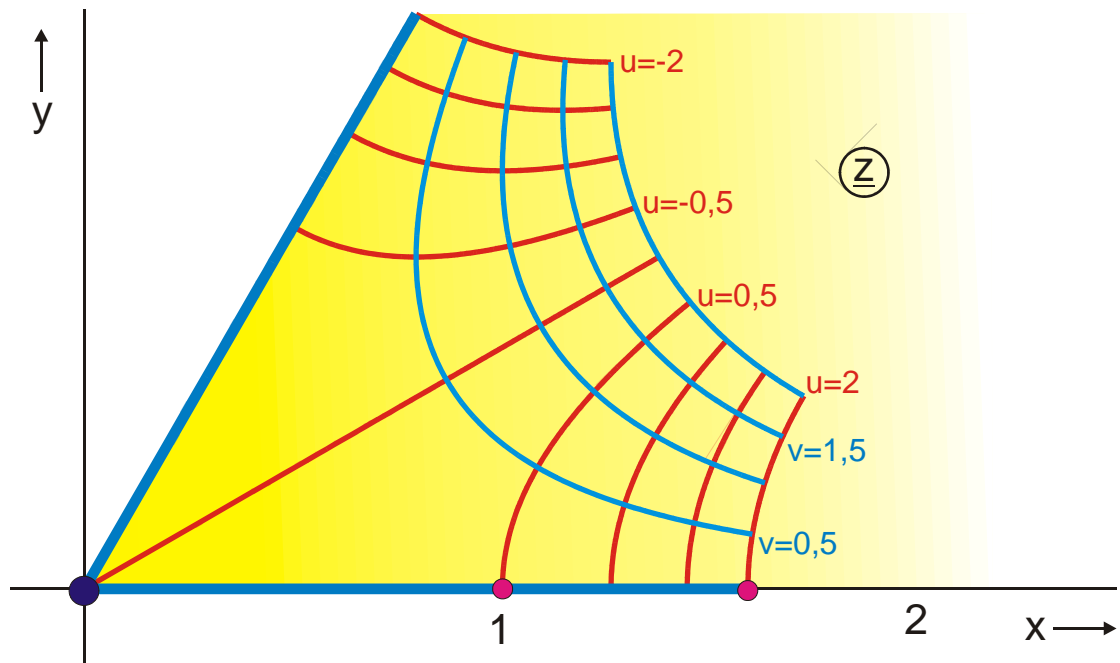


Figure 14.2: Solution for Exercise 1b

c) The lines $v = \text{const}$ are the lines of constant potential. Then it is true that:

$$\vec{E} = -E_0 \text{grad } v$$

$$\vec{E}(x, y) = -E_0 \left(\frac{\partial v}{\partial x} \vec{e}_x + \frac{\partial v}{\partial y} \vec{e}_y \right)$$

$$\text{from } u + jv = (x + jy)^3 \text{ follows } v = 3x^2y^2 - y^3$$

$$\vec{E}(x, y) = -E_0 \left(6xy \vec{e}_x + [3x^2 - 3y^2] \vec{e}_y \right)$$

$$E(x, y) = \sqrt{E_x^2 + E_y^2} = 3E_0(x^2 + y^2)$$

Exercise 2: Ohmic Resistance, Potential Distribution

A sector of an annulus ($r_i = 1 \text{ cm}$, $r_a = 10 \text{ cm}$) is cut out from a conductive sheet (conductivity $\sigma = 10^4 \text{ S/m}$) with thickness $d = 1 \text{ mm}$. The sector has electrical contacts at both ends, at $\varphi = 0^\circ$ and at $\varphi = 45^\circ$. Calculate the Ohmic resistance of this configuration by conformal mapping with the function $\underline{w} = \underline{C}_1 \ln(\underline{z}/\underline{C}_2)$.

- Choose two points of the boundary and determine the constants \underline{C}_1 and \underline{C}_2 .
- Calculate the Ohmic resistance of this configuration in the \underline{w} -plane with the equation $R = \frac{1}{d\sigma} \cdot \frac{\text{Length in the } w\text{-plane}}{\text{Width in the } w\text{-plane}}$.
- Sketch the field lines ($u=\text{const}$) and the lines of constant potential ($v=\text{const}$) in the \underline{z} -plane.
- Calculate the distribution of the electric potentials $U(\underline{w})$ and $U(\underline{z})$.
- For which value of r_i resp. r_a is the Ohmic resistance one half of the value calculated in b)?

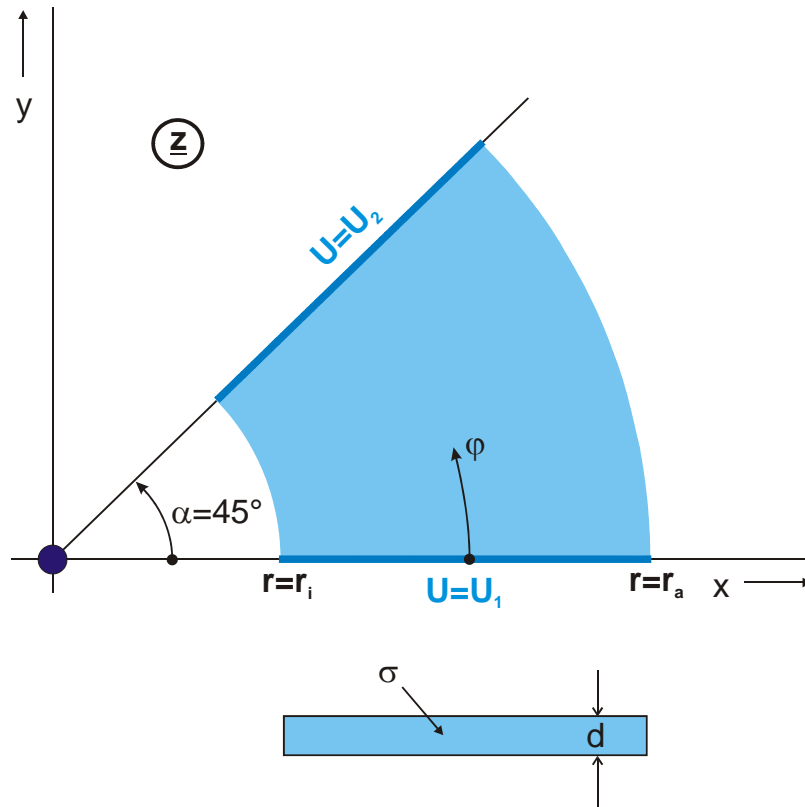


Figure 14.3: Exercise 2

Solution:

- Define the vertices in the \underline{z} -plane and the sense of circulation.
- The sector of the annulus in the \underline{z} -plane is mapped onto a rectangle in the \underline{w} -plane. Location and size of this rectangle in the \underline{w} -plane can be freely chosen. 2 points and the sense of circulation are determined:

$$A(\underline{w}) = 0 \quad \text{und} \quad D(\underline{w}) = \lambda$$

With this the constants can be calculated:

$$\text{Point A:} \quad 0 = \underline{C}_1 \ln(r_i / \underline{C}_2) \quad \Rightarrow \quad \underline{C}_2 = r_i$$

$$\text{Point D:} \quad \lambda = \underline{C}_1 \ln(r_i e^{j\alpha} / r_i) \quad \Rightarrow \quad \underline{C}_1 = \lambda / (j\alpha)$$

In order to get a simple mapping function the freely chosen constant λ is changed to $\lambda = \alpha$. Insertion into the mapping function results in:

$$\underline{w} = j \ln(r_i / \underline{z})$$

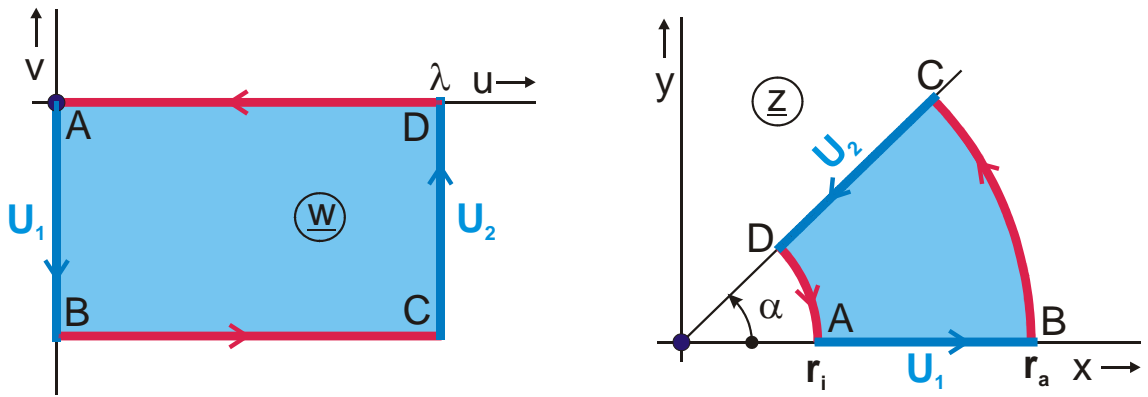


Figure 14.4: Exercise 2, solution a, b

Inserting the points $B(z) = r_a$ and $C(z) = r_a e^{j\alpha}$ reveals that the rectangle has the length α and the width $\ln(r_a / r_i)$ in the \underline{w} -plane. Therefore the Ohmic resistance R is:

$$R = \frac{1}{\sigma d} \cdot \frac{\alpha}{\ln(r_a / r_i)}$$

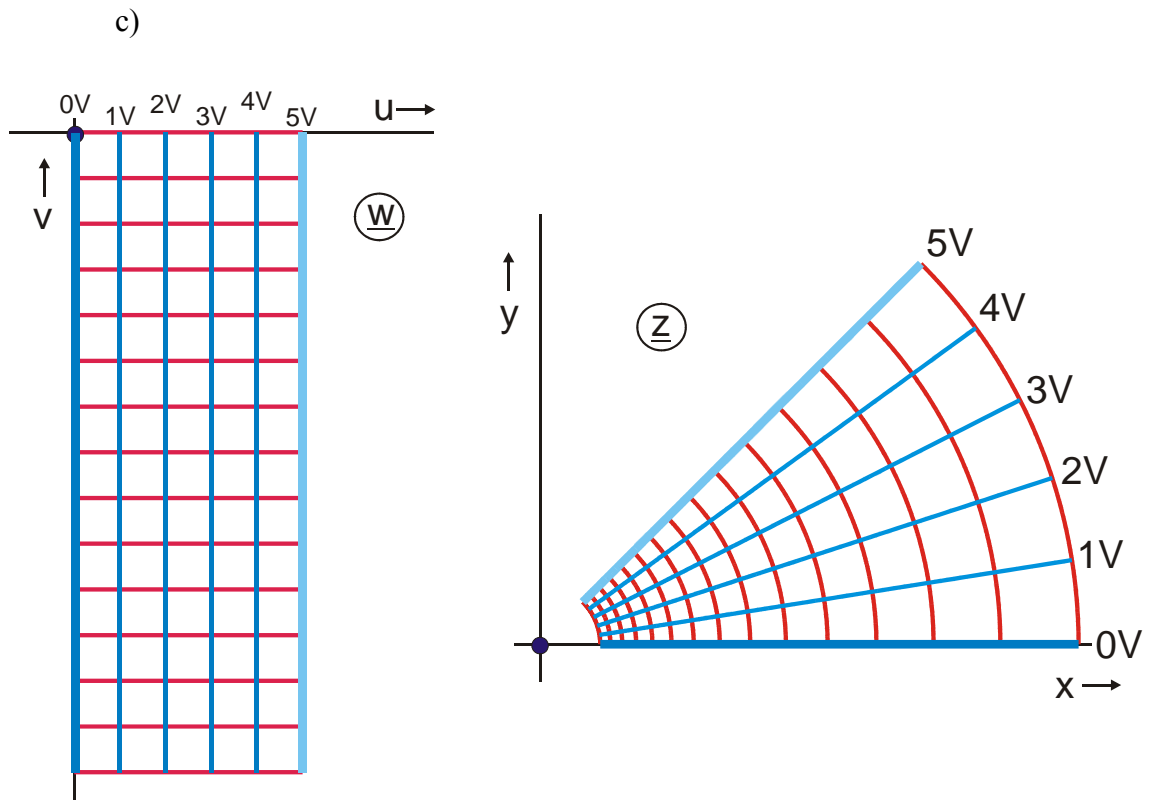


Figure 14.5: Field lines (red) and lines of constant potential (blue)

- d) In the \underline{w} -plane we have a linear distribution of the potential (equation of a straight line):

$$U(u) = U_1 + (U_2 - U_1) u/\alpha.$$

$U(z)$ is given in polar coordinates. With $r = \sqrt{x^2 + y^2}$ and $\varphi = \arctan \frac{y}{x}$ the mapping function is $\underline{w} = \varphi - j \ln (r/r_i)$ and:

$$U(\varphi) = U_1 + (U_2 - U_1) \varphi/\alpha.$$

- e) To divide the resistance by two you have to add the same amount of curvilinear squares at the inside resp. at the outside of the original sector (parallel connection):

- $R/2$ for $r_a = 10$ cm and $r_i = 0,1$ cm
- $R/2$ for $r_i = 1$ cm and $r_a = 100$ cm.

Exercise 3: Capacity, Characteristic Impedance

A thin conductive strip of width $w = 10 \text{ mm}$ runs in a height $h = 5 \text{ mm}$ parallel to a conductive plane. The strip is completely embedded in a dielectric material with the dielectric constant $\epsilon_r = 2$.

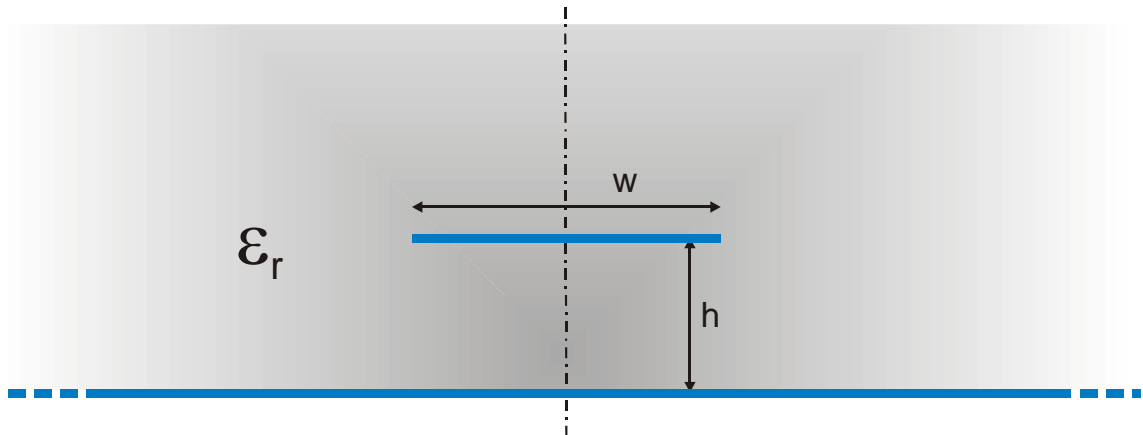


Figure 14.6: Exercise 3

- How large is the capacity per unit length C' ?
- How large is the characteristic impedance Z_L of this transmission line?

Solution:

- According to transformation E 2 the right half of the configuration is mapped onto a rectangle with the dimensions $K(k) \times K'(k)$.

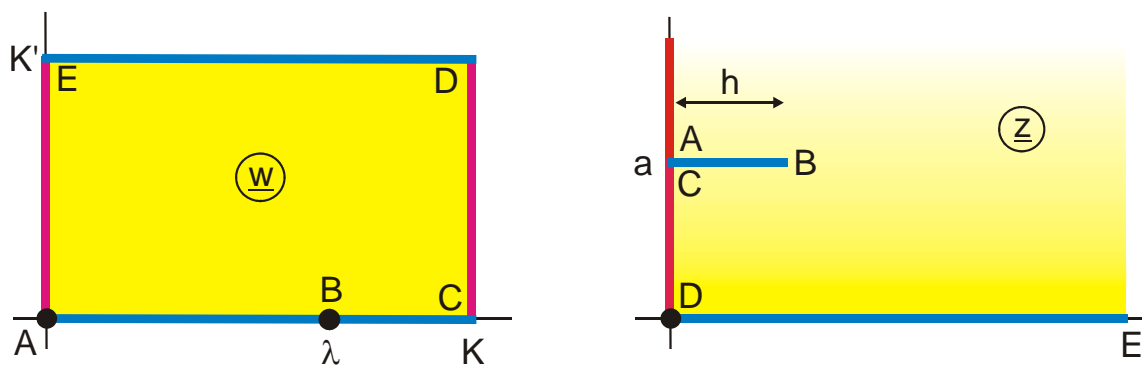


Figure 14.7: Mapping E 2

As the capacity has the same value in the \underline{z} -plane as in the \underline{w} -plane, it is calculated in the uniform field of the \underline{w} -plane:

$$C' = 2 \varepsilon_0 \varepsilon_r K(k)/K'(k)$$

The factor 2 takes into account the capacity of the left half of the line. As it is not possible to calculate the module k directly from h and a , k is determined with program E 2 by trial and error:

$$k = 0,98963 \text{ for } h = a = 0,47$$

The use of Eq. (13.37) yields $K(k)/K'(k) = 2,1$ and $C' = 74,9 \text{ pF/m}$ ($\varepsilon_0 = 8,854 \cdot 10^{-12} \text{ F/m}$).

b) The characteristic impedance Z_L of this type of transmission line is

$$Z_L = \frac{\sqrt{\varepsilon_r}}{c_0 C'}$$

and with $c_0 = 3 \cdot 10^8 \text{ m/s}$ the result is $Z_L = 62,95 \Omega$.

Exercise 4: Graphical Analysis of the Field Map

Given is the field map of a round conductor in air above a conductive plane resp. one half of the field map of a symmetrical two wire line (Figure 14.8). The properties of the field shall be determined using this pattern. The diameter of the conductor is $2r_0 = 10 \text{ mm}$. The distance between the center of the conductor and the plane is found by measuring the diameter and the distance to be $d = 15 \text{ mm}$. Between the conductor and the conductive plane is an RF-voltage of $U = 100 \text{ V}$ (extreme skin effect). The transmission line is terminated with its characteristic impedance.

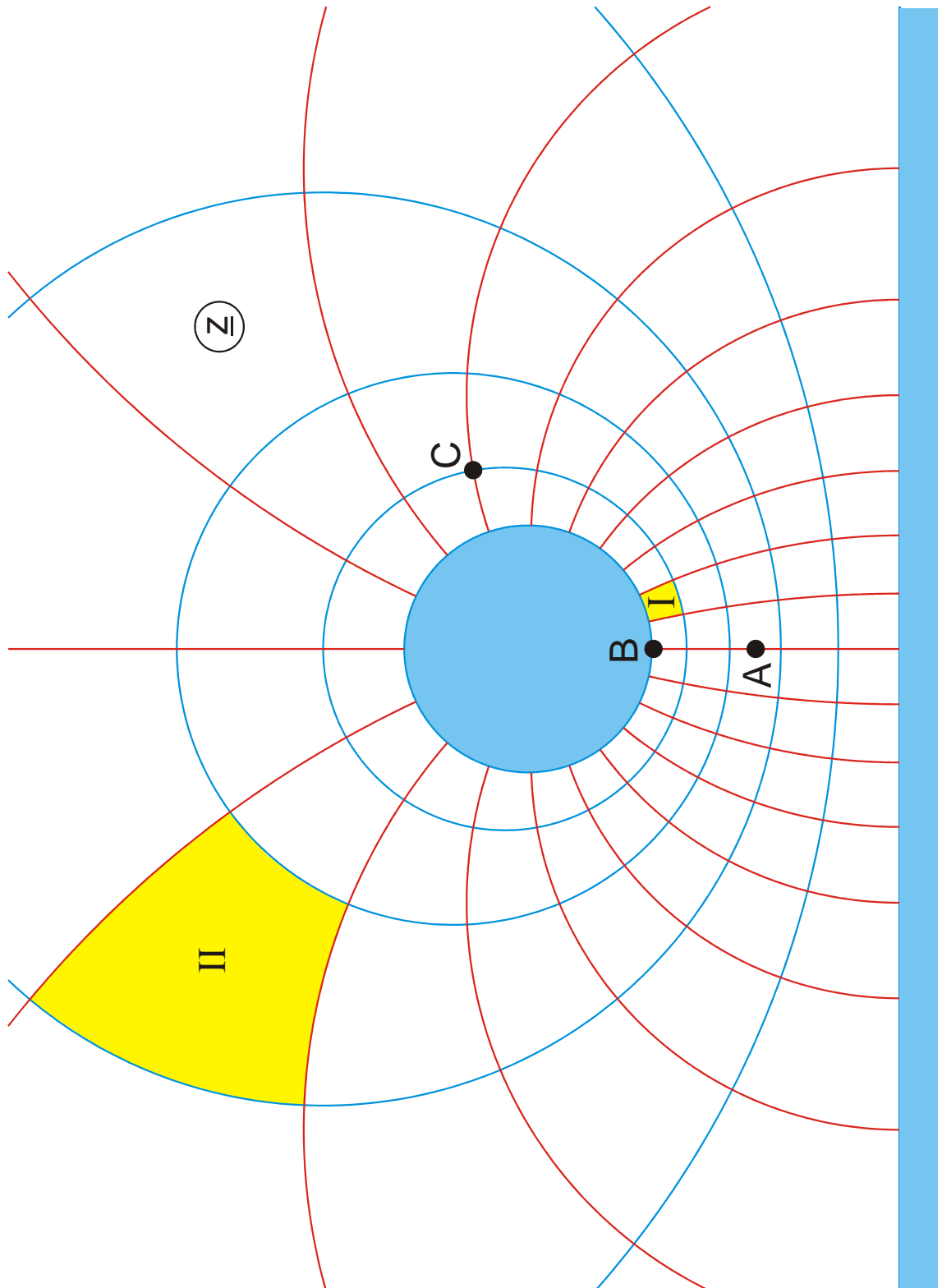


Figure 14.8: Exercise 4, mapping E 1.1 with $u_C = 0,28$

a) What is the capacity C' of the transmission line?

Solution:
$$C' = \varepsilon_0 \varepsilon_r \frac{m}{n} \frac{\Delta v}{\Delta u} = 31,6 \text{ pF} / m$$

with: $\varepsilon_0 = 8,854 \text{ pF/m}$ $\varepsilon_r = 1$
 $n = 5$ (Number of rectangles between conductor and plane)
 $m = 20$ (Number of rectangles around the conductor)
 $\Delta u / \Delta v = u_C / 0,25 = 1,12$ (ratio of the sides of the rectangles, same value in both planes)

In the uniform field of the \underline{w} -plane every rectangle is a parallel plate capacitor with the capacitance $C_0' = \varepsilon_0 \varepsilon_r \frac{\Delta v}{\Delta u} = 7,9 \text{ pF} / m$. There are n capacitors in series and m capacitors in parallel connection.

b) How large is the characteristic impedance?

Solution:
$$Z_L = \frac{Z_0}{\sqrt{\varepsilon_r}} \frac{n}{m} \frac{\Delta u}{\Delta v} = 105,6 \Omega$$

with: $Z_0 = 377 \Omega$

c) What is the conductor current I ?

Solution:
$$I = U / Z_L = 947 \text{ mA}$$

d) How large is the electric field strength in point A?

Solution:
$$E_A = \frac{20 \text{ V}}{8 \text{ mm} \cdot M} = 9,6 \text{ V} / \text{mm}$$

with: $M = 2 r_0 / 38,4 \text{ mm} = 0,26$ (scaling factor: reality/field map)

The voltage between two neighboring potential lines is 20 V. The distance is 8 mm in the field map and 8 mm \times M in reality.

e) Which value has the surface current density in point B?

Solution:
$$K_B = \frac{I}{m \Delta b} = \frac{947 \text{ mA}}{20 \cdot 4 \text{ mm} \cdot M} = 45,5 \text{ mA} / \text{mm}$$

The surface current between two neighboring field lines is constant in the whole field map. It is $\Delta I = I/m = 47,35 \text{ mA}$. For the sake of simplicity the assumption is made that the surface current density is constant in the small area between two field lines. This leads to a surface current density of $K_B = \Delta I / (\text{width of conductor}) \Delta b$. With 4 mm distance between two field lines, which is measured in the field map, Δb gets a value of 4 mm x M = 1,04 mm.

f) Calculate the energy density in point C?

Solution:
$$S_c = \frac{1}{2} \frac{E_c^2}{Z_0} = 48 \frac{\text{mW}}{\text{mm}^2} \quad \text{with} \quad E_c = \frac{20V}{M (10\text{mm} + 15,5\text{mm}) / 2} = 6 \frac{\text{V}}{\text{mm}}$$

g) Which amount of energy is transported in the curvilinear rectangle I and which amount of energy is transported in the curvilinear rectangle II?

Solution: In all curvilinear rectangles the same amount of power is transported, namely

$$\Delta P = \frac{P}{m \cdot n} = \frac{47,35 \text{ W}}{100} = 473,5 \text{ mW} \quad \text{with} \quad P = \frac{1}{2} U I .$$

h) Which part of the total power is transported in the total cross-section shown in Figure 14.8?

Solution: From a total of $m \times n = 100$ curvilinear rectangles are approximately $2 \times 45,5 = 91$ shown. Therefore about 91 % of the total power is transported in the cross-section shown. The remaining 9 % are distributed over the complete infinite half space above the conductive plane outside the drawing area.

15. Table of Conformal Mappings

Elementary und Special Functions

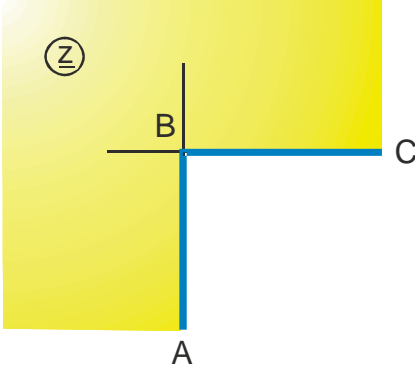
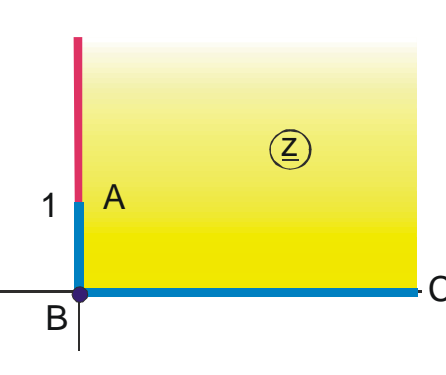
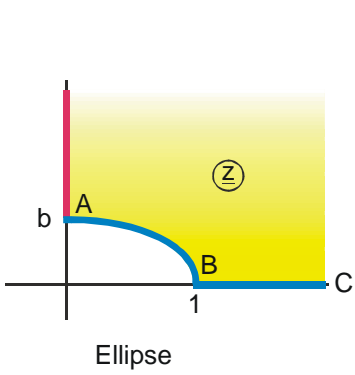
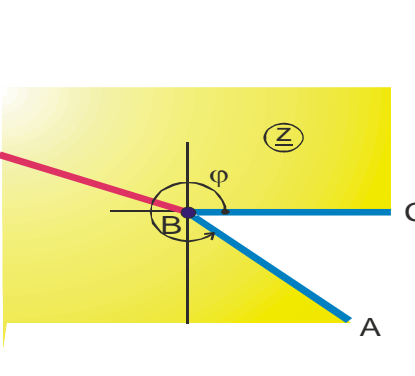
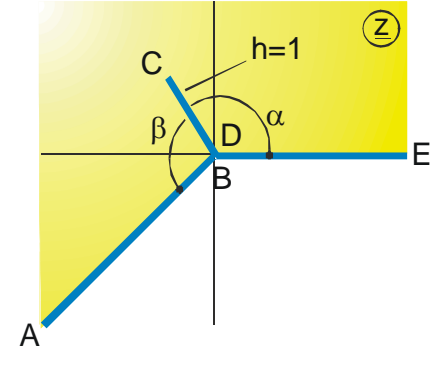
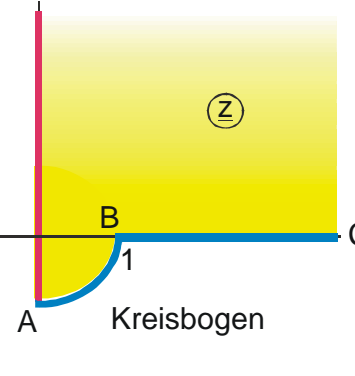
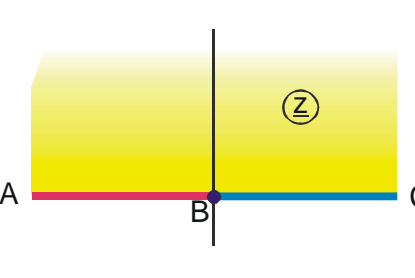
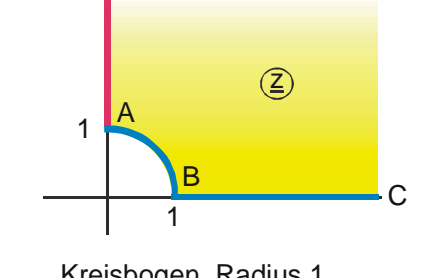
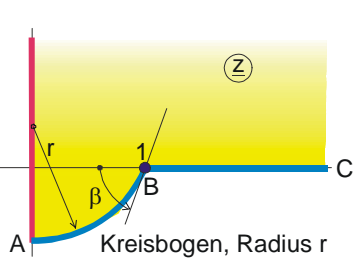
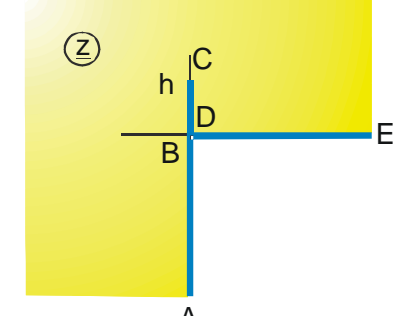
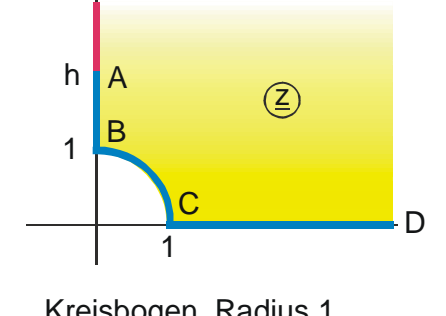
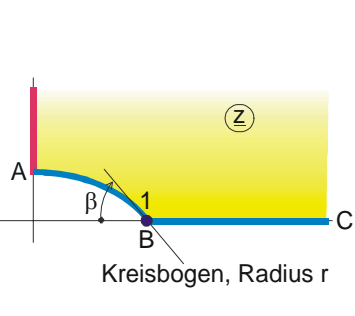
Function	Mapping Number
$1/w$	Q1
w^φ	A 1.1
e^φ	B 1
$\ln w$	H 1
\arcsin	H 1.5
\tanh	E 1
\sin	B 2
\cosh	B 2
$1/\sqrt{w}$	U 7.1
$1/w^2$	U 7
sn	E 3
cn	P 4
Z_e	E 2
Z_t	S 2
Z_a	A 11.1
Z_t	S 2
F_a	Q 4
F_t	I 1.2
E_t	C 3.1

Function	Mapping Number
E_a	A 10
E_e	U 5
B_t	U 1
B_a	A 10.2
B_e	U 1.1
D_t	U 2
D_a	U 2.1
D_e	U 2.2
Π_t	U 4.1
Π_a	U 4.2
Π_e	U 4.3
Π_j	U 3
Λ	C 3.2
\mathfrak{g}_1	U 6.1
\mathfrak{g}_2	U 6.2
\mathfrak{g}_3	U 6.3
\mathfrak{g}_4	U 6.4

Elementary und Special Curves

Name	Mapping Number
Concentric Circles	B1
Parabolas	A 1.2
Hyperbolas	A 1.1 with $\varphi = 90^\circ$
Confocal Ellipses	B 2
Confocal Hyperbolas	B 2
Bipolar Coordinate System	E 1
Inverse Ellipses	P 1.1
Cassinian Curves	S 1
Inverse Cassinian Curves	P 1
Lemniscate	S 1, Curve through $z = 0$
Cardioids	U 7
Maxwell-Curves	C 2; D 1.1 for $e = 0$
4-Leaf-Roses	U 7.1
Rogowski Profile	C 2, Center Line with $v = 0,5$
π –Borda Profile	N 2.2
$\pi/2$ -Borda Profile	N 2
Joukowski Profile	R 7.1 with $b = 0$
Kármán-Trefftz-Profile	R 7.2 with $b = 0$
Apollonian Circles	E1

Group A: One Conducting Boundary with Infinite Extension

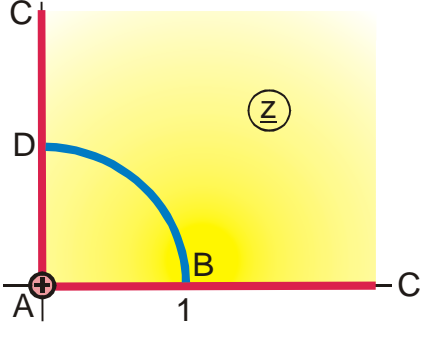
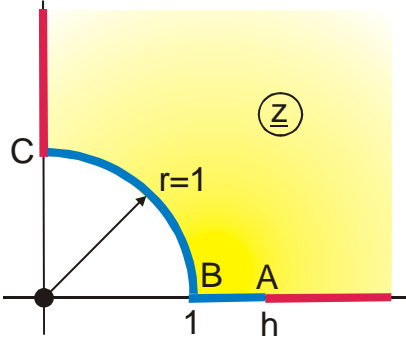
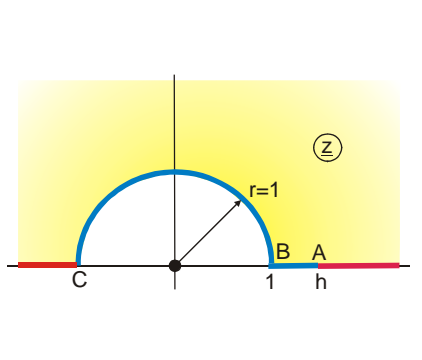
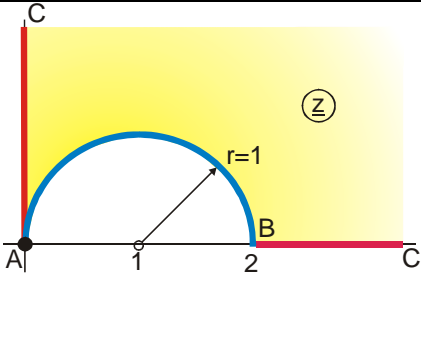
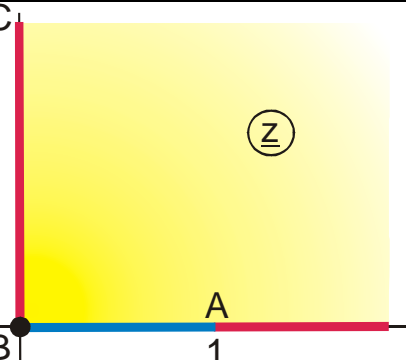
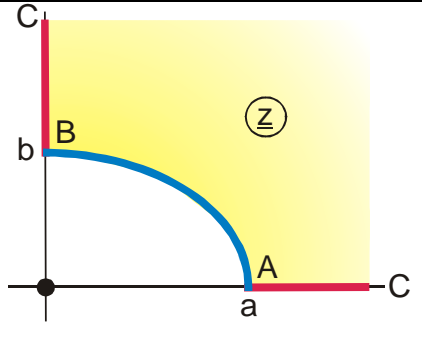
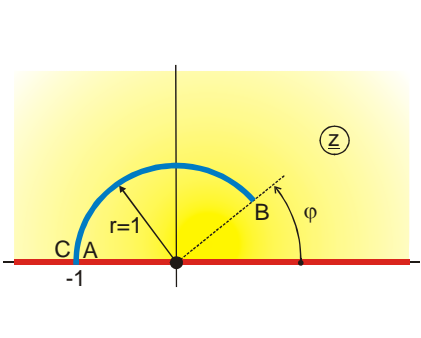
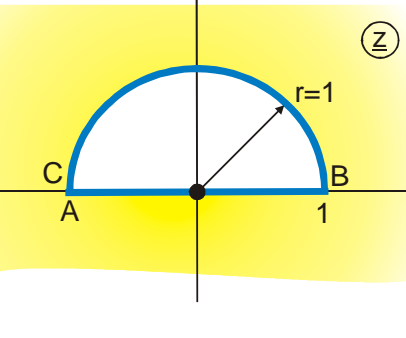
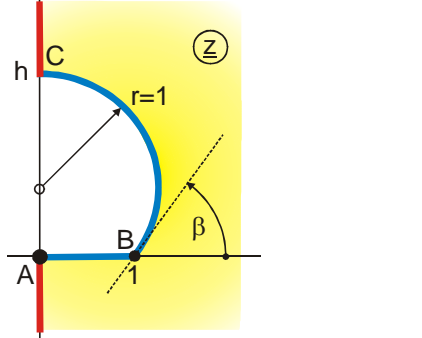
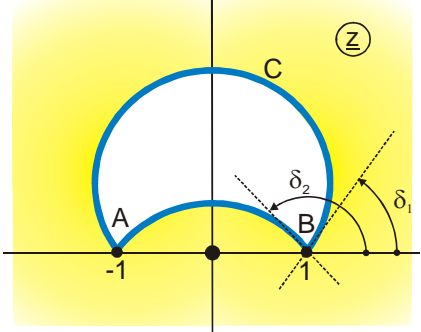
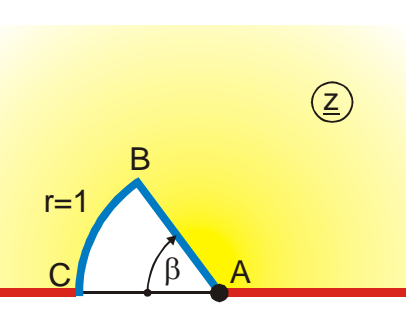
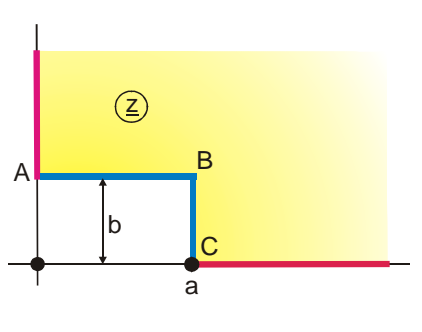
A 1	A 2.1	A 3.2
		 <p>Ellipse</p>
A 1.1	A 2.3	A 3.3
		 <p>Kreisbogen</p>
A 1.2	A 3	A 3.4
	 <p>Kreisbogen, Radius 1</p>	 <p>Kreisbogen, Radius r</p>
A 2	A 3.1	A 3.4
	 <p>Kreisbogen, Radius 1</p>	 <p>Kreisbogen, Radius r</p>

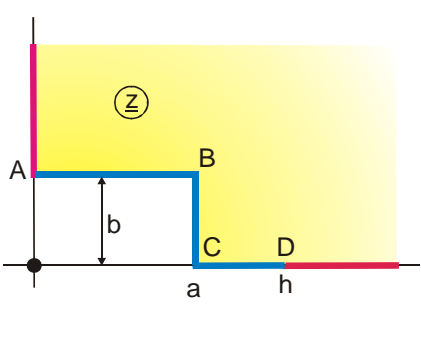
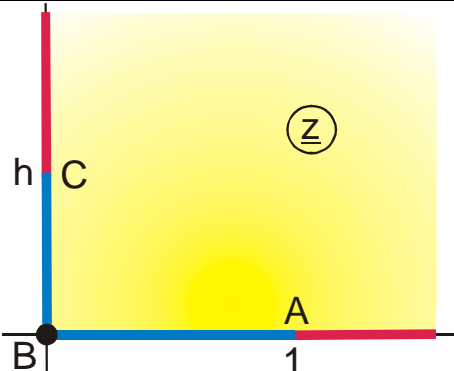
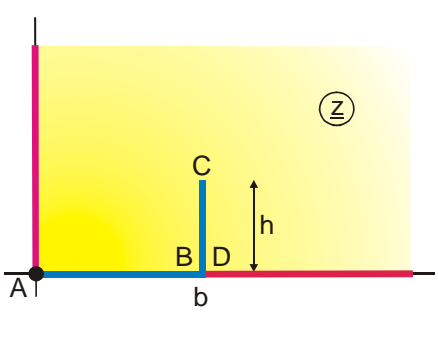
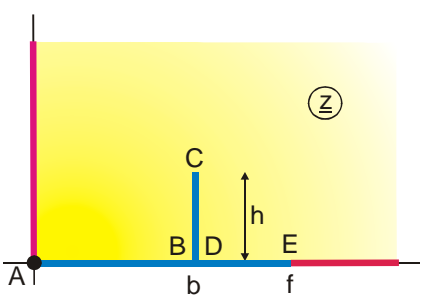
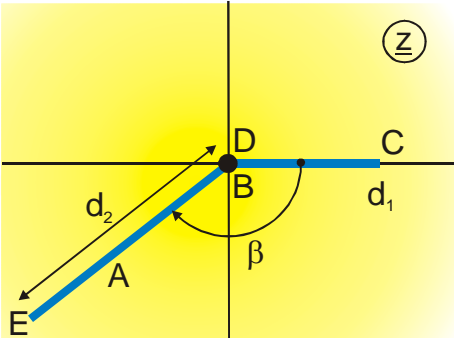
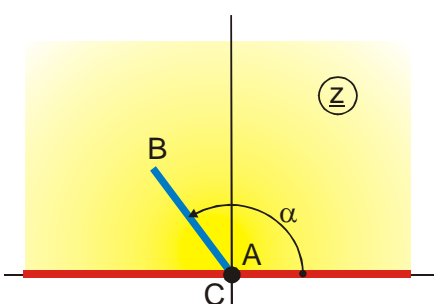
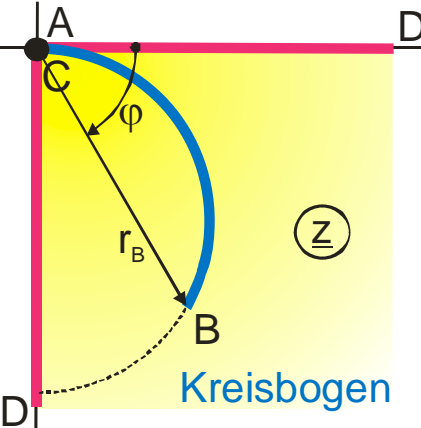
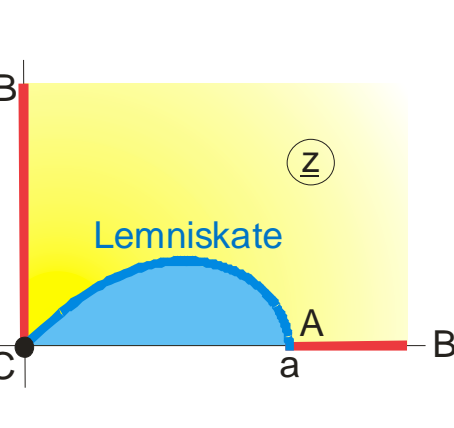
<p>A 3.5</p>	<p>A 3.6</p>	<p>A 3.7</p>
<p>A 3.8</p>	<p>A 4</p>	<p>A 4.1</p>
<p>A 5</p>	<p>A 5.1</p>	<p>A 5.2</p>
<p>A 5.3</p>	<p>A 5.4</p>	<p>A 5.5</p>
<p>A 5.6</p>	<p>A 5.7</p>	<p>A 6</p>
<p>A 6.1</p>	<p>A 6.2</p>	<p>A 6.3</p>

A 7	A 7.1	A 8
A 8.1	A 8.2	A 9
A 9.1	A 9.2	A 9.3
A 9.4	A 10	A 10.1
A 10.2	A 10.3	A 10.4

<p>A 10.5</p>	<p>A 10.6</p>	<p>A 10.7</p>
<p>A 10.8</p>	<p>A 10.9</p>	<p>A 11</p>
<p>A 11.1</p>	<p>A 11.2</p>	<p>A 11.3</p>
<p>A 3.10</p>	<p>A 2.4</p>	<p>A 8.3</p>
<p>A 3.9</p>	<p>A 3.11</p>	

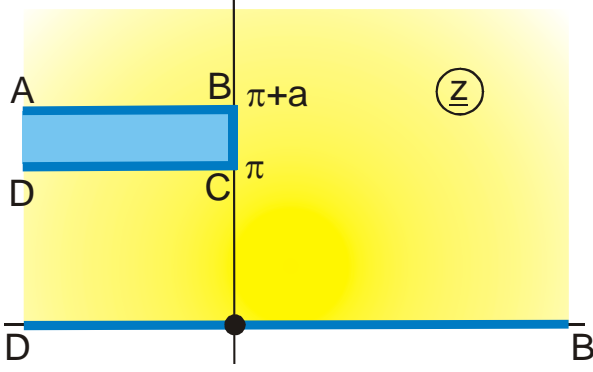
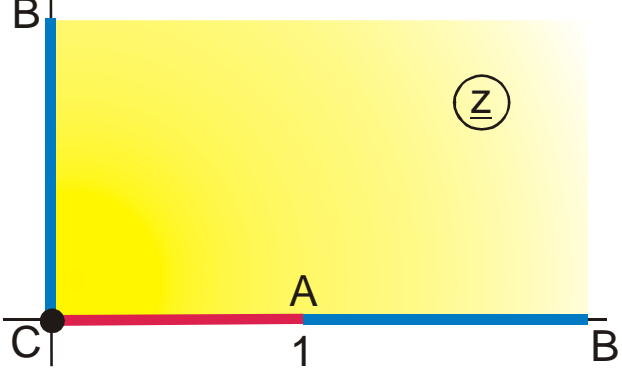
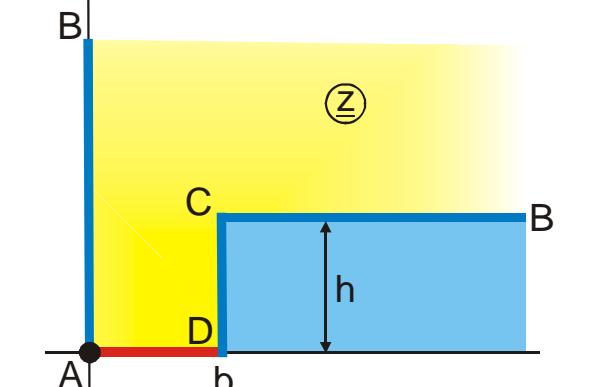
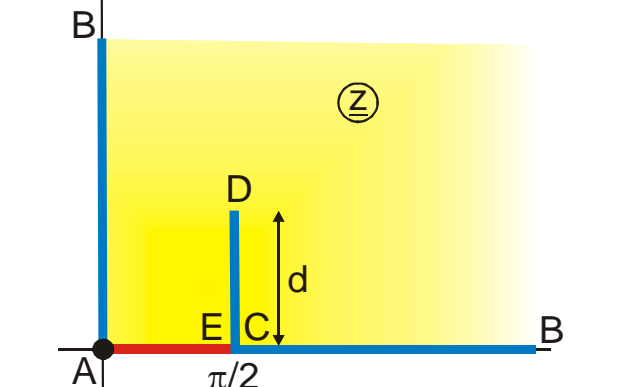
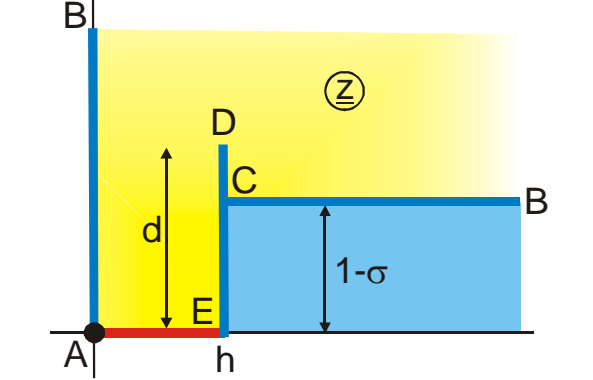
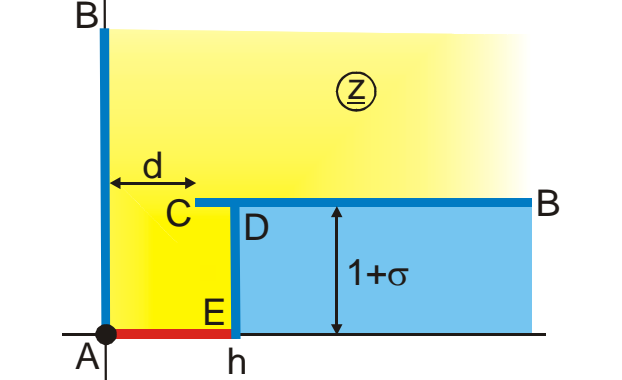
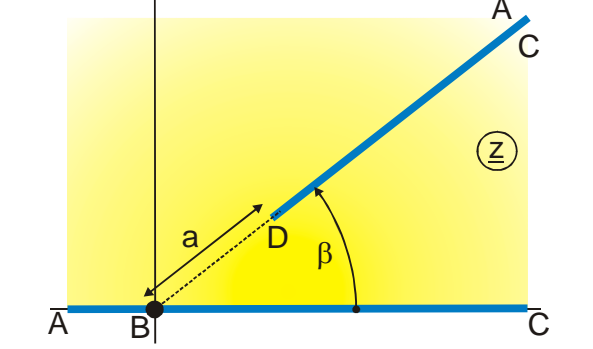
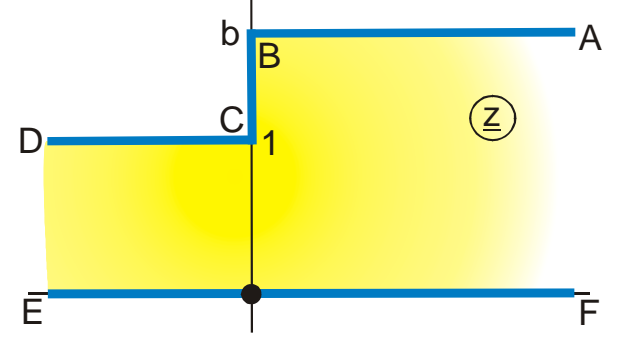
Group B: One Conducting Boundary with Finite Extension

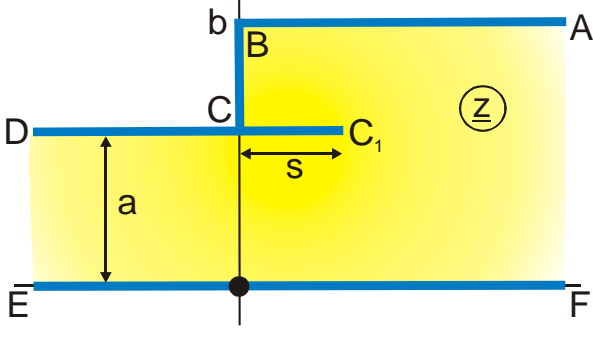
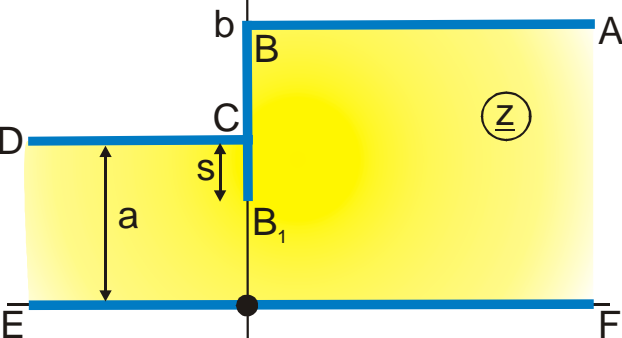
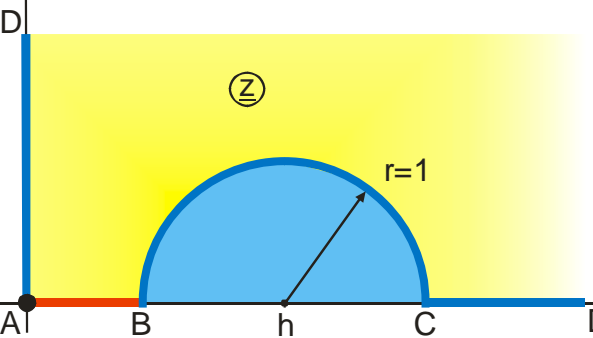
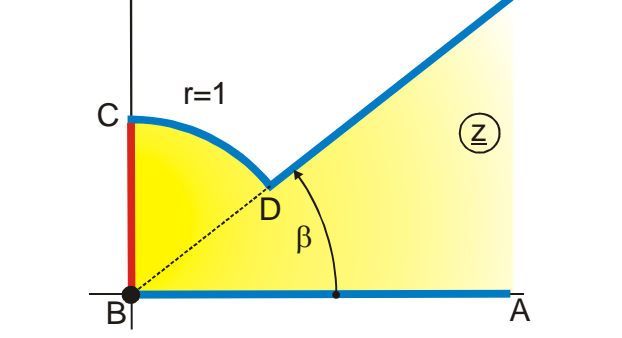
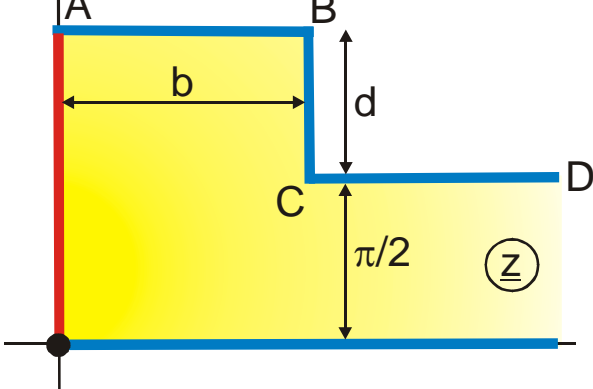
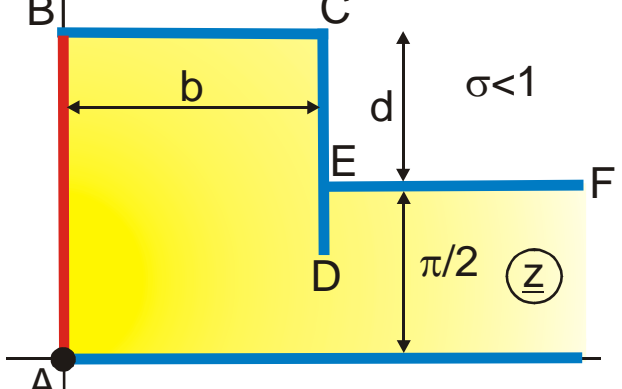
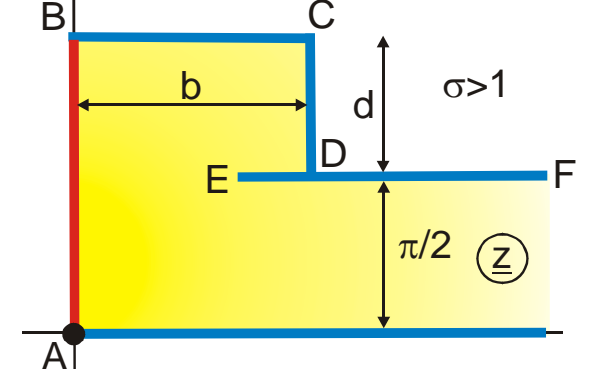
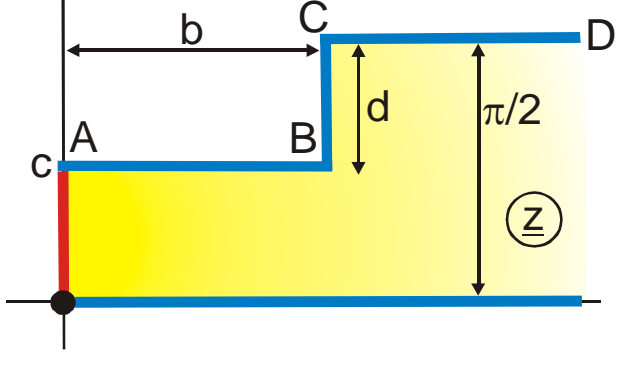
B 1	B 1.1	B 1.2
		
B 1.3	B 2	B 2.1
		
B 2.2	B 3	B 3.1
		
B 3.2	B 3.3	B 4
		

B 4.1	B 5	B 5.1
		
B 5.2	B 5.3	B 5.4
		
B3.4	B 3_5	
		

Group C: Two Conducting Boundaries with Infinite Extension, Symmetrically Arranged, Same Charge, Opposite Polarity

C 1	C 1.1
C 1.2	C1.3
C 1.4	C 2

C 2.1	C 3
	
C 3.1	C 3.2
	
C 3.3	C 3.4
	
C 4	C 5
	

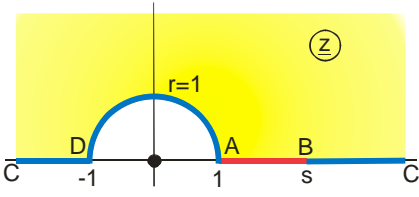
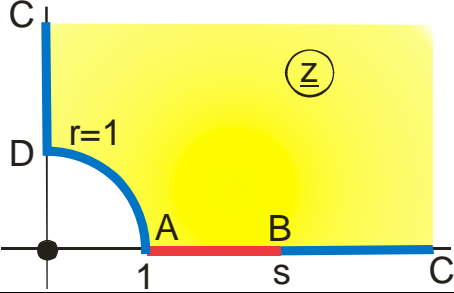
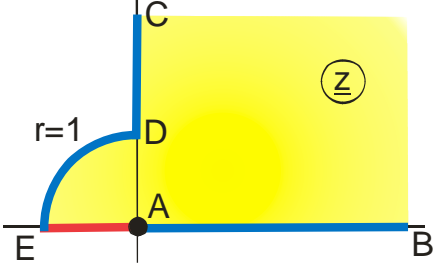
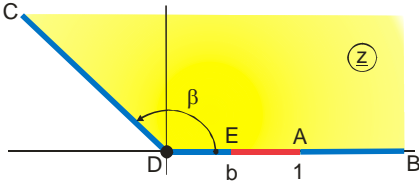
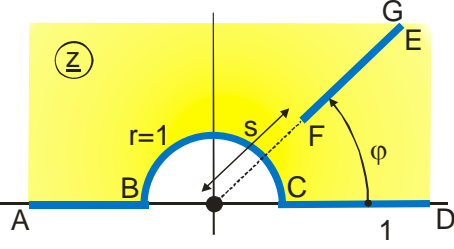
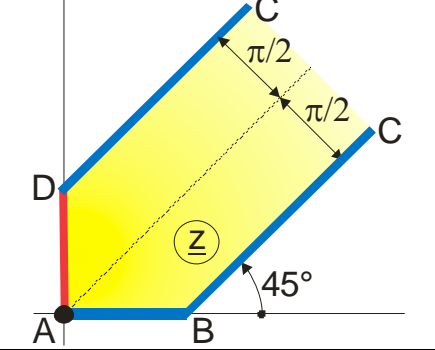
C 5.1	C 5.2
	
C 6	C 7
	
C 8	C 8.1
	
C 8.1	C 9
	

Group D: Two Conducting Boundaries with Infinite Extension, Same Charge, Opposite Polarity

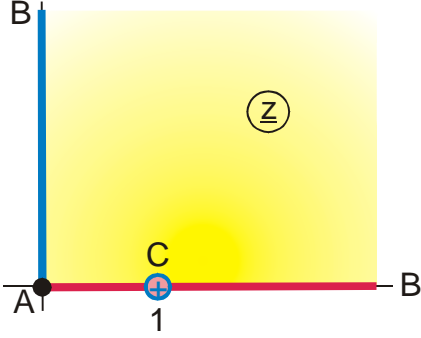
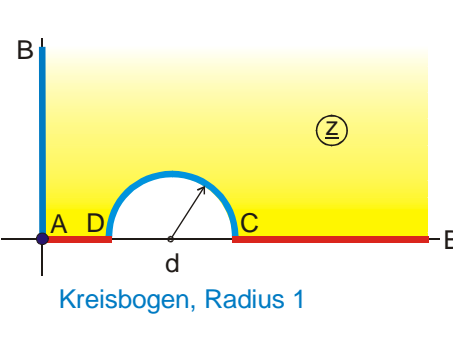
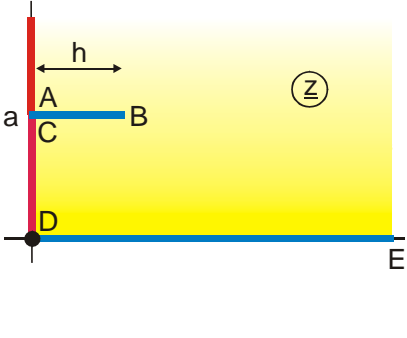
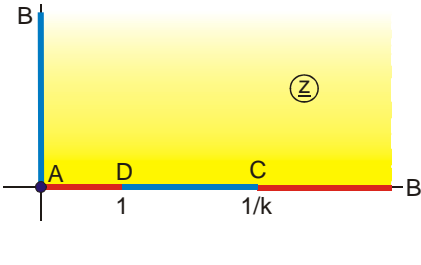
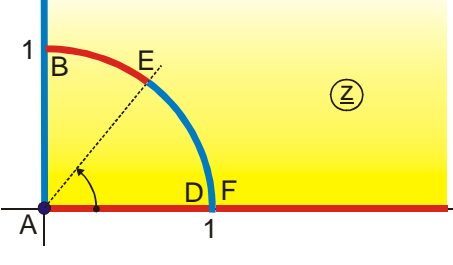
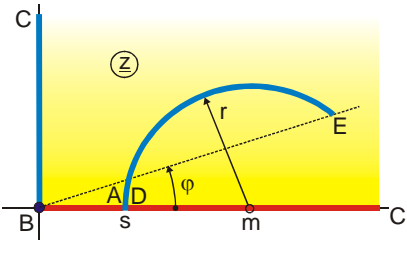
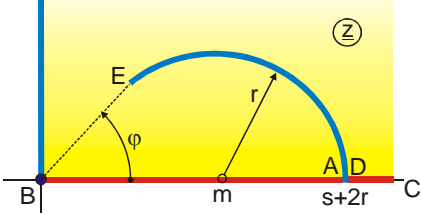
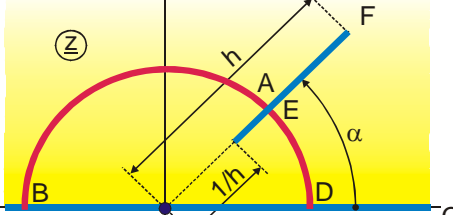
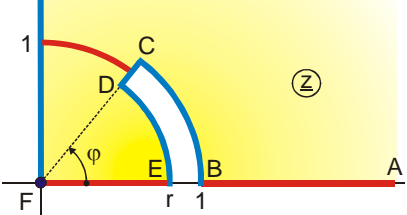
D 1	D 1.1	D 1.2
D 1.3	D 1.4	D 1.5
D 2	D 2.1	D 2.2
D 2.2	D 2.3	D 2.4

<p>D 2.5</p>	<p>D 2.6</p>	<p>D 3</p>
<p>D 3.1</p>	<p>D 4</p>	<p>D 4.1</p>
<p>D 4.2</p>	<p>D 5</p>	<p>D 6</p>
<p>D 6.1</p>	<p>D 6.2</p>	<p>D 6.3</p>

15. Table of Conformal Mappings

D 7	D 7.1	D 7.2
		
D 7.3	D 7.4	D 4.3
		

Group E: Two Conducting Boundaries with Finite Extension, Symmetrically Arranged, Same Charge, Opposite Polarity

E 1	E 1.1	E 2
		
E 3	E 4	E 4.1
		
E 4.2	E 5	E 6
		

Group F: Two Conducting Boundaries with Finite Extension, Same Charge, Opposite Polarity

F 1	F 1.1	F 1.2
F 1.3	F 2	F 2.1
F 2.2	F 2.3	F 2.4
F 2.5	F 2.6	F 2.7

F 2.8	F 3	F 3.1
F 3.2	F 3.3	F 3.4
F 3.5	F 3.6	F 3.7
F 3.8	F 4	F 4.1

F 4.2	F 4.3	F 4.4
F 5	F 5.1	F 5.2
F 5.3	F 5.4	F 5.5

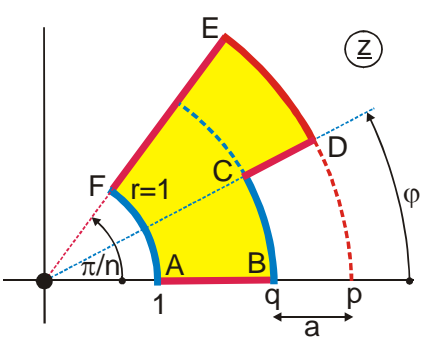
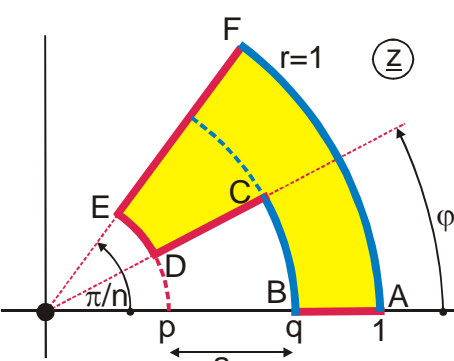
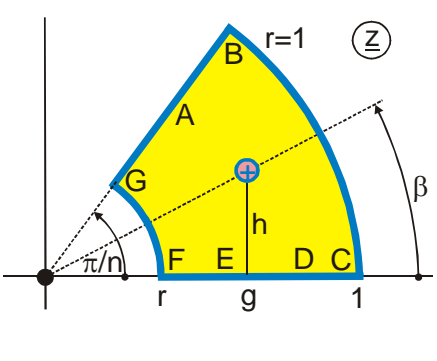
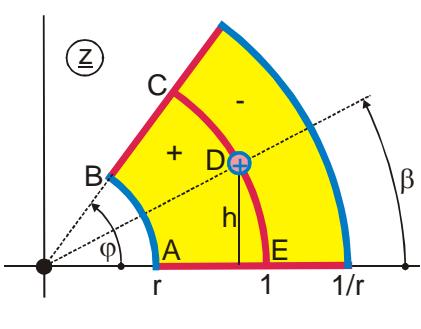
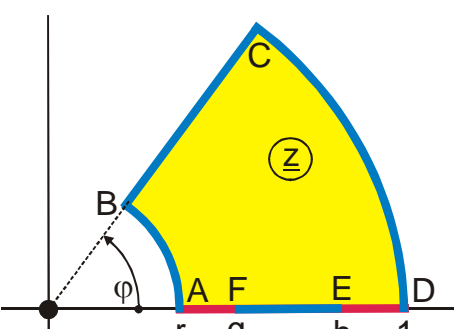
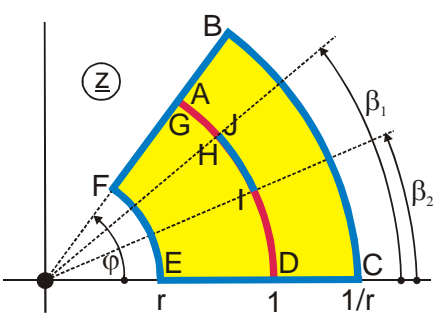
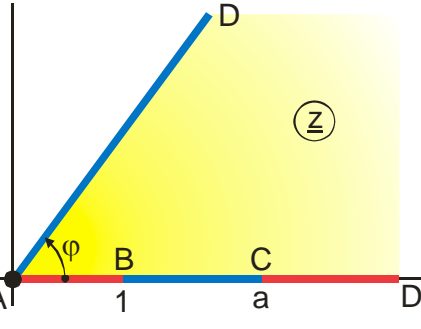
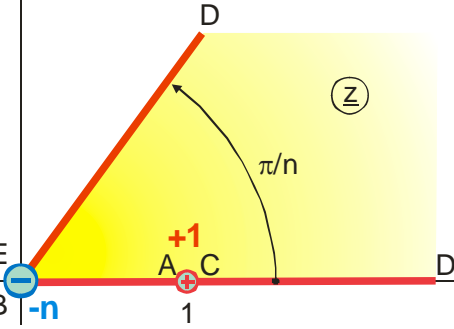
F 6	F 6.1	F 6.2
F 6.3	F 6.4	F 6.5
F 6.6	F 7	F 7.1

F 8	F 8.1	F 8.2
F 8.3	F 8.4	F 8.5
F 8.6	F 9	F 9.1
F 2.9	F 2.10	F 6.7

F 4.5	F 4.6	

Group G: Fields with Radial Symmetry

G 1	G 1.1	G 1.2
G 1.3	G 1.4	G 1.5
G 2	G 2.1	G 3
G 3.1	G 4	G 5

G 6	G 6.1	G 7
		
G 7.1	G 7.2	G 7.3
		
G 3.2	G 1.6	
		

Group H: Fields with Periodicity in One Dimension

H 1	H 1.1	H 1.2
H 1.3	H 1.4	H 1.5
H 1.6	H 2	H 2.1
H 2.2	H 2.3	H 3
H 3.1	H 3.2	H 3.3

15. Table of Conformal Mappings

<p>H 3.4</p>	<p>H 3.5</p>	<p>H 4</p>
<p>H 4.1</p>	<p>H 4.2</p>	<p>H 4.3</p>
<p>H 4.4</p>	<p>H 5</p>	<p>H 6</p>
<p>H 6.1</p>	<p>H 6.2</p>	<p>H 6.3</p>
<p>H 6.4</p>	<p>H 6.5</p>	<p>H 6.6</p>
<p>H 6.7</p>	<p>H 6.8</p>	<p>H 6.9</p>

15. Table of Conformal Mappings

<p>H 6.10</p>	<p>H 6.11</p>	<p>H 6.12</p>
<p>H 6.13</p>	<p>H 6.14</p>	<p>H 7</p>
<p>H 7.1</p>	<p>H 7.2</p>	<p>H 7.3</p>
<p>H 7.4</p>	<p>H 7.5</p>	<p>H 7.6</p>
<p>H 7.7</p>	<p>H 7.8</p>	<p>H 7.9</p>
<p>H 7.10</p>	<p>H 7.11</p>	<p>H 7.12</p>

15. Table of Conformal Mappings

<p>H 7.13</p>	<p>H 7.14</p>	<p>H 7.15</p>
<p>H 7.16</p>	<p>H 7.17</p>	<p>H 7.18</p>
<p>H 7.19</p>	<p>H 8</p>	<p>H 8.1</p>
<p>H 8.2</p>	<p>H 8.3</p>	<p>H 9</p>
<p>H 9.1</p>	<p>H 9.2</p>	<p>H 10</p>
<p>H 10.1</p>	<p>H 10.2</p>	<p>H 10.3</p>

15. Table of Conformal Mappings

H 11	H 11.1	H 12
H 12.1	H 12.2	H 12.3

Group I: Fields with Periodicity in Two Dimensions

I 1	I 1.1	I 1.2
I 1.3	I 1.4	I 1.5
I 1.6	I 1.7	I 1.8
I 1.9	I 2	I 2.1

I 2.2	I 2.3	I 2.4
I 2.5	I 2.6	I 2.7
I 2.8	I 3	I 3.1
I 3.2	I 4	I 4.1

15. Table of Conformal Mappings

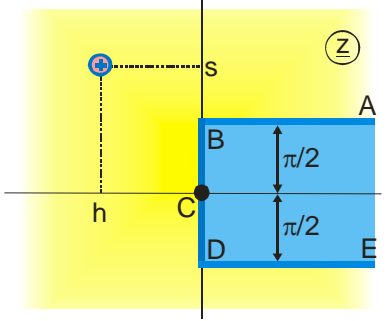
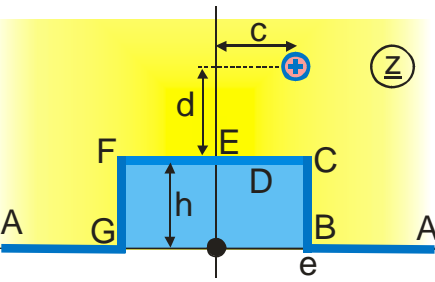
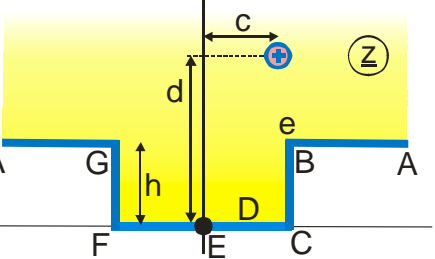
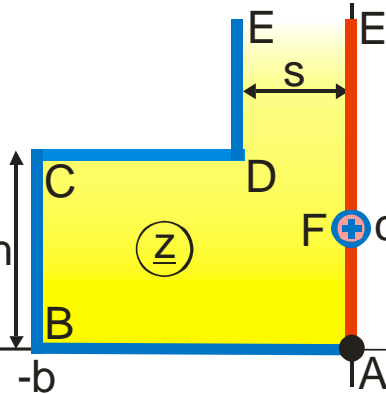
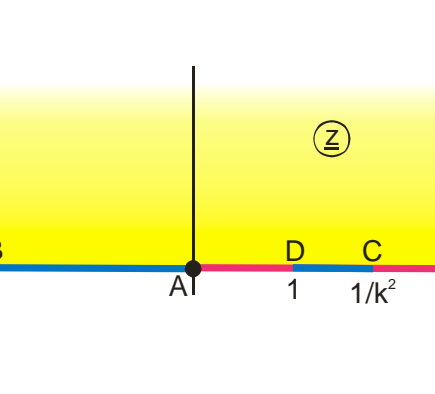
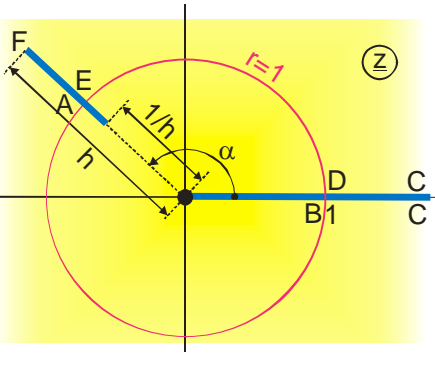
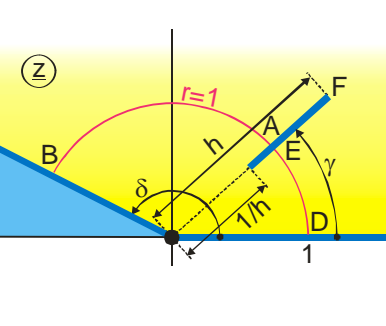
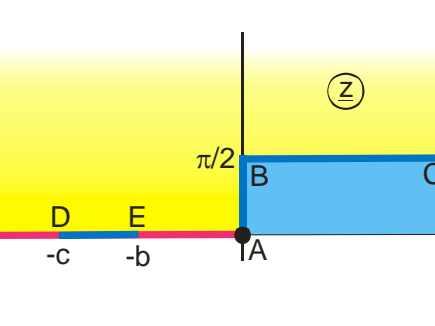
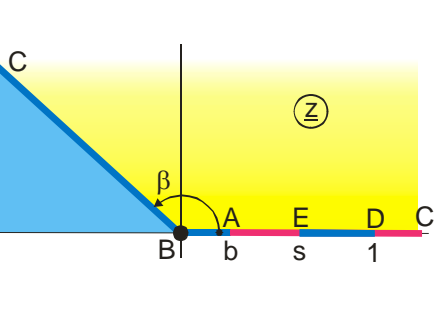
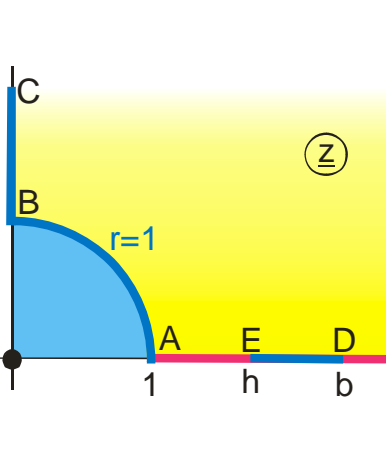
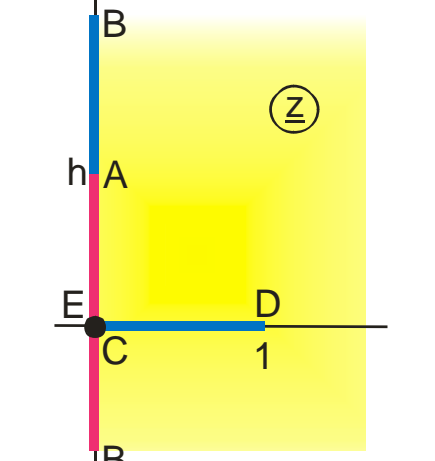
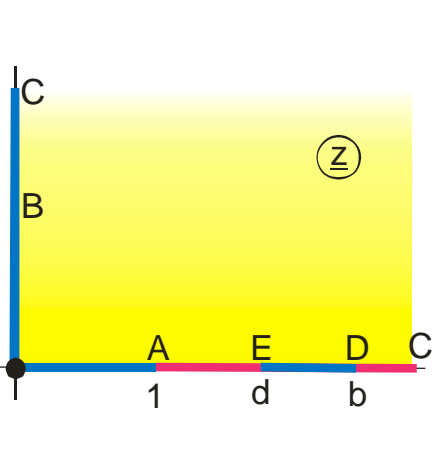
I 4.2	I 5	I 5.1
I 6	I 2.9	

Group J: Surfaces with Periodicity in One Dimension

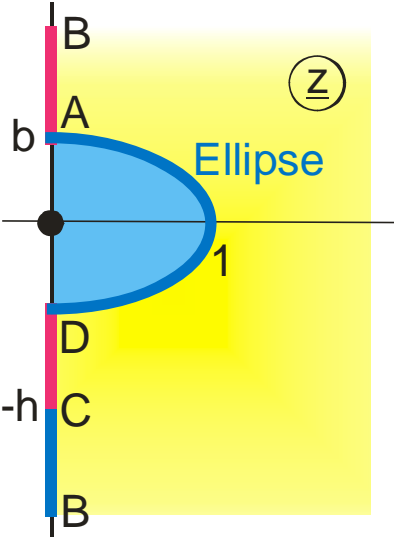
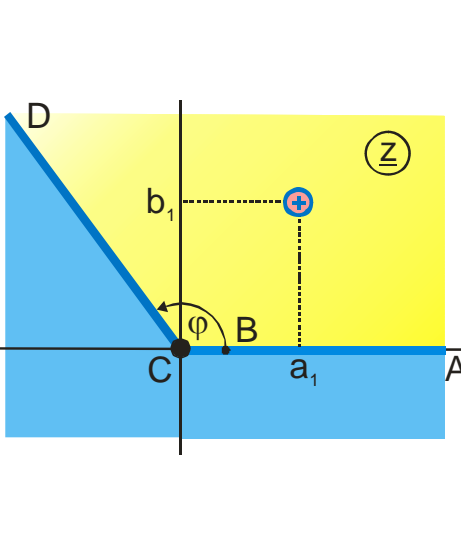
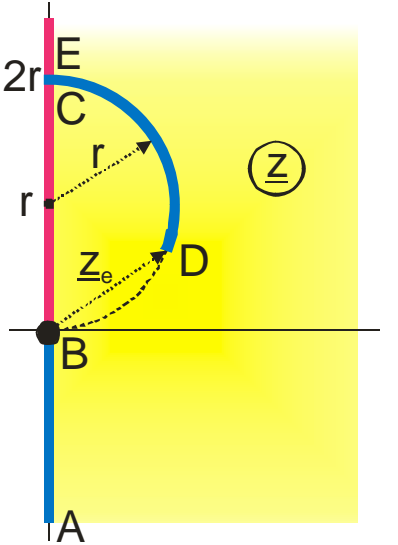
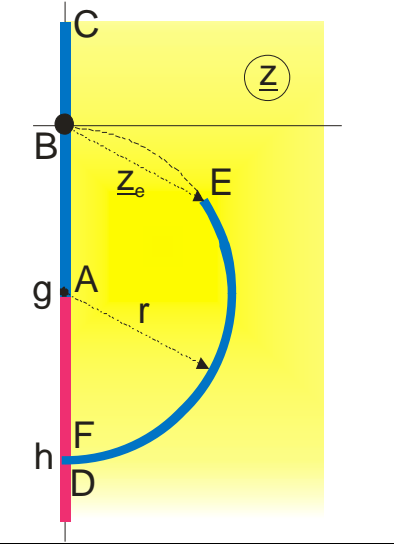
J 1	J 1.1	J 1.2
J 2	J 2.1	J 3
J 3.1	J 3.2	J 3.3

Group K: One Conducting Boundary with Finite Extension and One with Infinite Extension, Same Charge, Opposite Polarity

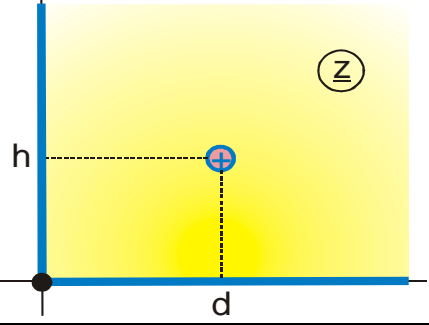
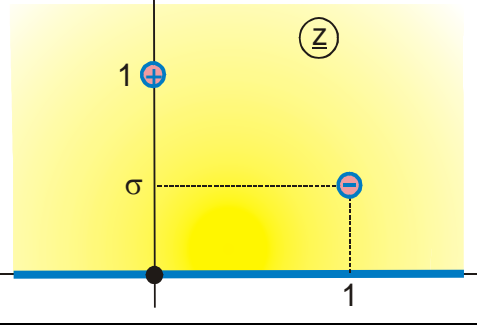
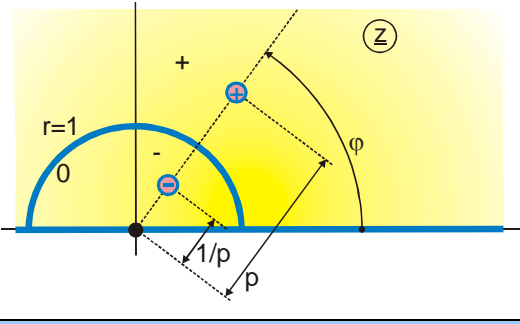
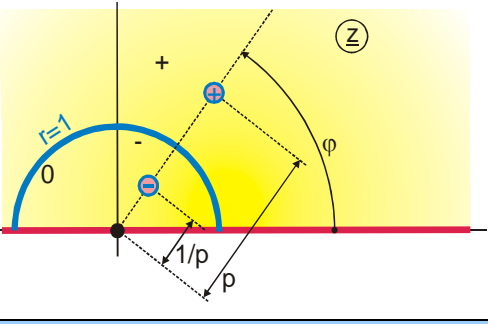
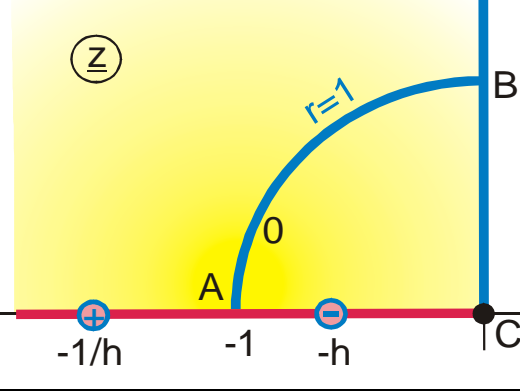
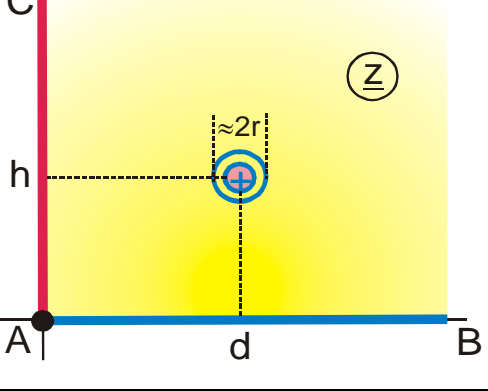
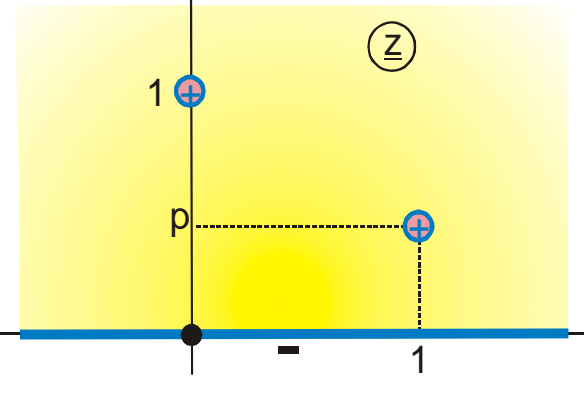
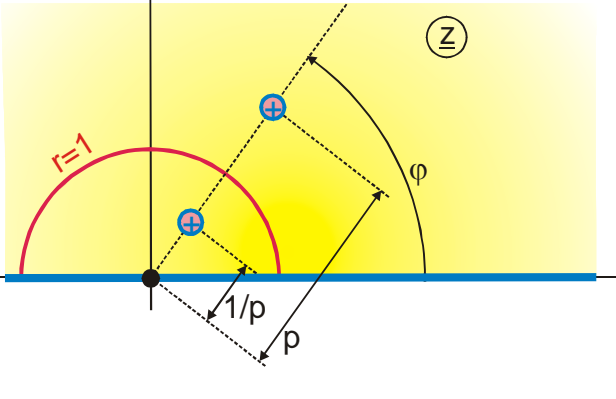
K 1	K 1.1	K 1.2
K 1.3	K 1.4	K 1.5
K 1.6	K 1.7	K 1.8
K 1.9	K 1.10	K 1.11

K 2	K 2.1	K 2.2
		
K 2.3	K 3	K 3.1
		
K 3.2	K 3.3	K 3.4
		
K 3.5	K 3.6	K 3.7
		

K 3.8	K 4	K 4.1
K 4.2	K 4.3	K 4.4
K 4.5	K 4.6	K 5

K 6	K 1.12	K 4.7
		
K 4.8		
		

Group L: More Fields with Line Charges

L 1	L 1.1
	
L 1.2	L 1.3
	
L 1.4	L 2
	
L 2.1	L 2.2
	

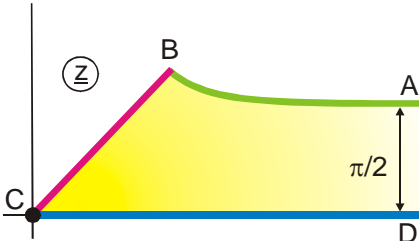
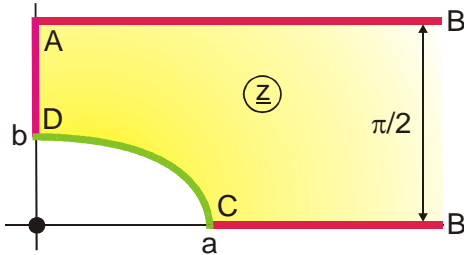
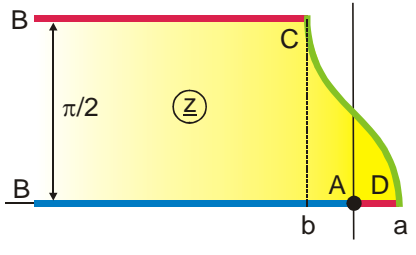
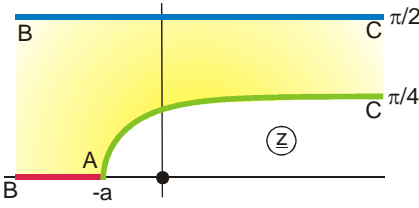
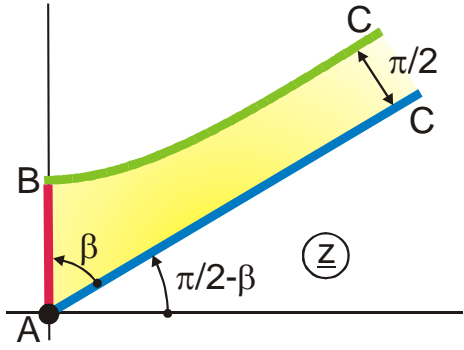
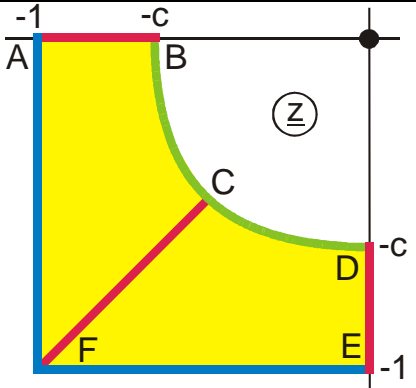
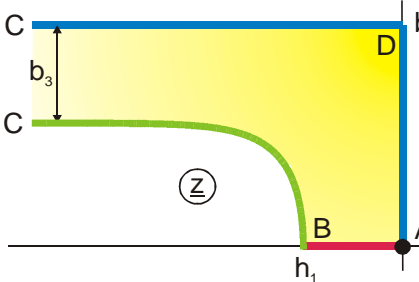
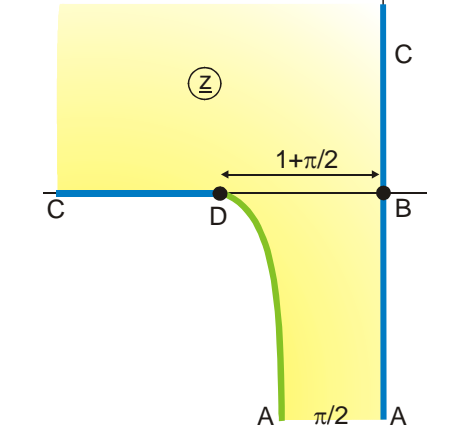
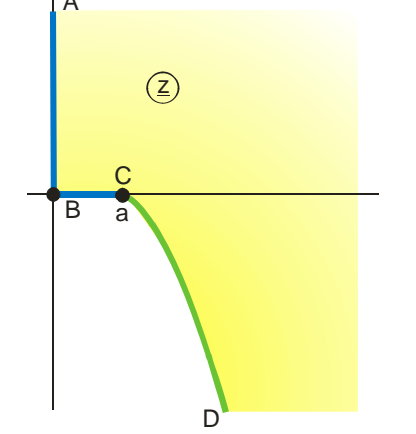
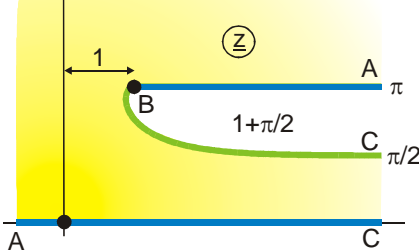
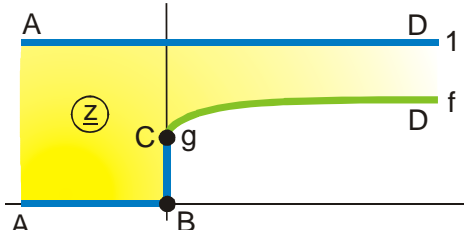
15. Table of Conformal Mappings

L 2.3	L 3
L 3.1	L 3.2
L4	

Group M: Boundaries with Rounded Corners

M 1	M 1.1	M 1.2
M 2	M 2.1	M 2.2
M 2.3	M 3	M 4
M 4.1	M 5	M 5.1

Group N: Conducting Boundaries with Constant Field Strength

N 1	N 1.1	N 1.2
		
N 1.3	N 1.4	N 1.5
		
N 1.6	N 2	N 2.1
		
N 2.2	N 3	
		

Group P: Three and More Conducting Boundaries

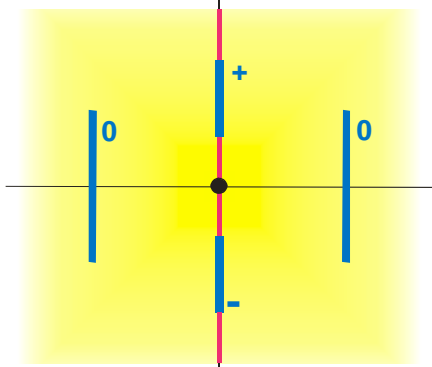
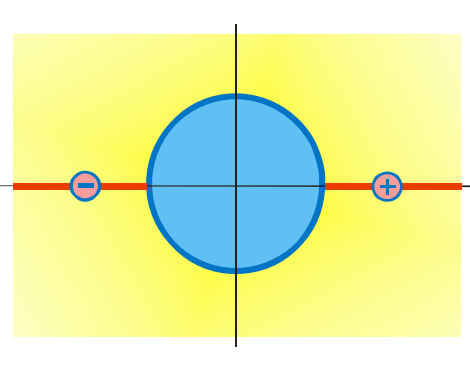
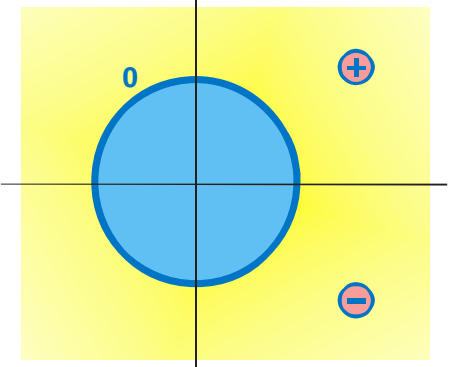
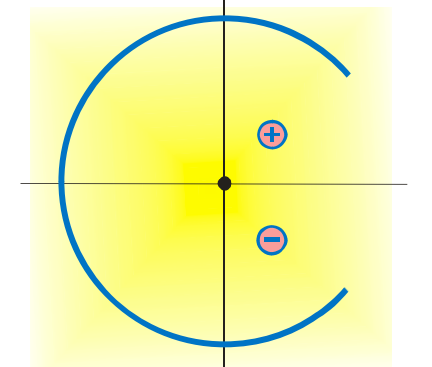
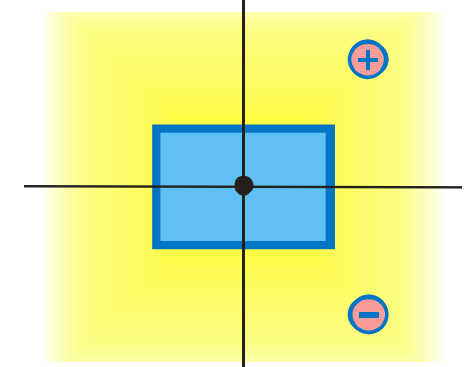
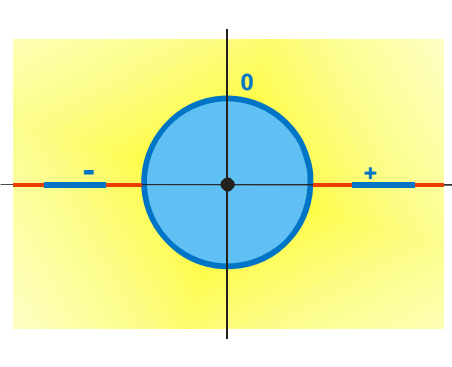
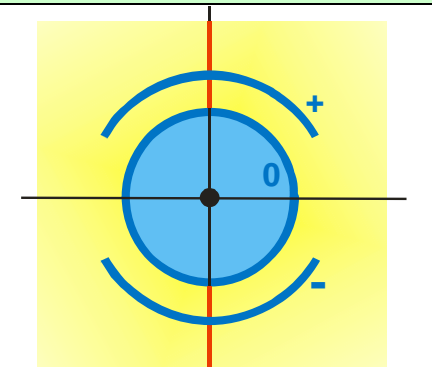
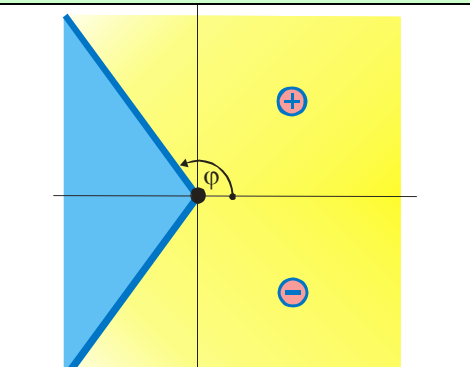
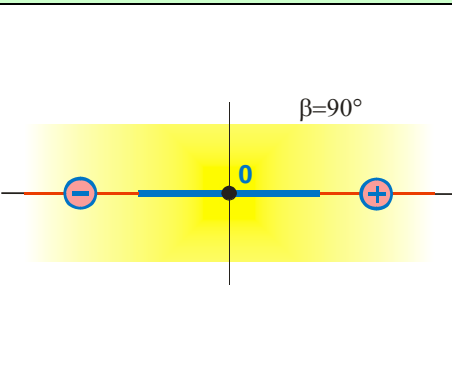
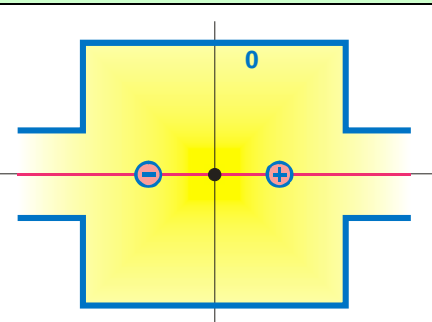
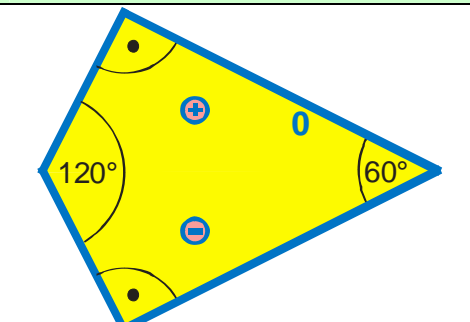
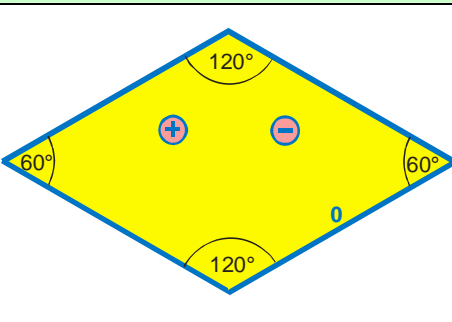
P 1	P 1.1	P 1.2
P 1.3	P 1.4	P 1.5
P 1.6	P 1.7	P 1.8
P 1.9	P 1.10	P 1.11

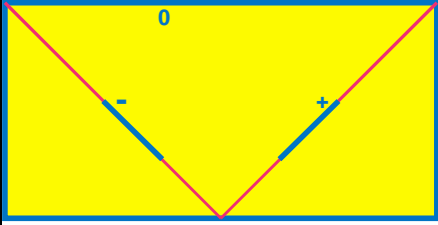
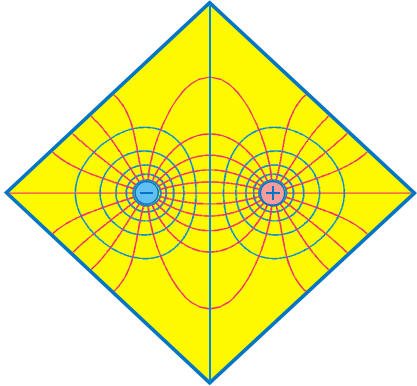
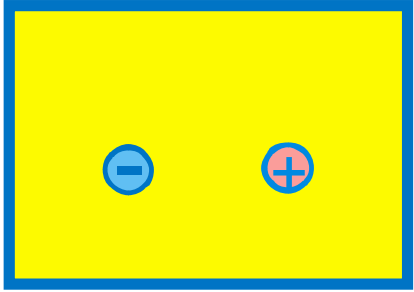
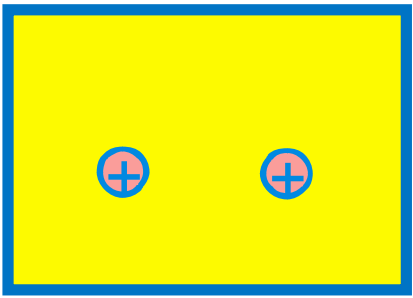
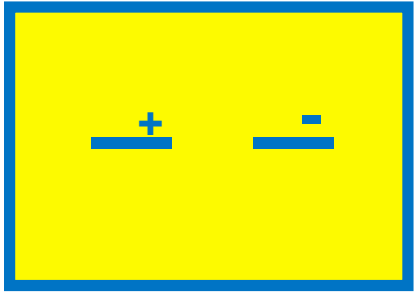
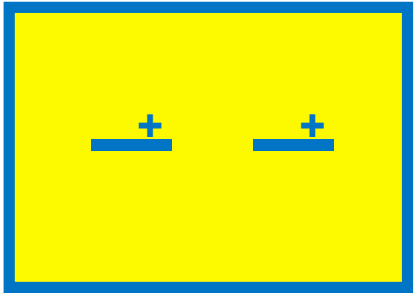
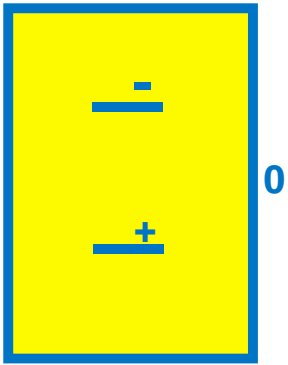
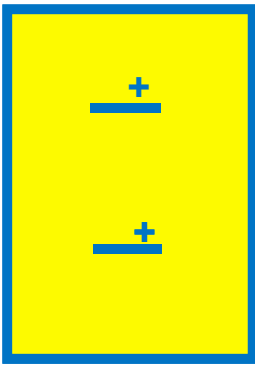
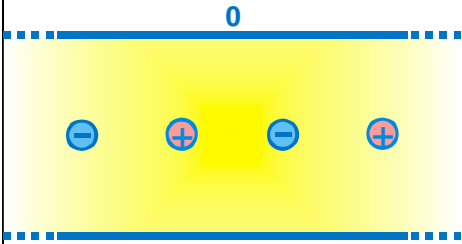
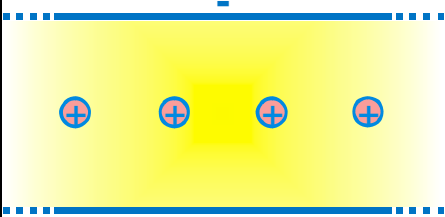
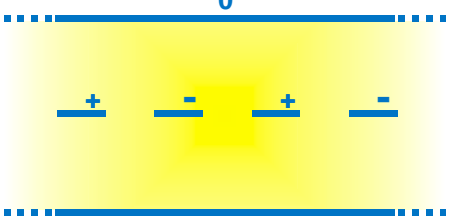
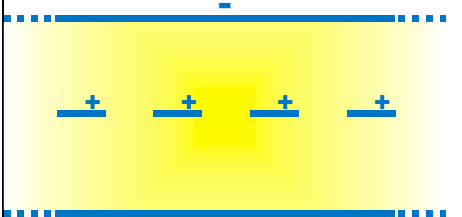
P 1.12	P 1.13	P 2
P 2.1	P 2.2	P 2.3
P 3	P 3.1	P 3.2
P 3.3	P 3.4	P 3.5

<p>P 3.6</p>	<p>P 3.7</p>	<p>P 4</p>
<p>P 4.1</p>	<p>P 4.2</p>	<p>P 4.3</p>
<p>P 4.4</p>	<p>P 4.5</p>	<p>P 4.6</p>
<p>P 4.7</p>	<p>P 4.8</p>	<p>P 4.9</p>

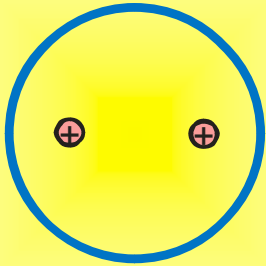
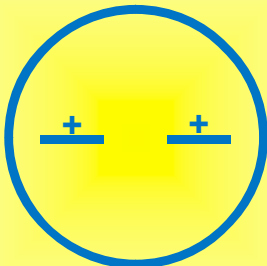
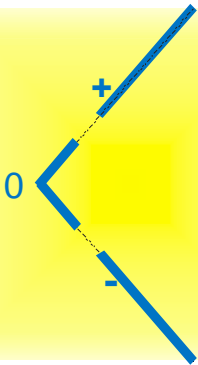

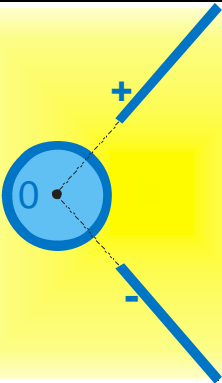
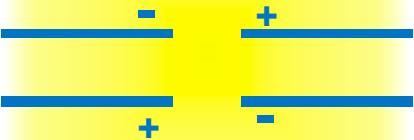

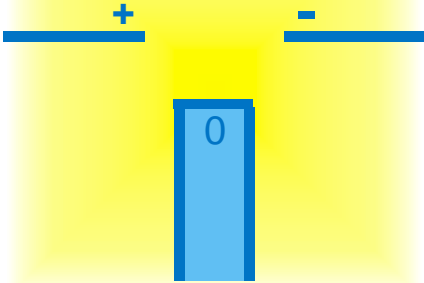
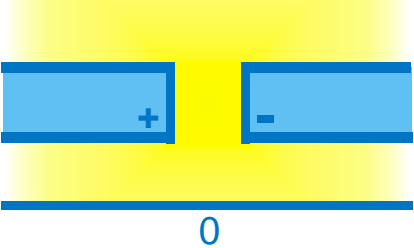
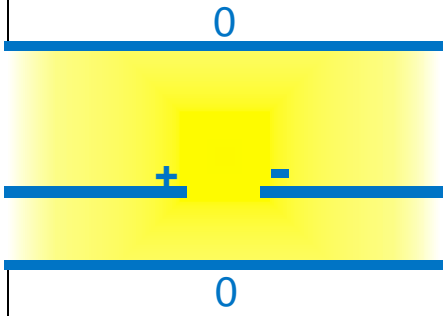
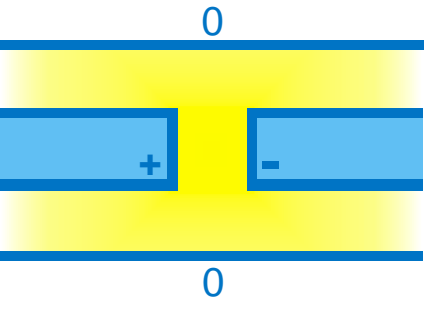
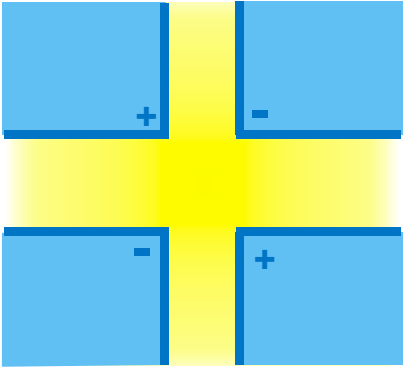
P 4.10	P 4.11	P 5
P 5.1	P 5.2	P 5.3
P 5.4	P 5.5	P 5.6
P 6	P 6.1	P 6.2

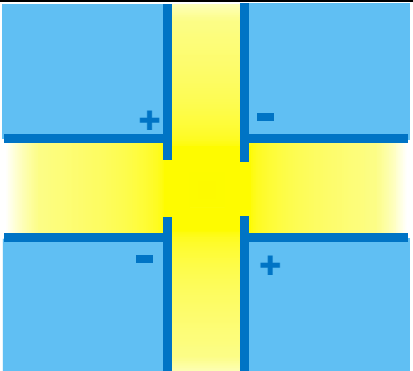
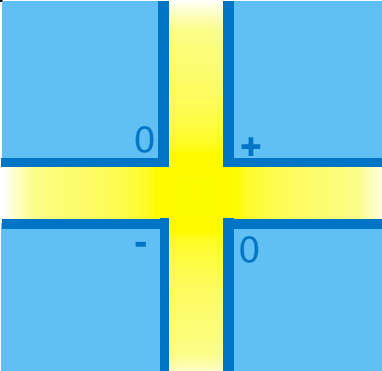
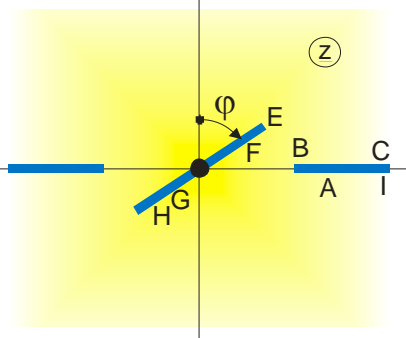
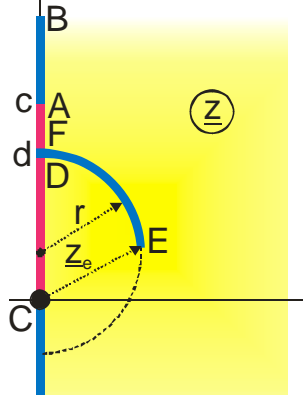
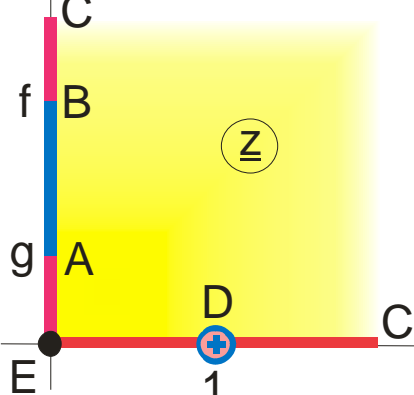
P 6.3	P 7	P 7.1
P 7.2	P 7.3	P 1.14
K 3.7	F 5.1	P 5.1
P 5.6	K 3.2	K 1.3

<p>K 3.8</p> 	<p>K 1.5</p> 	<p>K 1.6</p> 
<p>K 1.7</p> 	<p>K 2.1</p> 	<p>K 3.5</p> 
<p>K 4.5</p> 	<p>K 1.12</p> 	<p>K 1.4</p> 
<p>K 2.3</p> 	<p>F 8.1</p> 	<p>F 8.2</p> 

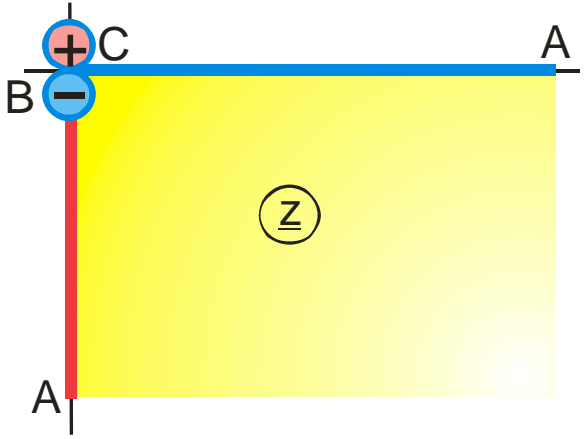
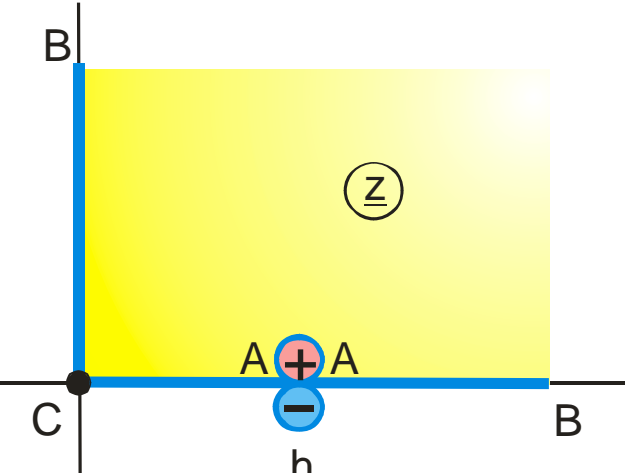
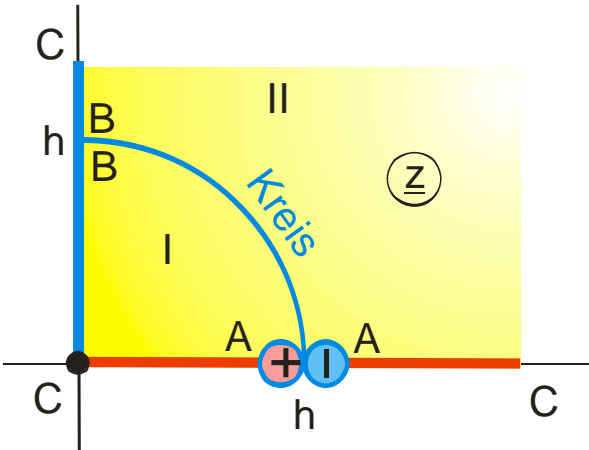
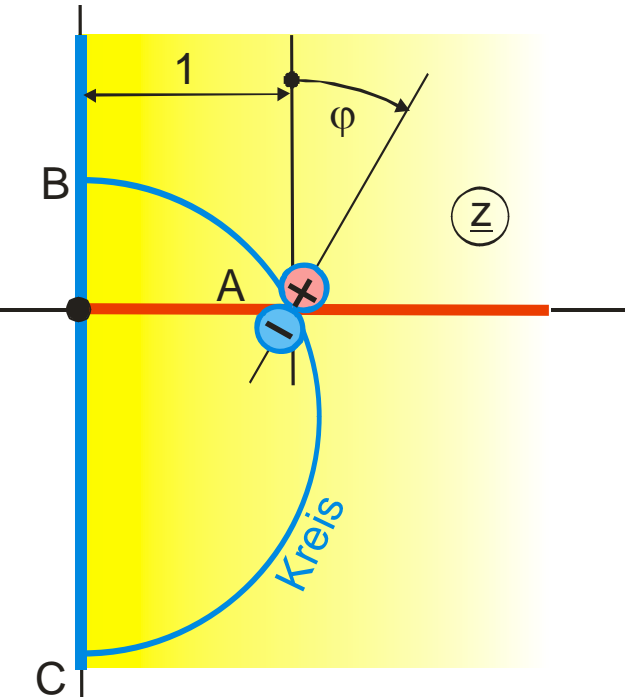
<p>F 8.3</p> 	<p>F 8.5</p> 	<p>I 1.1</p> <p>0</p> 
<p>I 1.4</p> <p>-</p> 	<p>I 2.1</p> <p>0</p> 	<p>I 2.4</p> <p>-</p> 
<p>I 1.2</p> 	<p>I 6</p>  <p>-</p>	<p>I 1</p> <p>0</p> 
<p>I 1.2</p> 	<p>I 2.1</p> <p>0</p> 	<p>I 2.2</p> <p>-</p> 

P 4.12	P 2.4	P 7.4
F 2.6	F 6.1	F 4.3
F 4.2	F 2.7	F 3.4
E 3	F 4.6	F 4.5

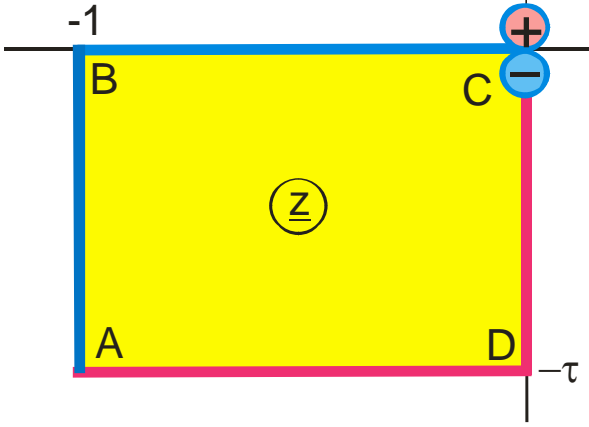
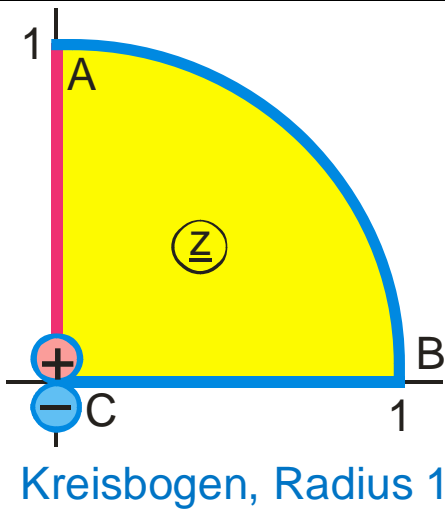
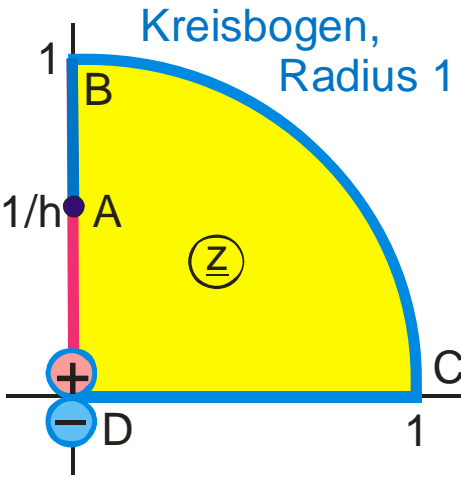
F 2.10	F 6.7	D 2.6
		
D 7.1	D 7.4	D 2
		
D 2.3	D 2.4	D 6.1
		
D 5	D 6	D 4
		

D 4.1	D 4.3	P 4.13
		
P 4.14	P 2.5	
		

Group Q: Fields with Dipoles

Q 1	Q 2
	
Q 2.1	Q 2.2
	






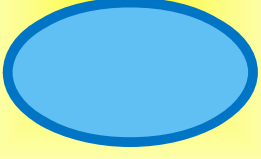
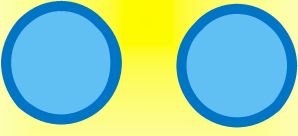





Q 3	Q 3.1
Q 4	Q 4.1
Q 4.2	Q 4.3

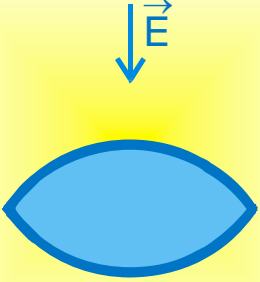

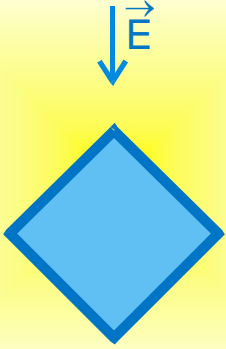
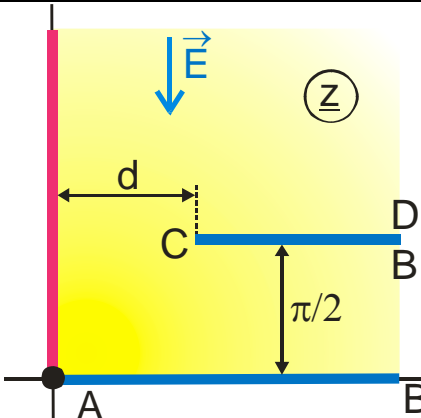


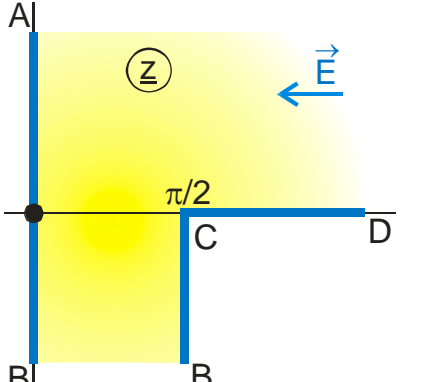
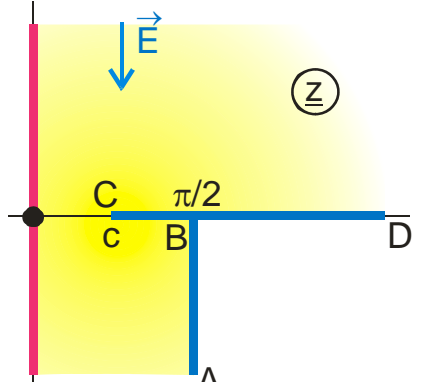
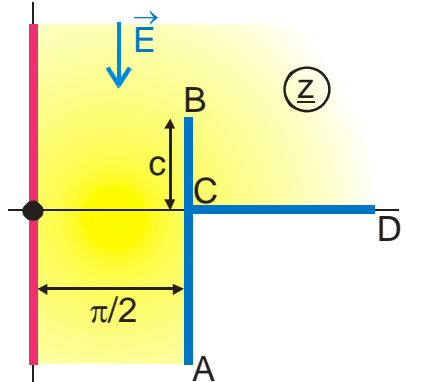
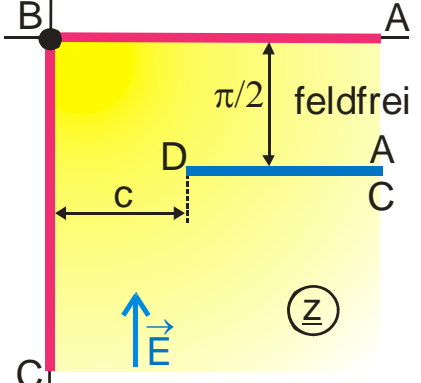
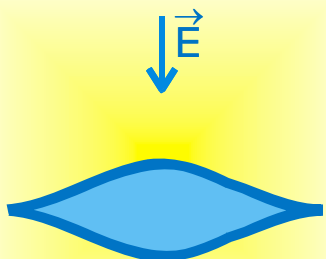
Q 4.4	Q 5
	 <p>Kreisbogen, Radius 1</p>
Q 5.1	
 <p>Kreisbogen, Radius 1</p>	

Group R: Conducting Boundaries in a Uniform Field

<p>R 1</p>	<p>R 2</p>	<p>R 2.1</p>
<p>R 3</p>	<p>R 3.1</p>	<p>R 3.2</p>
<p>R 3.3</p>	<p>R 3.4</p>	<p>R 4</p>
<p>R 4.1</p>	<p>R 4.2</p>	<p>R 4.3</p>

R 4.4	R 4.5	R 4.6
R 4.7	R 5	R 6
R 7	R 7.1	R 6
R 7.2	R 4.8	R 4.9

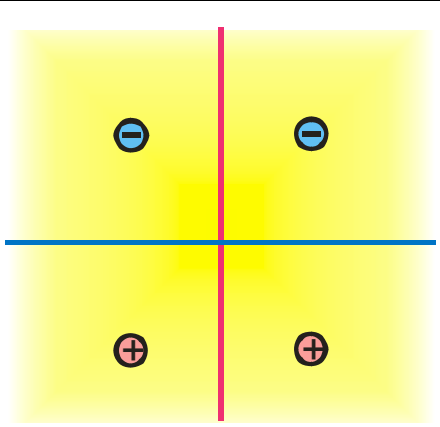
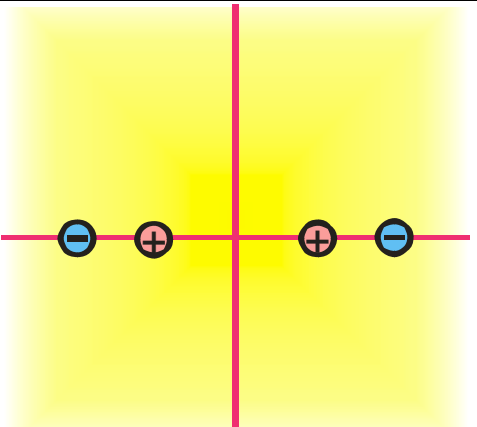
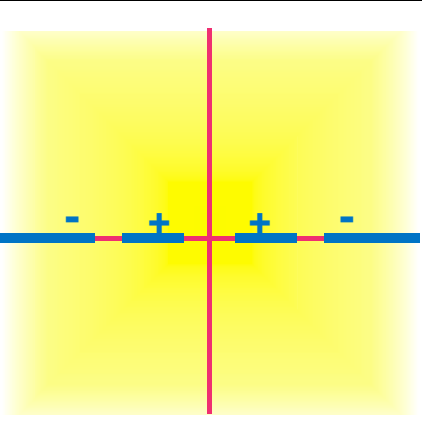
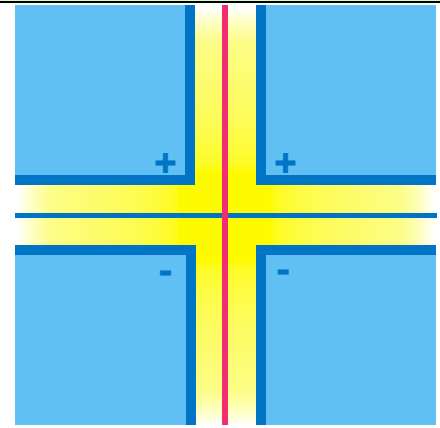
A 2.1	A 11	A 11.1
		
A 3	A 3.1	A 3.2
		 Ellipse
A 4	A 4.1	A 3.7
		
A 11.2	A 3.5	A 3.8
	 Kreissektor	 Kreisbogen

A 3.4	A 10.2	A 10.6
 <p>Kreispbogenzweieck, $\beta > 0$</p>		
R 5.1	A 3.10	R 2
 <p>2 Kreisbögen</p>		
R 4.10	R 4.11	R 4.12
		
R 5.2	A 3.11	
		

Group S: Conducting Boundaries, Symmetrically Arranged, Same Charge, Same Polarity

S 1	S 2	S 2.1
S 2.2	S 3	S 4
S 4.1	S 5	S 6
A 2.1	R 5.2	P 6.2

15. Table of Conformal Mappings

L 3	L 4	K 3.7
		
P 3.1		
		

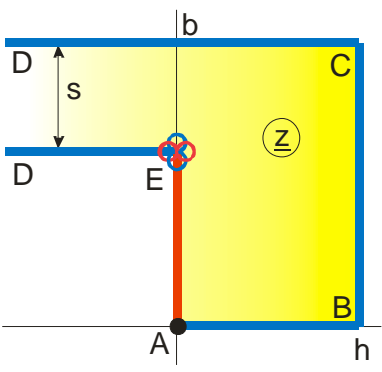
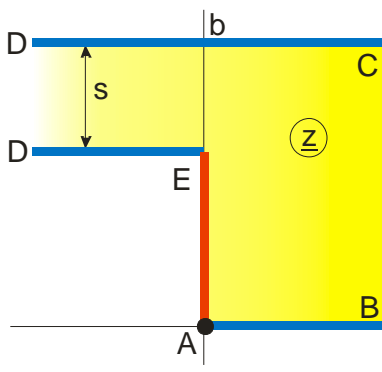
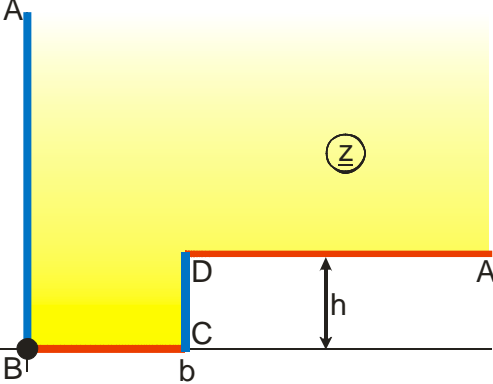
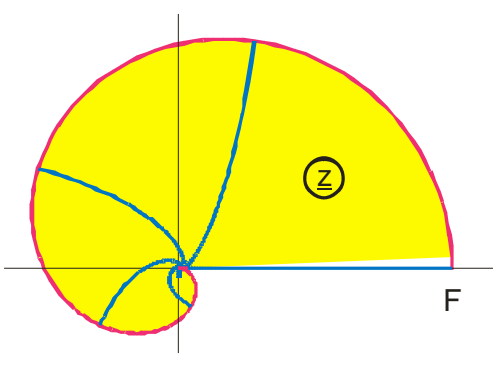
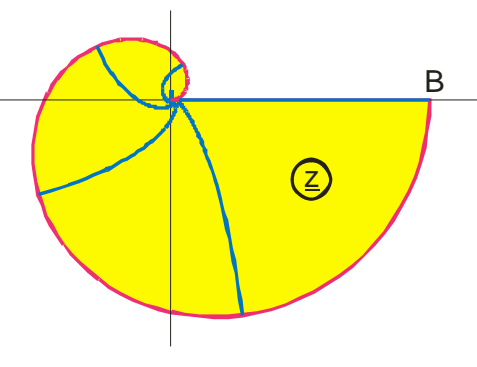
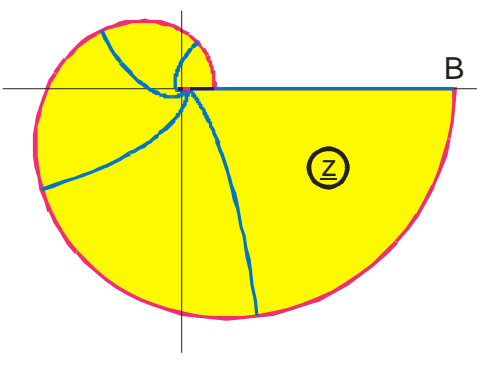
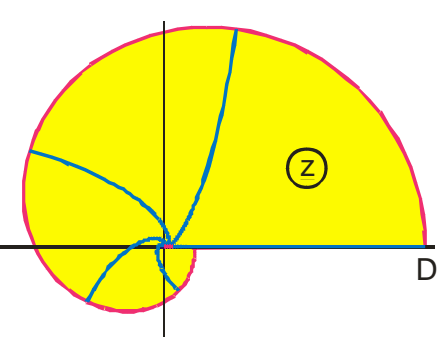
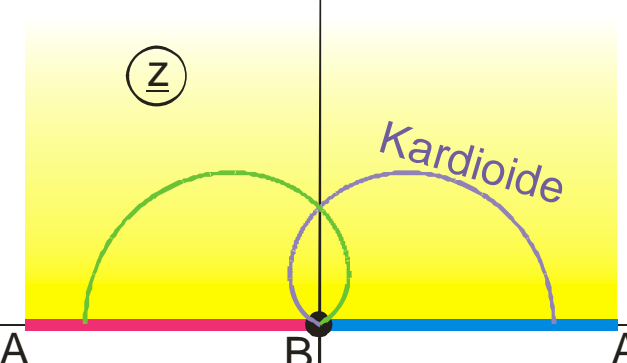
Group T: Mappings with Nonconducting Boundaries

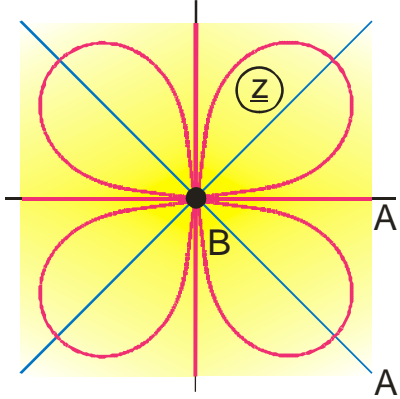
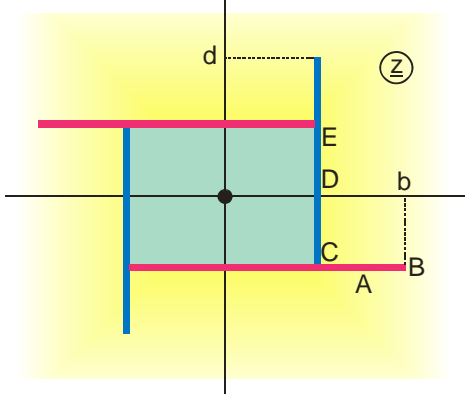
T 1	T 2
T 2.1	T 2.2
T 3	T 3.1
T 3.2	T 3.3

T 4	T 5
T 4.1	T 5.1
T 5.2	

Group U: More Mappings, Special Functions

U 1	U 1.1
U 2	U 2.1
U 2.2	U 3
U 4	U 4.1

U 4.2	U 4.3
	
U 5	U 6.1
	
U 6.2	U 6.3
	
U 6.4	U 7
	

U 7.1	U 7.2
	

16. BASIC-Subroutines

Conformal transformations whose mapping function contain elliptic functions, elliptic integrals or theta functions can be calculated using the following subroutines. In the program library these subroutines are listed as plain text in the program A_ELLI.bas. This chapter is a printout of A_ELLI.bas. In the individual BASIC mapping programs the subroutines are loaded from D_ELLI, the compiled version of A_ELLI.bas.

The sources for the applied algorithms are listed in the comments below.

These subroutines were written at a time, where the PC's were so slow, that it took several minutes to run some of the programs. Therefore they are optimized with respect to short runtime. Instead of e.g. $C1^2$ they use $C1*C1$, which is faster (see for instance line 285 below) etc.

16.1 Elliptic Functions

16.1.1 Elliptic Function sn (z,k)

```

195  SUB Csn(U,V,K,X,Y)    ! CALL Scdz
200  !
205  ! - sn MIT KOMPLEXEM ARGUMENT ----- Abramowitz 16.21.2 -----
210  ! EINGABE : u+jv  und  k
215  ! AUSGABE : x+jy
220  M=K*K
225  Kc=SQR(1-M)
230  CALL Scdz(U,K,K8,E8,S,C,D,Z)
235  CALL Scdz(V,Kc,K9,E9,S1,C1,D1,Z1)
240  IF V=K9 THEN
245  Y=0
250  IF U=0 THEN
255  X=0
260  Y=1.E+12
265  ELSE
270  X=1/(K*S)
275  END IF
280  ELSE

```

```

285      Nenn=C1*C1+M*S*S1*S*S1
290      X=S*D1/Nenn
295      Y=C*D*S1*C1/Nenn
300      END IF
305      SUBEND

```

16.1.2 Elliptic Function cn (z,k)

```

3190  SUB Ccn(U,V,K,X,Y)      ! CALL Scdz
3195  !
3200  ! cn mit komplexem Argument      Abramowitz 16.21.3
3205  ! EINGABE : u+jv   und   k
3210  ! AUSGABE : x+jy
3215  M=K*K
3220  Kc=SQR(1-M)
3225  CALL Scdz(U,K,K8,E8,S,C,D,Z)
3230  CALL Scdz(V,Kc,K9,E9,S1,C1,D1,Z1)
3235  Nenn=C1*C1+M*S*S1*S*S1
3240  Nenn1=C1*C1+M*S1*S1
3245  IF Nenn=0 THEN Nenn=1.E-7
3250  IF Nenn1=0 THEN Nenn1=1.E-7
3255  X=C*C1/Nenn
3260  Y=-S*D*S1*D1/Nenn
3265  IF U=K8 THEN
3270      X=0
3275      IF V=K9 THEN
3280          Y=-Kc/K
3285      ELSE
3290          Y=-Kc*S1*D1/Nenn1
3295      END IF
3300  END IF
3305  IF V=K9 AND U>0 THEN
3310      X=0
3315      IF U=K8 THEN
3320          Y=-Kc/K
3325      ELSE
3330          Y=-D/(K*S)
3335      END IF
3340  END IF
3345  IF U<0 THEN X=-X ! 4-Quadranten-Version
3350  IF U<0 THEN Y=-Y ! 4-Quadranten-Version
3355  SUBEND

```

16.1.3 Elliptic Function dn (z,k)

```

315  SUB Cdn(U,V,K,X,Y)      ! CALL Scdz
320  !
325  ! - dn MIT KOMPLEXEM ARGUMENT ----- Abramowitz 16.21.4 -----
330  ! EINGABE : u+jv   und   k

```

```

335    ! AUSGABE : x+jy
340    M=K*K
345    Kc=SQR(1-M)
350    CALL Scdz(U,K,K0,E0,S,C,D,Z)
355    CALL Scdz(V,Kc,K0,E0,S1,C1,D1,Z1)
360    Nenn=C1*C1+M*S*S*S1*S1
365    X=D*C1*D1/Nenn
370    Y=-M*S*C*S1/Nenn
375    SUBEND

```

16.1.4 Zeta Function $Z_a(z,k)$

```

3445    SUB Cza(Rt,It,K,Rz,Iz)    ! CALL Cea+Cfa+Ske
3450    !
3455    !      EINGABE : K ist Modul k
3460    !      ERGEBNIS : Z = Rz + j Iz
3465    ! Zeta-Funktion, algebraische Form
3470    CALL Ske(K,K8,E8)
3475    Ks=SQR(1-K*K)
3480    M9=Ks*Ks
3485    CALL Cea(Rt,It,Ks,1,M9,Re,Ie)
3490    CALL Cfa(Rt,It,K,Rf,If)
3495    Rz=Re-E8*Rf/K8
3500    Iz=Ie-E8*If/K8
3505    SUBEND

```

16.1.5 Zeta Function $Z_t(\varphi,k)$

```

3365    SUB Czt(Phi,Psi,K,Rz,Iz)    ! CALL CE+Cf+Ske
3370    !
3375    ! Zeta-Funktion, trigonometrische Form
3380    !      EINGABE : K ist Modul k
3385    !      ERGEBNIS : Z = Rz + j Iz
3390    !      Abramowitz 17.4.27
3395    IF Phi=PI/2 AND Psi=0 THEN Phi=PI/2-1.E-7
3400    CALL Ske(K,K8,E8)
3405    Ks=SQR(1-K*K)
3410    M9=Ks*Ks
3415    CALL Ce(Phi,Psi,Ks,1,M9,Re,Ie)
3420    CALL Cf(Phi,Psi,K,Rf,If)
3425    Rz=Re-E8*Rf/K8
3430    Iz=Ie-E8*If/K8
3435    SUBEND

```

16.1.6 Zeta Function $Z_e(z,k)$

```

385    SUB Cz(U,V,K,X,Y)    ! CALL Scdz
390    !

```

```

395      ! - Zeta-Funktion mit komplexem Argument (elliptische Form) -----
400      ! EINGABE : u+jv   und k   *** Abramowitz 17.4.35/6 *****
405      ! AUSGABE : x+jy
410      M=K*K
415      Kc=SQR(1-M)
420      CALL Scdz(U,K,K8,E,S,C,D,Z)
425      CALL Scdz(V,Kc,K9,E,Ss,Cs,Ds,Zs)
430      Nenn=1-D*Ss*D*Ss
435      IF Nenn=0 THEN Nenn=1.E-9
440      X=Z+M*S*C*D*Ss*Ss/Nenn
445      Y=-Zs-PI*V/(2*K8*K9)+D*D*Ss*Cs*Ds/Nenn
450      IF U=0 AND V=K9 THEN Y=1.E+7
455      SUBEND

```

16.1.7 Elliptic Functions sn, cn, dn, $Z_e(x,k)$ as well as $K(k)$ and $E(k)$

```

465      SUB Scdz(X,K,K1,E,S,C,D,Z)
470      ! **** Abramow. 16.4 / 16.35 / 17.6 *
475      C0=K
480      B0=SQR(1-C0*C0)
485      A1=(1+B0)/2
490      B1=SQR(B0)
495      C1=(1-B0)/2
500      A2=(A1+B1)/2
505      B2=SQR(A1*B1)
510      C2=(A1-B1)/2
515      A3=(A2+B2)/2
520      B3=SQR(A2*B2)
525      C3=(A2-B2)/2
530      A4=(A3+B3)/2
535      B4=SQR(A3*B3)
540      C4=(A3-B3)/2
545      A5=(A4+B4)/2
550      C5=(A4-B4)/2
555      !
560      K1=PI/(A5+A5)
565      E=PI*(2-C0*C0-2*C1*C1-4*C2*C2-8*C3*C3-16*C4*C4-
32*C5*C5)/(4*A5)
570      !
575      F5=32*A5*X
580      F4=(F5+ASN(C5*SIN(F5)/A5))/2
585      F3=(F4+ASN(C4*SIN(F4)/A4))/2
590      F2=(F3+ASN(C3*SIN(F3)/A3))/2
595      F1=(F2+ASN(C2*SIN(F2)/A2))/2
600      F0=(F1+ASN(C1*SIN(F1)/A1))/2
605      !
610      S=SIN(F0)
615      C=COS(F0)
620      D=C/COS(F1-F0)

```

```

625     IF ABS(X)=K1 THEN D=B0
630     Z=C1*SIN(F1)+C2*SIN(F2)+C3*SIN(F3)+C4*SIN(F4)+C5*SIN(F5)
635     SUBEND

```

16.1.8 Elliptic Functions sn, cn, dn and $Z_e(z,k)$

```

1655    SUB Cscdz(U,V,K,Rs,Is,Rc,Ic,Rd,Id,Rz,Iz)    ! CALL Scdz
1660    !
1665    ! - sn , cn , dn , Z - mit komplexem Argument
1670    ! EINGABE : u+jv  und  k
1675    ! AUSGABE : Re + j Im
1680    M=K*K
1685    Kc=SQR(1-M)
1690    CALL Scdz(U,K,K8,E8,S,C,D,Z)
1695    CALL Scdz(V,Kc,K9,E9,S1,C1,D1,Z1)
1700    Nenn=C1*C1+M*S*S1*S*S1
1705    Nenn1=C1*C1+M*S1*S1
1710    IF Nenn1=0 THEN Nenn1=1.E-9
1715    IF Nenn=0 THEN Nenn=1.E-9
1720    IF S=0 THEN S=1.E-9
1725    IF K=0 THEN K=1.E-9
1730    !                                sn
1735    IF V=K9 THEN
1740        Is=0
1745        IF U=0 THEN
1750            Rs=1.E+12
1755        ELSE
1760            Rs=1/(K*S)
1765        END IF
1770    ELSE
1775        Rs=S*D1/Nenn
1780        Is=C*D*S1*C1/Nenn
1785    END IF
1790    !                                cn
1795    Rc=C*C1/Nenn
1800    Ic=-S*D*S1*D1/Nenn
1805    IF U=K8 THEN
1810        Rc=0
1815        IF V=K9 THEN
1820            Ic=-Kc/K
1825        ELSE
1830            Ic=-Kc*S1*D1/Nenn1
1835        END IF
1840    END IF
1845    IF V=K9 AND U>0 THEN
1850        Rc=0
1855        IF U=K8 THEN
1860            Ic=-Kc/K
1865        ELSE

```

```

1870      Ic=-D/(K*S)
1875      END IF
1880      END IF
1885      !                      dn
1890      IF V=K9 THEN
1895          Rd=0
1900          Id=-C/S
1905      ELSE
1910          Rd=D*C1*D1/Nenn
1915          Id=-M*S*C*S1/Nenn
1920      END IF
1925      !                      cz
1930      Nenn=1-D*S1*D*S1
1935      IF Nenn=0 THEN Nenn=1.E-9
1940      Rz=Z+M*S*C*D*S1*S1/Nenn
1945      Iz=-Z1-PI*V/(2*K8*K9)+D*D*S1*C1*D1/Nenn
1950      SUBEND

```

16.2 Elliptic Integrals

16.2.1 Complete Elliptic Integrals K(k) and E(k)

```

2165      SUB Ske(K,K1,E)
2170      !-----
2175      DIM A(20),B(20),C(20)
2180      INTEGER I,J
2185      IF K=1 THEN
2190          K1=1.E+10
2195          E=1
2200      ELSE
2205          C(0)=K
2210          B(0)=SQR(1-C(0)*C(0))
2215          A(0)=1
2220          I=0
2225          LOOP
2230              I=I+1
2235              A(I)=(A(I-1)+B(I-1))/2
2240              B(I)=SQR(A(I-1)*B(I-1))
2245              C(I)=(A(I-1)-B(I-1))/2
2250              EXIT IF (I>14) OR ABS(C(I))<1.E-8
2255          END LOOP
2260          K1=PI/(2*A(I))
2265          E=2
2270          L=.5
2275          FOR J=0 TO I
2280              L=L+L
2285              E=E-L*C(J)*C(J)
2290          NEXT J
2295          E=PI/(4*A(I))*E

```



```

2300     END IF
2305     SUBEND

```

16.2.2 Complete Elliptic Integrals K , E , Π , $-\infty < k_c$, p , a , $b < +\infty$

```

2980     SUB Kep(Kc0,P0,A0,B0,Cei)
2985     !
2990         Kc=Kc0
2995         A=A0
3000         B=B0
3005         P=P0
3010         C=12
3015         Ca=10^(-C/2)
3020         IF Kc=0 THEN Kc=1.E-12
3025         D=ABS(Kc)
3030         M=1
3035         IF P>0 THEN
3040             P=SQR(P)
3045             B=B/P
3050         ELSE
3055             F=Kc*Kc
3060             Q=1-F
3065             G=1-P
3070             F=F-P
3075             Q=(B-A*P)*Q
3080             P=SQR(F/G)
3085             A=(A-B)/G
3090             B=-Q/(G*G*P)+A*P
3095         END IF
3100     Mar: F=A
3105         A=B/P+A
3110         G=D/P
3115         B=F*G+B
3120         B=B+B
3125         P=G+P
3130         G=M
3135         M=Kc+M
3140         !
3145         IF ABS(G-Kc)>G*Ca THEN
3150             Kc=SQR(D)
3155             Kc=Kc+Kc
3160             D=Kc*M
3165             GOTO Mar
3170         END IF
3175         Cei=PI/2*(A*M+B)/(M*M+M*P)
3180     SUBEND

```

16.2.3 Elliptic Integral of the First Kind $F_a(x,k)$, Real Argument

```

25  SUB F1(X,K0,F1)
30  !
35  !      BERECHNUNG DES ELLIPTISCHEN INTEGRALS 1.ART:
F1(X|K)
40  !      ARGUMENT X, MODUL K, ERGEBNIS F1
45  !      x = tan(Phi)
50      K=K0
55      D=8      ! AUF D STELLEN GENAU
60      IF X=0 THEN
65          F1=0
70      ELSE
75          IF K=1 THEN K=K-1.E-16
80          INTEGER B2
85          B5=ABS(1/X)
90          B0=SQR(1-K*K)
95          B1=1
100         B2=0
105 L1:   B3=B1*B0
110         B4=B1
115         B1=B0+B1
120         B5=-B3/B5+B5
125         IF B5=0 THEN B5=SQR(B3)*10^(-D+2)
130         IF ABS(B4-B0)>10^(-D/2)*B4 THEN L2
135         GOTO L3
140 L2:   B0=SQR(B3)*2
145         B2=B2+B2
150         IF B5<0 THEN B2=1+B2
155         GOTO L1
160 L3:   IF B5<0 THEN B2=1+B2
165         B3=(ATN(B1/B5)+PI*B2)/B1
170         F1=B3
175         IF X<0 THEN F1=-B3
180     END IF
185  SUBEND

```

16.2.4 Elliptic Integral of the First Kind $F_t(\phi, k)$, Real Argument

```

2315  SUB F(Phi,K0,F1)
2320  !=====
2325  !      BERECHNUNG DES ELLIPTISCHEN INTEGRALS 1.ART:
F1(Phi|k)
2330  !      ARGUMENT Phi, MODUL k, ERGEBNIS F1
2335      X=TAN(Phi)
2340      K=K0
2345      D=8      ! AUF D STELLEN GENAU
2350      IF X=0 THEN
2355          F1=0
2360      ELSE
2365          IF K=1 THEN K=K-1.E-16

```

```

2370      INTEGER B2
2375      B5=ABS(1/X)
2380      B0=SQR(1-K*K)
2385      B1=1
2390      B2=0
2395 L1:   B3=B1*B0
2400      B4=B1
2405      B1=B0+B1
2410      B5=-B3/B5+B5
2415      IF B5=0 THEN B5=SQR(B3)*10^(-D+2)
2420      IF ABS(B4-B0)>10^(-D/2)*B4 THEN L2
2425      GOTO L3
2430 L2:   B0=SQR(B3)*2
2435      B2=B2+B2
2440      IF B5<0 THEN B2=1+B2
2445      GOTO L1
2450 L3:   IF B5<0 THEN B2=1+B2
2455      B3=(ATN(B1/B5)+PI*B2)/B1
2460      F1=B3
2465      IF X<0 THEN F1=-B3
2470      END IF
2475      SUBEND

```

16.2.5 Elliptic Integral of the First Kind $F_a(z,k)$

```

5925      SUB Cfa(U,V,K,X,Y)          ! CALL F1
5930      !
5935      ! Ellipt. Integral 1.Art mit komplexem Argument
5940      ! EINGABE : u+jv   und k       Abramowitz
5945      ! AUSGABE : x+jy
5950      COMPLEX W1,W2
5955      IF ABS(V)<1.E-12 THEN V=0
5960      W1=CMPLX(U,V)
5965      IF ABS(U)=1 AND V=0 THEN
5970          W1=W1-1.E-7

5975      END IF
5980      W2=ASN(W1)
5985      H=REAL(W2)
5990      S=IMAG(W2)
5995      M=K*K
6000      Ms=1-M
6005      Kc=SQR(Ms)
6010      IF ABS(S)>100 THEN S=SGN(S)*100
6015      IF H=0 THEN
6020          X=0
6025          B=SINH(S)
6030          CALL F1(B,Kc,Y)
6035          GOTO L1

```

```

6040     END IF
6045     IF S=0 THEN
6050         L=TAN(H)
6055         B=0
6060         GOTO L2
6065     END IF
6070     H1=H
6075     IF ABS(H)=PI/2 THEN H1=H-1.E-6
6080     T1=TAN(H1)
6085     T2=T1*T1
6090     IF T2=0 THEN T2=1.E-5
6095     S1=SIN(H)
6100     IF S1=0 THEN S1=1.E-5
6105     P1=1/T2+M*SINH(S)*SINH(S)/(S1*S1)-Ms
6110     P2=Ms/T2
6115     X0=P1/2+SQR(P2+P1*P1/4)
6120     IF X0=0 THEN X0=1.E-8
6125     L=1/SQR(X0)
6130     A=(T2*X0-1)/M
6135     B=SQR(ABS(A))
6140 L2: CALL F1(L,K,X)
6145     CALL F1(B,Kc,Y)
6150     IF H<0 THEN X=-ABS(X)      ! ***
6155 L1: SUBEND

```

16.2.6 Elliptic Integral of the First Kind $F_t(\phi, k)$

```

1205     SUB Cf(Phi,Psi,K,X,Y)    ! CALL F1
1210     !
1215     ! Ellipt. Integral 1.Art mit komplexem Argument
1220     ! EINGABE : Phi+j Psi    und k *** Abramowitz 17.4.11
1225     ! AUSGABE : x+jy        *** benoetigt Sub F1(x,k,F1)
1230     M=K*K
1235     Ms=1-M
1240     Kc=SQR(Ms)
1245     IF ABS(Psi)>100 THEN Psi=SGN(Psi)*100
1250     IF Phi=0 THEN
1255         X=0
1260         Mue=SINH(Psi)
1265         CALL F1(Mue,Kc,Y)
1270         GOTO L2
1275     END IF
1280     IF Psi=0 THEN
1285         Lam=ABS(TAN(Phi))
1290         Mue=0
1295         GOTO L1
1300     END IF
1305     Phi1=Phi
1310     IF ABS(Phi)=PI/2 THEN Phi1=Phi-1.E-6

```

```

1315     Tanu=TAN(Phi1)
1320     Tanu2=Tanu*Tanu
1325     IF Tanu2=0 THEN Tanu2=1.E-5
1330     Sinu=SIN(Phi1)
1335     IF Sinu=0 THEN Sinu=1.E-5
1340     P1=1/Tanu2+M*SINH(Psi)*SINH(Psi)/(Sinu*Sinu)-Ms
1345     P2=Ms/Tanu2
1350     X0=P1/2+SQR(P2+P1*P1/4)
1355     IF X0=0 THEN X0=1.E-8
1360     Lam=1/SQR(X0)
1365     Arg=(Tanu2*X0-1)/M
1370     Mue=SQR(ABS(Arg))
1375 L1: CALL F1(Lam,K,X)
1380     CALL F1(Mue,Kc,Y)
1385     IF Phi<0 THEN X=-ABS(X)
1390     IF Psi<0 THEN Y=-ABS(Y)
1395 L2: SUBEND

```

16.2.7 Elliptic Integral of the Second Kind $E_a(z,k)$

```

3640     SUB Cea(U1,V1,Kc0,A0,B0,U,V)
3645     !
3650     COMPLEX Xy,X1,X2,Ff,E3,G,N,T,Q,P,Dd,R,Z
3655     COMPLEX Y1,Y2,X3,X4,W,Z1,Z2
3660     Kc=Kc0
3665     A=A0
3670     B=B0
3675     IF V1=0 THEN V1=1.E-7
3680     Z1=CMPLX(U1,V1)
3685     Z2=1-Z1*Z1
3690     R2=REAL(Z2)
3695     I2=IMAG(Z2)
3700     IF R2=0 AND I2=0 THEN
3705         Z2=Z2+1.E-7
3710     END IF
3715     W=Z1/SQR(Z2)
3720     X=REAL(W)
3725     Y=IMAG(W)
3730     !   BERECHNUNG DES ELLIPT. INTEGRALS 2.ART:  $E1(u1+jv1|kc)$ 
3735     !   PARAMETER   a, b
3740     !           a=1   b=kc*kc
3745     !   ERGEBNIS:   u+jv
3750     !   MODUL:      kc = SQR(1-k^2)
3755     !
3760     X=ABS(X)
3765     IF Kc=0 THEN Kc=Kc-1.E-7
3770     INTEGER I,J,L,Genau
3775     DIM D1(20),D2(20)
3780     Genau=8

```

```

3785      Cc=10^(-Genau)
3790      Sy=SGN(Y)
3795      Y=ABS(Y)
3800      Xy=CMPLX(X,Y)
3805      C=REAL(Xy*Xy)
3810      E2=IMAG(Xy*Xy)
3815      D=Kc*Kc
3820      K=1-D
3825      IF C=-1 THEN C=C+1.E-12
3830      E1=1+C
3835      X1=CMPLX(1+C*D,D*E2)
3840      X2=CMPLX(E1,E2)
3845      F1=REAL(X1/X2)
3850      F2=ABS(X2*X2)
3855      F2=-K*X*Y*2/F2
3860      Ff=CMPLX(F1,F2)
3865      D3=SQR((ABS(Ff)+ABS(REAL(Ff)))/2)
3870      IF D3=0 THEN D3=1.E-7
3875      D4=IMAG(Ff)/(D3+D3)
3880      IF F1<0 THEN
3885          F1=D3
3890          D3=-D4
3895          D4=-F1
3900      END IF
3905      IF K<0 THEN
3910          D3=ABS(D3)
3915          D4=ABS(D4)
3920      END IF
3925      C=1+D3
3930      E3=CMPLX(E1,E2)
3935      G=CMPLX(C,D4)
3940      F1=REAL(E3*G)
3945      F2=IMAG(E3*G)
3950      N=CMPLX(F1,F2)
3955      Rn=REAL(N)
3960      In=IMAG(N)
3965      IF Rn=0 AND In=0 THEN
3970          N=N+1.E-7
3975      END IF
3980      D1(0)=REAL(Xy/N)
3985      D2(0)=IMAG(Xy/N)
3990      H=A-B
3995      I=1
4000      D=1
4005      F=1
4010      M=1
4015      Kc=ABS(Kc)
4020      E=A
4025      A=B+A
4030      L=4

```

```

4035 L1: M1=(Kc+M)/2
4040     M2=M1*M1
4045     K=F*K/(4*M2)
4050     B=E*Kc+B
4055     E=A
4060     T=CMPLX(Kc+M*D3,M*D4)
4065     Q=CMPLX(C,D4)
4070     F1=REAL(T/Q)
4075     F2=ABS(Q*Q)
4080     P=CMPLX(F1/M1,K*D4*2/F2)
4085     D3=SQR((ABS(P)+ABS(REAL(P)))/2)
4090     IF D3=0 THEN D3=1.E-7
4095     D4=IMAG(P)/(D3+D3)
4100     Dd=CMPLX(D3,D4)
4105     X4=CMPLX(X,Y)
4110     F1=REAL(Dd*X4)
4115     F2=IMAG(Dd*X4)
4120     X=ABS(F1)
4125     Y=ABS(F2)
4130     A=B/M1+A
4135     L=L*2
4140     C=1+D3
4145     D=K*D/2
4150     X3=CMPLX(X,Y)
4155     E1=REAL(X3*X3)
4160     E2=IMAG(X3*X3)
4165     K=K*K
4170     Q=CMPLX(C,D4)
4175     R=CMPLX(E1*M2+1,E2*M2)
4180     F1=REAL(Q*R)
4185     F2=IMAG(Q*R)
4190     Z=CMPLX(D*X,D*Y)
4195     N=CMPLX(F1,F2)
4200     Rn=REAL(N)
4205     In=IMAG(N)
4210     IF Rn=0 AND In=0 THEN
4215         N=N+1.E-7
4220     END IF
4225     D1(I)=REAL(Z/N)
4230     D2(I)=IMAG(Z/N)
4235     IF K>Cc THEN
4240         Kc=SQR(M*Kc)
4245         F=M2
4250         M=M1
4255         I=1+I
4260         GOTO L1
4265     !
4270     END IF
4275     F1=0
4280     F2=0

```

```

4285     FOR J=I TO 0 STEP -1
4290         F1=D1(J)+F1
4295         F2=D2(J)+F2
4300     NEXT J
4305     X=M1*X
4310     Y=M1*Y
4315     Y1=CMPLX(1-Y,X)
4320     Y2=CMPLX(1+Y,-X)
4325     E1=REAL(Y1/Y2)
4330     E2=ABS(Y2*Y2)
4335     E2=X*2/E2
4340     D=A/(M1*L)
4345     IF E1=0 THEN
4350         U=PI/2
4355     ELSE
4360         A=E2/E1
4365         U=ATN(A)
4370         IF A<0 THEN U=PI+U
4375     END IF
4380     A=D*Sy/2
4385     U=D*U+F1*H
4390     V=(-1-LOG(E1*E1+E2*E2))*A+F2*H*Sy+A
4395     IF U1<0 THEN U=-U
4400 Ende: SUBEND

```

16.2.8 Elliptic Integral of the Second Kind $E_t(\phi, k)$

```

4410     SUB Ce(Phi,Psi,Kc0,A0,B0,U,V)
4415     !
4420     COMPLEX Xy,X1,X2,Ff,E3,G,N,T,Q,P,Dd,R,Z
4425     COMPLEX Y1,Y2,X3,X4,W,S
4430     Kc=Kc0
4435     A=A0
4440     B=B0
4445     IF ABS(Phi)-PI/2<1.E-5 AND Psi=0 THEN
4450         Phi=Phi-1.E-5
4455     END IF
4460     S=CMPLX((Phi),(Psi))
4465     W=TAN(S)
4470     X=ABS(REAL(W))
4475     Y=IMAG(W)
4480     !   Berechnung des ellipt. Integrals 2.Art:  $E_1(\Phi+j\Psi|k)$ 
4485     !   wenn      a=1   b=k*c*k
4490     !   Parameter   a, b
4495     !   Ergebnis:   u+jv
4500     !   kompl. Modul:  $k = \text{SQR}(1-k^2)$ 
4505     IF Kc=0 THEN Kc=Kc-1.E-7
4510     INTEGER I,J,L,Genau
4515     DIM D1(20),D2(20)

```

```

4520      Genau=8
4525      Cc=10^(-Genau)
4530      Sy=SGN(Y)
4535      Y=ABS(Y)
4540      Xy=CMPLX(X,Y)
4545      C=REAL(Xy*Xy)
4550      E2=IMAG(Xy*Xy)
4555      D=Kc*Kc
4560      K=1-D
4565      IF C=-1 THEN C=C+1.E-12
4570      E1=1+C
4575      X1=CMPLX(1+C*D,D*E2)
4580      X2=CMPLX(E1,E2)
4585      F1=REAL(X1/X2)
4590      F2=ABS(X2*X2)
4595      F2=-K*X*Y*2/F2
4600      Ff=CMPLX(F1,F2)
4605      N1=SQR((ABS(Ff)+ABS(REAL(Ff)))/2)
4610      IF N1=0 THEN N1=1.E-7
4615      N2=IMAG(Ff)/(N1+N1)
4620      IF F1<0 THEN
4625          F1=N1
4630          N1=-N2
4635          N2=-F1
4640      END IF
4645      IF K<0 THEN
4650          N1=ABS(N1)
4655          N2=ABS(N2)
4660      END IF
4665      C=1+N1
4670      E3=CMPLX(E1,E2)
4675      G=CMPLX(C,N2)
4680      F1=REAL(E3*G)
4685      F2=IMAG(E3*G)
4690      N=CMPLX(F1,F2)
4695      Ah=ABS(N)
4700      IF Ah=0 THEN
4705          N=N+1.E-7
4710      END IF
4715      D1(0)=REAL(Xy/N)
4720      D2(0)=IMAG(Xy/N)
4725      H=A-B
4730      I=1
4735      D=1
4740      F=1
4745      M=1
4750      Kc=ABS(Kc)
4755      E=A
4760      A=B+A
4765      L=4

```

```

4770 L1: M1=(Kc+M)/2
4775     M2=M1*M1
4780     K=F*K/(4*M2)
4785     B=E*Kc+B
4790     E=A
4795     T=CMPLX(Kc+M*N1,M*N2)
4800     Q=CMPLX(C,N2)
4805     F1=REAL(T/Q)
4810     F2=ABS(Q*Q)
4815     P=CMPLX(F1/M1,K*N2*2/F2)
4820     N1=SQR((ABS(P)+ABS(REAL(P))))/2)
4825     IF N1=0 THEN N1=1.E-7
4830     N2=IMAG(P)/(N1+N1)
4835     Dd=CMPLX(N1,N2)
4840     X4=CMPLX(X,Y)
4845     F1=REAL(Dd*X4)
4850     F2=IMAG(Dd*X4)
4855     X=ABS(F1)
4860     Y=ABS(F2)
4865     A=B/M1+A
4870     L=L*2
4875     C=1+N1
4880     D=K*D/2
4885     X3=CMPLX(X,Y)
4890     E1=REAL(X3*X3)
4895     E2=IMAG(X3*X3)
4900     K=K*K
4905     Q=CMPLX(C,N2)
4910     R=CMPLX(E1*M2+1,E2*M2)
4915     F1=REAL(Q*R)
4920     F2=IMAG(Q*R)
4925     Z=CMPLX(D*X,D*Y)
4930     N=CMPLX(F1,F2)
4935     Ah=ABS(N)
4940     IF Ah=0 THEN
4945         N=N+1.E-7
4950     END IF
4955     D1(I)=REAL(Z/N)
4960     D2(I)=IMAG(Z/N)
4965     IF K>Cc THEN
4970         Kc=SQR(M*Kc)
4975         F=M2
4980         M=M1
4985         I=1+I
4990         GOTO L1
4995     !.....
5000     END IF
5005     F1=0
5010     F2=0
5015     FOR J=I TO 0 STEP -1

```

```

5020      F1=D1(J)+F1
5025      F2=D2(J)+F2
5030      NEXT J
5035      X=M1*X
5040      Y=M1*Y
5045      Y1=CMPLX(1-Y,X)
5050      Y2=CMPLX(1+Y,-X)
5055      E1=REAL(Y1/Y2)
5060      E2=ABS(Y2*Y2)
5065      E2=X*2/E2
5070      D=A/(M1*L)
5075      IF E1=0 THEN
5080          U=PI/2
5085      ELSE
5090          A=E2/E1
5095          U=ATN(A)
5100          IF A<0 THEN U=PI+U
5105      END IF
5110      A=D*Sy/2
5115      U=D*U+F1*H
5120      V=(-1-LOG(E1*E1+E2*E2))*A+F2*H*Sy+A
5125      IF Phi<0 THEN U=-U
5130      Ende: SUBEND

```

16.2.9 Elliptic Integral of the Second Kind $E_e(z,k)$

```

3515      SUB Cee(U,V,K,Re,Ie)      ! CALL Scdz
3520      !
3525      ! ellipt. Integral 2.Art, elliptische Form
3530      ! EINGABE : u+jv  und k      Abramowitz 17.4.28
3535      ! AUSGABE : Re + j Ie
3540      M=K*K
3545      Kc=SQR(1-M)
3550      CALL Scdz(U,K,K8,E8,S,C,D,Z)
3555      CALL Scdz(V,Kc,K9,E9,Ss,Cs,Ds,Zs)
3560      Nenn=1-D*Ss*D*Ss
3565      IF Nenn=0 THEN Nenn=1.E-12
3570      X=Z+M*S*C*D*Ss*Ss/Nenn
3575      Y=-Zs-PI*V/(2*K8*K9)+D*D*Ss*Cs*Ds/Nenn
3580      Re=X+U*E8/K8
3585      Ie=Y+V*E8/K8
3590      IF U=0 AND V=K9 THEN
3595          Re=1.E+9
3600          Ie=1.E+9
3605      END IF
3610      IF U=K8 AND V=K9 THEN !**  ?
3615          Re=E8
3620          Ie=K9-E9
3625      END IF

```

3630 SUBEND

16.2.10 Elliptic Integral of the Second Kind $E_a(z, k_c, a, b)$, $B_a(z, k, a = 1, b = 0)$, $D_a(z, k, a = 0, b = 1)$

```

5140 SUB Cea4(U1,V1,Kc0,A0,B0,U,V) ! CALL Ske
5145 !
5150 COMPLEX Xy,X1,X2,Ff,E3,G,N,T,Q,P,Dd,R,Z
5155 COMPLEX Y1,Y2,X3,X4,W,Z1,Z2
5160 Kc=Kc0
5165 A=A0
5170 B=B0
5175 IF V1=0 THEN V1=1.E-7
5180 Z1=CMPLX(U1,V1)
5185 Z2=1-Z1*Z1
5190 A2=ABS(Z2)
5195 IF A2=0 THEN
5200     Z2=Z2+1.E-7
5205 END IF
5210 W=Z1/SQR(Z2)
5215 X=ABS-REAL(W))
5220 Y=IMAG(W)
5225 !   BERECHNUNG DES ELLIPT. INTEGRALS 2.ART: E1(u1+jv1|kc)
5230 !   PARAMETER   a, b
5235 !           a=1   b=kc*kc
5240 !   ERGEBNIS:   u+jv
5245 !   MODUL:      kc = SQR(1-k^2)
5250 !
5255 IF Kc=0 THEN Kc=Kc-1.E-7
5260 INTEGER I,J,L,Genau
5265 DIM D1(20),D2(20)
5270 Genau=8
5275 Cc=10^(-Genau)
5280 Sy=SGN(Y)
5285 Y=ABS(Y)
5290 Xy=CMPLX(X,Y)
5295 C=REAL(Xy*Xy)
5300 E2=IMAG(Xy*Xy)
5305 D=Kc*Kc
5310 K=1-D
5315 !
5320 IF A0=1 AND B0=0 THEN
5325     CALL Ske(Kc,K9,E9)
5330     B1=E9/K-K9
5335 END IF
5340 !
5345 IF C=-1 THEN C=C+1.E-12
5350 E1=1+C
5355 X1=CMPLX(1+C*D,D*E2)

```

```

5360      X2=CMPLX(E1,E2)
5365      F1=REAL(X1/X2)
5370      F2=ABS(X2*X2)
5375      F2=-K*X*Y*2/F2
5380      Ff=CMPLX(F1,F2)
5385      N1=SQR((ABS(Ff)+ABS(REAL(Ff)))/2)
5390      IF N1=0 THEN N1=1.E-7
5395      N2=IMAG(Ff)/(N1+N1)
5400      IF F1<0 THEN
5405          F1=N1
5410          N1=-N2
5415          N2=-F1
5420      END IF
5425      IF K<0 THEN
5430          N1=ABS(N1)
5435          N2=ABS(N2)
5440      END IF
5445      C=1+N1
5450      E3=CMPLX(E1,E2)
5455      G=CMPLX(C,N2)
5460      F1=REAL(E3*G)
5465      F2=IMAG(E3*G)
5470      N=CMPLX(F1,F2)
5475      Ah=ABS(N)
5480      IF Ah=0 THEN
5485          N=N+1.E-7
5490      END IF
5495      D1(0)=REAL(Xy/N)
5500      D2(0)=IMAG(Xy/N)
5505      H=A-B
5510      I=1
5515      D=1
5520      F=1
5525      M=1
5530      Kc=ABS(Kc)
5535      E=A
5540      A=B+A
5545      L=4
5550 L1: M1=(Kc+M)/2
5555      M2=M1*M1
5560      K=F*K/(4*M2)
5565      B=E*Kc+B
5570      E=A
5575      T=CMPLX(Kc+M*N1,M*N2)
5580      Q=CMPLX(C,N2)
5585      F1=REAL(T/Q)
5590      F2=ABS(Q*Q)
5595      P=CMPLX(F1/M1,K*N2*2/F2)
5600      N1=SQR((ABS(P)+ABS(REAL(P)))/2)
5605      IF N1=0 THEN N1=1.E-7

```

```

5610     N2=IMAG(P)/(N1+N1)
5615     Dd=CMPLX(N1,N2)
5620     X4=CMPLX(X,Y)
5625     F1=REAL(Dd*X4)
5630     F2=IMAG(Dd*X4)
5635     X=ABS(F1)
5640     Y=ABS(F2)
5645     A=B/M1+A
5650     L=L*2
5655     C=1+N1
5660     D=K*D/2
5665     X3=CMPLX(X,Y)
5670     E1=REAL(X3*X3)
5675     E2=IMAG(X3*X3)
5680     K=K*K
5685     Q=CMPLX(C,N2)
5690     R=CMPLX(E1*M2+1,E2*M2)
5695     F1=REAL(Q*R)
5700     F2=IMAG(Q*R)
5705     Z=CMPLX(D*X,D*Y)
5710     N=CMPLX(F1,F2)
5715     Ah=ABS(N)
5720     IF Ah=0 THEN
5725         N=N+1.E-7
5730     END IF
5735     D1(I)=REAL(Z/N)
5740     D2(I)=IMAG(Z/N)
5745     IF K>Cc THEN
5750         Kc=SQR(M*Kc)
5755         F=M2
5760         M=M1
5765         I=1+I
5770         GOTO L1
5775     !
5780     END IF
5785     F1=0
5790     F2=0
5795     FOR J=I TO 0 STEP -1
5800         F1=D1(J)+F1
5805         F2=D2(J)+F2
5810     NEXT J
5815     X=M1*X
5820     Y=M1*Y
5825     Y1=CMPLX(1-Y,X)
5830     Y2=CMPLX(1+Y,-X)
5835     E1=REAL(Y1/Y2)
5840     E2=ABS(Y2*Y2)
5845     E2=X*2/E2
5850     D=A/(M1*L)
5855     IF E1=0 THEN

```

```

5860      U=PI/2
5865      ELSE
5870      A=E2/E1
5875      U=ATN(A)
5880      IF A<0 THEN U=PI+U
5885      END IF
5890      A=D*Sy/2
5895      U=D*U+F1*H
5900      V=(-1-LOG(E1*E1+E2*E2))*A+F2*H*Sy+A+B1
5905      IF U1<0 THEN U=-U
5910      IF V1<0 THEN V=V-B1-B1
5915      Ende: SUBEND

```

16.2.11 Elliptic Integral of the Third Kind $\Pi_a(z,k,n)$

```

2680      SUB Cpia(Rt,It,L8,Rn,In,X,Y)      ! CALL Ske+Cscdz+Ce+Theta4
2685      !
2690      ! PI , algebraische Form, n komplex
2695      ! EINGABE : u+jv und k = L8      Abramowitz 17.7.3, Lawden S.68
2700      ! AUSGABE : x+jy
2705      COMPLEX Ltm,Ltp,Tm,Tp,Cn,Q,Scd,Cz,Cu,Z,W1,W2
2710      K=L8
2715      IF K=1 THEN K=1-1.E-8
2720      IF K>1 OR K<0 THEN L1
2725      Kc=SQR(1-K*K)
2730      !
2735      W1=CMPLX(Rt,It)
2740      Rw=ABS-REAL(W1))
2745      Iw=IMAG(W1)
2750      IF Rw=1 AND Iw=0 THEN
2755          W1=W1+1.E-7
2760      END IF
2765      W2=ASN(W1)
2770      U=REAL(W2)
2775      V=IMAG(W2)
2780      !
2785      Cn=CMPLX(Rn,In)
2790      Q=ASN(SQR(Cn)/K)
2795      !
2800      CALL Ske(K,K8,E8)
2805      CALL Ske(Kc,K9,E9)
2810      Pk=PI/(K8+K8)
2815      Rq=REAL(Q)
2820      Iq=ABS(IMAG(Q))
2825      CALL Ce(Rq,Iq,Kc,1,1,Rf,If)
2830      !
2835      CALL Cscdz(Rf,If,L8,Rs,Is,Rc,Ic,Rd,Id,Rz,Iz)
2840      Cz=CMPLX(Rz,Iz)
2845      Scd=CMPLX(Rs,Is)/(CMPLX(Rc,Ic)*CMPLX(Rd,Id))

```

```

2850      !
2855      CALL Ce(U,V,Kc,1,1,Uu,Vv)
2860      Cu=CMPLX(Uu,Vv)
2865      Tau=K9/K8
2870      !
2875      CALL Theta4(Tau,(Uu+Rf)*Pk,(Vv+If)*Pk,Rtp,Itp)
2880      CALL Theta4(Tau,(Uu-Rf)*Pk,(Vv-If)*Pk,Rtm,Itm)
2885      Tp=CMPLX(Rtp,Itp)
2890      Tm=CMPLX(Rtm,Itm)
2895      Ap=ABS(Tp)
2900      IF Ap=0 THEN
2905          Tp=Tp+1.E-7
2910      END IF
2915      Am=ABS(Tm)
2920      IF Am=0 THEN
2925          Tm=Tm+1.E-7
2930      END IF
2935      Ltp=LOG(Tp)
2940      Ltm=LOG(Tm)
2945      Z=Cu+Scd*(.5*(Ltm-Ltp)+Cu*Cz)
2950      X=REAL(Z)
2955      Y=IMAG(Z)
2960 L1: SUBEND

```

16.2.12 Elliptic Integral of the Third Kind $\Pi_t(\phi, k, n)$

```

1410      SUB Cpit(U,V,L8,Rn,In,X,Y)  ! CALL Cf+Ske+Scdz+Theta4
1415      !
1420      ! - PI mit komplexem Argument --- n komplex
1425      ! EINGABE : u+jv und k = L8 *** Abramowitz 17.7.3 + Lawden S.68
1430      ! AUSGABE : x+jy
1435      COMPLEX Ltm,Ltp,Tm,Tp,Cn,Q,Scd,Cz,Cu,Z
1440      K=L8
1445      IF K=1 THEN K=1-1.E-8
1450      IF K>1 OR K<0 THEN L1
1455      Kc=SQR(1-K*K)
1460      !
1465      Cn=CMPLX(Rn,In)
1470      Q=ASN(SQR(Cn)/K)
1475      !
1480      CALL Ske(K,K8,E8)
1485      CALL Ske(Kc,K9,E9)
1490      Pk=PI/(K8+K8)
1495      Rq=REAL(Q)
1500      Iq=IMAG(Q)
1505      CALL Cf(Rq,Iq,L8,Rf,If)
1510      !
1515      CALL Cscdz(Rf,If,L8,Rs,Is,Rc,Ic,Rd,Id,Rz,Iz)
1520      Cz=CMPLX(Rz,Iz)

```



```

1525     Scd=CMPLX(Rs,Is)/(CMPLX(Rc,Ic)*CMPLX(Rd,Id))
1530     !
1535     CALL Cf(U,V,K,Uu,Vv)
1540     Cu=CMPLX(Uu,Vv)
1545     Tau=K9/K8
1550     !
1555     CALL Theta4(Tau,(Uu+Rf)*Pk,(Vv+If)*Pk,Rtp,Itp)
1560     CALL Theta4(Tau,(Uu-Rf)*Pk,(Vv-If)*Pk,Rtm,Itm)
1565     Tp=CMPLX(Rtp,Itp)
1570     Tm=CMPLX(Rtm,Itm)
1575     Ap=ABS(Tp)
1580     IF Ap=0 THEN
1585         Tp=Tp+1.E-7
1590     END IF
1595     Am=ABS(Tm)
1600     IF Am=0 THEN
1605         Tm=Tm+1.E-7
1610     END IF
1615     Ltp=LOG(Tp)
1620     Ltm=LOG(Tm)
1625     Z=Cu+Scd*(.5*(Ltm-Ltp)+Cu*Cz)
1630     X=REAL(Z)
1635     Y=IMAG(Z)
1640 L1: SUBEND

```

16.2.13 Elliptic Integral of the Third Kind $\Pi_e(z,k,a)$

```

1960     SUB Cpie(U,V,L8,Ra,Ia,X,Y)    ! CALL Cscdz+Ske+Theta4
1965     !
1970     ! - PI MIT KOMPLEXEM ARGUMENT --- a komplex --- 31.7.92
1975     ! EINGABE : u+jv und k = L8   und Re a + j Im a
1980     ! AUSGABE : x+jy          ***   Pi (u,a)
1985     COMPLEX Ltm,Ltp,Tm,Tp,Cz,Cu,Z,Scd
1990     K=L8
1995     IF K=1 THEN K=1-1.E-8
2000     IF K>1 OR K<0 THEN Mcpie
2005     Kc=SQR(1-K*K)
2010     !
2015     CALL Ske(K,K8,E8)
2020     CALL Ske(Kc,K9,E9)
2025     Pk=PI/(K8+K8)
2030     !
2035     CALL Cscdz(Ra,Ia,L8,Rs,Is,Rc,Ic,Rd,Id,Rz,Iz)
2040     Scd=CMPLX(Rs,Is)/(CMPLX(Rc,Ic)*CMPLX(Rd,Id))
2045     Cz=CMPLX(Rz,Iz)
2050     !
2055     Cu=CMPLX(U,V)
2060     Tau=K9/K8
2065     !

```

```

2070      CALL Theta4(Tau,(U+Ra)*Pk,(V+Ia)*Pk,Rtp,Itp)
2075      CALL Theta4(Tau,(U-Ra)*Pk,(V-Ia)*Pk,Rtm,Itm)
2080      Tp=CMPLX(Rtp,Itp)
2085      Tm=CMPLX(Rtm,Itm)
2090      Ap=ABS(Tp)
2095      IF Ap=0 THEN
2100          Tp=Tp+1.E-7
2105      END IF
2110      Am=ABS(Tm)
2115      IF Am=0 THEN
2120          Tm=Tm+1.E-7
2125      END IF
2130      Ltp=LOG(Tp)
2135      Ltm=LOG(Tm)
2140      Z=Cu+Scd*(.5*(Ltm-Ltp)+Cu*Cz)
2145      X=REAL(Z)
2150      Y=IMAG(Z)
2155 Mcpie: SUBEND

```

16.2.14 Elliptic Integral of the Third Kind $\Pi_j(z,k,a)$

```

2485      SUB Cpij(U,V,L8,Ra,Ia,X,Y)    ! CALL Ske+Cscdz+Theta4
2490      !
2495      ! - PI mit komplexem Argument --- a komplex --- Jakobische Form ---
2500      ! EINGABE : u+jv und k = L8  und Re a + j Im a *****
2505      ! AUSGABE : x+jy          ***      Pi_j(u,a) *****
2510      COMPLEX Ltm,Ltp,Tm,Tp,Cn,Cz,Cu,Z,Tpm
2515      K=L8
2520      IF K=1 THEN K=1-1.E-8
2525      IF K>1 OR K<0 THEN L1
2530      Kc=SQR(1-K*K)
2535      !
2540      CALL Ske(K,K8,E8)
2545      CALL Ske(Kc,K9,E9)
2550      Pk=PI/(K8+K8)
2555      !
2560      CALL Cscdz(Ra,Ia,L8,Rs,Is,Rc,Ic,Rd,Id,Rz,Iz)
2565      Cz=CMPLX(Rz,Iz)
2570      Cu=CMPLX(U,V)
2575      Tau=K9/K8
2580      !
2585      CALL Theta4(Tau,(U+Ra)*Pk,(V+Ia)*Pk,Rtp,Itp)
2590      CALL Theta4(Tau,(U-Ra)*Pk,(V-Ia)*Pk,Rtm,Itm)
2595      Tp=CMPLX(Rtp,Itp)
2600      Tm=CMPLX(Rtm,Itm)
2605      Ap=ABS(Tp)
2610      IF Ap=0 THEN
2615          Tp=Tp+1.E-7
2620      END IF

```

```

2625     Tpm=Tm/Tp
2630     Am=ABS(Tpm)
2635     IF Am=0 THEN
2640         Tpm=Tpm+1.E-7
2645     END IF
2650     Z=.5*LOG(Tpm)+Cu*Cz
2655     X=REAL(Z)
2660     Y=IMAG(Z)
2665 L1: SUBEND

```

16.3 Theta Functions

16.3.1 Theta Function $\vartheta_1(z,k)$

```

645     SUB Theta1(Tau,X,Y,Re,Im)
650     !
655     ! **** Abramowitz Nr. 16.27.1 ****
660     COMPLEX Delta,Sum_neu,Sum_alt,Z
665     INTEGER N,M
670     N=-1
675     M=0
680     Q=EXP(-PI*Tau)
685     IF ABS(Q)>=1 THEN L1
690     Sum_neu=CMPLX(0,0)
695     Z=CMPLX(X,Y)
700     WHILE M<4
705         N=N+1
710         Sum_alt=Sum_neu
715         Delta=(-1)^N*Q^(N*(N+1))*SIN((N+N+1)*Z)
720         Sum_neu=Sum_alt+Delta
725         Bd=ABS(Delta)
730         IF Bd<1.E-8 THEN
735             M=M+1
740         ELSE
745             M=0
750         END IF
755     END WHILE
760     Sum_neu=2*SQR(SQR(Q))*Sum_neu
765     Re=REAL(Sum_neu)
770     Im=IMAG(Sum_neu)
775 L1: SUBEND

```

16.3.2 Theta Function $\vartheta_2(z,k)$

```

785     SUB Theta2(Tau,X,Y,Re,Im)
790     !
795     ! **** Abramowitz Nr. 16.27.2 ****
800     COMPLEX Delta,Sum_neu,Sum_alt,Z

```

```

805     INTEGER N,M
810     N=-1
815     M=0
820     Q=EXP(-PI*Tau)
825     IF ABS(Q)>=1 THEN L1
830     Sum_neu=CMPLX(0,0)
835     Z=CMPLX(X,Y)
840     WHILE M<4
845         N=N+1
850         Sum_alt=Sum_neu
855         Delta=Q^(N*(N+1))*COS((N+N+1)*Z)
860         Sum_neu=Sum_alt+Delta
865         Bd=ABS(Delta)
870         IF Bd<1.E-8 THEN
875             M=M+1
880         ELSE
885             M=0
890         END IF
895     END WHILE
900     Sum_neu=2*SQR(SQR(Q))*Sum_neu
905     Re=REAL(Sum_neu)
910     Im=IMAG(Sum_neu)
915 L1: SUBEND

```

16.3.3 Theta Function $\vartheta_3(z,k)$

```

925     SUB Theta3(Tau,X,Y,Re,Im)
930     !
935     ! ***** Abramowitz Nr. 16.27.3 *****
940     COMPLEX Delta,Sum_neu,Sum_alt,Z
945     INTEGER N,M
950     N=0
955     M=0
960     Q=EXP(-PI*Tau)
965     IF ABS(Q)>=1 THEN L1
970     Sum_neu=CMPLX(0,0)
975     Z=CMPLX(X,Y)
980     WHILE M<4
985         N=N+1
990         Sum_alt=Sum_neu
995         Delta=Q^(N*N)*COS(2*N*Z)
1000        Sum_neu=Sum_alt+Delta
1005        Bd=ABS(Delta)
1010        IF Bd<1.E-8 THEN
1015            M=M+1
1020        ELSE
1025            M=0
1030        END IF
1035    END WHILE

```

```

1040      Sum_neu=1+Sum_neu+Sum_neu
1045      Re=REAL(Sum_neu)
1050      Im=IMAG(Sum_neu)
1055 L1: SUBEND

```

16.3.4 Theta Function $\vartheta_4(z,k)$

```

1065      SUB Theta4(Tau,X,Y,Re,Im)
1070      !
1075      ! **** Abramowitz Nr. 16.27.4 ****
1080      COMPLEX Delta,Sum_neu,Sum_alt,Z
1085      INTEGER N,M
1090      N=0
1095      M=0
1100      Q=EXP(-PI*Tau)
1105      IF ABS(Q)>=1 THEN L1
1110      Sum_neu=CMPLX(0,0)
1115      Z=CMPLX(X,Y)
1120      WHILE M<4
1125          N=N+1
1130          Sum_alt=Sum_neu
1135          Delta=(-1)^N*Q^(N*N)*COS(2*N*Z)
1140          Sum_neu=Sum_alt+Delta
1145          Bd=ABS(Delta)
1150          IF Bd<1.E-8 THEN
1155              M=M+1
1160          ELSE
1165              M=0
1170          END IF
1175      END WHILE
1180      Sum_neu=1+Sum_neu+Sum_neu
1185      Re=REAL(Sum_neu)
1190      Im=IMAG(Sum_neu)
1195 L1: SUBEND

```

REFERENCES

- [1] Prinz, H.: Hochspannungsfelder.
München: Oldenbourg 1969.
- [2] Abramowitz, M.; Stegun, I.A.: Handbook of mathematical functions.
New York: Dover Publ., 9. Auflage 1970.
- [3] Betz, A.: Konforme Abbildung.
Berlin: Springer, 2. Auflage 1964.
- [4] Buchholz, H.: Elektrische und magnetische Potentialfelder.
Berlin: Springer 1957.
- [5] Nehari, Z.: Conformal mapping.
New York: Dover Publ. 1975; New York: Mc Graw-Hill 1952
- [6] v. Koppenfels, W.; Stallmann, F.: Praxis der konformen Abbildung.
Berlin: Springer 1959.
- [7] Kober, H.: Dictionary of conformal representations.
New York: Dover Publ. 1957.
- [8] Binns, K.J.; Lawrenson, P.L.: Analysis and computation of electric and magnetic field problems. Oxford: Pergamon Press 1963.*
- [9] Ollendorf, F.: Berechnung magnetischer Felder.
Berlin: Springer 1952.
- [10] Weber, E.: Electromagnetic fields, Vol.I., Mapping of fields.
New York: Wiley 1960.
- [11] Lawden, D.F.: Elliptic functions and applications.
Berlin: Springer 1989.
- [12] Jahnke/Emde/Lösch: Tafeln höherer Funktionen.
Stuttgart: Teubner 7. Auflage 1966.
- [13] Moon, P.; Spencer, D.E.: Field theory handbook.
Berlin: Springer, 2. Auflage 1971.
- [14] Churchill, R.V.; Brown J.W.: Complex variables and applications.
London: Mc Graw-Hill, 4. Auflage 1984.
- [15] Lawrentjew, M.A.; Schabat, B.W.: Methoden der komplexen Funktionentheorie.

-
- Berlin: VEB Deutscher Verlag der Wissenschaften 1967.
- [16] Spiegel, M.R.: Complex variables (Schaum's outline series)
New York: Mc Graw-Hill 1964.
- [17] Gaier, D.: Konstruktive Methoden der konformen Abbildung.
Berlin: Springer 1964.*
- [18] Tölke, F.: Praktische Funktionenlehre, Bd. II - V.
Berlin: Springer 1966/68.
- [19] Kaden, H.: Open circularly cylindrical metal strip as shield and return circuit of a single-wire line. Siemens Forschungs- und Entwicklungs-Berichte Bd.7 (1978) Nr. 2, S. 82-90.
- [20] Bowman, F.: Introduction to elliptic functions with applications.
New York: Dover Publ. 1961.
- [21] Byrd, P.F.; Friedmann, M.D.: Handbook of elliptical integrals for engineers and scientists. Berlin: Springer, 2.Auflage 1971.
- [22] Gibbs, W.J.: Conformal transformations in electrical engineering.
London: Capman & Hall, 1958.
- [23] Whittaker, E.T.; Watson, G.N.: A course of modern analysis.
Cambridge: Cambridge University Press, 4. Auflage, 1973 (1927).
- [24] Waldron, R.A.: Theory of guided electromagnetic waves.
London: van Nostrand Reinhold 1970.
- [25] Simonyi, K.: Theoretische Elektrotechnik.
Berlin: VEB Deutscher Verlag der Wissenschaften, 6.Auflage 1977.
- [26] Bulirsch, R.: Numerical calculation of elliptic integrals and elliptic functions.
Numerische Mathematik Bd.7 (1965), S.78-90 und Bd.13 (1969) S.305-313, S.353-354, (Handbook series special functions).
- [27] Morath, E.: Nutkontraktionsfaktoren für halbgeschlossene Nuten.
Archiv für Elektrotechnik 54 (1971), S. 164-169.
- [28] Gurevich, M.I.: Theory of jets in ideal fluids.
London: Academic Press, 1965.
- [29] Milne-Thomson, L.M.: Theoretical aerodynamics.
New York: Dover Publ., 4. Aufl. 1973.
- [30] Milne-Thomson, L.M.: Theoretical hydrodynamics.
London: MacMillan, 5. Aufl. 1976.

-
- [31] Erdélyi, A.; Magnus, W.; Oberhettinger, F.; Tricomi, F.G.: Higher transcendental functions, Vol. II., New York: Mc Graw-Hill 1953.
- [32] Birkhoff, G.; Zarantonello, E.H.: Jets, wakes and cavities.
London: Academic Press, 1957.

* : with extensive references